Taming Secondary Benzylic Cations *via* Asymmetric Counteranion-Directed Catalysis

Inaugural-Dissertation

Zur

Erlangung des Doktorgrades

der Mathematisch-Naturwissenschaftlichen Fakultät

der Universität zu Köln

vorgelegt von

Vikas Kumar Singh

aus Varanasi (Indien)

Köln 2024

Berichterstatter: Prof. Dr. Benjamin List

Prof. Dr. Hans-Günther Schmalz

Tag der mündlichen Prüfung: 12.03.2024

“I have no special talent. I am only passionately curious.”

A. Einstein

Acknowledgements

Special thanks to Prof. Dr. Benjamin List for giving me opportunity to work on my Ph.D. thesis in his group. The freedom I got to work on my own ideas and his philosophy going after ‘gold’ showed me how capable I am of doing things. His continuous enthusiasm about tackling major and minor synthetic challenges in the course of developing new methods and thinking about the problems from the basic has created an encouraging working environment.

I thank to Prof. Dr. Hans-Günther Schmalz for kindly accepting the role as second referee and examiner of this Ph.D. thesis and my Ph.D. defense and Prof. Dr. Axel Klein for serving on my defense committee.

I sincerely thanks to Dr. Chendan Zhu, Dr. Chandra Kanta De, Prof. Dr. Raja Mitra, Lorenzo Baldinelli and Prof. Dr. Giovanni Bistoni for their contributions and helpful discussions to the projects and collaboration discussed in this thesis.

I also thanks to Dr. Markus Leutzsch with low temperature NMR experiments and kinetics experiments.

I also thank Anna Iniutina, Sebastian Brunen, Benjamin Mitschke and Wencke Leinung for careful reviewing and proof reading of this thesis.

I would like to thank Alexandra Kaltsidis, Dr. Monika Lindner, former and present student assistants for administrative concern.

I thank Dr. Martin Klußmann for his teaching efforts in our POC seminars.

I would like to thank all current and former technicians of the List group for their valuable contributions in terms of providing important synthetic intermediates and the maintenance of and support with the technical equipment in the laboratory.

I thank all members of the Chromatography, Mass Spectrometry, and NMR Spectroscopy Department for their assistance in the analysis of the compounds.

I would like to thank all the former and present List group members for sharing catalysts, reagents and insightful discussions.

I would like to thank Dr. Oleg Grossmann for his constant support and helpful discussions.

Last, but not least, I thank to my parents for their unconditional support and belief in me.

Table of Contents

Acknowledgements

Table of contents

Abstract

Kurzzusammenfassung

List of Abbreviations

1 Introduction 1

2 Background 2

- 2.1 Chiral Acids in Asymmetric Catalysis 2
- 2.2 Development of Strong Asymmetric Brønsted Acid Catalysts 3
- 2.3 Brønsted Acid Catalysis 10
- 2.4 Lewis Acid Catalysis 11
- 2.5 Modularity of BINOL-derived Dimeric Catalysts (IDP, *i*IDP, IDPi) 13
- 2.6 Asymmetric Counteranion-Directed Catalysis (ACDC) 15
- 2.7 Taming Benzylic Carbocations 17
- 2.8 Chiral β–branched Esters 20
- 2.8.1 Asymmetric Conjugate Reduction 21
- 2.8.2 Asymmetric Conjugate Addition 23
- 2.8.3 Asymmetric Hydrogenation 24

3 Objectives 27

4 Results and Discussion 29

- 4.1 Results and Discussion for C–O Bond Formation 29
- 4.2 Results and Discussion for C–N Bond Formation 39
- 4.3 Results and Discussion for C–C Bond Formation 44
- 4.4 Mechanism Study 52

5 Summary 66

6 Outlook 68

7 Experimental Section 73

- 7.1 General Information 73
- 7.2 Synthesis of Substrates 76
- 7.3.1 Synthesis and Characterization of Catalysts 81
- 7.3.2 Synthesis and Characterization of C–O Bond Products 103
- 7.3.3 Synthesis and Characterization of C–N Bond Products 108
- 7.3.4 Synthesis and Characterization of C–C Bond Products 111
- 7.4 Mechanistic Study Data 116
- 7.5 NMR Spectra 125
- 7.6 HPLC/GC Chromatograms 194
- 7.7 Computational Study Data 215

8 References 230

Appendix 239

Erklärung zur Dissertation 239

CV 240

Abstract

Reactions that proceed *via* carbocations play a big role in various chemical transformations for over a century. Their applications range from drug discovery, commercial compounds to petroleum industry. Despite their vast reactions in chemical synthesis, taming carbocations in asymmetric synthesis is rather limited. Hydrocarbon-based carbocations lack polarized bonds, which diminishes possible interactions with catalysts.

The main objective of this thesis is reaction development, optimization, design and synthesis of enantiomerically pure Brønsted acids, which are capable of generating and stabilizing benzylic carbocations from the corresponding racemic sp^3 starting materials.

The developed methodology provides a general approach to the synthesis of chiral benzylic compounds with high enantioselectivity. The use of confined counteranions allows for the stabilization of the carbocation intermediate, which is crucial for achieving high enantioselectivity in the subsequent C–C-, C–O- and C–N-bond forming reactions. The highly reactive cationic intermediate can be accessed from different precursors *via* Lewis- or Brønsted acid catalysis.

In conclusion, this work represents a significant contribution to the field of asymmetric synthesis and has the potential to impact the development of new drugs and materials. The design and synthesis of enantiomerically pure Brønsted acids capable of generating and stabilizing benzylic carbocations has opened up new possibilities for the synthesis of enantioenriched benzylic compounds. The use of confined counteranions has proven to be a highly effective strategy for catalytic asymmetric reactions with excellent enantioselectivity. This research has significant implications for the development of new drugs and compounds in the pharmaceutical industry.

Kurzzusammenfassung

Reaktionen, die über Carbokationen ablaufen, spielen seit über einem Jahrhundert eine große Rolle bei verschiedenen chemischen Umwandlungen. Ihre Anwendungen reichen von der Arzneimittelentwicklung über kommerzielle Verbindungen bis hin zur Erdölindustrie. Trotz ihrer umfangreichen Reaktionen in der chemischen Synthese ist die Zähmung von Carbokationen in der asymmetrischen Synthese eher begrenzt. Carbokationen auf Kohlenwasserstoffbasis weisen keine polarisierten Bindungen auf, was mögliche Wechselwirkungen mit Katalysatoren verringert.

Das Hauptziel dieser Arbeit ist die Reaktionsentwicklung, -optimierung, das Design und die Synthese von enantiomerenreinen Brønsted-Säuren, die in der Lage sind, benzylische Carbokationen aus den entsprechenden racemischen sp^3-Ausgangsmaterialien zu erzeugen und zu stabilisieren.

Die entwickelte Methodik bietet einen allgemeinen Ansatz zur Synthese chiraler Benzylverbindungen mit hoher Enantioselektivität. Die Verwendung begrenzter Gegenanionen ermöglicht die Stabilisierung des Carbokation-Zwischenprodukts, was für das Erreichen einer hohen Enantioselektivität in den nachfolgenden C–C-, C–O- und C–N-Bindungsbildungsreaktionen entscheidend ist. Das hochreaktive kationische Zwischenprodukt kann aus verschiedenen Vorläufern durch Lewis- oder Brønsted-Säure-Katalyse gewonnen werden.

Zusammenfassend lässt sich sagen, dass diese Arbeit einen bedeutenden Beitrag auf dem Gebiet der asymmetrischen Synthese darstellt und das Potenzial hat, die Entwicklung neuer Medikamente und Materialien zu beeinflussen. Das Design und die Synthese enantiomerenreiner Brønsted-Säuren, die benzylische Carbokationen erzeugen und stabilisieren können, haben neue Möglichkeiten für die Synthese enantiomerenangereicherter benzylischer Verbindungen eröffnet. Die Verwendung begrenzter Gegenanionen hat sich als äußerst effektive Strategie für katalytische asymmetrische Reaktionen mit ausgezeichneter Enantioselektivität erwiesen. Diese Forschung hat erhebliche Auswirkungen auf die Entwicklung neuer Medikamente und Verbindungen in der Pharmaindustrie.

List of Abbreviations

*	designation of chiral centers
ACDC	asymmetric counteranion-directed catalysis
alk	alkyl
ar	aryl
aq.	aqueous
BINOL	1,1’-bi-2-naphthol
Bu	butyl
cat.	catalyst or catalytic
conv.	conversion
d	days
DBU	1,8-diazabicyclo[5.4.0]undec-7-ene
DCE	1,2-dichloroethane
DCM	dichloromethane
DMF	dimethylformamide
DMSO	dimethylsulfoxide
dr	diastereomeric ratio
DSI	disulfonimide
E	electrophile
EDG	electron donating group
e.e.	enantiomeric excess

e.r.	enantiomeric ratio
equiv.	equivalents
Et	ethyl
EWG	electron withdrawing group
GC	gas chromatography
h	hours
HPLC	high performance liquid chromatography
Hdf	$SO_2{}^nC_8F_{17}$
i	iso
IDP	imidodiphosphoric acid/imidodiphosphate
IDPi	imidodiphosphorimidic/imidodiphosphorimidate
*i*IDP	imino-imidodiphosphoric acid/imino-imidodiphosphate
LUMO	lowest unoccupied molecular orbital
m	meta
min	minutes
M	molar
Me	methyl
MOM	methoxymethyl
MS	mass spectrometry or molecular sieves
MTBE	methyl *tert*-butyl ether
MW	molecular weight
NMR	nuclear magnetic resonance

Nu/NuH	nucleophile
Nf	$SO_2{}^nC_4F_9$
o	ortho
P	product
p	para
Pr	propyl
quant.	quantitative
rac	racemic
r.t.	room temperature
SKA	silyl ketene acetal
t	*tert*, tertiary
T	temperature
TBS	*tert*-butyldimethylsilyl
TES	triethylsilyl
TIPS	triisopropylsilyl
TMS	trimethylsilyl
Tf	trifluoromethylsulfonyl
THF	tetrahydrofuran
TLC	thin layer chromatography
TMS	trimethylsilyl

1. Introduction

Benzylic stereocenters are highly prevalent in a wide range of natural products and drugs[1], making their asymmetric construction a topic of great interest. Numerous methods have been reported for the asymmetric formation of the crucial benzylic C−C or C–X (X = heteroatom) bond, including the use of chiral auxiliaries, metal catalysts, organocatalysts, and enzymes, among others[2-5]. However, a more general approach would be the catalytic enantioselective reaction of a nucleophile with *in situ* generated benzylic cations, where enantiocontrol is provided by the chiral catalyst.

Benzylic cations can be generated from readily available and cheap starting materials like styrenes or benzylic alcohols (and corresponding derivatives) upon protonation by strong chiral Brønsted acids. By effectively controlling benzylic cations using this approach, it would be possible to access readily these crucial (sub)structures by selecting suitable nucleophiles (**Figure 1.1**).

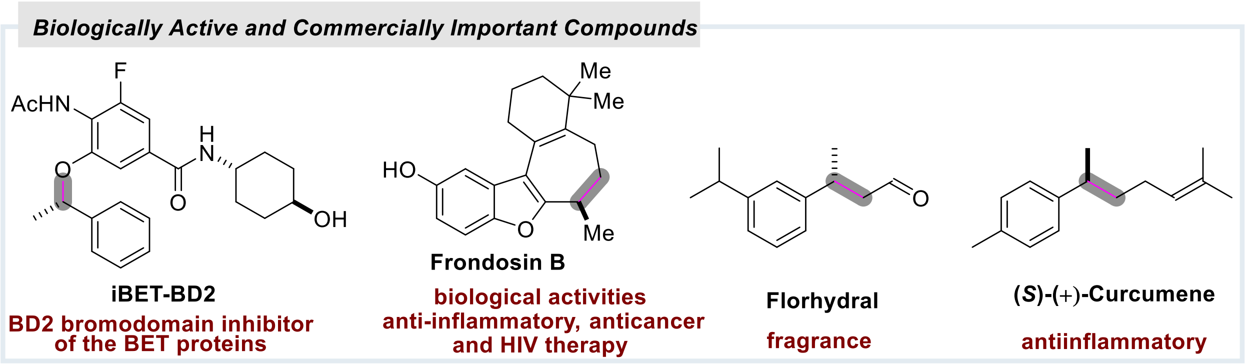
Biologically Active and Commercially Important Compounds
F
AcHN
H
N
O
O
OH
iBET-BD2
BD2 bromodomain inhibitor of the BET proteins
Me
Me
HO
O
Me
Frondosin B
biological activities anti-inflammatory, anticancer and HIV therapy
O
Florhydral
fragrance
(S)-(+)-Curcumene
antiinflammatory

Figure 1.1: Important representative structures containing benzylic stereocenters

The development of this approach would also have applications in the field of drug discovery and development. Many natural products and drugs contain benzylic stereocenters, and the ability to construct efficiently and selectively these stereocenters would facilitate the synthesis of analogs and derivatives for structure-activity relationship studies. This could lead to the discovery of new and improved pharmaceuticals.

Overall, the development of this approach would fill a significant gap in the synthetic toolbox and provide a powerful method for the construction of benzylic stereocenters. Despite the potential of this approach as a general method for constructing benzylic stereocenters, the catalytic enantioselective reaction of a nucleophile with a benzylic cation was underdeveloped at the beginning of my doctoral work.

2. Background

2.1 Chiral Acids in Asymmetric Catalysis:

In the early in 20th century Brønsted[6] and Lowry[7] independently reported a theory in which acids are defined as proton donors and bases are defined as proton acceptors. According to the IUPAC definition, a Brønsted acid is "a molecular entity capable of donating a proton to a base". Historically, acids have been classified into two major groups: Brønsted acids and Lewis acids. IUPAC defines Lewis acids as "a molecular entity that is an electron-pair acceptors." The proton itself is the simplest Lewis acid. When an acid interacts with the Lewis basic moiety of the substrate, it changes the electronic nature of the substrate by lowering the LUMO, thus increasing the electrophilic character of the substrate or activation of substrate. Acids have been used as catalysts in organic reactions by exploiting these acid-base interactions. Depending on the acidity of the catalyst and the basicity of the substrate, the acid-base interactions vary. Based on theseinteractions, acid catalysis is divided into two subclasses (**Figure2.1**).

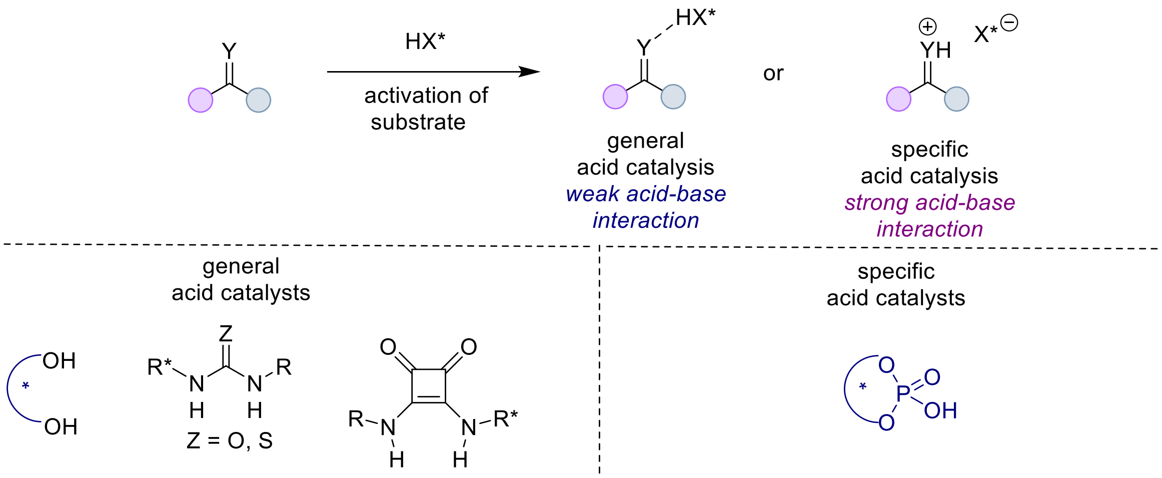
Y
HX*
activation of substrate
HX*
Y
or
YH
X*
general acid catalysis
weak acid-base interaction
specific acid catalysis
strong acid-base interaction
general acid catalysts
OH
OH
R*
N
H
Z
N
H
R
Z = O, S
O
O
R
N
H
N
H
R*
specific acid catalysts
O
P
O
O
OH

Figure 2.1: General and specific Brønsted acid catalysis

In 1998, Jacobsen and Sigman developed (thio)urea catalysts for an asymmetric Strecker reaction.[8] This work laid the foundation for the development of hydrogen bond donors (HBDs) as general catalysts.[9,10] An enantioselective hetero Diels-Alder reaction catalyzed by TADDOL-derived diol was reported by Rawal in 2003.[11] Despite several successes of HBDs as asymmetric organocatalysts, this strategy presents an inherent limitation. Due to the weak substrate-catalyst interaction, these catalysts could only activate imines and carbonyl groups. To achieve better activation of less basic substrates, a strong acid-base interaction needed.

In 2004, Akiyama and Terada independently developed BINOL (1,1'-binaphthalene-2,2'-diol) derived chiral phosphoric acids (CPAs), and their use as catalysts for enantioselective Mannich reactions between aromatic imines and carbon nucleophiles.[12] It was later revealed that the actual catalyst in the case of Terada was the calcium salt of the phosphoric acid, however reaction still could be catalyzed by using phosphoric acid, albeit with giving the opposite enantioselectivity of the product. Nevertheless, these reports laid the foundation for the development of several strong chiral Brønsted acids. With numerous reports of different CPAs, mainly based on BINOL backbones or similar chiral biphenols, such as H_8-BINOL, SPINOL, SPHENOL, VANOL, TADDOL, planar chiral diols (ferrocene-based or cyclophane-based) and among others. While strongly Lewis basic substrates such as imines were successfully activated by phosphoric acid catalysts for the addition of highly nucleophilic silyl ketene acetals[12] phosphoric acids remained insufficiently acidic for less basic substrates such as aldehydes, ketones, unsaturated carboxylic acid derivatives, and olefins. The List group developed one of the most general CPA catalysts with broad applications in asymmetric organocatalysis in 2005.[13] Although the ability to impart stereochemical information can be attributed to the catalyst structure, the propensity to initiate the reactions and modulate their rates lies mainly on the acidity of the catalyst. Thus, the focus shifted toward stronger organic Brønsted acids or as precatalysts for silylium ion based Lewis acids as potential catalysts for activating such substrates.

2.2 Development of Strong Asymmetric Brønsted Acid Catalysts:

In 2002, Yagupolskii et al. showed that the replacement of oxygen atoms by NTf groups in benzoic acid dramatically increases the acidity.[14]

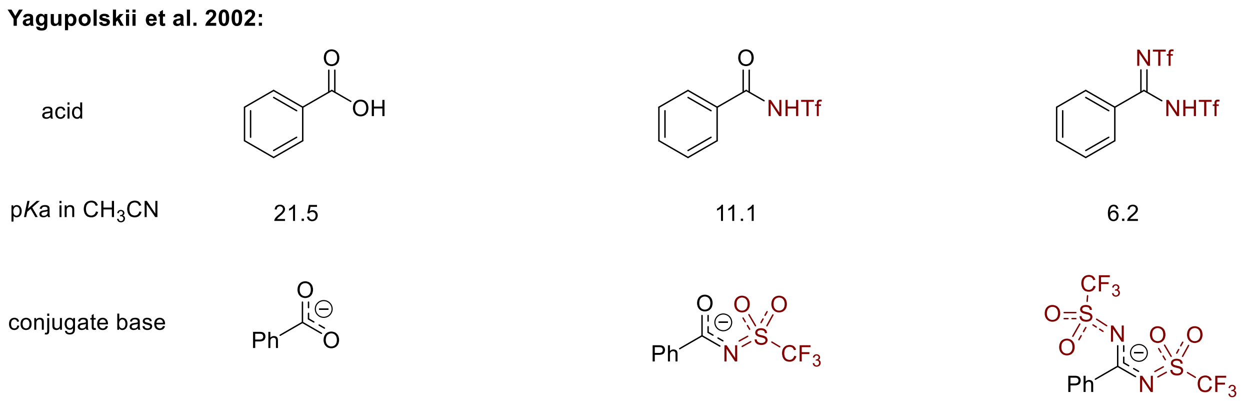
Yagupolskii et al. 2002:
acid
OH
NHTf
NTf
NHTf
pKa in CH3CN
21.5
11.1
6.2
conjugate base
Ph
Ph
CF3
Ph
CF3
CF3

Figure 2.2: Application of Yagupolskii principle on benzoic acid

Yamamoto applied the Yagupolskii principle to BINOL-derived phosphoric acids to develop *N*-triflyl-phosphoramides (NTPAs). The acidity of this phosphoramide **2.3** was sufficient to promote the catalytic enantioselective Diels–Alder reaction of α,β-unsaturated ketone **2.2** with silyloxydienes **2.1** (**Scheme2.1**).[15]

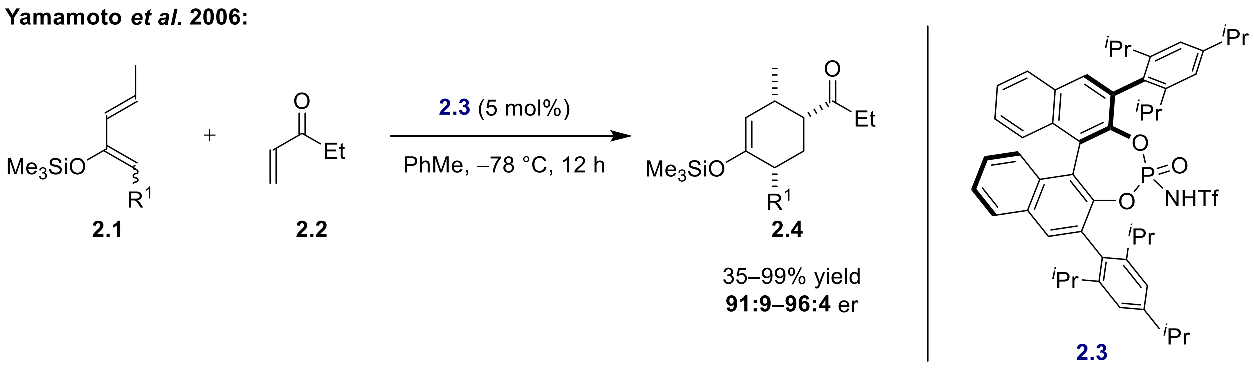
Yamamoto et al. 2006:
Me3SiO
R1
2.1
+
Et
2.2
2.3 (5 mol%)
PhMe, –78 °C, 12 h
Et
Me3SiO
R1
2.4
35–99% yield
91:9–96:4 er
iPr
iPr
iPr
NHTf
iPr
iPr
iPr
2.3

Scheme2.1: Showcase of Yagupolskii principle on BINOL-derived phosphoric acids.

Applying the similar concept towards stronger acids, the List group reported *N*-phosphinyl-phosphoramides (NPPAs) replacing the acidic hydroxyl group in the CPA structure with the phosphinylamino group.[16] Several other strategies have been applied to achieve higher acidic catalysts such as introducing electron withdrawing group on the BINOL backbone[17], replacement of oxygen atoms with sulfur/selenium in the CPAs or NTPAs translate into stronger acids.[18,19] Later, the List group extended the Yagupolskii concept to the second oxygen atom of the BINOL derived phosphoramide and synthesized highly acidic phosphoramidimidic acid **2.6**.[20] Its high acidity allows the diastereoselective addition of trimethylhydroquinone **2.4** to (7R, 11R)-isophytol

2.5, to give α-tocopherol **2.7**, albeit with low diastereoselectivity probably due to the open active site of the catalyst (Scheme 2.2).

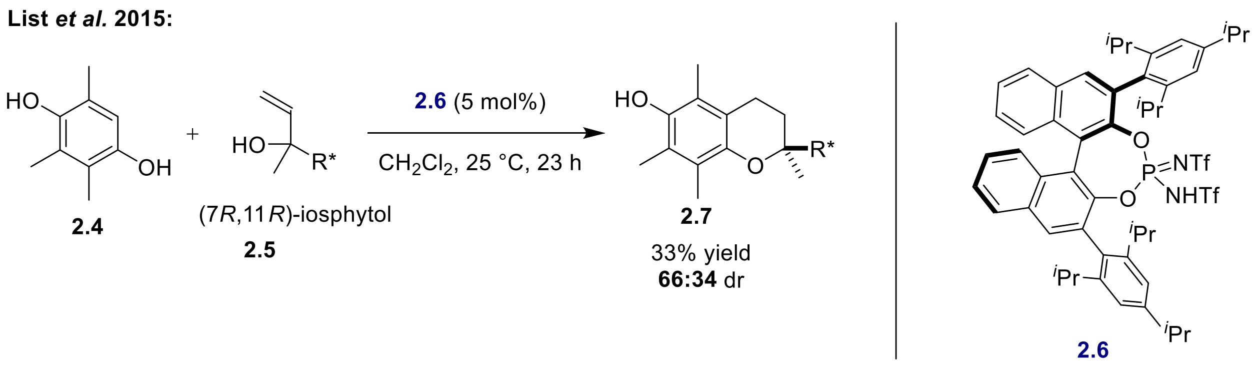
List et al. 2015:
HO
OH
2.4
+
HO
R*
(7R,11R)-iosphytol
2.5
2.6 (5 mol%)
CH2Cl2, 25 °C, 23 h
HO
O
R*
2.7
33% yield
66:34 dr
iPr
iPr
iPr
O
P=NTf
NHTf
O
iPr
iPr
iPr
2.6

Scheme 2.2: Showcase of Yagupolskii principle on BINOL-derived phosphoric acids.

In search for stronger chiral acid catalysts, moving to sulfur as central element, several chiral sulfonic acids and derivatives have been developed, which display higher reactivity and selectivity compared to CPA. In 2009, List[21] and Giernoth[22] independently reported a new class of more acidic chiral Brønsted acids, disulfonimides (DSI). List et al. demonstrated an enantioselective Mukaiyama aldol reaction between aromatic aldehyde **2.7** and silyl ketene acetal **2.8** to give the

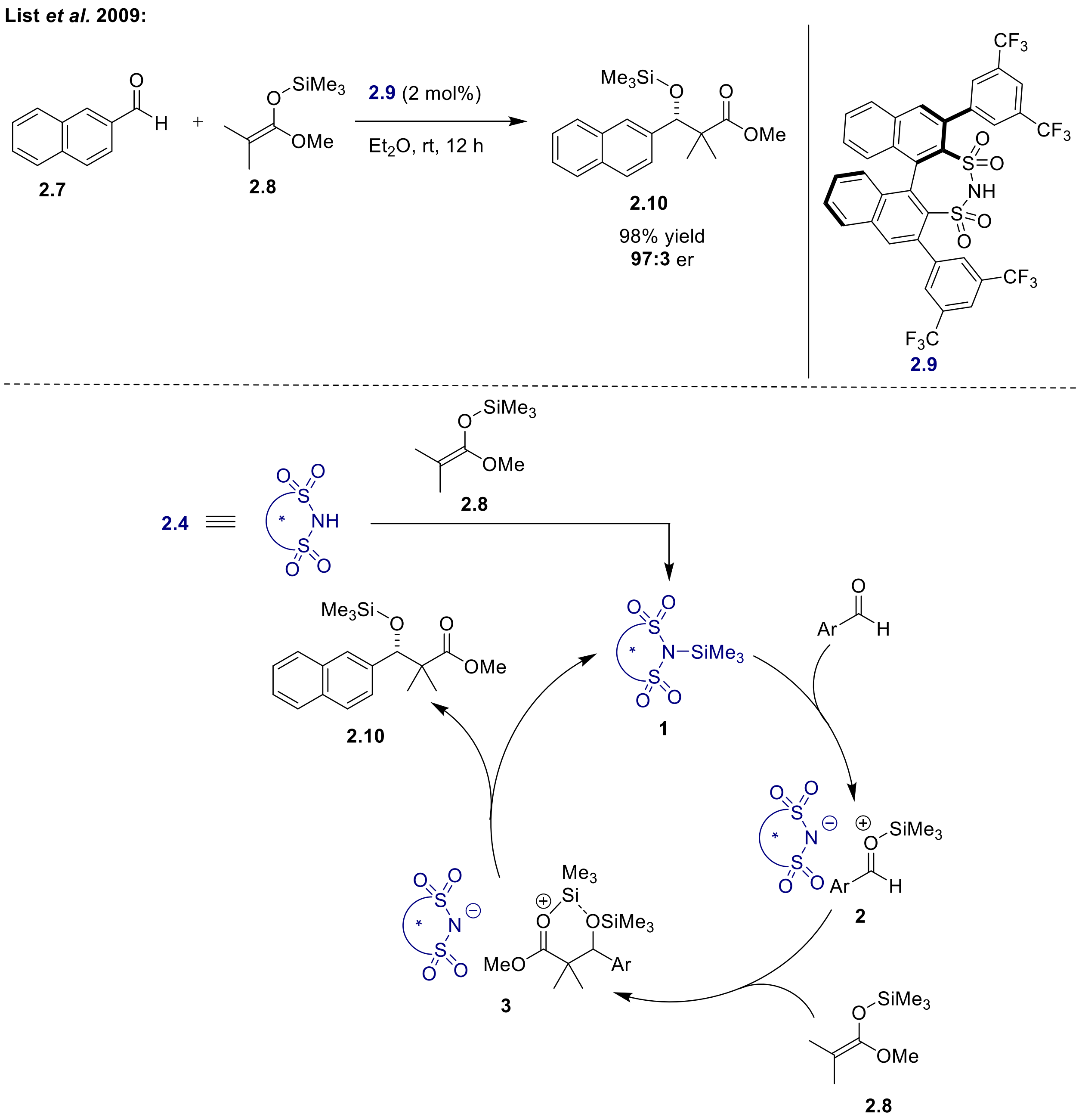
List et al. 2009:
2.7
2.8
2.9 (2 mol%)
Et_2O, rt, 12 h
2.10
98% yield
97:3 er
2.9
2.4
2.8
1
2
3
2.10
2.8

Scheme 2.3: A Mukaiyama aldol reaction between silyl ketene acetals and aldehydes catalyzed by DSI. Proposed catalytic cycle.

corresponding product in excellent yield and enantioselectivity using DSI **2.9** as precatalyst. Mechanistically, the reaction proceeds through silylation of DSI **2.9** by silyl ketene acetal **2.8** to generate active Lewis acid catalyst **1**. Lewis acid **1** then activates aldehyde to form ion pair **2**, which is attacked by nucleophile **2.8** to give intermediate **3**. The catalytic cycle is completed by the liberation of product **2.10** and the regeneration of active catalyst **1** (**Scheme2.3**). DSI catalysts have proven to be powerful Brønsted and Lewis acids that can effectively catalyze various asymmetric transformations, including alkylations, condensations, cyclizations, cascade reactions, reductions, and more.[23,24]

Several limitations remained in spite of the numerous applications of DSI catalysts in both Brønsted and Lewis acid catalyzed reactions. For example, due to their lower reactivity and challenging enantiofacial discrimination, the transformation of small, unbiased aliphatic aldehydes proceeded with significantly diminished efficiency and enantioselectivity compared to aromatic aldehydes.[24] By substituting the disulfonimide functionality with analogous bis(sulfuryl)imides (JINJLE), introduced by Berkessel et al. [25], a higher catalytic efficiency was achieved. Alternatively, List et al. used disulfonic acid (BINSA) [26,27]. The most acidic catalysts of this class have not found application with high enantioselectivity[24], although BINSA has been used in asymmetric transformations, either as its pyridinium salt, as reported by Ishihara et al.[28], or as a ligand in the presence of Lewis acidic metals.[29] The spatial discrimination that these catalysts provide around the active site in the absence of additional interactions with the substrate is likely to be insufficient to allow for efficient enantiodifferentiation. A breakthrough in this regard, which also limited the applicability of BINOL-derived phosphoric acids in Brønsted acid catalysis, was subsequently achieved by Čorić and List by the developing imidodiphosphate (IDP) Brønsted acids[30]. They increased the confinement around the catalytically active site by linking two units of BINOL-derived phosphate *via* a P−N−P bridge. IDPs are sterically highly confined acids with the active core buried within two 3,3´-disubstituted BINOL units, allowing for exceptionally high levels of stereoinduction even with unfunctionalized, aliphatic substrates[31-34], in contrast to the open active site of both BINOL-based phosphoric acids and DSIs. The newly synthesized BINOL-derived dimeric catalysts have some key features; they are modular in nature with tunable acidity and functionality, in addition to having a confined structure. The spiroacetalization of electronically and sterically unbiased substrate **2.11** in high yield and enantioselectivity demonstrated by the potential of the confined IDP[30]. The Nargony group achieved the same transformation with high enantioselectivity using **TRIP 2.14**. However, in contrast to the IDP system, they modified the substrate for enhancing the Thrope-Ingold effect (two germinal phenyl groups) and possible π-interactions between aromatic groups and the catalyst (**Scheme 2.4**).[35]

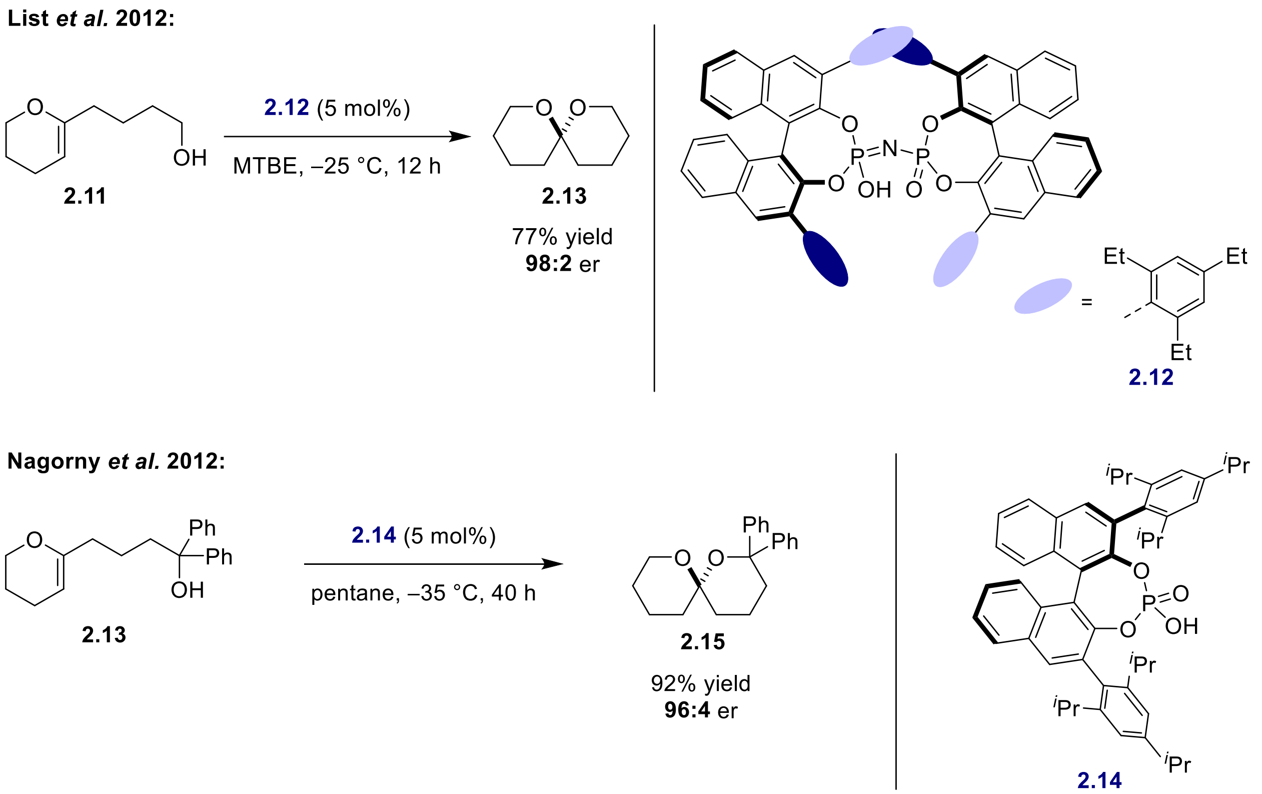
List et al. 2012:
2.12 (5 mol%)
MTBE, −25 °C, 12 h
OH
2.11
2.13
77% yield
98:2 er
O
P=N
P
OH
O
Et
Et
Et
=
2.12
Nagorny et al. 2012:
Ph
Ph
OH
2.14 (5 mol%)
pentane, −35 °C, 40 h
2.13
2.15
92% yield
96:4 er
^{i}Pr
P=O
OH
2.14

Scheme 2.4: Comparison of IDP with (*S*)-TRIP for the enantioselective spiroacetalization.

In spite of the fact that IDPs addressed some of the previous limitations of an open active site and therefore insufficient space discrimination of DSI, which solved several reactions with unfunctionalized, aliphatic substrates[31-34] nevertheless other limitations of DSIs like insufficient catalytic activity for less Lewis basic substrates remained. The reduced acidity of IDPs (p*K*a = 11.3 in MeCN) as compared to DSIs (p*K*a = 8.5 in MeCN) limited their applicability in Brønsted acid catalysis and made them incompatible for silylium Lewis acid catalysis as well.[36]

Successful efforts were made to increase the acidity of the IDP catalyst by installing an electron-withdrawing group (NO_2) into the BINOL backbone, which was able to provide the required reactivity as well as control the enantioselectivity for the oxa-Pictet-Spengler reaction (**Scheme 2.5**).[37] However this increase in reactivity still was not sufficient for less basic substrates.

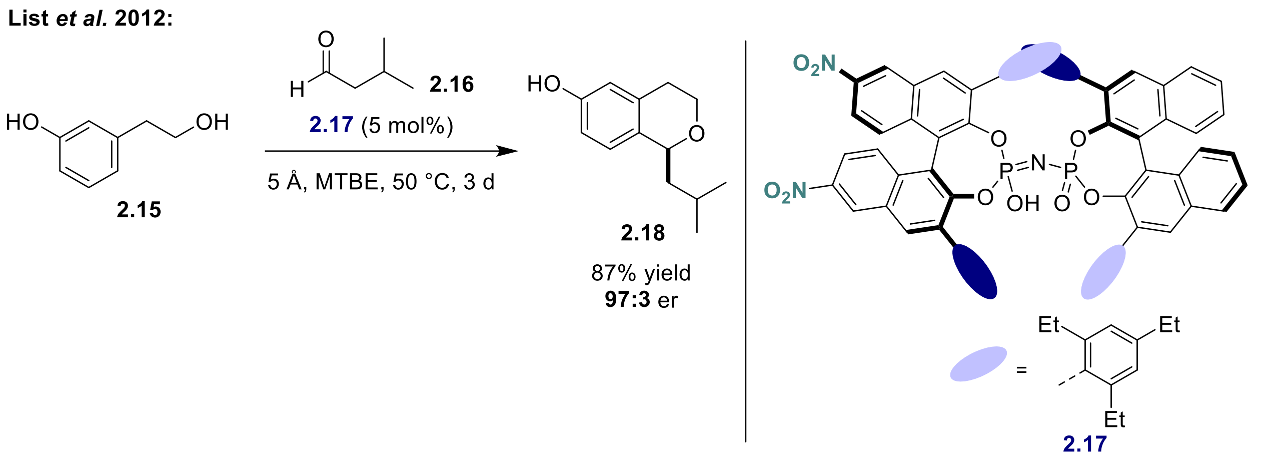
List et al. 2012:
HO
OH
2.15
H
O
2.16
2.17 (5 mol%)
5 Å, MTBE, 50 °C, 3 d
HO
O
2.18
87% yield
97:3 er
O₂N
O₂N
O
P=N
P
O
OH
O
O
O
=
Et
Et
Et
2.17

Scheme 2.5: oxa-Pictet-Spengler reaction: modification of BINOL backbone.

Within the dimeric architectural framework, the List and coworkers applied the Yagupolskii principle for the next generation of confined and highly acidic catalysts. Replacement of one oxygen atom with NTf group in IDP led to imino-imidodiphosporic acids (*i*IDPs)[38] bifunctional catalyst with improved acidity (pKa in CH3CN ~ 7−9) compared to IDPs. Substitution of the second oxygen atom led to imidodiphosphorimidic acids (IDPi), highly confined and acidic chiral organic acids. (p*K*a in CH_3CN ~ 2–5)[39]. Due to the lack of a basic site in IDPis, they can act not only as Brønsted acid catalysis but also as precursors for silylium Lewis acid catalysis. In 2016, List et al. reported Hosomi−Sakurai allylation of aromatic and aliphatic aldehydes with excellent

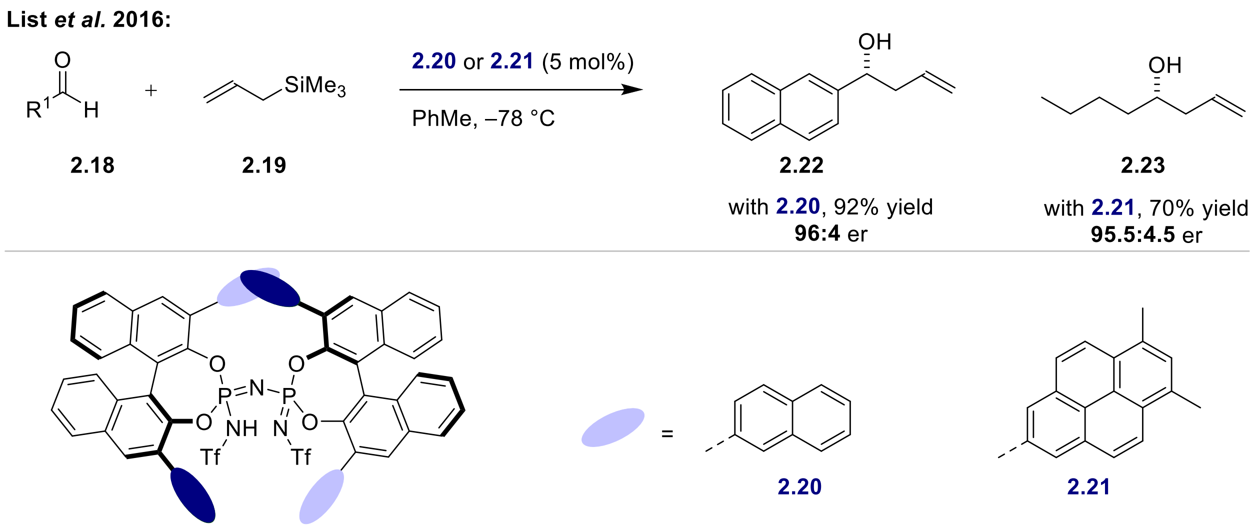
List et al. 2016:
O
R¹
H
2.18
+
SiMe₃
2.19
2.20 or 2.21 (5 mol%)
PhMe, –78 °C
OH
2.22
with 2.20, 92% yield
96:4 er
OH
2.23
with 2.21, 70% yield
95.5:4.5 er
O
P=N
P
O
O
NH
Tf
N
Tf
O
=
2.20
2.21

Scheme 2.6: Silylium Lewis acid-catalyzed Hosomi-Sakurai reactions with aromatic.

yields and enantioselectivities using very poorly reactive allyltrimethylsilane as nucleophile overcoming the limitations of the DSI catalysts in both reactivity and selectivity (**Scheme 2.6**).[40]

As a result of the increase in acidity and confinement, IDPis have been able to activate and enantiodiscriminate several unbiased and extremely unreactive functionalities in Brønsted acid .[39,41]

2.3 Bronsted Acid Catalysis:

BINOL-derived chiral Brønsted acid catalysts have evolved into a catalyst class that successfully enables the spatial discrimination of several cationic intermediates. Lee and coworkers demonstrated that DSI is an effective Brønsted acid catalyst for

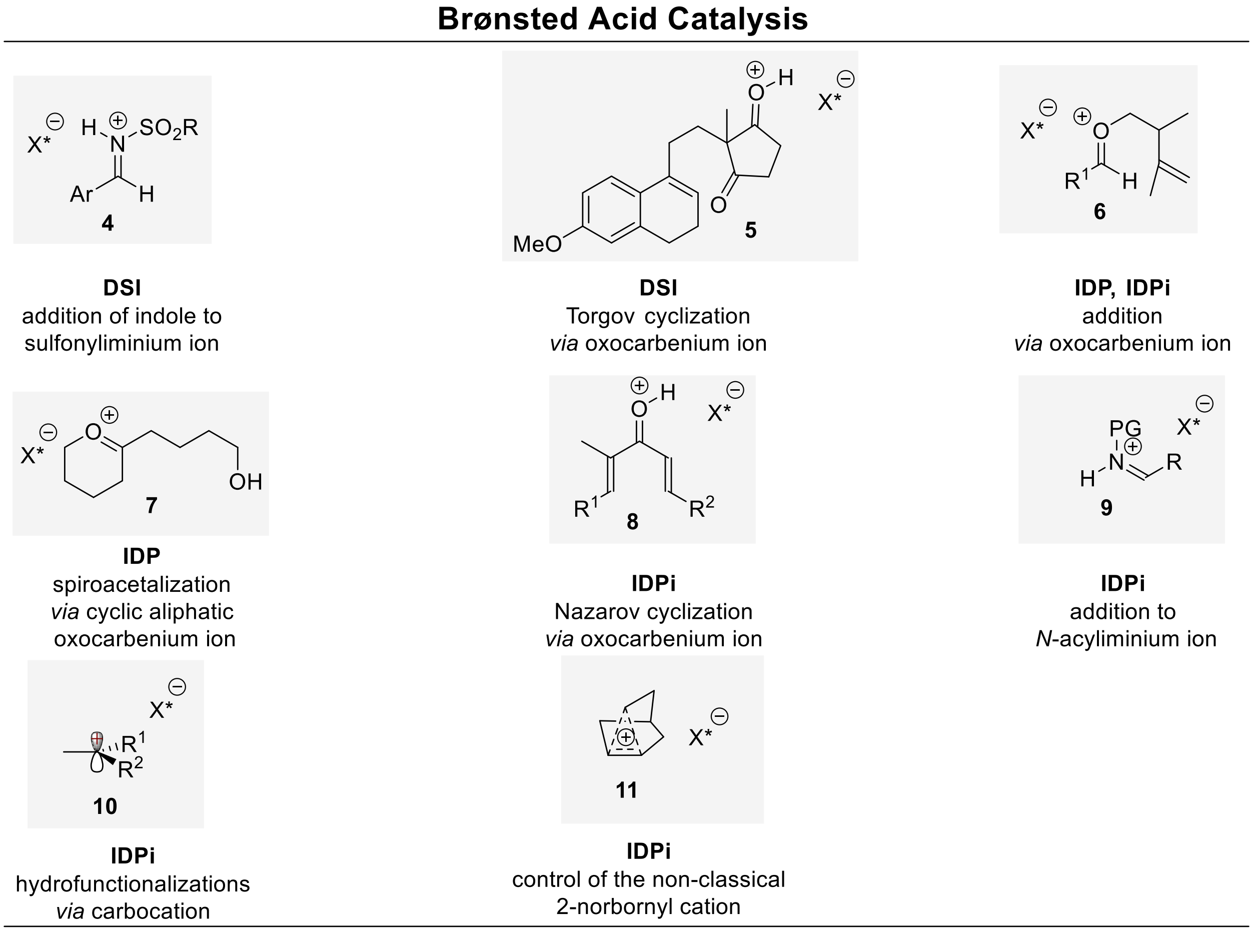
Brønsted Acid Catalysis
X*
H
SO2R
N
Ar
H
4
DSI
addition of indole to
sulfonyliminium ion
O
H
X*
O
MeO
5
DSI
Torgov cyclization
via oxocarbenium ion
X*
O
R1
H
6
IDP, IDPi
addition
via oxocarbenium ion
X*
O
OH
7
IDP
spiroacetalization
via cyclic aliphatic
oxocarbenium ion
O
H
X*
R1
8
R2
IDPi
Nazarov cyclization
via oxocarbenium ion
PG
X*
H
N
R
9
IDPi
addition to
N-acyliminium ion
X*
R1
R2
10
IDPi
hydrofunctionalizations
via carbocation
X*
11
IDPi
control of the non-classical
2-norbornyl cation

Figure 2.3: Overview of representative examples of controlled cationic intermediates *via* Brønsted acid catalysis.

the addition of indoles to sulfonyliminium ion **4**[42]. In 2014, List et al. reported an efficient asymmetric Torgov cyclization, an example of acid catalyzed cascade reactions, controlling the intramolecular Prins reaction of oxocarbenium ion **5**[43]. In this case, an additional increase in acidity was achieved by introducing NO_2 groups at the 5,5´-positions of the BINOL backbone. The increased confinement in the IDP catalyst allowed the control of oxocarbenium ion **6** in an acetalization reaction[32], the Prins cyclization[34]. IDP catalyst could also have a controlled of cyclic, aliphatic oxocarbenium ion **7** in an intramolecular spiroacetalization[30]. The combined effect of high acidity and confinement in the IDPi catalysts enables high diastreo- and enantioselectivities *via* oxocarbenium ion **6** in a vinylogous Prins cyclization[44] and a *hetero*-Diels–Alder reaction.[45] Furthermore, the confinement effect of IDPis was also observed in the Nazarov cyclization with cation **8** as intermediate *via* an 'induced fit' mechanism[46]. Since the reaction takes place in the confinement space, the catalyst enforces the highly reactive, though thermodynamically disfavored *s-trans*/*s-trans* conformation of **8**. In addition, a less basic counteranion of IDPi could control the highly reactive *N*-acyliminium ion **9** for the Pictet-Spengler reaction[41m] and the addition of less nucleophilic arenes (like toluene or benzene) for Friedel−Crafts reactions.[41r] The high acidity of IDPi catalysts enables the activation of less basic substrates like olefins. Generated under acid conditions, carbocations **10** were engaged with multiple nucleophiles, including intramolecular hydroalkoxylation[47], hydrolactonization[41p], and hydroarylations[41d] with indoles. The potential of IDPi catalysis was further shown by controlling the non-classical 2-norbornyl cation **11** in an arylation reaction[41c]. The authors showed that this cation could be accessed via different precursors, like the choice of suitable leaving group, activating C−C π-bond, C−C σ-bond, and cation−π cyclization in Brønsted acid catalysis and C−F bond activation, forming the same major enantiomer with almost same enantioselectivity of the product.

2.4 Lewis acid Catalysis:

To employ both silyl activation and ion pairing, List and coworkers envisioned the use of chiral disulfonimides (DSIs) as uniquely active Lewis acid catalysts. Aromatic aldehydes and imines were utilized in addition reactions with various silyl nucleophiles. List et al. reported an enantioselective Mukaiyama aldol reaction of silyl oxocarbenium ion **12**[21]. For the Mukaiyama aldol methodology, the authors extended the applicability of DSI not only to silyl ketene acetals but also to vinylogous[48], bis-vinylogous[48], and alkynylogous[49] variants. Other examples include a hetero-Diels-Alder reaction[50], their alkynylogous analogs[50], a cyanosilylation[51], allylation (Hosomi-Sakurai reaction) with methallyl silanes[52] and the Abramov reaction[53] with silylated phosphites to form α-hydroxyphosphonates. As previously discussed, DSI catalysts could not be

Lewis Acid Catalysis

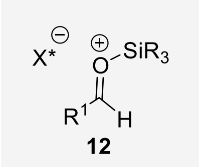

12

DSI, IDPi
additions to
silyl oxocarbenium ion

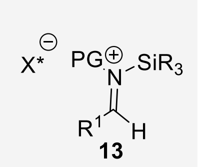

13

DSI
additions
to silyl *N*-acyliminium ions

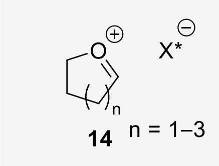

14

IDPi
addition of silyl ketene acetals
to cyclic aliphatic
oxocarbenium ion

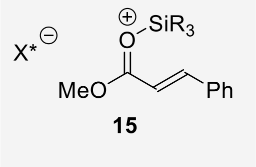

15

IDPi
Mukaiyama–Michael
addition/Diels-alder cycloaddition
via silyl oxocarbenium ion

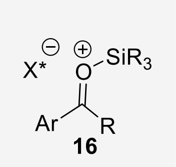

16

IDPi
Mukaiyama aldol
addition *via* silyl
oxocarbenium ion

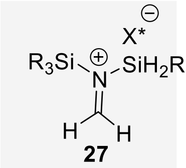

27

IDPi
Mukaiyama Mannich
addition *via* bis-silyl
iminium ion

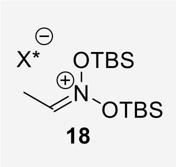

18

IDPi
addition of silyl ketene acetals
to bis(siloxy)iminium ion

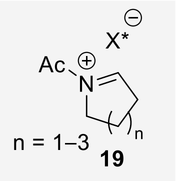

19

IDPi
addition to
N–acyliminium ion

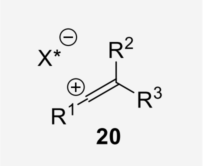

20

IDPi
C–H insertion
via vinyl cation

Figure 2.4: Overview of representative examples of controlled cationic intermediates *via* silylium Lewis acid catalysis.

used for the addition of poorly nucleophilic allyltrimethylsilane to silyl oxocarbenium ion **12** and required more acidic IDPi catalysts[40]. It is worth mentioning that the confined Si-IDPi system also enables the use of aliphatic silyl oxocarbenium ion **12**. The simultaneous generation of a stereocenter and a C–C bond formation is an attractive endeavor in the Mukaiyama-Mannich reaction between imines and silyl ketene acetals; however, the facile decomposition of imines *via* hydrolysis often inhibits the application of this method. List et al. reported the use of *N*-Boc–amino sulfones as electrophile and the *in situ* generation of silyl *N*- acyliminium ion **13** for the addition of silyl ketene acetals to circumvent the decomposition of imines.[54] Expansion of this methodology to its vinylogous variant to access amino-β-ketoesters[55] as well as an aza-Hosomi–Sakurai allylation with allyltrimethylsilane as nucleophile[56], in which Fmoc as a protecting group is required to achieve high enantioselectivities were also successful. The high reactivity and confinement of IDPi enable the enantiodiscrimination of several small and unbiased substrates. Due to the lack of Lewis basic site or aromatic sites, it is challenging to enantiodiscriminate oxocarbenium ion **14**. The IDPi enables the addition of silyl ketene acetals, vinylogous, and silyl enol ethers to cyclic, aliphatic oxocarbenium ion **14**[57]. Aside from differently substituted THFs, substituted tetrahydropyrans, oxepanes, and chromanes could also be accessed. While the addition of silyl ketene acetals to cyclic, aliphatic oxocarbenium ions was challenged by their enantiofacial discrimination, α,β-unsaturated esters additionally suffer from low electrophilicity in enantioselective Mukaiyama-Michael reactions[58]. Silylated methyl cinnamate cation **15** was controlled in both Mukaiyama–Michael[59] and in the Diels–Alder[60] reactions with excellent enantioselectivity. The high catalytic activity of the IDPi was further demonstrated for the addition of silyl ketene acetals to silyl oxocarbenium ion **16** in the Mukaiyama-Aldol reaction, where as little as 2.8 ppm of the catalyst completely converted the substrate to the desired product[61]. The enzyme-like confinement properties of IDPi catalysts were highlighted in the single aldolization of silyl oxocarbenium ion **12** with acetaldehyde-derived enol silane for the Mukaiyama aldol reaction.[62] Another success for IDPi catalysis was the control of the bis-silyl iminium ion **17** generated from silylated aminomethyl ether for the direct formation of β^2-amino acids with bis-silyl ketene acetals as nucleophiles[41e]. Some other examples of success of IDPi include the control of bis(siloxy)iminium ions **18**[41g] and *N*-acyliminium ions **19**[41h] for the addition of silyl ketene acetals and silyl enol ethers, respectively. Furthermore, Nelson et al. showed that IDPi catalysts could generate and control highly reactive vinylic carbocation **20** for an enantioselective intramolecular C–H insertion reaction[41n]; however, this method limited to only six membered substrates.

2.5 Modularity of BINOL-derived Dimeric Catalysts (IDP, *i*IDP, IDPi):

The key features of BINOL-derived dimeric catalysts IDP, *i*IDP, IDPi are their modular structure with tunable acidity, which is highly required for the success of each particular transformation. To demonstrate the modularity of these catalysts, the List group modified the 6,6´-position of the BINOL backbone in the IDP and introduced a NO_2 group to achieve higher reactivity and selectivity for the oxa-Pictet-Spengler reaction[37]. A similar effect was observed when the perfluororisopropyl group was introduced at the 6,6´-position of the BINOL backbone in the IDPi for the addition of acetone-derived silyl enol ether to *N*-acyliminium ions **19**[41h]. To increase the acidity of IDPi even further, the List group applied the Yagupolskii principle to replace both the oxygen atoms in the NTf group with the NTf group to give the next generation of highly acidic IDPii[63] catalysts.

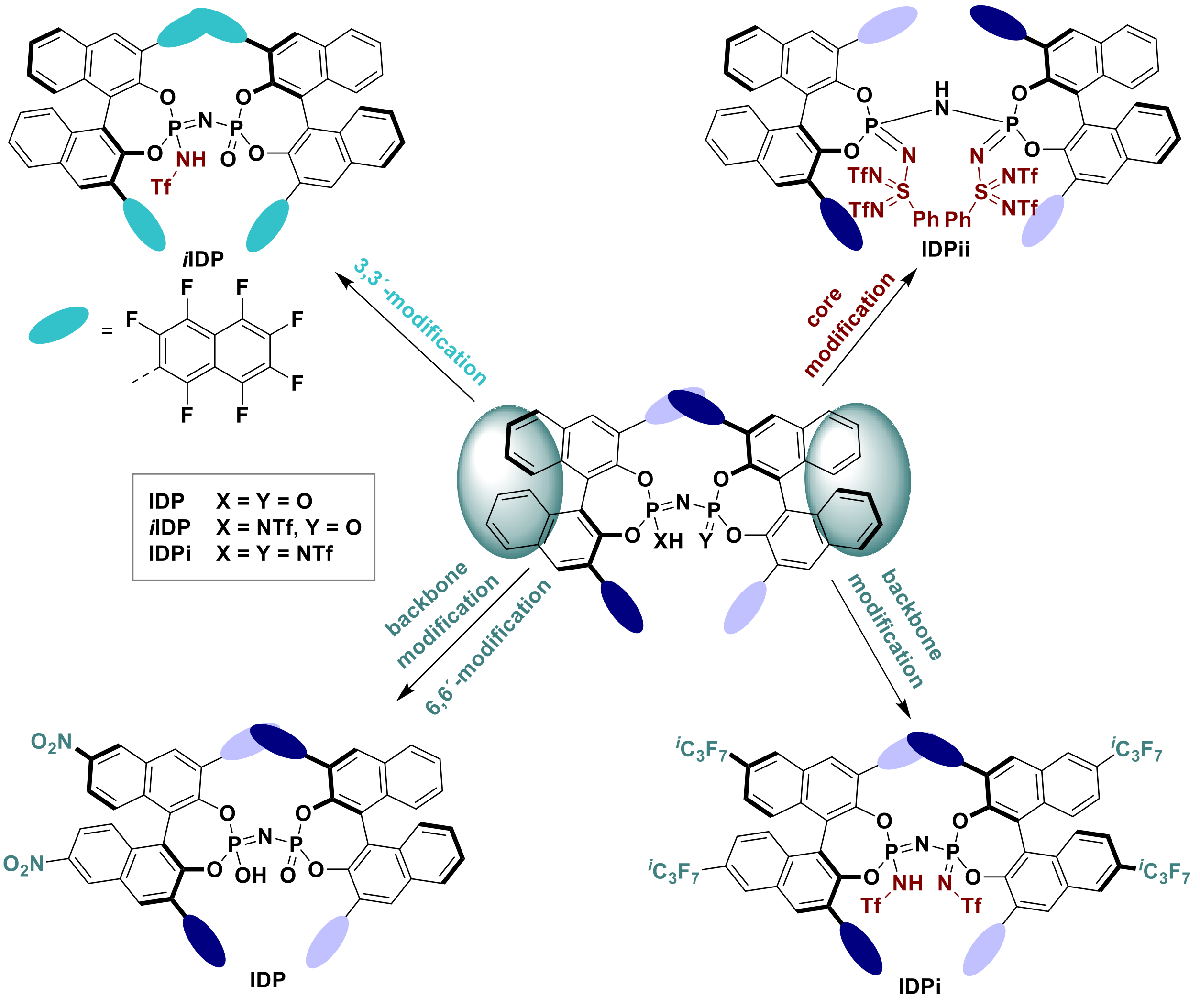
iIDP
IDPii
IDP
IDPi
3,3´-modification
core modification
backbone modification
6,6´-modification
backbone modification
IDP X = Y = O
iIDP X = NTf, Y = O
IDPi X = Y = NTf
O₂N
ⁱC₃F₇
TfN
NTf
Ph Ph
Tf
XH
Y

Figure 2.6: Showcase of modularity of BINOL-derived dimeric catalysts.

Lewis acidity of this catalyst was powerful enough for the α-methylation of silyl ketene acetal with methanol as an electrophile, which was previously impossible using pre-Lewis Acid Organocatalysts. Another example of catalyst modification on the requirement of the reaction conditions is replacing the 3,3´-position of the BINOL backbone with perfluoronaphthalene in the *i*IDP catalyst. The generated catalyst was confined and active enough for cyclization of neral to isopiperitenol.[64]

2.6 Asymmetric Counteranion-Directed Catalysis (ACDC):

The concept of asymmetric counteranion-directed catalysis involves the use of a chiral anion to direct the enantioselectivity of a reaction by forming an ion pair with a cationic species. The List group coined the term asymmetric counteranion-directed catalysis (ACDC) in 2006, stating ‘the induction of enantioselectivity in a reaction proceeding through a cationic intermediate by means of ion pairing with an enantiomerically pure anion provided by the catalyst’.[65] One of the key advantages of ACDC is its ability to control the stereochemistry of reactions involving cationic intermediates. The subsequent transformation can be made enantioselective by the use of chiral enantiopure counteranions with sufficient ion pair association. According to Anslyn and Dougherty, the term ion pair defined ‘An ion pair is defined to exist when a cation and anion are close enough in space that the energy associated with their electrostatic attraction is larger than the thermal energy (RT) available to separate them’.[66] In addition to the Coulombic attraction, further attractive interactions between cation and anion may be involved in the context of ACDC[6]. A proof of concept on the feasibility of ACDC as a powerful strategy for asymmetric catalysis beyond Brønsted acid catalysis was provided by List and coworkers in 2006 for the highly enantioselective transfer hydrogenations of enals using a Hantzsch ester as the reductant (**Scheme 2.7**).[67] The morpholinium salt of (R)-3,3′-Bis(2,4,6-triisopropylphenyl)-1,1′-binaphthyl-2,2′-diyl hydrogenphosphate (TRIP) **2.22** forms a chiral ion pair upon condensation with the enal substrate.

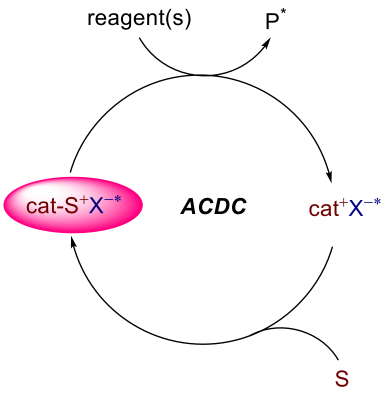

Figure 2.7: Schematic representation of asymmetric counteranion-directed catalysis (ACDC). P^* = enantioenriched product; X^{-*} = enantiopure anion; cat$^+$ = achiral cation.

The chiral anion directs the approach of the hydride source to the reactive iminium intermediate by enantiofacial steric shielding. The ACDC concept has become a powerful tool for achieving enantioselective transformations in an expanding range of catalytic fields, including aminocatalysis[67], transition metal catalysis[68,69], and anion-binding catalysis[70], among many others.

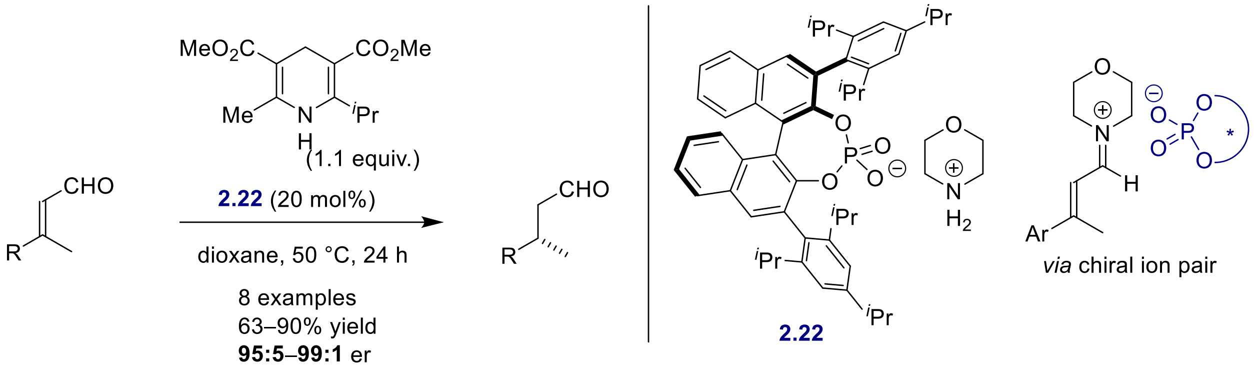
MeO2C
CO2Me
Me
N
H
iPr
(1.1 equiv.)
CHO
R
2.22 (20 mol%)
dioxane, 50 °C, 24 h
8 examples
63–90% yield
95:5–99:1 er
CHO
R
iPr
iPr
iPr
O
P=O
O
O⊖
iPr
iPr
iPr
2.22
O
⊕
N
H2
O
⊕
N
H
Ar
⊖
O
O
P
O
O
*
via chiral ion pair

Scheme 2.7: The catalytic asymmetric transfer hydrogenation of enals with the salt of morpholine and TRIP phosphoric acid.

Strong organic Brønsted and Lewis acids catalyze reactions also find application in ACDC by formation of chiral ion pair intermediates.[46,60] By applying the ACDC concept various highly reactive cationic intermediates could be controlled in asymmetric catalysis using strong organic Brønsted and Lewis acids, which were were discussed earlier in this chapter.

2.7 Taming Benzylic Carbocations:

During the past decade, early attempts towards the enantioselective reaction of a nucleophile with a benzylic cation typically involved oxygenated arenes, stabilizing the corresponding benzylic cation as *ortho*- or *para*-quinone methides.[71-77]

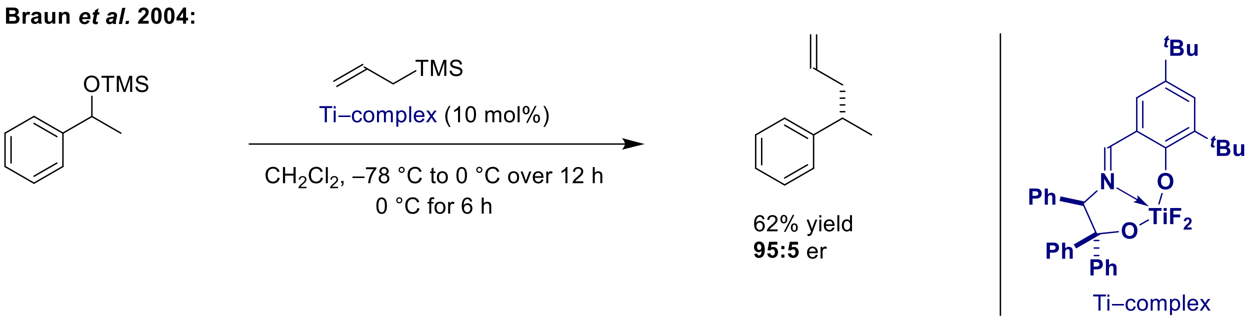

Scheme 2.8: Titanium catalyzed control of secondary benzylic carbocation in asymmetric catalysis.

In 2004, the Braun group reported Titanium-complex as Lewis acid for allylation of TMS-protected secondary benzylic alcohol using allyltrimethylsilane as nucleophile (**Scheme 2.8**).[78]. The authors achieved remarkable selectivity for the desired products; however, a TMS-protected substrate was required for the catalytic cycle to complete as the Ti-complex decomposes when free benzylic alcohol was used as a substrate, requiring the equivalent amount of Ti-complex. It is also worth mentioning that the authors showed only one example for controlling secondary benzylic cation.

A decade later, Toste et al. reported solvolysis of 1-phenylethyl 2,2,2-trichloroacetimidate derived from benzylic alcohol using supramolecular host-guest catalysis (**Scheme 2.9**)[79]. While the authors achieved good yield, enantioselectivity suffered, and kinetic resolution was observed at the beginning of the reaction.

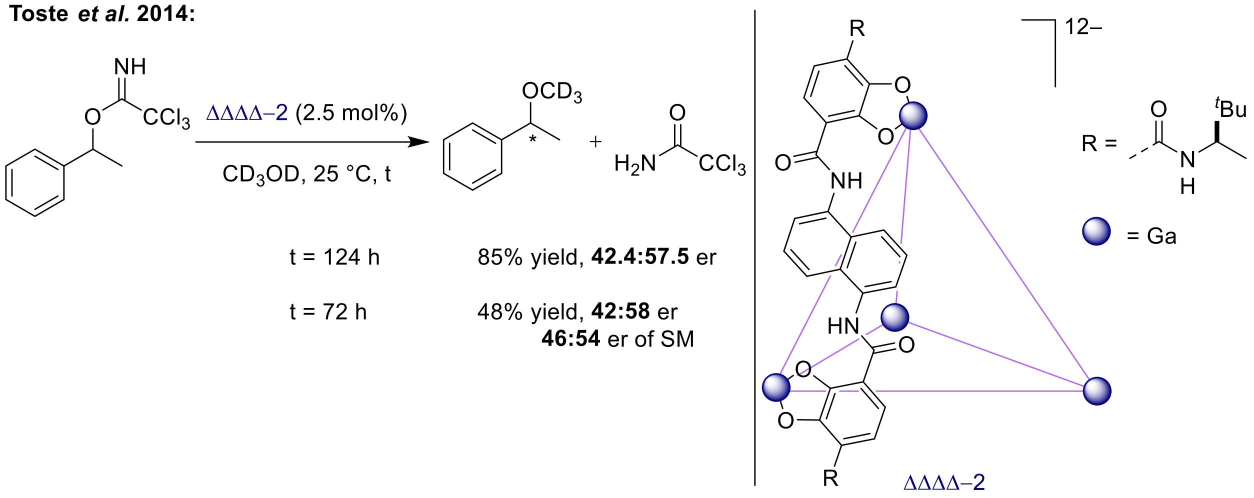
Toste et al. 2014:
NH
O
CCl3
ΔΔΔΔ–2 (2.5 mol%)
CD3OD, 25 °C, t
OCD3
*
+
O
H2N
CCl3
t = 124 h
85% yield, 42.4:57.5 er
t = 72 h
48% yield, 42:58 er
46:54 er of SM
R
12–
O
O
O
NH
HN
O
O
O
R
R =
O
tBu
N
H
= Ga
ΔΔΔΔ–2

Scheme 2.9: Supramolecular host-guest catalysis for control of secondary benzylic carbocation in asymmetric catalysis.

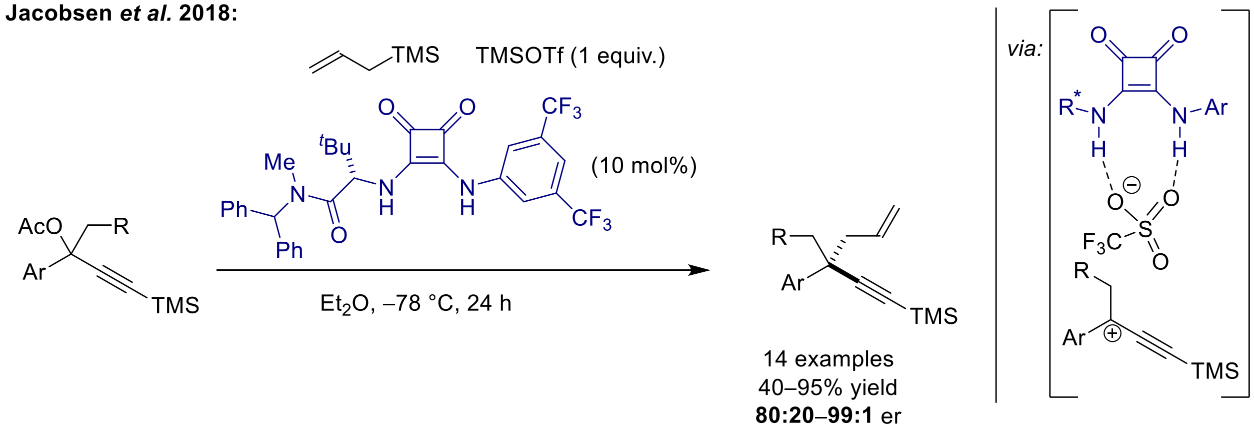
Jacobsen et al. 2018:
TMS
TMSOTf (1 equiv.)
O
O
CF3
tBu
Me
N
N
H
N
H
Ph
Ph
O
CF3
(10 mol%)
AcO
R
Ar
TMS
Et2O, –78 °C, 24 h
R
Ar
TMS
14 examples
40–95% yield
80:20–99:1 er
via:
O
O
R*
N
H
N
Ar
H
O
O
F3C
S
O
R
Ar
TMS

Scheme 2.10: anion-binding catalysis for control of tertiary benzylic carbocations in asymmetric catalysis.

The advancement came from the Jacobsen group for controlling the tertiary benzylic carbocation in an intermolecular reaction. The Jacobsen group reported an allylation of tertiary benzylic cations to construct quaternary stereogenic centers using anion-binding hydrogen bond-donor catalysis (**Scheme2.10**)[80] for several different substrates. Although the reaction gave moderate to excellent enantioselectivity and yield, the success of the reaction was achieved by using TMS protected alkyne substituent as the substrate, which additionally stabilized the carbocation. Subsequently, the Sun group explored tertiary benzylic cations as intermediates in asymmetric catalysis (**Scheme**

2.11).[81] However, the authors mainly employed *o*-oxygenated substituents to one of the arene substituents as substrate.

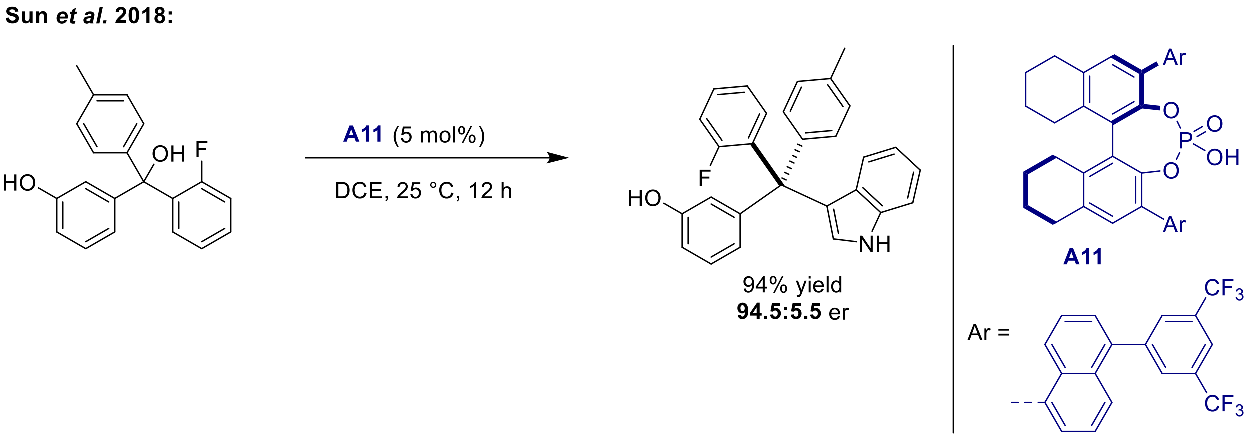
Sun *et al.* 2018:
HO
OH
F
A11 (5 mol%)
DCE, 25 °C, 12 h
HO
F
NH
94% yield
94.5:5.5 er
Ar
O
P
O
OH
O
Ar
A11
Ar =
CF3
CF3

Scheme 2.11: Brønsted acid catalyzed control of tertiary benzylic carbocations in asymmetric catalysis.

2.8 Chiral β–branched Esters:

Chiral β–branched esters are prevalent moieties in pharmaceuticals, fragrances, materials, and agrochemicals and esters themselves serve as versatile synthetic handles for further functionalization to access important structures[82] (**figure 2.8**). Early efforts towards accessing chiral β-branched esters rely on chiral-auxiliaries or chiral additives which require stoichiometric reagents and potentially an additional deprotection step of chiral-auxiliary[83]. In an effort to diversify the pool of β–branched esters that are easily accessible, chemist have utilized three main strategies to access such structures in enantiomerically pure form, from α,β–unsaturated esters by small molecule catalysis.

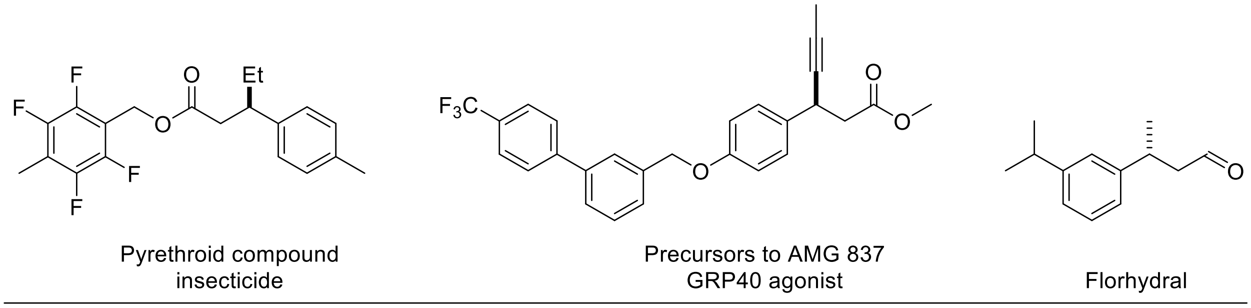
F
F
F
F
O
Et
O
Pyrethroid compound
insecticide
F$_3$C
O
O
O
Precursors to AMG 837
GRP40 agonist
O
Florhydral

Figure 2.8: Biologically active and commercially important compounds

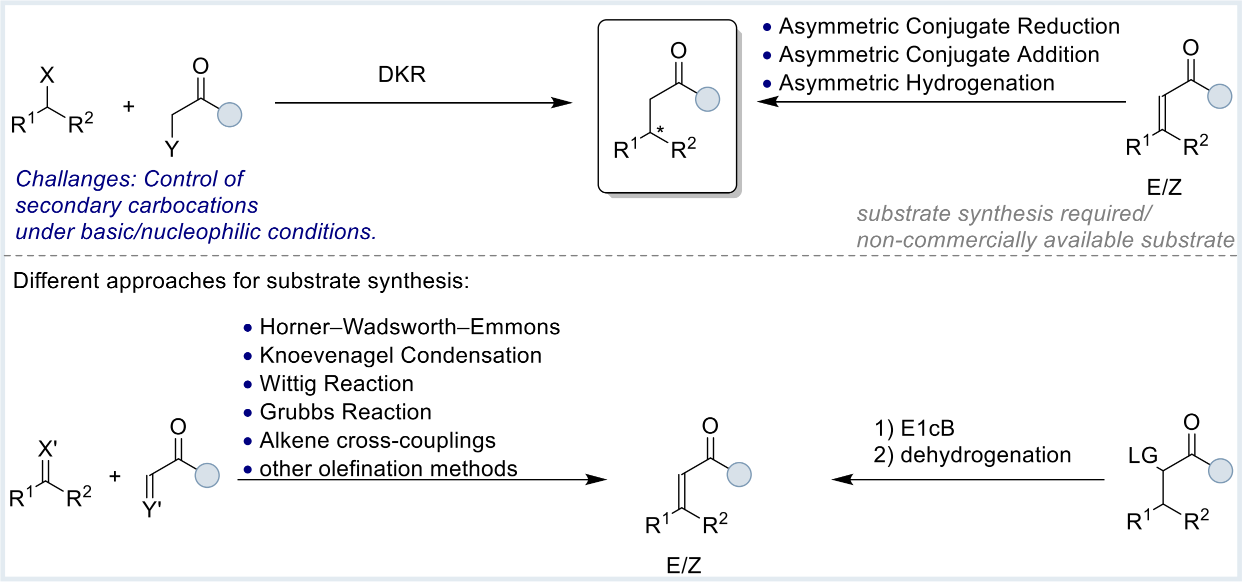
X
R1 R2
+
O
Y
DKR
O
*
R1 R2
• Asymmetric Conjugate Reduction
• Asymmetric Conjugate Addition
• Asymmetric Hydrogenation
O
R1 R2
E/Z
Challanges: Control of
secondary carbocations
under basic/nucleophilic conditions.
substrate synthesis required/
non-commercially available substrate
Different approaches for substrate synthesis:
X'
R1 R2
+
O
Y'
• Horner–Wadsworth–Emmons
• Knoevenagel Condensation
• Wittig Reaction
• Grubbs Reaction
• Alkene cross-couplings
• other olefination methods
O
R1 R2
E/Z
1) E1cB
2) dehydrogenation
LG
O
R1 R2

Figure 2.9: Strategies towards synthesis of chiral β–branched esters

Asymmetric Conjugate Reduction

Asymmetric Conjugate Addition

Asymmetric Hydrogenation

2.8.1 Asymmetric Conjugate Reduction:

Asymmetric conjugate reduction of β,β-disubstituted α,β-unsaturated esters is a very important practical synthetic method, leading to a variety of optically active compounds bearing an asymmetric center at the β-position. In order to resolve this issue, several chiral transition-metal catalysts in combination with hydride donors, such as borohydride or hydrosilanes, have been developed to demonstrate their high efficiency.[84]. Some of these methods were also applied in total synthesis.[85,86] In 1989 Pfaltz et al. reported first example of catalytic asymmetric conjugate reduction of α,β-unsaturated esters to obtain enantioenriched β-branched esters (**Scheme 2.12**). The authors found that cobalt complex of the ligand L_1 was effective in the reduction of β,β-dialkyl substrate using sodium borohydride as reductant.[87] On the other hand, as for copper catalyst, chiral copper–hydride species generated by reaction of CuCl/NaO^{t}Bu/tolBINAP and PMHS (PMHS=polymethyl-hydrosiloxane) was reported by Buchwald et al. in 1999 to show higher enantioselectivity for esters.[88] Development of chiral phosphine–copper catalysts, modified on the basis of Stryker´s discovery for copper–hydride complex $[(Ph_3P)CuH]_6$ and its application to the conjugate reduction. In these processes, hydrosilane derivatives such as poly(methylhydrosilane), phenylsilane or tetramethyldisiloxane are preferably used as efficient hydrogen donors. Around the same time, Lipshutz et al. also reported that copper catalysts bearing a chiral bisphosphine, DTBM-SEGPHOS, were effective in the asymmetric conjugate reduction of esters with excellent enantioselectivity.[89] Hydrosilane derivatives such as poly(methylhydrosilane) require a high amount of silanes (4 equiv.) compared to substrates in a copper-phosphine-based catalytic system. Nishiyama et al. adopted Rh-Phebox-based catalytic system for the asymmetric conjugate reduction of α,β-unsaturated esters in the combination with ethoxymethylsilane as hydrogen donor, which requires only slight excess compared to the substrate and delivered the product with high catalytic efficiency.[90] Although excellent results were achieved employing chiral ligands in the Cu-catalyzed asymmetric 1,4-reduction, only a few diphosphine ligand types, such as BINAP, DTBM-SEGPHOS, have been found to be efficient for this important transformation. In the search

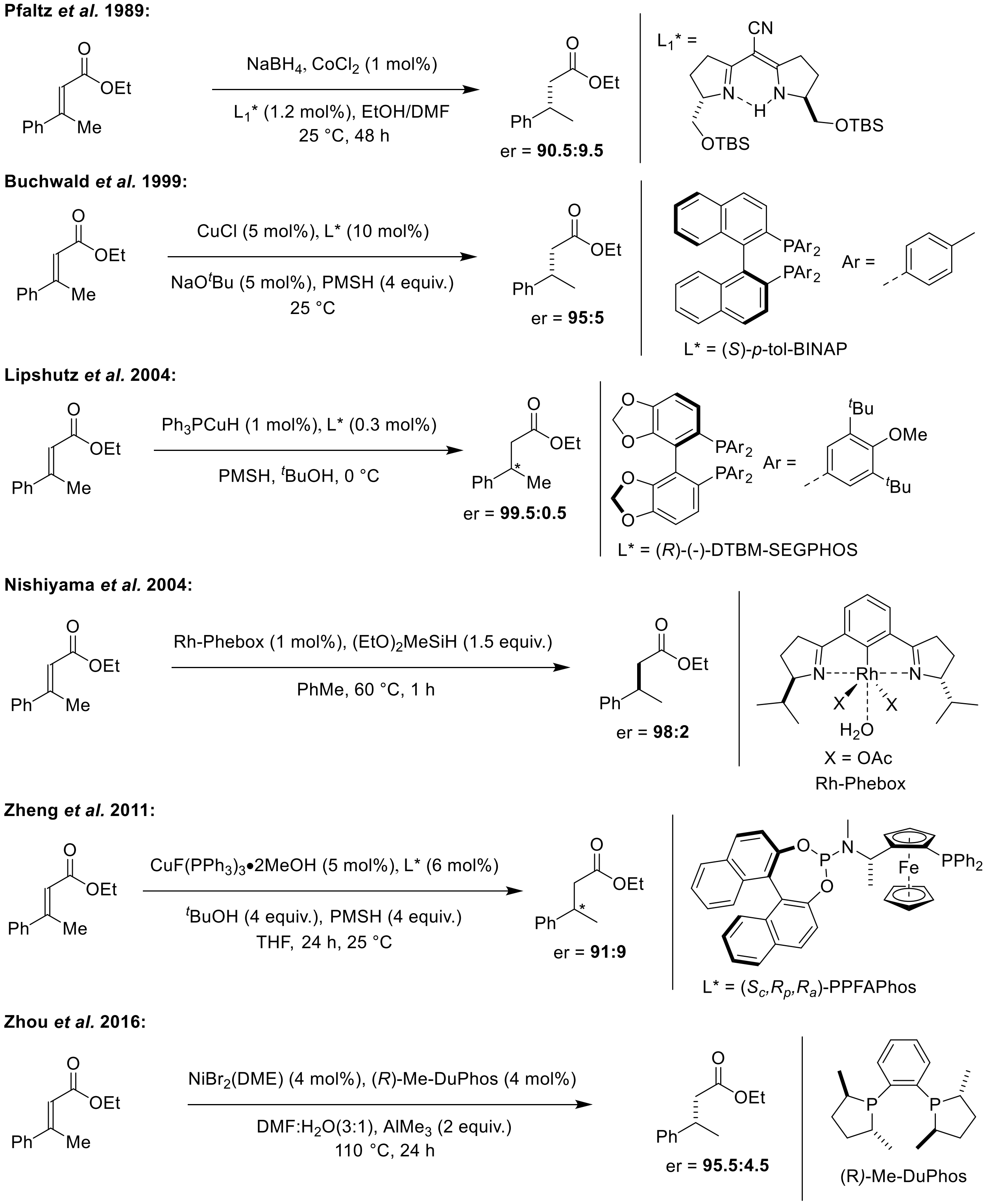
Pfaltz et al. 1989:
NaBH4, CoCl2 (1 mol%)
L1* (1.2 mol%), EtOH/DMF
25 °C, 48 h
er = 90.5:9.5
L1* =
CN
OTBS
Buchwald et al. 1999:
CuCl (5 mol%), L* (10 mol%)
NaOtBu (5 mol%), PMSH (4 equiv.)
25 °C
er = 95:5
PAr2
Ar =
L* = (S)-p-tol-BINAP
Lipshutz et al. 2004:
Ph3PCuH (1 mol%), L* (0.3 mol%)
PMSH, tBuOH, 0 °C
er = 99.5:0.5
tBu
OMe
L* = (R)-(-)-DTBM-SEGPHOS
Nishiyama et al. 2004:
Rh-Phebox (1 mol%), (EtO)2MeSiH (1.5 equiv.)
PhMe, 60 °C, 1 h
er = 98:2
H2O
X = OAc
Rh-Phebox
Zheng et al. 2011:
CuF(PPh3)3•2MeOH (5 mol%), L* (6 mol%)
tBuOH (4 equiv.), PMSH (4 equiv.)
THF, 24 h, 25 °C
er = 91:9
PPh2
Fe
L* = (Sc,Rp,Ra)-PPFAPhos
Zhou et al. 2016:
NiBr2(DME) (4 mol%), (R)-Me-DuPhos (4 mol%)
DMF:H2O(3:1), AlMe3 (2 equiv.)
110 °C, 24 h
er = 95.5:4.5
(R)-Me-DuPhos
Ph
Me
OEt

Scheme 2.12: Overview of Asymmetric Conjugate Reduction

for new chiral ligands for Cu-catalyzed asymmetric 1,4-reduction, Zheng et al. reported PPFAPhos ligand for Cu-catalyzed asymmetric 1,4-reduction.[91] In 2016 Zhou *et al.* reported the asymmetric transfer hydrogenation of α,β-unsaturated esters using a nickel/bisphosphine catalyst and *N*,*N*-dimethylformamide (DMF) as the hydride source (**Scheme 2.12**).[92]

2.8.2 Asymmetric Conjugate Addition:

While remarkable progress has been made with asymmetric 1,4-additions to enones, lactones, and nitroalkenes, progress has been limited in the case of acyclic α,β-unsaturated esters, despite the enormous synthetic potential of the resulting enantiopure β-substituted esters as building blocks

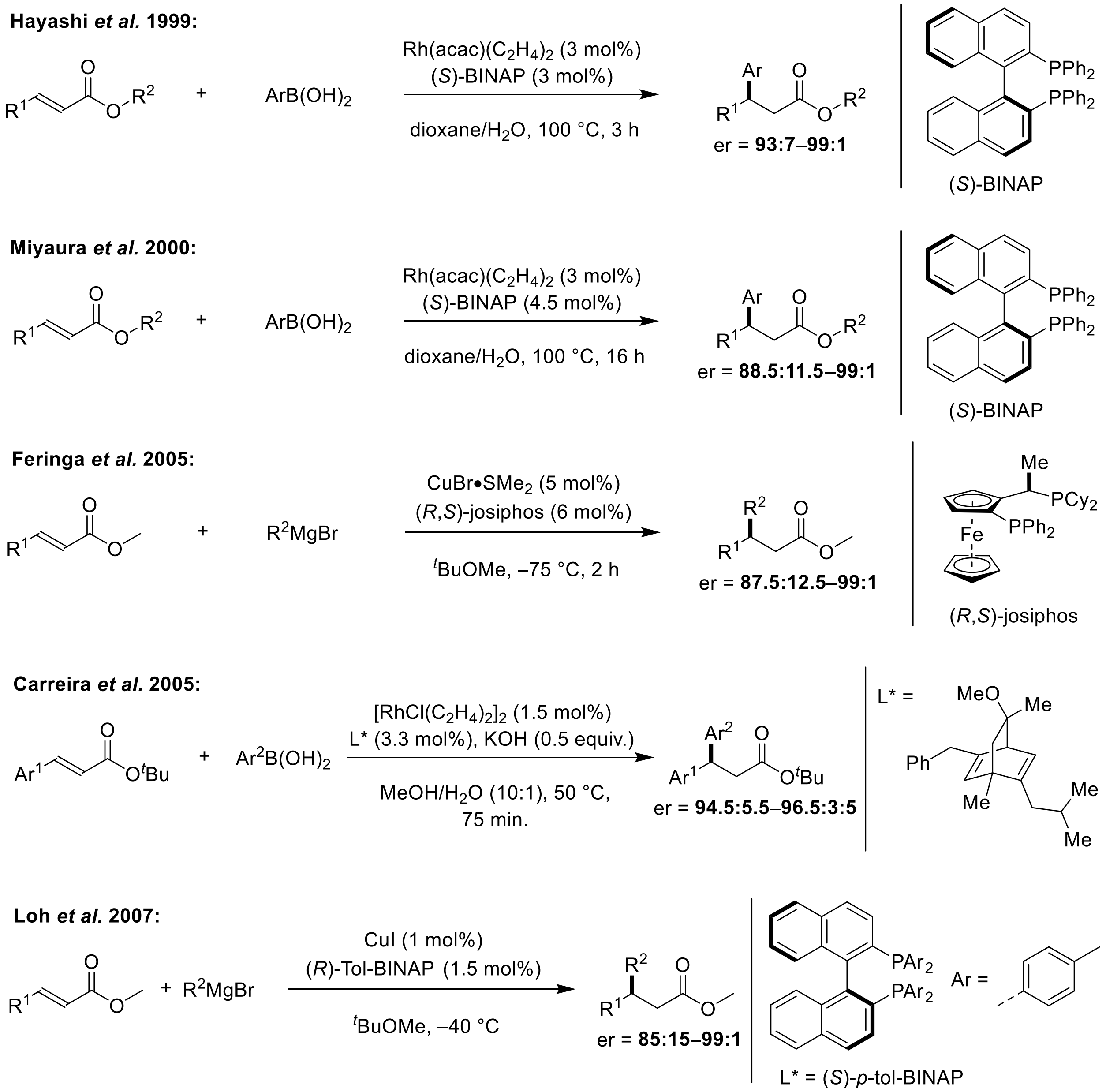
Hayashi *et al.* 1999:
R^1, R^2, O
+ $ArB(OH)_2$
$Rh(acac)(C_2H_4)_2$ (3 mol%)
(*S*)-BINAP (3 mol%)
dioxane/H_2O, 100 °C, 3 h
Ar, O, R^1, R^2
er = **93:7–99:1**
PPh_2
PPh_2
(*S*)-BINAP
Miyaura *et al.* 2000:
R^1, R^2, O
+ $ArB(OH)_2$
$Rh(acac)(C_2H_4)_2$ (3 mol%)
(*S*)-BINAP (4.5 mol%)
dioxane/H_2O, 100 °C, 16 h
Ar, O, R^1, R^2
er = **88.5:11.5–99:1**
PPh_2
PPh_2
(*S*)-BINAP
Feringa *et al.* 2005:
R^1, O
+ R^2MgBr
$CuBr•SMe_2$ (5 mol%)
(*R*,*S*)-josiphos (6 mol%)
^{t}BuOMe, –75 °C, 2 h
R^2, O, R^1
er = **87.5:12.5–99:1**
Me
PCy_2
Fe
PPh_2
(*R*,*S*)-josiphos
Carreira *et al.* 2005:
Ar^1, O, O^tBu
+ $Ar^2B(OH)_2$
$[RhCl(C_2H_4)_2]_2$ (1.5 mol%)
L* (3.3 mol%), KOH (0.5 equiv.)
MeOH/H_2O (10:1), 50 °C,
75 min.
Ar^2, O, Ar^1, O^tBu
er = **94.5:5.5–96.5:3:5**
L* =
MeO
Me
Ph
Me
Me
Me
Loh *et al.* 2007:
R^1, O
+ R^2MgBr
CuI (1 mol%)
(*R*)-Tol-BINAP (1.5 mol%)
^{t}BuOMe, –40 °C
R^2, O, R^1
er = **85:15–99:1**
PAr_2
PAr_2
Ar =
L* = (*S*)-*p*-tol-BINAP

Scheme 2.13: Overview of Asymmetric Conjugate Addition for natural product synthesis. This paucity of versatile methods may be due to the lower intrinsic reactivity of α,β-unsaturated esters compared to enones and the challenge to controlling the various conformers present in acyclic unsaturated systems. In 1997, Miyaura et al. showed that organoboronic acids could be used for conjugate addition to α,β-unsaturated ketones catalyzed by a rhodium(I)–phosphine complex in an aqueous solution.[93] Based on the findings of Miyaura, Hayashi et al. reported in 1999 the rhodium(I) catalyzed 1,4-addition of arylboronic acids to α,β-unsaturated aliphatic esters using the BINAP ligand with excellent enantioselectivity (**Scheme 2.13**).[94] Around the same time the Miyaura group also reported similar reaction conditions for the 1,4-addition of arylboronic acid to α,β-unsaturated esters.[95] Although only a few reports on 1,4-addition for α,β-unsaturated esters were already published, in 2005 Feringa et al. reported inexpensive copper based catalytic system for the conjugate addition to acyclic α,β-unsaturated methyl esters using readily available Grignard reagents.[96] A limitation of this method is the addition of the relatively unreactive methyl Grignard reagent which gave low conversion albeit high enantioselectivity. In the same year, the Carreira group reported rhodium catalyzed 1,4-addition of arylboronic acids to α,β-unsaturated esters using chiral dienes as ligands with good enantioselectivity.[97] In 2007, Loh and co-workers reported a complementary and efficient catalyst system for the conjugate addition of Grignard reagents to α.β-unsaturated esters (**Scheme 2.13**).[98] The catalyst is based on CuI complexed with Tol-BINAP. was reported by copper catalyzed asymmetric conjugate addition of Grignard reagents to α,β-unsaturated esters using BINAP ligand.

2.8.3 Asymmetric Hydrogenation:

Although many methods were already developed to access enantioenriched β-branched esters these

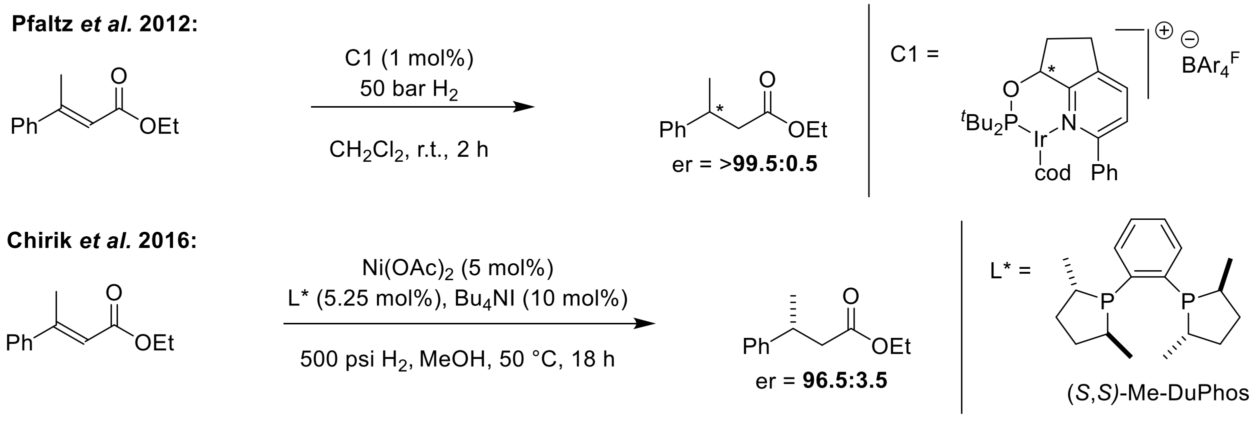

Scheme 2.14: Overview of Asymmetric Hydrogenation

methods requires multiple chemicals for the transformation. Probably another better approach would be the asymmetric hydrogenation of β,β-disubstituted esters using hydrogen gas which is an inexpensive, readily available, and atom economical reagent that produces no waste. Many reports have been published on the asymmetric hydrogenation of β,β-disubstituted esters with excellent enantioselectivity, however, only a limited number of substrates have been investigated with these methods.[99] Pfaltz et al. reported Ir complex with chiral N,P ligand in the asymmetric hydrogenation of a wide range of α,β-unsaturated esters with excellent enantioselectivity (**Scheme 2.14**).[100] Moving away from precious metal catalysts based on rhodium, ruthenium, or iridium, Chirik *et al.* reported a nickel based catalyst for the asymmetric hydrogenation of a range of α,β-unsaturated esters (**Scheme 2.14**).[101]

In addition to these three general approaches, there are more other methods have been reported[84], which are not discussed in this thesis. However, it is worth mentioning two other approaches for the synthesis of chiral β-branched esters.

The Arnold group reported enzyme-catalyzed carbene C–H insertion to construct C–C bonds.[102] Although this method is of great importance, as C–H bonds are ubiquitous and this method enables the direct synthesis of chiral β-branched esters, nevertheless C–H insertion is reported only with electron rich C–H bonds (**Scheme 2.15)**.

Arnold *et al.* 2016:

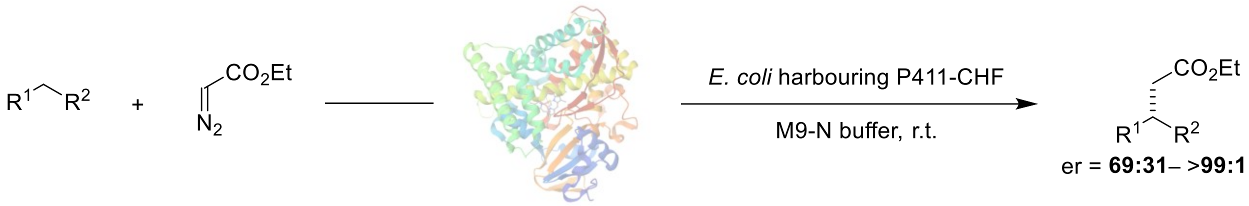

Scheme 2.15: Carbene C–H insertion to chiral, β-branched esters

In 2018, the Hull group reported the conversion of allylic amines to chiral, β-branched esters under rhodium catalysis in the presence of alcohol nucleophiles.[103] The authors used an isomerization strategy that allowed enantioinduction that was not limited by the steric differentiation of the substituents at the stereogenic center formed (**Scheme 2.16)**.

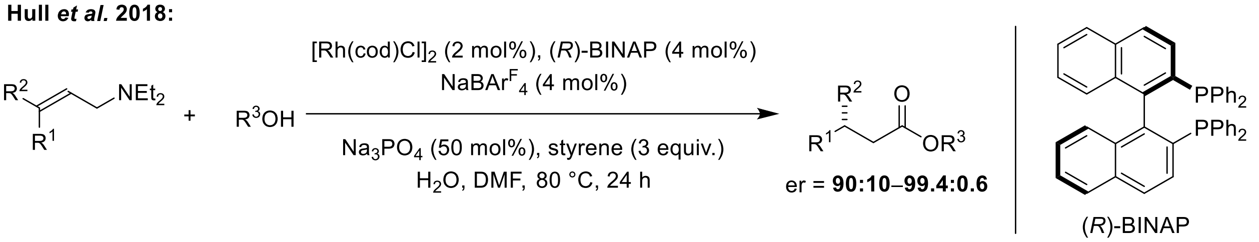
Hull *et al.* 2018:
R^2
NEt_2
R^1
+
R^3OH
$[Rh(cod)Cl]_2$ (2 mol%), (*R*)-BINAP (4 mol%)
$NaBAr^F_4$ (4 mol%)
Na_3PO_4 (50 mol%), styrene (3 equiv.)
H_2O, DMF, 80 °C, 24 h
R^2
O
R^1
OR^3
er = **90:10–99.4:0.6**
PPh_2
PPh_2
(*R*)-BINAP

Scheme 2.16: isomerization of allylic amines to chiral, β-branched esters

3. Objectives

Comparing the hydride ion affinity of various cations[104,105] (which also represents stability of carbocations) non-classical 2-norbornyl cation and a simple secondary benzylic carbocation have similar hydride ion affinity (**Figure 3.1**). Since IDPi catalysts could control non-classical 2-norbornyl cation[41c] and are highly modular, since our group previously demonstrated the IDPi catalysts' ability to control the non-classical 2-norbornyl cation, we were eager to test their potential regarding the control of secondary benzylic carbocations for various bond-forming reactions. As benzylic stereocenters are ubiquitous in numerous natural products, pharmaceuticals, and agrochemicals products. Asymmetric catalysis of reactions proceeding through unstabilized secondary benzylic cations has previously been reported by the Braun[78] and the Toste[79] groups, albeit each with only a single example.

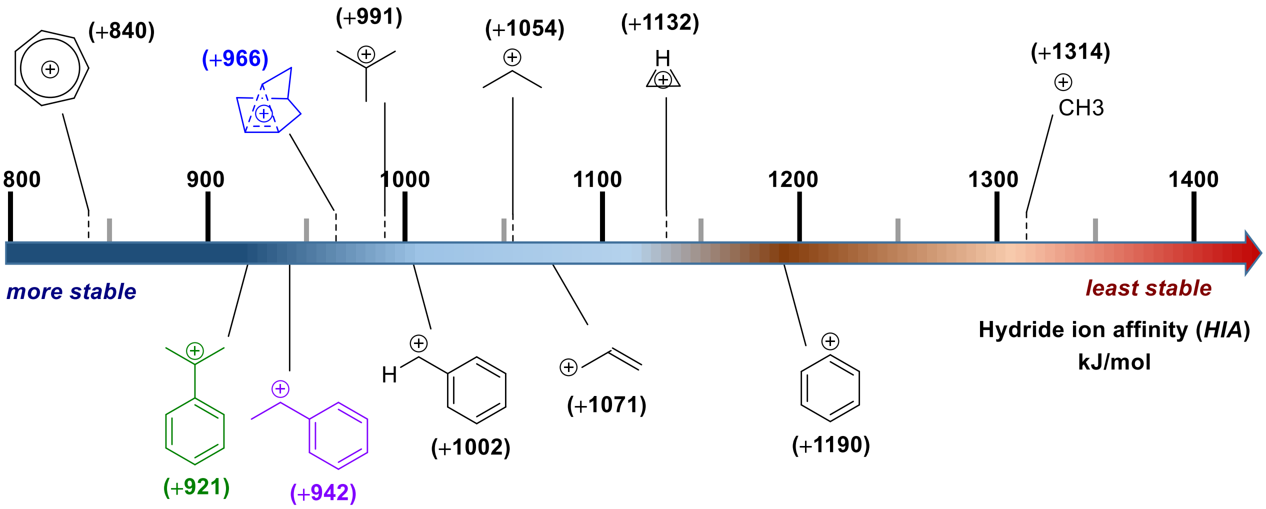

Figure 3.1: Hydride ion affinity of various carbocations.

Initially, we expected three fundamental challenges toward applying our design to unstabilized secondary benzylic cations:

(i) The differentiation between two faces of an only hydrocarbon-based planar cationic intermediate

(ii) The exclusion of unproductive reaction pathways, such as deprotonation or rearrangement, and

(iii) Potential catalyst deactivation by alkylation from the benzylic cation.

We postulated that essential cation stabilization could be achieved using a less basic, weakly coordinating anion, which at the same time can also provide a chiral microenvironment for further nucleophilic attack to achieve high enantiocontrol (**Scheme 3.1**). We hypothesized that engaging unbiased secondary benzylic carbocationic intermediates with a wide range of nucleophiles could provide a general solution to the problem of constructing benzylic stereocenters. The aim of this PhD thesis is to design and develop an IDPi-catalyzed S_N1 platform that enables the conversion of racemic *sp*^{3} starting materials into valuable enantioenriched benzylic stereocenter-containing products in a dynamic kinetic asymmetric transformation.

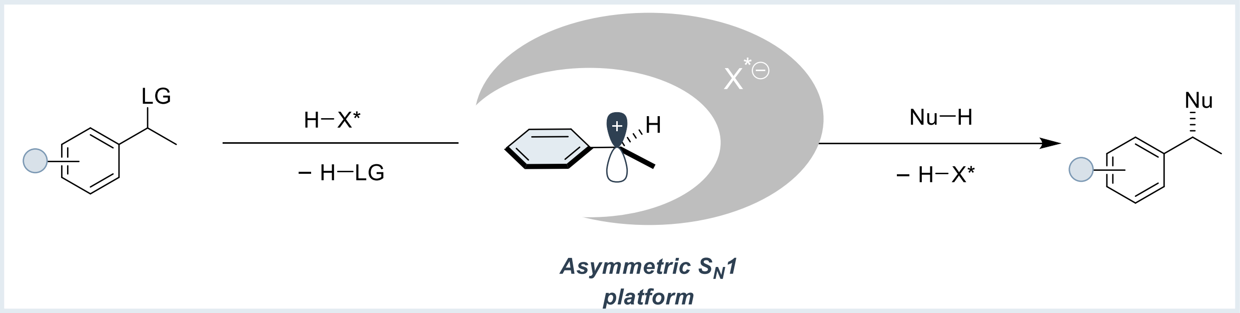

Scheme 3.1: confined counteranions tame secondary benzylic cations for asymmetric catalysis.

4 Results and Discussion:

4.1 Results and Discussion for C–O Bond formation:

4.1.1 Reaction development and optimization studies (C–O bond formation):

Our investigation started with an intermolecular reaction between trichloroacetimidate **4.1.1a** as a cation precursor and acetic acid **4.1.2a** as a nucleophile. When testing different Brønsted acids, the desired acetate **4.1.4a** product formation was observed only in the case of IDPi **4.1.3a** with 85% NMR yield albeit moderate enantiomeric ratio (61:39) (**Scheme 4.1.1**).

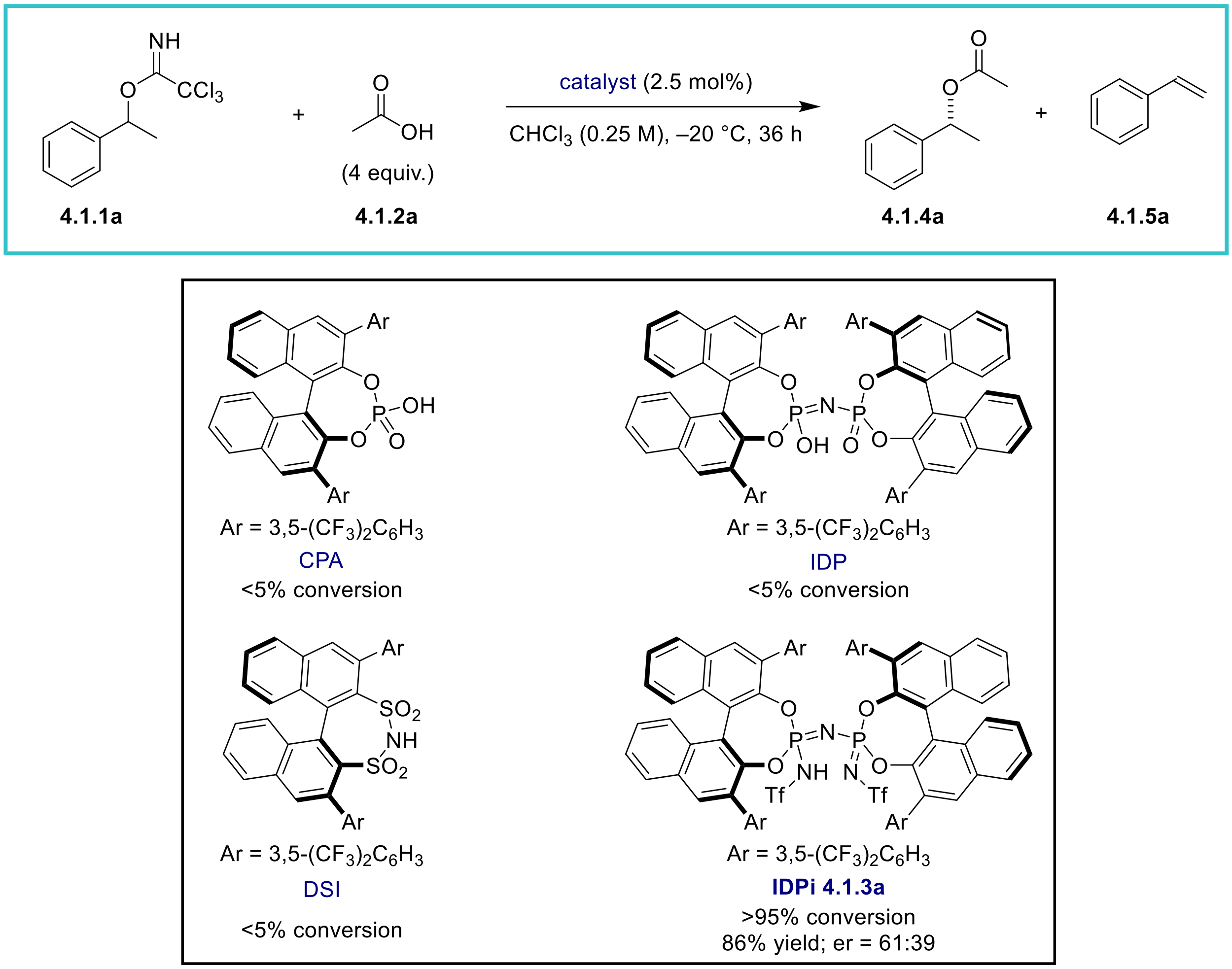
NH
O
CCl$_3$
4.1.1a
+
O
OH
(4 equiv.)
4.1.2a
catalyst (2.5 mol%)
CHCl$_3$ (0.25 M), –20 °C, 36 h
O
O
4.1.4a
+
4.1.5a
Ar
O
P
OH
O
O
Ar
Ar = 3,5-(CF$_3$)$_2$C$_6$H$_3$
CPA
<5% conversion
Ar
Ar
O
O
P=N–P
O
OH
O
O
Ar
Ar
Ar = 3,5-(CF$_3$)$_2$C$_6$H$_3$
IDP
<5% conversion
Ar
SO$_2$
NH
SO$_2$
Ar
Ar = 3,5-(CF$_3$)$_2$C$_6$H$_3$
DSI
<5% conversion
Ar
Ar
O
O
P=N–P
O
NH
N
O
Tf
Tf
Ar
Ar
Ar = 3,5-(CF$_3$)$_2$C$_6$H$_3$
IDPi 4.1.3a
>95% conversion
86% yield; er = 61:39

Scheme 4.1.1: Initial catalyst screening of chiral Brønsted acid catalysts

With this initial promising result, we focused on improving the enantioselectivity of the reaction. Subsequently, the solvent effect and amount of acetic acid were investigated. The result of the solvent study showed that the ether was the best solvent in order to achieve high yield and selectivity (Table 4.1.1).

Table 4.1.1: Solvent and equivalents screening for the reaction between trichloroacetimidate **4.1.1a** and nucleophile **4.1.2a**:

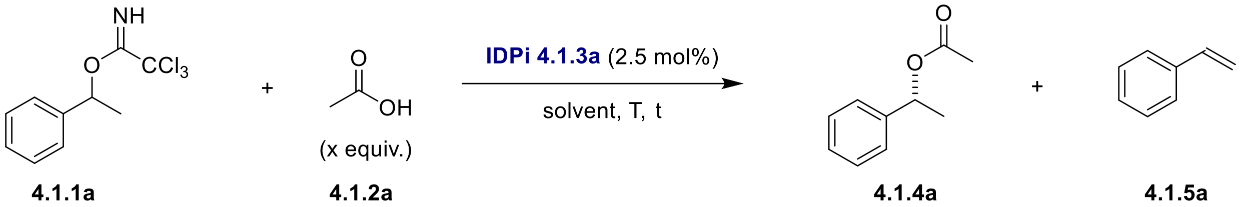
NH
CCl3
O
+
O
OH
(x equiv.)
IDPi 4.1.3a (2.5 mol%)
solvent, T, t
O
O
+
4.1.1a
4.1.2a
4.1.4a
4.1.5a

entry	X equiv.	solvent	T (°C)	time (t)	%Yield(conv.)	er
1.	1	CHCl$_3$	–20	36 h	60(>95%)	61.5:38.5
2.	2	CHCl$_3$	–20	36 h	75(>95%)	61:39
3.	3	CHCl$_3$	–20	36 h	85(>95%)	60.5:39.5
4.	4	CHCl$_3$	–20	36 h	85(>95%)	61:39
5.	4	CHCl$_3$	–80	3 d	90(>95%)	69:31
6.	4	CHCl$_3$:Et$_2$O (1:1)	–80	3 d	81(>95%)	71.5:28.5
7.	4	CHCl$_3$:MeCy (1:1)	–80	3 d	88(>95%)	72:28
8	4	Et$_2$O	–80	3 d	92(>95%)	71.5:28.5

To see the effect of the choice of nucleophile has on the enantioselectivity, we tested different carboxylic acids as a nucleophile; however, it turned out that acetic acid was still the best nucleophile for the enantiomeric ratio.

Table 4.1.2: Effect of nucleophiles on enantioselectivity:

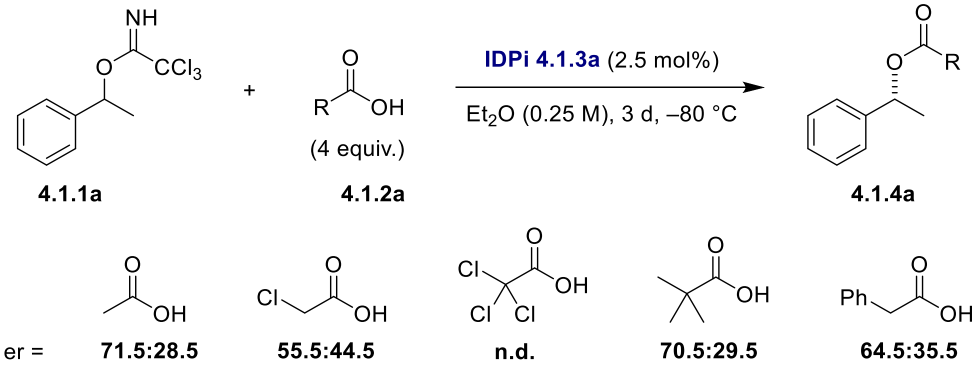
NH
CCl3
O
+
O
R
OH
(4 equiv.)
IDPi 4.1.3a (2.5 mol%)
Et2O (0.25 M), 3 d, –80 °C
O
O
R
4.1.1a
4.1.2a
4.1.4a
O
OH
O
Cl
OH
O
Cl
Cl
Cl
OH
O
OH
O
Ph
OH
er =
71.5:28.5
55.5:44.5
n.d.
70.5:29.5
64.5:35.5

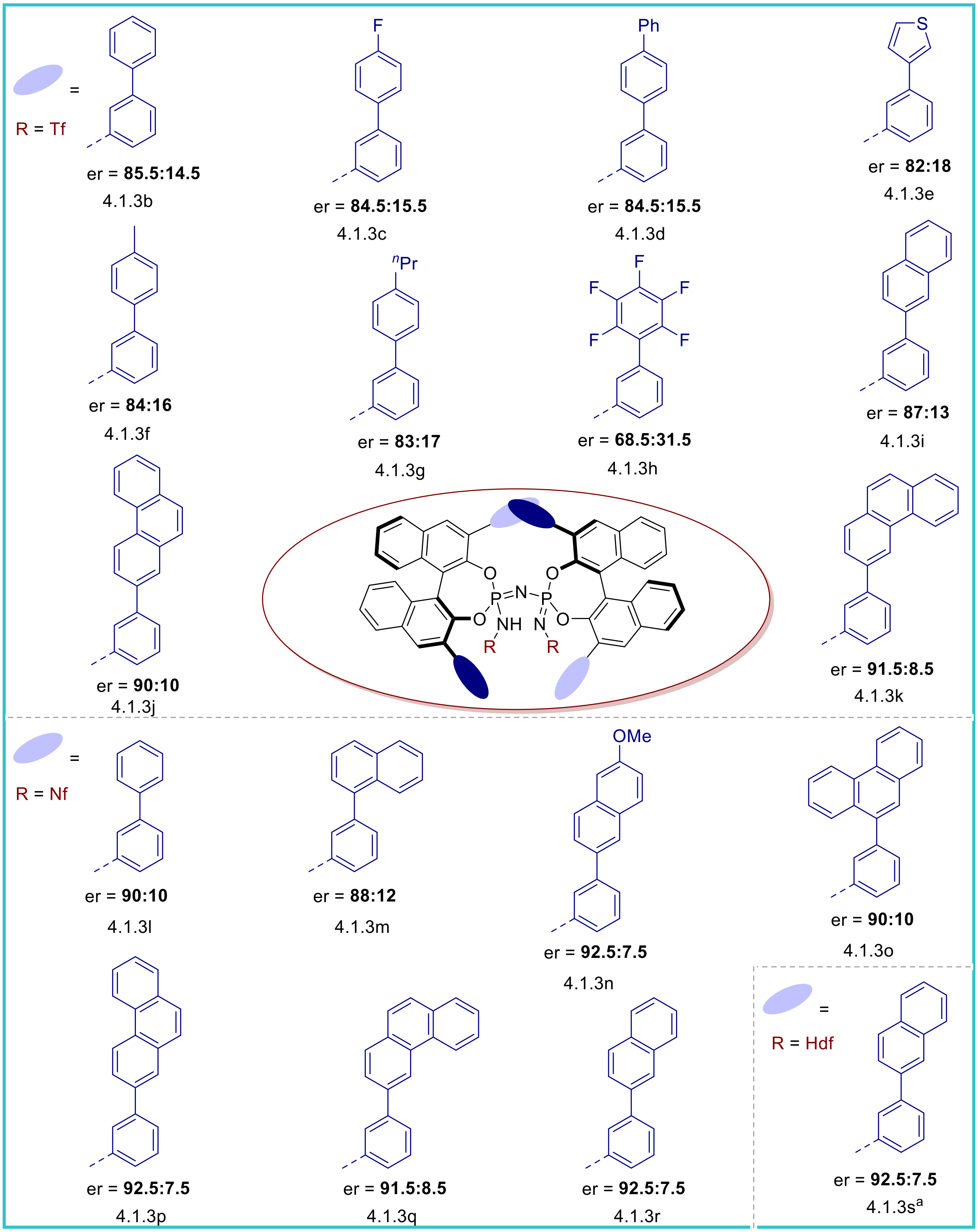
=
R = Tf
er = 85.5:14.5
4.1.3b
F
er = 84.5:15.5
4.1.3c
Ph
er = 84.5:15.5
4.1.3d
S
er = 82:18
4.1.3e
er = 84:16
4.1.3f
ⁿPr
er = 83:17
4.1.3g
F
F
F
F
F
er = 68.5:31.5
4.1.3h
er = 87:13
4.1.3i
er = 90:10
4.1.3j
O
P=N-P
O
NH
N
O
O
R
R
er = 91.5:8.5
4.1.3k
=
R = Nf
er = 90:10
4.1.3l
er = 88:12
4.1.3m
OMe
er = 92.5:7.5
4.1.3n
er = 90:10
4.1.3o
er = 92.5:7.5
4.1.3p
er = 91.5:8.5
4.1.3q
er = 92.5:7.5
4.1.3r
=
R = Hdf
er = 92.5:7.5
4.1.3s[a]

Figure 4.1.1: Selected overview of tested catalysts for the reaction between trichloroacetimidate **4.1.1a** and nucleophile **4.1.2a**, Tf = SO_2CF_3, Nf = $SO_2C_4F_9$, Hdf = $SO_2C_8F_{17}$. [a]IDPi 4.1.3s was chosen for further optimization due to better solubility at low temperature

Encouraged by the initial results, we turned our attention to catalyst screening by fine-tuning the 3,3´-substituents of the BINOL framework and the active core of the catalyst. We investigated the effect of *m*-substituents of the phenyl ring using our group´s internal catalyst library. Irrespective of the steric (4.1.3b–4.1.3h), no increase in enantioselectivity was observed, with the highest enantioselectivity being obtained only for *meta*-biphenyl substituent. Nevertheless, a gradual increase in enantioselectivity was observed when polyaromatic groups (4.1.3i–4.1.3k) (Figure 4.1.1) were introduced at the *meta* position of the phenyl substituent. We believe that the cation–π interaction is stabilizing the carbocation inside the catalyst core and the carbocation is not accessible to nucleophilic attack from another side. Next, we focused on investigating the inner core of the catalyst. To our delight, a noticeable improvement in enantioinduction was observed when moving to a longer perfluoroalkyl chain (4.1.3–4.1.3s). Yet, no improvement in enantioselectivity was observed when moving from the C_4F_9 to the C_8F_{17} core (4.1.3s). With this promising enantioselectivity, we turned our attention to reinvestigating the effect of solvents.

Table 4.1.3: Solvent screening for the reaction between trichloroacetimidate **4.1.1a** and nucleophile **4.1.2a** with IDPi **4.1.3s** catalyst:

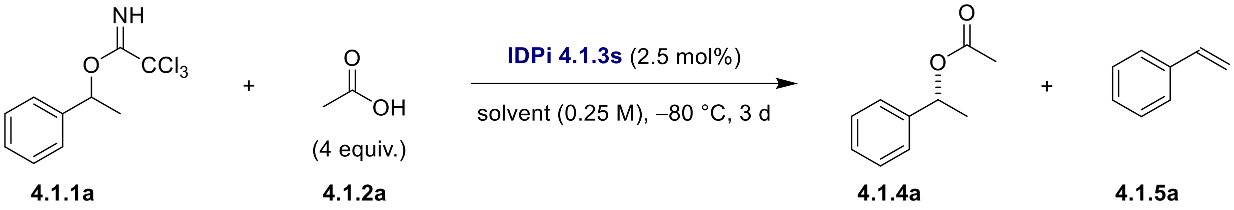

entry	solvent	%Yield(conv.)	er
1.	Et_2O	85(>95%)	92.5:7.5
2.	Et_2O:MeCy (1:1)	56(>95%)	94:6
3.	Et_2O:CyH (1:1)	50(>95%)	94:6
4.	Et_2O:MeCyclopentane (1:1)	<10(>95%)	n.d.
5.	Et_2O:pentane (1:1)	<10(>95%)	n.d.
6.	Et_2O:hexane (1:1)	<10(>95%)	n.d.

Investigation of solvents showed that hydrocarbon-based solvents in combination with Et_2O were good for enantioselectivity, but it was not good for the yield of the desired product. We hypothesized that in the presence of hydrocarbon-based solvents, the interaction between cation and anion is much stronger, leading to higher enantioselectivity. In addition to the ionic interaction between the cation and the catalyst counteranion, solvent interaction also takes place when a Lewis basic solvent is used, distorting the ion pairing and leading to slightly lower enantioselectivity.

Table 4.1.4: Effect of temperature on enantioselectivity for the reaction between trichloroacetimidate **4.1.1a** and nucleophile **4.1.2a** using **IDPi 4.1.3s** catalyst:

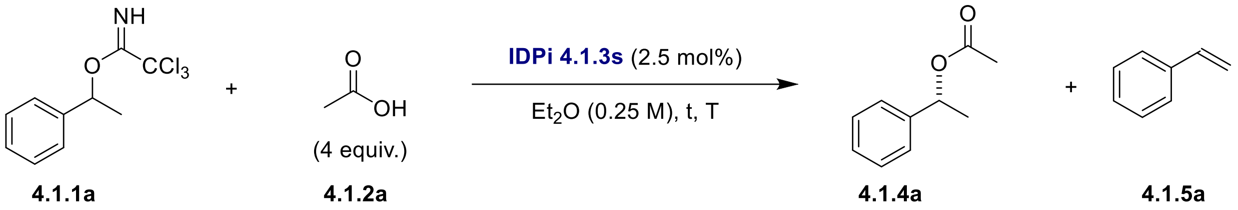

entry	T (°C)	time (t)	%Yield(conv.)	er
1.	–80	3 d	85(>95%)	92.5:7.5
2.	–90	5 d	85(>95%)	95:5

Having failed to improve enantioselectivity and yield, we decided to lower the reaction temperature further. Lowering the reaction temperature (from –80 °C to –90 °C) increased the enantiomeric ratio from 92.5:7.5 to 95:5 (Table 4.1.4). With these optimal conditions, we turned our attention toward the scope of the reaction.

Preliminary substrate scope: For the preliminary scope of the substrates, **IDPi 4.1.3r** was chosen for convenience, as the result does not change (Figure 4.1.1).

Several electronically substituted substrates were tested and we found that all of them gave good to excellent yields (63–90% yield). However, the enantioselectivity was highly dependent on the steric and electronic properties of the arene ring. The enantioselectivities decreased significantly when electron–donating groups were introduced at the *para* position (entry 4.1.4b–4.1.4d; Scheme 4.1.2). We believe that the electron–donating groups stabilize the cation, loosening the ion pair and exposing the cation to the nucleophile. When the electron–donating groups were introduced at the *meta* position, no change in enantioselectivity was observed, as the *meta* substituents have no stabilizing or destabilizing effect on the benzylic cation (entries 4.1.4g, 4.1.4h). A substrate with a substituent at the *ortho* position gave good yield with poor enantioselectivity (entry 4.1.4i).

From this preliminary screening, two main challenges were realized:

i) electron-donating groups at the para position hampers the enantioselectivity.

ii) The presence of substituent close to the reactive center also hampers enantioselectivity.

From this preliminary screening, we also concluded that substituents at the *meta* position do not affect enantioselectivity (Scheme 4.1.2).

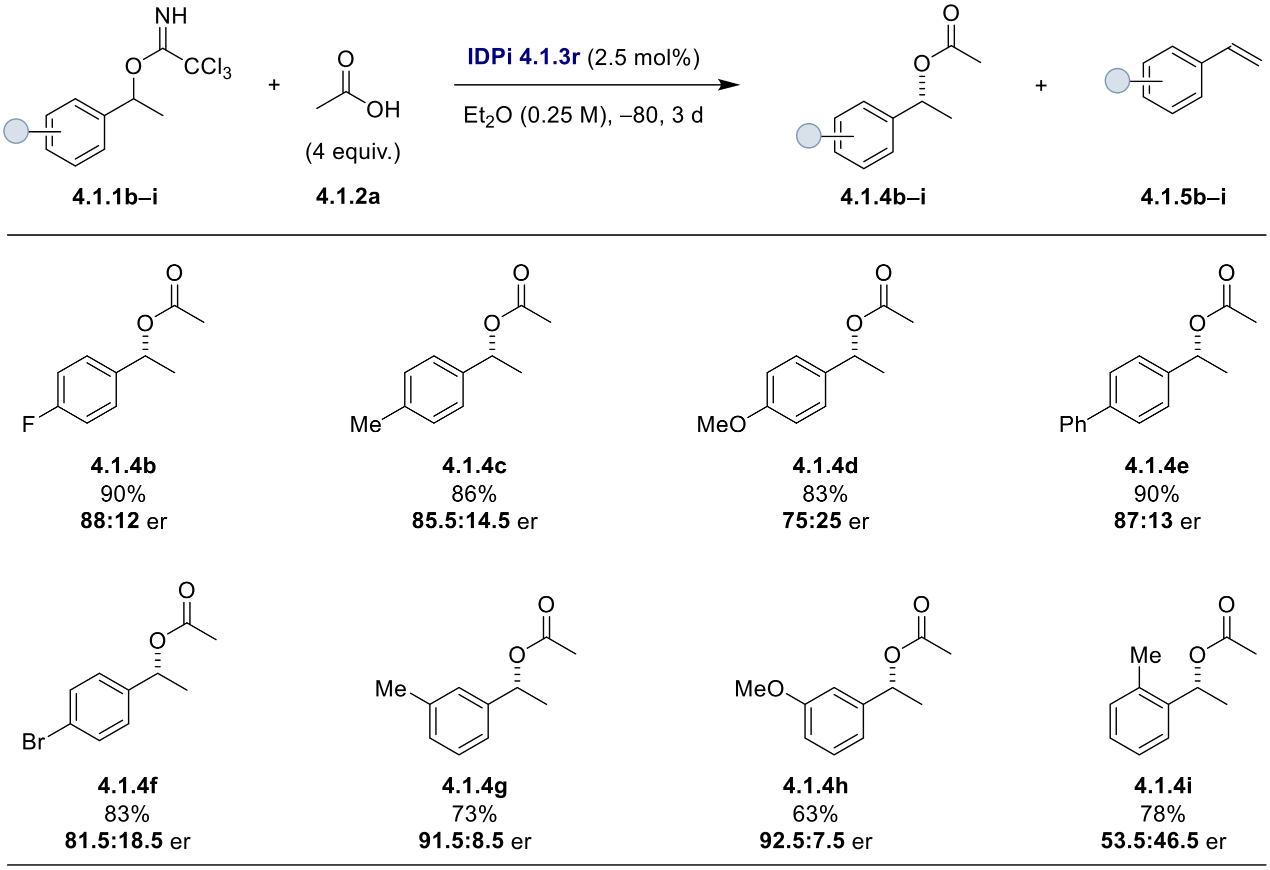
NH
CCl3
+
(4 equiv.)
IDPi 4.1.3r (2.5 mol%)
Et2O (0.25 M), –80, 3 d
+
4.1.1b–i
4.1.2a
4.1.4b–i
4.1.5b–i
F
4.1.4b
90%
88:12 er
Me
4.1.4c
86%
85.5:14.5 er
MeO
4.1.4d
83%
75:25 er
Ph
4.1.4e
90%
87:13 er
Br
4.1.4f
83%
81.5:18.5 er
Me
4.1.4g
73%
91.5:8.5 er
MeO
4.1.4h
63%
92.5:7.5 er
Me
4.1.4i
78%
53.5:46.5 er

Scheme 4.1.2: Preliminary substrate scope of different carbocation precursor using **IDPi 4.1.3r**

Since the electron-donating groups at *the para* position hamper the enantioselectivity, we decided to reinvestigate the catalysts to improve the enantioselectivity for these substrates. In order to find out the best catalyst for substrates having electron-donating groups at the *para* position, we tested several of our group´s internal catalyst library; we elaborated on the effect of the *meta*-substituents on the phenyl ring and spiro fluorene type as 3,3´-substituents. When we tested several *meta*-substituents on the phenyl ring, we found that these catalysts were not fruitful for higher enantioselectivity and gave moderate enantioselectivity (4.1.3t–4.1.3aa) (Scheme 4.1.3). For the 3,3´-substituted spiro fluorene type catalysts, the enantioselectivity increased with increasing ring size (4.1.3ab–4.1.3ad). Finally, enantioselectivity was further improved (4.1.3ae–4.1.3af) by a phenyl substitution at C_7 of the spiro fluorene wing and modification of the active core improves. We decided to investigate the effect of nucleophile on enantioselectivity with this promising enantioselectivity.

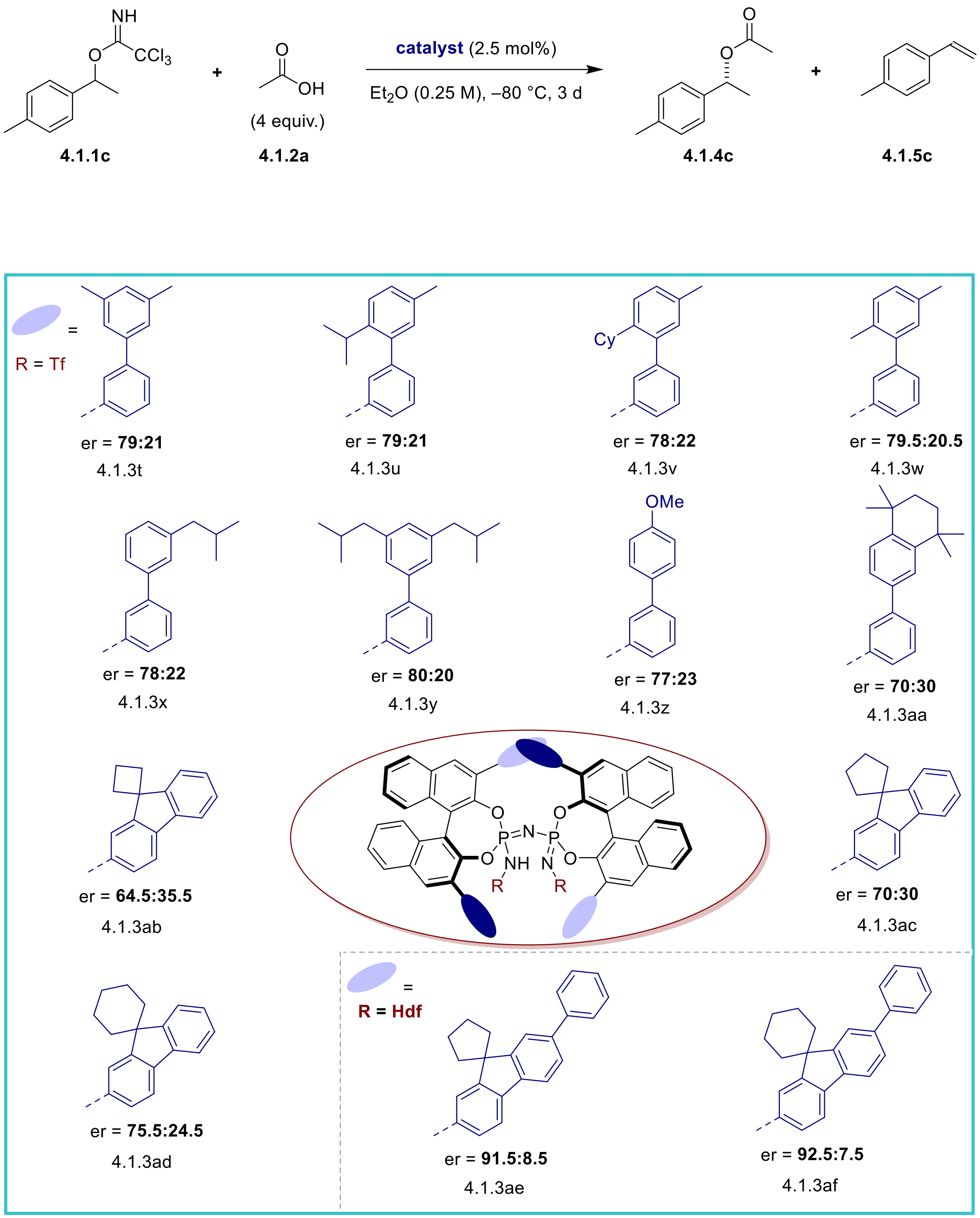
NH
O
CCl3
+
O
OH
(4 equiv.)
catalyst (2.5 mol%)
Et2O (0.25 M), –80 °C, 3 d
O
O
+
4.1.1c
4.1.2a
4.1.4c
4.1.5c
=
R = Tf
er = 79:21
4.1.3t
er = 79:21
4.1.3u
Cy
er = 78:22
4.1.3v
er = 79.5:20.5
4.1.3w
er = 78:22
4.1.3x
er = 80:20
4.1.3y
OMe
er = 77:23
4.1.3z
er = 70:30
4.1.3aa
er = 64.5:35.5
4.1.3ab
O
P=N–P
O
O
NH
N
O
R
R
er = 70:30
4.1.3ac
er = 75.5:24.5
4.1.3ad
=
R = Hdf
er = 91.5:8.5
4.1.3ae
er = 92.5:7.5
4.1.3af

Scheme 4.1.3: Selected overview of tested catalysts for the reaction between trichloroacetimidate **4.1.1c** and nucleophile **4.1.2a**, Tf = SO_2CF_3, Hdf = $SO_2C_8F_{17}$

Table 4.1.5: Effect of nucleophiles on enantioselectivity:

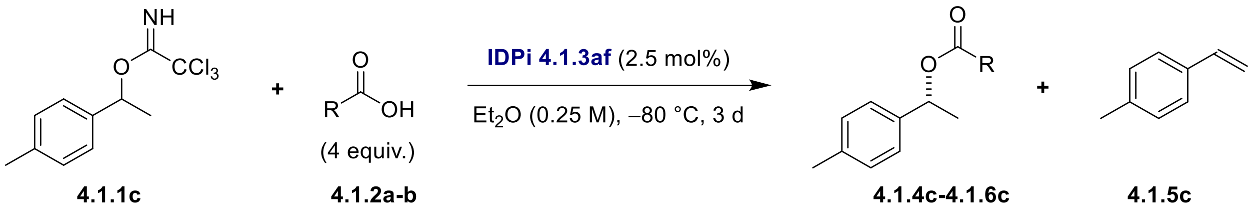
NH
CCl3
O
+
R
OH
(4 equiv.)
IDPi 4.1.3af (2.5 mol%)
Et2O (0.25 M), –80 °C, 3 d
O
R
+
4.1.1c
4.1.2a-b
4.1.4c-4.1.6c
4.1.5c

entry	R	%Yield(conv.)	er
1.	Me	85(>95%)	92.5:7.5
2.	Et	86(>95%)	95.5:4.5

The effect of nucleophile on the enantioselectivity was investigated by testing different carboxylic acids as nucleophile, and it turned out that propionic acid was the best compared to acetic acid for the enantioselectivity, giving 95.5:4.5 enantiomeric ratio (Table 4.1.5). With this promising selectivity, we turned our attention to the scope of the reaction with electron–donating groups at the *para* position.

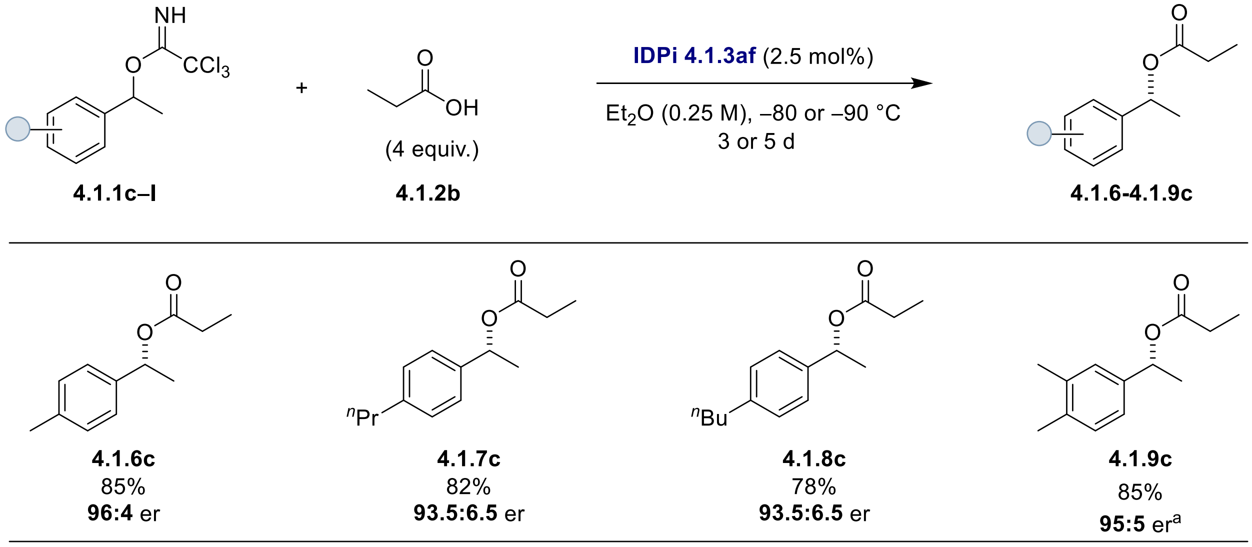
NH
CCl3
O
+
O
OH
(4 equiv.)
IDPi 4.1.3af (2.5 mol%)
Et2O (0.25 M), –80 or –90 °C
3 or 5 d
4.1.1c–l
4.1.2b
4.1.6-4.1.9c
nPr
nBu
4.1.6c
85%
96:4 er
4.1.7c
82%
93.5:6.5 er
4.1.8c
78%
93.5:6.5 er
4.1.9c
85%
95:5 er[a]

Scheme 4.1.4: Scope for substrates having Electron–donating group at the *para*-position using **IDPi 4.1.3af**. [a]reaction was performed at –90 °C for 5 d.

Several *para*-alkyl substituted as well as *meta*-, *para*-disubstituted substrates were tested. The desired products were yielded with a good to excellent enantiomeric ratio (4.1.6c–4.1.9c) (Scheme 4.1.4).

Fine-tuning of the scope: After screening several catalysts and reaction conditions to find which substrates were tolerated in this developed methodology to get the desired reactivity and selectivity, improved results are summarized in **Scheme 4.1.5**.

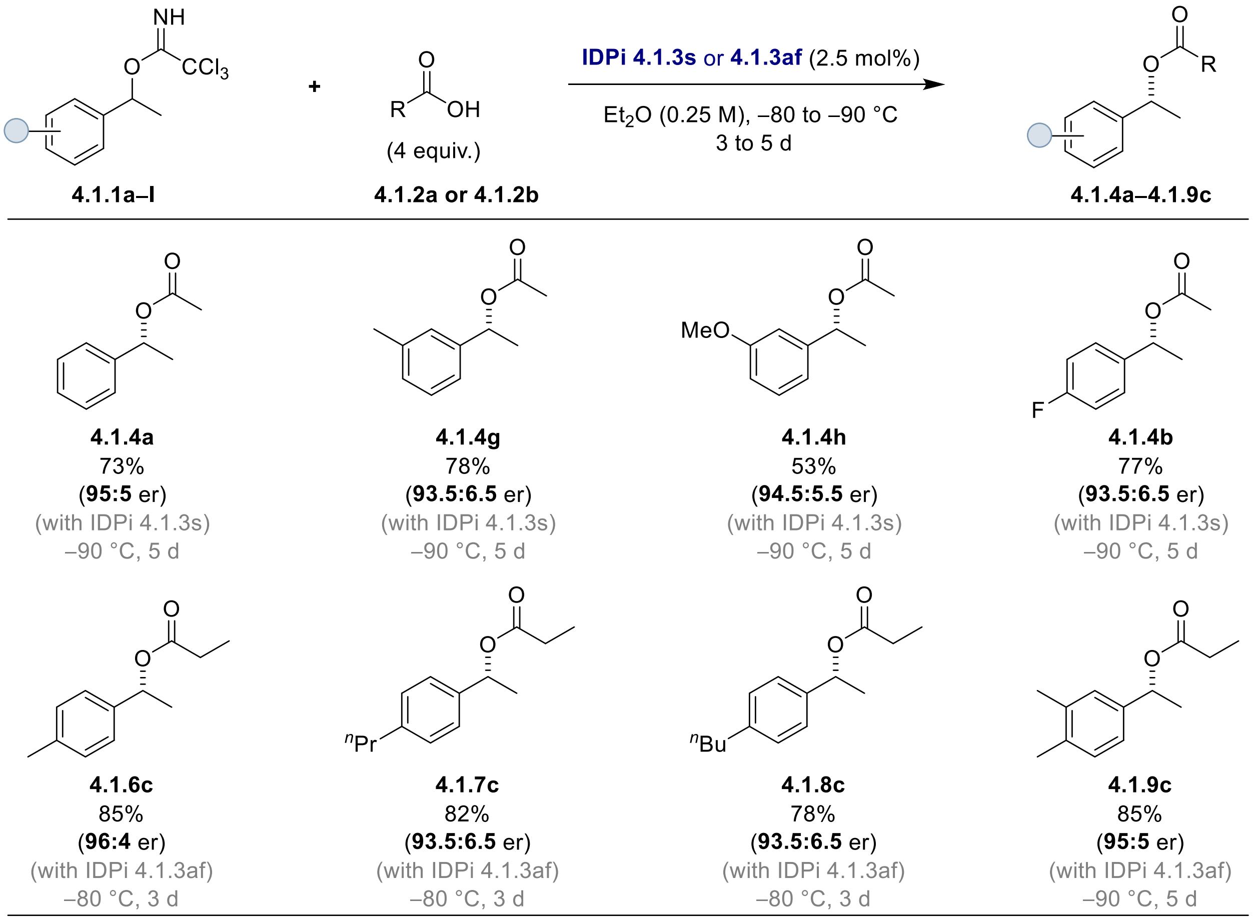
NH
O
CCl3
+
O
R
OH
(4 equiv.)
IDPi 4.1.3s or 4.1.3af (2.5 mol%)
Et2O (0.25 M), –80 to –90 °C
3 to 5 d
O
O
R
4.1.1a–l
4.1.2a or 4.1.2b
4.1.4a–4.1.9c
4.1.4a
73%
(95:5 er)
(with IDPi 4.1.3s)
–90 °C, 5 d
4.1.4g
78%
(93.5:6.5 er)
(with IDPi 4.1.3s)
–90 °C, 5 d
MeO
4.1.4h
53%
(94.5:5.5 er)
(with IDPi 4.1.3s)
–90 °C, 5 d
F
4.1.4b
77%
(93.5:6.5 er)
(with IDPi 4.1.3s)
–90 °C, 5 d
4.1.6c
85%
(96:4 er)
(with IDPi 4.1.3af)
–80 °C, 3 d
nPr
4.1.7c
82%
(93.5:6.5 er)
(with IDPi 4.1.3af)
–80 °C, 3 d
nBu
4.1.8c
78%
(93.5:6.5 er)
(with IDPi 4.1.3af)
–80 °C, 3 d
4.1.9c
85%
(95:5 er)
(with IDPi 4.1.3af)
–90 °C, 5 d

Scheme 4.1.5: Scope for IDPi catalyzed C–O bond formation reaction.

Limitations of the scope:

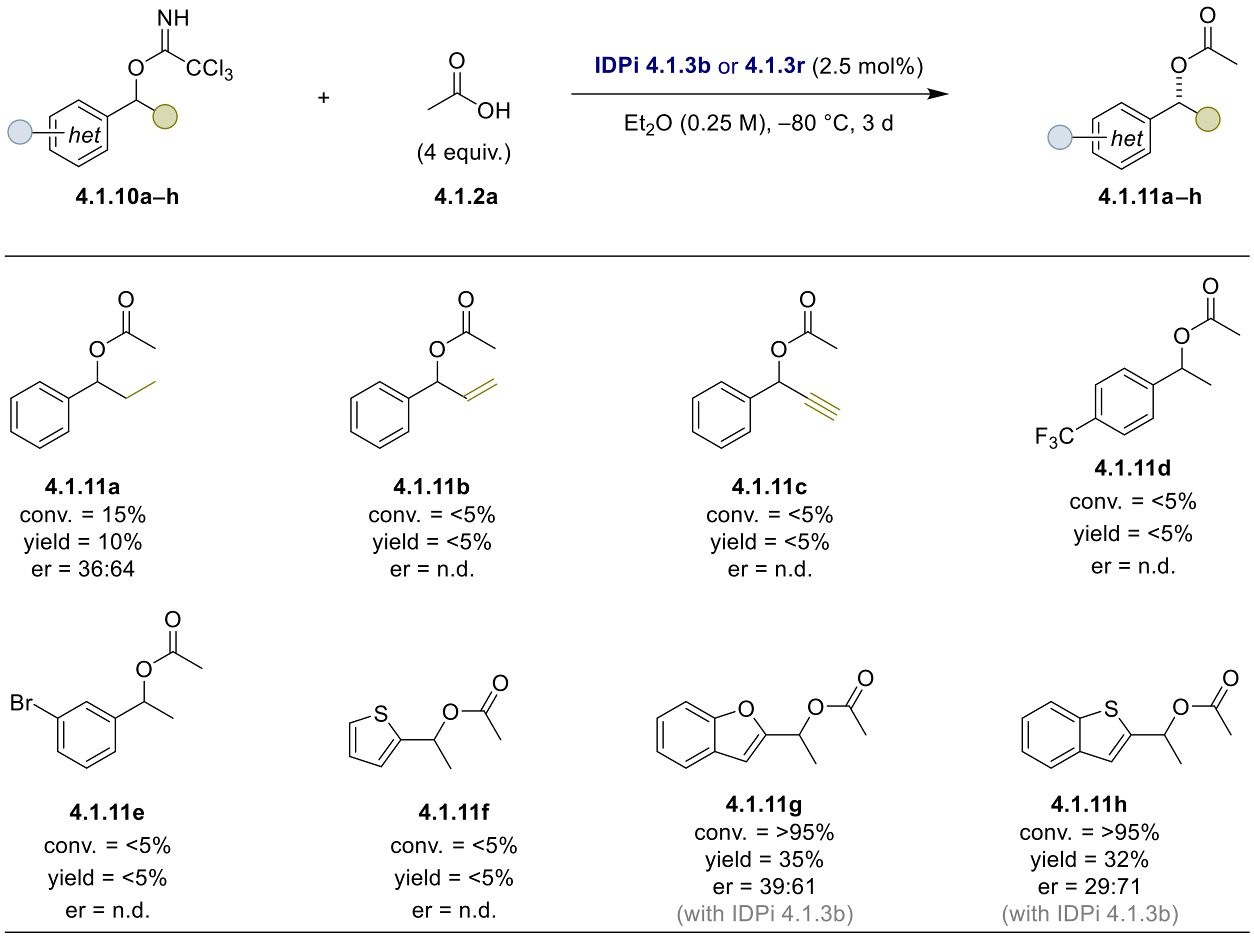
NH
O
CCl3
het
4.1.10a–h
+
O
OH
(4 equiv.)
4.1.2a
IDPi 4.1.3b or 4.1.3r (2.5 mol%)
Et2O (0.25 M), –80 °C, 3 d
O
O
het
4.1.11a–h
4.1.11a
conv. = 15%
yield = 10%
er = 36:64
4.1.11b
conv. = <5%
yield = <5%
er = n.d.
4.1.11c
conv. = <5%
yield = <5%
er = n.d.
F3C
4.1.11d
conv. = <5%
yield = <5%
er = n.d.
Br
4.1.11e
conv. = <5%
yield = <5%
er = n.d.
S
4.1.11f
conv. = <5%
yield = <5%
er = n.d.
4.1.11g
conv. = >95%
yield = 35%
er = 39:61
(with IDPi 4.1.3b)
S
4.1.11h
conv. = >95%
yield = 32%
er = 29:71
(with IDPi 4.1.3b)

Scheme 4.1.6: Limitations of scope for IDPi catalyzed C–O bond formation reaction.

4.2 Results and Discussion for C–N Bond formation:

The work presented in this section was performed in cooperation with Dr. Chandra Kanta De and Dr. Raja Mitra.

4.2.1 Reaction development and optimization studies:

We were inspired by the promising results on the C–O bond formation, where we used external nucleophiles to trap the reactive benzylic carbocation intermediate. We wonder whether *in situ* generated trichloroacetamide can recombine with generated carbocation to form the corresponding C–N rearrangement product. Such a transformation might be an attractive approach to the enantioselective formation of benzylic C–N bonds from benzylic alcohols or derivatives.[102-110] However, the availability of nucleophiles will always be equivalent in amount to the generated cation. In addition, styrene **4.1.5a** cannot regenerate carbocation on protonation at such a low temperature.

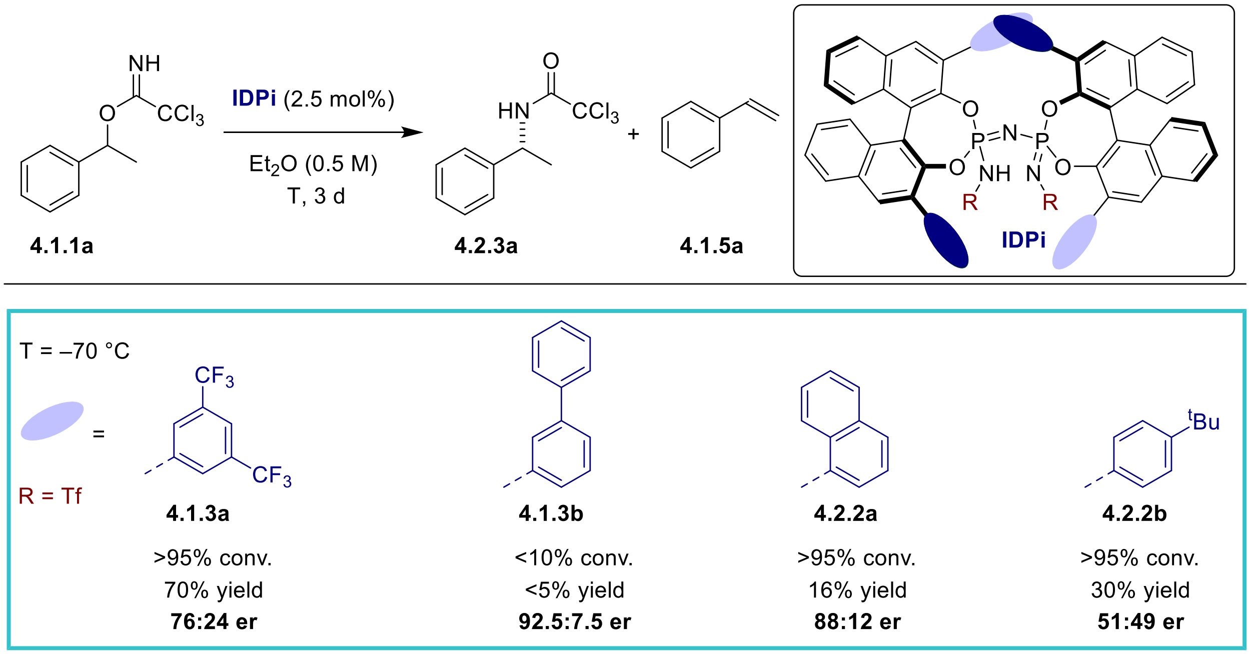
NH
O
CCl3
4.1.1a
IDPi (2.5 mol%)
Et2O (0.5 M)
T, 3 d
O
HN
CCl3
4.2.3a
+
4.1.5a
O
P=N–P
O
NH
N
O
O
R
R
IDPi
T = –70 °C
=
R = Tf
CF3
CF3
4.1.3a
>95% conv.
70% yield
76:24 er
4.1.3b
<10% conv.
<5% yield
92.5:7.5 er
4.2.2a
>95% conv.
16% yield
88:12 er
tBu
4.2.2b
>95% conv.
30% yield
51:49 er

Scheme 4.2.1: Initial catalyst screening of chiral Brønsted acid catalysts for C–N bond formation.

Upon testing various IDPi catalysts from our group's internal catalyst library, we found that only the acidic catalyst **4.1.3a** (electron-withdrawing group at the substituents of 3,3´-position) gave a good yield of the desired product **4.2.3a**, albeit with moderate enantioselectivity. When less acidic catalysts **4.1.3b**, **4.2.2a** and **4.2.2b** were tested, they gave poor yield with moderate to good enantiomeric ratio. We hypothesize that more Lewis basic counteranions (electron neutral or electron-rich 3,3´-substituents) deprotonate the *in situ* generated cation faster, leading to significant styrene **4.1.5a** formation. With these preliminary results, we investigated the effect of temperature, 3,3´-substituents on the BINOL backbone, and active core for desired product formation and enantioselectivity (Table 4.2.1). With extensive screening of the catalysts (Table 4.2.1) and lowering the reaction temperature (from –70 °C to –80 °C), we did not observe a significant improvement in the selectivity. It is worth noting that longer perfluoro-alkyl chains in the active core of the catalyst **4.1.3l** improve the enantioselectivity, although with poor yield of the product.

Table 4.2.1: Effect of temperature, 3,3´-substituents and active core :

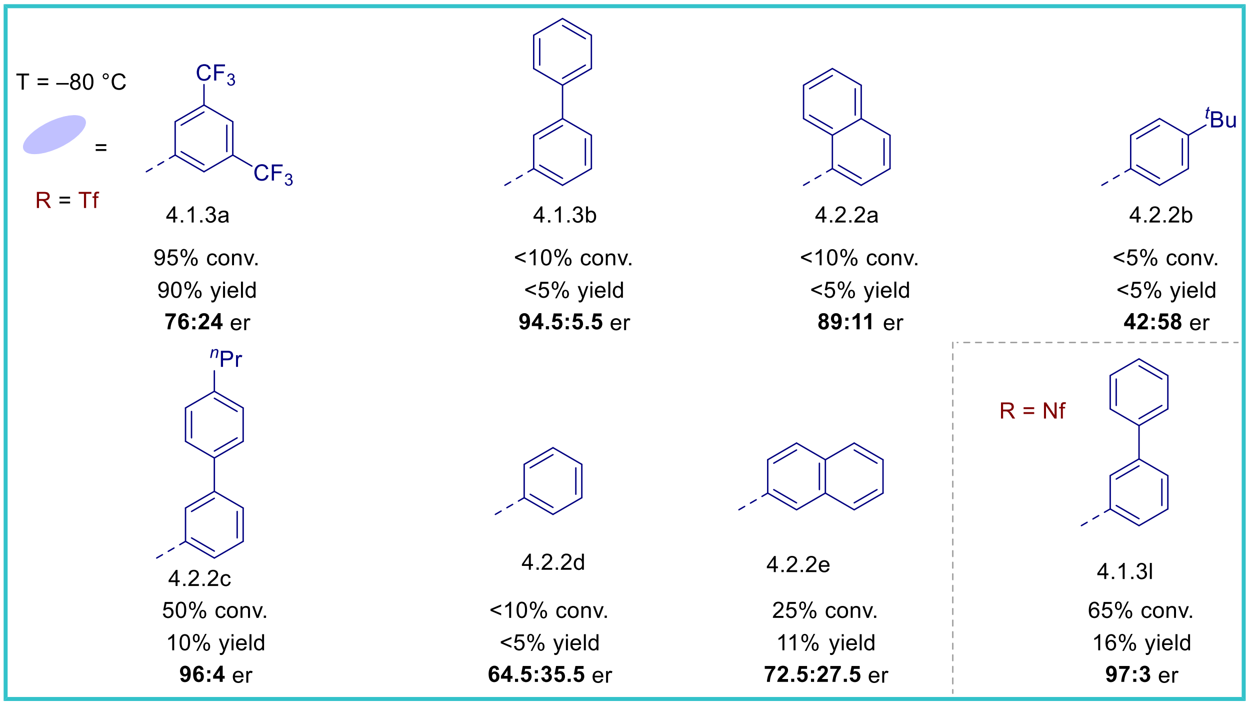
T = –80 °C
=
R = Tf
CF3
CF3
4.1.3a
95% conv.
90% yield
76:24 er
4.1.3b
<10% conv.
<5% yield
94.5:5.5 er
4.2.2a
<10% conv.
<5% yield
89:11 er
tBu
4.2.2b
<5% conv.
<5% yield
42:58 er
nPr
4.2.2c
50% conv.
10% yield
96:4 er
4.2.2d
<10% conv.
<5% yield
64.5:35.5 er
4.2.2e
25% conv.
11% yield
72.5:27.5 er
R = Nf
4.1.3l
65% conv.
16% yield
97:3 er

We decided to move forward by developing more acidic IDPi catalysts to enhance the yield of the desired product, however, without changing the microenvironment of the active core of the catalyst. Previously, we have shown that electron-withdrawing groups on the BINOL backbone enhance the acidity of the IDPi catalyst.[41h] Therefore, attempts to modulate the electronic properties of the catalyst were made to diminish the deprotonation pathway.

Based on the reports[111] for the substitution of hydrogens by fluorines at the 5, 5′, 6, 6′, 7, 7′, 8, and 8′ positions (F_8-BINOL) for substituted BINOL derivatives, we used the corresponding F_8-

BINOL for the synthesis of IDPi derivatives **4.1.3b** and **4.1.3l**. When we tested these two catalysts (**4.2.2f**, **4.2.2g**) in the reaction, we found improved conversion and NMR yield for the desired product although, a decrease in the enantiomeric ratio was observed (Scheme 4.2.2). We believe substituting hydrogens with fluorines at 8, 8´ of BINOL changes the bi-angle, making the catalyst core more open.

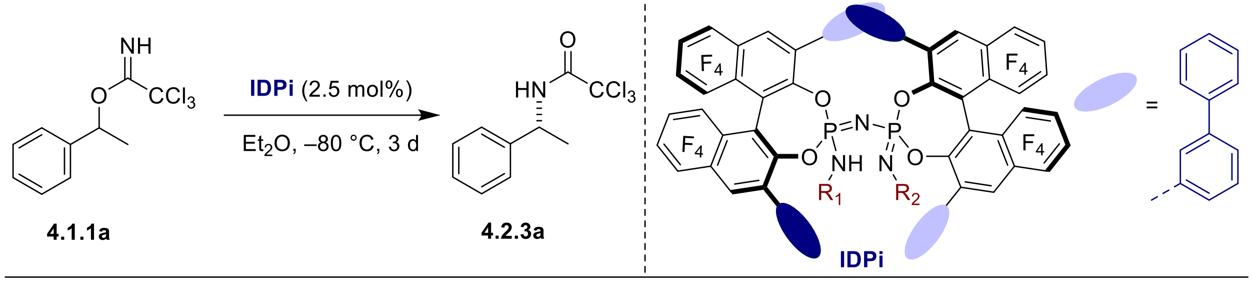
NH
O
CCl3
IDPi (2.5 mol%)
Et2O, –80 °C, 3 d
O
HN
CCl3
4.1.1a
4.2.3a
F4
F4
F4
F4
O
O
P=N–P
O
O
NH
N
R1
R2
IDPi
=

R$_1$ = Tf; R$_2$ = Tf (**4.2.2f**)

>95% conv.
91% yield
9.5:90.5 er

R$_1$ = Nf; R$_2$ = Nf (**4.2.2g**)

>95% conv.
71% yield
13:87 er

Scheme 4.2.2: Effect of perfluorinated IDPi catalysts for C–N bond formation

The improved yield hinted the correct direction for the catalyst development. To improve the enantioselectivity in addition to the better yield, we decided to replace one of the F$_8$-BINOL with BINOL in the IDPi catalyst (Scheme 4.2.3).

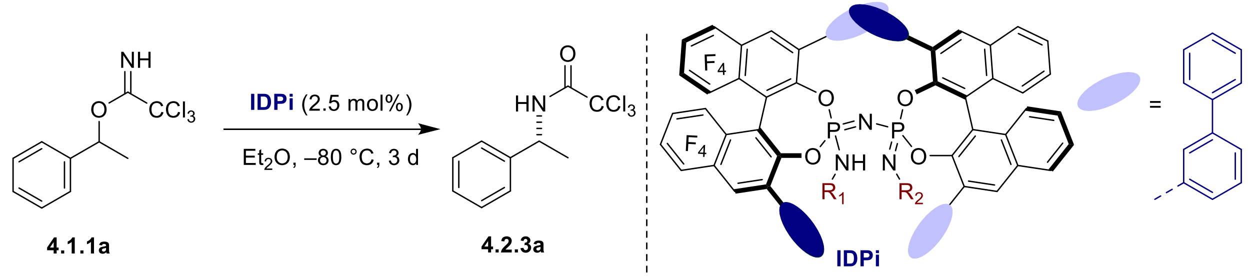
NH
O
CCl3
IDPi (2.5 mol%)
Et2O, –80 °C, 3 d
O
HN
CCl3
4.1.1a
4.2.3a
F4
F4
O
O
P=N–P
O
O
NH
N
R1
R2
IDPi
=

R$_1$ = Tf; R$_2$ = Tf (**4.2.2h**)

>95% conv.
72% yield
90.5:9.5 er

R$_1$ = Nf; R$_2$ = Tf (**4.2.2i**)

>95% conv.
70% yield
92.5:7.5 er

R$_1$ = Tf; R$_2$ = Nf (**4.2.2j**)

>95% conv.
75% yield
95:5 er

Scheme 4.2.3: Effect of different electronically substituted BINOL derived IDPi catalysts for C–N bond formation

After systematic fine-tuning of the active core, we obtained 75% yield with 95:5 er of the desired product using catalyst **4.2.2j** (Scheme 4.2.3). Using these conditions, we turned our attention toward the scope of C–N bond formation.

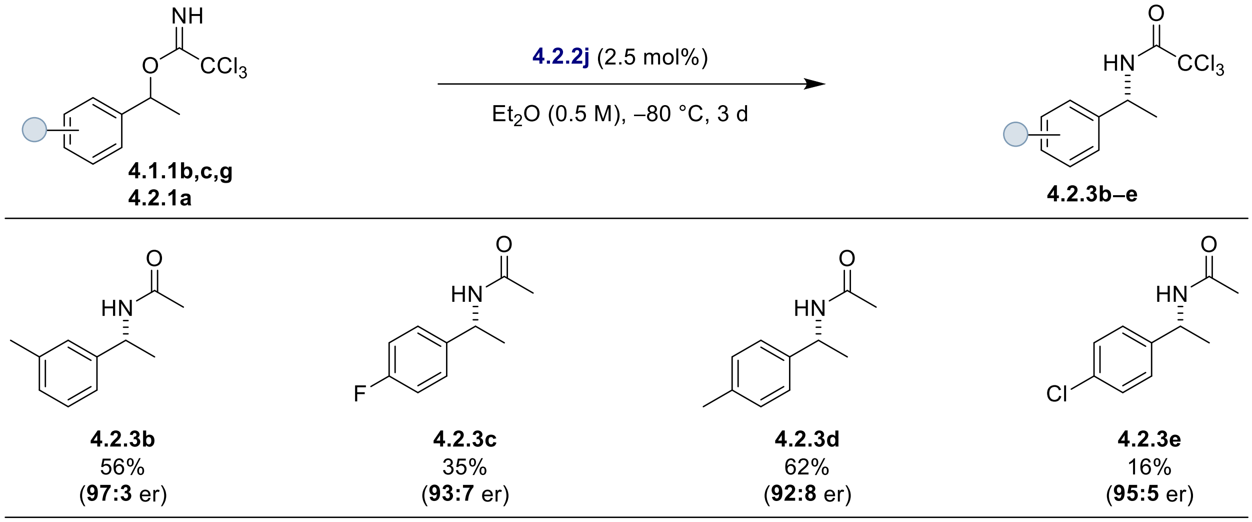
NH
O
CCl3
4.1.1b,c,g
4.2.1a
4.2.2j (2.5 mol%)
Et2O (0.5 M), –80 °C, 3 d
O
HN
CCl3
4.2.3b–e
4.2.3b
56%
(97:3 er)
4.2.3c
35%
(93:7 er)
F
4.2.3d
62%
(92:8 er)
4.2.3e
16%
(95:5 er)
Cl

Scheme 4.2.4: Preliminary substrate scope for C–N bond formation.

Preliminary screening of substrates showed that substrate with *meta* substituent gave slightly increased enantiomeric ratio **97:3** with moderate yield for product **4.2.3b**. While for substrates (4.1.1b, 4.1.1c) having electron–donating group at *para* position the enantioselectivity dropped. The corresponding product **4.2.3e** was obtained with the same enantioselectivity but in poor yield when the electron-withdrawing group at the *para* position was used as substrate (Scheme 4.2.4).

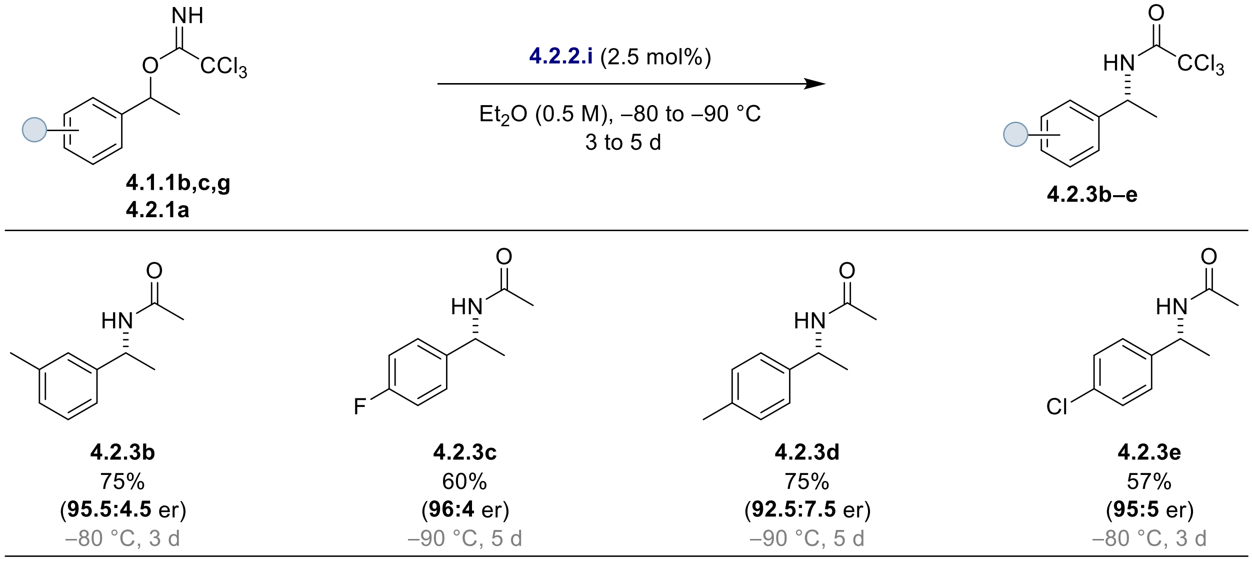
NH
O
CCl3
4.1.1b,c,g
4.2.1a
4.2.2.i (2.5 mol%)
Et2O (0.5 M), –80 to –90 °C
3 to 5 d
O
HN
CCl3
4.2.3b–e
4.2.3b
75%
(95.5:4.5 er)
–80 °C, 3 d
4.2.3c
60%
(96:4 er)
–90 °C, 5 d
F
4.2.3d
75%
(92.5:7.5 er)
–90 °C, 5 d
4.2.3e
57%
(95:5 er)
–80 °C, 3 d
Cl

Scheme 4.2.5: Scope of different electronically substituted substrates for IDPi catalyzed C–N bond formation reaction.

In order to improve the enantioselecivity and yield we further optimized the reaction conditions. On optimization of the reaction conditions, we found that substrates **4.1.1b**, **4.1.1c**, **4.1.1g & 4.2.1a** bearing alkyl groups and halogen atoms at the *meta* or *para* positions provided the corresponding products with good to excellent enantioselectivities and moderate to good yields using catalyst **4.2.2i** (**Scheme 4.2.5**).

Fine-tuning of the scope: After screening several catalysts and reaction conditions to find which substrates were tolerated in this developed methodology to get the desired reactivity and selectivity, improved results are summarized in **Scheme 4.2.6**.

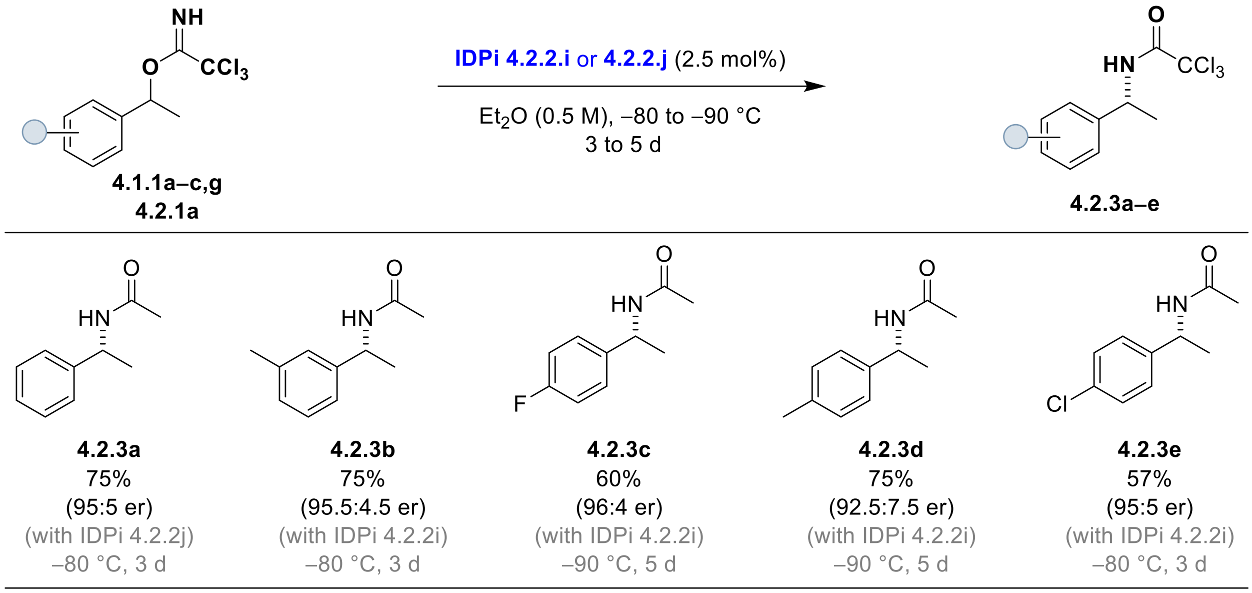
NH
O
CCl3
4.1.1a–c,g
4.2.1a
IDPi 4.2.2.i or 4.2.2.j (2.5 mol%)
Et2O (0.5 M), –80 to –90 °C
3 to 5 d
O
HN
CCl3
4.2.3a–e
O
HN
4.2.3a
75%
(95:5 er)
(with IDPi 4.2.2j)
–80 °C, 3 d
O
HN
4.2.3b
75%
(95.5:4.5 er)
(with IDPi 4.2.2i)
–80 °C, 3 d
O
HN
F
4.2.3c
60%
(96:4 er)
(with IDPi 4.2.2i)
–90 °C, 5 d
O
HN
4.2.3d
75%
(92.5:7.5 er)
(with IDPi 4.2.2i)
–90 °C, 5 d
O
HN
Cl
4.2.3e
57%
(95:5 er)
(with IDPi 4.2.2i)
–80 °C, 3 d

Scheme 4.2.6: Scope for IDPi catalyzed C–N bond formation reaction.

4.3 Results and Discussion for C−C Bond Formation:

4.3.1 Result and discussion:

After the successful implementation of the Brønsted acid-catalyzed asymmetric C−O and C−N bond-forming S_N1 reactions, we were keen on exploring the exciting potential to create C−C bonds *via* a similar pathway. We envisioned the previously unknown reaction of secondary benzylic alcohol derivatives with silyl ketene acetals toward the formation of β-branched esters as particularly attractive target. A somewhat related copper-catalyzed enantioselective substitution of benzylic propargylic acetates using silyl ketene acetal has been described[112]. However, only 10% yield and no enantioinduction was achieved with silyl ketene acetal. Similarly, our initial attempts at reacting trichloroacetimidate **4.1.1a** with silyl ketene acetals (SKAs) using IDPi catalysts did not lead to the desired C−C bond-forming product, and only the substrate **4.1.1a** was recovered. We speculate that imidate **4.1.1a** engages in a deprotosilylation[41b], the product of which, however, is unreactive toward ionization to the reactive benzylic carbocation. The List group had previously shown that heteroatom-stabilized cations (oxocarbenium ions and iminium ions) could be generated under (oxophilic) silylium Lewis acid catalysis conditions when acetate was used as leaving group[57]. We therefore commenced our investigation with commercially available 1-phenylethyl acetate **4.3.1a** as electrophile and tert-butyl((1-methoxyvinyl)oxy)dimethylsilane (SKA) **4.3.2a** as nucleophile. On initial catalysts screening using our group´s internal catalyst

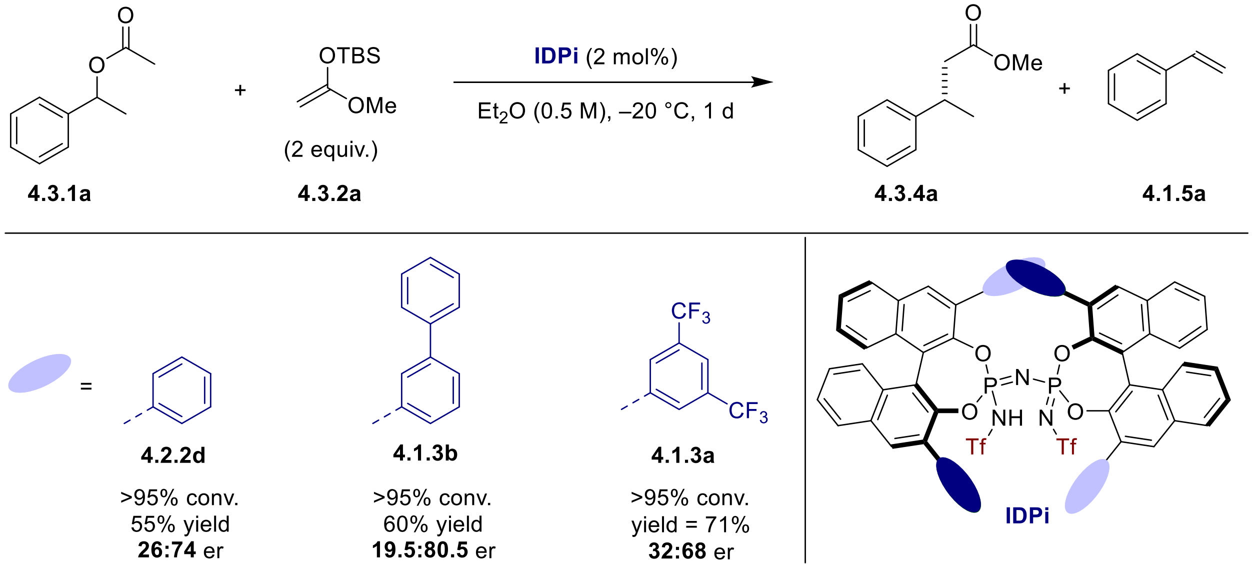

Scheme 4.3.1: Initial catalyst screening for C–C bond formation.

library we were pleased to find desired product **4.3.4a** formation in moderate yield with promising er (**Scheme 4.3.1**).

Initial investigation revealed a strong decline in the yield of the desired product **4.3.4a** and upon closer examination; we found that product was being used as a starting material for Mukaiyama–Claisen-type condensation reaction as the catalyst could not sterically discriminate between structurally similar starting material and product (Scheme 4.3.2). Owing to this reactivity, kinetic resolution was observed leading to increased er of the product. In order to avoid such kinetic resolution, we decided to use bulkier ester-derived SKA, the product of which would not be the part of the Mukaiyama–Claisen-type condensation reaction. For this purpose we decided to use ((1-(benzyloxy)vinyl)oxy)(tert-butyl)dimethylsilane **4.3.2b** (SKA) as nucleophile. To our delight, when we used SKA **4.3.2b**, we didn´t observe any Mukaiyama–Claisen-type product from the crude NMR as the product **4.3.7a** was sterically bulky compared to the starting material and the catalyst was able to discriminate between the starting material and the product (Scheme 4.3.3). After the realization of these initial results, our focus was on the optimization of the reaction conditions in order to improve the enantioselectivity of the reaction.

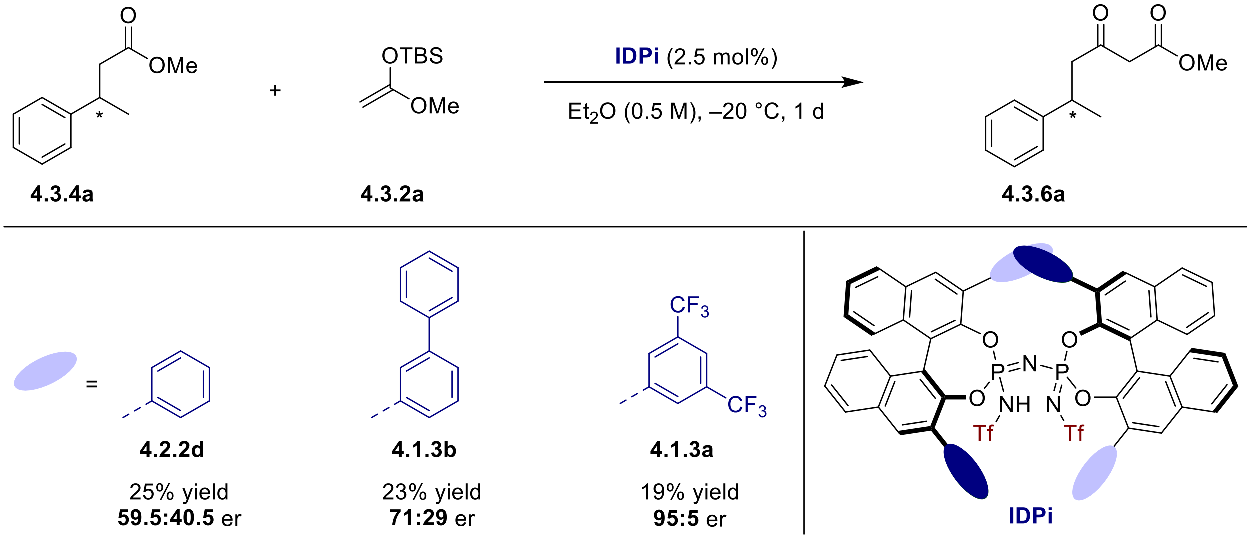

Scheme 4.3.2: Initial catalyst screening for C–C bond formation.

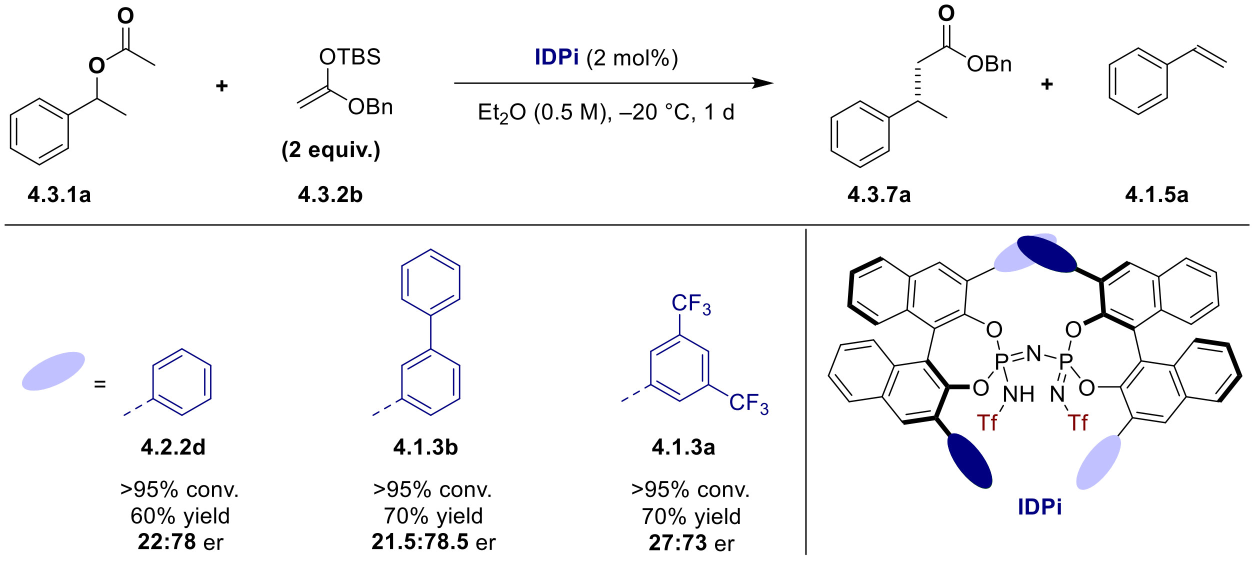
IDPi (2 mol%)
Et$_2$O (0.5 M), –20 °C, 1 d
(2 equiv.)
4.3.1a
4.3.2b
4.3.7a
4.1.5a
OTBS
OBn
4.2.2d
4.1.3b
4.1.3a
CF$_3$
IDPi
Tf
NH

4.2.2d: >95% conv., 60% yield, **22:78** er

4.1.3b: >95% conv., 70% yield, **21.5:78.5** er

4.1.3a: >95% conv., 70% yield, **27:73** er

Scheme 4.3.3: Initial catalyst screening for C–C bond formation

A temperature study showed that the enantiomeric ratio increased from 21.5:79.5 to 15.5:84.5 when the reaction temperature was lowered from –20 °C to –60 °C.

Table 4.3.2: Effect of temperature on enantioselectivity:

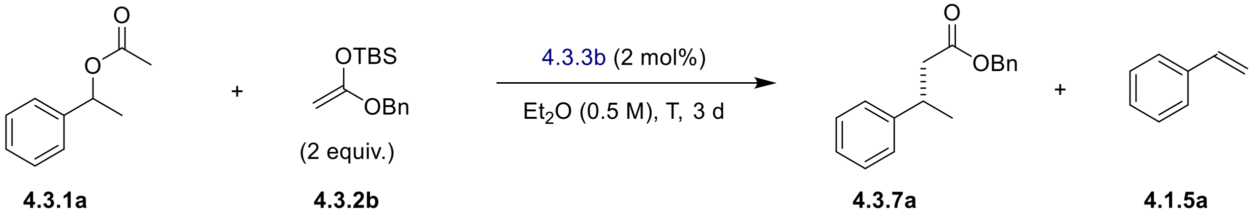
4.3.3b (2 mol%)
Et$_2$O (0.5 M), T, 3 d
(2 equiv.)
OTBS
OBn
4.3.1a
4.3.2b
4.3.7a
4.1.5a

entry	T (°C)	%Yield(conv.)	er
1.	–20	70(>95%)	**21.5:79.5**
2.	–30	75(>95%)	**21:79**
3.	–40	95(>95%)	**18:82**
4.	–50	95(>95%)	**16.5:83.5**
5.	–60	95(>95%)	**15.5:84.5**

Next, we wanted to investigate the effect of concentration nonetheless, almost identical enantiomeric ratios were observed and only a change in yield of the desired product was observed (Table 4.3.3).

Table 4.3.3: Effect of concentration on enantioselectivity:

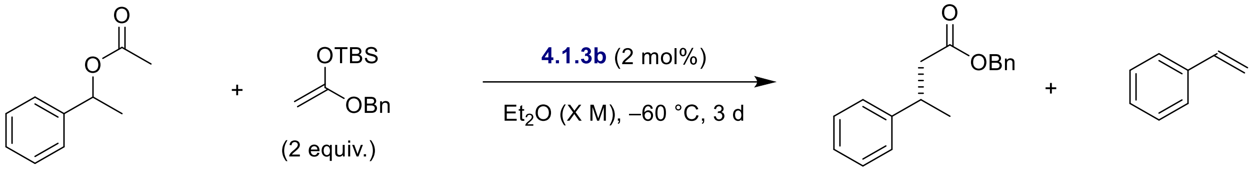

4.3.1a **4.3.2b** **4.3.7a** **4.1.5a**

entry	X (M)	%Yield(conv.)	er
1.	0.1	63(>95%)	**15.5:84.5**
2.	0.2	74(>95%)	**15.5:84.5**
3.	0.25	84(>95%)	**14.5:85.5**
4.	0.5	89(>95%)	**15.5:84.5**

As the concentration was gradually increased (from 0.1 M to 0.5 M) the yield of the desired product gradually increased (from 63% to 89%). At this point, we turned our attention to optimizing the catalyst structure by fine-tuning the 3,3´-substituents of the BINOL framework of the catalyst. We tested several catalysts using our group´s internal catalyst library, while the polycyclic aromatic hydrocarbon-substituted IDPi (4.3.3a–4.3.3c) gave moderate enantioselectivities (35:65–22:78), the polycyclic aromatic unit attached with thiophene as a 3,3´-substituent **4.3.3d** gave poor enantiomeric ratio 41:59. Catalyst with polycyclic aromatics groups as substituents at the *meta* position of the phenyl ring (4.3.3e–4.3.3j), as we observed previously (for C–O & C–N bonds formation), were good to achieve high enantiomeric ratio (Figure 4.3.2).

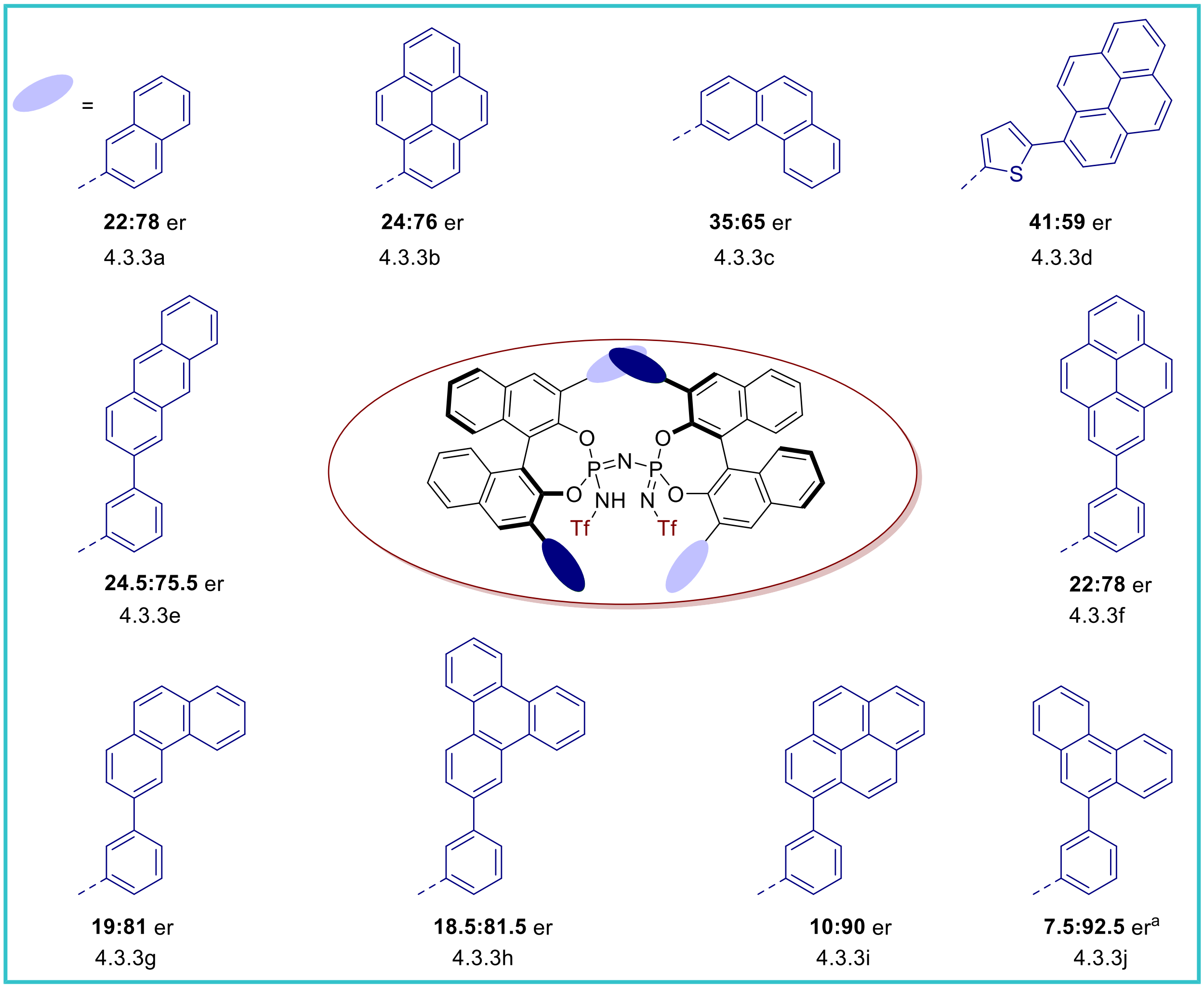
=
22:78 er
4.3.3a
24:76 er
4.3.3b
35:65 er
4.3.3c
S
41:59 er
4.3.3d
O
P=N
P
O
O
NH
N
O
Tf
Tf
24.5:75.5 er
4.3.3e
22:78 er
4.3.3f
19:81 er
4.3.3g
18.5:81.5 er
4.3.3h
10:90 er
4.3.3i
7.5:92.5 er[a]
4.3.3j

Figure 4.3.2: Selected overview of tested catalysts for the C-C bond formation, Tf = SO_2CF_3.
[a]reaction was performed at –65 °C for 4 d.

Moving from 2-position substitution (4.3.3e–4.3.3h) to 1-position substitution (4.3.3i–4.3.3j) of the polycyclic aromatic group, a gradual increase in enantioselectivity was observed, giving a satisfactory enantiomeric ratio of 7.5:92.5 for catalyst **4.3.3j** (Figure 4.3.2). With these optimized conditions, we turned our attention to the scope of the reaction.

As we previously observed for C–O bond formation, the enantioselectivity for C–C bond formation was also highly dependent on the steric and electronic properties on the arene ring. Several electronically substituted substrates were tested, and we found that all of them gave good to excellent yields (80–96%). The enantioselectivity decreases significantly with the introduction of the electron–donating groups at the *para* position (entry 4.3.7b–4.3.7d; scheme 4.3.4). When the electron–donating groups were introduced at the *meta* position almost identical enantiomeric ratio was observed as the substituents at *meta* position does not stabilize or destabilize the benzylic cation (entry 4.3.7e).

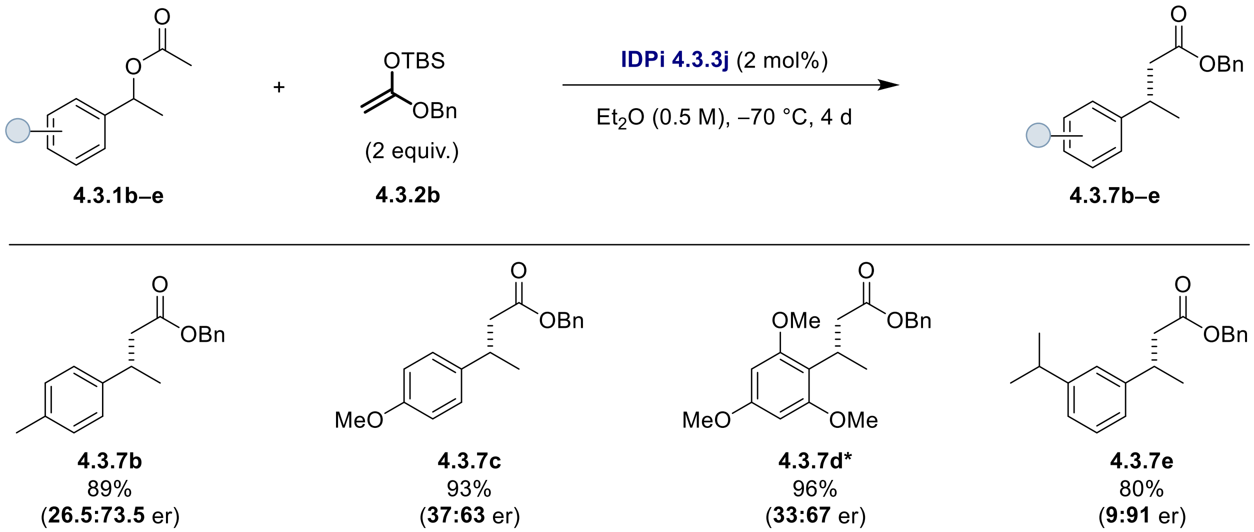

4.3.1b–e + **4.3.2b** → **4.3.7b–e**

4.3.7b 89% (**26.5:73.5** er)

4.3.7c 93% (**37:63** er)

4.3.7d* 96% (**33:67** er)

4.3.7e 80% (**9:91** er)

*OMe group in place of acetate was used as the leaving group

Scheme 4.3.4: Preliminary substrate scope for C−C bond formation

At this point, we resumed the exploration of the catalysts to improve the enantioselectivity for substrates with electron−donating groups. We decided to use substrate **4.3.7b** as a model substrate and tested several IDPis catalysts. Nevertheless, catalysts only with spiro fluorene type as 3,3´-substituents were fruitful to give high enantioselectivity (4.3.3l-p) and giving a satisfactory enantiomeric ratio (95.5:4.5) for catalyst **4.3.3p** (Scheme 4.3.5). Under these conditions, other substrates with alkyl substituents at the *para* position, linear or branched and with different chain lengths were tested, giving products **4.3.7f–j** (scheme 4.3.6) in 84–91% yields with high enantiomeric ratios (95:5–96.5:3.5) using the fluorenyl substituted 4.3.3s catalyst. Substrate **4.3.1j** with *meta*, *para* disubstitution afforded product **4.3.7j** in 92% yield with 95:5 er.

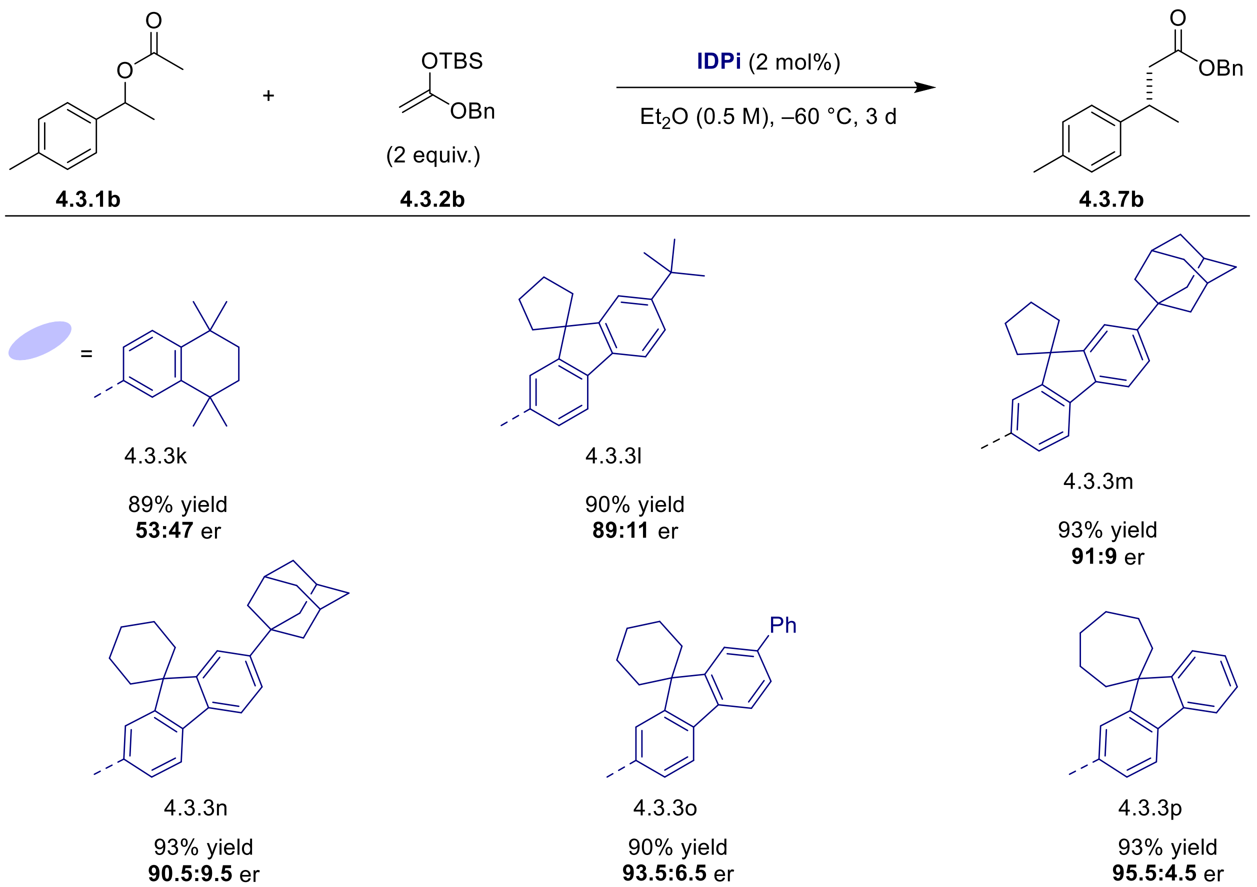
O
O
OTBS
OBn
(2 equiv.)
IDPi (2 mol%)
Et_2O (0.5 M), –60 °C, 3 d
O
OBn
4.3.1b
4.3.2b
4.3.7b
=
4.3.3k
89% yield
53:47 er
4.3.3l
90% yield
89:11 er
4.3.3m
93% yield
91:9 er
4.3.3n
93% yield
90.5:9.5 er
Ph
4.3.3o
90% yield
93.5:6.5 er
4.3.3p
93% yield
95.5:4.5 er

Scheme 4.3.5: Selected overview of tested catalysts for the reaction between benzylic acetate **4.3.1b** and SKA **4.3.2b**.

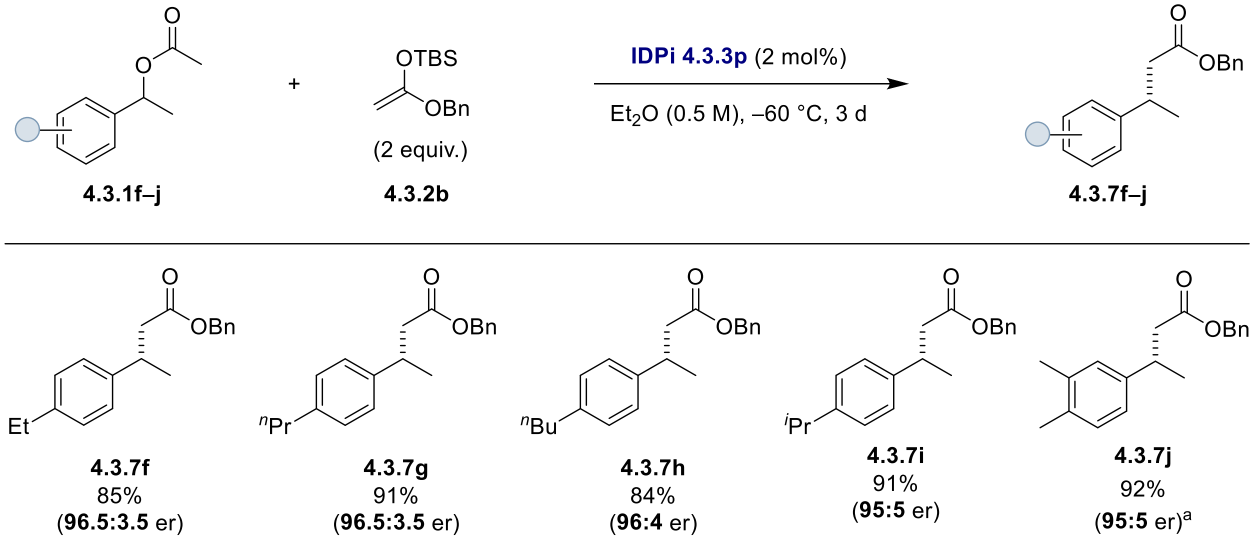
O
O
OTBS
OBn
(2 equiv.)
IDPi 4.3.3p (2 mol%)
Et_2O (0.5 M), –60 °C, 3 d
O
OBn
4.3.1f–j
4.3.2b
4.3.7f–j
O
OBn
Et
4.3.7f
85%
(96.5:3.5 er)
O
OBn
^{n}Pr
4.3.7g
91%
(96.5:3.5 er)
O
OBn
^{n}Bu
4.3.7h
84%
(96:4 er)
O
OBn
^{i}Pr
4.3.7i
91%
(95:5 er)
O
OBn
4.3.7j
92%
(95:5 er)^a

[a] reaction was performed at –70 °C for 4 d

Scheme 4.3.6: Scope of substrates having Electron-donating group at *para*-position using IDPi **4.3.3p**. ^{a}reaction was performed at –70 °C for 4 d.

Fine-tuning of the scope: After screening several catalysts and reaction conditions to find which substrates were tolerated in this developed methodology to get desired reactivity and selectivity, improved results are summarized in **Scheme 4.3.7**.

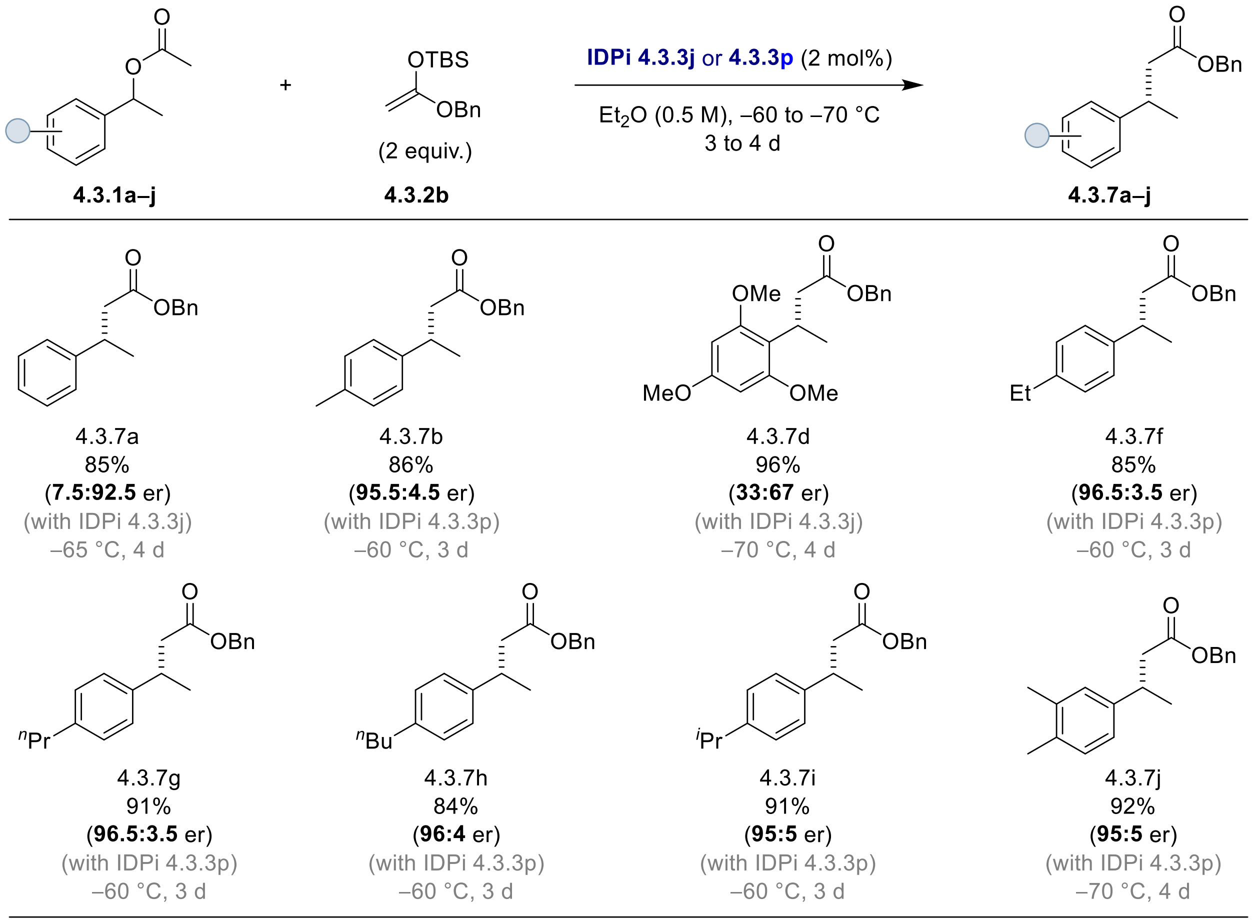

4.3.1a–j
OTBS
OBn
(2 equiv.)
4.3.2b
IDPi 4.3.3j or 4.3.3p (2 mol%)
Et2O (0.5 M), –60 to –70 °C
3 to 4 d
OBn
4.3.7a–j
4.3.7a
85%
(7.5:92.5 er)
(with IDPi 4.3.3j)
–65 °C, 4 d
4.3.7b
86%
(95.5:4.5 er)
(with IDPi 4.3.3p)
–60 °C, 3 d
OMe
MeO
OMe
4.3.7d
96%
(33:67 er)
(with IDPi 4.3.3j)
–70 °C, 4 d
Et
4.3.7f
85%
(96.5:3.5 er)
(with IDPi 4.3.3p)
–60 °C, 3 d
nPr
4.3.7g
91%
(96.5:3.5 er)
(with IDPi 4.3.3p)
–60 °C, 3 d
nBu
4.3.7h
84%
(96:4 er)
(with IDPi 4.3.3p)
–60 °C, 3 d
iPr
4.3.7i
91%
(95:5 er)
(with IDPi 4.3.3p)
–60 °C, 3 d
4.3.7j
92%
(95:5 er)
(with IDPi 4.3.3p)
–70 °C, 4 d

Scheme 4.3.7: Scope for IDPi catalyzed C–C bond formation reaction.

4.4 Results and Discussion:

4.4.1 Mechanistic Investigation:

In order to elucidate the mechanism of the reaction and our benzylic cation S_N1–hypothesis, we carried out a detailed experimental and computational study. As a model reaction for our mechanistic study, we chose C–O bond formation reaction. First, the optimized reaction conditions were applied individually to *rac*–**4.1.1a** and either of the enantiopure starting materials (*S*)–**4.1.1a** or (*R*)–**4.1.1a**. It was found that all three reactions gave same major enantiomer of the product **4.1.4a** in nearly equal NMR yields (**Scheme 4.4.1**). These results suggest the formation of common benzylic carbocation intermediate.

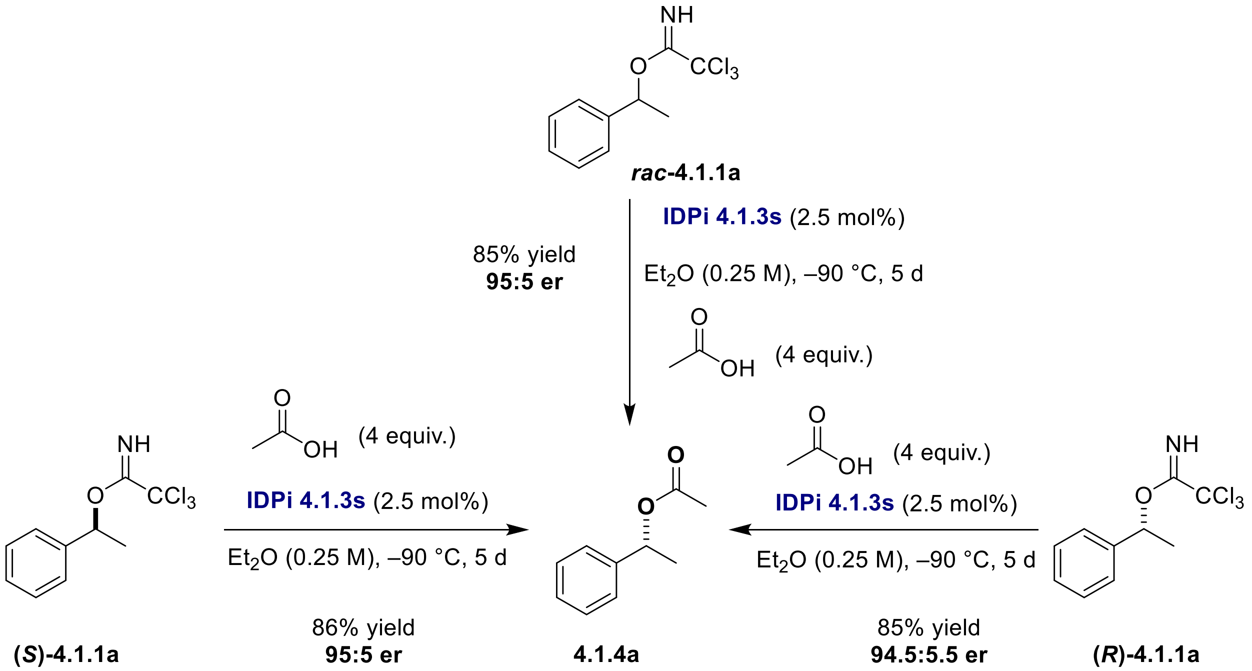

NH
O
CCl3
***rac*-4.1.1a**
IDPi 4.1.3s (2.5 mol%)
Et2O (0.25 M), –90 °C, 5 d
O
OH
(4 equiv.)
85% yield
95:5 er
NH
O
CCl3
(*S*)-4.1.1a
O
OH
(4 equiv.)
IDPi 4.1.3s (2.5 mol%)
Et2O (0.25 M), –90 °C, 5 d
86% yield
95:5 er
O
O
4.1.4a
O
OH
(4 equiv.)
IDPi 4.1.3s (2.5 mol%)
Et2O (0.25 M), –90 °C, 5 d
85% yield
94.5:5.5 er
NH
O
CCl3
(*R*)-4.1.1a

Scheme 4.4.1: Enantioselectivity and NMR yield comparison of *rac*-4.1.1a with and enantiopure 4.1.1a substrate

We then monitor the progress of the reaction by ^{1}H NMR at –60 °C (Figure 4.4.1) for racemic and enantiopure substrates separately and found that they react at similar rates, with very little to no kinetic resolution. We went one-step further and decided to characterize the ion-pair or covalent adduct between benzylic carbocation and the catalyst anion. Attempts to characterize either an ion pair or a covalent adduct in the reaction of substrate **4.1.1a** with **IDPi 4.1.4s** were unsuccessful, yielding only product

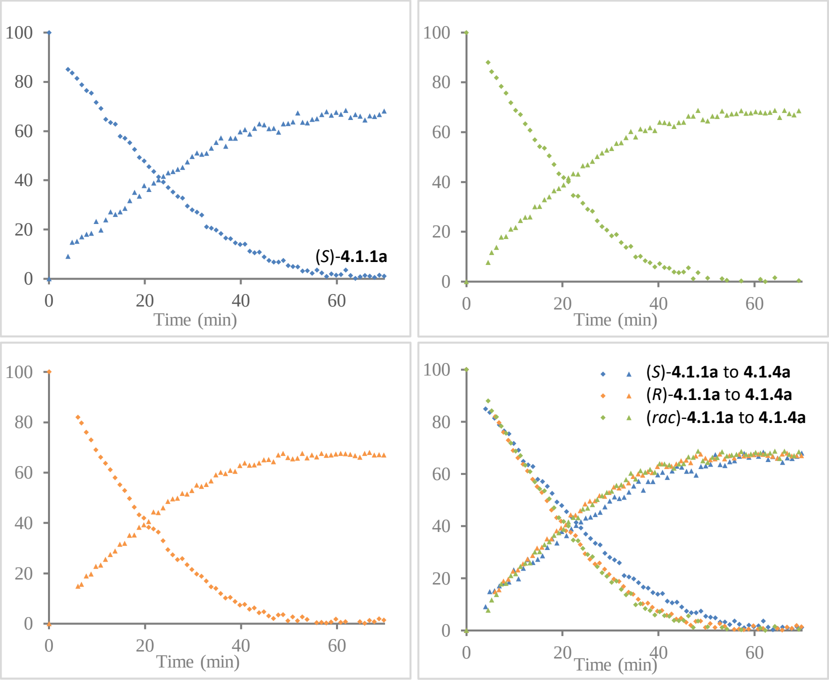

Figure 4.4.1: Reactivity measurements of *rac*-4.1.1a and enantiopure 4.1.1a

4.2.3a and styrene under the reaction conditions. Indeed, these highly reactive, short-lived reaction intermediates are unlikely to be detectable under experimental conditions, given the sensitivity limitations of the spectroscopic method employed. Therefore, a series of substrates (benzyl alcohols) featuring different substitution patterns were investigated. These substrates were ionized with $HNTf_2$ as a strong achiral acid to gain further insight into the cationic intermediates and their lifetime.

4.4.2 Interaction of Various Substrates with HNTf$_2$:

Reaction of 1-(4-methoxyphenyl)ethan-1-ol with HNTf$_2$: No ion pair formation was detected only decomposition of starting material was observed.

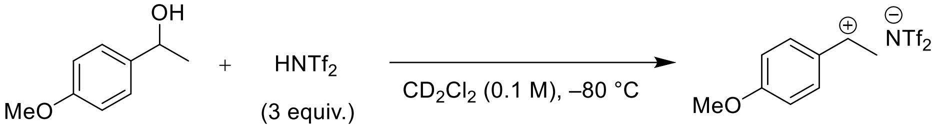
OH
MeO
+
HNTf$_2$
(3 equiv.)
CD$_2$Cl$_2$ (0.1 M), –80 °C
MeO
NTf$_2$

4.4.1a **4.4.2a** **4.4.3a** not detected

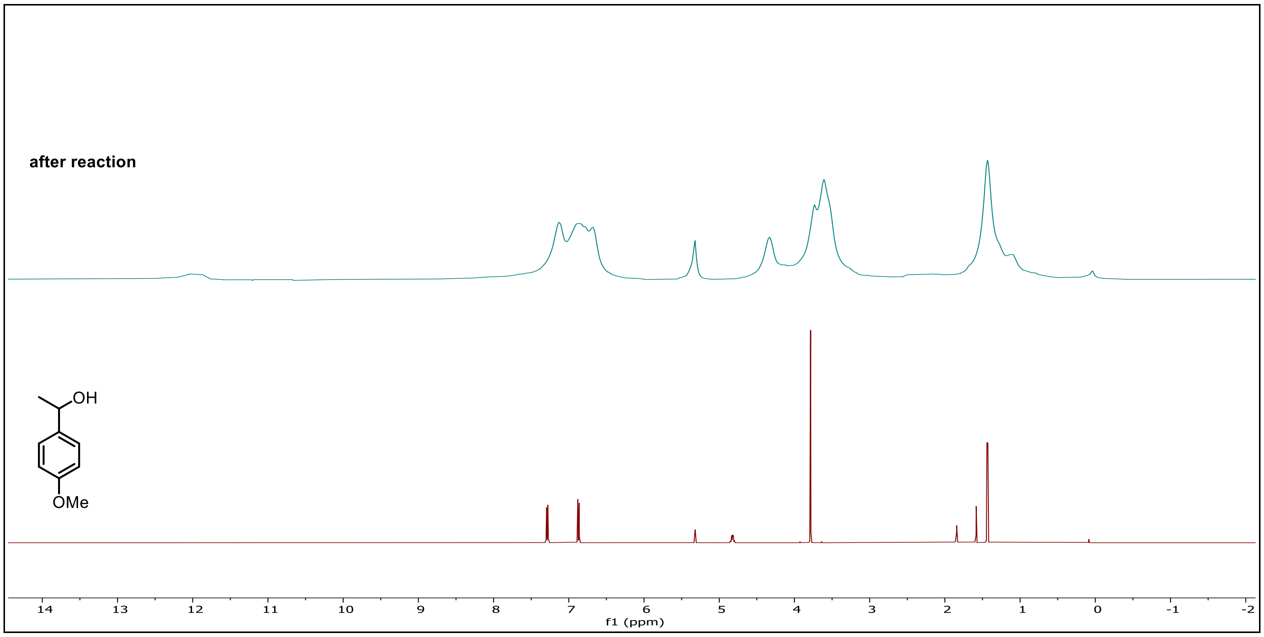

Reaction of 1-(2,4-dimethoxyphenyl)ethan-1-ol with HNTf₂: No ion pair formation was detected only decomposition of starting material was observed.

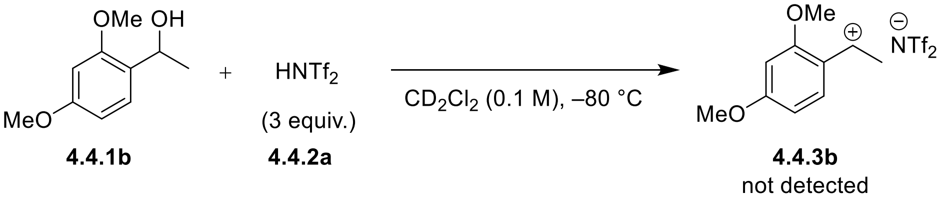
OMe OH
MeO
4.4.1b
+
HNTf$_2$
(3 equiv.)
4.4.2a
CD_2Cl_2 (0.1 M), –80 °C
OMe
MeO
NTf$_2$
4.4.3b
not detected

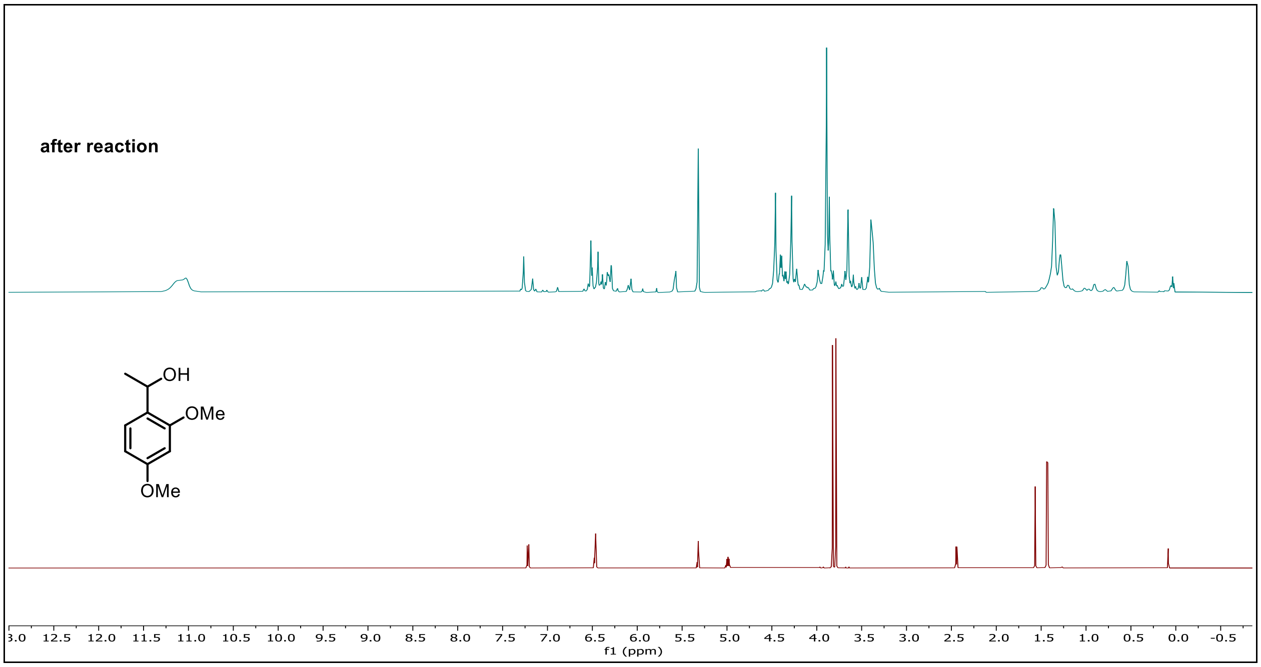

Reaction of 1-(2,6-dimethoxyphenyl)ethan-1-ol with HNTf$_2$: No ion pair formation was detected only decomposition of starting material was observed.

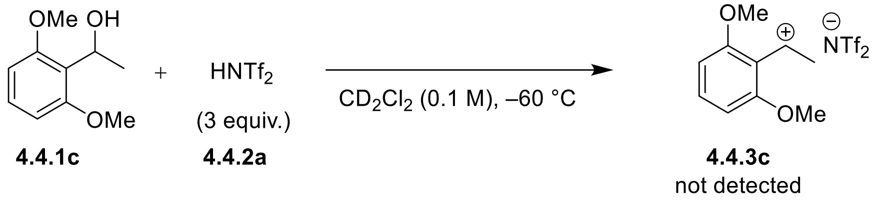
OMe OH
OMe
4.4.1c
+
HNTf2
(3 equiv.)
4.4.2a
CD2Cl2 (0.1 M), –60 °C
OMe
NTf2
OMe
4.4.3c
not detected

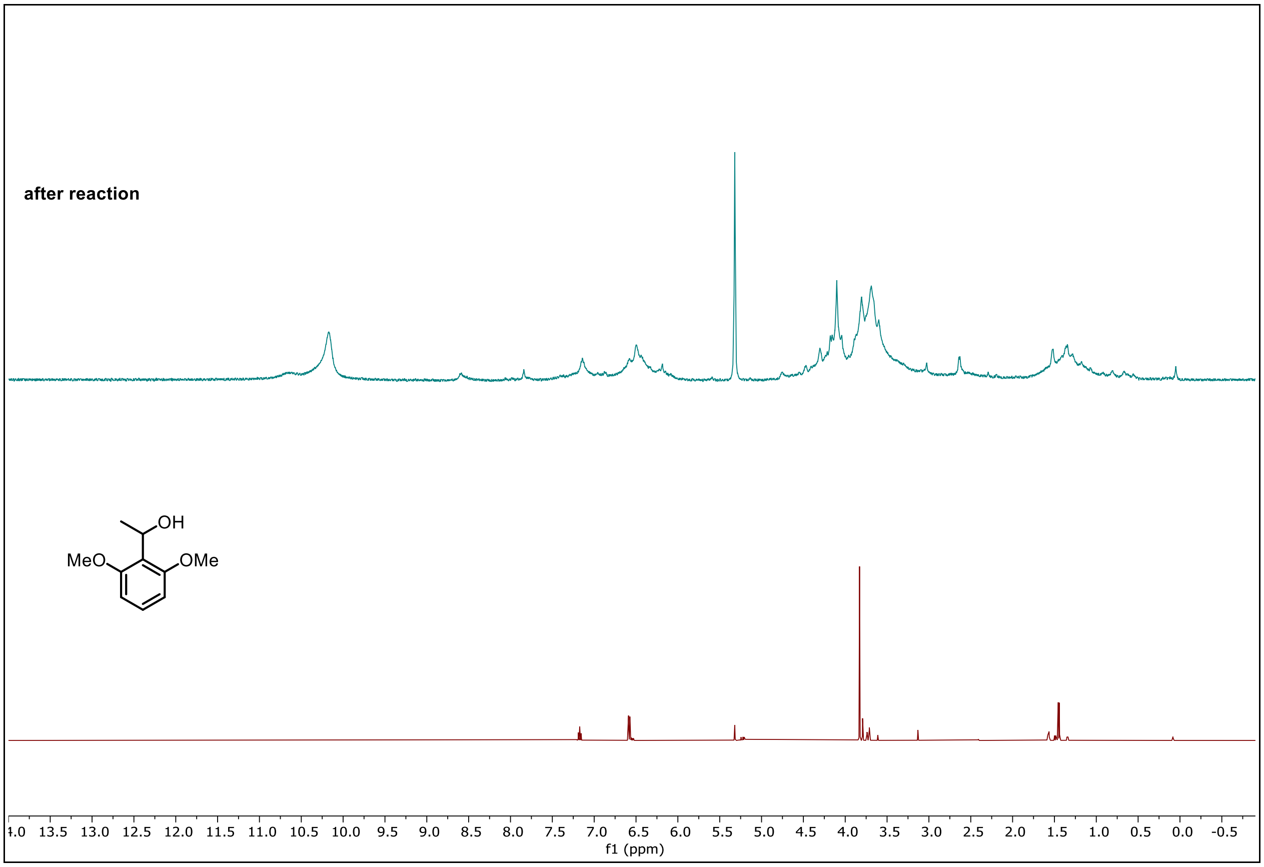

Reaction of 1-(2,6-dimethoxy-4-methylphenyl)ethan-1-ol with $HNTf_2$: Formation of the ion pair was detected however it was decomposing slowly over the time at –60 °C.

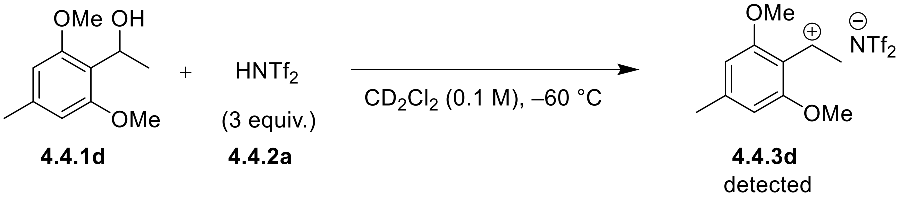
OMe OH
OMe
+
HNTf2
(3 equiv.)
CD2Cl2 (0.1 M), –60 °C
OMe
NTf2
OMe
4.4.1d
4.4.2a
4.4.3d
detected

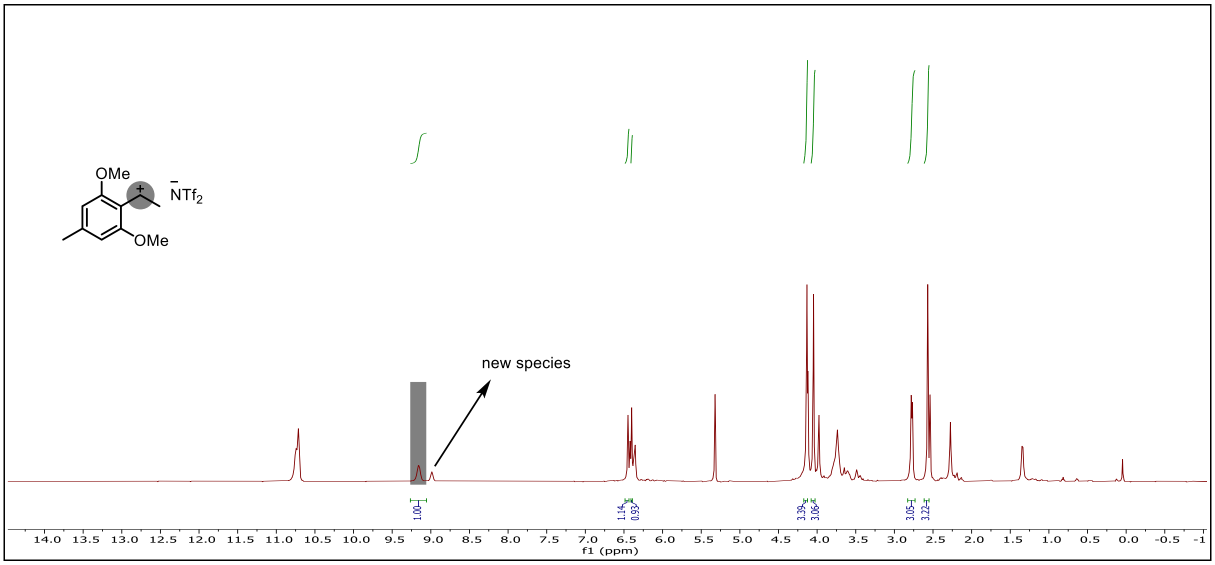

Decomposition of ion pair 4.4.3d over time:

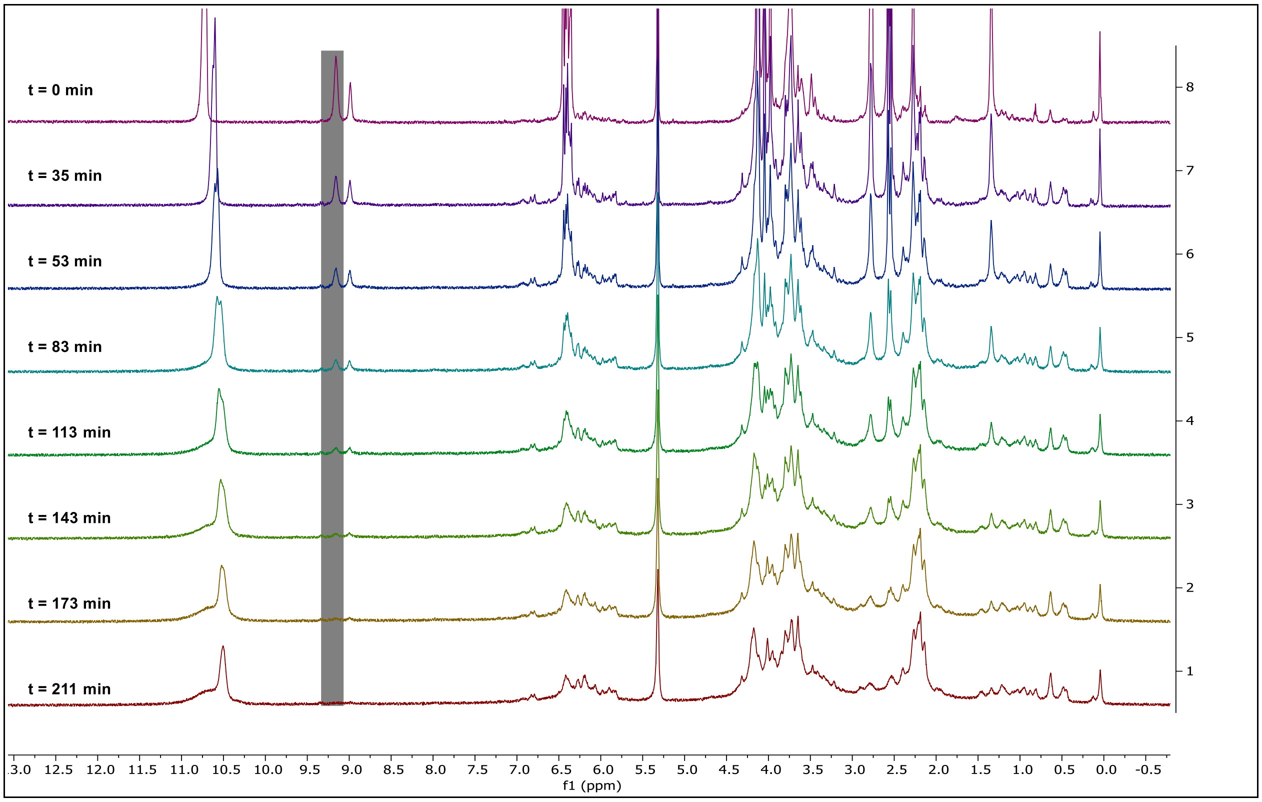

We anticipated the ion pair resulting from the reaction of 1-(2,4,6-trimethoxyphenyl)ethan-1-ol (4.4.1e) and $HNTf_2$ would have a sufficiently long lifetime to allow its characterization. Indeed, when **4.4.1e** was treated with $HNTf_2$ (3 equiv.) in DCM-d_2 at –60 °C in an NMR tube, the formation of the ion pair was observed and characterized by NMR spectroscopy (^{1}H, ^{13}C, and 2D NMR experiments).

Reaction of 1-(2,4,6-trimethoxyphenyl)ethan-1-ol with $HNTf_2$:

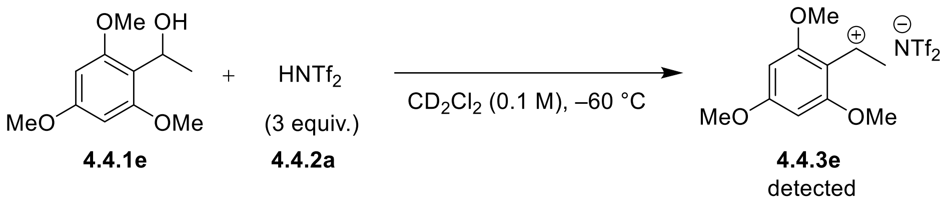
OMe OH
MeO
OMe
+
HNTf2
(3 equiv.)
CD2Cl2 (0.1 M), –60 °C
OMe
NTf2
MeO
OMe
4.4.1e
4.4.2a
4.4.3e
detected

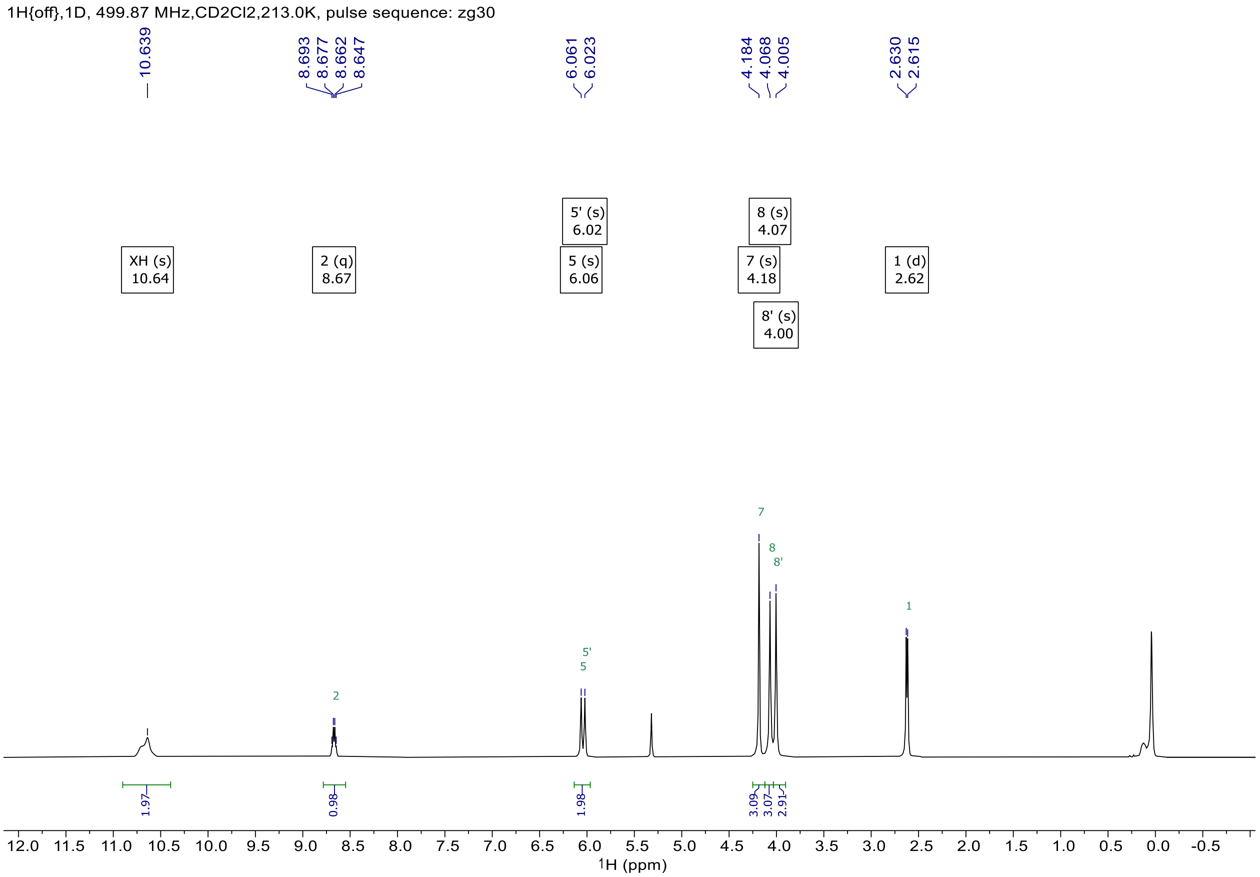

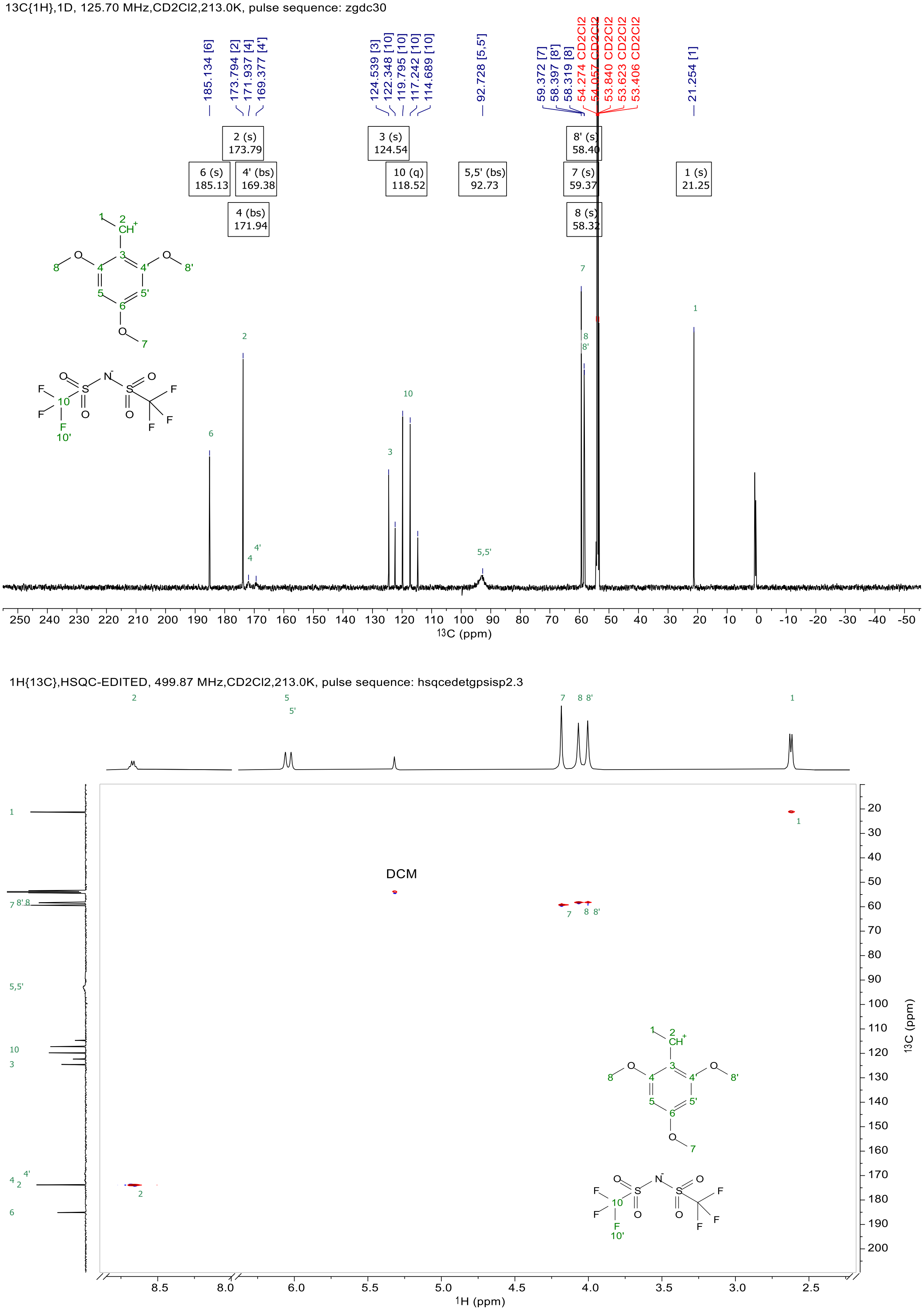

Figure 4.4.2: Characterization of ion pair 4.4.3e at –60 °C

Next, we wanted to gain insight into the stability of this ion pair. We gradually increased the temperature from –60 °C to –20 °C, and found that the ion pair was stable in this range, and only started to decompose at higher temperatures.

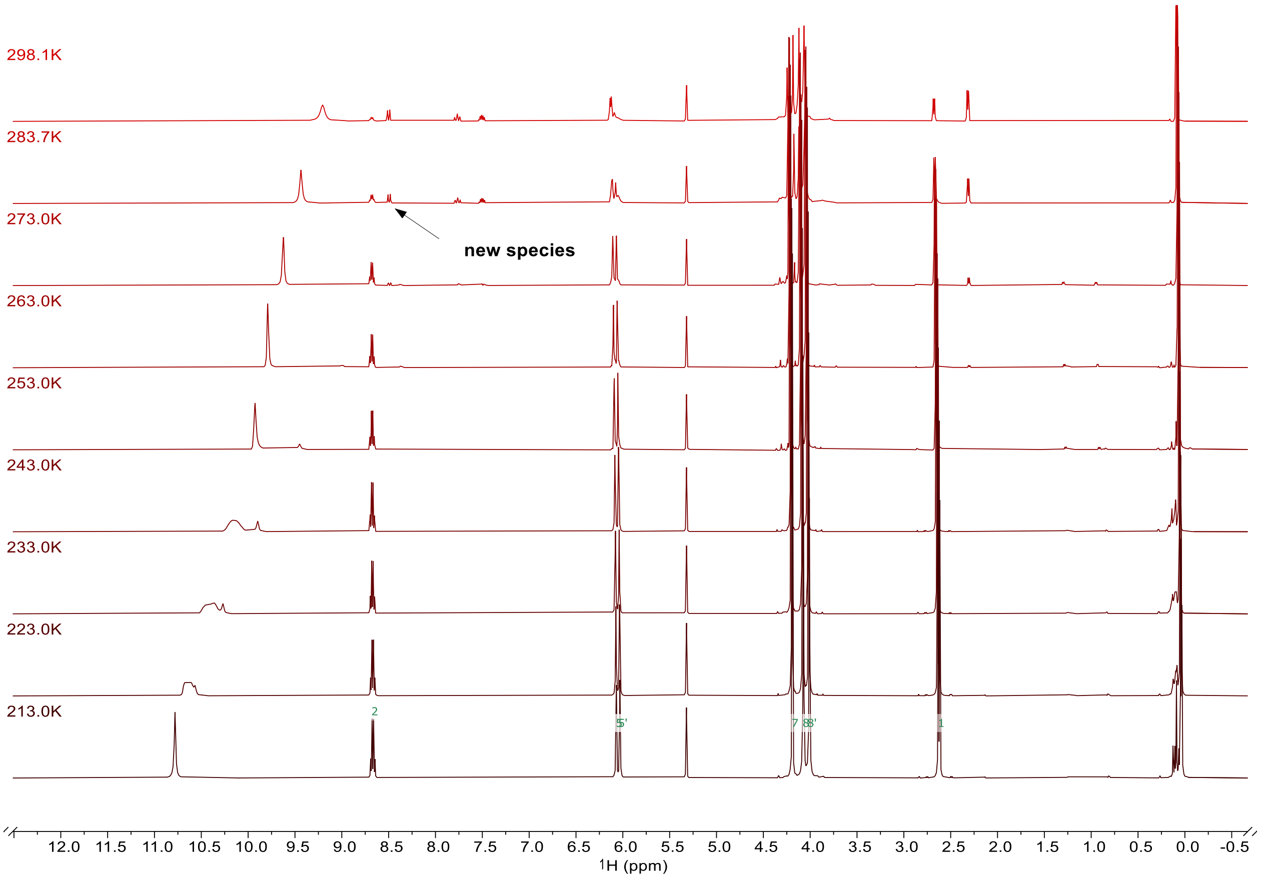

Figure 4.4.3: Variable Temperature NMR experiments of ion pair 4.4.3e from –60 °C to room temperature

Next, we were interested in whether one can generate the same ion pair in silylium Lewis acid conditions. To generate this ion pair, we used 1,3,5-trimethoxy-2-(1-methoxyethyl)benzene as substrate and 1,1,1-trifluoro-N-((trifluoromethyl)sulfonyl)-N-(trimethylsilyl)methanesulfonamide (TMSNTf$_2$) as Lewis acid and reacted both species in same reaction conditions. We found that the same ion pair **4.4.3e** could also be generated under silylium-Lewis acid conditions, and a similar behavior was observed in this case.

Formation of ion pair 4.4.3e under Lewis acid conditions:

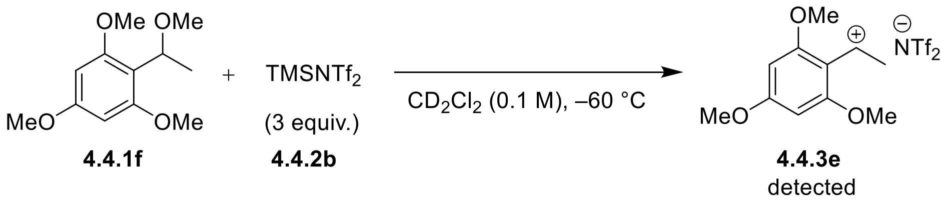
OMe OMe
MeO
OMe
4.4.1f
+
TMSNTf2
(3 equiv.)
4.4.2b
CD2Cl2 (0.1 M), –60 °C
OMe
⊕
⊖
NTf2
MeO
OMe
4.4.3e
detected

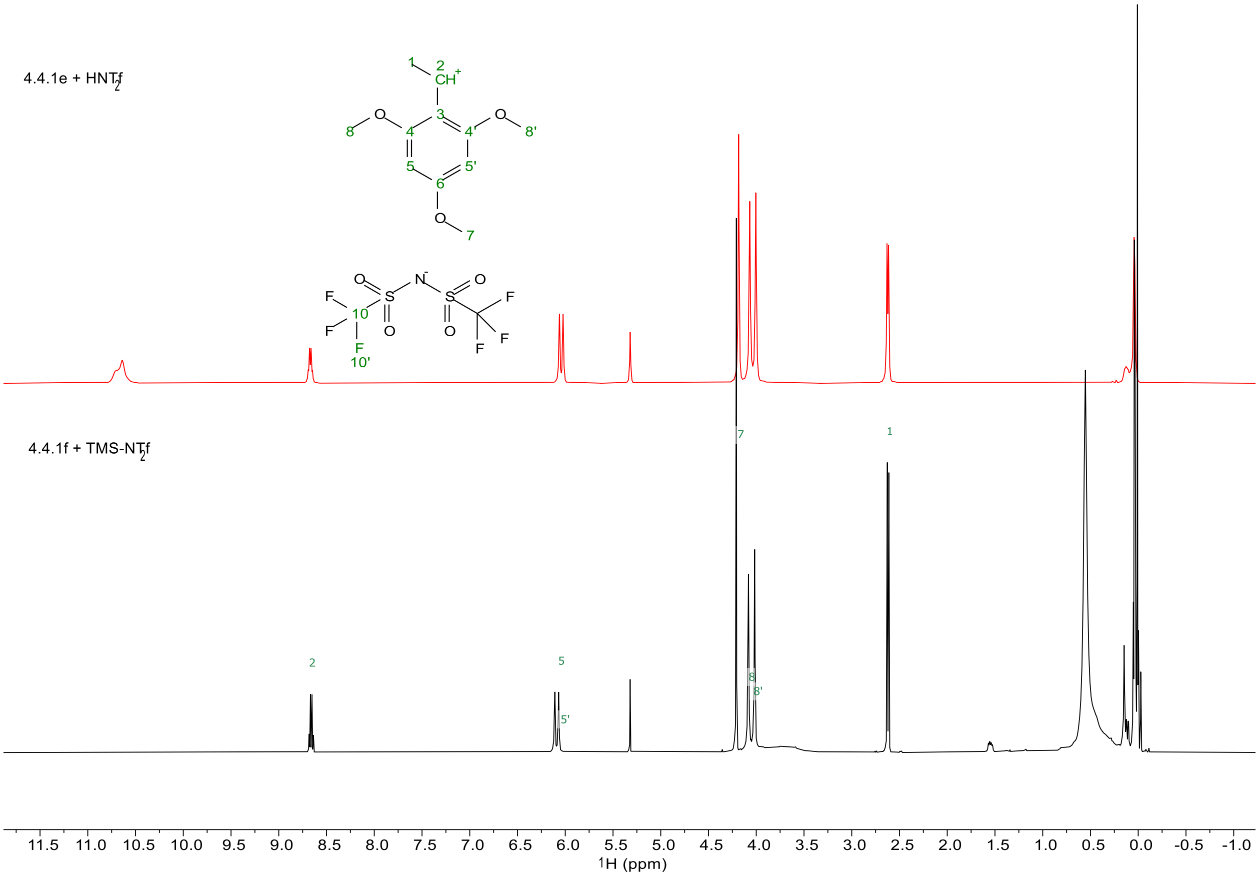

Figure 4.4.4: Comparison of the ion pair 4.4.3e formed under Lewis and Brønsted acid conditions

Since this cation has a significant lifetime, we wondered if this cation could also be generated and characterized using our IDPi catalyst. When we treated IDPi **4.1.3a** with 1-(2,4,6-trimethoxyphenyl)ethan-1-ol, indeed, we found the formation of an ion pair. A shift in the ^{1}H and ^{13}C NMR (benzylic proton from 8.7 to 8.5 ppm and benzylic carbon from 173.8 to 172.8 ppm) was observed, clearly indicating different counteranions in the close proximity to the cation.

Decomposition of this ion-pair species **4.4.3f** was observed at –60 °C, presumably due to the relatively higher basicity of the IDPi counteranion compared to the NTf$_2$ anion.

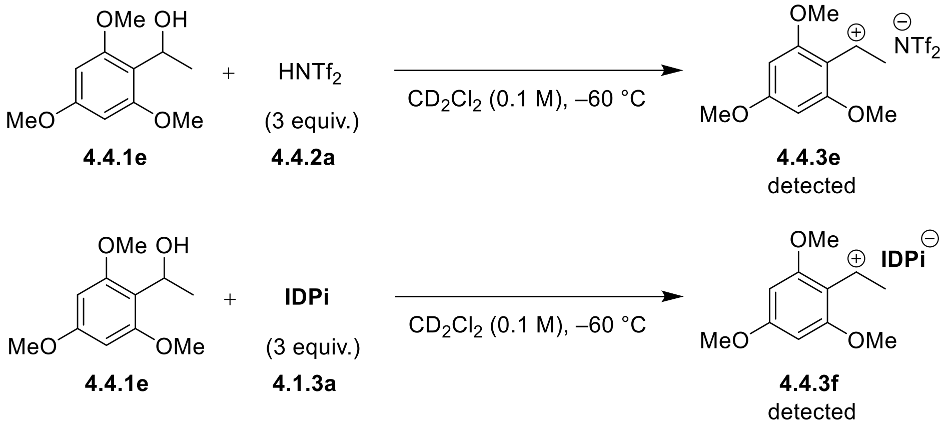
OMe OH
MeO
OMe
4.4.1e
+
HNTf2
(3 equiv.)
4.4.2a
CD2Cl2 (0.1 M), –60 °C
OMe
⊕
⊖
NTf2
MeO
OMe
4.4.3e
detected
OMe OH
MeO
OMe
4.4.1e
+
IDPi
(3 equiv.)
4.1.3a
CD2Cl2 (0.1 M), –60 °C
OMe
⊕
IDPi⊖
MeO
OMe
4.4.3f
detected

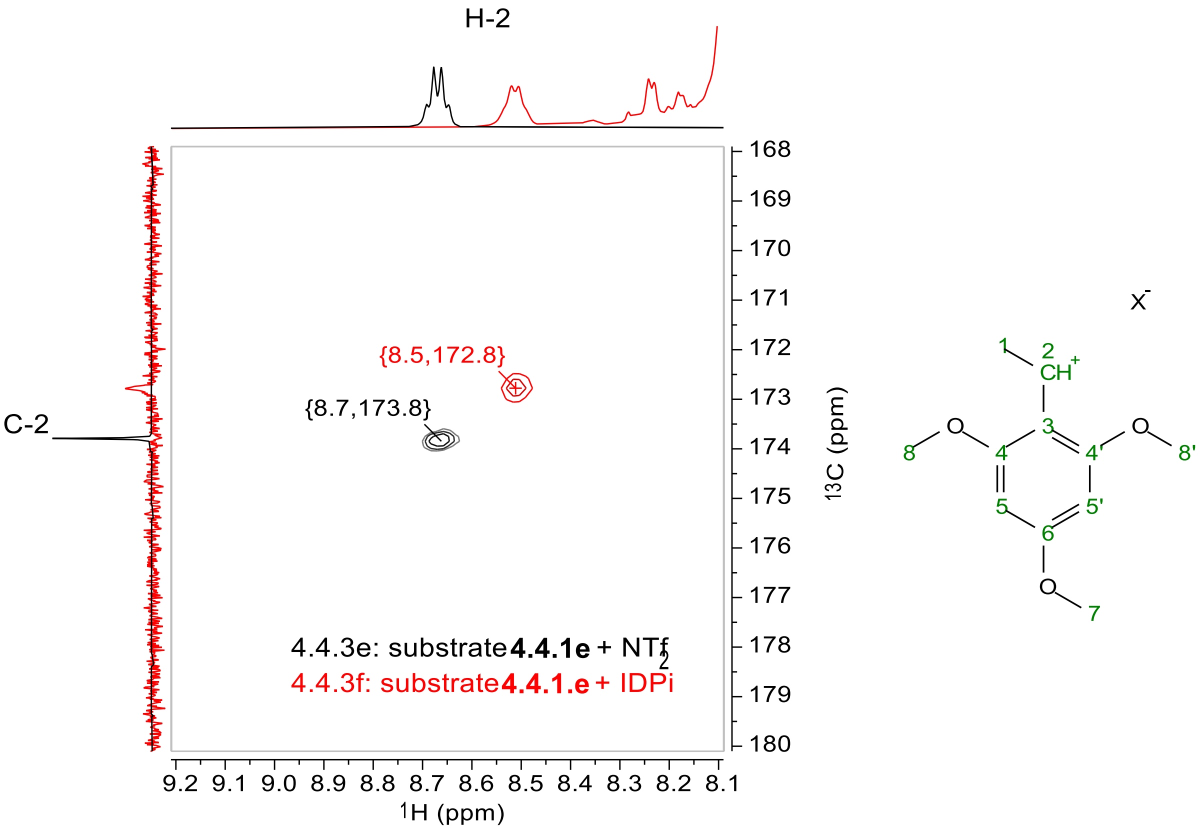

Figure 4.4.5: Comparison of heteronuclearsingle quantum coherence (HSQC) spectrum for bistriflimide and IDPi (4.1.3a) anions

To the best of our knowledge, this is the first spectroscopic characterization of an ion pair consisting of a highly reactive carbocationic intermediate with a chiral counteranion.

In addition, density functional theory (DFT) was used to optimize the ion-pair structure (see supplementary materials for details). A large number of conformers was initially generated at various levels of GFNn-FF/XTB theory, and the low-energy structures were refined at the PBE-D3 level. Analysis of the electrostatic potential surfaces reveals that the ion pair structure is held together by directional electrostatic interactions between the IDPi anion and the benzylic carbocation.

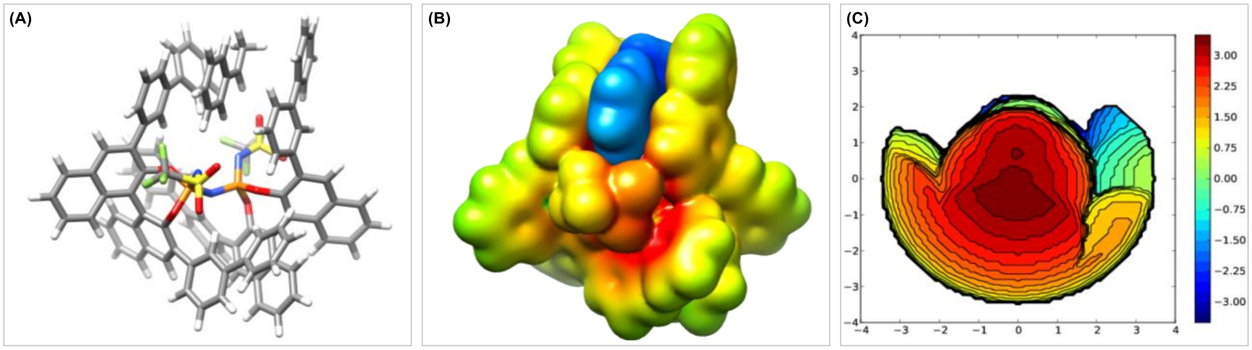

Figure 4.4.6: (A) DFT-optimized ion-pair structure. (B) Electrostatic potential map (MEP) of the ion pair. (C) Topographic steric map of the ion pair

The computed association free energy between the IDPi anion and benzylic carbocation (ΔG) is slightly negative (-2.3 kcal/mol), however, the internal energy (ΔEint = -22.35 kcal/mol)

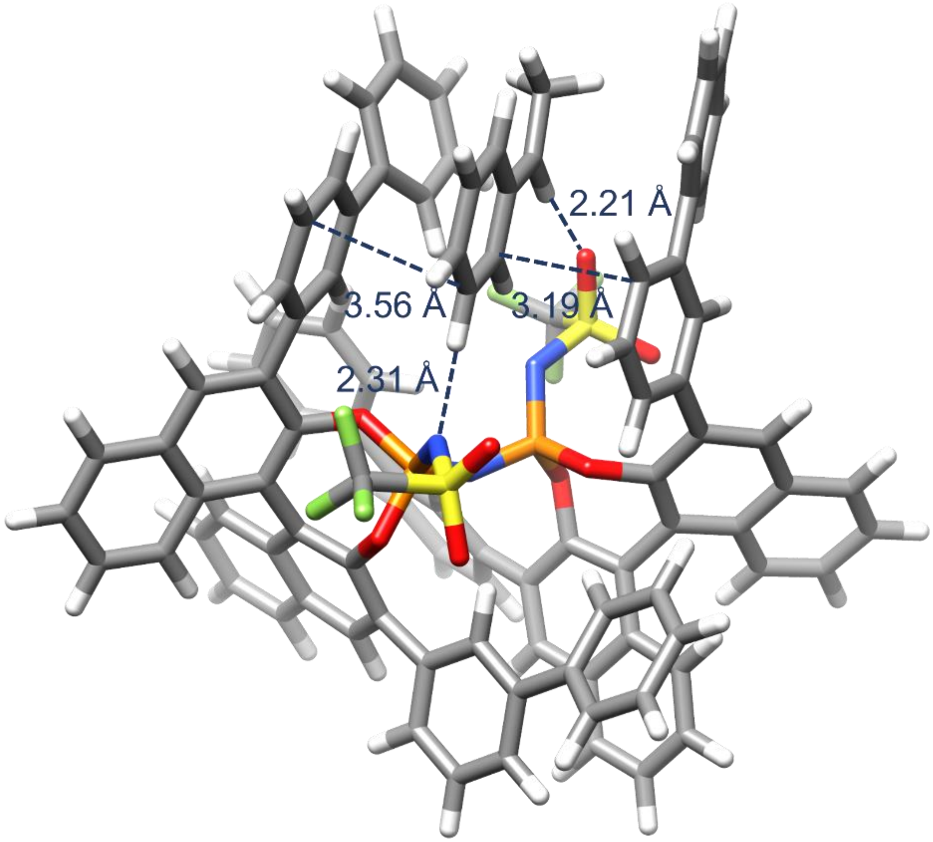

Figure 4.4.7: Graphic of the ion pair showing crucial interactions between the benzylic cation and the IDPi anion. The distances for the cation–p interaction were chosen so that the atoms of substrate and catalyst are in a as parallel as possible arrangement.

demonstrating that the system is held together by strong and attractive noncovalent interactions. While the interaction between the anion and the cation is clearly electrostatically dominated, the decomposition of ΔEint into dispersive (ΔEdisp) and steric/electrostatic components (ΔEster/elec) shows that dispersion alone plays a crucial role in favoring the formation of the chiral ion pair, contributing with -18.46 kcal/mol to the overall interaction energy. The negative interaction is at least partially counterbalanced by: (i) the energy penalty required to distort the catalyst to maximize the electrostatic interaction with the cation, (ii) entropy and temperature effects. Most notably, the cation resides between the 3-biphenyl substituents of the BINOL skeleton (3.56 Å and 3.2 Å, respectively) that aid in stabilizing the reactive intermediate by virtue of cation-π interactions. Additionally, the benzylic CH group clearly interacts with a sulfonyl oxygen atom (2.2 Å), as well as the phenyl 3-CH with an inner core nitrogen atom (2.31 Å) (**Figure 4.4.7**). It is plausible to assume that all of these interactions can be expected to play a vital role in the stabilization of the respective transition states leading to the major enantiomer.

5 Summary:

Benzylic stereogenic centers are ubiquitous in natural products and pharmaceuticals. A potentially general though challenging approach toward their selective creation would be asymmetric S_N1 reactions that proceed through highly reactive benzylic cations. We have developed a broadly applicable solution to this problem by identifying chiral counteranions that pair with secondary benzylic cations to engage in catalytic asymmetric C–C-, C–O-, and C–N-bond forming reactions. The reactions proceed through highly reactive benzylic cations, which can be challenging to control in terms of selectivity. However, our method has demonstrated excellent enantioselectivity, making it a promising solution to this problem. These transformations benefit from the ability of IDPi catalysts to either function as Brønsted acids or as precatalysts for silylium ion-based Lewis acid catalysis. Overall, our work provides a new and effective strategy for the asymmetric synthesis of benzylic stereogenic centers.

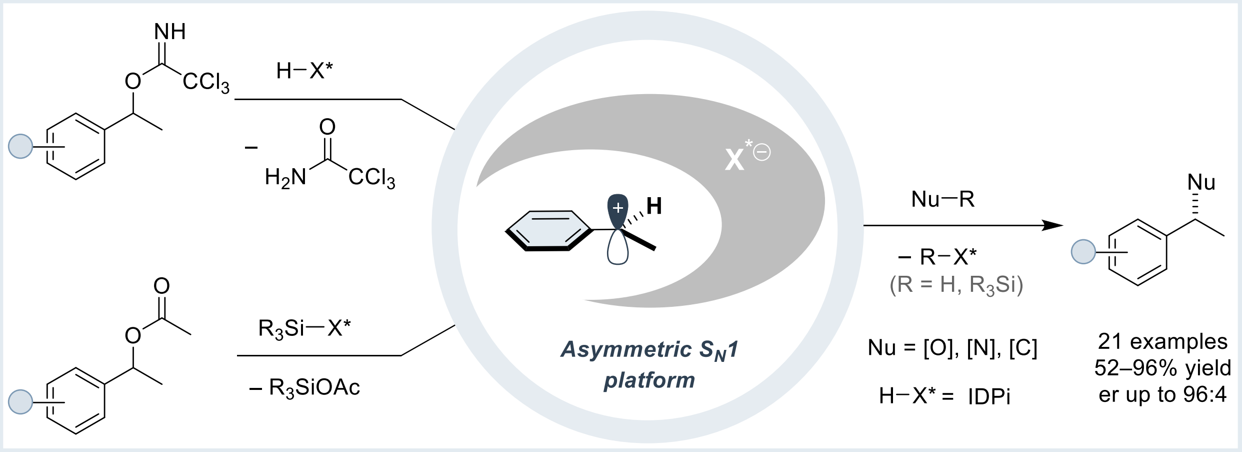

Scheme 5.1: IDPi catalyzed S_N1 platform for creation of benzylic stereocenters

High levels of enantioselectivity across a broad range of substrates and nucleophiles have been achieved. This methodology demonstrates versatility and potential usefulness of this method in creation of benzylic stereocenters. In addition to that, we have used different benzylic cation precursors to generate benzylic carbocation in different reaction conditions.

We did extensive experimental and computational analysis to understand the mechanism of the reaction. At first, substrate *rac*-4.1.1a or either of the enantiopure starting materials, (*S*)-4.1.1a or (*R*)- 4.1.1a were individually subjected to the optimized reaction conditions. Consistent with the ion pair formation followed by nucleophilic attack on the benzylic cation in a S_N1 like mechanism,

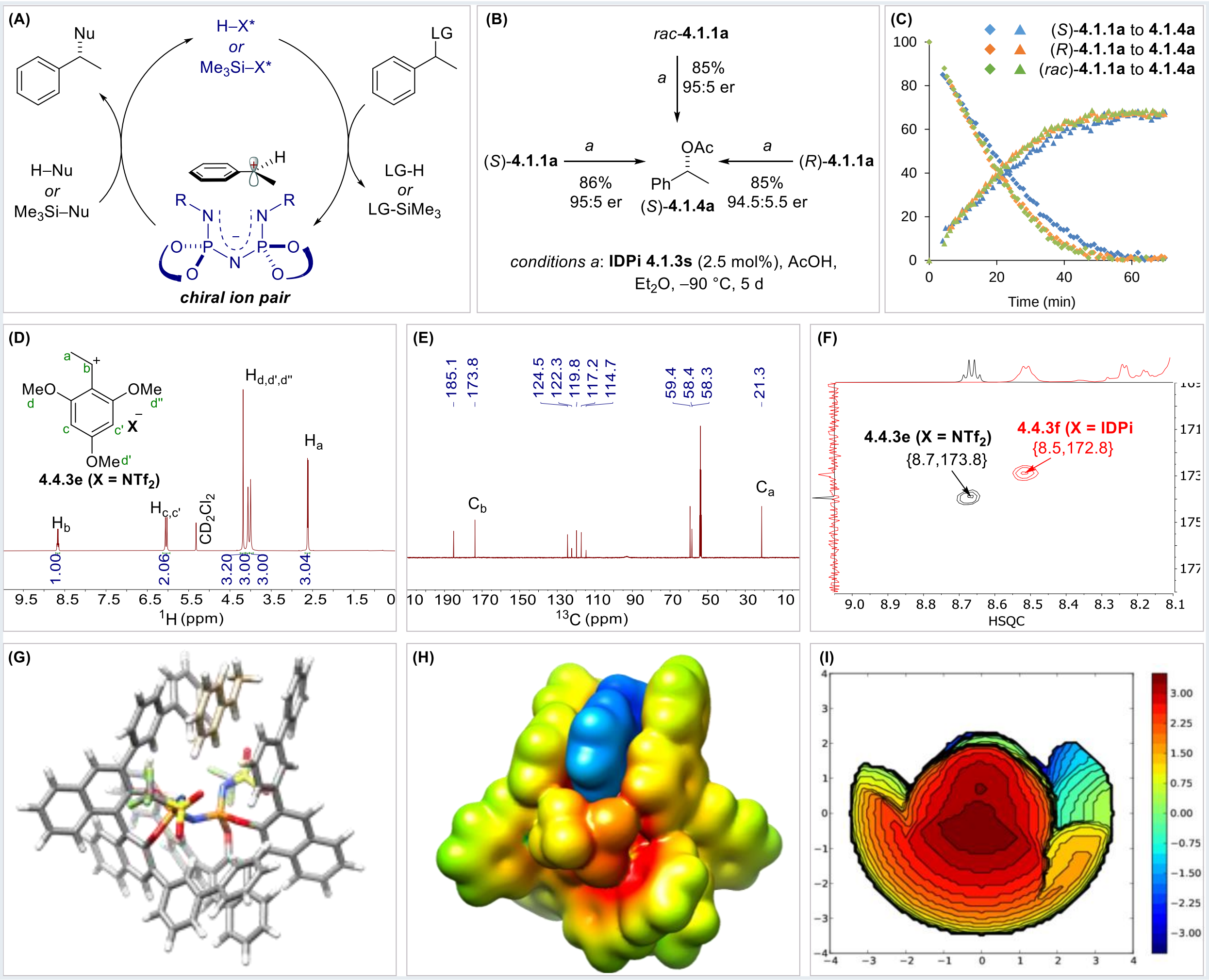

we found that all three reactions delivered the same major enantiomer of product 4.1.4a with essentially identical yield (85%, 86%, and 85% by NMR) and enantioselectivity (95:5, 95:5, and 94.5:5.5 er). Interestingly, when the progress of the C–O bond forming reaction was monitored by ^{1}H NMR at –60 °C for each substrate separately (*rac*-4.1.1a, enantiopure (*S*)-4.1.1a, and (*R*)-4.1.1a), both enantiomers were found to react with similar rates showing very little to no kinetic resolution. Moreover, we characterized the achiral as well as the chiral ion pair and gained insight into the lifetime of the ion pair by NMR spectroscopy.

Based on the above experimental and computational data, we propose a reaction mechanism where the substrate gets ionized in the presence of a catalyst to form the ion pair in either Brønsted acid or Lewis acid conditions followed by nucleophilic attack on the benzylic cation to deliver the product.

6 Outlook:

6.1 Other nucleophiles

Having disclosed the catalytic, asymmetric silyl ketene acetal addition to benzylic carbocations, we envisioned expanding the scope of this transformation to other alpha-substituted silyl ketene acetals (E/Z) addition, giving acyclic carboxylic acid derivatives with contiguous stereogenic centers with vicinal-dialkyl groups as products in a one-step. The development of efficient methods to access complex molecules with multistereogenic centers has been a substantial challenge.

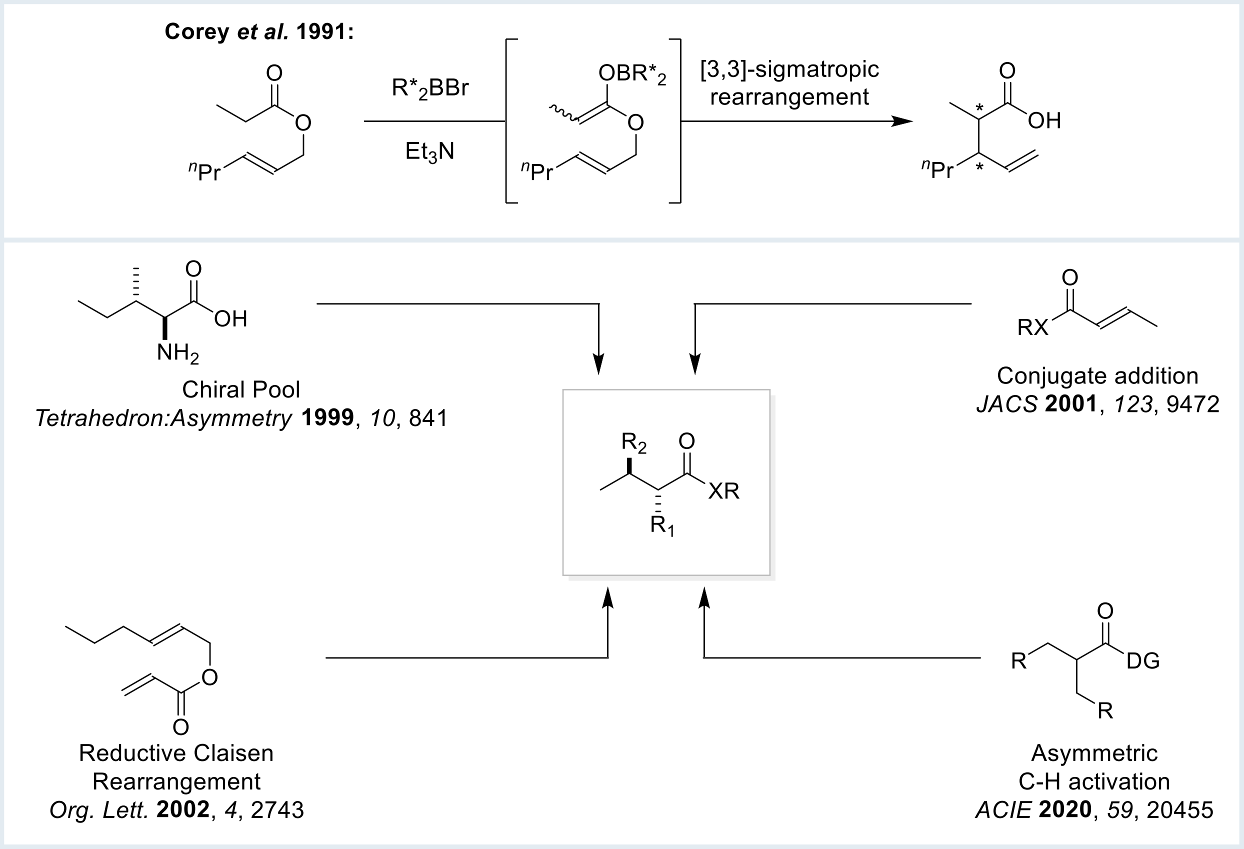
Corey *et al.* 1991:
O
O
ⁿPr
R*₂BBr
Et₃N
OBR*₂
O
ⁿPr
[3,3]-sigmatropic
rearrangement
O
OH
ⁿPr
*
*
O
OH
NH₂
Chiral Pool
Tetrahedron:Asymmetry **1999**, *10*, 841
O
RX
Conjugate addition
JACS **2001**, *123*, 9472
R₂
O
XR
R₁
O
O
Reductive Claisen
Rearrangement
Org. Lett. **2002**, *4*, 2743
O
R
DG
R
Asymmetric
C-H activation
ACIE **2020**, *59*, 20455

Scheme 6.1.1: Different approaches towards synthesis of acyclic aliphatic carboxylic acid derivatives with contiguous stereogenic centers with vicinal-dialkyl groups

Current strategies rely on the multiple transformations from the use of chiral reagents[113], chiral pool precursors[114], asymmetric conjugate addition[115], reductive Claisen rearrangement[116], and enantioselective desymmetrizing C–H activation[117]. These methods rely on substrate design, the use of enantioenriched starting materials/reagents, or expensive metals.

As a proof of concept, we used benzylic acetate 4.2.1a as an electrophile and silyl ketene acetal 6.1.2a as a nucleophile. On initial catalyst screening, it was found that most of the catalysts gave the desired product formation in moderate to good e.r. with moderate diastereomeric ratio (d.r.).

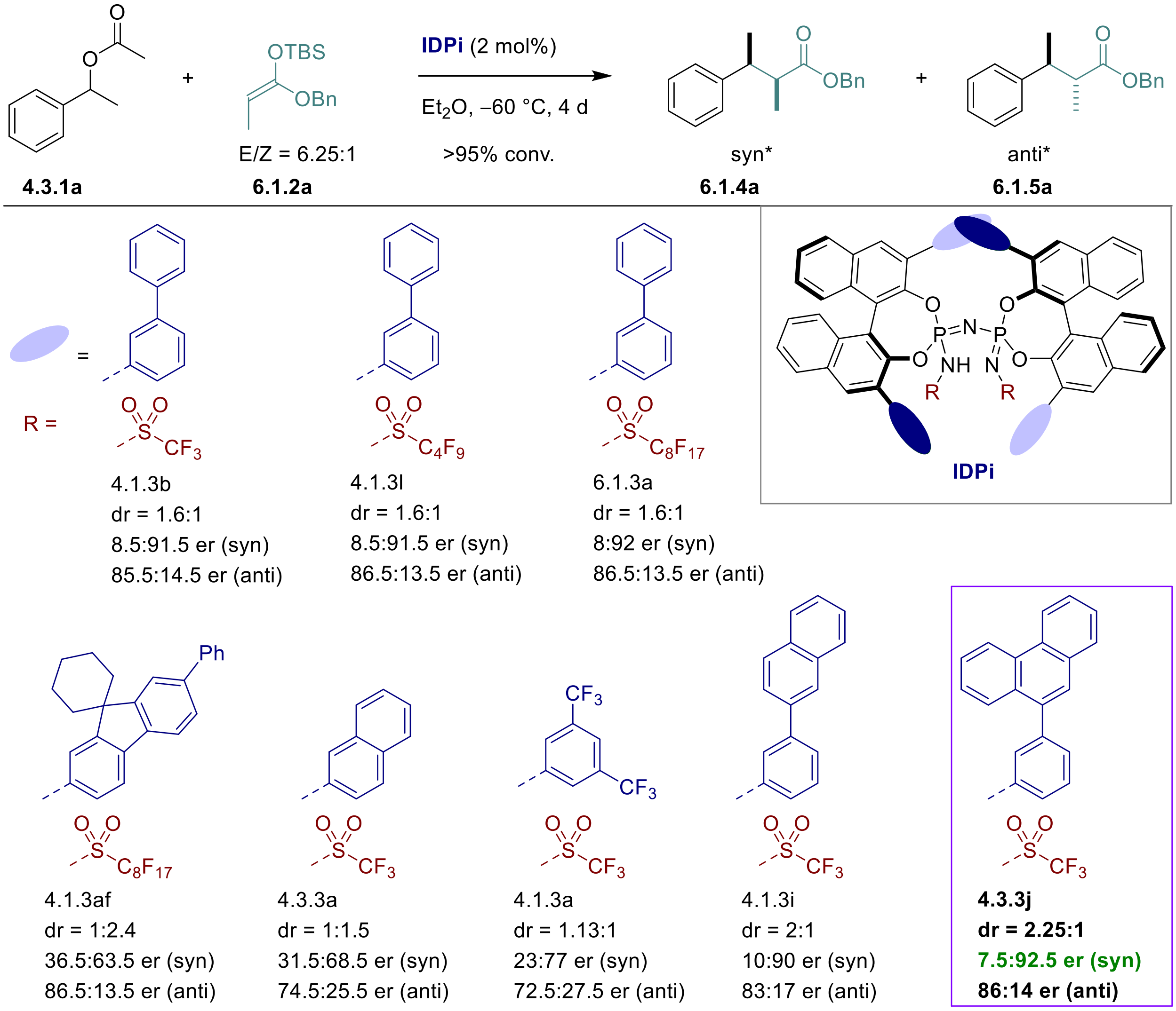
OTBS
OBn
E/Z = 6.25:1
4.3.1a
6.1.2a
IDPi (2 mol%)
Et2O, –60 °C, 4 d
>95% conv.
OBn
syn*
6.1.4a
anti*
6.1.5a
R =
CF3
C4F9
C8F17
4.1.3b
dr = 1.6:1
8.5:91.5 er (syn)
85.5:14.5 er (anti)
4.1.3l
dr = 1.6:1
8.5:91.5 er (syn)
86.5:13.5 er (anti)
6.1.3a
dr = 1.6:1
8:92 er (syn)
86.5:13.5 er (anti)
IDPi
Ph
4.1.3af
dr = 1:2.4
36.5:63.5 er (syn)
86.5:13.5 er (anti)
4.3.3a
dr = 1:1.5
31.5:68.5 er (syn)
74.5:25.5 er (anti)
4.1.3a
dr = 1.13:1
23:77 er (syn)
72.5:27.5 er (anti)
4.1.3i
dr = 2:1
10:90 er (syn)
83:17 er (anti)
4.3.3j
dr = 2.25:1
7.5:92.5 er (syn)
86:14 er (anti)

* relative stereochemistry is given

Scheme 6.1.2: Initial catalyst screening for enantio- and diastereoselective synthesis of acyclic aliphatic esters with contiguous stereogenic centers

Although these are very early results, preliminary results indicate that the diastereomeric ratio is possible to control, which will enable us to synthesize of enantio- and diastereoselective synthesis of acyclic aliphatic esters with contiguous stereogenic centers. The improvement of the enantio- and diastereoselective variant of this reaction has proven challenging and requires further work.

6.2 Tertiary benzylic carbocations (for creation of quaternary stereocentres):

Organic compounds containing all-carbon quaternary stereogenic centers are important structural motifs in natural products, and biologically active compounds endow with valuable structural, conformational, and metabolic properties. Due to its high importance, it has received significant attention for its synthesis in recent decades[118]. Notable examples include cycloadditions[119], α- and β-alkylation, and arylation of carbonyls[120], 3,3´-additions[121], $S_N2´$reactions[122] and Heck-type cross-couplings[123]. However, these methods rely on enantiofacial addition across a prochiral substrate and, therefore, require the synthesis of stereochemically well-defined starting materials. Since we already could control secondary benzylic carbocations using our IDPi catalysts, we thought about the addition of carbon nucleophiles to tertiary (benzylic) carbocations. Previously on quaternary stereocentres formation, Braun[78] and Jacobsen[80] using carbon nucleophiles reported *via* S_N1 like pathway. Despite that, these methods could only solve tertiary benzylic carbocations, or heteroatom stabilized cations. Therefore, we decided to explore this area using our methodology developed for C–C bond formation.

To commence our study, we decided to use tertiary benzylic acetate **6.2.1a** as an electrophile and silyl ketene acetal **4.3.2b** as a nucleophile. On testing some catalysts from our group's internal catalyst library, we found that most of the catalysts gave the desired product with a promising enantiomeric ratio. The combination of *meta*, *para*-substitution pattern (spiro fluorene), or *para*-substitution pattern was fruitful for the enantioselectivity. We further fine-tune the 3,3´-substitution to improve the enantioselectivity; however, it does not lead to any significant improvement in enantioselectivity.

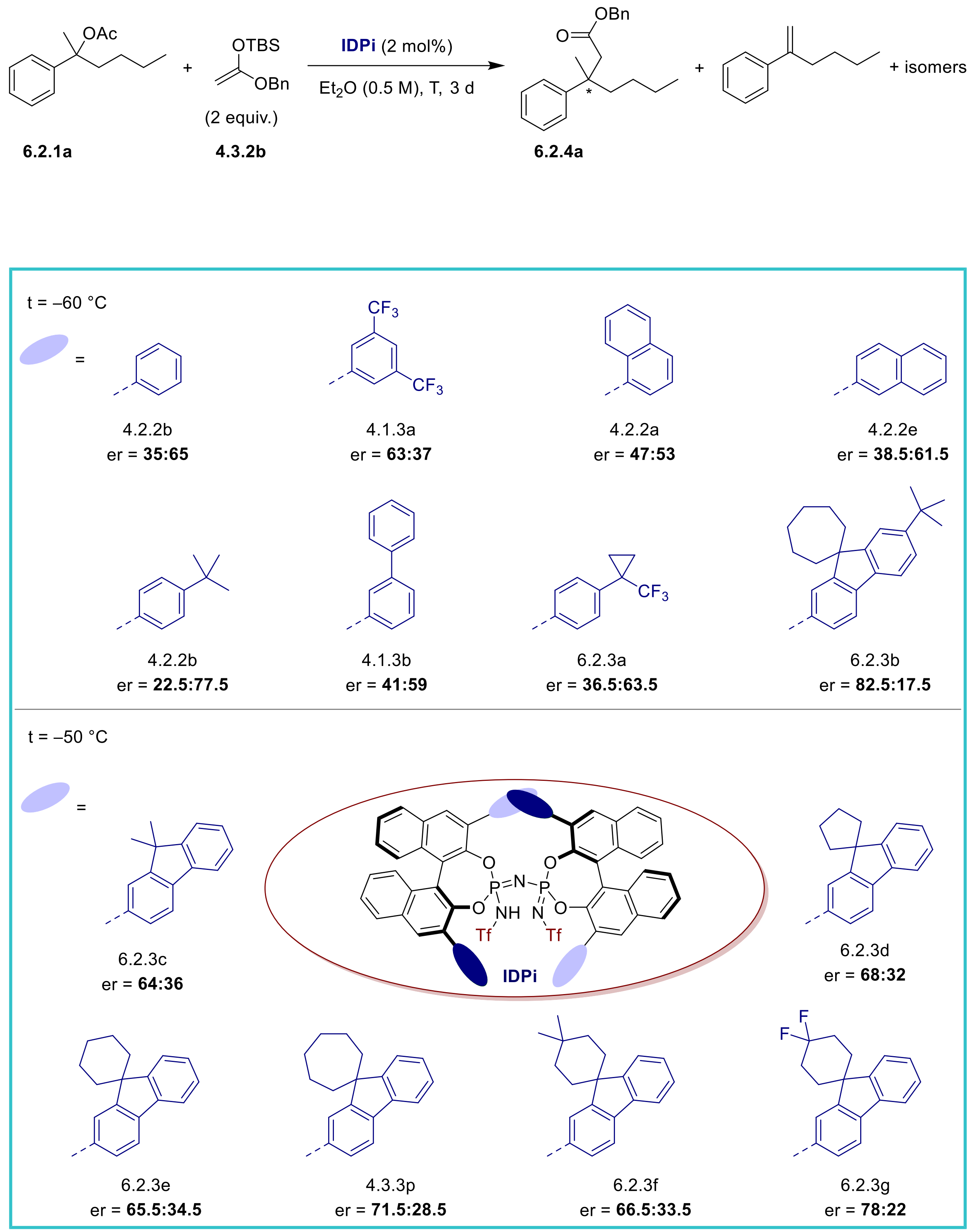
OAc
6.2.1a
+
OTBS
OBn
(2 equiv.)
4.3.2b
IDPi (2 mol%)
Et$_2$O (0.5 M), T, 3 d
OBn
O
*
6.2.4a
+
+ isomers
t = –60 °C
=
4.2.2b
er = 35:65
CF$_3$
CF$_3$
4.1.3a
er = 63:37
4.2.2a
er = 47:53
4.2.2e
er = 38.5:61.5
4.2.2b
er = 22.5:77.5
4.1.3b
er = 41:59
CF$_3$
6.2.3a
er = 36.5:63.5
6.2.3b
er = 82.5:17.5
t = –50 °C
=
6.2.3c
er = 64:36
O
P=N–P
O
NH
N
O
O
Tf
Tf
IDPi
6.2.3d
er = 68:32
6.2.3e
er = 65.5:34.5
4.3.3p
er = 71.5:28.5
6.2.3f
er = 66.5:33.5
F
F
6.2.3g
er = 78:22

Scheme 6.2.1: Initial catalyst screening for creation of quaternary stereocentres

To extend this methodology further to aliphatic tertiary cations, we used substrate **6.2.5a** as cation precursors and silyl ketene acetal **6.2.6a** as a nucleophile. Initial results suggest that it is possible to form a C–C bond to generate quaternary stereogenic centers for aliphatic substrates *via* an S_N1 like pathway.

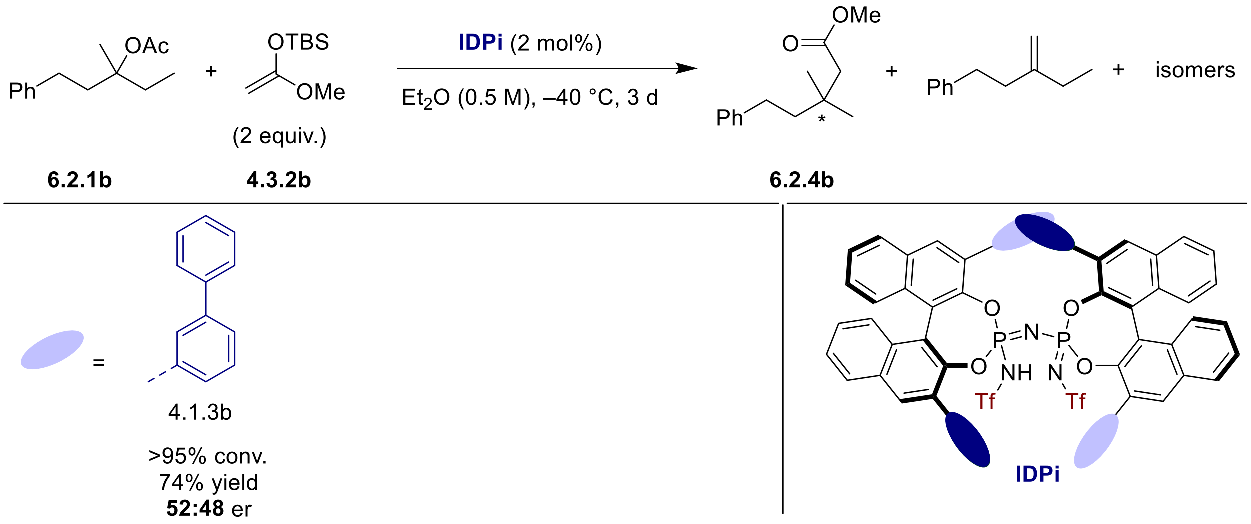
OAc
Ph
OTBS
OMe
(2 equiv.)
IDPi (2 mol%)
Et₂O (0.5 M), –40 °C, 3 d
OMe
O
Ph
*
Ph
isomers
6.2.1b
4.3.2b
6.2.4b
=
4.1.3b
>95% conv.
74% yield
52:48 er
O
P=N-P
O
NH
N
Tf
Tf
IDPi

Scheme 6.2.2: Initial catalyst screening for creation of quaternary stereocentres for aliphatic substrate

These initial experiments show promising results and the potential of this methodology compared to other existing methodologies on the creation of quaternary stereogenic centers *via* S_N1 reaction. Furthermore, reaction optimization is required to achieve better results, and mechanistic studies could be beneficial to gain insight into the reaction mechanism.

7 Experimental Section

7.1 General Information

Unless otherwise stated, all reactions were magnetically stirred and conducted in oven-dried (80 °C) or flame-dried glassware in anhydrous solvents under argon, applying standard Schlenk techniques. Solvents and liquid reagents, as well as solutions of solid or liquid reagents were added via syringes, stainless steel or polyethylene cannulas through rubber septa or through a weak argon counter-flow. Solid reagents were added through a weak argon counter-flow. Cooling baths were prepared in Dewar vessels, filled with ice/water (0 °C), cooled acetone (> –78 °C), ethanol/liquid nitrogen (< –78 °C) or dry ice/acetone (–78 °C). Heated oil baths were used for reactions requiring elevated temperatures. Solvents were removed under reduced pressure at 40 °C using a rotary evaporator, and unless otherwise stated, the remaining compound was dried in high vacuum (10^{-3} mbar) at ambient temperature. All given yields are isolated yields of chromatographically and nuclear magnetic resonance (NMR) spectroscopically pure materials, unless otherwise stated.

***Chemicals*:** Unless otherwise stated, chemicals were purchased from commercial suppliers (Sigma-Aldrich, ABCR-GmbH, TCI, Acros, Alfa Aser and fluorochem) and used without further purification.

***Solvents*:** Solvents (dichloromethane, diethyl ether, tetrahydrofuran, toluene, chloroform and benzene) were dried by distillation from an appropriate drying agent in the technical department of the Max-Planck-Institut für Kohlenforschung and received in Schlenk flasks under argon. Other anhydrous solvents (1,4-dioxane, dimethyl sulfoxide, ethyl acetate, ethanol, acetonitrile, methanol, methyl *tert*-butyl ether, and hexane and pentane) were purchased from commercial suppliers and dried over molecular sieves.

***Inert Gas*:** Dry argon was purchased from Air Liquide with > 99.5% purity.

***Thin Layer Chromatography*:** Thin-layer chromatography (TLC) was performed using silica gel pre-coated glass plates (SIL G-25, with fluorescent indicator UV254; Macherey-Nagel) and aluminium oxide pre-coated plastic sheets (Polygram Alox N, 0.2 mm, with fluorescent indicator UV254; Macherey-Nagel), which were visualized by irradiation with UV light (λ = 254 or 366 nm), basic $KMnO_4$, phosphomolybdic acid (PMA) and/or anisaldehyde. Preparative thin-layer chromatography was performed on silica gel pre-coated glass plates SIL G-100, with fluorescent indicator UV254 (Macherey-Nagel).

Nomenclature**:** Nomenclature follows the suggestions proposed by the computer program ChemBioDraw (15.0.0.106) of CBD/cambridgesoft.

Nuclear Magnetic Resonance (NMR) Spectroscopy**:** ^{1}H, ^{13}C, ^{19}F, ^{31}P NMR spectra were recorded on a Bruker AVIII 500 MHz, Bruker AVIII HD 300 MHz or Bruker AVNeo 600 MHz spectrometer in a suitable deuterated solvent. The solvent employed and respective measuring frequency are indicated for each experiment. Chemical shifts are reported with Me_4Si serving as a universal reference of all nuclides and with two or one digits after the comma. The resonance multiplicity is described as s (singlet), d (doublet), t (triplet), q (quadruplet), p (pentet), hept (heptet), m (multiplet), and br. (broad). All spectra were recorded at 298 K unless otherwise noted, processed with the program MestReNova 14.1.2, and coupling constants are reported as observed. The residual deuterated solvent signal relative to tetramethylsilane (TMS) was used as the internal reference in ^{1}H NMR spectra ($CDCl_3$ δ 7.26, CD_2Cl_2 δ 5.32), and are reported as follows: chemical shift δ in ppm (multiplicity, coupling constant J in Hz, number of protons). ^{13}C NMR spectra reported in ppm from tetramethylsilane (TMS) with the solvent resonance as the internal standard ($CDCl_3$ δ 77.16, CD_2Cl_2 δ 53.84).

Mass Spectrometry (MS)**:** Electron impact (EI) MS was performed on a Finnigan MAT 8200 (70 eV) or MAT 8400 (70 eV) spectrometer. Electrospray ionization (ESI) MS was conducted on a Bruker ESQ 3000 spectrometer. High resolution mass spectrometry (HRMS) was performed on a Finnigan MAT 95 (EI) or Bruker APEX III FTMS (7T magnet, ESI). The ionization method and mode of detection employed is indicated for the respective experiment and all masses are reported in atomic units per elementary charge (m/z) with an intensity normalized to the most intense peak.

Specific Rotation**:** Specific rotations $[\alpha]_D^T$ were measured with a Rudolph RA Autopol IV Automatic Polarimeter at the indicated temperature (T) with a sodium lamp (sodium D line, λ = 589 nm). Measurements were performed in an acid resistant 1 mL cell (50 mm length) with concentrations (g/100 mL) reported in the corresponding solvent.

High-Performance Liquid Chromatography (HPLC)**:** HPLC was performed on Shimadzu LC-20AD liquid chromatograph (SIL-20AC auto sampler, CMB-20A communication bus module, DGU-20A5 degasser, CTO-20AC column oven, SPD-M20A diode array detector), Shimadzu LC-20AB liquid chromatograph (SIL-20ACHT auto sampler, DGU20A5 degasser, CTO-20AC column oven, SPD-M20A diode array detector), or Shimadzu LC-20AB liquid chromatograph (reversed phase, SIL-20ACHT auto sampler, CTO-20AC column oven, SPD-M20A diode array detector) using Daicel columns with chiral stationary phases. All solvents used were HPLC-grade solvents, purchased from Merck. The column employed and respective solvent mixture are indicated for each experiment.

***Gas Chromatography (GC)*:** GC analyses on a chiral stationary phase were performed on HP 6890 and 5890 series instruments (split-mode capillary injection system, flame ionization detector (FID), hydrogen carrier gas). All of these analyses were conducted in the GC department of the Max-Planck-Institut für Kohlenforschung. The conditions employed are described in detail for the individual experiments. Liquid Chromatography-Mass Spectrometry Liquid chromatography-mass spectrometry (LC-MS) was performed on Shimadzu LC-MS 2020 liquid chromatograph. All solvents used were HPLC-grade solvents purchased from Sigma-Aldrich. The column employed, the respective solvent mixture, and the MS parameters are indicated for each experiment.

7.2. Synthesis of Substrates

The trichloroacetimidates **4.1.1a**[79], **4.1.1c**[124], and **4.2.1e**[125] were synthesized according to the literature procedure[126] and the characterizing data were matched with known literature data. The acetates **4.3.1a**[126], **4.3.1b**[127], **4.3.1f**[128], **4.3.1g**[129], **4.3.1i**[130], and **4.3.1j**[131] were synthesized according to the literature procedure[132] and the characterizing data were matched with known literature data.

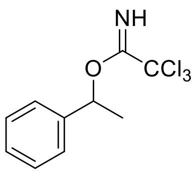

4.1.1a

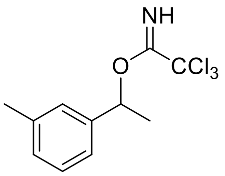

4.1.1g

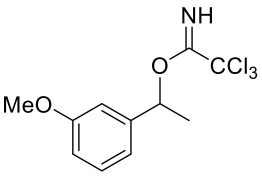

4.1.1h

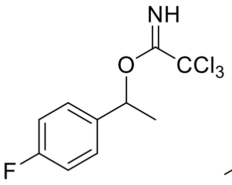

4.1.1b

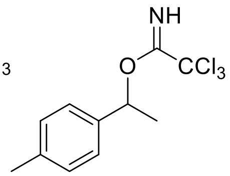

4.1.1c

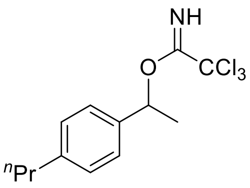

4.1.1j

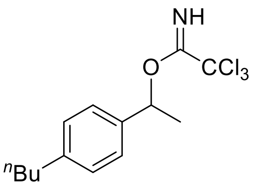

4.1.1k

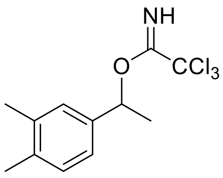

4.1.1l

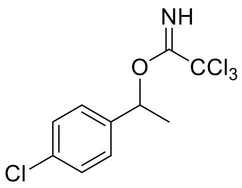

4.2.1a

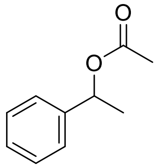

4.3.1a

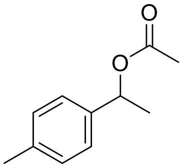

4.3.1b

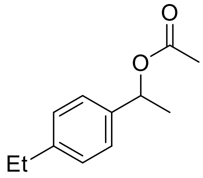

4.3.1f

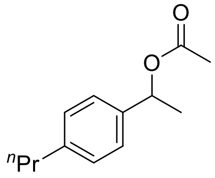

4.3.1g

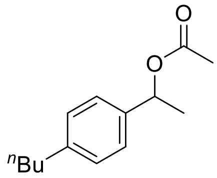

4.3.1h

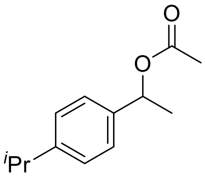

4.3.1i

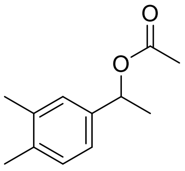

4.3.1j

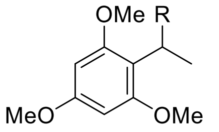

R = OMe, **4.3.1d**
R = OH, **4.3.1k**

Figure 7.1: Structure of substrates.

Procedure for synthesis of trichloroacetimidates:

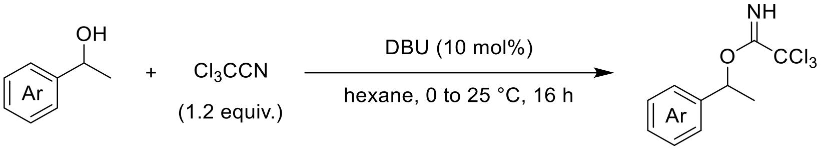

Following the literature procedure[126]: To a solution of benzylic alcohols (1.0 equiv.) and trichloroacetonitrile (1.2 equiv.) in hexane was added DBU (10 mol%) at 0 °C. The mixture was allowed to warm to room temperature and stirred for 16 h. After stirring for 16 h reaction mixture was washed with saturated NH_4Cl and then brine, dried over anhydrous Na_2SO_4. After concentration in *vacuo*, the crude product was purified on silica gel with presoaked Et_3N, using 1–5% Et_3N in hexane.

1-(*m*-tolyl)ethyl 2,2,2-trichloroacetimidate (4.1.1g):

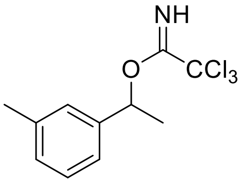

Prepared following the procedure using 1-(*m*-tolyl)ethan-1-ol (2.5 mmol, 340 mg) and obtained after column chromatography as a colorless liquid (550 mg, 78%).

^{1}H NMR (501 MHz, CD_2Cl_2) δ 8.34 (s, 1H), 7.27–7.20 (m, 3H), 7.12 (ddq, *J* = 7.2, 1.8, 0.9 Hz, 1H), 5.94 (q, *J* = 6.6 Hz, 1H), 2.36 (s, 3H), 1.62 (d, *J* = 6.6 Hz, 3H). **^{13}C NMR** (126 MHz, CD_2Cl_2) δ 161.9, 141.9, 138.6, 129.0, 128.7, 126.9, 123.2, 92.2, 77.7, 22.4, 21.6. **HRMS (EI)**: calculated for $C_{11}H_{12}NOCl_3^+$ (M^+): 278.997898, found: 278.9977780.

1-(3-methoxyphenyl)ethyl 2,2,2-trichloroacetimidate (4.1.1h):

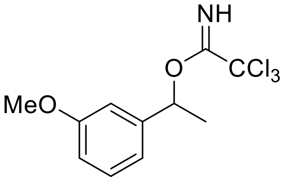

Prepared following the procedure using 1-(3-methoxyphenyl)ethan-1-ol (3.3 mmol, 500 mg) and obtained after column chromatography as a colorless liquid (700 mg, 72%).

^{1}H NMR (501 MHz, CD_2Cl_2) δ 8.36 (s, 1H), 7.28 (t, *J* = 7.9 Hz, 1H), 7.03–6.95 (m, 2H), 6.84 (ddd, *J* = 8.2, 2.7, 0.9 Hz, 1H), 5.95 (q, *J* = 6.6 Hz, 1H), 3.79 (s, 3H), 1.63 (d, *J* = 6.6 Hz, 3H). **^{13}C NMR** (126 MHz, CD_2Cl_2) δ 161.8, 160.2, 143.6, 129.9, 118.4, 113.6, 111.7, 92.1, 77.4, 55.6, 22.4. **HRMS (EI)**: calculated for $C_{11}H_{12}NO_2Cl_3^+$ (M^+): 294.992813, found: 294.992820.

1-(4-fluorophenyl)ethyl 2,2,2-trichloroacetimidate (4.1.1b):

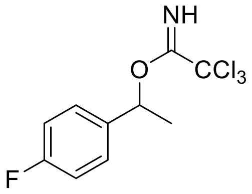

Prepared following the procedure using 1-(4-fluorophenyl)ethan-1-ol (15.8 mmol, 2.2 g) and obtained after column chromatography as a colorless liquid (3.7 g, 82%).

^{1}H NMR (501 MHz, CD_2Cl_2) δ 8.36 (s, 1H), 7.47–7.34 (m, 2H), 7.09–7.01 (m, 2H), 5.97 (q, *J* = 6.6 Hz, 1H), 1.63 (d, *J* = 6.6 Hz, 3H). **^{13}C NMR** (126 MHz, CD_2Cl_2) δ 162.7 (d, *J* = 245.1 Hz), 161. 8, 137.75 (d, *J* = 3.2 Hz), 128.22 (d, *J* = 8.2 Hz), 115.59 (d, *J* = 21.6 Hz), 92.1, 76.9, 22.2. **^{19}F NMR** (471 MHz, CD_2Cl_2) δ –115.2. **HRMS (ESI)**: calculated for $C_{10}H_9NOFCl_3Na^+$ ($[M+Na]^+$): 305.962595, found: 305.962800.

1-(4-propylphenyl)ethyl 2,2,2-trichloroacetimidate (4.1.1j):

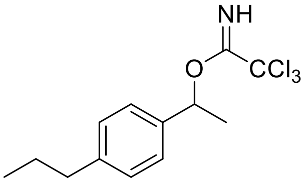

Prepared following the procedure using 1-(4-propylphenyl)ethan-1-ol (6.1 mmol, 1.0 g) and obtained after column chromatography as a white solid (1.5 g, 80%).

^{1}H NMR (501 MHz, CD_2Cl_2) δ 8.34 (s, 1H), 7.37–7.31 (m, 2H), 7.21–7.16 (m, 2H), 5.96 (q, *J* = 6.6 Hz, 1H), 2.65–2.51 (m, 2H), 1.6 (dq, *J* = 15.0, 7.4 Hz, 2H), 1.6 (d, *J* = 6.5 Hz, 3H), 0.95 (t, *J* = 7.3 Hz, 3H). **^{13}C NMR** (126 MHz, CD_2Cl_2) δ 161.9, 143.0, 139.1, 128.9, 126.2, 92.2, 77.6, 38.1, 25.0, 22.2, 14.1. **HRMS (ESI)**: calculated for $C_{13}H_{16}NOCl_3Na^+$ ($[M+Na]^+$): 330.018967, found: 330.019250.

1-(4-butylphenyl)ethyl 2,2,2-trichloroacetimidate (4.1.1k):

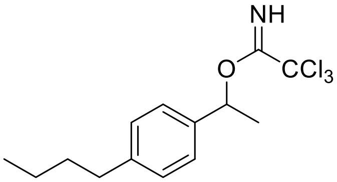

Prepared following the procedure using 1-(4-butylphenyl)ethan-1-ol (5.6 mmol, 1.0 g) and obtained after column chromatography as a white solid (1.5 g, 83%).

^{1}H NMR (501 MHz, CD_2Cl_2) δ 8.34 (s, 1H), 7.33 (dd, *J* = 8.3, 2.0 Hz, 2H), 7.22–7.15 (m, 2H), 5.96 (q, *J* = 6.6 Hz, 1H), 2.73–2.50 (m, 2H), 1.67–1.56 (m, 5H), 1.42–1.31 (m, 2H), 0.93 (t, *J* = 7.3 Hz, 3H). **^{13}C NMR** (126 MHz, CD_2Cl_2) δ 161.9, 143.2, 139.1, 128.8, 126.2, 77.6, 35.7, 34.1, 22.8, 22.2, 14.1. **HRMS (ESI)**: calculated for $C_{14}H_{19}NOCl_3^+$ ($[M+H]^+$): 322.052672, found: 322.052590.

1-(3,4-dimethylphenyl)ethyl 2,2,2-trichloroacetimidate (4.1.1l):

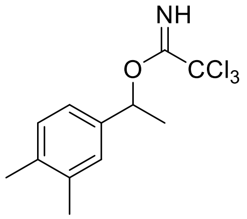

Prepared following the procedure using 1-(3,4-dimethylphenyl)ethan-1-ol (7.1 mmol, 1.1 g) and obtained after column chromatography as a colorless liquid (1.5 g, 71%).

^{1}H NMR (501 MHz, CD_2Cl_2) δ 8.32 (s, 1H), 7.18 (d, *J* = 1.8 Hz, 1H), 7.17–7.11 (m, 2H), 5.91 (q, *J* = 6.6 Hz, 1H), 2.27 (s, 3H), 2.25 (s, 3H), 1.61 (d, *J* = 6.6 Hz, 3H). **^{13}C NMR** (126 MHz, CD_2Cl_2) δ 161.9, 139.3, 137.1, 136.8, 130.0, 127.5, 123.6, 92.2, 77.7, 22.3, 20.0, 19.6. **HRMS (EI)**: calculated for $C_{12}H_{14}NOCl_3^+$ (M^+): 293.013548, found: 293.013590.

1-(4-butylphenyl)ethyl acetate (4.3.1h):

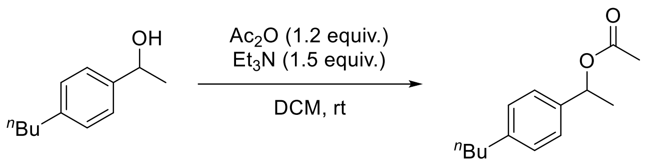

Prepared following the literature procedure[132] from 1-(4-butylphenyl)ethan-1-ol (5.6 mmol, 1.0 g) and obtained after column chromatography (eluent: pentane/Et_2O 95:5→85:15) as a colorless liquid (1.19 g, 96%)

^{1}H NMR (501 MHz, CD_2Cl_2) δ 7.27–7.22 (m, 2H), 7.18–7.13 (m, 2H), 5.80 (q, *J* = 6.6 Hz, 1H), 2.63–2.57 (m, 2H), 2.03 (s, 3H), 1.58 (tt, *J* = 7.7, 6.6 Hz, 2H), 1.50 (d, *J* = 6.6 Hz, 3H), 1.35 (h, *J* = 7.4 Hz, 2H), 0.93 (t, *J* = 7.4 Hz, 3H). **^{13}C NMR** (126 MHz, CD_2Cl_2) δ 170.5, 143.1, 139.6, 128.8, 126.4, 72.5, 35.7, 34.1, 22.8, 22.3, 21.5, 14.1. **HRMS (EI)**: calculated for $C_{14}H_{20}O_2^+$ (M^+): 220.145780, found: 220.145700.

1-(2,4,6-trimethoxyphenyl)ethan-1-ol (4.3.1k):

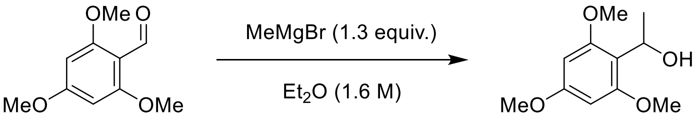

5i

To a flame-dried schlenk tube was charged with 2,4,6-trimethoxybenzaldehyde (1 equiv., 3.15 g, 16.1 mmol), Et_2O (10 mL) under argon, and the reaction was cooled to 0 °C. After 10 min, MeMgBr (1.3 equiv., 7 mL, 20.8 mmol) was added dropwise to the reaction mixture *via* cannula, and then the reaction mixture was warmed up to room temperature and continued stirring for 2 h. On completion of the reaction, saturated NH_4Cl was added, and the organic layer was extracted with DCM three times, dried over Na_2SO_4, and concentrated under reduced pressure. The crude product was purified by column chromatography (eluent: pentane/EtOAc 80:20→70:30) to give the product 1-(2,4,6-trimethoxyphenyl)ethan-1-ol (**4.3.1k**) as a white solid (3.4 g, quantitative).

^{1}H NMR (501 MHz, $CDCl_3$) δ 6.13 (s, 2H), 5.24 (dq, *J* = 11.4, 6.7 Hz, 1H), 3.82 (s, 3H), 3.82 (s, 3H), 3.80 (s, 3H), 3.66 (d, *J* = 11.4 Hz, 1H), 1.47 (d, *J* = 6.7 Hz, 3H). **^{13}C NMR** (126 MHz, $CDCl_3$) δ 160.2, 158.3, 113.9, 91.2, 63.9, 55.8, 55.5, 24.0. **HRMS (EI)**: calculated for $C_{11}H_{16}O_4^+$ (M^+): 212.104310, found: 212.104100.

1,3,5-trimethoxy-2-(1-methoxyethyl)benzene (4.3.1d):

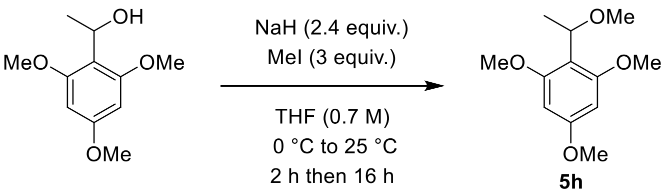

To a flame-dried schlenk tube was charged with 1-(2,4,6-trimethoxyphenyl)ethan-1-ol (1 equiv., 750 mg, 3.5 mmol), THF (5 mL) under argon and the reaction was cooled to 0 °C. After 10 min, NaH (2.4 equiv., 339 mg, 8.5 mmol) was added to the reaction mixture, and the reaction mixture was stirred for 2 h. Then MeI (3 equiv., 0.67 mL, 10.6 mmol) was added, and the reaction was warmed to room temperature and continued stirring for an additional 16 h. On completion of the reaction, saturated NH_4Cl was added, and the organic layer was extracted with DCM three times, dried over Na_2SO_4, and concentrated under reduced pressure. The crude product was purified by column chromatography (eluent: pentane/Et_2O 90:10→60:40) to give the product 1,3,5-trimethoxy-2-(1-methoxyethyl)benzene (**4.3.1d**) as a white solid (600 mg, 75%).

^{1}H NMR (501 MHz, CD_2Cl_2) δ 6.13 (s, 2H), 4.92 (q, *J* = 6.7 Hz, 1H), 3.79 (s, 3H), 3.78 (s, 6H), 3.11 (s, 3H), 1.47 (s, 3H). **^{13}C NMR** (126 MHz, CD_2Cl_2) δ 160.99, 160.40, 110.97, 91.40, 70.79, 56.16, 56.04, 55.61, 19.84. **HRMS (ESI)**: calculated for $C_{12}H_{18}O_4Na^+$ ($[M+Na]^+$): 249.10973, found: 249.10960.

7.3.1 Synthesis and Characterization of Catalysts

2',7'-dibromospiro[cyclohexane-1,9'-fluorene]:

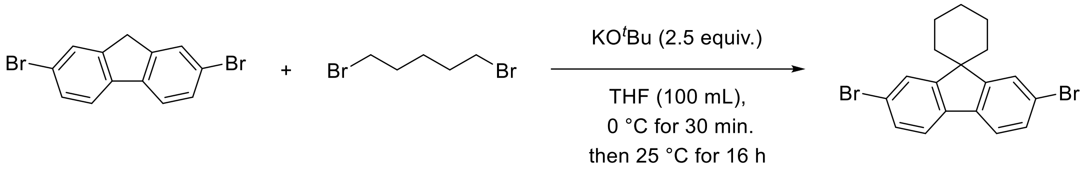

A flame-dried two-neck round bottom flask was charged with potassium *tert*-butoxide (2.5 equiv., 4.3 g, 38.6 mmol), THF (80 mL) under argon, and the reaction was cooled to 0 °C. In another flame-dried flask 2,7-dibromo-9*H*-fluorene (1 equiv., 5 g, 15.4 mmol) was added and dissolved in THF (20 mL) under argon and then dropwise added to the reaction mixture *via* cannula and stirred the reaction mixture for 30 min at 0 °C. After 30 min, 1,5-dibromopentane was added at same temperature, and then the reaction mixture was warmed up to room temperature and stirred for an additional 16 h. On completion of the reaction, water was added and organic layer was extracted with DCM three times, dried over Na_2SO_4, concentrated under reduced pressure. The crude product was purified by column chromatography (eluent: hexane/DCM 100:0→90:10) on activated alumina to give the product as a white solid (6.05 g, 80%).

^{1}H NMR (501 MHz, $CDCl_3$) δ 7.77 (d, J = 1.7 Hz, 1H), 7.55 (d, J = 8.0 Hz, 1H), 7.48 (dd, J = 8.1, 1.7 Hz, 1H), 1.88 (q, J = 6.5 Hz, 2H), 1.79 (q, J = 6.3 Hz, 1H), 1.76–1.67 (m, 2H). **^{13}C NMR** (126 MHz, $CDCl_3$) δ 154.9, 137.7, 130.3, 128.0, 121.30, 121.25, 50.9, 35.4, 25.4, 22.6. **HRMS (EI)**: calculated for $C_{18}H_{16}Br_2^+$ (M^+): 389.961350, found: 389.961210.

2'-bromo-7'-phenylspiro[cyclohexane-1,9'-fluorene]:

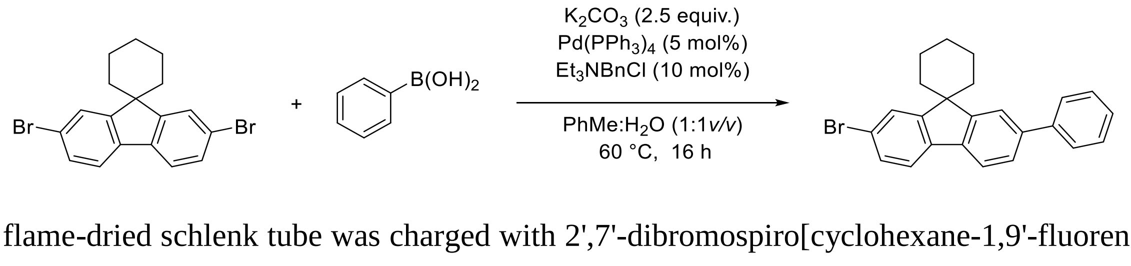

To a flame-dried schlenk tube was charged with 2',7'-dibromospiro[cyclohexane-1,9'-fluorene] (1 equiv., 4.5 g, 11.5 mmol), potassium carbonate (2.5 equiv., 4 g, 28.7 mmol), benzyltriethylammonium chloride (0.1 equiv., 261.4 mg, 1.1 mmol), phenyl boronic acid (1 equiv., 1.4 g, 11.5 mmol), and tetrakis(triphenylphosphine) palladium (0) (0.05 equiv., 663.0 mg, 0.6 mmol) under argon. Degassed toluene (10 mL) and water (10 mL) were added and heated to 60 °C for 16 h. On completion of the reaction, the mixture was cooled to room temperature water was added, and the organic layer was extracted with DCM three times and then combined organic layer was washed with 10% HCl solution, dried over Na_2SO_4, concentrated under reduced pressure. The crude product was purified by column chromatography (eluent: hexane/DCM 100:0→95:5) on activated alumina to give the product as a white solid (1.5 g, 33.5%).

^{1}H NMR (501 MHz, $CDCl_3$) δ 7.85 (d, *J* = 1.7 Hz, 1H), 7.81 (d, *J* = 1.9 Hz, 1H), 7.76 (d, *J* = 7.8 Hz, 1H), 7.69–7.64 (m, 2H), 7.63–7.58 (m, 2H), 7.52–7.45 (m, 3H), 7.41–7.36 (m, 1H), 2.04–1.87 (m, 4H), 1.87–1.73 (m, 6H). **^{13}C NMR** (126 MHz, $CDCl_3$) δ 155.5, 153.7, 141.8, 140.6, 138.4, 137.9, 130.2, 129.0, 128.0, 127.42, 127.40, 126.5, 123.5, 121.3, 120.8, 120.2, 50.8, 35.7, 25.6, 22.8. **HRMS (EI)**: calculated for $C_{24}H_{21}Br^+$ (M^+): 388.082125, found: 388.082860.

2'-bromospiro[cycloheptane-1,9'-fluorene]:

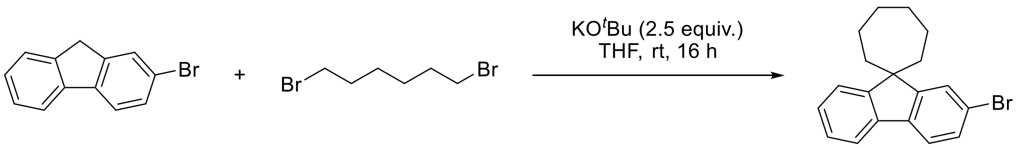

In a flame-dried round bottom flask potassium *tert*-butoxide (2.80 g, 25 mmol, 2.5 equiv.) was added under argon and dissolved in THF (80 mL), then cooled to 0 °C. In another flask 2-bromofluorene (2.45 g, 10 mmol, 1 equiv.) was dissolved in THF (10 mL) under argon. This solution was added dropwise for 5 min to the reaction mixture. The inner surface of the reaction flask was washed with THF (10 mL), and the reaction was stirred at 0 °C for 15 min. 1,6-dibromohexane (1.69 mL, 11 mmol, 1.1 equiv.) was added dropwise for 10 min. The reaction was stirred at 0 °C for 20 min, and then the cooling bath was removed and allowed to stir at room temperature for 16 h. The mixture was quenched with aqueous HCl (10%) at 0 °C and extracted three times with MTBE. The combined organic layers were dried over Na_2SO_4, concentrated under reduced pressure. The crude residue was purified by column chromatography on alumina (eluent: hexane) to provide the desired product (95 mg, 3% yield).

^{1}H NMR (501 MHz, $CDCl_3$) δ 7.72 (d, *J* = 1.8 Hz, 1H), 7.69–7.65 (m, 1H), 7.61–7.58 (m, 1H), 7.55 (d, *J* = 8.1 Hz, 1H), 7.45 (dd, *J* = 8.1, 1.8 Hz, 1H), 7.37–7.29 (m, 2H), 1.97–1.77 (m, 12H). **^{13}C NMR** (126 MHz, $CDCl_3$) δ 157.4, 154.9, 138.2, 138.2, 130.0, 127.8, 127.2, 127.0, 123.6, 121.2, 121.1, 119.9, 53.8, 39.5, 32.0, 25.5. **HRMS (EI)**: calculated for $C_{19}H_{19}Br^+$ (M^+): 326.066475, found: 326.066840.

(*S*)-3,3'-di([1,1'-biphenyl]-3-yl)-5,5',6,6',7,7',8,8'-octafluoro-[1,1'-binaphthalene]-2,2'-diol:

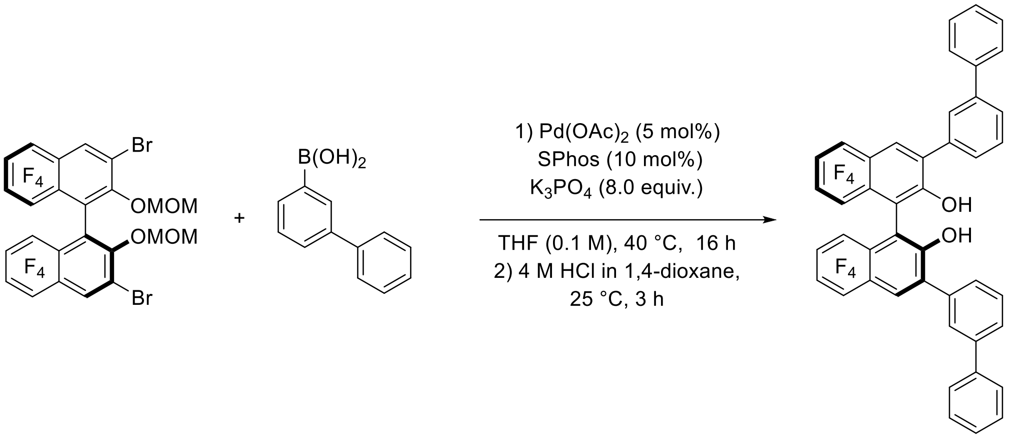

(*S*)-3,3'-dibromo-5,5',6,6',7,7',8,8'-octafluoro-2,2'-bis(methoxymethoxy)-1,1'-binaphthalene[17,111] was prepared following literature known procedure.

To a flame-dried schlenk tube equipped with a magnetic stir bar was charged with (S)-3,3'-dibromo-5,5',6,6',7,7',8,8'-octafluoro-2,2'-bis(methoxymethoxy)-1,1'-binaphthalene (1 equiv., 260 mg, 1.0 mmol), potassium phosphate (8.0 equiv., 653 mg, 3.1 mmol), [1,1'-biphenyl]-3-ylboronic acid (4.0 equiv., 304 mg, 1.5 mmol), SPhos (0.1 equiv., 16 mg, 0.04 mmol) and palladium acetate (0.05 equiv., 4.3 mg, 0.02 mmol) under argon. Degassed THF (4 mL) was added and heated to 40 °C for 16 h. On completion of the reaction, the mixture was cooled to room temperature and water was added, and the organic layer was extracted with DCM three times, and then combined organic layer was washed with 10% HCl solution, dried over Na_2SO_4, concentrated under reduced pressure. Subsequently, HCl (4 M in 1,4-dioxane, 5 mL) was added to this mixture and stirred at room temperature for 3 h. The solvent was removed under reduced pressure, and the crude product was purified by column chromatography (eluent: hexane/EtOAc 93:7→85:15) to afford the desired BINOL as a yellow solid (260 mg, 90%).

^{1}H NMR (501 MHz, $CDCl_3$) δ 8.19 (d, *J* = 1.3 Hz, 2H), 7.85 (q, *J* = 1.3 Hz, 2H), 7.70 (dh, *J* = 4.4, 1.9 Hz, 2H), 7.66–7.60 (m, 8H), 7.47 (dd, *J* = 8.4, 6.9 Hz, 4H), 7.42–7.35 (m, 2H), 5.59 (s, 2H). **^{13}C NMR** (126 MHz, $CDCl_3$) δ 150.9, 143.6, 142.6, 140.6, 136.2, 132.0, 129.8, 129.1, 128.4, 128.3, 127.9, 127.8, 127.4, 123.0, 119.7, 115.8 (d, *J* = 13.4 Hz), 111.4. **^{19}F NMR** (471 MHz, $CDCl_3$) δ –147.76 (t, *J* = 16.4 Hz, 2F), –148.95 (dd, *J* = 19.2, 15.1 Hz, 2F), –156.82 (t, *J* = 18.6 Hz, 2F), –161.50 (t, *J* = 19.2 Hz, 2F). **HRMS (ESI)**: calculated for $C_{44}H_{21}O_2F_8^-$ ($[M–H]^-$): 733.141933, found: 733.142220.

(*S*)-3,3'-bis(3-(naphthalen-2-yl)phenyl)-[1,1'-binaphthalene]-2,2'-diol:

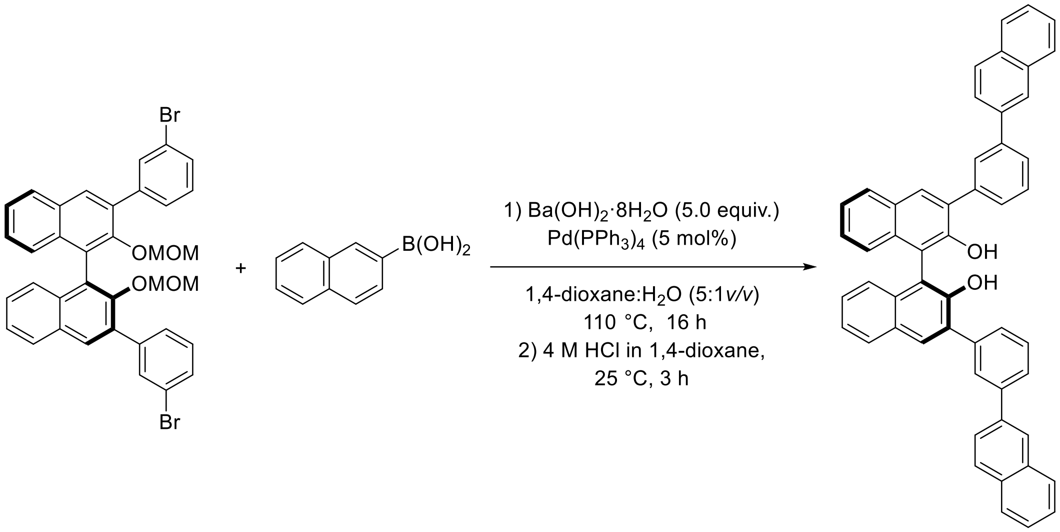

(*S*)-3,3'-bis(3-bromophenyl)-2,2'-bis(methoxymethoxy)-1,1'-binaphthalene[41h] was prepared following literature known procedure.

To a flame-dried schlenk tube equipped with a magnetic stir bar was charged with (S)-3,3'-bis(3-bromophenyl)-2,2'-bis(methoxymethoxy)-1,1'-binaphthalene (1 equiv., 700 mg, 1.0 mmol), Barium hydroxide octahydrate (5.0 equiv., 1.6 g, 5.1 mmol), 2-naphthyl boronic acid (3.5 equiv., 615 mg, 3.6 mmol), and tetrakis(triphenylphosphine)palladium (0) (0.075 equiv., 88.6 mg, 0.08 mmol) under argon. Degassed 1,4-dioxane (3 mL) and water (0.6 mL) were added and heated to 110 °C for 16 h. On completion of the reaction, the mixture was cooled to room temperature and water was added, and organic layer was extracted with DCM three times, and then combined organic layer was washed with 10% HCl solution, dried over Na_2SO_4, concentrated under reduced pressure. Subsequently, HCl (4 M in 1,4-dioxane, 5 mL) was added to this mixture and stirred at room temperature for 3 h. The solvent was removed under reduced pressure, and the crude product was purified by column chromatography (eluent: hexane/DCM 75:25→50:50) to afford the desired BINOL as a white solid (706 mg, 85.6%).

^{1}H NMR (501 MHz, $CDCl_3$) δ 8.15–8.10 (m, 6H), 7.99–7.90 (m, 6H), 7.89–7.86 (m, 2H), 7.83 (dd, *J* = 8.5, 1.9 Hz, 2H), 7.78 (tdt, *J* = 6.2, 3.3, 1.5 Hz, 4H), 7.62 (t, *J* = 7.7 Hz, 2H), 7.53–7.47 (m, 4H), 7.43 (ddd, *J* = 8.1, 6.7, 1.3 Hz, 2H), 7.36 (ddd, *J* = 8.2, 6.8, 1.4 Hz, 2H), 7.30 (dd, *J* = 8.4, 1.2 Hz, 2H), 5.47 (s, 2H). **^{13}C NMR** (126 MHz, $CDCl_3$) δ 150.4, 141.6, 138.5, 138.2, 133.8, 133.2, 132.9, 131.7, 130.8, 129.7, 129.2, 129.0, 128.8, 128. 7, 128.6, 128.4, 127.8, 127.7, 127.0, 126.5, 126.14, 126.12, 125.8, 124.6, 124.5, 112.6. **HRMS (ESI)**: calculated for $C_{52}H_{33}O_2^-$ ([M–H]$^-$): 689.248605, found: 689.248880.

(*S*)-3,3'-bis(3-(phenanthren-9-yl)phenyl)-[1,1'-binaphthalene]-2,2'-diol:

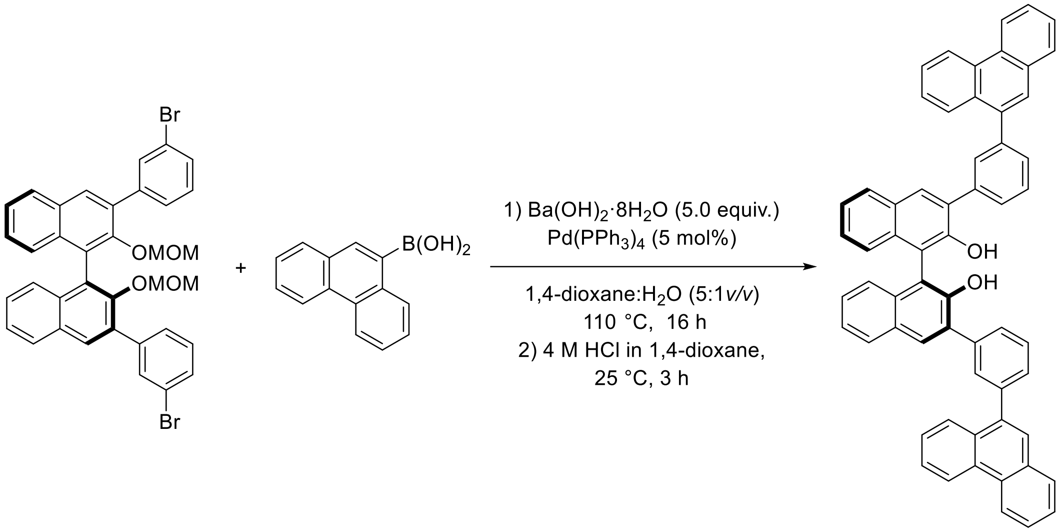

(*S*)-3,3'-bis(3-bromophenyl)-2,2'-bis(methoxymethoxy)-1,1'-binaphthalene[41h] was prepared following literature known procedure.

To a flame-dried schlenk tube equipped with a magnetic stir bar was charged with (*S*)-3,3'-bis(3-bromophenyl)-2,2'-bis(methoxymethoxy)-1,1'-binaphthalene (1 equiv., 250 mg, 0.36 mmol), barium hydroxide octahydrate (5.0 equiv., 576 mg, 1.83 mmol), 9-phenanthrene boronic acid (3.5 equiv., 284 mg, 1.28 mmol), and tetrakis(triphenylphosphine)palladium (0) (0.05 equiv., 21.1 mg, 0.02 mmol) under argon. Degassed 1,4-dioxane (1 mL) and water (0.2 mL) were added and heated to 110 °C for 16 h. On completion of the reaction, the mixture was cooled to room temperature and water was added, and organic layer was extracted with DCM three times, and then combined organic layer was washed with 10% HCl solution, dried over Na_2SO_4, concentrated under reduced pressure. Subsequently, HCl (4 M in 1,4-dioxane, 2 mL) was added to this mixture and stirred at room temperature for 3 h. The solvent was removed under reduced pressure, and the crude product was purified by column chromatography (eluent: hexane/DCM 80:20→65:35) to afford the desired BINOL as a white solid (289 mg, 86%).

^{1}H NMR (501 MHz, $CDCl_3$) δ 8.79 (d, J = 8.4 Hz, 2H), 8.74 (d, J = 8.2 Hz, 2H), 8.16 (d, J = 2.1 Hz, 2H), 8.06 (dt, J = 8.2, 1.9 Hz, 2H), 7.99 (t, J = 1.8 Hz, 2H), 7.95 (d, J = 8.2 Hz, 2H), 7.91 (dd, J = 7.9, 1.4 Hz, 2H), 7.87 (dq, J = 7.5, 1.8 Hz, 2H), 7.79 (d, J = 2.1 Hz, 2H), 7.72–7.59 (m, 10H), 7.56 (ddd, *J* = 8.2, 6.9, 1.3 Hz, 2H), 7.40 (ddd, *J* = 8.0, 6.7, 1.3 Hz, 2H), 7.33 (ddd, *J* = 8.1, 6.8, 1.3 Hz, 2H), 7.26 (s, 2H), 5.47 (d, *J* = 2.7 Hz, 2H). **^{13}C NMR** (126 MHz, $CDCl_3$) δ 150.4, 141.1, 138.7, 137.7, 133.2, 131.8, 131.7, 131.4, 131.3, 130.8, 130.6, 130.2, 129.7, 129.6, 128.8, 128.7, 128.64, 128.55, 127.8, 127.7, 127.1, 127.0, 126.76, 126.7, 126.6, 124.6, 124.4, 123.1, 122.7, 112.5. **HRMS (ESI)**: calculated for $C_{60}H_{37}O_2^-$ ([M–H]$^-$): 789.279904, found: 789.280370.

(*S*)-3,3'-bis(3-(naphthalen-1-yl)phenyl)-[1,1'-binaphthalene]-2,2'-diol:

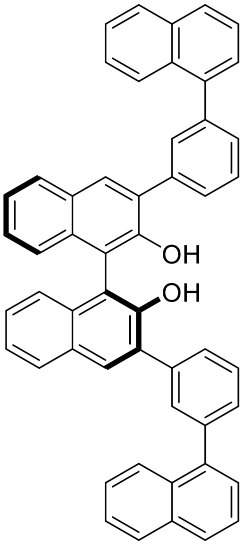

The crude product was purified by column chromatography (eluent: hexane/EtOAc 97:3→95: 5) to afford the desired BINOL as a white solid (370 mg, 92%).

^{1}H NMR (501 MHz, $CDCl_3$) δ 8.13 (s, 2H), 8.04 (d, *J* = 8.3 Hz, 2H), 7.96–7.89 (m, 6H), 7.87 (dd, *J* = 7.6, 2.0 Hz, 2H), 7.83 (dt, *J* = 7.7, 1.6 Hz, 2H), 7.62 (t, *J* = 7.6 Hz, 2H), 7.58–7.47 (m, 8H), 7.44 (ddd, *J* = 8.3, 6.8, 1.4 Hz, 2H), 7.41–7.36 (m, 2H), 7.32 (td, *J* = 7.6, 1.3 Hz, 2H), 7.25 (d, *J* = 8.4 Hz, 2H), 5.46 (s, 2H). **HRMS (ESI)**: calculated for $C_{52}H_{33}O_2^-$ ([M–H]$^-$): 689.24860, found: 689.24814.

(*S*)-3,3'-bis(3-(6-methoxynaphthalen-2-yl)phenyl)-[1,1'-binaphthalene]-2,2'-diol:

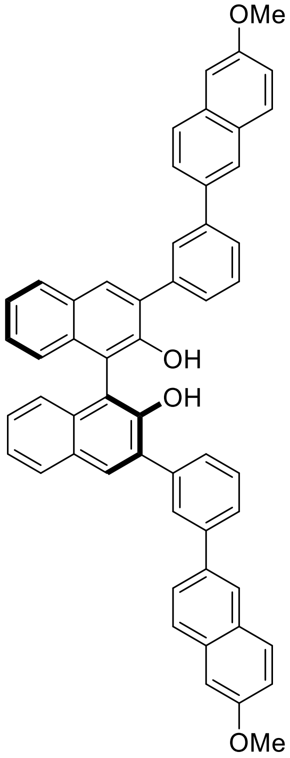

The crude product was purified by column chromatography (eluent: hexane/DCM 60:40→25:75) to afford the desired BINOL as a white solid (250 mg, 57%).

^{1}H NMR (501 MHz, $CDCl_3$) δ 8.13 (s, 2H), 8.09 (d, *J* = 1.9 Hz, 2H), 8.05 (d, *J* = 1.8 Hz, 2H), 7.96 (d, *J* = 8.1 Hz, 2H), 7.85–7.77 (m, 6H), 7.75 (ddt, *J* = 7.5, 5.8, 1.3 Hz, 4H), 7.60 (t, *J* = 7.7 Hz, 2H), 7.42 (ddd, *J* = 8.1, 6.7, 1.3 Hz, 2H), 7.35 (ddd, *J* = 8.2, 6.8, 1.3 Hz, 2H), 7.31 – 7.27 (m, 2H), 7.21–7.14 (m, 4H), 5.46 (s, 2H), 3.94 (s, 6H). **^{13}C NMR** (126 MHz, $CDCl_3$) δ 158.0, 150.4, 141.7, 138.2, 136.3, 134.0, 133.2, 131.7, 130.8, 129.9, 129.7, 129.3, 129.1, 128.75, 128.66, 128.5, 127.6, 127.5, 126.8, 126.3, 125.9, 124.56, 124.50, 119.3, 112.6, 105.8, 55.5. **HRMS (ESI)**: calculated for $C_{54}H_{37}O_4^-$ ($[M–H]^-$): 749.26973, found: 749.27071.

Procedure for cross-coupling reactions and subsequent MOM-deprotection and IDPi synthesis[41e]:

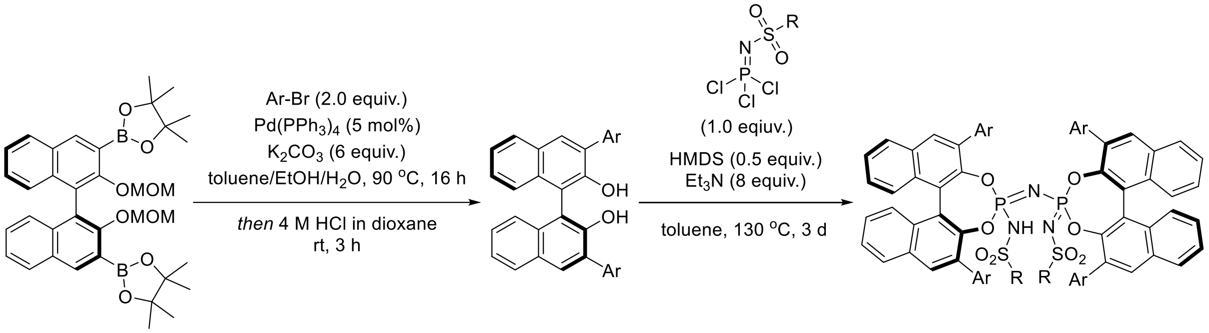

To a two-neck round-bottom flask with a condenser was added (*S*)-2,2'-(2,2'-bis(methoxymethoxy)-1,1'binaphthyl-3,3'-diyl)bis(4,4,-5,5-tetramethyl-1,3,2-dioxaborolane) (1.0 equiv.), bromide (2.0 equiv.), tetrakis(triphenylphosphine)palladium (0.5 equiv.) and K_2CO_3 (6 equiv.) under argon atmosphere. Degassed toluene/ethanol/water (3/2/1 *v*/*v*/*v* 0.2 M) were sequentially added. The mixture was then heated to 90 °C and stirred overnight. After cooling the reaction to room temperature, the organic layer was separated and the aqueous phase was extracted with EtOAc (3 times). The organic phase was combined and filtered through a thin layer of silica gel using a Büchner funnel, and the silica gel layer washed with EtOAc. The solvent was removed under reduced pressure and the crude MOM-protected diol was obtained. Subsequently, the crude product was dissolved in a small amount of DCM. A solution of HCl (4 M in 1,4-dioxane, 20 equiv.) was added at room temperature and the mixture was stirred for 3 h. The solvent was removed under reduced pressure and the crude was purified by column chromatography to afford the corresponding diol.

In a Schlenk tube under argon, a suspension of 3,3’-substituted (*S*,*S*)-BINOL (2.1 equiv.) in toluene (0.15 M) was treated with sulfonyl phosphorimidoyl trichloride (2.1 equiv.) and Et_3N (16 equiv.). The reaction mixture was stirred for 45 min at room temperature, then neat hexamethyldisilazane (HMDS, 1 equiv.) was added dropwise. The reaction mixture was stirred for additional 15 min at room temperature, then the Schlenk tube was subsequently sealed and heated to 130 °C for 3 d. On completion of the reaction, the mixture was cooled to room temperature, aq. HCl (10%) was added and the mixture was extracted with DCM. The combined organic layers were washed with brine, dried over $MgSO_4$ and concentrated under reduced pressure. The crude material was purified by column chromatography on silica gel to afford the desired product as a salt. The corresponding

IDPi Brønsted acids were obtained after acidification in DCM with aq. HCl (6 M) or ion exchange resin DOWEX 50WX8 (H-form), and evaporation of the solvent followed by drying under high vacuum as typically off-white solids. [Acidification procedure: The product as a salt was dissolved in 5 mL DCM, then aq. HCl (6 M, 8 mL) was added, and the mixture was stirred vigorously for 10 min. The organic layer was separated and the aqueous phase was extracted with DCM for several times until there was no product could be detected by TLC in the last DCM extract. The organic layers were combined and the solvent was removed under reduced pressure. The obtained IDPi solid was dried under high vacuum for 16 h at room temperature. Optionally, IDPi Brønsted acids were acidified by passing over a short plug of DOWEX 50WX8 (H-form) in DCM and obtained after removing the solvent.]

(*S*)-3,3'-bis(2'-phenylspiro[cyclohexane-1,9'-fluoren]-7'-yl)-[1,1'-binaphthalene]-2,2'-diol:

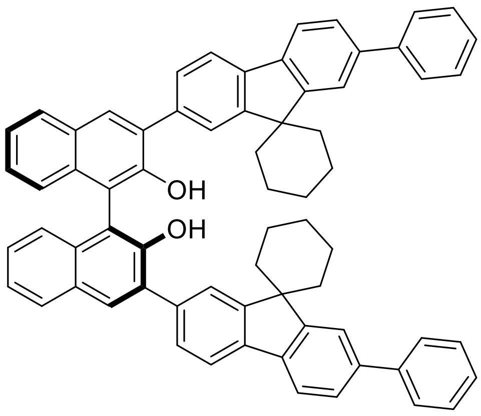

The crude product was purified by column chromatography (eluent: hexane/EtOAc 100:0→94:6) to afford the desired BINOL as a white solid (1.2 g, 94.5%).

^{1}H NMR (501 MHz, $CDCl_3$) δ 8.14 (s, 2H), 8.09 (d, *J* = 1.6 Hz, 2H), 8.02–7.97 (m, 2H), 7.91 (d, *J* = 1.6 Hz, 2H), 7.89 (d, *J* = 7.9 Hz, 2H), 7.86 (d, *J* = 7.9 Hz, 2H), 7.78 (dd, *J* = 7.9, 1.5 Hz, 2H), 7.72–7.66 (m, 4H), 7.63 (dd, *J* = 7.9, 1.6 Hz, 2H), 7.49 (t, *J* = 7.7 Hz, 4H), 7.44 (ddd, *J* = 8.1, 6.8, 1.3 Hz, 2H), 7.41–7.35 (m, 4H), 7.31 (dd, *J* = 8.4, 1.2 Hz, 2H), 5.52 (s, 2H), 2.05–1.96 (m, 4H), 1.94–1.87 (m, 4H), 1.86–1.80 (m, 2H). **^{13}C NMR** (126 MHz, $CDCl_3$) δ 154.3, 153.9, 150.4, 141.9, 140.3, 139.2, 138.7, 136.1, 133.1, 131.5, 131.3, 129.7, 128.9, 128.7, 128.6, 127.5, 127.3, 126.4, 126.0, 124.56, 124.52, 123.6, 120.4, 120.0, 112.8, 67.2, 50.7, 35.9, 35.9, 25.7, 23.0. **HRMS (ESI)**: calculated for $C_{68}H_{53}O_2^-$ ([M–H]$^-$): 901.40510, found: 901.40558.

(*S*)-3,3'-di(spiro[cycloheptane-1,9'-fluoren]-2'-yl)-[1,1'-binaphthalene]-2,2'-diol:

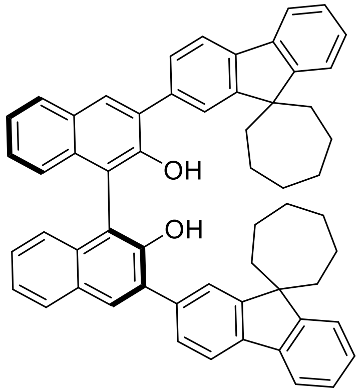

The crude product was purified by column chromatography (eluent: hexane/DCM 2:1) to afford the desired BINOL as a white solid (890 mg, 94%).

^{1}H NMR (501 MHz, CDCl$_3$) δ 8.11 (s, 2H), 8.00–7.95 (m, 4H), 7.82 (d, *J* = 7.9 Hz, 2H), 7.74 (ddd, *J* = 15.1, 7.6, 1.5 Hz, 4H), 7.66–7.61 (m, 2H), 7.42 (ddd, *J* = 8.0, 6.7, 1.3 Hz, 2H), 7.38–7.27 (m, 8H), 5.50 (s, 2H), 2.08–1.89 (m, 16H), 1.81 (d, *J* = 3.9 Hz, 8H). **^{13}C NMR** (126 MHz, CDCl$_3$) δ 155.7, 155.6, 150.4, 139.0, 138.8, 136.4, 133.2, 131.4, 131.3, 129.7, 128.6, 127.5, 127.4, 127.0, 125.0, 124.6, 124.5, 123.7, 120.1, 119.9, 112.8, 53.8, 39.7, 31.9, 25.6. **HRMS (ESI)**: calculated for $C_{58}H_{49}O_2^-$ ([M–H]$^-$): 777.37380, found: 777.37388.

(*S*,*S*)–Imidodiphosphorimidate 4.2.2i (IDPi 4.2.2i):

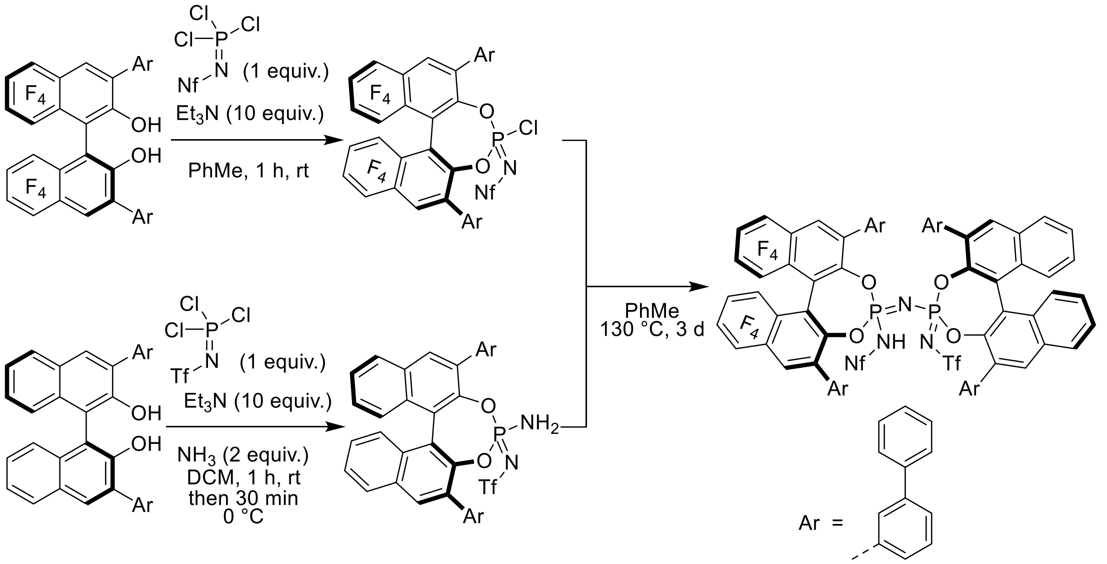

In a schlenk tube 1 a suspension of (*S*)-3,3'-di([1,1'-biphenyl]-3-yl)-5,5',6,6',7,7',8,8'-octafluoro-[1,1'-binaphthalene]-2,2'-diol (0.082 mmol, 1 equiv., 60 mg) in toluene (0.25 M) was added perfluorobutylsulfonylphosphorimidoyl trichloride (1 equiv.) and trimethylamine (10 equiv.) under argon and stirred for 1 h at room temperature. In another schlenk tube 2 (*S*)-3,3'-di([1,1'-biphenyl]-3-yl)-[1,1'-binaphthalene]-2,2'-diol (0.´082 mmol, 1 equiv., 48 mg) in DCM (0.25 M) was added trifluoromethylsulfonylphosphorimidoyl trichloride (1 equiv.) and trimethylamine (10 equiv.) under argon and stirred for 1 h at room temperature. The reaction mixture was cooled to 0 °C and then NH_3 (2 equiv., 0.5 M in 1,4 dioxane) was added and stirred for 30 min at the same temperature. After that DCM, Et_3N and excess NH_3 was removed from schlenk tube 2 under high vacuum. The reaction mixture from schlenk tube 1 was transferred to schlenk tube 2 via cannula, additional toluene (0.25 M) added and schlenk tube was sealed before heating the schlenk tube 2 at 130 °C for 3 d. After cooling to room temperature, aq. HCl (10%) was added and the mixture was extracted with DCM thrice. The combined organic layer was dried over Na_2SO_4 and concentrated under reduced pressure. The crude material was purified by column chromatography on silica gel (eluent: hexane/EtOAc 90:10→75:25) to afford the desired IDPi as a salt. The product was acidified by passing over a short plug of DOWEX 50WX8 (H-form) in DCM and obtained as a yellow solid after removing the solvent (33% yield, 50 mg).

^{1}H NMR (501 MHz, $CDCl_3$) δ 8.34 (s, 1H), 8.13 (s, 1H), 8.00 (t, *J* = 7.6 Hz, 2H), 7.82 (t, *J* = 7.7 Hz, 1H), 7.72 (d, *J* = 2.2 Hz, 2H), 7.62–7.25 (m, 34H), 7.07–6.86 (m, 6H), 6.13 (ddd, *J* = 24.7, 7.1, 1.3 Hz, 2H). **^{13}C NMR** (126 MHz, $CDCl_3$) δ 145.0, 143.4, 142.5, 142.4, 141.7, 141.4, 141.2, 141.0, 140.0, 140.0, 136.1, 135.3, 135.0, 133.4, 132.4, 132.4, 132.0, 131.9, 131.7, 131.2, 129.2, 129.0, 128.9, 128.8, 128.7, 128.6, 128.5, 128.3, 128.2, 128.1, 127.9, 127.8, 127.7, 127.6, 127.5, 127.5, 127.5, 127.4, 127.3, 127.3, 127.1, 126.9, 126.9, 124.2, 123.7, 123.3, 121.1, 119.5, 118.3. **^{31}P NMR** (203 MHz, $CDCl_3$) δ –13.95, –14.57, –15.93, –16.57. **^{19}F NMR** (471 MHz, $CDCl_3$) δ –77.90 (s, 3F), –80.76 (t, *J* = 10.1 Hz, 3F), –112.62 (t, *J* = 13.8 Hz, 2F), –120.66 – –121.10 (m, 2F), –125.96 (dt, *J* = 15.9, 10.1 Hz, 2F), –140.23 (s, 1F), –141.07 (t, *J* = 16.4 Hz, 1F), –145.44 (s, 1F), –146.72 (d, *J* = 17.0 Hz, 1F), –153.31 (s, 1F), –154.76 (s, 1F), –155.60 (s, 1F), –156.64 (s, 1F). **HRMS (ESI)**: calculated for $C_{93}H_{48}F_{20}N_3O_8P_2S_2^-$ ([M–H]$^-$): 1840.204435, found: 1840.206000.

(*S*,*S*) –Imidodiphosphorimidate 4.2.2j (IDPi 4.2.2j):

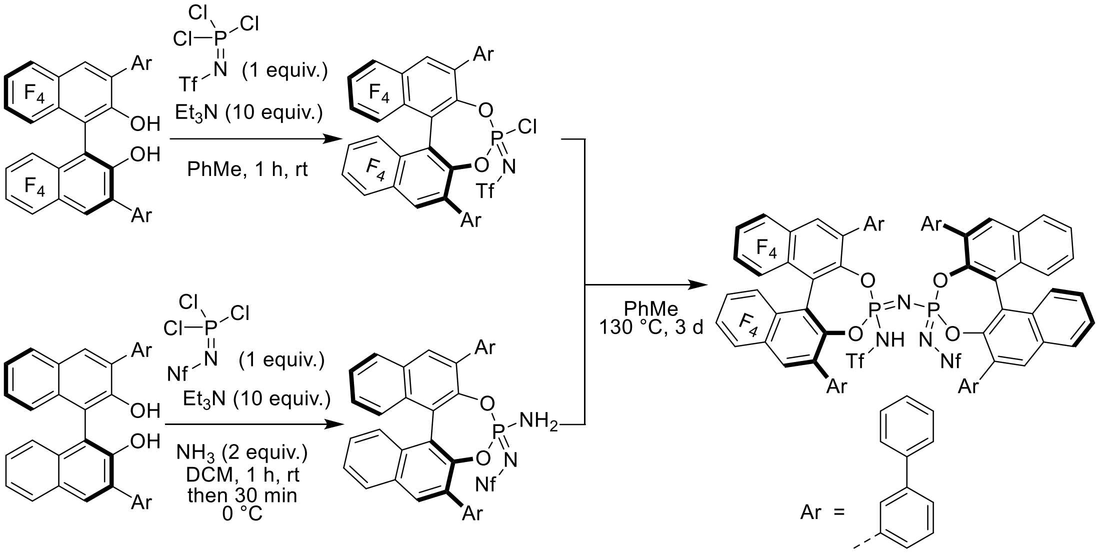

In a schlenk tube 1 a suspension of (*S*)-3,3'-di([1,1'-biphenyl]-3-yl)-5,5',6,6',7,7',8,8'-octafluoro-[1,1'-binaphthalene]-2,2'-diol (0.136 mmol, 1 equiv., 100 mg) in toluene (0.25 M) was added trifluoromethylsulfonylphosphorimidoyl trichloride (1 equiv.) and trimethylamine (10 equiv.) under argon and stirred for 1 h at room temperature. In another schlenk tube 2 (*S*)-3,3'-di([1,1'-biphenyl]-3-yl)-[1,1'-binaphthalene]-2,2'-diol (0.136 mmol, 1 equiv., 80 mg) in DCM (0.25 M) was added perfluorobutylsulfonylphosphorimidoyl trichloride (1 equiv.) and trimethylamine (10 equiv.) under argon and stirred for 1 h at room temperature. The reaction mixture was cooled to 0 °C and then NH_3 (2 equiv., 0.5 M in 1,4 dioxane) was added and stirred for 30 min at the same temperature. After that DCM, Et_3N and excess NH_3 was removed from schlenk tube 2 under high vacuum. The reaction mixture from schlenk tube 1 was transferred to schlenk tube 2 via cannula, additional toluene (0.25 M) added and schlenk tube was sealed before heating the schlenk tube 2 at 130 °C for 3 d. After cooling to room temperature, aq. HCl (10%) was added and the mixture was extracted with DCM thrice. The combined organic layer was dried over Na_2SO_4 and concentrated under reduced pressure. The crude material was purified by column chromatography on silica gel (eluent: hexane/EtOAc 90:10→75:25) to afford the desired IDPi as a salt. The product was acidified by passing over a short plug of DOWEX 50WX8 (H-form) in DCM and obtained as a yellow solid after removing the solvent (34% yield, 86 mg).

^{1}H NMR (501 MHz, $CDCl_3$) δ 8.35 (s, 1H), 8.13 (s, 1H), 8.01 (d, *J* = 8.2 Hz, 2H), 7.84 (t, *J* = 7.6 Hz, 1H), 7.74 (d, *J* = 1.9 Hz, 1H), 7.70 (t, *J* = 1.8 Hz, 1H), 7.60 (ddt, *J* = 8.0, 3.3, 1.8 Hz, 3H), 7.55 (ddd, *J* = 12.6, 6.9, 1.7 Hz, 7H), 7.50 (dd, *J* = 9.1, 2.2 Hz, 4H), 7.46 (ddt, *J* = 7.9, 6.5, 1.7 Hz, 4H), 7.43–7.38 (m, 4H), 7.38–7.34 (m, 4H), 7.34–7.27 (m, 9H), 7.04 (t, *J* = 8.0 Hz, 1H), 7.01–6.90 (m, 4H), 6.85 (t, *J* = 7.8 Hz, 1H), 6.14 (d, *J* = 7.7 Hz, 1H), 5.95 (d, *J* = 7.7 Hz, 1H). **^{13}C NMR** (126 MHz, $CDCl_3$) δ 143.4 (d, *J* = 10.6 Hz), 142.4, 141.5, 141.2, 141.1, 140.0, 135.5 (d, *J* = 13.5 Hz), 133.4 (d, *J* = 35.2 Hz), 132.7, 132.0, 131.4, 129.4, 129.1–128.5 (m), 128.5–127.4 (m), 127.4–127.1 (m), 127.1–126.7 (m), 123.9 (d, *J* = 54.2 Hz), 123.1, 119.6 (other signals not detected or observed)**.** **^{31}P NMR** (203 MHz, $CDCl_3$) δ –13.17, –13.81, –17.03, –17.67. **^{19}F NMR** (471 MHz, $CDCl_3$) δ –79.44 (s, 3F), –80.69 (t, *J* = 9.9 Hz, 3F), –109.38 – –111.92 (m, 2F), –120.74 (d, *J* = 73.6 Hz, 2F), –126.11 (dd, *J* = 14.2, 7.0 Hz, 2F), –140.12 (t, *J* = 16.8 Hz, 1F), –141.15 (t, *J* = 16.5 Hz, 1F), –145.67 (t, *J* = 16.7 Hz, 1F), –146.79 (t, *J* = 17.1 Hz, 1F), –153.37 (t, *J* = 19.3 Hz, 1F), –154.88 (t, *J* = 19.1 Hz, 1F), –155.71 (t, *J* = 19.6 Hz, 1F), –156.71 (t, *J* = 19.3 Hz, 1F). **HRMS (ESI)**: calculated for $C_{93}H_{48}F_{20}N_3O_8P_2S_2^-$ ([M–H]$^-$): 1840.20442, found: 1840.20142.

(*S*,*S*)-Imidodiphosphorimidate (IDPi 4.1.3s):

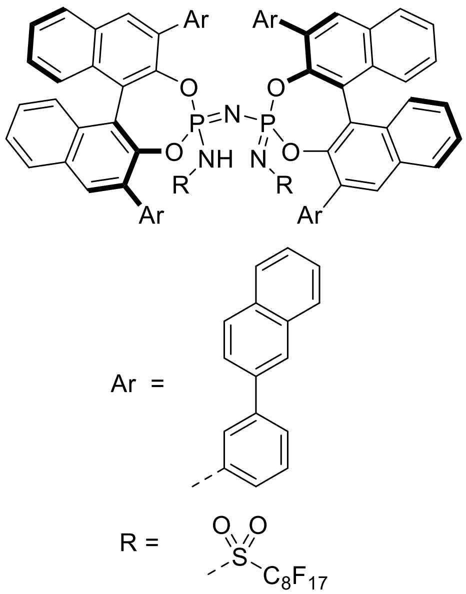

IDPi 4.3.1s was prepared following the procedure with diol (300 mg). The crude product was purified by column chromatography (eluent: pentane/DCM 50:50→30:70) to afford the desired IDPi as a salt. The product was acidified by passing over a short plug of DOWEX 50WX8 (H-form) in DCM and obtained as a white solid after removing the solvent (47% yield, 263 mg).

^{1}H NMR (501 MHz, $CDCl_3$) δ 8.04 (s, 2H), 8.01 (s, 2H), 7.92 (d, *J* = 8.2 Hz, 2H), 7.83 (td, *J* = 11.8, 4.4 Hz, 14H), 7.75–7.71 (m, 4H), 7.66 (t, *J* = 8.8 Hz, 4H), 7.62 (d, *J* = 7.8 Hz, 2H), 7.58 (t, *J* = 7.7 Hz, 2H), 7.55–7.51 (m, 4H), 7.49–7.41 (m, 14H), 7.30–7.23 (m, 5H), 7.19–7.13 (m, 4H), 7.08 (t, *J* = 7.7 Hz, 2H), 7.03 (d, *J* = 7.8 Hz, 2H), 6.64 (d, *J* = 7.7 Hz, 2H). **^{13}C NMR** (126 MHz, $CDCl_3$) δ 143.9, 143.1, 142.2, 141.6, 138.9, 137.8, 136.5, 135.9, 133.8, 133.5, 133.3, 132.8 (d, *J* = 3.2 Hz), 132.1, 132.0–131.6 (m), 131.4, 129.4 (d, *J* = 18.8 Hz), 128.9, 128.5–128.0 (m), 127.9–127.2 (m), 126.8 (d, *J* = 27.4 Hz), 126.5–125.6 (m), 123.6, 121.7 (other signals not detected or observed). **^{31}P NMR** (203 MHz, $CDCl_3$) δ –16.60. **^{19}F NMR** (471 MHz, $CDCl_3$) δ –80.78 (d, *J* = 10.6 Hz, 3F), –111.47 – –112.03 (m, 2F), –119.79 – –120.25 (m, 2F), –121.50 – –122.29 (m, 6F), –122.81 (s, 2F), –126.15 (d, *J* = 16.0 Hz, 2F). **HRMS (ESI)**: calculated for $C_{120}H_{64}F_{34}N_3O_8P_2S_2^-$ ([M–H]$^-$): 2446.307284, found: 2446.308180.

(*S*,*S*)-Imidodiphosphorimidate (IDPi 4.1.3af):

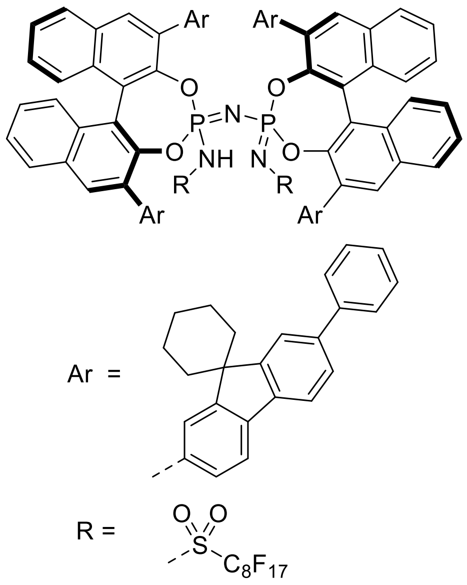

IDPi 4.1.3af was prepared following the procedure with diol (520 mg). The crude product was purified by column chromatography (eluent: hexane/DCM 70:30→50:50) to afford the desired IDPi as a salt. The product was acidified by passing over a short plug of DOWEX 50WX8 (H-form) in DCM and obtained as a white solid after removing the solvent (60% yield, 500 mg).

^{1}H NMR (501 MHz, $CDCl_3$) δ 8.11–8.04 (m, 4H), 8.01–7.85 (m, 8H), 7.81–7.77 (m, 2H), 7.75–7.66 (m, 6H), 7.62–7.52 (m, 12H), 7.48–7.44 (m, 2H), 7.44–7.27 (m, 22H), 6.96 (d, *J* = 3.3 Hz, 2H), 6.86–6.72 (m, 4H), 6.56–6.47 (m, 2H), 2.05–1.35 (m, 40H). **^{13}C NMR** (126 MHz, $CDCl_3$) δ 154.5, 154.4, 154.0, 153.9, 144.4, 143.2, 142.3, 141.9, 140.3, 139.8, 139.4, 139.0, 138.7, 138.5, 135.1, 134.8, 133.9, 133.8, 132.4, 132.1, 131.8, 131.3, 129.7, 129.3, 128.9, 128.7, 127.5, 127.5, 127.3, 127.2, 127.1, 126.9, 126.8, 126.5, 125.8, 124.3, 124.0, 123.6, 123.2, 121.8, 120.5, 119.8, 118.9, 118.7, 50.7, 35.9, 35.3, 35.0, 25.8, 25.4, 23.3, 22.7, 22.6 (other signals not detected or observed). **^{31}P NMR** (203 MHz, $CDCl_3$) δ –16.44. **^{19}F NMR** (471 MHz, $CDCl_3$) δ –80.79 (t, *J* = 10.1 Hz, 3F), –110.35 – –112.27 (m, 2F), –119.73 – –120.20 (m, 2F), –121.39 (td, *J* = 15.9, 9.5 Hz, 2F), –121.70 – –122.14 (m, 4F), –122.70 (tt, *J* = 14.8, 6.4 Hz, 2F), –125.94 – –126.43 (m, 2F). **HRMS (ESI)**: calculated for $C_{152}H_{104}F_{34}N_3O_8P_2S_2^-$ ([M–H]$^-$): 2870.620284, found: 2870.619720.

(*S*,*S*)-Imidodiphosphorimidate (IDPi 4.3.3j):

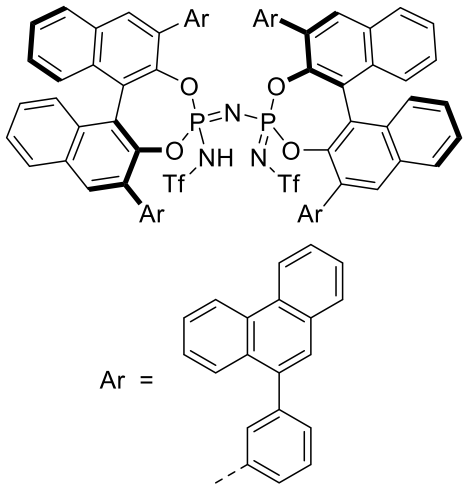

IDPi 4.3.3j was prepared following the procedure with diol (600 mg). The crude product was purified by column chromatography (eluent: hexane/EtOAc 80:20→65:35) to afford the desired IDPi as a salt. The product was acidified by passing over a short plug of DOWEX 50WX8 (H-form) in DCM and obtained as a white solid after removing the solvent (70% yield, 520 mg).

^{1}H NMR (501 MHz, $CDCl_3$) δ 8.86–8.55 (m, 8H), 8.52–5.51 (m, 64H). **^{13}C NMR** (126 MHz, $CDCl_3$) δ 143.7, 142.6, 141.7, 140.7, 138.6, 138.0, 135.9, 133.2, 132.5, 132.0, 131.8, 131.6, 131.5, 131.1, 130.7, 130.6, 130.1, 129.9, 129.7, 129.3, 129.1, 128.8, 128.8, 128.5, 128.0, 127.1, 126.9, 126.6, 126.5, 126.4, 126.3, 123.5, 123.0, 122.5, 122.3, 122.1, 120.6, 118.0 (other signals not detected or observed). **^{31}P NMR** (203 MHz, $CDCl_3$) δ –16.93. **^{19}F NMR** (471 MHz, $CDCl_3$) δ –77.84. **HRMS (ESI)**: calculated for $C_{122}H_{72}F_6N_3O_8P_2S_2^-$ ([M–H]$^-$): 1946.414586, found: 1946.414586.

(*S*,*S*)-Imidodiphosphorimidate (IDPi 4.3.3p):

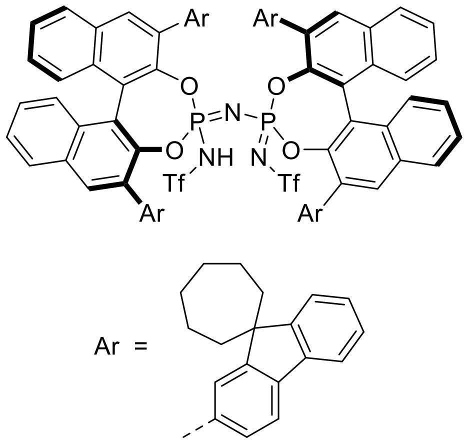

IDPi 4.3.3p was prepared following the procedure with diol (200 mg). The crude product was purified by column chromatography (eluent: hexane/EtOAc 90:10→75:25) to afford the desired IDPi as a salt. The product was acidified by passing over a short plug of DOWEX 50WX8 (H-form) in DCM and obtained as off-white amorphous solid after removing the solvent (41% yield, 102 mg).

^{1}H NMR (501 MHz, CD_2Cl_2) δ 8.16 (s, 2H), 8.12 (d, *J* = 8.4 Hz, 2H), 8.04 (d, *J* = 8.2 Hz, 2H), 7.90–7.81 (m, 4H), 7.72 (d, *J* = 1.7 Hz, 2H), 7.70–7.59 (m, 6H), 7.52 (dq, *J* = 7.9, 2.8 Hz, 6H), 7.48–7.39 (m, 4H), 7.38–7.33 (m, 2H), 7.31 (d, *J* = 7.9 Hz, 2H), 7.28–7.17 (m, 10H), 6.65 (d, *J* = 8.0 Hz, 2H), 6.61–6.50 (m, 2H), 6.15 (d, *J* = 8.0 Hz, 2H), 2.13–1.84 (m, 18H), 1.80–1.59 (m, 28H), 1.53–1.46 (m, 2H). **^{13}C NMR** (126 MHz, CD_2Cl_2) δ 156.2, 155.9, 155.8, 144.3, 143.5, 139.4, 139.0, 138.9, 135.5, 135.1, 134.8, 134.6, 132.8, 132.5, 132.4, 132.3, 132.2, 132.0, 129.8, 129.3, 129.2, 129.0, 128.1, 128.1, 127.7, 127.5, 127.4, 127.4, 127.2, 125.0, 124.7, 124.3, 123.9, 123.8, 122.5, 120.4, 119.8, 119.4, 119.0, 40.4, 40.3, 39.5, 39.0, 32.5, 32.5, 32.1, 31.8, 26.1, 25.9, 25.8, 25.8 (other signals not detected or observed). **^{31}P NMR** (203 MHz, $CDCl_3$) δ –16.76. **^{19}F NMR** (471 MHz, $CDCl_3$) δ –78.69. **HRMS (ESI)**: calculated for $C_{118}H_{96}F_6N_3O_8P_2S_2^-$ ([M–H]$^-$): 1922.602386, found: 1922.601990.

(*S*,*S*)-Imidodiphosphorimidate (IDPi 4.1.3m):

IDPi 4.1.3m was prepared following the procedure with diol (100 mg). The crude product was purified by column chromatography (eluent: hexane/EtOAc 95:5→85:15) to afford the desired

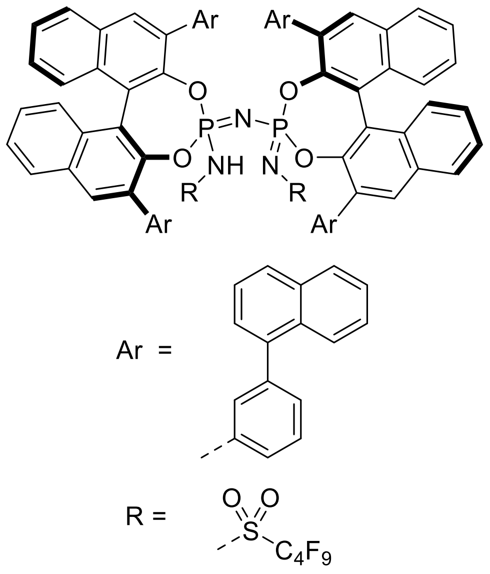

IDPi as a salt. The product was acidified by passing over a short plug of DOWEX 50WX8 (H-form) in DCM and obtained as a white solid after removing the solvent (31% yield, 47 mg).

^{1}H NMR (501 MHz, CD$_2$Cl$_2$) δ 8.38 (s, 2H), 8.09 (dd, J = 15.8, 8.4 Hz, 4H), 8.03–7.83 (m, 9H), 7.77 (d, J = 8.3 Hz, 2H), 7.69–7.29 (m, 32H), 7.28–7.10 (m, 5H), 7.02 (d, J = 8.6 Hz, 2H), 6.90 (d, J = 27.9 Hz, 6H), 6.38 (s, 2H). **^{19}F NMR** (471 MHz, CD2Cl2) δ –80.92 (t, J = 9.6 Hz), –111.05 – –112.45 (m), –120.95 (h, J = 9.6 Hz), –125.77 (tt, J = 18.2, 10.7 Hz). **^{31}P NMR** (203 MHz, CD$_2$Cl$_2$) δ –17.45. **HRMS (ESI)**: calculated for $C_{112}H_{64}F_{18}N_3O_8P_2S_2^-$ ([M–H]$^-$): 2046.33281, found: 2046.33193.

(*S*,*S*)-Imidodiphosphorimidate (IDPi 4.1.3n):

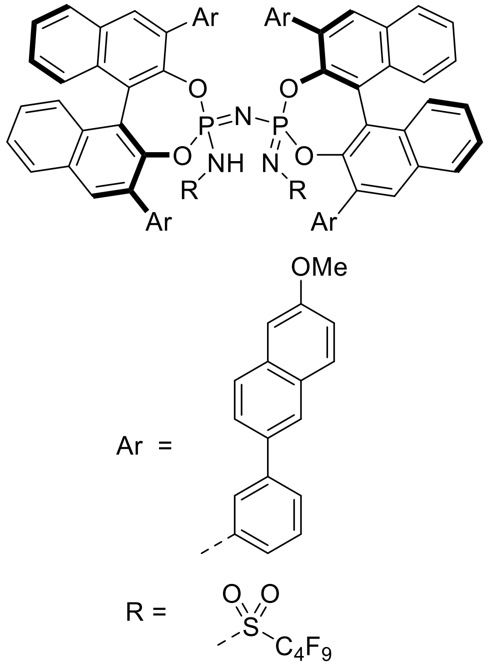

IDPi 4.1.3n was prepared following the procedure with diol (100 mg). The crude product was purified by column chromatography (first column eluent: hexane/Acetone 100:0→90:10; second column eluent: MTBE/DCM 0:100→2:98) to afford the desired IDPi as a salt. The product was acidified by passing over a short plug of DOWEX 50WX8 (H-form) in DCM and obtained as a white solid after removing the solvent (24% yield, 34 mg).

^{1}H NMR (501 MHz, CD$_2$Cl$_2$) δ 8.07–7.98 (m, 4H), 7.93–7.88 (m, 2H), 7.88–7.83 (m, 6H), 7.82–7.74 (m, 6H), 7.70 (d, J = 1.8 Hz, 2H), 7.61 (ddt, J = 14.7, 8.0, 1.5 Hz, 6H), 7.56 (d, J = 8.5 Hz, 2H), 7.53–7.48 (m, 4H), 7.48–7.43 (m, 3H), 7.40 (d, J = 8.5 Hz, 2H), 7.30 (q, J = 1.6 Hz, 2H), 7.29–7.19 (m, 6H), 7.17 (dd, J = 7.2, 2.5 Hz, 3H), 7.15–7.12 (m, 4H), 7.10 (dd, J = 8.9, 2.5 Hz, 2H), 7.06 (d, J = 2.6 Hz, 2H), 7.00 (dt, J = 8.2, 1.4 Hz, 2H), 6.87 (d, J = 7.8 Hz, 2H), 3.92 (d, J = 3.7 Hz, 12H). **^{19}F NMR** (471 MHz, CD$_2$Cl^2) δ −81.09 (t, J = 9.8 Hz), −111.94 (dt, J = 56.8, 13.7 Hz), −121.17 (dt, J = 36.3, 9.8 Hz), −125.69 – −126.57 (m). **^{31}P NMR** (203 MHz, CD$_2$Cl$_2$) δ −17.32. **HRMS (ESI)**: calculated for $C_{116}H_{72}F_{18}N_3O_{12}P_2S_2^-$ ([M–H]$^-$): 2166.37507, found: 2166.37368.

(*S*,*S*)-Imidodiphosphorimidate (IDPi 4.1.3o):

IDPi 4.1.3o was prepared following the procedure with diol (110 mg). The crude product was purified by column chromatography (eluent: pentane/EtOAc 95:5→80:20) to afford the desired IDPi as a salt. The product was acidified by passing over a short plug of DOWEX 50WX8 (H-form) in DCM and obtained as a white solid after removing the solvent (35% yield, 50 mg).

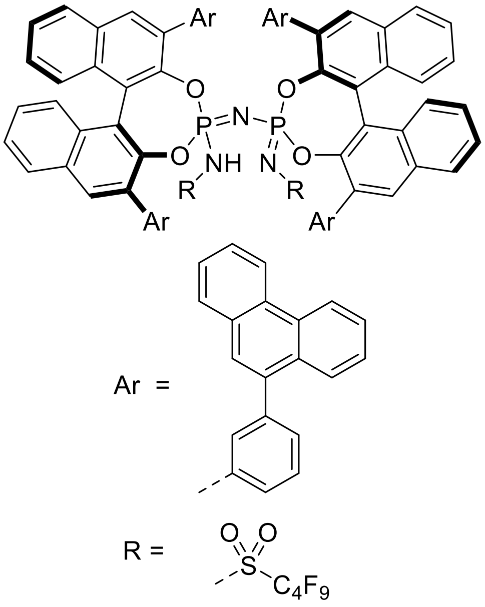

^{1}**H NMR** (600 MHz, CDCl$_3$) δ 8.87–8.69 (m, 6H), 8.60 (d, J = 8.3 Hz, 2H), 8.39–8.14 (m, 4H), 7.96 (d, J = 29.4 Hz, 6H), 7.86–7.25 (m, 43H), 6.98 (d, J = 81.8 Hz, 6H), 6.45 (s, 2H), 5.93 (d, J = 149.6 Hz, 3H). ^{13}**C NMR** (151 MHz, CDCl$_3$) δ 135.6 (d, J = 84.7 Hz), 132.9, 132.4, 132.0 (d, J = 10.7 Hz), 131.7–130.5 (m), 130.4–129.9 (m), 129.7, 129.4–128.3 (m), 128.0, 127.5–125.7 (m), 123.5, 123.1, 122.8, 122.2 (d, J = 33.4 Hz), 118.1 (d, J = 33.0 Hz), 116.3 (t, J = 33.1 Hz), 113.7 (t, J = 34.6 Hz), 112.4–111.5 (m), 110.3 (t, J = 31.5 Hz), 108.3 (t, J = 31.9 Hz) (other signals not detected or observed). ^{19}**F NMR** (565 MHz, CDCl$_3$) δ −80.73, −111.62, −120.85, −125.77. ^{31}**P NMR** (243 MHz, CDCl$_3$) δ −17.23. **HRMS (ESI)**: calculated for $C_{128}H_{72}F_{18}N_3O_8P_2S_2^-$ ([M–H]$^-$): 2246.39541, found: 2246.39551.

(*S*,*S*)-Imidodiphosphorimidate (IDPi 4.1.3p):

IDPi 4.1.3p was prepared following the procedure with diol (88 mg). The crude product was purified by column chromatography (eluent: Toluene/DCM 80:20→60:40) to afford the desired

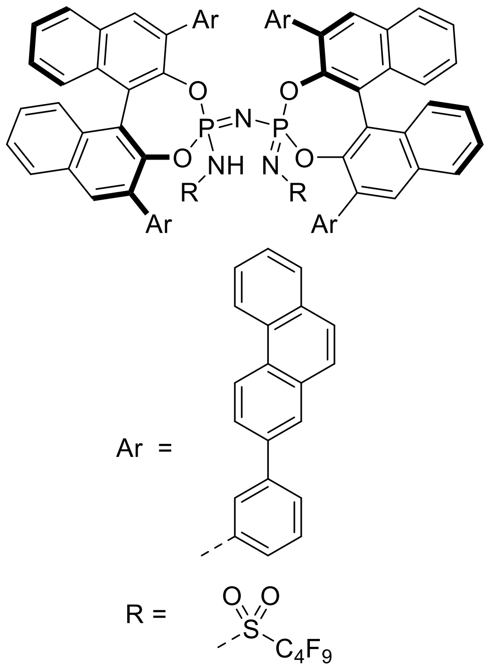

IDPi as a salt. The product was acidified by passing over a short plug of DOWEX 50WX8 (H-form) in DCM and obtained as a white solid after removing the solvent (43% yield, 53 mg).

^{1}H NMR (501 MHz, CD_2Cl_2) δ 8.64 (d, J = 8.7 Hz, 2H), 8.59 (d, J = 8.2 Hz, 2H), 8.46 (d, J = 8.1 Hz, 2H), 8.34 (d, J = 8.6 Hz, 2H), 8.06 (d, J = 2.1 Hz, 2H), 7.89–7.84 (m, 4H), 7.80 (ddt, J = 12.9, 10.4, 4.3 Hz, 10H), 7.75–7.72 (m, 2H), 7.71–7.64 (m, 4H), 7.63–7.51 (m, 16H), 7.51–7.45 (m, 4H), 7.42 (d, J = 8.9 Hz, 2H), 7.33 (d, J = 8.5 Hz, 2H), 7.24 (s, 2H), 7.19 (ddd, J = 8.8, 6.7, 3.7 Hz, 4H), 7.14–7.06 (m, 6H), 7.03 (s, 2H), 6.96 (d, J = 7.9 Hz, 2H), 6.86 (d, J = 7.9 Hz, 2H). **^{19}F NMR** (471 MHz, CD_2Cl_2) δ –81.11 (t, J = 10.0 Hz), −111.88 (dt, J = 43.5, 15.1 Hz), −120.86 – −121.41 (m), −126.08 (qd, J = 14.7, 6.6 Hz). **^{31}P NMR** (203 MHz, CD_2Cl_2) δ –17.19. **HRMS (ESI)**: calculated for $C_{128}H_{72}F_{18}N_3O_8P_2S_2^-$ ([M–H]$^-$): 2246.39541, found: 2246.39672.

(*S*,*S*)-Imidodiphosphorimidate (IDPi 4.1.3q):

IDPi 4.1.3q was prepared following the procedure with diol (100 mg). The crude product was purified by column chromatography (eluent: Toluene/DCM 80:20→60:40) to afford the desired IDPi as a salt. The product was acidified by passing over a short plug of DOWEX 50WX8 (H-form) in DCM and obtained as a white solid after removing the solvent (40% yield, 56 mg).

^{1}H NMR (501 MHz, CD_2Cl_2) δ 8.93 (d, J = 1.7 Hz, 2H), 8.78–8.71 (m, 2H), 8.58 (s, 2H), 8.15 (d, J = 8.3 Hz, 2H), 8.04–7.94 (m, 4H), 7.90 (dd, J = 5.3, 3.0 Hz, 8H), 7.83–7.74 (m, 12H), 7.69 (dd, J = 8.4, 4.2 Hz, 4H), 7.63–7.54 (m, 10H), 7.48–7.41 (m, 4H), 7.40–7.35 (m, 4H), 7.31 (dt, J = 17.0, 7.9 Hz, 4H), 7.26–7.11 (m, 10H), 7.11–7.04 (m, 4H). **^{19}F NMR** (471 MHz, CD_2Cl_2) δ –81.03 (t, J = 10.0 Hz), –111.86 (dt, J = 26.3, 14.8 Hz), –121.14 (dd, J = 46.9, 11.3 Hz), –126.04 (dtd, J = 20.2, 12.8, 6.0 Hz). **^{31}P NMR** (203 MHz, CD_2Cl_2) δ –17.82.

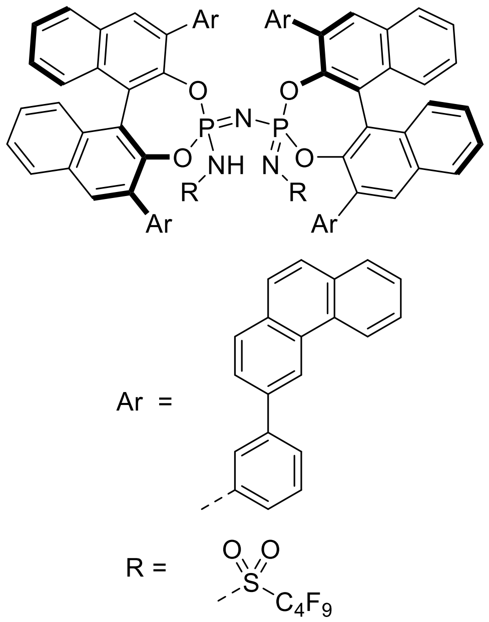

(*S*,*S*)-Imidodiphosphorimidate (IDPi 4.1.3r):

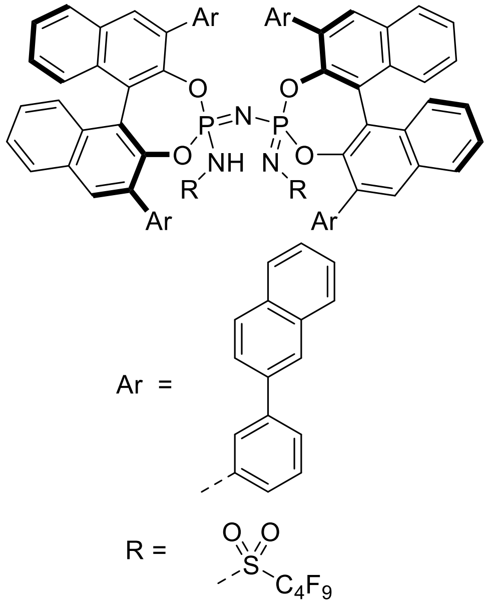

IDPi 4.1.3r was prepared following the procedure with diol (100 mg). The crude product was purified by column chromatography (eluent: Toluene/DCM 80:20→60:40) to afford the desired IDPi as a salt. The product was acidified by passing over a short plug of DOWEX 50WX8 (H-form) in DCM and obtained as a white solid after removing the solvent (40% yield, 56 mg).

^{1}H NMR (501 MHz, CD_2Cl_2) δ 8.10 (d, J = 1.8 Hz, 2H), 8.01 (s, 2H), 7.94–7.73 (m, 21H), 7.68–7.58 (m, 10H), 7.47 (dddd, J = 15.5, 13.6, 6.6, 3.2 Hz, 13H), 7.38 (d, J = 8.5 Hz, 2H), 7.33 (s, 2H), 7.27 (q, J = 7.9 Hz, 4H), 7.21 (d, J = 8.4 Hz, 2H), 7.18–7.11 (m, 4H), 7.03 (d, J = 7.9 Hz, 2H). **^{13}C NMR** (126 MHz, CD_2Cl_2) δ 138.1, 134.1, 133.8, 133.1, 133.0, 132.2 (d, J = 29.9 Hz), 131.8, 130.0, 129.6, 129.2 (d, J = 30.1 Hz), 128.8–128.2 (m), 127.9 (d, J = 12.8 Hz), 127.7, 127.6–126.8 (m), 126.8–126.4 (m), 126.4–126.0 (m), 123.7 (other signals not detected or observed). **^{19}F NMR** (471 MHz, CD_2Cl_2) δ –81.13 (t, J = 10.3 Hz), –111.19 – –112.69 (m), –121.00 – –121.55 (m), –126.17 (dt, J = 23.2, 12.7 Hz) **^{31}P NMR** (203 MHz, CD_2Cl_2) δ –17.26. **HRMS (ESI)**: calculated for $C_{112}H_{64}F_{18}N_3O_8P_2S_2^-$ ([M–H]$^-$): 2046.33281, found: 2046.33268.

(*S*,*S*)-Imidodiphosphorimidate (IDPi 4.2.2f):

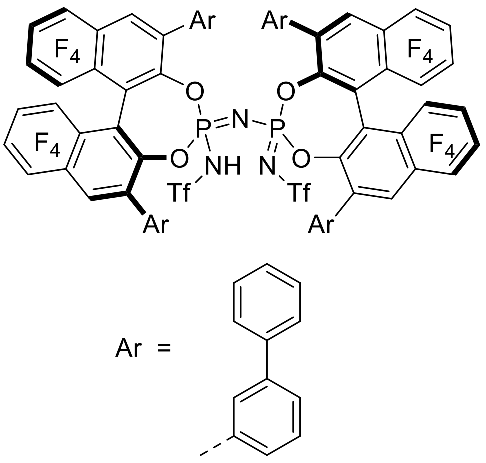

IDPi 4.2.2f was prepared following the procedure with diol (105 mg). The crude product was purified by column chromatography (eluent: hexanes/EtOAc 95:5→70:30) to afford the desired IDPi as a salt. The product was acidified by passing over a short plug of DOWEX 50WX8 (H-form) in DCM and obtained as a white solid after removing the solvent (24% yield, 30 mg).

^{1}H NMR (501 MHz, $CDCl_3$) δ 8.35 (s, 2H), 7.77–7.67 (m, 4H), 7.67–7.51 (m, 12H), 7.50–7.45 (m, 2H), 7.44–7.28 (m, 12H), 7.05 (t, J = 7.7 Hz, 2H), 6.94 (dd, J = 11.8, 7.4 Hz, 4H), 6.05 (d, J = 7.8 Hz, 2H). **^{19}F NMR** (471 MHz, $CDCl_3$) δ −78.40, −140.34 (t, J = 15.9 Hz), −140.79 (t, J = 16.4 Hz), −146.26 (t, J = 16.7 Hz), −146.41 (q, J = 12.3 Hz), −152.14 (t, J = 18.4 Hz), −153.53 – −154.24 (m), −155.95 (t, J = 18.7 Hz). **^{31}P NMR** (203 MHz, $CDCl_3$) δ −13.94.

(*S*,*S*)-Imidodiphosphorimidate (IDPi 4.2.2g):

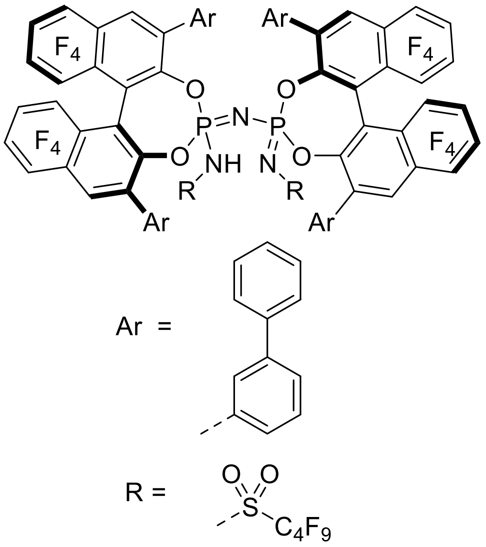

IDPi 4.2.2g was prepared following the procedure with diol (370 mg). The crude product was purified by column chromatography (first column eluent: Acetone/Et_2O 5:95→15:85; second column eluent: Acetone/pentane 0:100→20:80) to afford the desired IDPi as a salt. The product was acidified by passing over a short plug of DOWEX 50WX8 (H-form) in DCM and obtained as a white solid after removing the solvent (22% yield, 120 mg).

^{1}H NMR (501 MHz, CD_2Cl_2) δ 8.38 (s, 2H), 7.75 (d, J = 7.3 Hz, 4H), 7.62–7.55 (m, 8H), 7.54–7.49 (m, 4H), 7.45–7.38 (m, 7H), 7.32 (qd, J = 6.6, 5.0 Hz, 8H), 7.11 (t, J = 7.9 Hz, 2H), 6.99 (d, J = 4.9 Hz, 4H), 6.38 (d, J = 7.7 Hz, 2H). **^{19}F NMR** (471 MHz, CD_2Cl_2) δ −81.12 (t, J = 10.1 Hz), −112.18 (dd, J = 40.5, 17.5 Hz), −121.27, −125.70 – −126.33 (m), −140.71, −141.33 (t, J = 16.4 Hz), −146.91 – −147.74 (m), −153.67, −155.38 –

−156.26 (m), −157.75. **^{31}P NMR** (203 MHz, CD_2Cl_2) δ -12.51. **HRMS (ESI)**: calculated for $C_{96}H_{40}F_{34}N_3O_8P_2S_2^-$ ($[M–H]^-$): 2134.11946, found: 2134.12009.

7.3.2 Synthesis and Characterization of C–O Bond Products

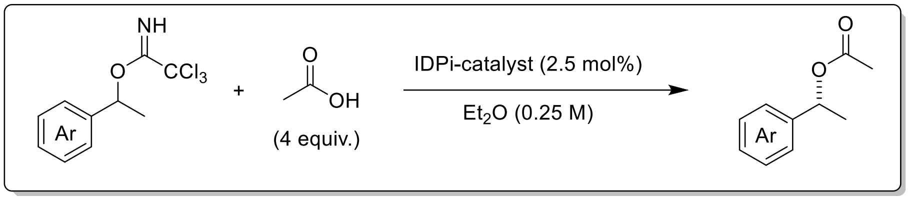

General Procedure A: IDPi-catalyzed C–O bond formation:

An oven-dried glass vial (10 mL) was charged with (*S*,*S*)-IDPi catalyst (2.5 mol%), carboxylic acid (4 equiv.), dry Et_2O, cooled to the reaction temperature (indicated in each case) and then substrate (trichloroacetimidate) (0.25 mmol) was added as a stock solution slowly under argon. The reaction mixture was stirred at the reaction temperature for a certain time (indicated in each case). The reaction was stopped by adding wet Et_3N (4.5 equiv.) at the reaction temperature and warmed to room temperature, solvent was removed under reduced pressure. Corresponding product was purified by flash column chromatography on silica gel (pentane/Et_2O mixtures).

(*R*)-1-phenylethyl acetate (4.1.4a)

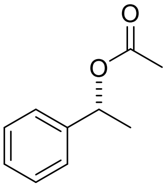

Prepared following General Procedure A, from 1-phenylethyl 2,2,2-trichloroacetimidate (**4.1.1a**, 0.25 mmol), acetic acid (1 mmol, 4 equiv.), with (*S*,*S*)-catalyst (**4.1.3s**, 2.5 mol%), in dry Et_2O (0.25 M), at –90 °C for 5 d. Purification by flash column chromatography (eluent: pentane/Et_2O 100:0→98:2) to give **4.1.4a** as a colorless liquid (30 mg, 73%, er = 95:5).

^{1}H NMR (501 MHz, CD_2Cl_2) δ 7.38–7.26 (m, 5H), 5.83 (q, *J* = 6.6 Hz, 1H), 2.05 (s, 3H), 1.52 (d, *J* = 6.6 Hz, 3H). **^{13}C NMR** (126 MHz, CD_2Cl_2) δ 170.5, 142.5, 128.8, 128.1, 126.4, 72.6, 22.5, 21.5. **HRMS (EI)**: calculated for $C_{10}H_{12}O_2^+$ (M^+): 164.083180, found: 164.083300. $[\boldsymbol{\alpha}]_D^{25}$ = +90.50 (*c* = 0.4, $CHCl_3$). (Lit. [133] $[\boldsymbol{\alpha}]_D^{20}$ = +82.30 (*c* = 1.1, $CHCl_3$)).

GC: Column: 25.0 m Lipodex G, Temperature: 220/80 1/min 5min iso/350, Gas: 0.5 bar He(g), t_R (minor) = 14.24 min., t_R (major) = 15.85 min., er = 95:5.

(*R*)-1-(*m*-tolyl)ethyl acetate (4.1.4g)

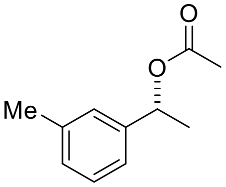

Prepared following General Procedure A, from 1-(*m*-tolyl)ethyl 2,2,2-trichloroacetimidate (**4.1.1g**, 0.25 mmol), acetic acid (1 mmol, 4 equiv.), with (*S*,*S*)-catalyst (**4.1.3s**, 2.5 mol%), in dry Et_2O (0.25 M), at –90 °C for 5 d.

Purification by flash column chromatography (eluent: pentane/Et_2O 100:0→98:2) to give **4.1.4g** as a colorless liquid (35 mg, 78%, er = 93.5:6.5).

^{1}H NMR (501 MHz, CD_2Cl_2) δ 7.23 (t, *J* = 7.6 Hz, 1H), 7.16 (dq, *J* = 2.4, 1.2 Hz, 1H), 7.15–7.08 (m, 2H), 5.78 (q, *J* = 6.6 Hz, 1H), 2.35 (d, *J* = 0.7 Hz, 3H), 2.04 (s, 3H), 1.50 (d, *J* = 6.6 Hz, 3H). **^{13}C NMR** (126 MHz, CD_2Cl_2) δ 170.5, 142.4, 138.6, 128.8, 128.7, 127.1, 123.4, 72.6, 22.5, 21.54, 21.51. **HRMS (EI)**: calculated for $C_{11}H_{14}O_2^+$ (M^+): 178.098830, found: 178.098760. $[\boldsymbol{\alpha}]_{\boldsymbol{D}}^{\mathbf{25}}$ = +83.43 (*c* = 0.4, $CHCl_3$). (Lit.[134] $[\boldsymbol{\alpha}]_{\boldsymbol{D}}^{\mathbf{26}}$ = +215.00 (*c* = 1.0, $CHCl_3$)).

GC: Column: 25.0 m Lipodex G, Temperature: 110/80 1/min 220/110 5/min 5min iso/350, Gas: 0.4 bar He(g), t_R (minor) = 20.52 min., t_R (major) = 22.37 min., er = 93.5:6.5.

(*R*)-1-(3-methoxyphenyl)ethyl acetate (4.1.4h)

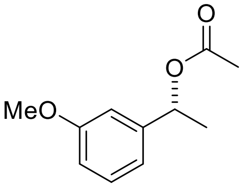

Prepared following General Procedure A, from 1-(3-methoxyphenyl)ethyl 2,2,2-trichloroacetimidate (**4.1.1h**, 0.25 mmol), acetic acid (1 mmol, 4 equiv.), with (*S*,*S*)-catalyst (**4.1.3s**, 2.5 mol%), in dry Et_2O (0.25 M), at –90 °C for 5 d. Purification by flash column chromatography (eluent: pentane/Et_2O 100:0→97:3) to give **4.1.4h** as a colorless liquid (26 mg, 53%, er = 94.5:5.5).

^{1}H NMR (501 MHz, CD_2Cl_2) δ 7.26 (t, *J* = 7.9 Hz, 1H), 6.92 (ddt, *J* = 7.6, 1.5, 0.7 Hz, 1H), 6.88 (t, *J* = 2.1 Hz, 1H), 6.82 (ddd, *J* = 8.2, 2.7, 0.9 Hz, 1H), 5.79 (q, *J* = 6.6 Hz, 1H), 3.80 (s, 3H), 2.05 (s, 3H), 1.50 (d, *J* = 6.6 Hz, 3H). **^{13}C NMR** (126 MHz, CD_2Cl_2) δ 170.5, 160.2, 144.2, 129.9, 118.5, 113.3, 112.1, 72.5, 55.6, 22.5, 21.5. **HRMS (EI)** calculated for $C_{11}H_{14}O_3^+$ (M^+):194.093580, found: 194.093745. $[\boldsymbol{\alpha}]_{\boldsymbol{D}}^{\mathbf{25}}$ = +85.46 (*c* = 0.3, $CHCl_3$).

GC: Column: 25.0 m Lipodex G, Temperature: 110/80 1/min 220/110 5/min 5min iso/350, Gas: 0.4 bar He(g), t_R (minor) = 34.20 min., t_R (major) = 35.01 min., er = 94.5:5.5.

(*R*)-1-(4-fluorophenyl)ethyl acetate (4.1.4b)

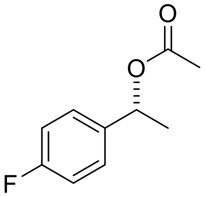

Prepared following General Procedure A, from 1-(4-fluorophenyl)ethyl 2,2,2-trichloroacetimidate (**4.1.1b**, 0.25 mmol), acetic acid (1 mmol, 4 equiv.), with (*S*,*S*)-catalyst (**4.1.3s**, 2.5 mol%), in dry Et2O (0.25 M), at –90 °C for 5 d. Purification by flash column chromatography (eluent: pentane/Et_2O 100:0→98:2) to give **4.1.4b** as a colorless liquid (35 mg, 77%, er = 93.5:6.5).

^{1}H NMR (501 MHz, CD_2Cl_2) δ 7.37–7.31 (m, 2H), 7.08–7.00 (m, 2H), 5.82 (q, *J* = 6.6 Hz, 1H), 2.03 (s, 3H), 1.50 (d, *J* = 6.6 Hz, 3H). **^{13}C NMR** (126 MHz, CD_2Cl_2) δ 170.4, 162.7 (d, *J* = 245.3 Hz), 138.4 (d, *J* = 3.2 Hz), 128.3 (d, *J* = 8.5 Hz), 115.6 (d, *J* = 21.7 Hz), 71.9, 22.4, 21.5. **^{19}F NMR** (471 MHz, CD_2Cl_2) δ –115.46. **HRMS (ESI)**: calculated for $C_{10}H_{11}O_2FNa^+$ ($[M+Na]^+$):205.063527, found: 205.063700. $[\boldsymbol{\alpha}]_{\boldsymbol{D}}^{\mathbf{25}}$ = +84.74 (*c* = 0.4, $CHCl_3$).

GC: Column: 25.0 m Lipodex G, Temperature: 110/80 1/min 220/110 5/min 5min iso/350, Gas: 0.5 bar He(g), t_R (minor) = 15.23 min., t_R (major) = 16.83 min., er = 93.5:6.5.

(*R*)-1-(*p*-tolyl)ethyl propionate (4.1.6c)

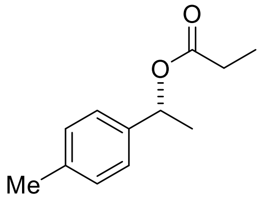

Prepared following General Procedure A, from 1-(*p*-tolyl)ethyl 2,2,2-trichloroacetimidate (**4.1.1c**, 0.25 mmol), propionic acid (1 mmol, 4 equiv.), with (*S*,*S*)-catalyst (**4.1.3af**, 2.5 mol%), in dry Et_2O (0.25 M), at –80 °C for 3 d. Purification by flash column chromatography (eluent: pentane/Et_2O 100:0→98:2) to give **4.1.6c** as a colorless liquid (41 mg, 85%, er = 96:4).

^{1}H NMR (501 MHz, CD_2Cl_2) δ 7.26–7.20 (m, 2H), 7.15 (d, *J* = 7.8 Hz, 2H), 5.80 (q, *J* = 6.6 Hz, 1H), 2.38–2.26 (m, 2H), 2.33 (s, $3ArCH_3$), 1.49 (d, *J* = 6.6 Hz, 3H), 1.10 (t, *J* = 7.6 Hz, 3H). **^{13}C NMR** (126 MHz, CD_2Cl_2) δ 173.9, 139.6, 137.9, 129.4, 126.3, 72.3, 28.2, 22.4, 21.2, 9.3. **HRMS (EI)**: calculated for $C_{12}H_{16}O_2^+$ (M^+: 192.114480, found: 192.114560. $[\boldsymbol{\alpha}]_{\boldsymbol{D}}^{\mathbf{25}}$ = +100.98 (*c* = 0.3, $CHCl_3$).

GC: Column: 25.0 m Lipodex G, Temperature: 110/80 1/min 220/110 5/min 5min iso/350, Gas: 0.5 bar He(g), t_R (minor) = 28.96 min., t_R (major) = 30.15 min., er = 96:4.

(*R*)-1-(4-propylphenyl)ethyl propionate (4.1.7c)

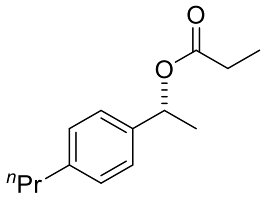

Prepared following General Procedure A, from 1-(4-propylphenyl)ethyl 2,2,2-trichloroacetimidate (**4.1.1j**, 0.25 mmol), propionic acid (1 mmol, 4 equiv.), with (*S*,*S*)-catalyst (**4.1.3af**, 2.5 mol%), in dry Et_2O (0.25 M), at –80 °C for 3 d. Purification by flash column chromatography (eluent: pentane/Et_2O 100:0→98:2) to give **4.1.7c** as a colorless liquid (48 mg, 82%, er = 93.5:6.5).

^{1}H NMR (501 MHz, CD_2Cl_2) δ 7.29–7.23 (m, 2H), 7.21–7.16 (m, 2H), 5.82 (q, *J* = 6.6 Hz, 1H), 2.64 (q, *J* = 7.6 Hz, 2H), 2.32 (qd, *J* = 7.6, 4.4 Hz, 2H), 1.50 (d, *J* = 6.5 Hz, 3H), 1.22 (t, *J* = 7.6 Hz, 3H), 1.10 (t, *J* = 7.6 Hz, 3H). **^{13}C NMR** (126 MHz, CD_2Cl_2) δ 173.9, 144.4, 139.9, 128.3, 126.4, 72.3, 28.9, 28.2, 22.4, 15.8, 9.3. **HRMS (EI)**: calculated for $C_{14}H_{20}O_2^+$ (M^+: 220.145780, found: 220.145750. $[\alpha]_D^{25}$ = +79.44 (*c* = 0.4, $CHCl_3$).

HPLC: chiral pack OJ-3R column, acetonitrile/water 50:50, 1 mL/min, 25 °C, 254 nm, t_R (major) = 14.75 min., t_R (minor) = 18.44 min., er = 93.5:6.5.

(*R*)-1-(4-butylphenyl)ethyl propionate (4.1.8c)

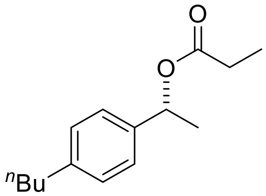

Prepared following General Procedure A, from 1-(4-butylphenyl)ethyl 2,2,2-trichloroacetimidate (**4.1.1k**, 0.25 mmol), propionic acid (1 mmol, 4 equiv.), with (*S*,*S*)-catalyst (**4.1.3af**, 2.5 mol%), in dry Et_2O (0.25 M), at –80 °C for 3 d. Purification by flash column chromatography (eluent: pentane/Et_2O 100:0→98:2) to give **4.1.8c** as a colorless liquid (46 mg, 78%, er = 93.5:6.5).

^{1}H NMR (501 MHz, CD_2Cl_2) δ 7.28–7.23 (m, 2H), 7.17–7.14 (m, 2H), 5.82 (q, *J* = 6.6 Hz, 1H), 2.63–2.56 (m, 2H), 2.32 (qd, *J* = 7.6, 4.2 Hz, 2H), 1.64–1.54 (m, 2H), 1.50 (d, *J* = 6.6 Hz, 3H), 1.36 (dq, *J* = 14.7, 7.3 Hz, 2H), 1.10 (t, *J* = 7.6 Hz, 3H), 0.93 (t, *J* = 7.3 Hz, 3H). **^{13}C NMR** (126 MHz, CD_2Cl_2) δ 173.9, 143.0, 139.8, 128.6, 125.7, 72.3, 35.7, 34.1, 28.2, 22.8, 22.4, 14.1, 9.3. **HRMS (EI)**: calculated for $C_{15}H_{22}O_2^+$ (M^+: 234.161430, found: 234.161620. $[\alpha]_D^{25}$ = +83.37 (*c* = 0.4, $CHCl_3$).

HPLC: chiral pack OJ-3R column, acetonitrile/water 50:50, 1 mL/min, 25 °C, 254 nm, t_R (major) = 19.35 min., t_R (minor) = 26.99 min., er = 93.5:6.5.

(*R*)-1-(3,4-dimethylphenyl)ethyl propionate (4.1.9c)

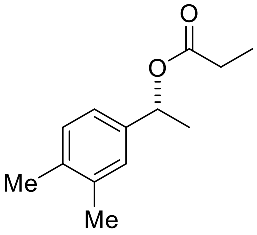

Prepared following General Procedure A, from 1-(3,4-dimethylphenyl)ethyl 2,2,2-trichloroacetimidate (**4.1.1l**, 0.25 mmol), propionic acid (1 mmol, 4 equiv.), with (*S*,*S*)-catalyst (**4.1.3af**, 2.5 mol%), in dry Et_2O (0.25 M), at –90 °C for 5 d. Purification by flash column chromatography (eluent: pentane/Et_2O 100:0→98:2) to give **4.1.9c** as a colorless liquid (44 mg, 85%, er = 95: 5).

^{1}H NMR (501 MHz, CD_2Cl_2) δ 7.12–7.08 (m, 2H), 7.05 (dd, *J* = 7.7, 1.9 Hz, 1H), 5.77 (q, *J* = 6.6 Hz, 1H), 2.32 (qd, *J* = 7.5, 4.1 Hz, 2H), 2.26 (s, 3H), 2.24 (s, 3H), 1.48 (d, *J* = 6.6 Hz, 3H), 1.10 (t, *J* = 7.5 Hz, 3H). **^{13}C NMR** (126 MHz, CD_2Cl_2) δ 173.9, 140.0, 137.1, 136.6, 129.9, 127.6, 123.7, 72.4, 28.2, 22.5, 19.9, 19.5, 9.3. **HRMS (EI)**: calculated for $C_{13}H_{18}O_2^+$ (M^+): 206.130130, found: 206.130170. $[\boldsymbol{\alpha}]_{\boldsymbol{D}}^{\mathbf{25}}$ = +100.57 (*c* = 0.4, $CHCl_3$)

HPLC: chiral pack IC-3R column, acetonitrile/water 50:50, 0.5 mL/min, 25 °C, 254 nm, t_R (major) = 15.32 min., t_R (minor) = 17.15 min., er = 95: 5.

7.3.3 Synthesis and Characterization of C–N Bond Products

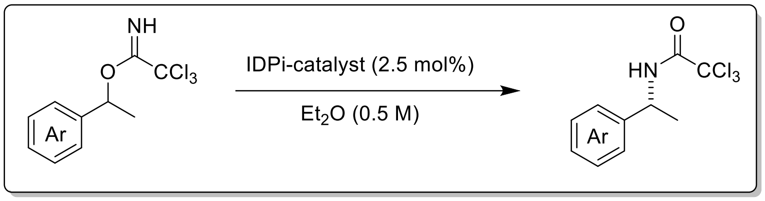

General Procedure B: IDPi-catalyzed C–N bond formation

An oven-dried glass vial (1.5 mL) was charged with substrate (0.1 mmol), dry Et_2O, cooled to the reaction temperature (indicated in each case) and then catalyst (2.5 mol%) was added as a stock solution slowly. The reaction mixture was stirred at the reaction temperature for a certain time (indicated in each case). The reaction was stopped by adding wet Et_3N (4.5 equiv.) at the reaction temperature and warmed to room temperature. Corresponding product was purified by flash column chromatography on silica gel (pentane/Et_2O mixtures).

(*R*)-2,2,2-trichloro-*N*-(1-phenylethyl)acetamide (4.2.3a):

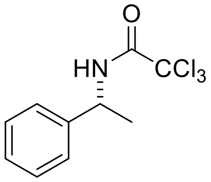

Prepared following General Procedure B, from 1-phenylethyl 2,2,2-trichloroacetimidate (**4.1.1a**, 0.1 mmol), with (*S*,*S*)-catalyst (**4.2.2i**, 2.5 mol%), in dry Et_2O (0.5 M), at –80 °C for 3 d. Purification by flash column chromatography (eluent: pentane/Et_2O 100:0→97:3) to give **4.2.3a** as a colorless solid (20 mg, 75%, er = 95:5).

^{1}H NMR (501 MHz, CD_2Cl_2) δ 7.36 (ddt, *J* = 19.5, 12.7, 7.3 Hz, 5H), 6.90 (s, 1H), 5.04 (p, *J* = 7.1 Hz, 1H), 1.59 (d, *J* = 6.9 Hz, 3H). **^{13}C NMR** (126 MHz, CD_2Cl_2) δ 161.2, 142.1, 129.2, 128.2, 126.4, 93.1, 51.6, 21.6. **HRMS (ESI)**: calculated for $C_{10}H_{10}NOCl_3Na^+$ ($[M+Na]^+$): 287.97202, found: 287.97189. $[\boldsymbol{\alpha}]_{\boldsymbol{D}}^{\mathbf{25}}$ = +64.44 (*c* = 0.3, $CHCl_3$).

HPLC: chiral pack IG-3R column, acetonitrile/water 50:50, 1 mL/min, 25 °C, 204 nm, t_R (major) = 5.45 min., t_R (minor) = 6.51 min., er = 95:5.

(*S*)-2,2,2-trichloro-*N*-(1-(*m*-tolyl)ethyl)acetamide (4.2.3b):

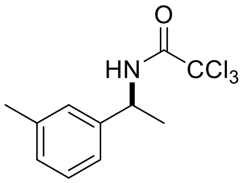

Prepared following General Procedure B, from 1-(*m*-tolyl)ethyl 2,2,2-trichloroacetimidate (**4.1.1g**, 0.1 mmol), with (*R*,*R*)-catalyst (**4.2.2j**, 2.5 mol%), in dry Et_2O (0.5 M), at –80 °C for 3 d. Purification by flash column chromatography (eluent: pentane/Et_2O 100:0→97:3) to give **4.2.3b** as a colorless solid (21 mg, 75%, er = 95.5:4.5).

^{1}H NMR (501 MHz, CD_2Cl_2) δ 7.27 (t, *J* = 7.6 Hz, 1H), 7.19–7.09 (m, 3H), 6.90 (s, 1H), 5.00 (p, *J* = 7.1 Hz, 1H), 2.36 (s, 3H), 1.57 (d, *J* = 7.0 Hz, 3H). **^{13}C NMR** (126 MHz, CD_2Cl_2) δ 161.1, 142.1, 139.1, 129.1, 128.9, 127.2, 123.3, 93.2, 51.6, 21.7, 21.6. **HRMS (ESI)**: calculated for $C_{11}H_{12}NOCl_3Na^+$ ($[M+Na]^+$): 301.98767, found: 301.98749. $[\boldsymbol{\alpha}]_{\boldsymbol{D}}^{\mathbf{25}}$ = –60.64 (*c* = 0.31, $CHCl_3$).

HPLC: chiral pack IG-3 column heptane/isopropanol 98:2, 1 mL/min, 25 °C, 254 nm, t_R (minor) = 5.26 min., t_R (major) = 6.01 min., er = 4.5:95.5.

(*S*)-2,2,2-trichloro-*N*-(1-(4-fluorophenyl)ethyl)acetamide (4.2.3c):

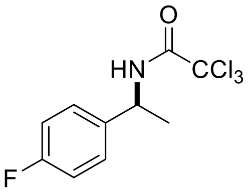

Prepared following General Procedure B, from 1-(4-fluorophenyl)ethyl 2,2,2-trichloroacetimidate (**4.1.1b**, 0.1 mmol), with (*R*,*R*)-catalyst (**4.2.2j**, 2.5 mol%), in dry Et_2O (0.5 M), at –90 °C for 5 d. Purification by flash column chromatography (eluent: pentane/Et_2O 100:0→97:3) to give **4.2.3c** as a colorless solid (17 mg, 60%, er = 96:4).

^{1}H NMR (501 MHz, CD_2Cl_2) δ 7.39–7.29 (m, 2H), 7.14–7.03 (m, 2H), 6.86 (s, 1H), 5.03 (p, *J* = 7.1 Hz, 1H), 1.58 (d, *J* = 6.9 Hz, 3H). **^{13}C NMR** (126 MHz, CD_2Cl_2) δ 162.7 (d, *J* = 245.3 Hz), 161.2, 138.0 (d, *J* = 3.4 Hz), 128.2 (d, *J* = 8.4 Hz), 116.0 (d, *J* = 21.5 Hz), 93.0, 51.0, 21.6. **^{19}F NMR** (471 MHz, CD_2Cl_2) δ –115.29. **HRMS (ESI)**: calculated for $C_{10}H_9NOFCl_3Na^+$ ($[M+Na]^+$): 305.96260, found: 305.96269. $[\boldsymbol{\alpha}]_{\boldsymbol{D}}^{\mathbf{25}}$ = –53.75 (*c* = 0.32, $CHCl_3$).

HPLC: chiral pack IG-3 column heptane/isopropanol 98:2, 1 mL/min, 25 °C, 254 nm, t_R (minor) = 6.30 min., t_R (major) = 8.06 min., er = 4:96.

(*S*)-2,2,2-trichloro-*N*-(1-(p-tolyl)ethyl)acetamide (4.2.3d):

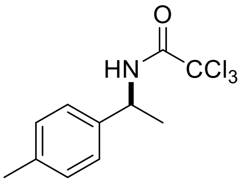

Prepared following General Procedure B, from 1-(p-tolyl)ethyl 2,2,2-trichloroacetimidate (**4.1.1c**, 0.1 mmol), with (*R*,*R*)-catalyst (**4.2.2j**, 2.5 mol%), in dry Et_2O (0.5 M), at –90 °C for 5 d. Purification by flash column chromatography (eluent: pentane/Et_2O 100:0→97:3) to give **4.2.3d** as a colorless solid (21 mg, 75%, er = 92.5:7.5).

^{1}H NMR (501 MHz, CD_2Cl_2) δ 7.24 (d, *J* = 8.3 Hz, 2H), 7.20 (d, *J* = 8.1 Hz, 2H), 6.88 (s, 1H), 5.00 (p, *J* = 7.1 Hz, 1H), 2.34 (s, 3H), 1.57 (d, *J* = 7.0 Hz, 3H). **^{13}C NMR** (126 MHz, CD_2Cl_2) δ 161.10, 139.07, 138.12, 129.86, 126.29, 93.17, 51.37, 21.52, 21.17. **HRMS (ESI)**: calculated for $C_{11}H_{12}NOCl_3Na^+$ ($[M+Na]^+$): 301.98767, found: 301.98753. $[\alpha]_D^{25}$ = –66.23 (*c* = 0.305, $CHCl_3$).

HPLC: chiral pack IG-3 column heptane/isopropanol 98:2, 1 mL/min, 25 °C, 254 nm, t_R (minor) = 5.78 min., t_R (major) = 7.94 min., er = 7.5:92.5.

(*S*)-2,2,2-trichloro-*N*-(1-(4-chlorophenyl)ethyl)acetamide (4.2.3e):

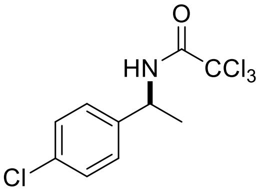

Prepared following General Procedure B, from 1-(4-chlorophenyl)ethyl 2,2,2-trichloroacetimidate (**4.2.1a**, 0.1 mmol), with (*R*,*R*)-catalyst (**4.2.2j**, 2.5 mol%), in dry Et_2O (0.5 M), at –80 °C for 3 d. Purification by flash column chromatography (eluent: pentane/Et_2O 100:0→97:3) to give **4.2.3e** as a colorless solid (17 mg, 57%, er = 95:5).

^{1}H NMR (501 MHz, CD_2Cl_2) δ 7.40–7.33 (m, 2H), 7.3–7.27 (m, 2H), 6.90 (s, 1H), 5.02 (p, *J* = 7.1 Hz, 1H), 1.57 (d, *J* = 7.0 Hz, 3H). **^{13}C NMR** (126 MHz, CD_2Cl_2) δ 161.24, 140.78, 133.86, 127.92, 92.98, 51.04, 21.50. **HRMS (ESI)**: calculated for $C_{10}H_9NOCl_4Na^+$ ($[M+Na]^+$): 321.93305, found: 321.93291. $[\alpha]_D^{25}$ = –63.23 (*c* = 0.31, $CHCl_3$).

HPLC: chiral pack IG-3 column heptane/isopropanol 98:2, 1 mL/min, 25 °C, 254 nm, t_R (minor) = 6.76 min., t_R (major) = 9.01 min., er = 5:95.

7.3.4 Synthesis and Characterization of SKA Alkylation Products

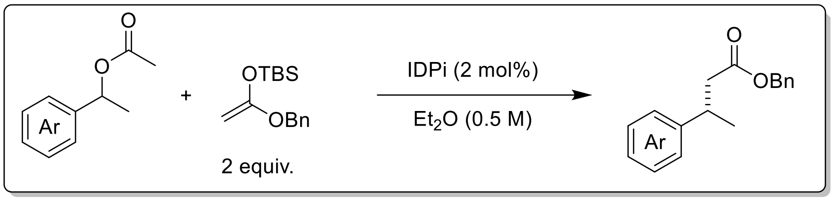

General Procedure C: IDPi-catalyzed SKA alkylation reaction

An oven-dried glass vial (1.5 mL) was charged with (*S*,*S*)-IDPi catalyst (2 mol%), SKA (2 equiv.), dry Et_2O, cooled to the reaction temperature (indicated in each case) and then after 10 min substrate (0.1 mmol) was added as a stock solution slowly under argon. The reaction mixture was stirred at the reaction temperature for a certain time (indicated in each case). The reaction was stopped by adding Et_3N in MeOH (20 µL) at the reaction temperature and warmed to room temperature. Corresponding product was purified by flash column chromatography on silica gel (pentane/Et_2O mixtures).

benzyl (*S*)-3-phenylbutanoate (4.3.7a):

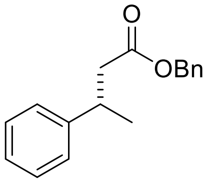

Prepared following General Procedure C, from 1-phenylethyl acetate (**4.3.1a**, 0.1 mmol), SKA (0.2 mmol, 2 equiv.), with (*S*,*S*)-catalyst (**4.3.3j**, 2.0 mol%), in dry Et_2O (0.5 M), at –65 °C for 4 d. Purification by flash column chromatography (eluent: pentane/toluene 30:70→10:90) to give **4.3.7a** as a colorless liquid (25 mg, 85%, er = 92.5:7.5).

^{1}H NMR (501 MHz, CD_2Cl_2) δ 7.36–7.26 (m, 5H), 7.26–7.17 (m, 5H), 5.03 (s, 2H), 3.28 (h, *J* = 7.2 Hz, 1H), 2.64 (qd, *J* = 15.2, 7.6 Hz, 2H), 1.29 (d, *J* = 7.0 Hz, 3H). **^{13}C NMR** (126 MHz, CD_2Cl_2) δ 172.4, 146.2, 136.7, 128.85, 128.83, 128.43, 128.41, 127.2, 126.7, 66.4, 43.2, 37.0, 22.2. **HRMS (EI)**: calculated for$C_{17}H_{19}O_2^+$ (M^+):255.137955, found: 255.138310. $[\boldsymbol{\alpha}]_{\boldsymbol{D}}^{\mathbf{25}}$ = +17.14 (*c* = 0.3, $CHCl_3$). (Lit.[135] $[\boldsymbol{\alpha}]_{\boldsymbol{D}}^{\mathbf{25}}$ = –11.90 (*c* = 0.52, $CHCl_3$) for (*R*)-enantiomer).

HPLC: chiral pack OD-3 column, heptane/isopropanol 98:2, 0.7 mL/min, 25 °C, 254 nm, t_R (minor) = 6.33 min., t_R (major) = 11.03 min., er = 92.5:7.5

benzyl (*S*)-3-(*p*-tolyl)butanoate (4.3.7b):

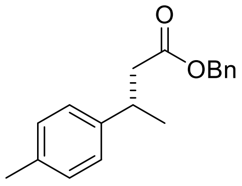

Prepared following General Procedure C, from 1-(*p*-tolyl)ethyl acetate (**4.3.1b**, 0.1 mmol), SKA (0.2 mmol, 2 equiv.), with (*S*,*S*)-catalyst (**4.3.3p**, 2.0 mol%), in dry Et_2O (0.5 M), at –60 °C for 3 d. Purification by flash column chromatography (eluent: pentane/Et_2O 100:0→98:2) to give **4.3.7b** as a colorless liquid (23 mg, 86%, er = 95.5:4.5).

^{1}H NMR (501 MHz, CD_2Cl_2) δ 7.39–7.21 (m, 5H), 7.10 (s, 4H), 5.03 (s, 2H), 3.23 (h, *J* = 7.2 Hz, 1H), 2.70–2.52 (m, 2H), 2.31 (s, 3H), 1.26 (d, *J* = 7.0 Hz, 3H). **^{13}C NMR** (126 MHz, CD_2Cl_2) δ 172.4, 143.1, 136.7, 136.3, 129.5, 128.8, 128.4, 127.0, 66.4, 43.3, 36.6, 22.3, 21.1. **HRMS (ESI)**: calculated for $C_{18}H_{24}NO_2^+$ ($[M+NH_4]^+$): 286.180154, found: 286.180180. $[\boldsymbol{\alpha}]_{\boldsymbol{D}}^{\boldsymbol{25}}$ = +18.46 (*c* = 0.3, $CHCl_3$). (Lit.[136] $[\boldsymbol{\alpha}]_{\boldsymbol{D}}^{\boldsymbol{20}}$ = –16.20 (*c* = 1.0, $CHCl_3$) for (*R*)-enantiomer).

HPLC: chiral pack IG-3R column, acetonitrile/water 40:60, 1 mL/min, 25 °C, 204 nm, t_R (major) = 112.81 min., t_R (minor) = 119.79 min., er = 95.5:4.5

benzyl (*S*)-3-(4-ethylphenyl)butanoate (4.3.7f):

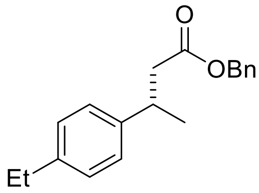

Prepared following General Procedure C, from 1-(4-ethylphenyl)ethyl acetate (**4.3.1f**, 0.1 mmol), SKA (0.2 mmol, 2 equiv.), with (*S*,*S*)-catalyst (**4.3.3p**, 2.0 mol%), in dry Et_2O (0.5 M), at –60 °C for 3 d. Purification by flash column chromatography (eluent: pentane/Et_2O 100:0→98:2) to give **4.3.7f** as a colorless liquid (24 mg, 85%, er = 96.5:3.5).

^{1}H NMR (501 MHz, CD_2Cl_2) δ 7.39–7.21 (m, 5H), 7.12 (s, 4H), 5.03 (s, 2H), 3.25 (h, *J* = 7.2 Hz, 1H), 2.69–2.55 (m, 4H), 1.27 (d, *J* = 7.0 Hz, 3H), 1.22 (t, *J* = 7.6 Hz, 3H). **^{13}C NMR** (126 MHz, CD_2Cl_2) δ 172.5, 143.4, 142.8, 136.7, 128.8, 128.4, 128.3, 127.1, 66.4, 43.3, 36.6, 28.8, 22.3, 15.8. **HRMS (ESI)**: calculated for $C_{19}H_{23}O_2^+$ ($[M+H]^+$): 283.169255, found: 283.169410. $[\boldsymbol{\alpha}]_{\boldsymbol{D}}^{\boldsymbol{25}}$ = +15.27 (*c* = 0.3, $CHCl_3$).

HPLC: chiral pack IG-3R column, acetonitrile/water 50:50, 0.5 mL/min, 25 °C, 204 nm, t_R (major) = 72.10 min., t_R (minor) = 76.54 min., er = 96.5:3.5

benzyl (*S*)-3-(4-propylphenyl)butanoate (4.3.7g):

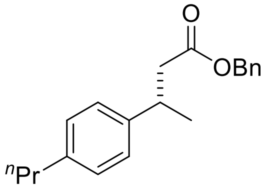

Prepared following General Procedure C, from 1-(4-propylphenyl)ethyl acetate (**4.3.1g**, 0.1 mmol), SKA (0.2 mmol, 2 equiv.), with (*S*,*S*)-catalyst (**4.3.3p**, 2.0 mol%), in dry Et_2O (0.5 M), at –60 °C for 3 d. Purification by flash column chromatography (eluent: pentane/Et_2O 100:0→98:2) to give **4.3.7g** as a colorless liquid (27 mg, 91%, er = 96.5:3.5).

^{1}H NMR (501 MHz, CD_2Cl_2) δ 7.38–7.29 (m, 3H), 7.27–7.23 (m, 2H), 7.14–7.08 (m, 4H), 5.03 (s, 2H), 3.24 (h, *J* = 7.2 Hz, 1H), 2.68–2.52 (m, 4H), 1.70–1.57 (m, 2H), 1.27 (d, *J* = 7.0 Hz, 3H), 0.94 (t, *J* = 7.3 Hz, 3H). **^{13}C NMR** (126 MHz, CD_2Cl_2) δ 172.5, 143.4, 141.2, 136.7, 128.9, 128.8, 128.4, 127.0, 66.4, 43.3, 38.0, 36.6, 25.1, 22.3, 14.1. **HRMS (ESI):** calculated for $C_{20}H_{28}NO_2^+$ ($[M+NH_4]^+$: 314.211454, found: 314.211260. $[\boldsymbol{\alpha}]_{\boldsymbol{D}}^{\mathbf{25}}$ = +15.86 (*c* = 0.3, $CHCl_3$)

HPLC: chiral pack IG-3R column, acetonitrile/water 70:30, 1 mL/min, 25 °C, 204 nm, t_R (major) = 8.50 min., t_R (minor) = 9.57 min., er = 96.5:3.5

benzyl (*S*)-3-(4-butylphenyl)butanoate (4.3.7h):

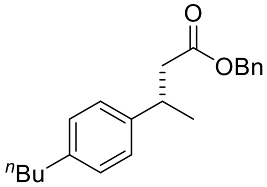

Prepared following General Procedure C, from 1-(4-butylphenyl)ethyl acetate (**4.3.1h**, 0.1 mmol), SKA (0.2 mmol, 2 equiv.), with (*S*,*S*)-catalyst (**4.3.3p**, 2.0 mol%), in dry Et_2O (0.5 M), at –60 °C for 3 d. Purification by flash column chromatography (eluent: pentane/Et_2O 100:0→98:2) to give **4.3.7h** as a colorless liquid (26 mg, 84%, er = 96:4).

^{1}H NMR (501 MHz, CD_2Cl_2) δ 7.39–7.27 (m, 3H), 7.27–7.22 (m, 2H), 7.14–7.08 (m, 4H), 5.03 (s, 2H), 3.24 (h, *J* = 7.2 Hz, 1H), 2.68–2.54 (m, 4H), 1.63–1.55 (m, 2H), 1.36 (h, *J* = 7.3 Hz, 2H), 1.27 (d, *J* = 7.0 Hz, 3H), 0.93 (t, *J* = 7.3 Hz, 3H). **^{13}C NMR** (126 MHz, CD_2Cl_2) δ 172.5, 143.3, 128.8, 128.4, 127.0, 66.4, 43.3, 36.6, 35.6, 34.2, 22.9, 22.3, 14.1. **HRMS (ESI):** calculated for $C_{21}H_{30}NO_2^+$ ($[M+NH_4]^+$: 328.227104, found: 328.227480. $[\boldsymbol{\alpha}]_{\boldsymbol{D}}^{\mathbf{25}}$ = +16.00 (*c* = 0.2, $CHCl_3$)

HPLC: chiral pack IG-3R column, acetonitrile/water 70:30, 1 mL/min, 25 °C, 204 nm, t_R (major) = 11.17 min., t_R (minor) = 13.21 min., er = 96:4

benzyl (*S*)-3-(4-isopropylphenyl)butanoate (4.3.7i):

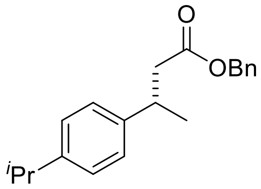

Prepared following General Procedure C, from 1-(4-isopropylphenyl)ethyl acetate (**4.3.1i**, 0.1 mmol), SKA (0.2 mmol, 2 equiv.), with (*S*,*S*)-catalyst (**4.3.3p**, 2.0 mol%), in dry Et_2O (0.5 M), at –60 °C for 3 d. Purification by flash column chromatography (eluent: pentane/Et_2O 100:0→98:2) to give **4.3.7i** as a colorless liquid (27 mg, 91%, er = 95.0:5.0).

^{1}H NMR (501 MHz, CD_2Cl_2) δ 7.39–7.29 (m, 3H), 7.25 (dd, *J* = 7.8, 1.8 Hz, 2H), 7.18–7.11 (m, 4H), 5.04 (s, 2H), 3.25 (h, *J* = 7.2 Hz, 1H), 2.88 (hept, *J* = 6.9 Hz, 1H), 2.72–2.55 (m, 2H), 1.27 (d, *J* = 7.0 Hz, 3H), 1.23 (d, *J* = 6.9 Hz, 6H). **^{13}C NMR** (126 MHz, CD_2Cl_2) δ 172.5, 147.4, 143.5, 136.7, 128.8, 128.43, 128.44, 127.0, 126.8, 66.4, 43.2, 36.5, 34.1, 24.2, 22.3. **^{13}C NMR** (126 MHz, CD_2Cl_2) δ 172.5, 147.4, 143.5, 136.7, 128.8, 128.43, 128.44, 127.0, 126.8, 66.4, 43.2, 36.5, 34.1, 24.2, 22.3. **HRMS (ESI):** calculated for $C_{20}H_{28}NO_2^+$ ($[M+NH_4]^+$): 314.211454, found: 314.211250. $[\boldsymbol{\alpha}]_{\boldsymbol{D}}^{\mathbf{25}}$ = +14.07 (*c* = 0.3, $CHCl_3$)

HPLC: chiral pack IG-3R column, acetonitrile/water 70:30, 1 mL/min, 25 °C, 204 nm, t_R (major) = 7.77 min., t_R (minor) = 8.96 min., er = 95.0:5.0

benzyl (*S*)-3-(3,4-dimethylphenyl)butanoate (4.3.7j):

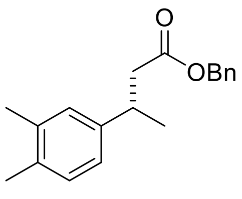

Prepared following General Procedure C, from 1-(3,4-dimethylphenyl)ethyl acetate (**4.3.1j**, 0.1 mmol), SKA (0.2 mmol, 2 equiv.), with (*S*,*S*)-catalyst (**4.3.3p**, 2.0 mol%), in dry Et_2O (0.5 M), at –70 °C for 4 d. Purification by flash column chromatography (eluent: pentane/Et_2O 100:0→98:2) to give **4.3.7j** as a colorless liquid (26 mg, 92%, er = 95:5).

^{1}H NMR (501 MHz, CD_2Cl_2) δ 7.39–7.20 (m, 5H), 7.04 (d, *J* = 7.7 Hz, 1H), 6.98 (d, *J* = 1.9 Hz, 1H), 6.93 (dd, *J* = 7.7, 2.0 Hz, 1H), 5.03 (d, *J* = 1.0 Hz, 2H), 3.20 (h, *J* = 7.2 Hz, 1H), 2.61 (qd, *J* = 15.1, 7.6 Hz, 2H), 2.23 (s, 6H), 1.25 (d, *J* = 7.0 Hz, 3H). **^{13}C NMR** (126 MHz, CD_2Cl_2) δ 172.5, 143.6, 137.0, 136.7, 134.9, 130.0, 128.8, 128.45, 128.40, 124.4, 66.3, 43.3, 36.6, 22.4, 19.9, 19.4. **HRMS (ESI)**: calculated for $C_{19}H_{23}O_2^+$ ($[M+H]^+$): 283.169255, found: 283.169120. $[\boldsymbol{\alpha}]_{\boldsymbol{D}}^{\mathbf{25}}$ = +20.31 (*c* = 0.3, $CHCl_3$)

HPLC: chiral pack IG-3R column, methanol/water 90:10, 1 mL/min, 25 °C, 220 nm, t_R (minor) = 8.76 min., t_R (major) = 9.75 min., er = 5:95.

benzyl (*S*)-3-(2,4,6-trimethoxyphenyl)butanoate (4.3.7d):

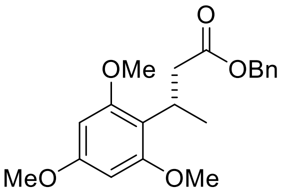

Prepared following General Procedure C, from 1,3,5-trimethoxy-2-(1-methoxyethyl)benzene (**4.3.1d**, 0.1 mmol), SKA (0.2 mmol, 2 equiv.), with (*S*,*S*)-catalyst (**4.3.3j**, 2.0 mol%), in dry Et_2O (0.5 M), at –70 °C for 3 d. Purification by flash column chromatography (eluent: pentane/Et_2O 100:0→98:2) to give **4.3.7d** as a colorless liquid (33 mg, 96%, er = 67:33).

^{1}H NMR (501 MHz, CD_2Cl_2) δ 7.43–7.14 (m, 5H), 6.10 (d, *J* = 1.6 Hz, 2H), 5.04–4.97 (m, 2H), 3.90–3.80 (m, 1H), 3.78 (d, *J* = 1.0 Hz, 3H), 3.75 (d, *J* = 1.1 Hz, 6H), 2.77 (dt, *J* = 7.5, 1.9 Hz, 2H), 1.22 (dd, *J* = 7.0, 1.9 Hz, 3H). **^{13}C NMR** (126 MHz, CD_2Cl_2) δ 173.6, 159.9, 159.5, 137.0, 128.8, 128.3, 128.3, 114.1, 91.4, 66.1, 56.0, 55.6, 40.1, 26.5, 19.3. **HRMS (EI):** calculated for $C_{20}H_{24}O_5^+$ (M^+): 344.161825, found: 344.161780. $[\boldsymbol{\alpha}]_{\boldsymbol{D}}^{\mathbf{25}}$ = +8.73 (*c* = 0.3, $CHCl_3$)

HPLC: chiral pack OJ-3 column, heptane/isopropanol 95:5, 1 mL/min, 25 °C, 204 nm, t_R (minor) = 14.91 min., t_R (major) = 16.68 min., er = 67:33

7.4 Mechanistic Study Data

Synthesis of 1-(2,6-dimethoxy-4-methylphenyl)ethan-1-ol (S5m):

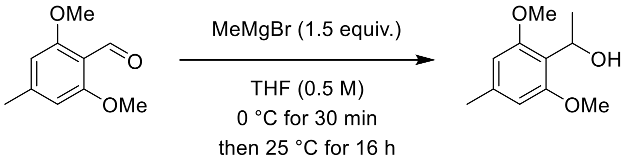

To a flame dried schlenk tube equipped with a magnetic stir bar was charged with 2,6-dimethoxy-4-methylbenzaldehyde (1 equiv., 1.0 g, 5.5 mmol) under argon. Anhydrous THF (10 mL) was added and cooled to 0 °C. 3 M MeMgBr in THF(1.5 equiv., 2.7 mL, 8.3 mmol) was added slowly and stirred at 0 °C for 30 min. The reaction mixture was warmed to room temperature and continued stirring for additional 16 h. After completion of the reaction, the reaction mixture was quenched with saturated NH_4Cl solution and organic layer was extracted with Et_2O three times and then combined organic layer was dried over Na_2SO_4, concentrated under reduced pressure. The crude product was purified by column chromatography (eluent: pentane/Et_2O 90:10→60:40) to afford the desired product as a white solid in quantitative yield (1080 mg, 99%).

^{1}H NMR (501 MHz, CD_2Cl_2) δ 6.41 (s, 2H), 5.24–5.09 (m, 1H), 3.81 (s, 6H), 3.68 (ddd, *J* = 11.6, 3.3, 1.7 Hz, 1H), 2.36–2.28 (m, 3H), 1.43 (d, *J* = 6.7 Hz, 3H). **^{13}C NMR** (126 MHz, CD_2Cl_2) δ 157.67, 138.75, 118.54, 105.53, 64.01, 56.00, 23.97, 22.02. **HRMS (EI)**: calculated for $C_{11}H_{16}O_3^+$ (M^+): 196.109395, found: 196.109280.

7.1 Interaction of Various Substrates with HNTf₂:

7.2 NMR Characterization of Ion Pair 9

Sample preparation: In an oven-dried (80 °C, overnight) NMR tube under argon equipped with a J. Young valve, substrate (10 mg) and anhydrous CD_2Cl_2 (300 µL) was added then cooled to –80 °C. $HNTf_2$ (40.0–55.0 mg, 3 equiv.) in CD_2Cl_2 (200 µL) was added to NMR tube slowly as a stock solution and then sample was mixed to make it homogenous. The sample was quickly transferred to the NMR spectrometer and the measurement was started.

Reaction of 1-(2,4,6-trimethoxyphenyl)ethan-1-ol with $HNTf_2$: Formation of the ion pair **9** was detected at –60 °C and characterized by NMR spectroscopy.

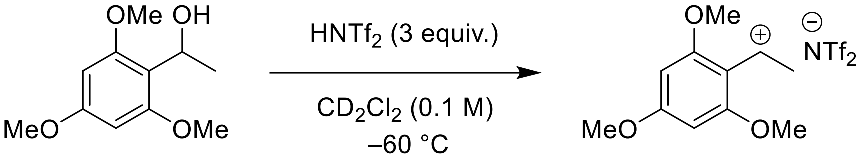

5i

9
detected

NMR data supports the following formal structure of the cation:

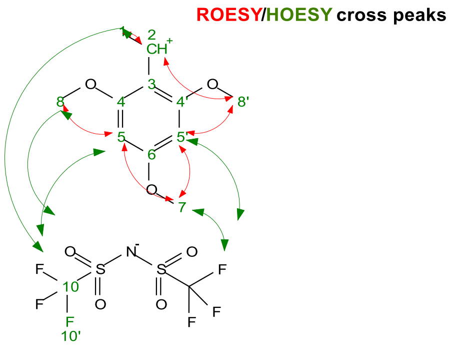

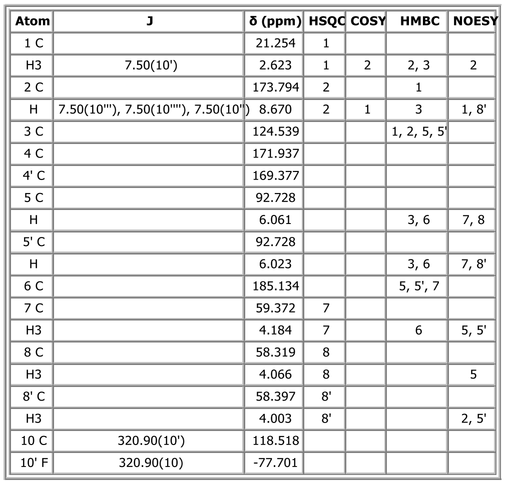

Atom	J	δ (ppm)	HSQC	COSY	HMBC	NOESY
1 C		21.254	1			
H3	7.50(10')	2.623	1	2	2, 3	2
2 C		173.794	2		1	
H	7.50(10'''), 7.50(10''''), 7.50(10'')	8.670	2	1	3	1, 8'
3 C		124.539			1, 2, 5, 5'	
4 C		171.937				
4' C		169.377				
5 C		92.728				
H		6.061			3, 6	7, 8
5' C		92.728				
H		6.023			3, 6	7, 8'
6 C		185.134			5, 5', 7	
7 C		59.372	7			
H3		4.184	7		6	5, 5'
8 C		58.319	8			
H3		4.066	8			5
8' C		58.397	8'			
H3		4.003	8'			2, 5'
10 C	320.90(10')	118.518				
10' F	320.90(10)	-77.701				

Remarks:

Positions C4,C4', C5 and C5' are broadened at lower temperatures. The origin could be a hinderes roation around the C6-O bond at this temperat
There is no interconversion of pos. 8 and 8' observed. The rotational barrier around the C3-C2 bond might be rather high.

The sample is rather stable at lower temperatures. Only from 0°C significant decomposition occures.

HOESY data revealed cross correlation peaks between the anion and cation.

1H{off},1D, 499.87 MHz,CD2Cl2,213.0K, pulse sequence: zg30

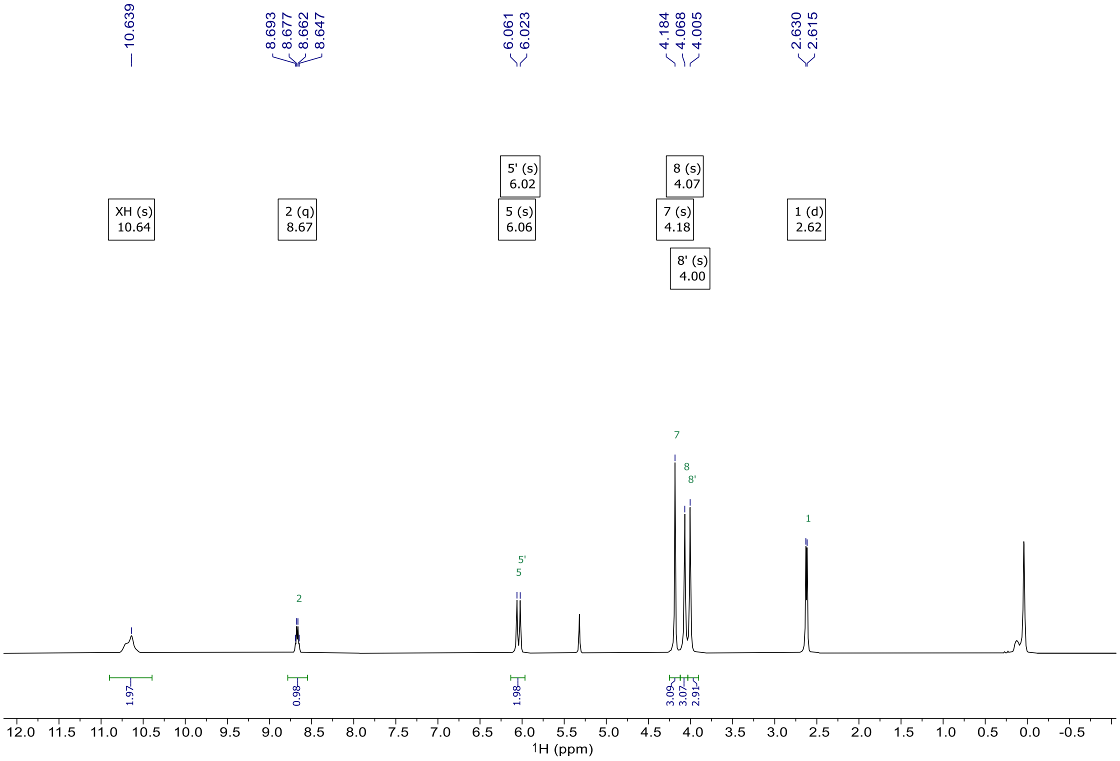

13C{1H},1D, 125.70 MHz,CD2Cl2,213.0K, pulse sequence: zgdc30

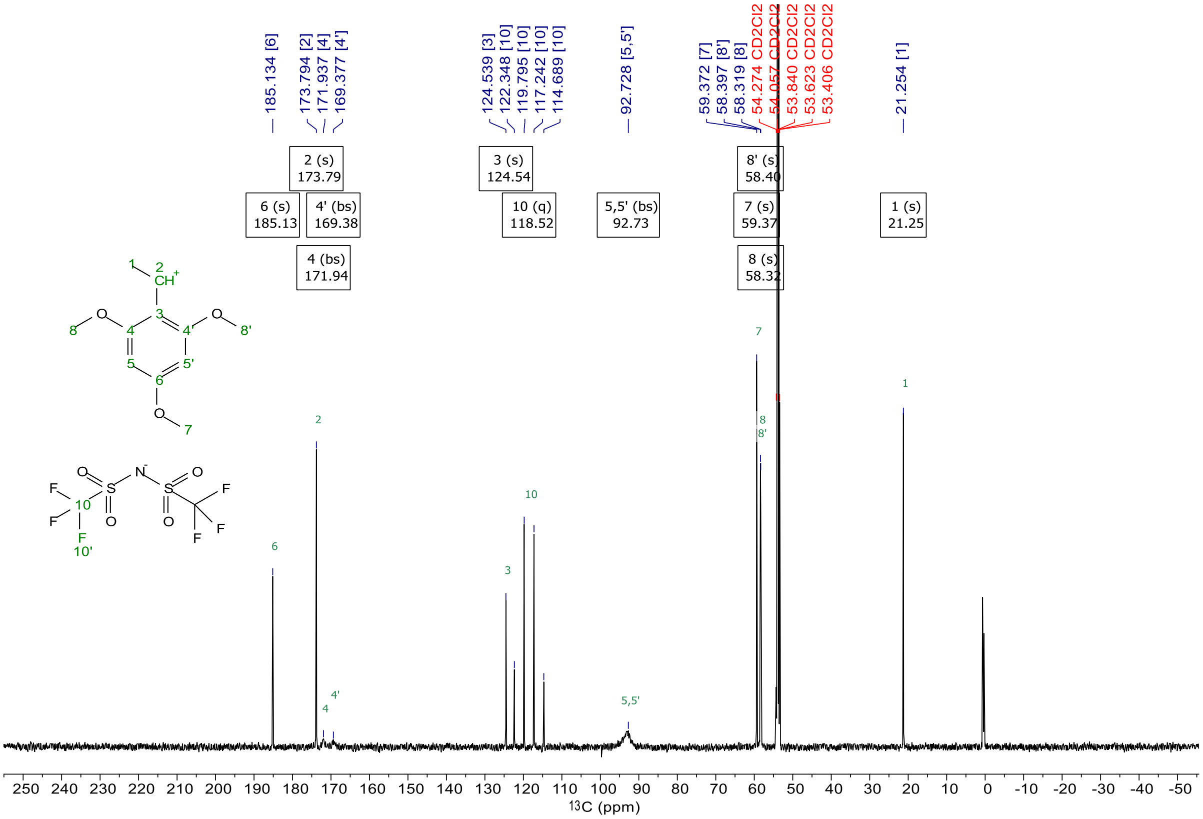

1H{13C},HSQC-EDITED, 499.87 MHz,CD2Cl2,213.0K, pulse sequence: hsqcedetgpsisp2.3

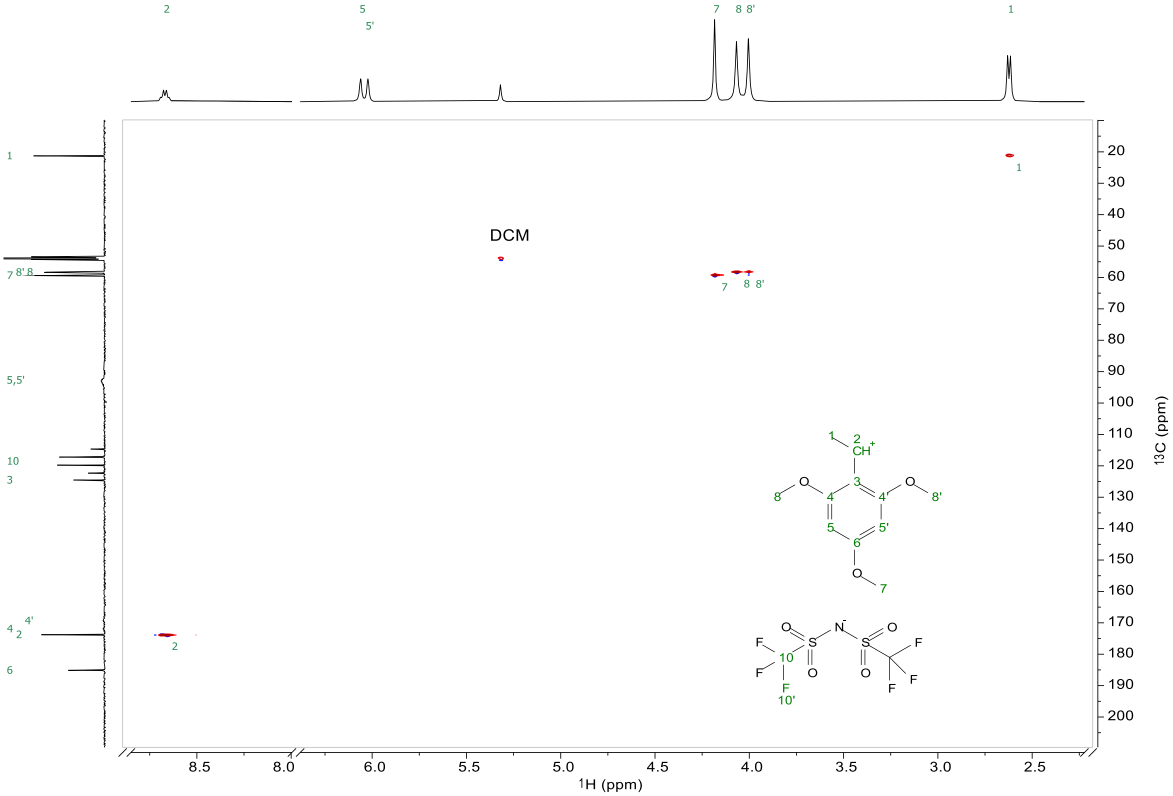

1H{13C},HMBC, 499.87 MHz,CD2Cl2,213.0K, pulse sequence: hmbcetgpl3nd

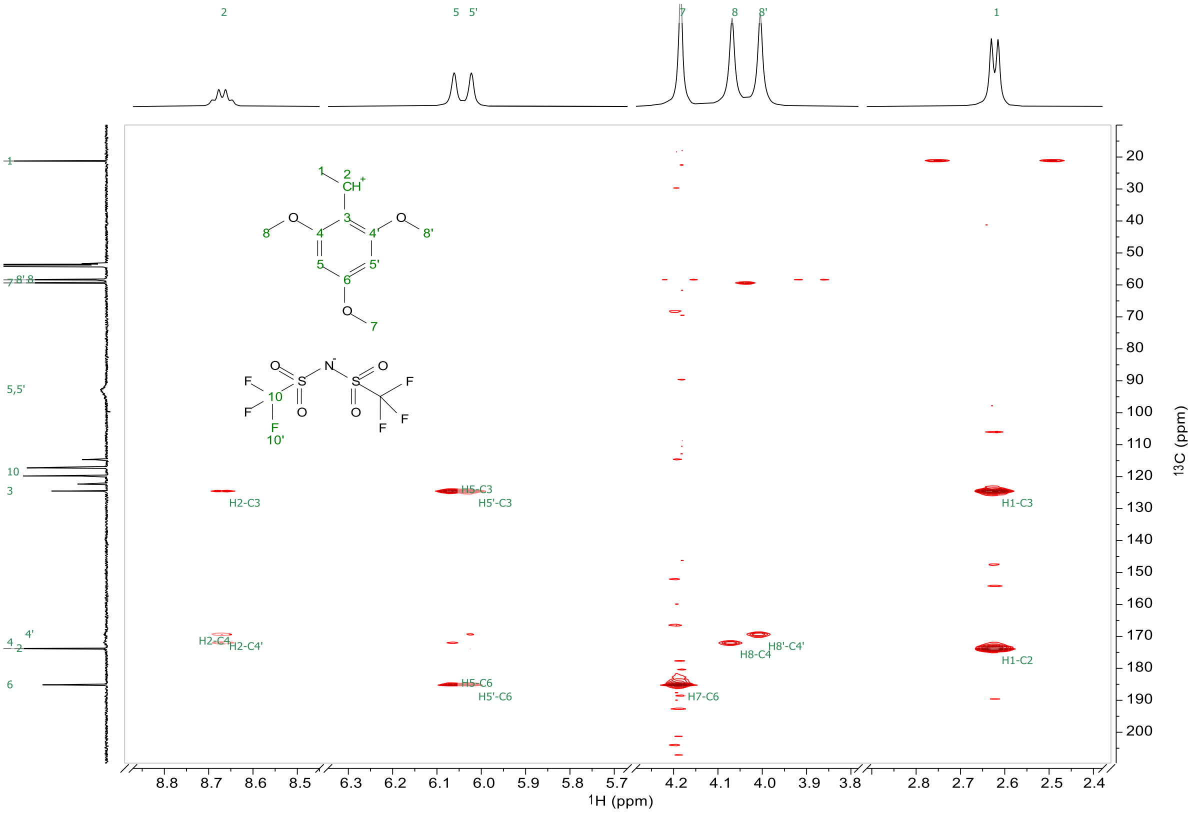

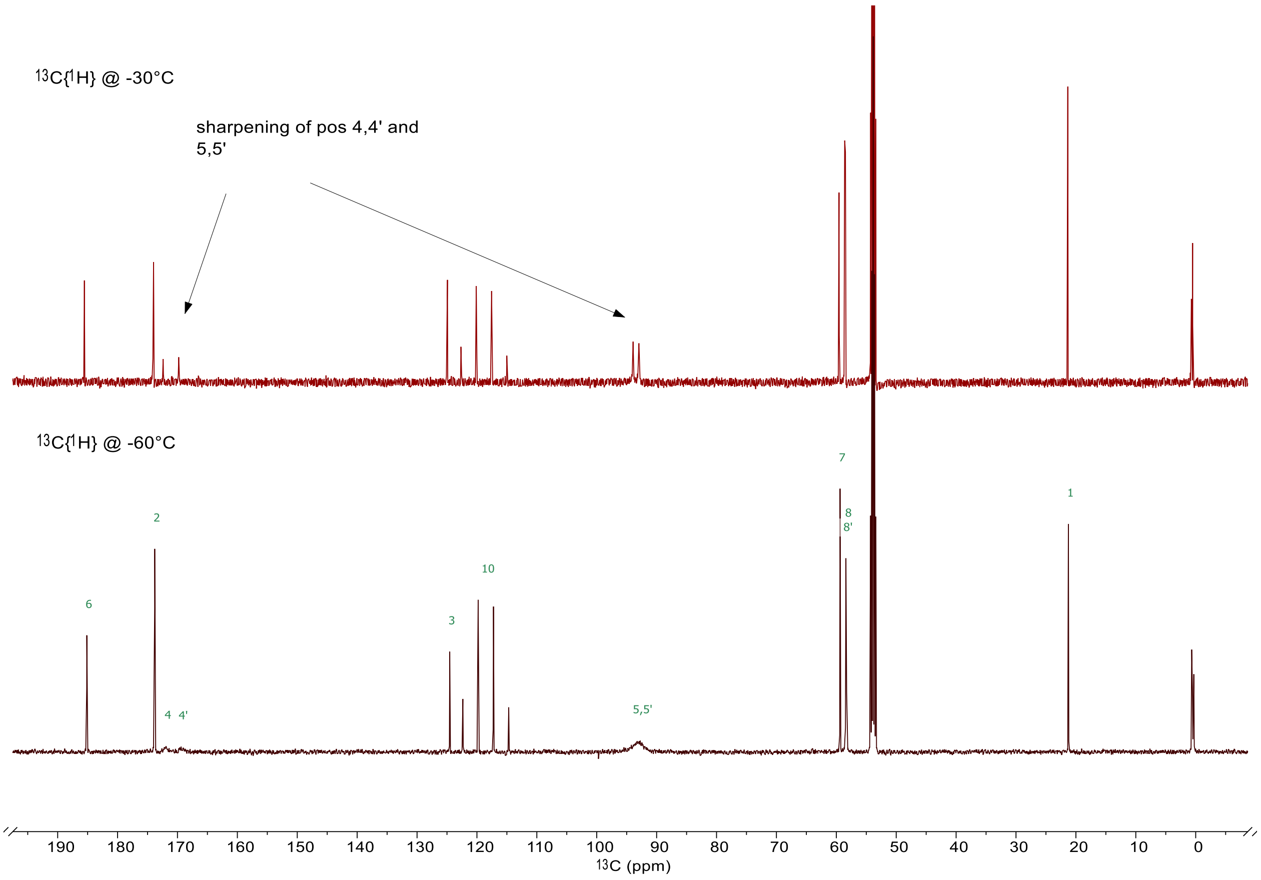

1H{off},ROESY, 499.87 MHz,CD2Cl2,213.0K, pulse sequence: roesyadjsph

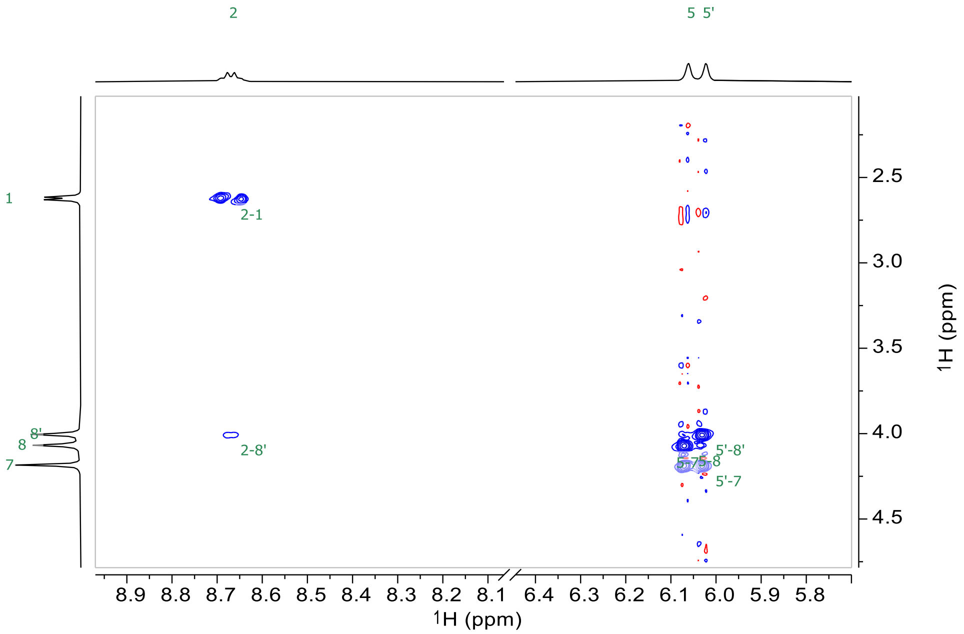

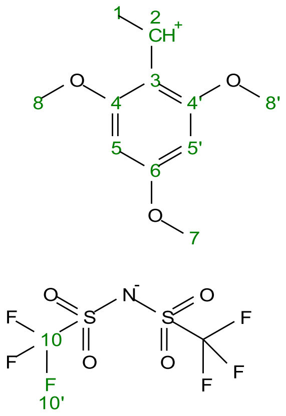
1
2
CH+
3
4
4'
5
5'
6
7
8
8'
10
10'

Variable Temperature NMR experiments of ion pair 9 from –60 °C to room temperature:

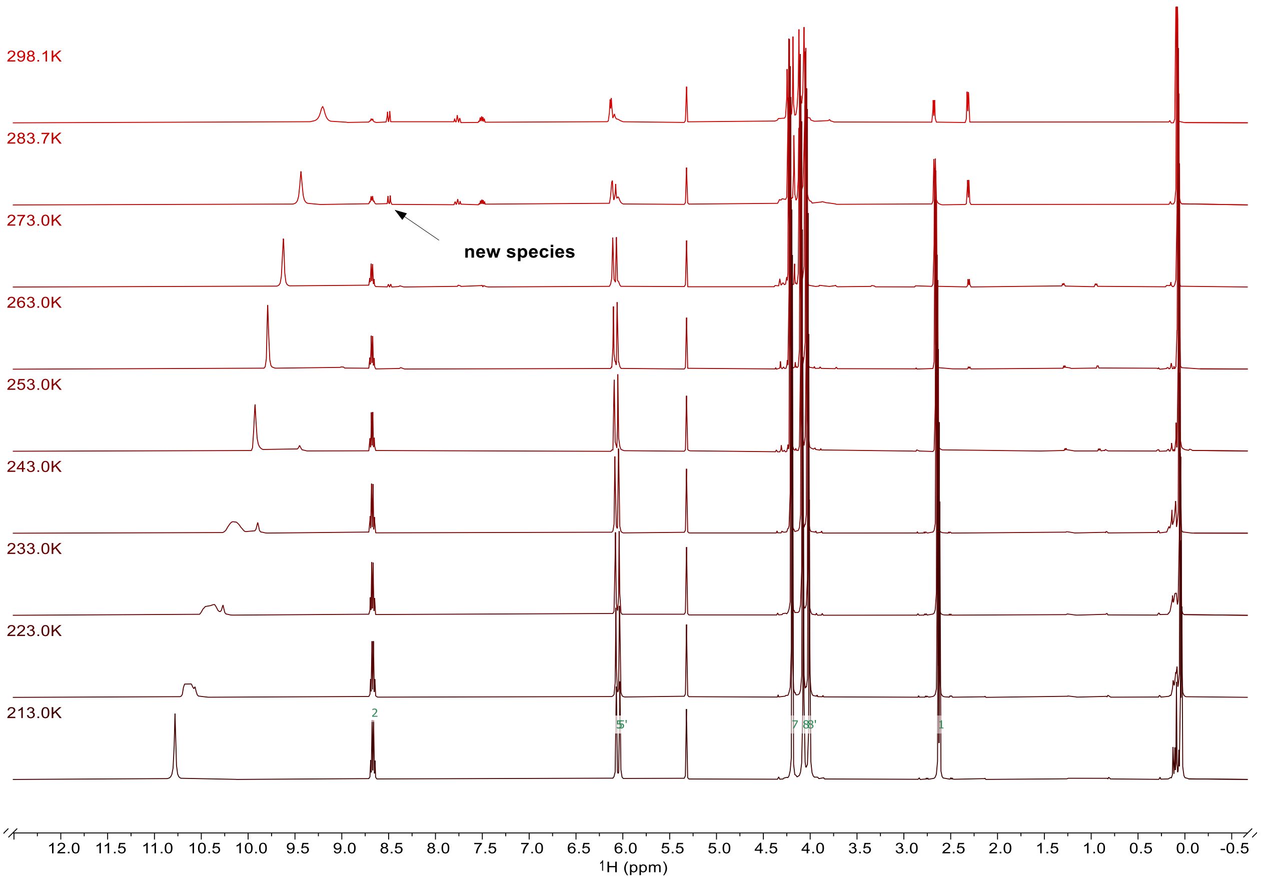

Comparison of the ion pair 9 formed under Lewis and Brønsted acid conditions:

Formation of ion pair **9** under Lewis acid conditions:

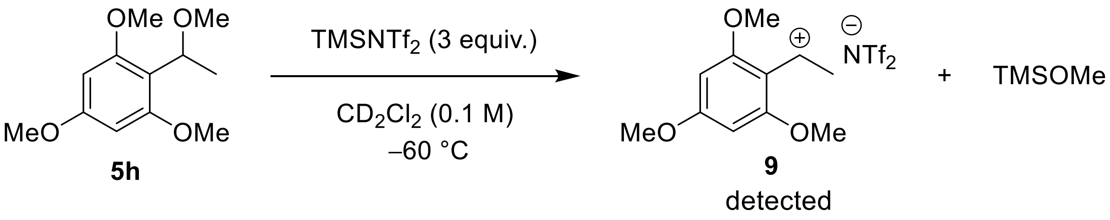
OMe OMe
MeO
OMe
5h
TMSNTf2 (3 equiv.)
CD2Cl2 (0.1 M)
–60 °C
OMe
NTf2
MeO
OMe
9
detected
+
TMSOMe

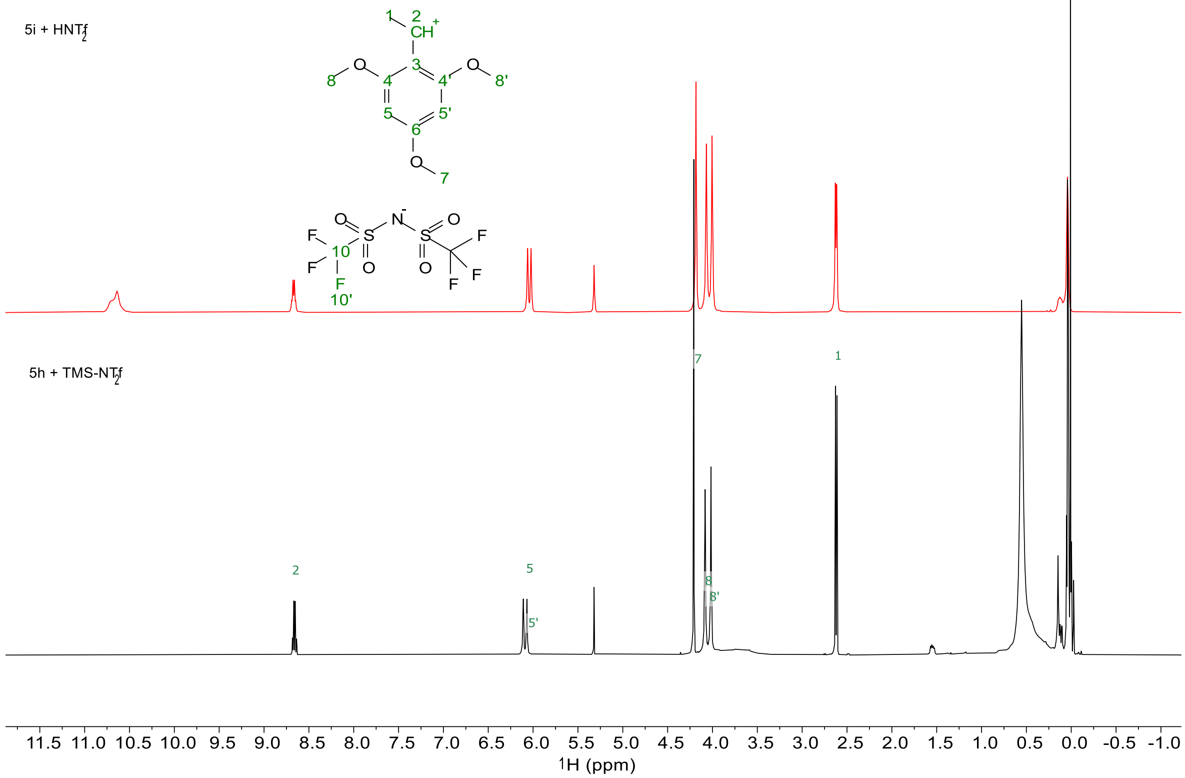
5i + HNTf2
5h + TMS-NTf2
1
2
CH+
3
4
4'
5
5'
6
7
8
8'
10
10'
F
O
S
N-
2
5
5'
7
8
8'
1
11.5 11.0 10.5 10.0 9.5 9.0 8.5 8.0 7.5 7.0 6.5 6.0 5.5 5.0 4.5 4.0 3.5 3.0 2.5 2.0 1.5 1.0 0.5 0.0 -0.5 -1.0
1H (ppm)

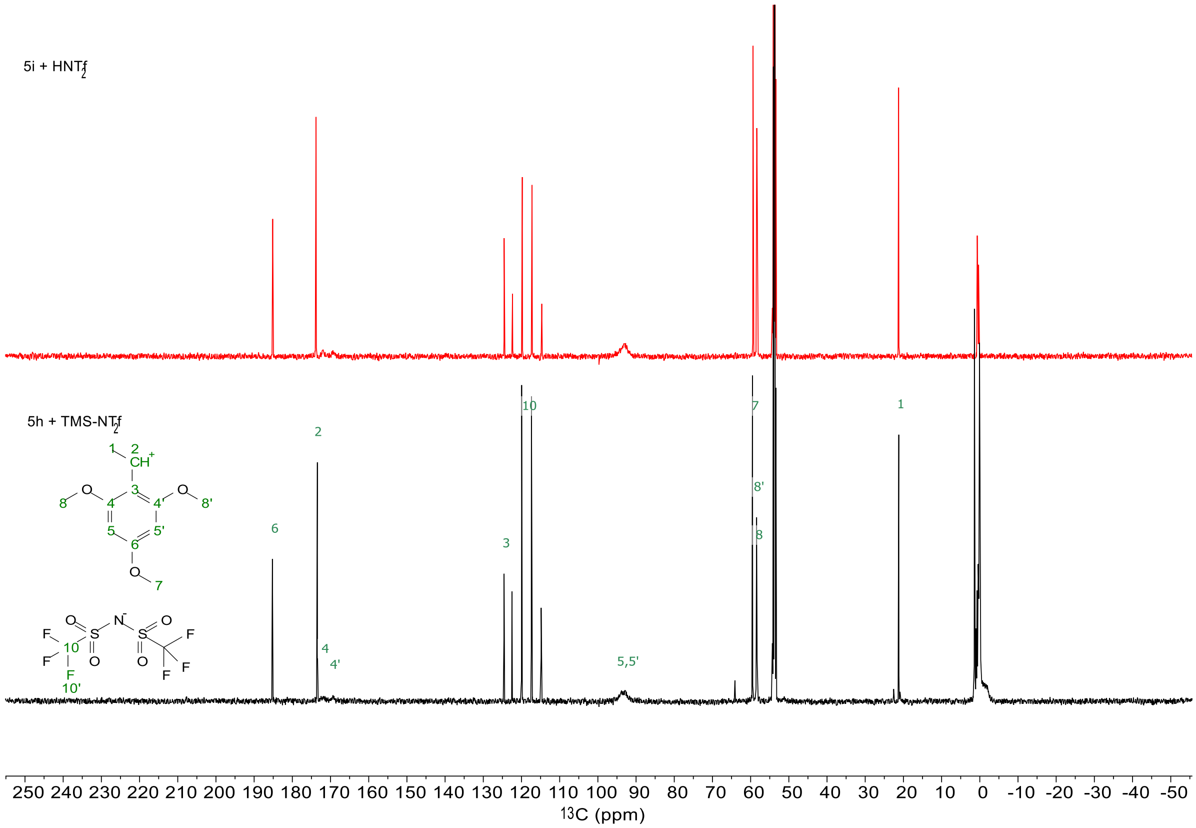
5i + HNTf2
5h + TMS-NTf2
1
2
CH+
3
4
4'
5
5'
6
7
8
8'
10
10'
F
O
S
N-
2
6
4
4'
3
10
5,5'
7
8'
8
1
250 240 230 220 210 200 190 180 170 160 150 140 130 120 110 100 90 80 70 60 50 40 30 20 10 0 -10 -20 -30 -40 -50
13C (ppm)

7.3 Comparison of Ion Pairs 9 and 10

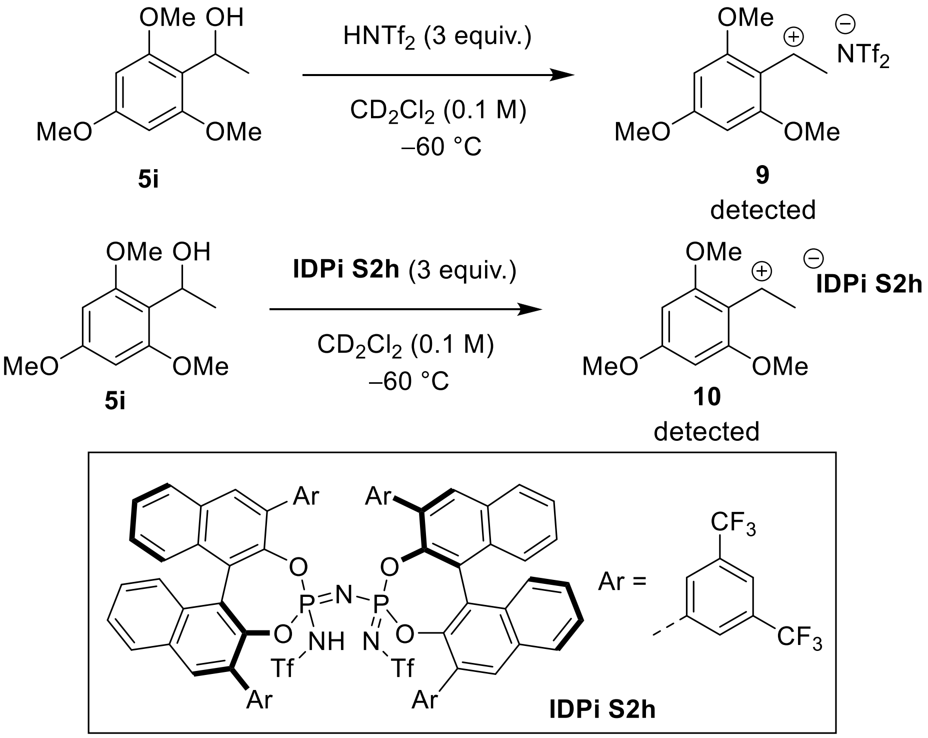
OMe OH
MeO
OMe
5i
HNTf$_2$ (3 equiv.)
CD$_2$Cl$_2$ (0.1 M)
−60 °C
OMe
⊕
⊖
NTf$_2$
MeO
OMe
9
detected
OMe OH
MeO
OMe
5i
IDPi S2h (3 equiv.)
CD$_2$Cl$_2$ (0.1 M)
−60 °C
OMe
⊕
⊖
IDPi S2h
MeO
OMe
10
detected
Ar
Ar
O
P=N–P
O
O
NH
N
O
Tf
Tf
Ar
Ar
Ar =
CF$_3$
CF$_3$
IDPi S2h

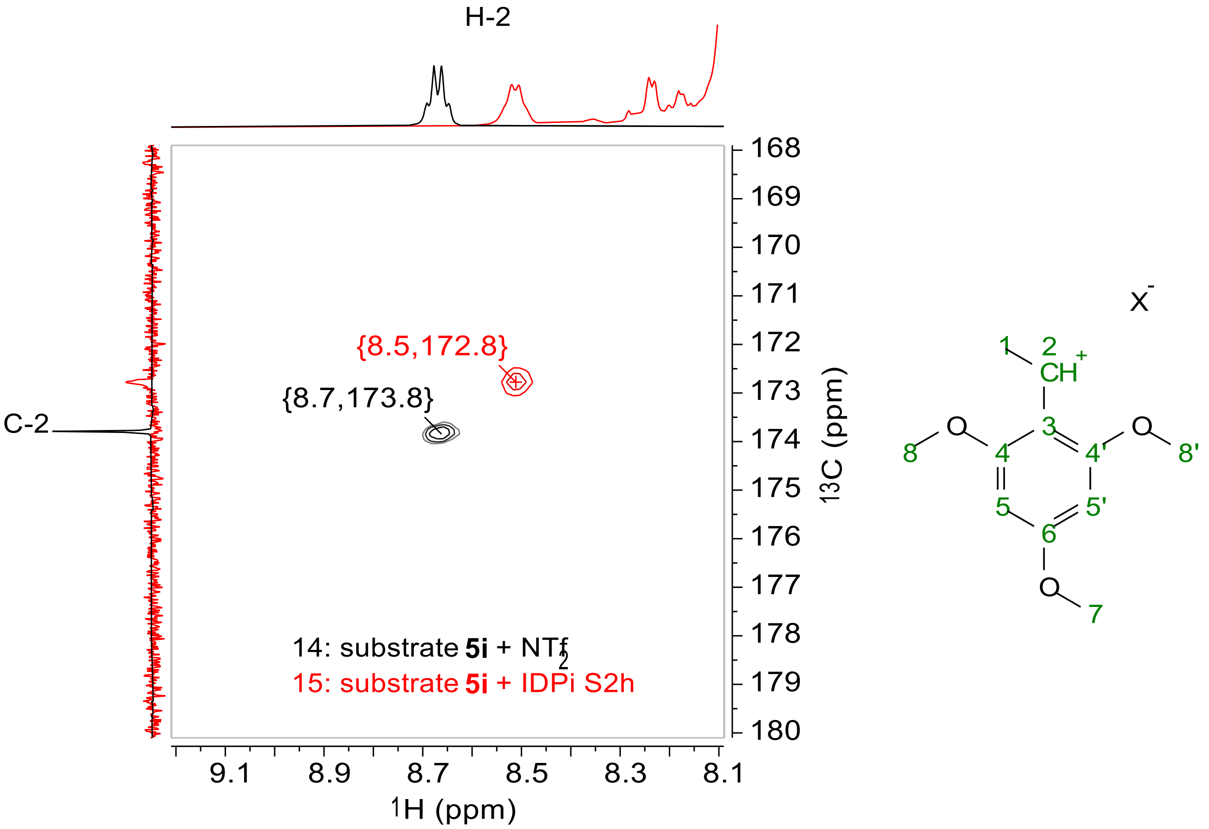

7.4 Reactivity Measurements of *rac*-1a and enantiopure 1a substrates

Reaction setup: In a dried NMR tube (flushed with argon), *rac*-**1a** (or enantiopure **1a**, 0.1 mmol, 1 equiv.) and solvent (Et_2O, 0.4 mL) were added and cooled down to –80 °C, and then acetic acid (50 µL, 4 equiv. stock solution in Et_2O) was added. An inner tube with acetone-d6 was used to lock the NMR field. The sample was cooled to –60 °C and ^1H NMR was measured. Then pre-cooled the catalyst **2a** solution (50 µL, 2.5 mol% stock solution in Et_2O) was added *via* a 50 µL Hamilton syringe having a long needle, and then reaction profile was measured at –60 °C over time.

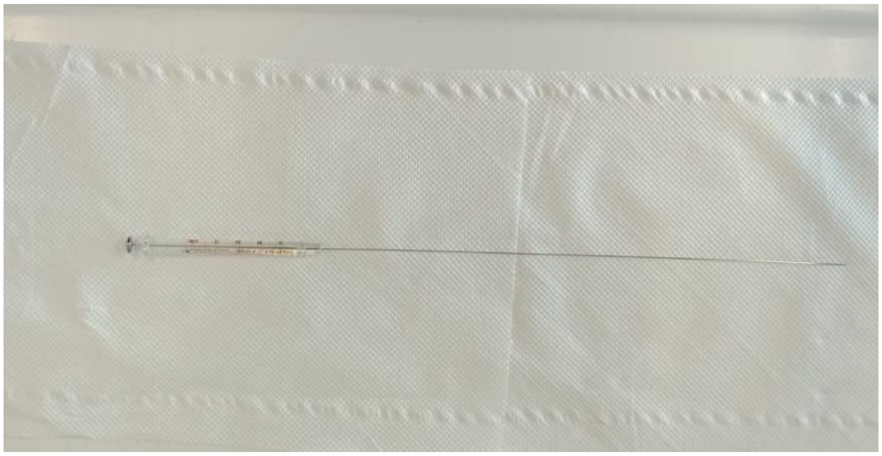

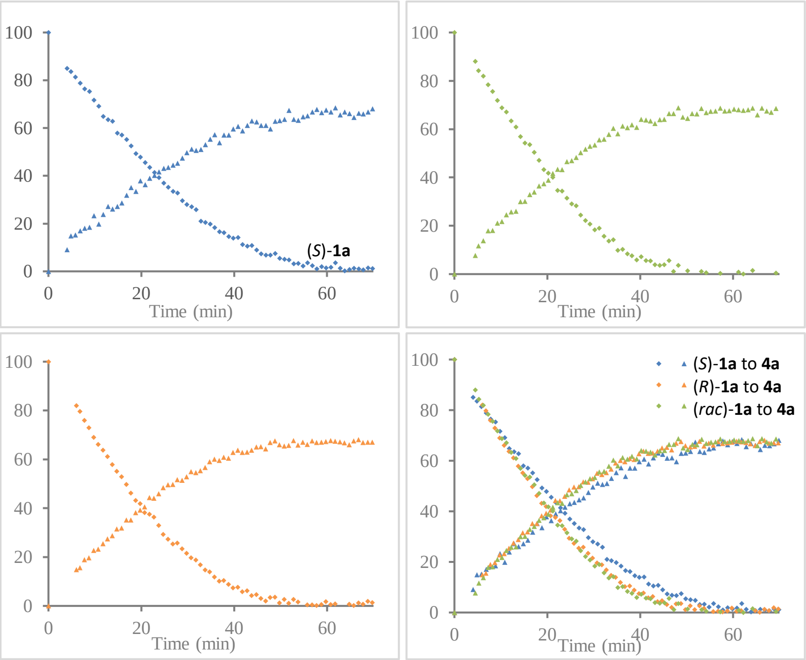

7.5. NMR Spectra:

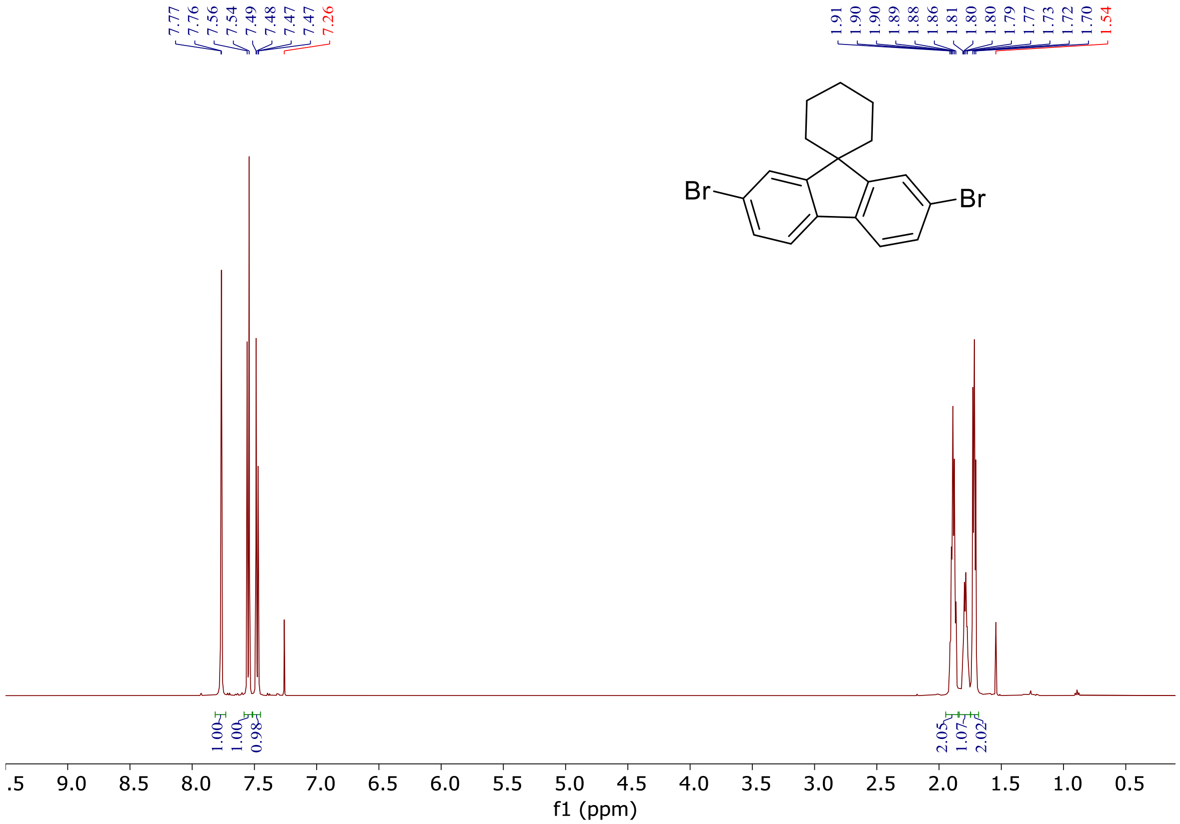

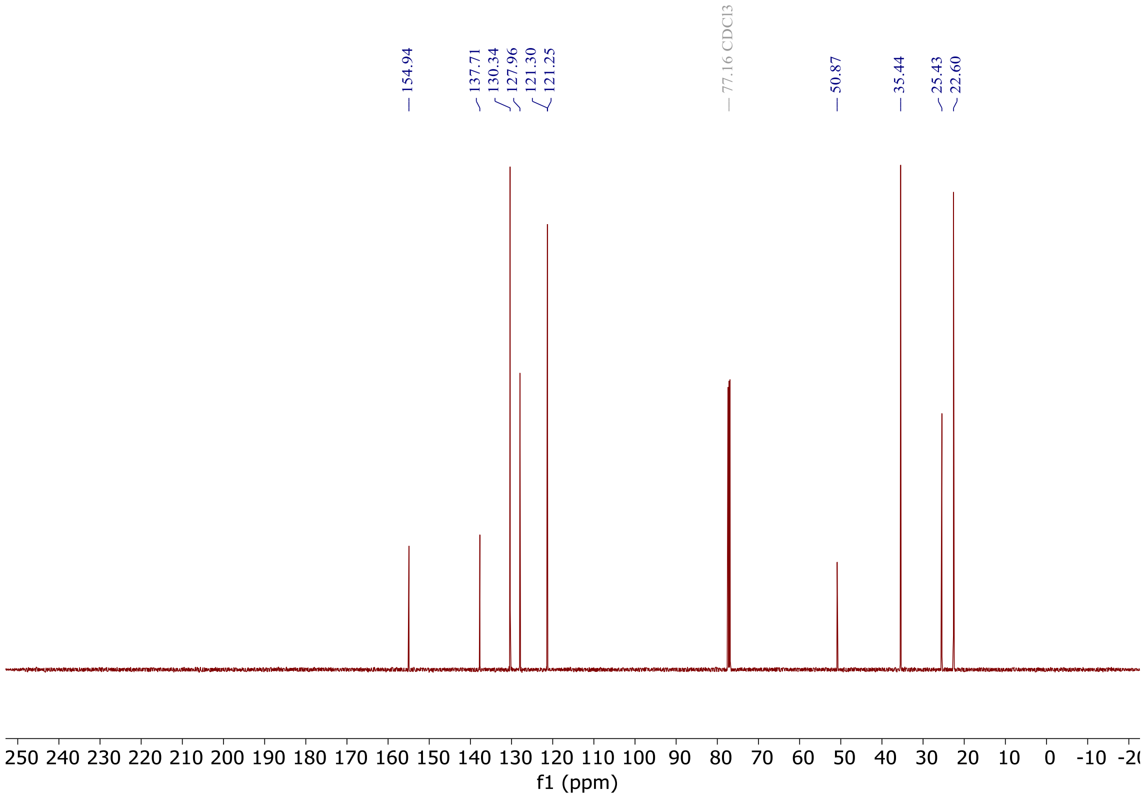

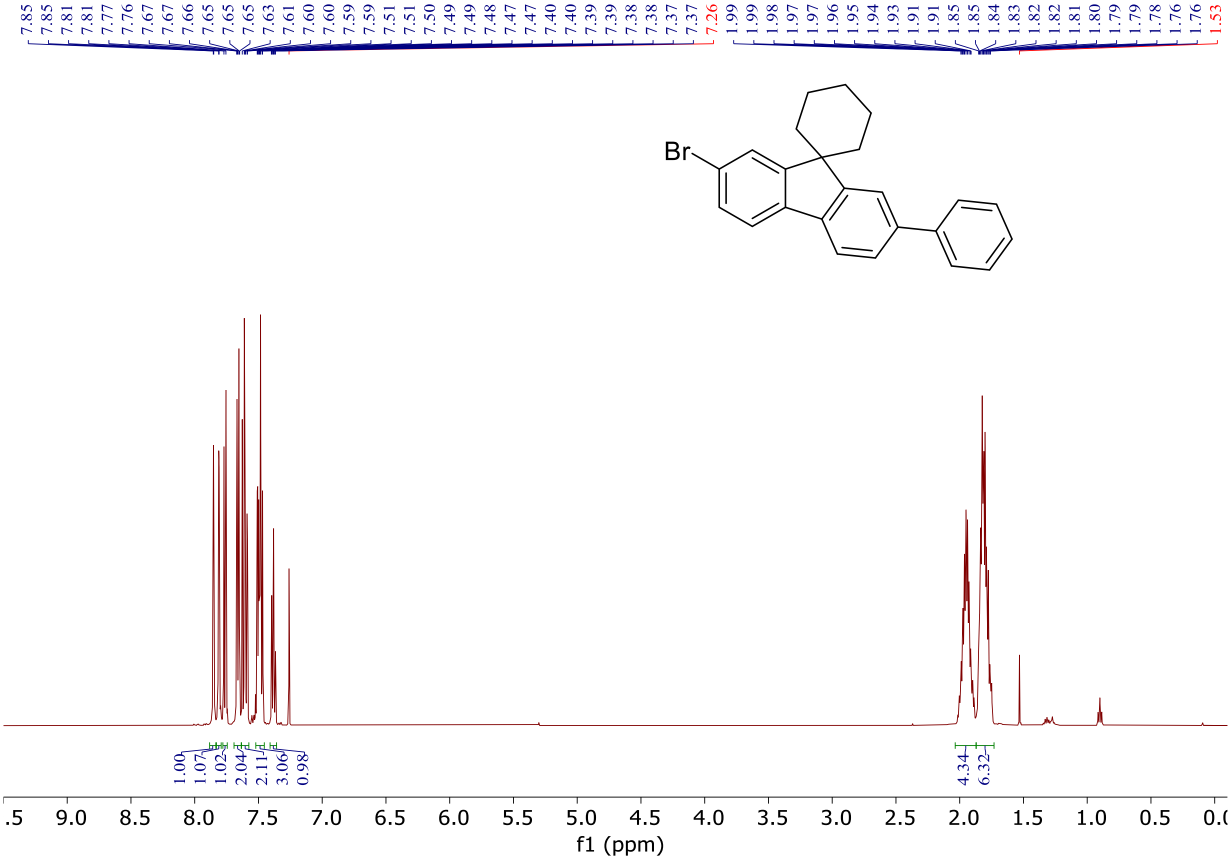
7.85
7.85
7.81
7.81
7.77
7.76
7.67
7.67
7.66
7.65
7.65
7.65
7.63
7.61
7.60
7.60
7.59
7.59
7.51
7.51
7.50
7.49
7.49
7.48
7.47
7.47
7.40
7.40
7.39
7.39
7.38
7.38
7.37
7.37
7.26
1.99
1.99
1.98
1.97
1.97
1.96
1.95
1.94
1.93
1.91
1.91
1.85
1.85
1.84
1.83
1.82
1.82
1.81
1.80
1.79
1.79
1.78
1.76
1.76
1.53
Br
1.00
1.07
1.02
2.04
2.11
3.06
0.98
4.34
6.32
.5
9.0
8.5
8.0
7.5
7.0
6.5
6.0
5.5
5.0
4.5
4.0
3.5
3.0
2.5
2.0
1.5
1.0
0.5
0.0
f1 (ppm)

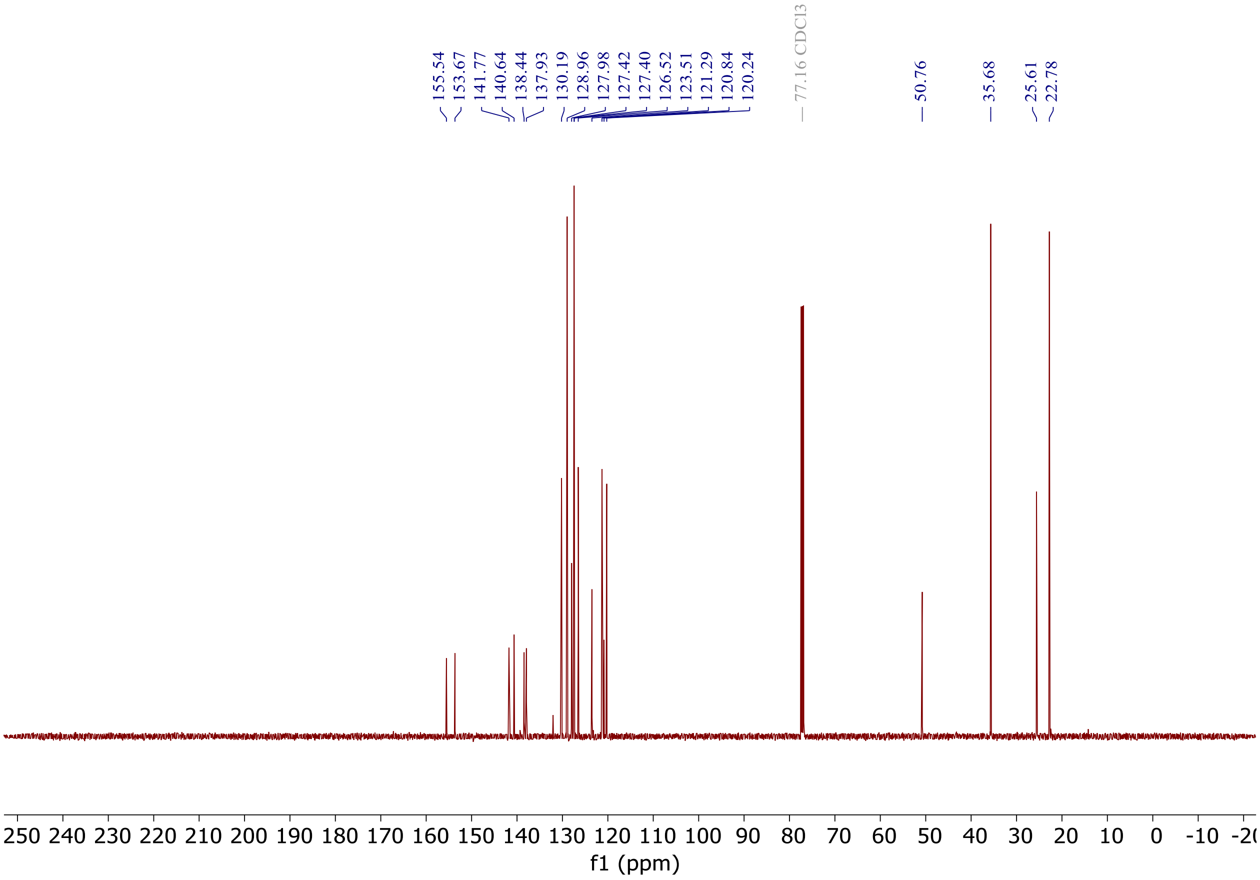
155.54
153.67
141.77
140.64
138.44
137.93
130.19
128.96
127.98
127.42
127.40
126.52
123.51
121.29
120.84
120.24
77.16 CDCl3
50.76
35.68
25.61
22.78
250
240
230
220
210
200
190
180
170
160
150
140
130
120
110
100
90
80
70
60
50
40
30
20
10
0
-10
-20
f1 (ppm)

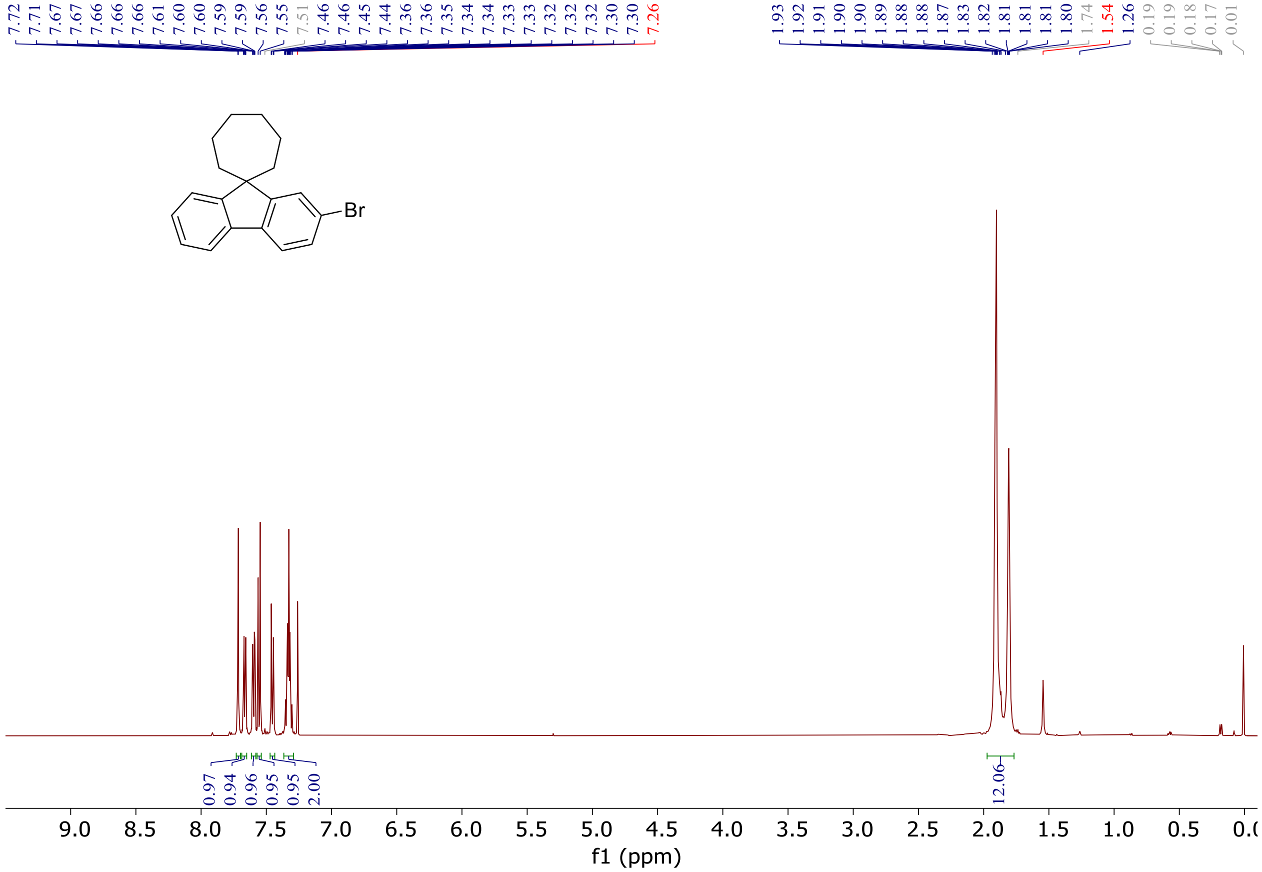
7.72
7.71
7.67
7.67
7.66
7.66
7.66
7.61
7.60
7.60
7.59
7.59
7.56
7.55
7.51
7.46
7.46
7.45
7.44
7.36
7.36
7.35
7.34
7.34
7.33
7.33
7.32
7.32
7.32
7.30
7.30
7.26
1.93
1.92
1.91
1.90
1.90
1.89
1.88
1.88
1.87
1.83
1.82
1.81
1.81
1.81
1.80
1.74
1.54
1.26
0.19
0.19
0.18
0.17
0.01
Br
0.97
0.94
0.96
0.95
0.95
2.00
12.06
9.0
8.5
8.0
7.5
7.0
6.5
6.0
5.5
5.0
4.5
4.0
3.5
3.0
2.5
2.0
1.5
1.0
0.5
0.0
f1 (ppm)

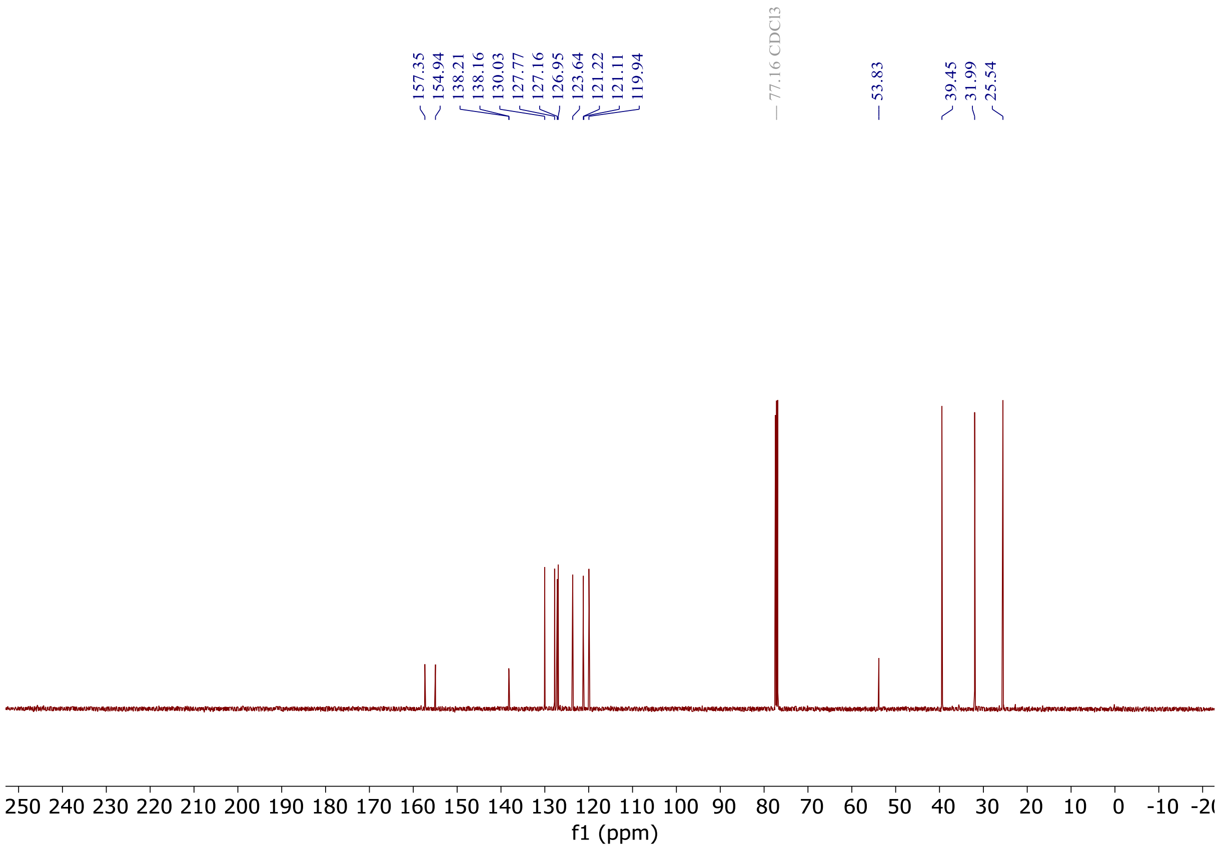
157.35
154.94
138.21
138.16
130.03
127.77
127.16
126.95
123.64
121.22
121.11
119.94
77.16 CDCl3
53.83
39.45
31.99
25.54
250
240
230
220
210
200
190
180
170
160
150
140
130
120
110
100
90
80
70
60
50
40
30
20
10
0
-10
-20
f1 (ppm)

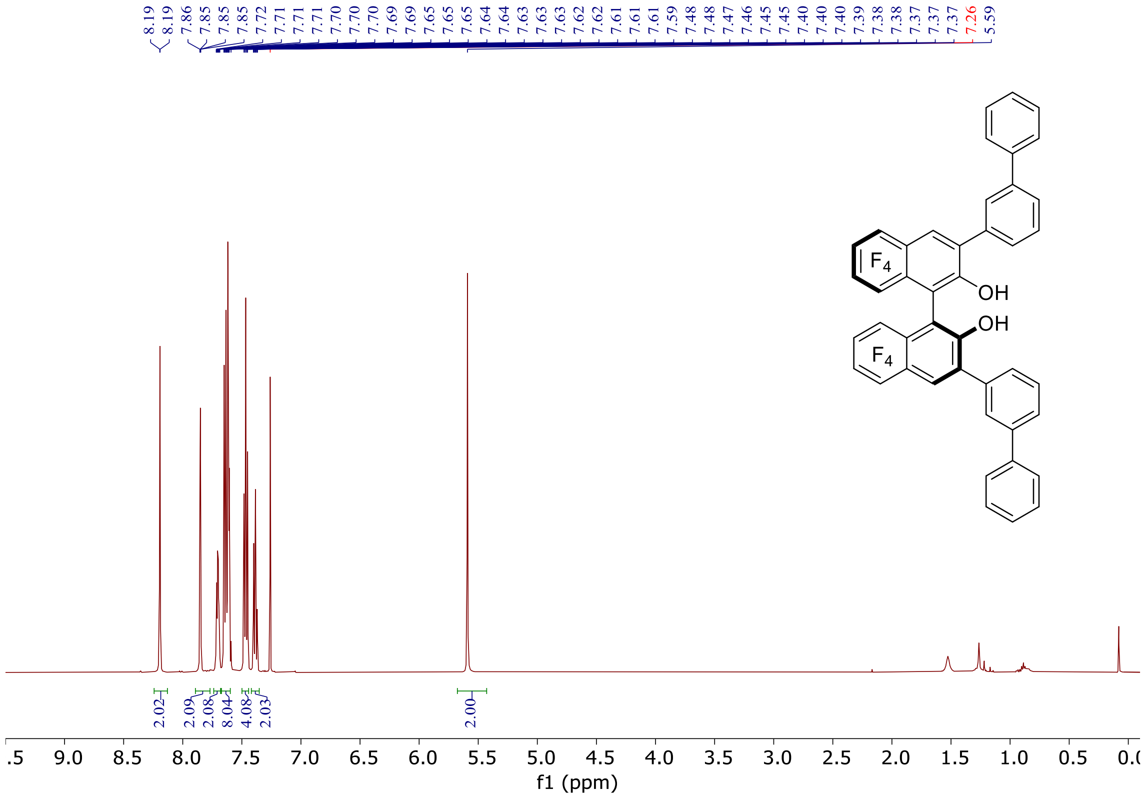
8.19
8.19
7.86
7.85
7.85
7.85
7.72
7.71
7.71
7.71
7.70
7.70
7.69
7.69
7.65
7.65
7.65
7.65
7.64
7.63
7.63
7.63
7.62
7.61
7.61
7.61
7.59
7.48
7.47
7.46
7.45
7.45
7.40
7.40
7.40
7.39
7.38
7.38
7.37
7.37
7.37
7.26
5.59
F4
OH
OH
F4
2.02
2.09
2.08
8.04
4.08
2.03
2.00
.5 9.0 8.5 8.0 7.5 7.0 6.5 6.0 5.5 5.0 4.5 4.0 3.5 3.0 2.5 2.0 1.5 1.0 0.5 0.(
f1 (ppm)

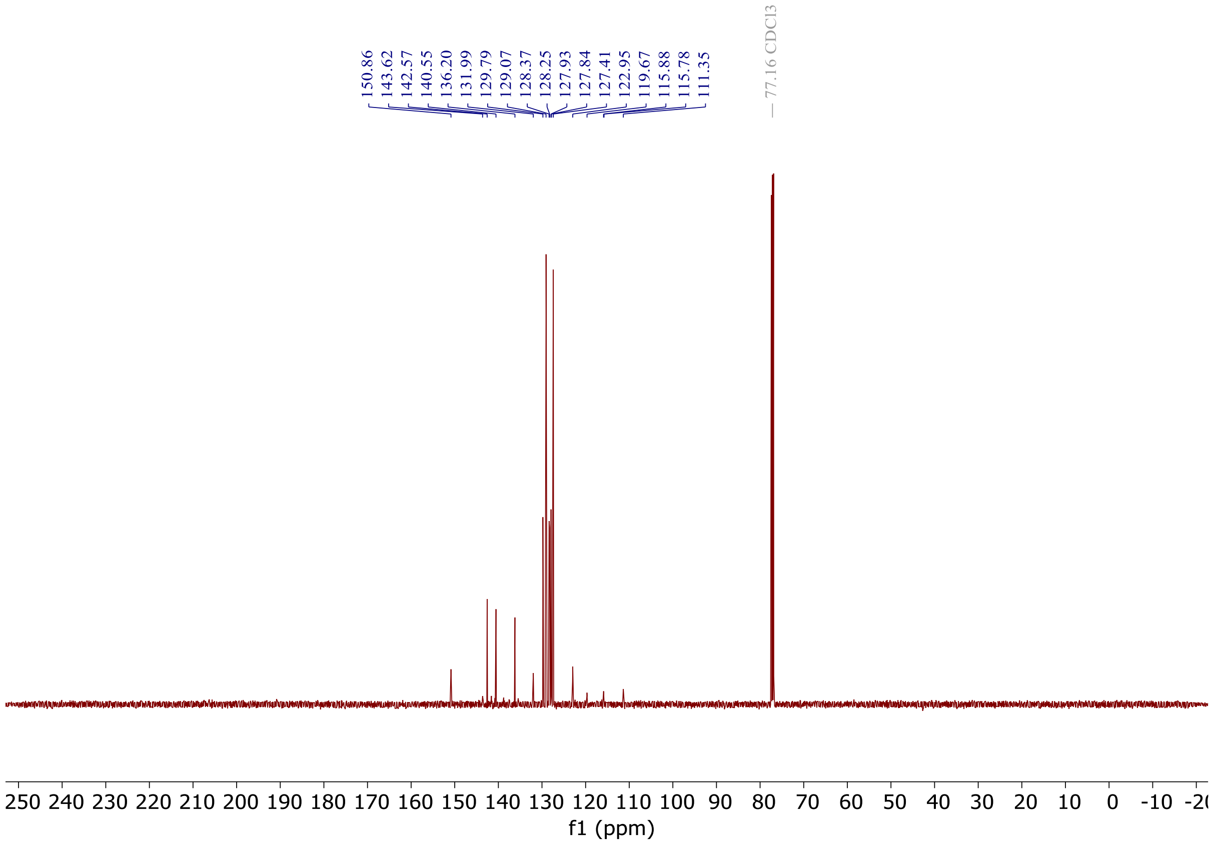
150.86
143.62
142.57
140.55
136.20
131.99
129.79
129.07
128.37
128.25
127.93
127.84
127.41
122.95
119.67
115.88
115.78
111.35
77.16 CDCl3
250 240 230 220 210 200 190 180 170 160 150 140 130 120 110 100 90 80 70 60 50 40 30 20 10 0 -10 -2(
f1 (ppm)

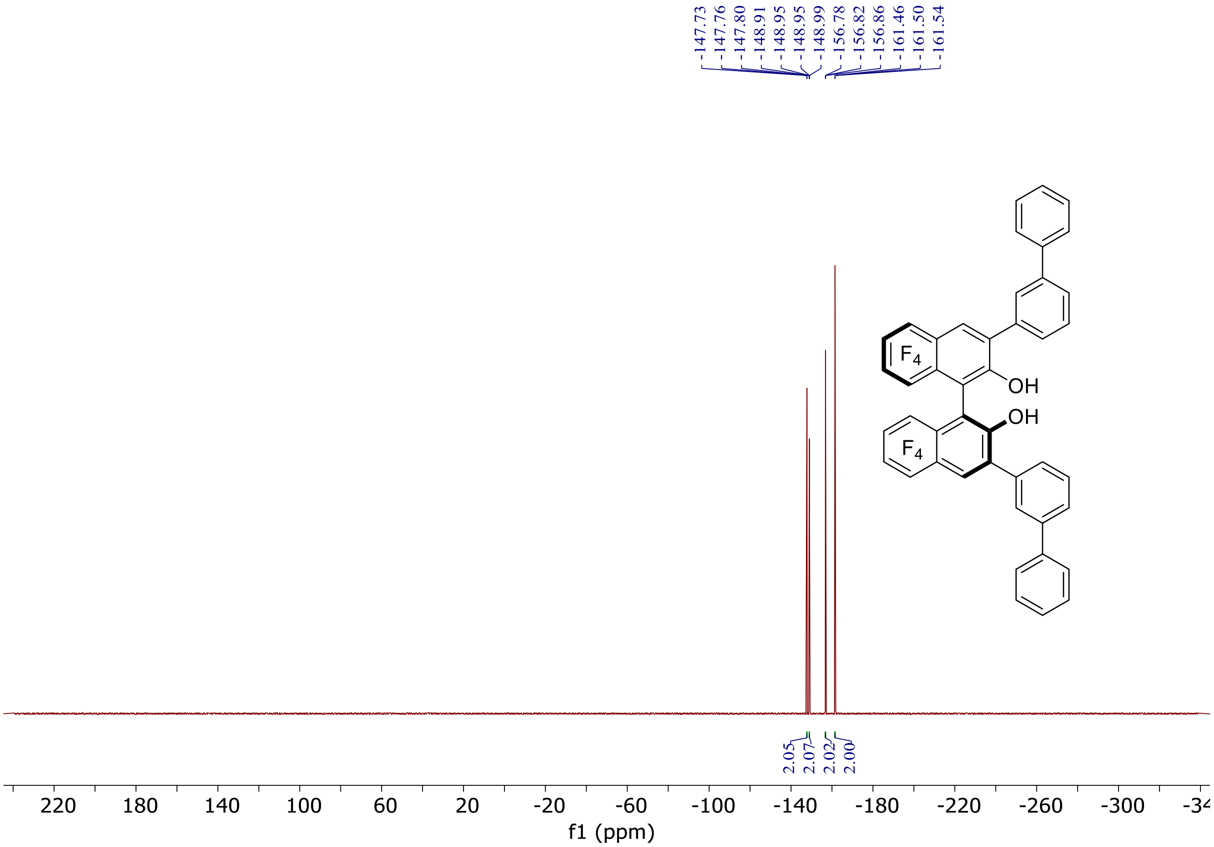
-147.73
-147.76
-147.80
-148.91
-148.95
-148.95
-148.99
-156.78
-156.82
-156.86
-161.46
-161.50
-161.54
F4
OH
OH
F4
2.05
2.07
2.02
2.00
220
180
140
100
60
20
-20
-60
-100
-140
-180
-220
-260
-300
f1 (ppm)

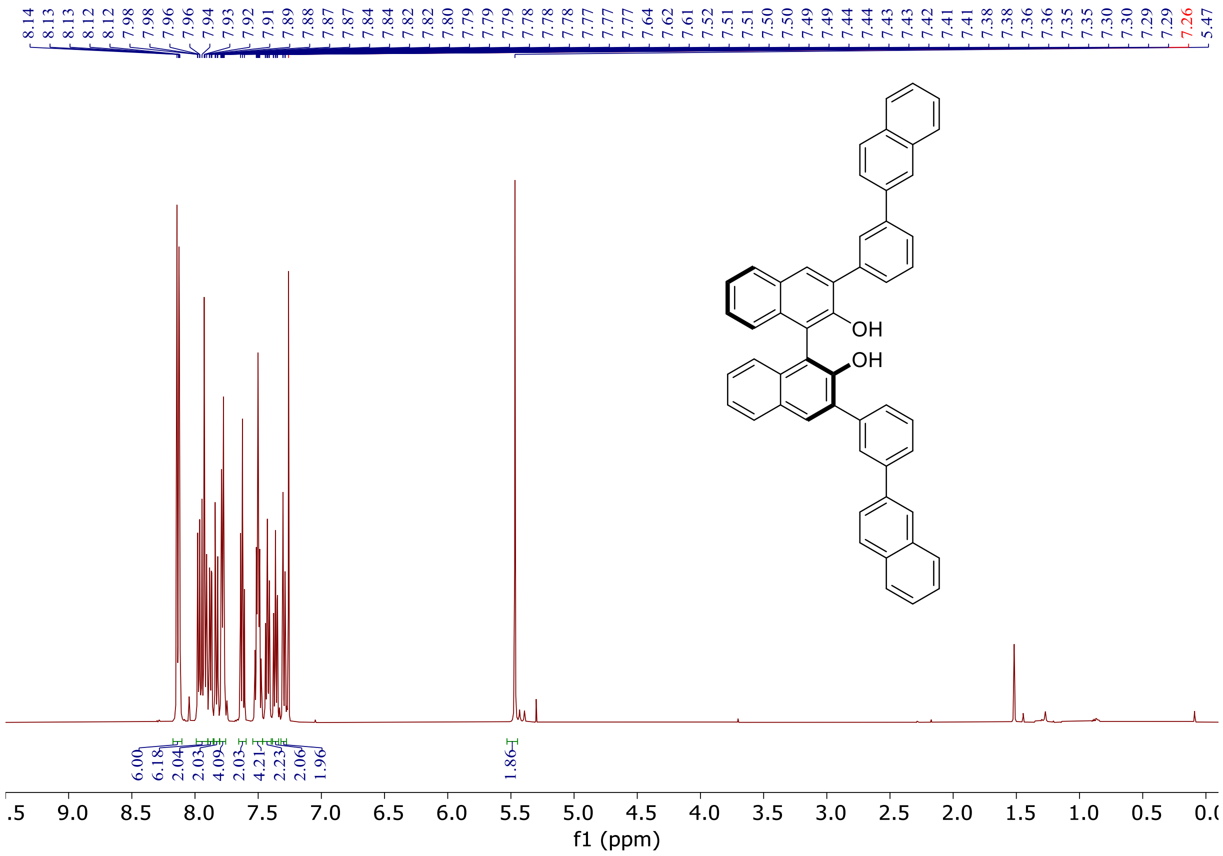
8.14
8.13
8.13
8.12
8.12
7.98
7.98
7.96
7.94
7.93
7.92
7.91
7.89
7.88
7.87
7.87
7.84
7.84
7.82
7.82
7.80
7.79
7.79
7.79
7.78
7.78
7.78
7.77
7.77
7.77
7.64
7.62
7.61
7.52
7.51
7.51
7.50
7.50
7.49
7.49
7.44
7.44
7.43
7.43
7.42
7.41
7.41
7.38
7.38
7.36
7.36
7.35
7.35
7.30
7.30
7.29
7.29
7.26
5.47
OH
OH
6.00
6.18
2.04
2.03
4.09
2.03
4.21
2.23
2.06
1.96
1.86
.5
9.0
8.5
8.0
7.5
7.0
6.5
6.0
5.5
5.0
4.5
4.0
3.5
3.0
2.5
2.0
1.5
1.0
0.5
0.(
f1 (ppm)

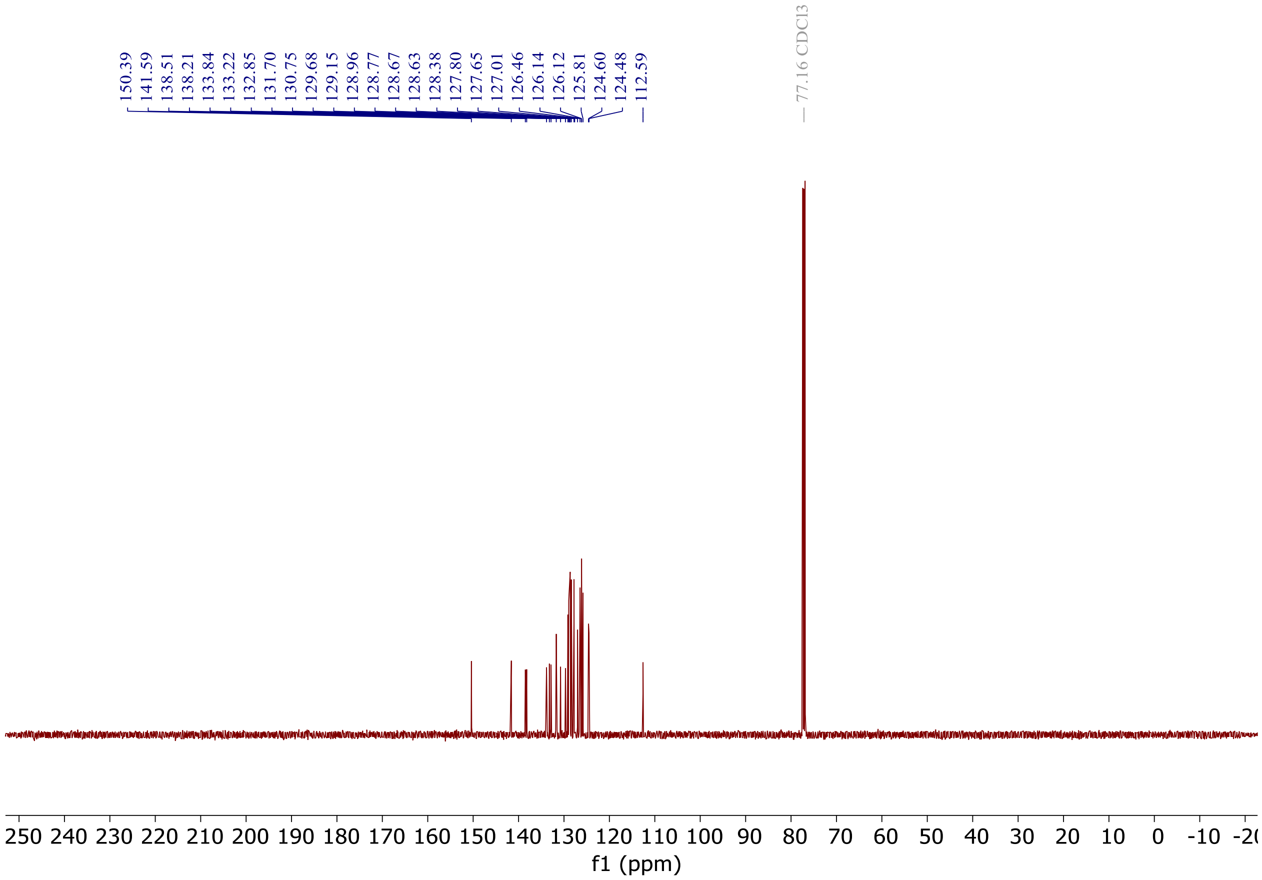
150.39
141.59
138.51
138.21
133.84
133.22
132.85
131.70
130.75
129.68
129.15
128.96
128.77
128.67
128.63
128.38
127.80
127.65
127.01
126.46
126.14
126.12
125.81
124.60
124.48
112.59
77.16 CDCl3
250
240
230
220
210
200
190
180
170
160
150
140
130
120
110
100
90
80
70
60
50
40
30
20
10
0
-10
-2(
f1 (ppm)

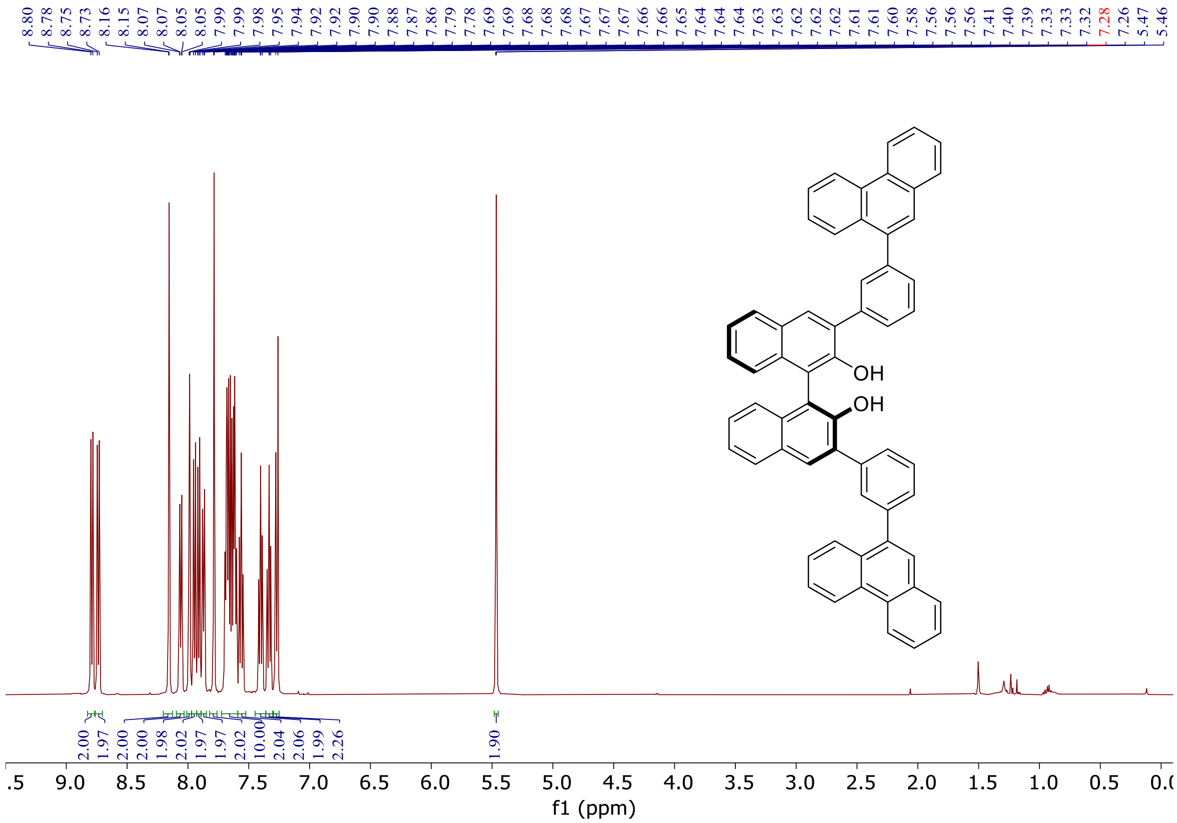
8.80
8.78
8.75
8.73
8.16
8.15
8.07
8.07
8.05
8.05
7.99
7.99
7.98
7.95
7.94
7.92
7.92
7.90
7.90
7.88
7.87
7.86
7.79
7.78
7.69
7.69
7.68
7.68
7.67
7.67
7.67
7.66
7.66
7.65
7.64
7.64
7.64
7.63
7.63
7.62
7.62
7.62
7.61
7.61
7.60
7.58
7.56
7.56
7.56
7.41
7.40
7.39
7.33
7.33
7.32
7.28
7.26
5.47
5.46
OH
OH
2.00
1.97
2.00
2.00
1.98
2.02
1.97
1.97
2.02
10.00
2.04
2.06
1.99
2.26
1.90
.5
9.0
8.5
8.0
7.5
7.0
6.5
6.0
5.5
5.0
4.5
4.0
3.5
3.0
2.5
2.0
1.5
1.0
0.5
0.(
f1 (ppm)

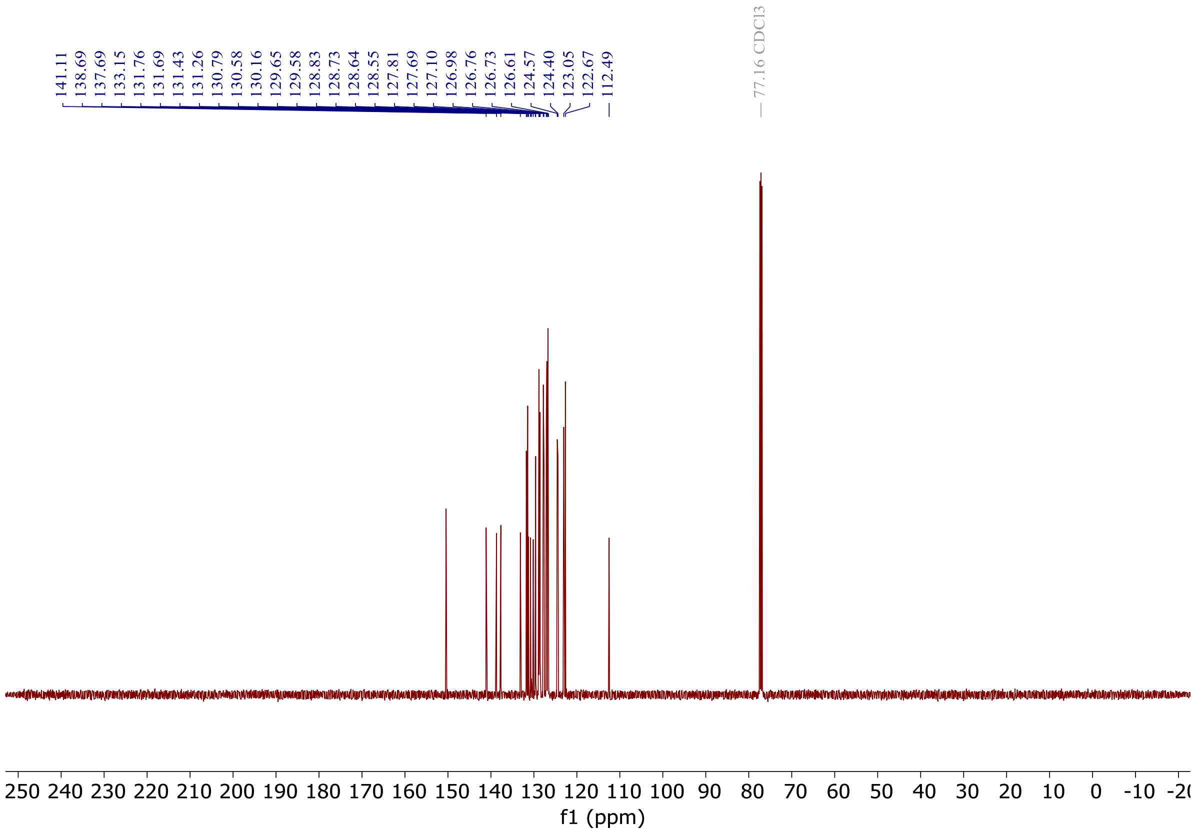
141.11
138.69
137.69
133.15
131.76
131.69
131.43
131.26
130.79
130.58
130.16
129.65
129.58
128.83
128.73
128.64
128.55
127.81
127.69
127.10
126.98
126.76
126.73
126.61
124.57
124.40
123.05
122.67
112.49
77.16 CDCl3
250
240
230
220
210
200
190
180
170
160
150
140
130
120
110
100
90
80
70
60
50
40
30
20
10
0
-10
-2(
f1 (ppm)

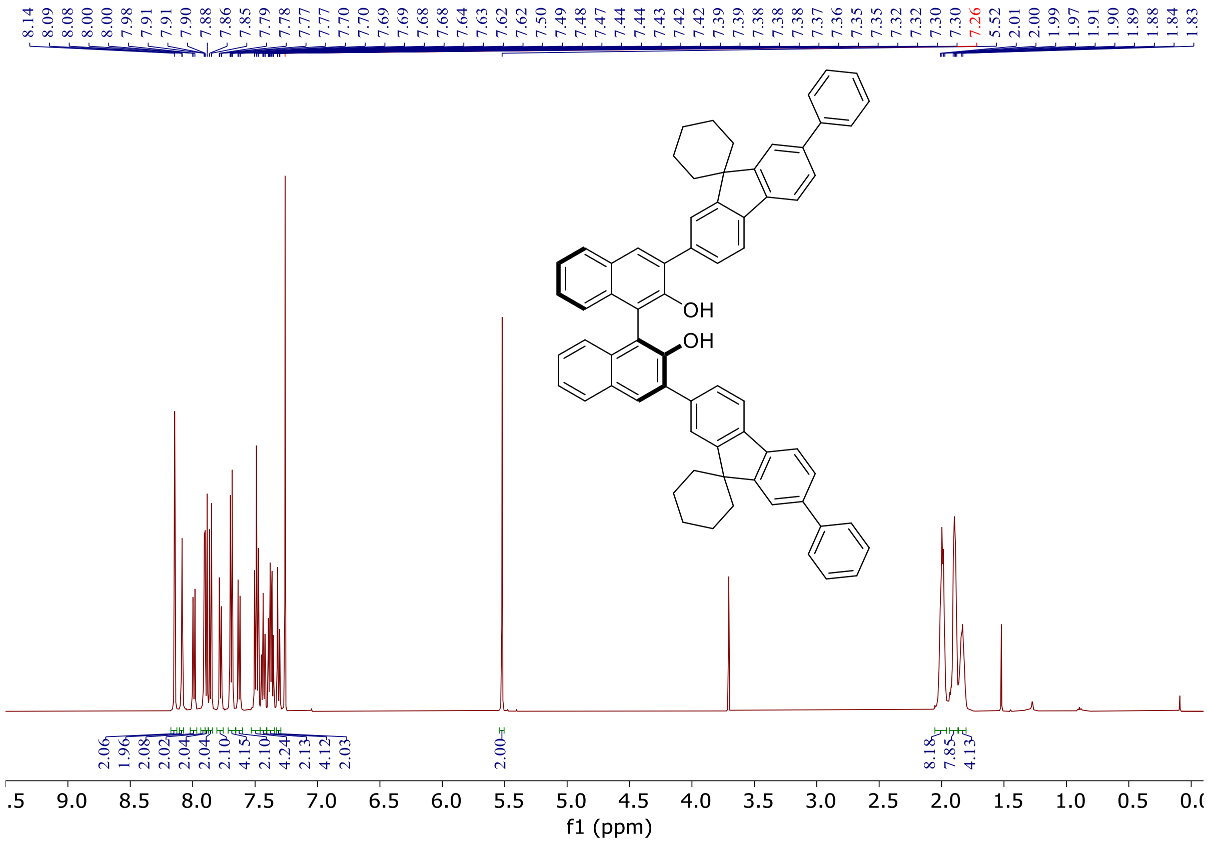
8.14
8.09
8.08
8.00
8.00
7.98
7.91
7.91
7.90
7.88
7.86
7.85
7.79
7.78
7.77
7.77
7.70
7.70
7.69
7.69
7.68
7.68
7.64
7.63
7.62
7.62
7.50
7.49
7.48
7.47
7.44
7.44
7.43
7.42
7.42
7.39
7.39
7.38
7.38
7.38
7.37
7.36
7.35
7.35
7.32
7.32
7.30
7.30
7.26
5.52
2.01
2.00
1.99
1.97
1.91
1.90
1.89
1.88
1.84
1.83
OH
OH
2.06
1.96
2.08
2.02
2.04
2.04
2.10
4.15
2.10
4.24
2.13
4.12
2.03
2.00
8.18
7.85
4.13
.5
9.0
8.5
8.0
7.5
7.0
6.5
6.0
5.5
5.0
4.5
4.0
3.5
3.0
2.5
2.0
1.5
1.0
0.5
0.(
f1 (ppm)

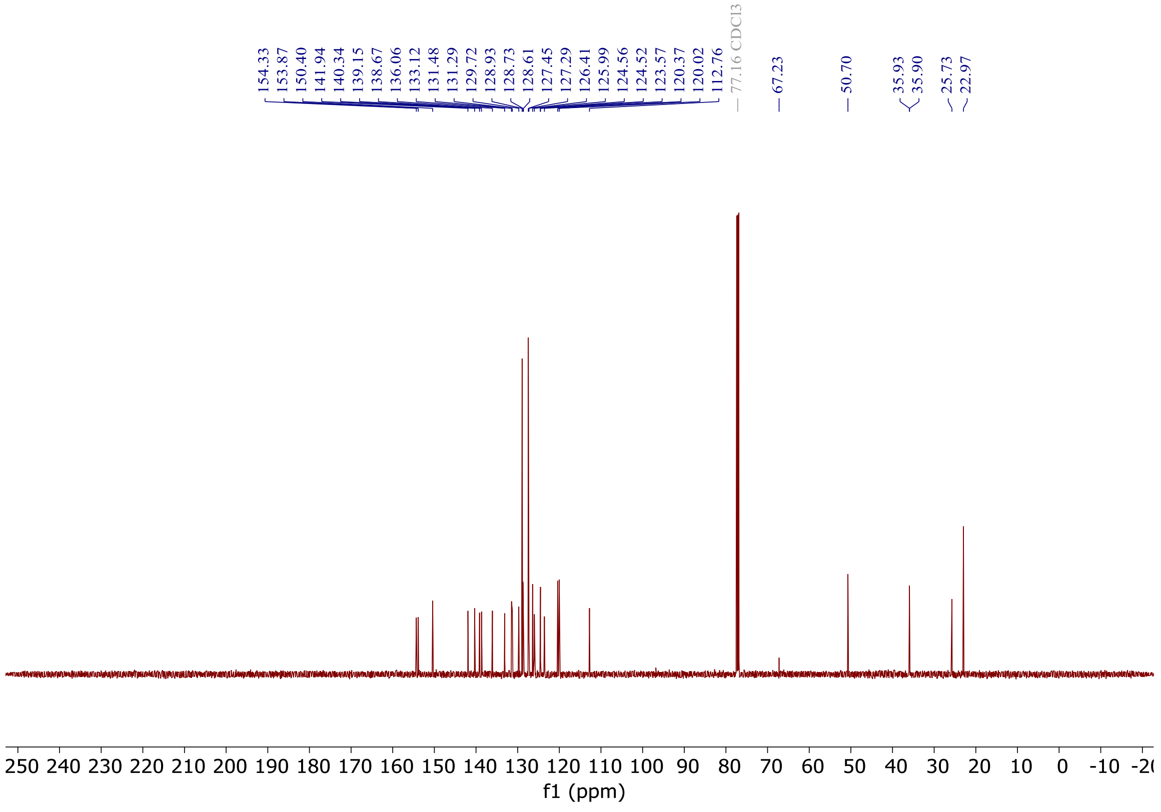
154.33
153.87
150.40
141.94
140.34
139.15
138.67
136.06
133.12
131.48
131.29
129.72
128.93
128.73
128.61
127.45
127.29
126.41
125.99
124.56
124.52
123.57
120.37
120.02
112.76
77.16 CDCl3
67.23
50.70
35.93
35.90
25.73
22.97
250
240
230
220
210
200
190
180
170
160
150
140
130
120
110
100
90
80
70
60
50
40
30
20
10
0
-10
-2(
f1 (ppm)

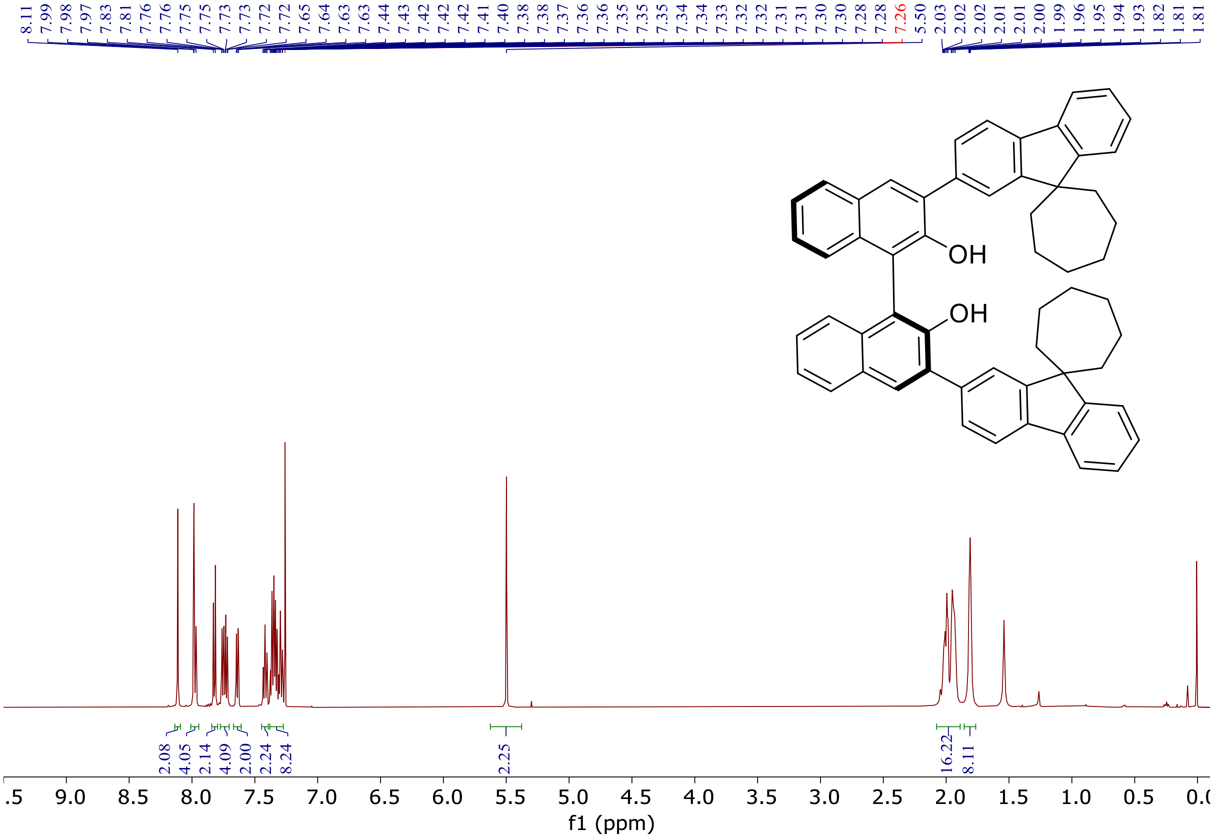
8.11
7.99
7.98
7.97
7.83
7.81
7.76
7.76
7.75
7.75
7.73
7.73
7.72
7.72
7.65
7.64
7.63
7.63
7.44
7.43
7.42
7.42
7.42
7.41
7.40
7.38
7.38
7.37
7.36
7.36
7.35
7.35
7.35
7.34
7.34
7.33
7.32
7.32
7.31
7.31
7.30
7.30
7.28
7.28
7.26
5.50
2.03
2.02
2.02
2.01
2.01
2.00
1.99
1.96
1.95
1.94
1.93
1.82
1.81
1.81
OH
OH
2.08
4.05
2.14
4.09
2.00
2.24
8.24
2.25
16.22
8.11
.5 9.0 8.5 8.0 7.5 7.0 6.5 6.0 5.5 5.0 4.5 4.0 3.5 3.0 2.5 2.0 1.5 1.0 0.5 0.0
f1 (ppm)

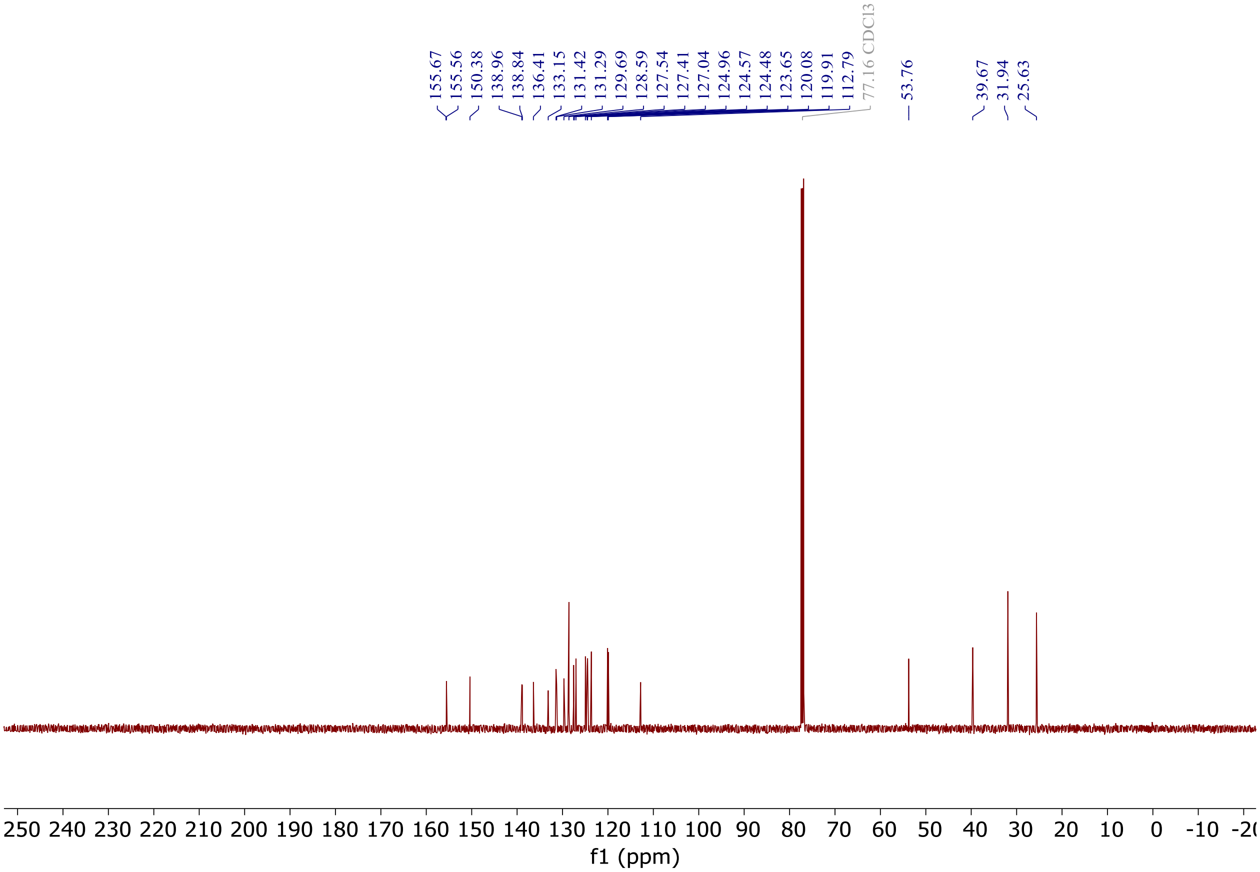
155.67
155.56
150.38
138.96
138.84
136.41
133.15
131.42
131.29
129.69
128.59
127.54
127.41
127.04
124.96
124.57
124.48
123.65
120.08
119.91
112.79
77.16 CDCl3
53.76
39.67
31.94
25.63
250 240 230 220 210 200 190 180 170 160 150 140 130 120 110 100 90 80 70 60 50 40 30 20 10 0 -10 -20
f1 (ppm)

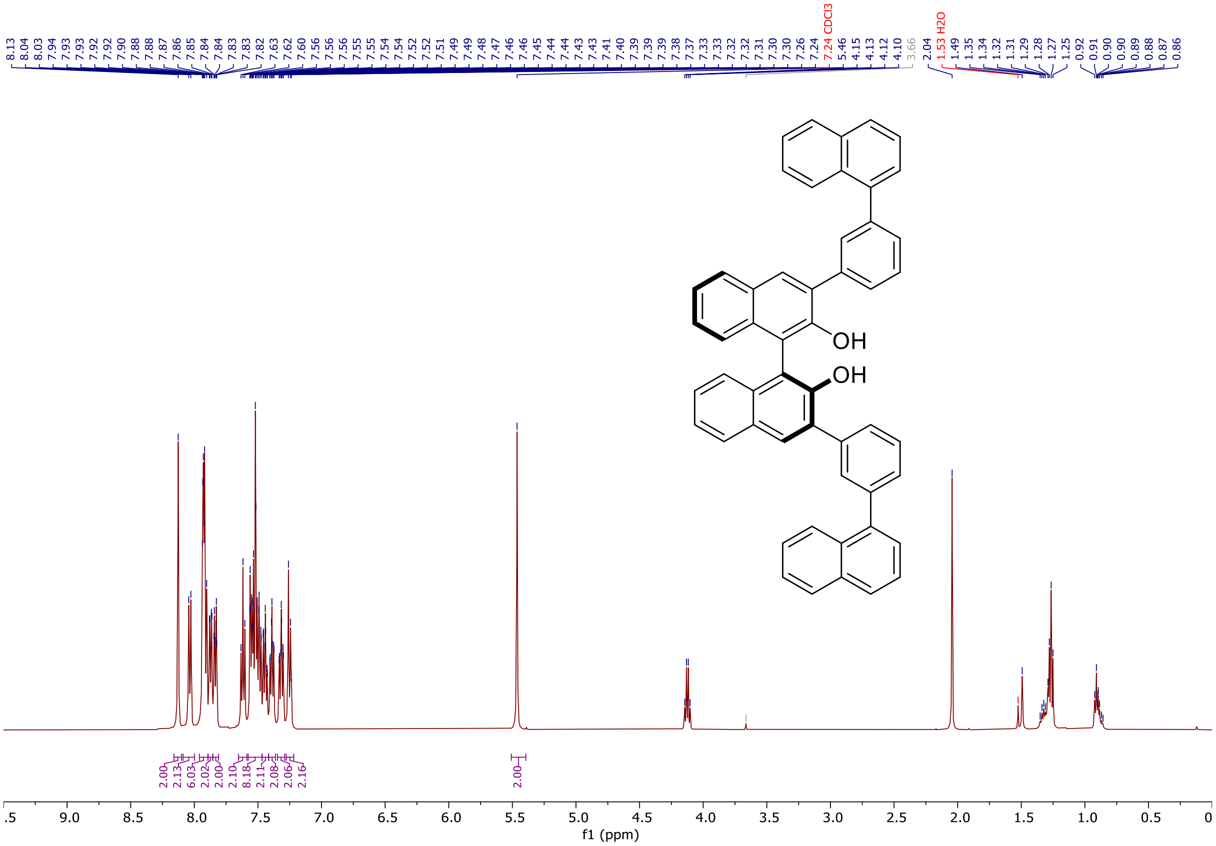
8.13 8.04 8.03 7.94 7.93 7.93 7.92 7.92 7.90 7.88 7.88 7.87 7.86 7.85 7.84 7.84 7.83 7.83 7.82 7.63 7.62 7.60 7.56 7.56 7.56 7.55 7.55 7.54 7.54 7.52 7.52 7.51 7.49 7.49 7.48 7.47 7.46 7.46 7.45 7.44 7.44 7.43 7.43 7.41 7.40 7.39 7.39 7.39 7.38 7.37 7.33 7.33 7.32 7.32 7.31 7.30 7.30 7.26 7.24
7.24 CDCl3
5.46 4.15 4.13 4.12 4.10 3.66 2.04
1.53 H2O
1.49 1.35 1.34 1.32 1.31 1.29 1.28 1.27 1.25 0.92 0.91 0.90 0.90 0.89 0.88 0.87 0.86
OH
OH
2.00 2.13 6.03 2.02 2.00 2.10 8.18 2.11 2.08 2.06 2.16
2.00
.5 9.0 8.5 8.0 7.5 7.0 6.5 6.0 5.5 5.0 4.5 4.0 3.5 3.0 2.5 2.0 1.5 1.0 0.5 0
f1 (ppm)

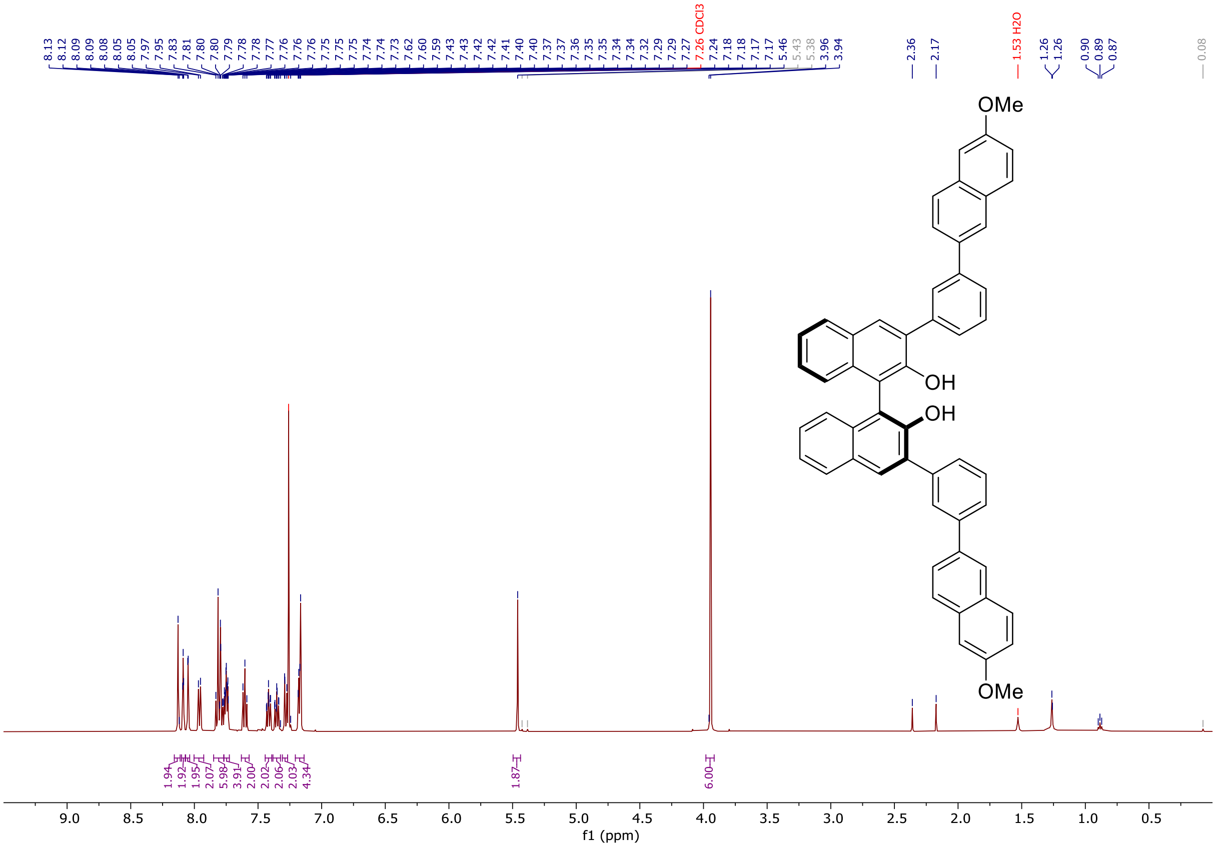
8.13 8.12 8.09 8.09 8.08 8.05 8.05 7.97 7.95 7.83 7.81 7.80 7.80 7.79 7.78 7.78 7.77 7.76 7.76 7.76 7.75 7.75 7.75 7.74 7.74 7.73 7.62 7.60 7.59 7.43 7.43 7.42 7.42 7.41 7.40 7.40 7.37 7.37 7.36 7.35 7.35 7.34 7.34 7.32 7.29 7.29 7.27
7.26 CDCl3
7.24 7.18 7.18 7.17 7.17 5.46 5.43 5.38 3.96 3.94
2.36 2.17
1.53 H2O
1.26 1.26 0.90 0.89 0.87 0.08
OMe
OH
OH
OMe
1.94 1.92 1.95 2.07 5.98 3.91 2.00 2.02 2.06 2.03 4.34
1.87
6.00
9.0 8.5 8.0 7.5 7.0 6.5 6.0 5.5 5.0 4.5 4.0 3.5 3.0 2.5 2.0 1.5 1.0 0.5
f1 (ppm)

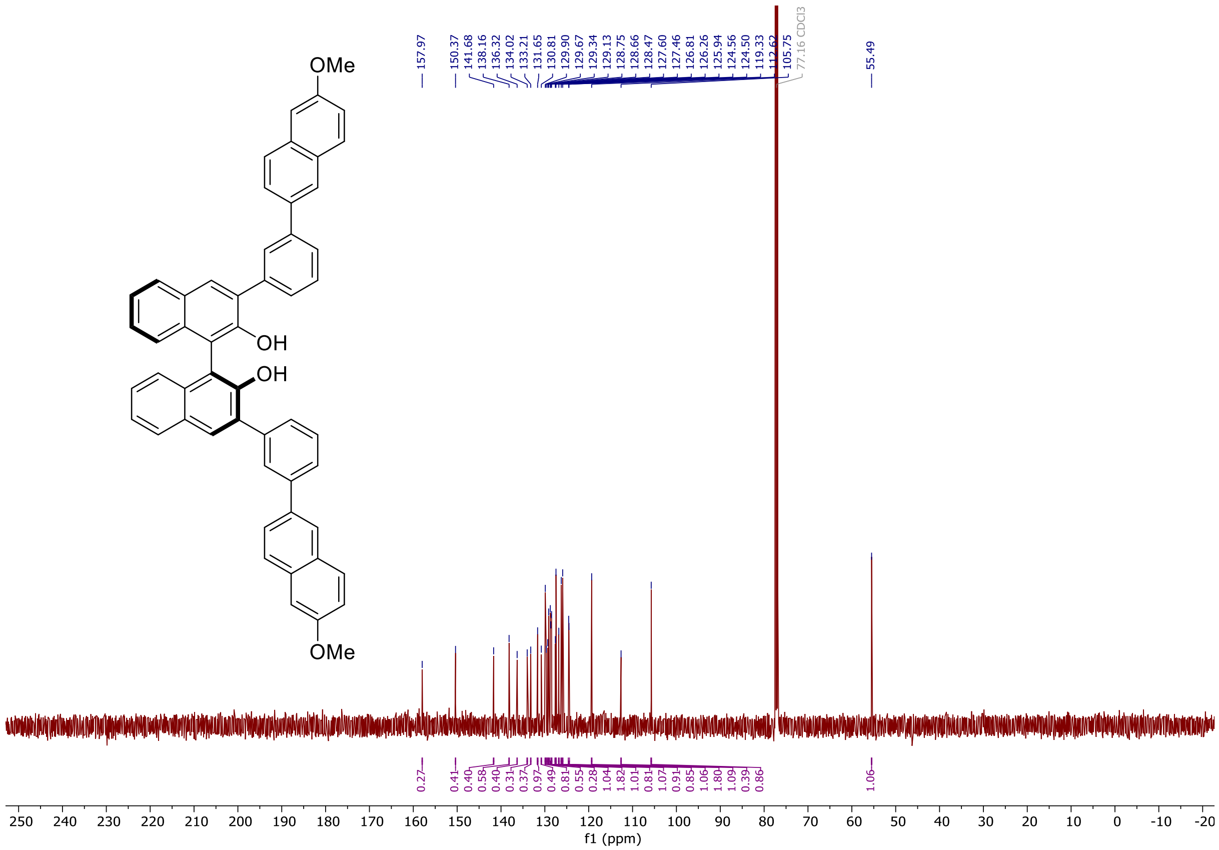
157.97
150.37
141.68
138.16
136.32
134.02
133.21
131.65
130.81
129.90
129.67
129.34
129.13
128.75
128.66
128.47
127.60
127.46
126.81
126.26
125.94
124.56
124.50
119.33
112.62
105.75
77.16 CDCl3
55.49
OMe
OH
OH
OMe
0.27
0.41
0.40
0.58
0.40
0.31
0.37
0.97
0.49
0.81
0.55
0.28
1.04
1.82
1.01
0.81
1.07
0.91
0.85
1.06
1.80
1.09
0.39
0.86
1.06
250 240 230 220 210 200 190 180 170 160 150 140 130 120 110 100 90 80 70 60 50 40 30 20 10 0 -10 -20
f1 (ppm)

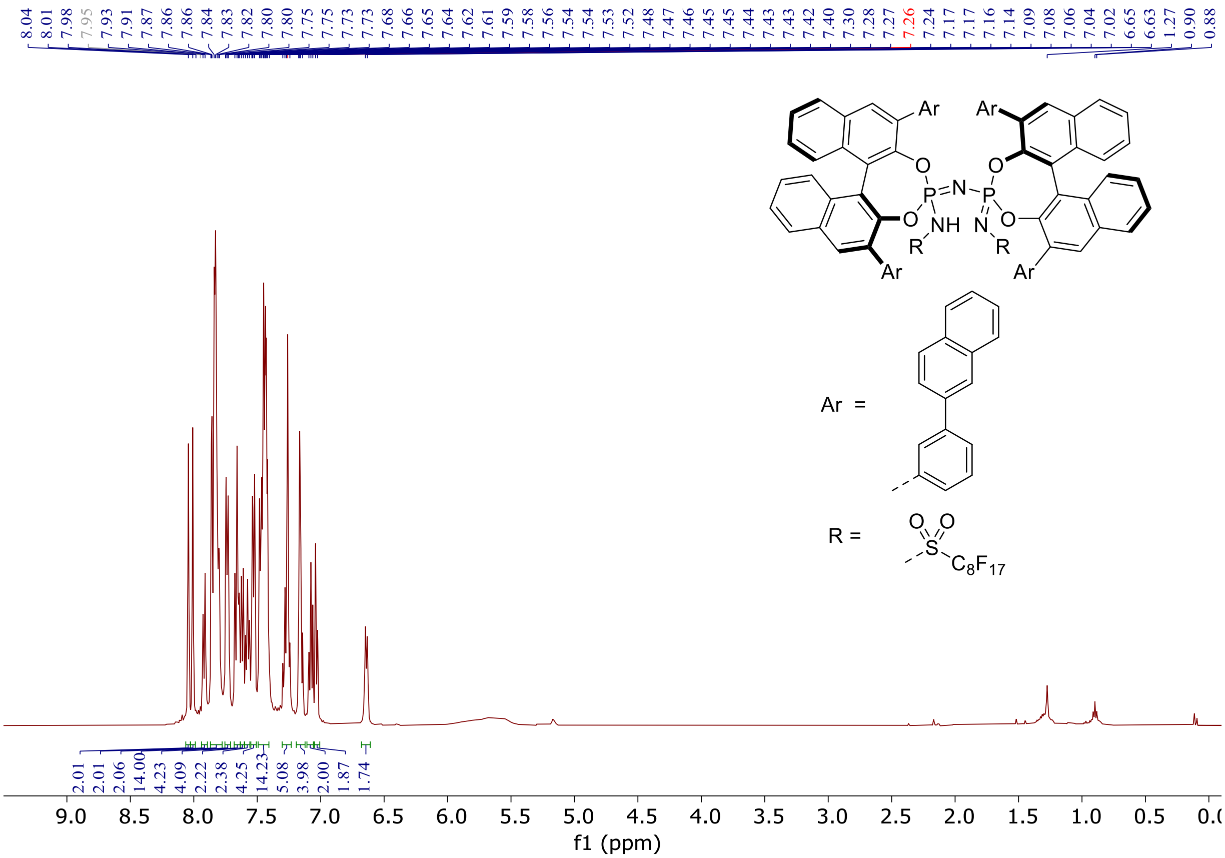
8.04
8.01
7.98
7.95
7.93
7.91
7.87
7.86
7.84
7.83
7.82
7.80
7.80
7.75
7.75
7.73
7.73
7.68
7.66
7.65
7.64
7.62
7.61
7.59
7.58
7.56
7.54
7.54
7.53
7.52
7.48
7.47
7.46
7.45
7.45
7.44
7.43
7.43
7.42
7.40
7.30
7.28
7.27
7.26
7.24
7.17
7.17
7.16
7.14
7.09
7.08
7.06
7.04
7.02
6.65
6.63
1.27
0.90
0.88
Ar
Ar
O
O
P
N
P
O
O
NH
N
R
R
Ar
Ar
Ar =
R =
O
O
S
C_8F_{17}
2.01
2.01
2.06
14.00
4.23
4.09
2.22
2.38
4.25
14.23
5.08
3.98
2.00
1.87
1.74
9.0
8.5
8.0
7.5
7.0
6.5
6.0
5.5
5.0
4.5
4.0
3.5
3.0
2.5
2.0
1.5
1.0
0.5
f1 (ppm)

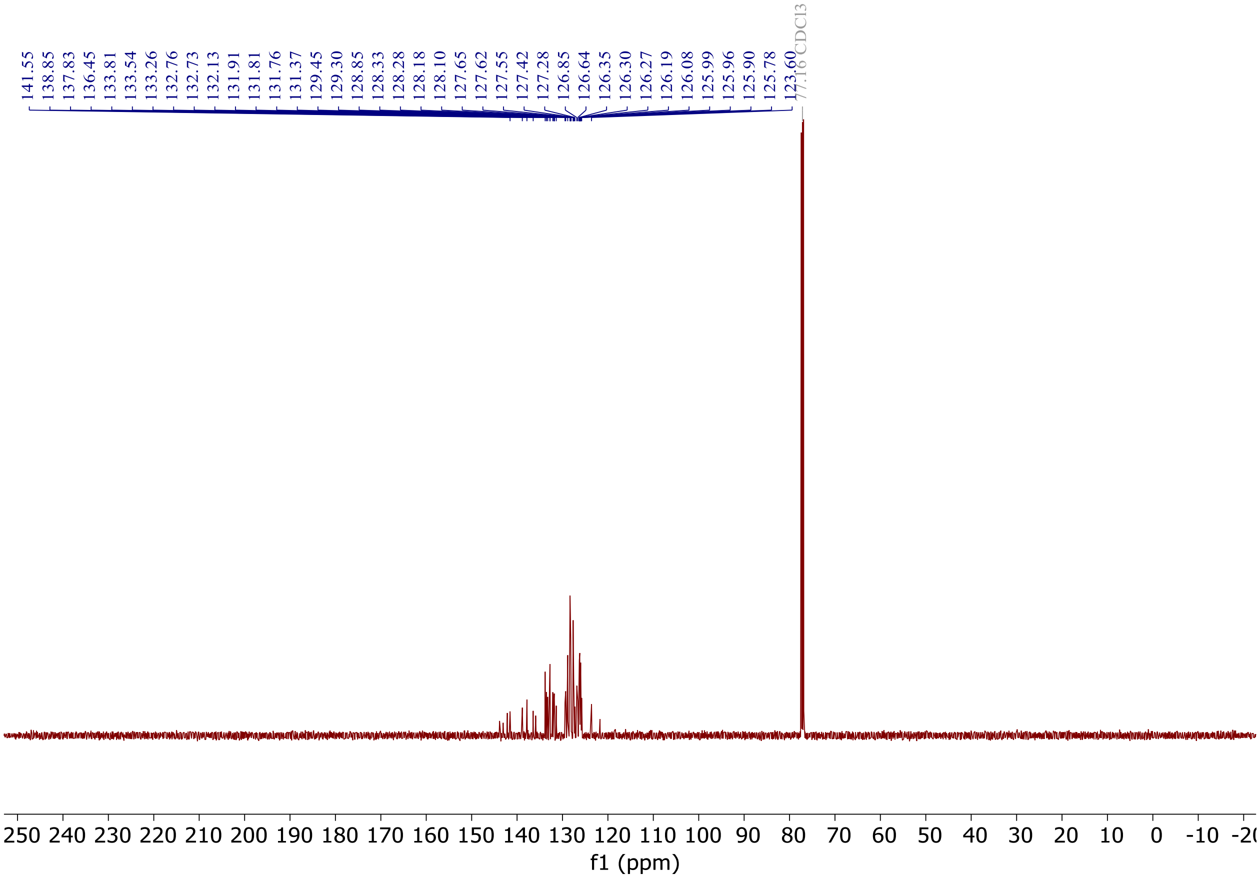
141.55
138.85
137.83
136.45
133.81
133.54
133.26
132.76
132.73
132.13
131.91
131.81
131.76
131.37
129.45
129.30
128.85
128.33
128.28
128.18
128.10
127.65
127.62
127.55
127.42
127.28
126.85
126.64
126.35
126.30
126.27
126.19
126.08
125.99
125.96
125.90
125.78
123.60
77.16 CDCl3
250
240
230
220
210
200
190
180
170
160
150
140
130
120
110
100
90
80
70
60
50
40
30
20
10
0
-10
f1 (ppm)

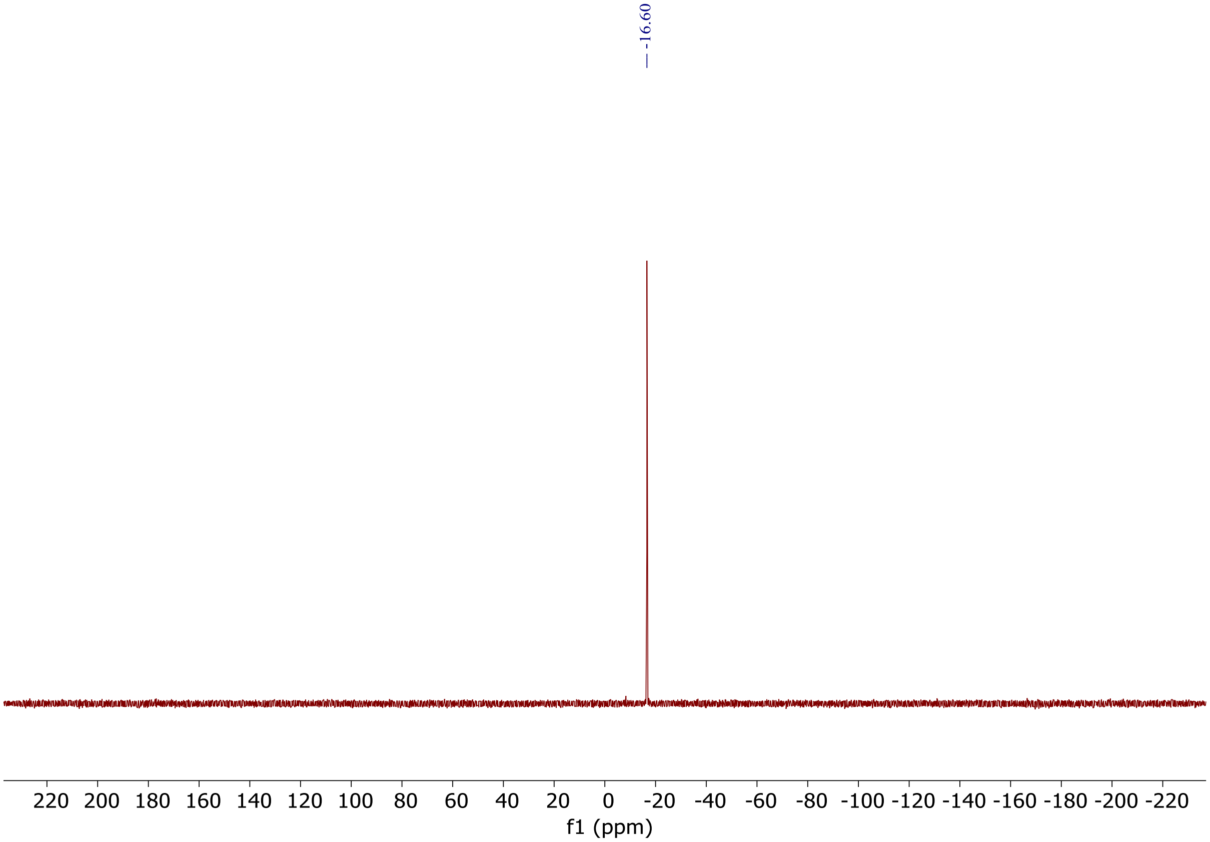
-16.60
220 200 180 160 140 120 100 80 60 40 20 0 -20 -40 -60 -80 -100 -120 -140 -160 -180 -200 -220
f1 (ppm)

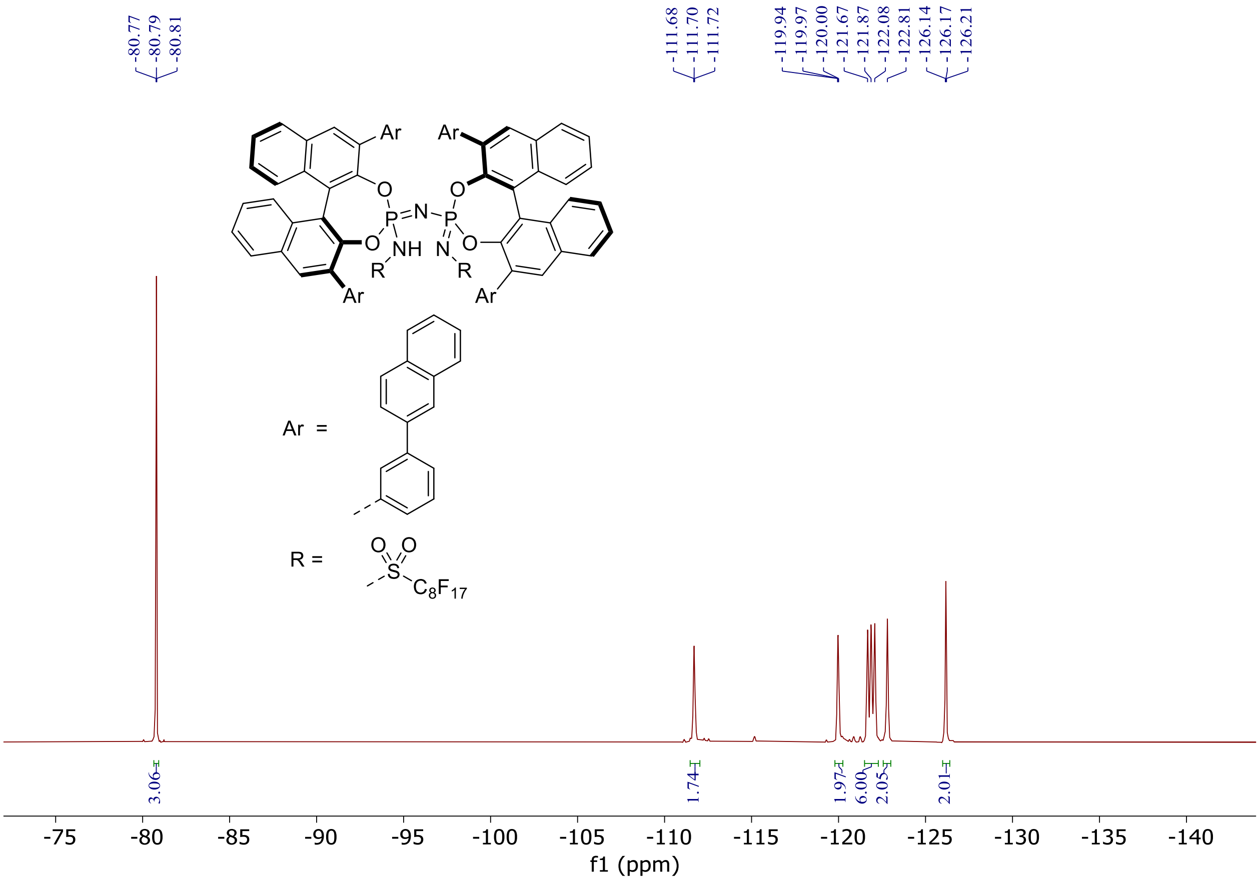
-80.77
-80.79
-80.81
-111.68
-111.70
-111.72
-119.94
-119.97
-120.00
-121.67
-121.87
-122.08
-122.81
-126.14
-126.17
-126.21
Ar
Ar
O
O
P
N
P
O
O
NH
N
R
R
Ar
Ar
Ar =
R =
O
O
S
C_8F_{17}
3.06
1.74
1.97
6.00
2.05
2.01
-75 -80 -85 -90 -95 -100 -105 -110 -115 -120 -125 -130 -135 -140
f1 (ppm)

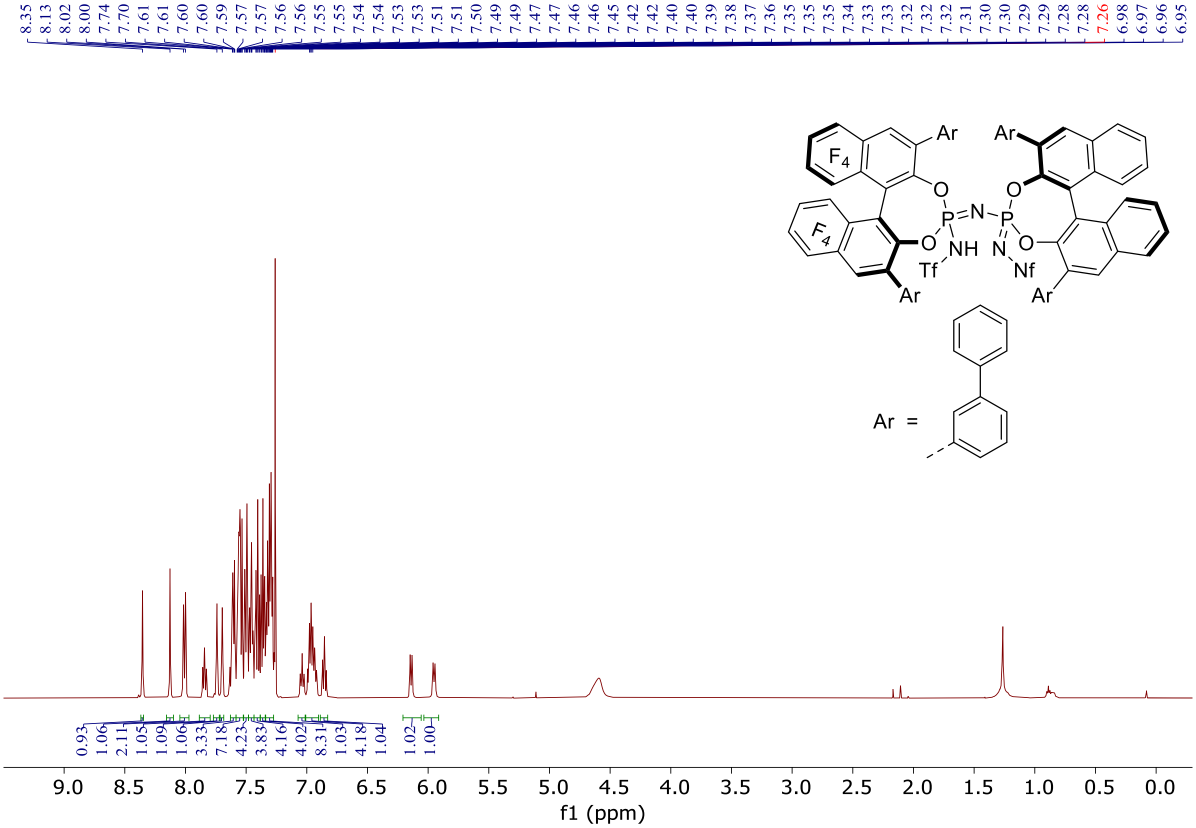
8.35
8.13
8.02
8.00
7.74
7.70
7.61
7.61
7.60
7.60
7.59
7.57
7.57
7.56
7.56
7.55
7.55
7.54
7.54
7.53
7.53
7.51
7.51
7.50
7.49
7.49
7.47
7.47
7.46
7.45
7.42
7.42
7.40
7.40
7.39
7.38
7.37
7.36
7.35
7.35
7.35
7.34
7.33
7.33
7.32
7.32
7.32
7.31
7.30
7.30
7.29
7.29
7.28
7.28
7.26
6.98
6.97
6.96
6.95
Ar
Ar
F4
F4
O
O
P
N
P
O
O
NH
N
Tf
Nf
Ar
Ar
Ar =
0.93
1.06
2.11
1.05
1.09
1.06
3.33
7.18
4.23
3.83
4.16
4.02
8.31
1.03
4.18
1.04
1.02
1.00
9.0
8.5
8.0
7.5
7.0
6.5
6.0
5.5
5.0
4.5
4.0
3.5
3.0
2.5
2.0
1.5
1.0
0.5
0.0
f1 (ppm)

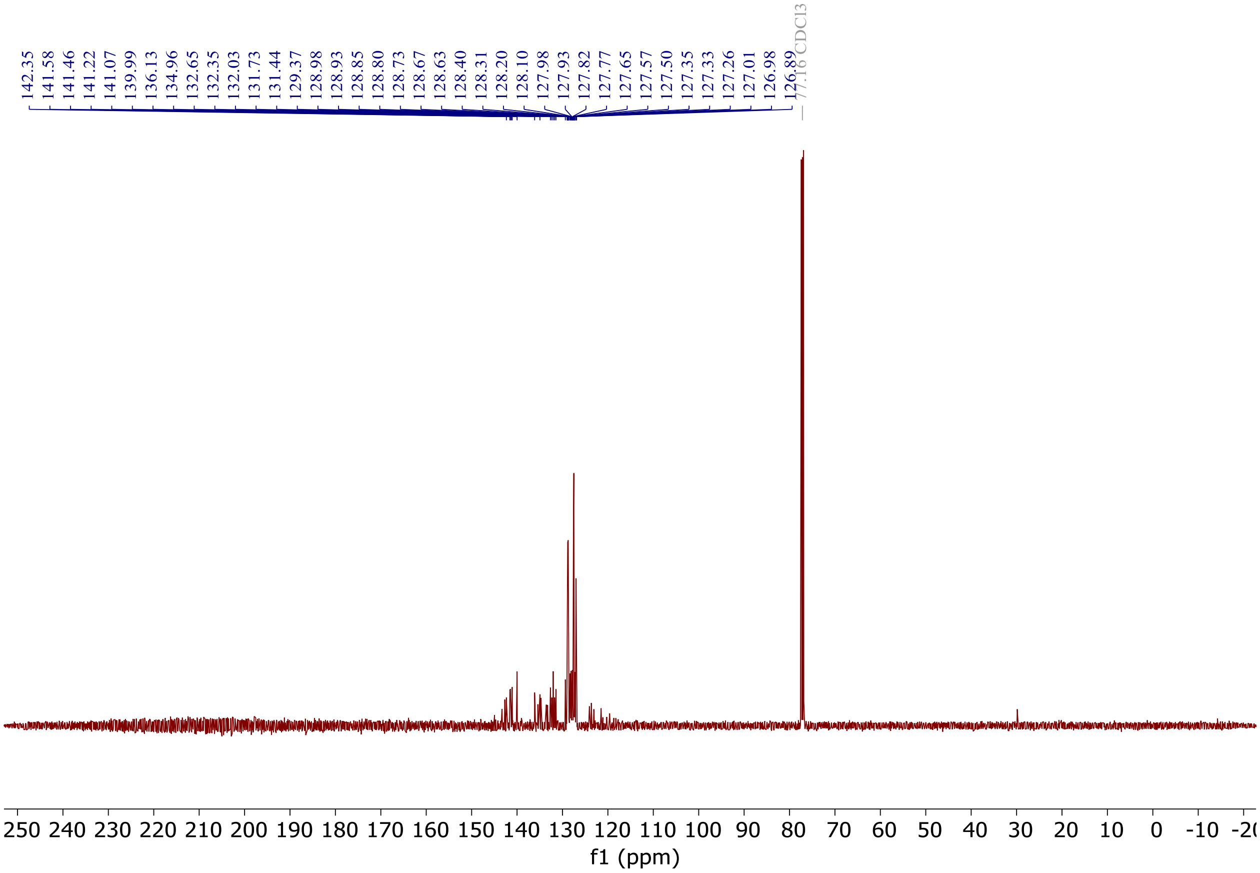
142.35
141.58
141.46
141.22
141.07
139.99
136.13
134.96
132.65
132.35
132.03
131.73
131.44
129.37
128.98
128.93
128.85
128.80
128.73
128.67
128.63
128.40
128.31
128.20
128.10
127.98
127.93
127.82
127.77
127.65
127.57
127.50
127.35
127.33
127.26
127.01
126.98
126.89
77.16 CDCl3
250
240
230
220
210
200
190
180
170
160
150
140
130
120
110
100
90
80
70
60
50
40
30
20
10
0
-10
f1 (ppm)

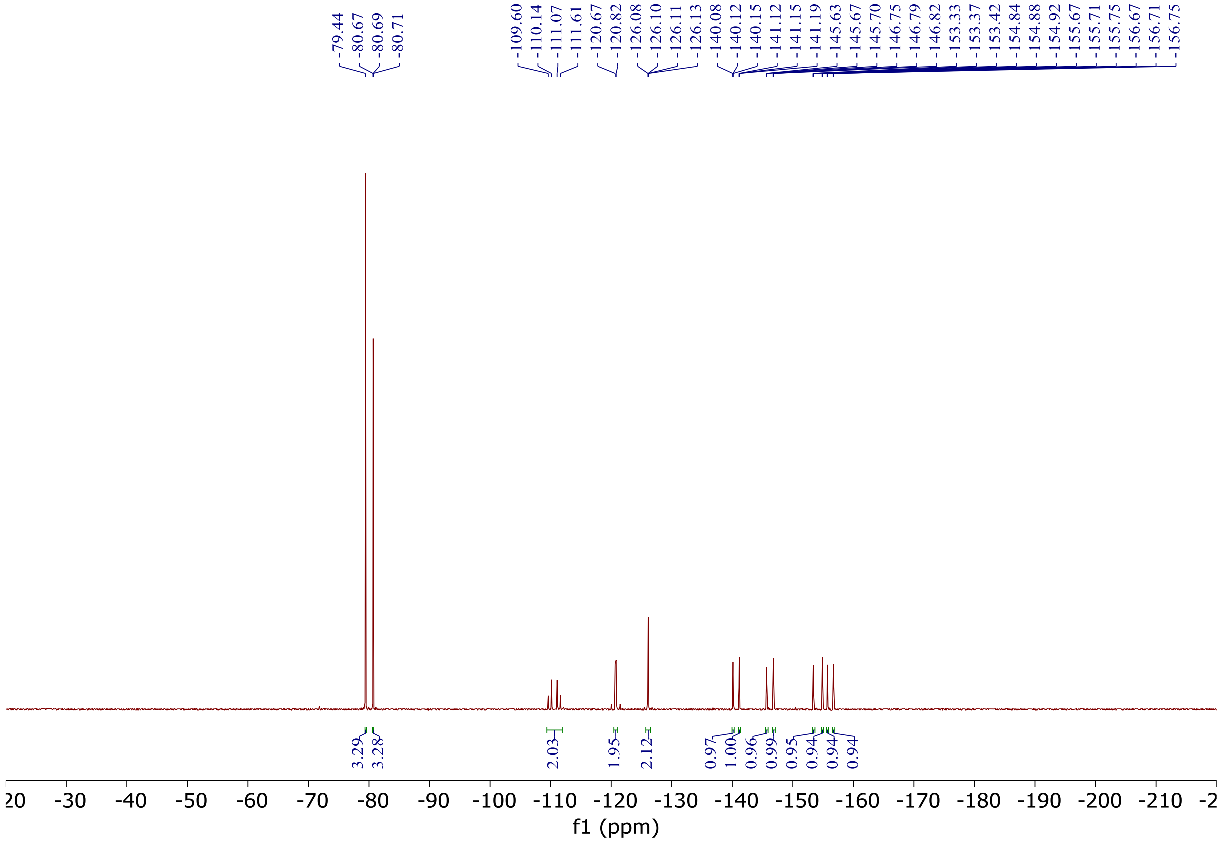
-79.44
-80.67
-80.69
-80.71
-109.60
-110.14
-111.07
-111.61
-120.67
-120.82
-126.08
-126.10
-126.11
-126.13
-140.08
-140.12
-140.15
-141.12
-141.15
-141.19
-145.63
-145.67
-145.70
-146.75
-146.79
-146.82
-153.33
-153.37
-153.42
-154.84
-154.88
-154.92
-155.67
-155.71
-155.75
-156.67
-156.71
-156.75
3.29
3.28
2.03
1.95
2.12
0.97
1.00
0.96
0.99
0.95
0.94
0.94
0.94
20 -30 -40 -50 -60 -70 -80 -90 -100 -110 -120 -130 -140 -150 -160 -170 -180 -190 -200 -210 -2
f1 (ppm)

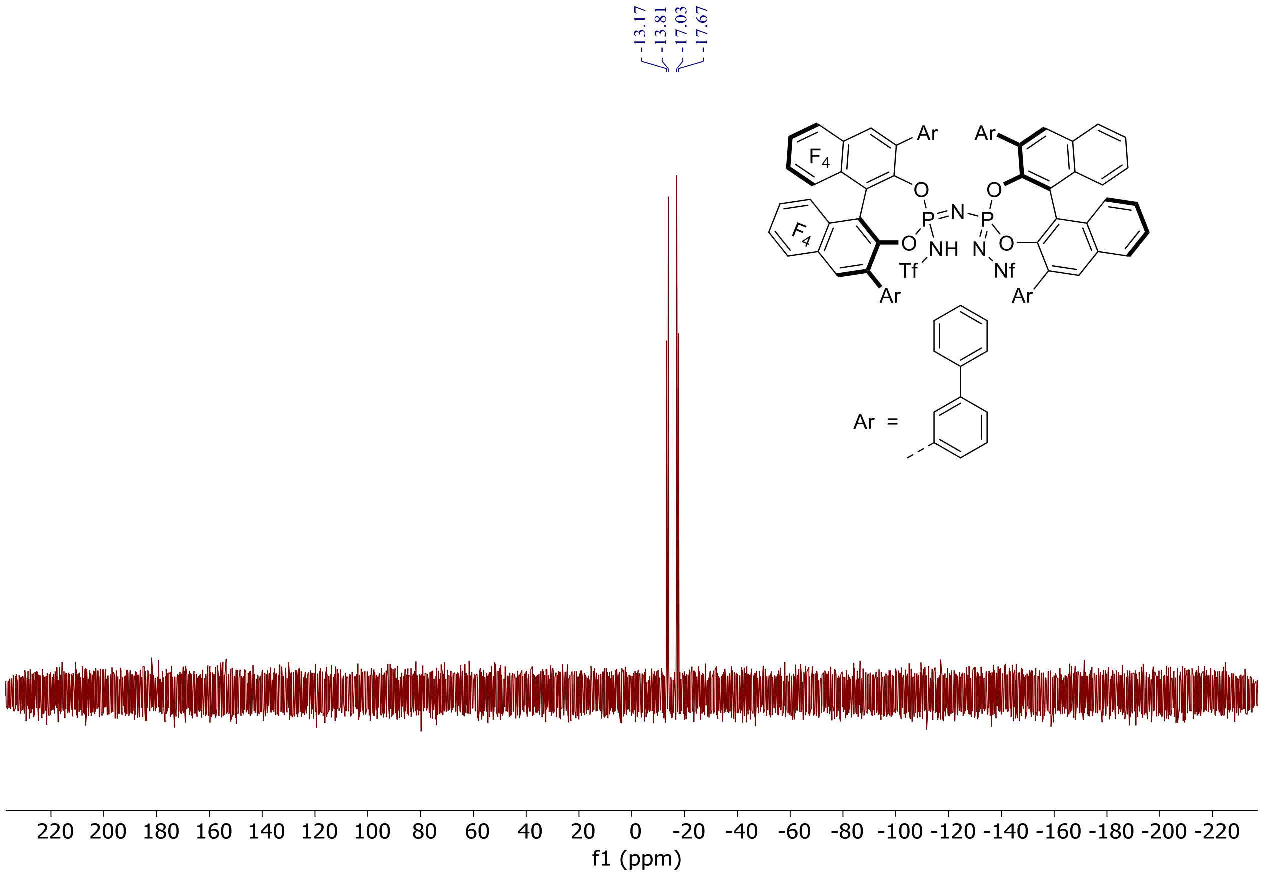
-13.17
-13.81
-17.03
-17.67
Ar
Ar
F4
F4
O
P
N
P
O
O
NH
N
O
Tf
Nf
Ar
Ar
Ar =
220 200 180 160 140 120 100 80 60 40 20 0 -20 -40 -60 -80 -100 -120 -140 -160 -180 -200 -220
f1 (ppm)

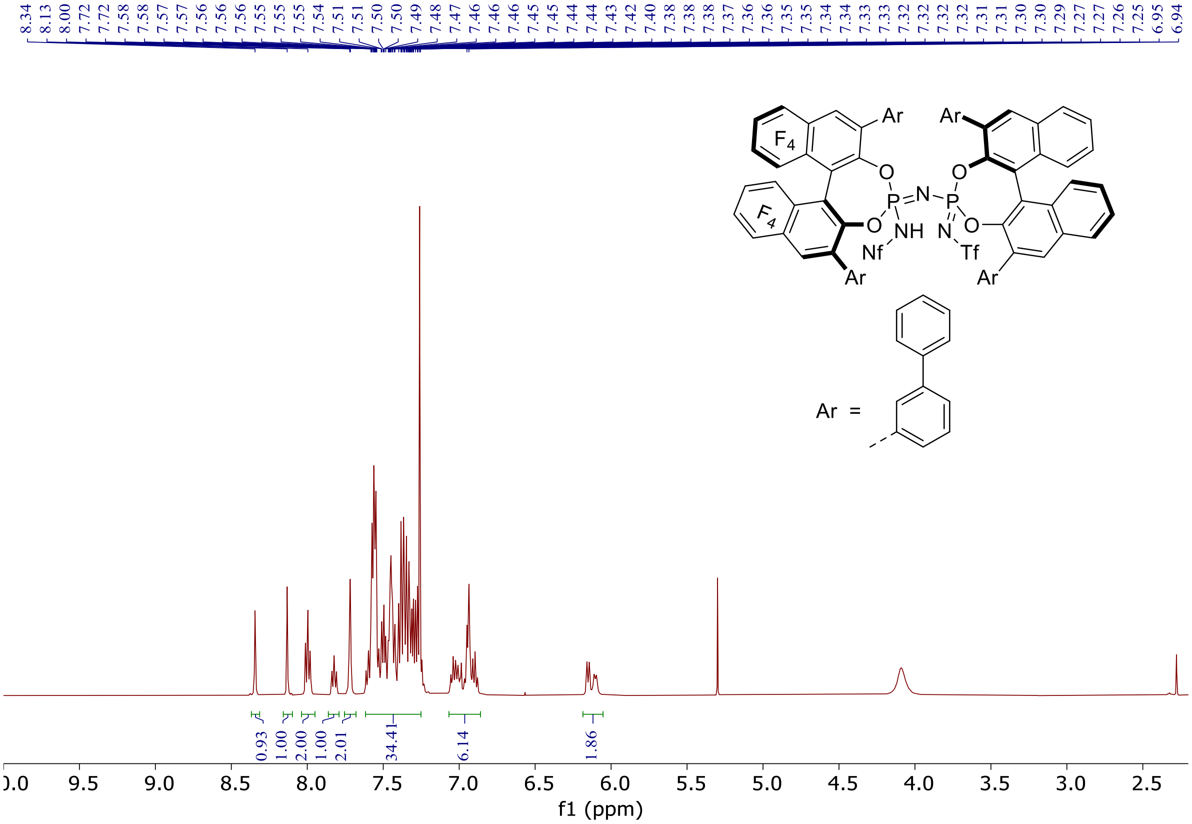
8.34
8.13
8.00
7.72
7.72
7.58
7.58
7.57
7.57
7.56
7.56
7.56
7.55
7.55
7.55
7.54
7.51
7.51
7.50
7.50
7.49
7.48
7.47
7.46
7.46
7.46
7.45
7.45
7.44
7.44
7.43
7.42
7.40
7.38
7.38
7.38
7.37
7.36
7.36
7.35
7.35
7.34
7.34
7.33
7.33
7.32
7.32
7.32
7.32
7.31
7.31
7.30
7.30
7.29
7.27
7.27
7.26
7.25
6.95
6.94
F4
Ar
Ar
O
P
N
P
O
F4
O
NH
N
O
Nf
Tf
Ar
Ar
Ar =
0.93
1.00
2.00
1.00
2.01
34.41
6.14
1.86
0.0
9.5
9.0
8.5
8.0
7.5
7.0
6.5
6.0
5.5
5.0
4.5
4.0
3.5
3.0
2.5
f1 (ppm)

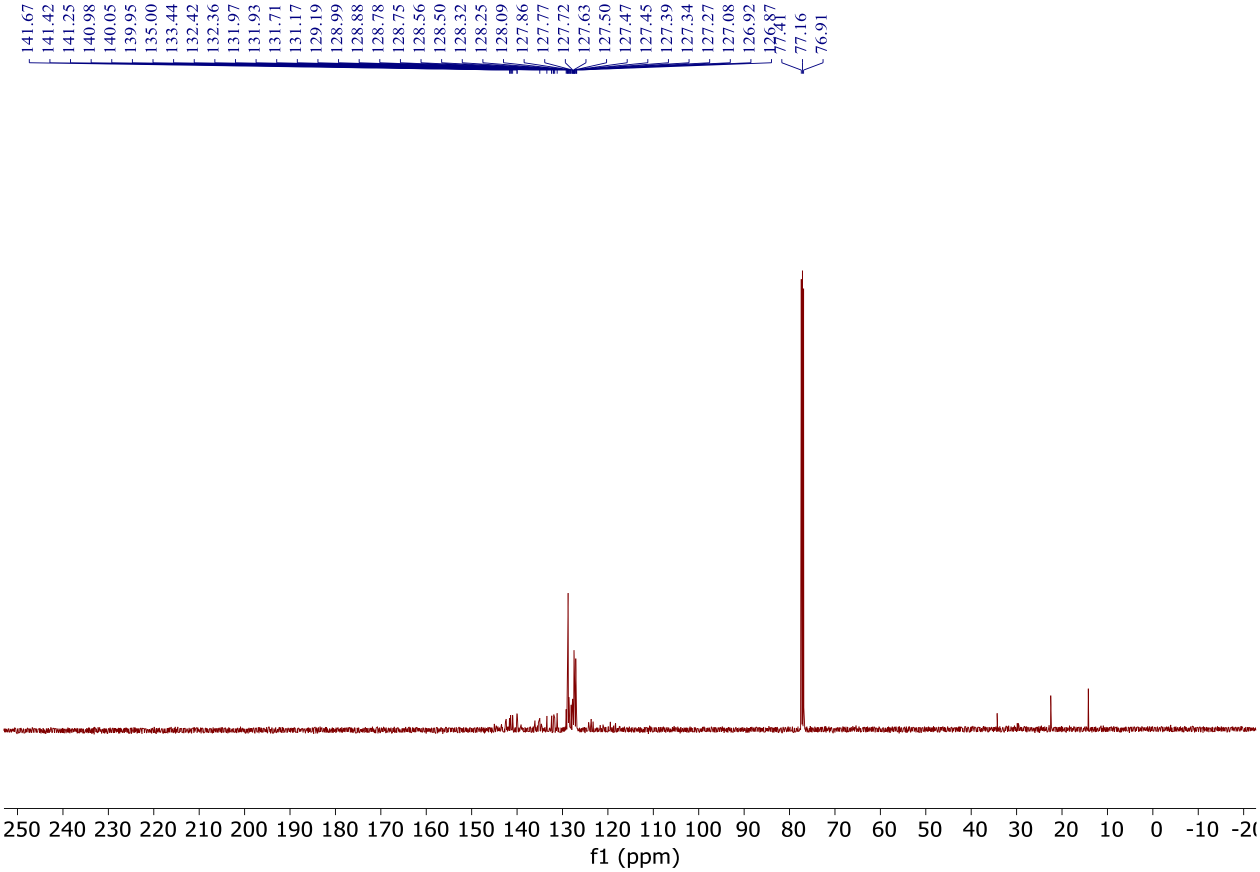
141.67
141.42
141.25
140.98
140.05
139.95
135.00
133.44
132.42
132.36
131.97
131.93
131.71
131.17
129.19
128.99
128.88
128.78
128.75
128.56
128.50
128.32
128.25
128.09
127.86
127.77
127.72
127.63
127.50
127.47
127.45
127.39
127.34
127.27
127.08
126.92
126.87
77.41
77.16
76.91
250
240
230
220
210
200
190
180
170
160
150
140
130
120
110
100
90
80
70
60
50
40
30
20
10
0
-10
-2
f1 (ppm)

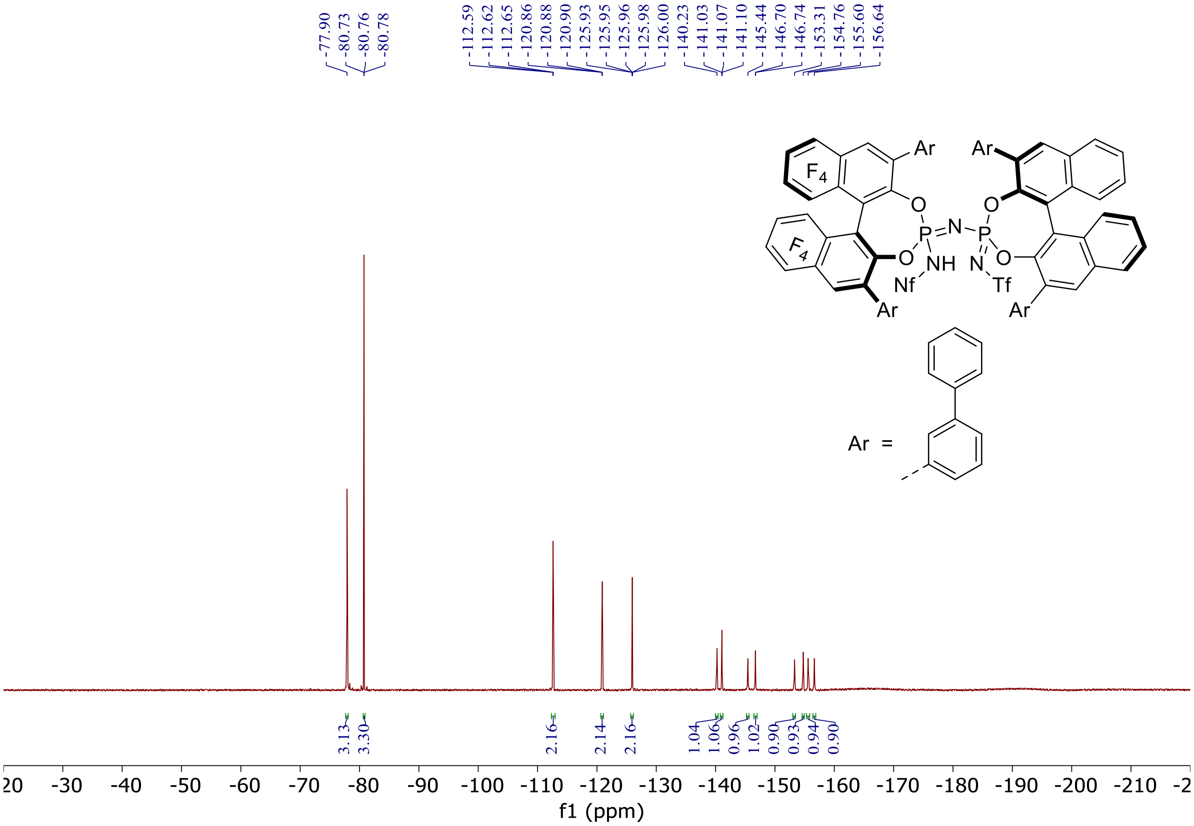
-77.90
-80.73
-80.76
-80.78
-112.59
-112.62
-112.65
-120.86
-120.88
-120.90
-125.93
-125.95
-125.96
-125.98
-126.00
-140.23
-141.03
-141.07
-141.10
-145.44
-146.70
-146.74
-153.31
-154.76
-155.60
-156.64
F4
Ar
O
P
N
NH
Nf
Tf
Ar =
3.13
3.30
2.16
2.14
2.16
1.04
1.06
0.96
1.02
0.90
0.93
0.94
0.90
20
-30
-40
-50
-60
-70
-80
-90
-100
-110
-120
-130
-140
-150
-160
-170
-180
-190
-200
-210
-2
f1 (ppm)

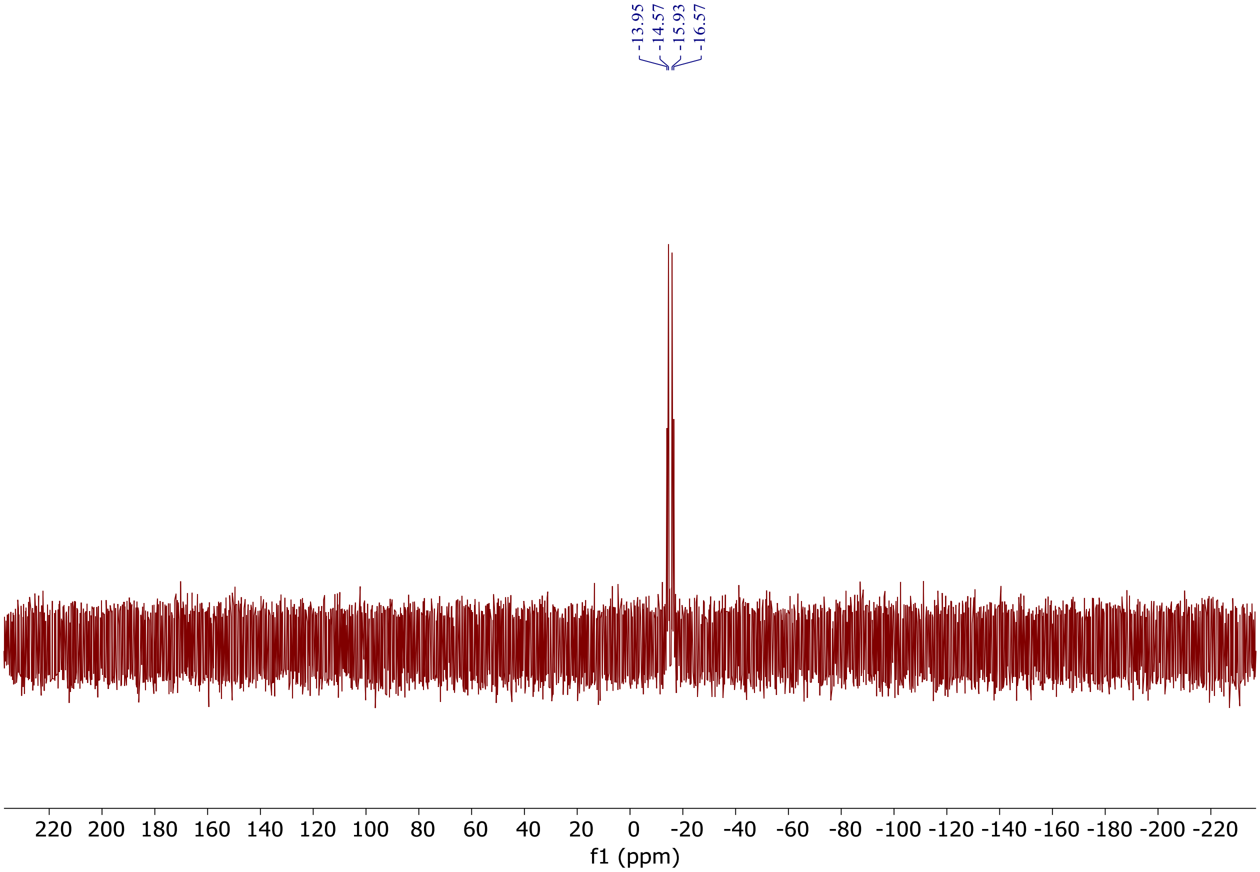
-13.95
-14.57
-15.93
-16.57
220
200
180
160
140
120
100
80
60
40
20
0
-20
-40
-60
-80
-100
-120
-140
-160
-180
-200
-220
f1 (ppm)

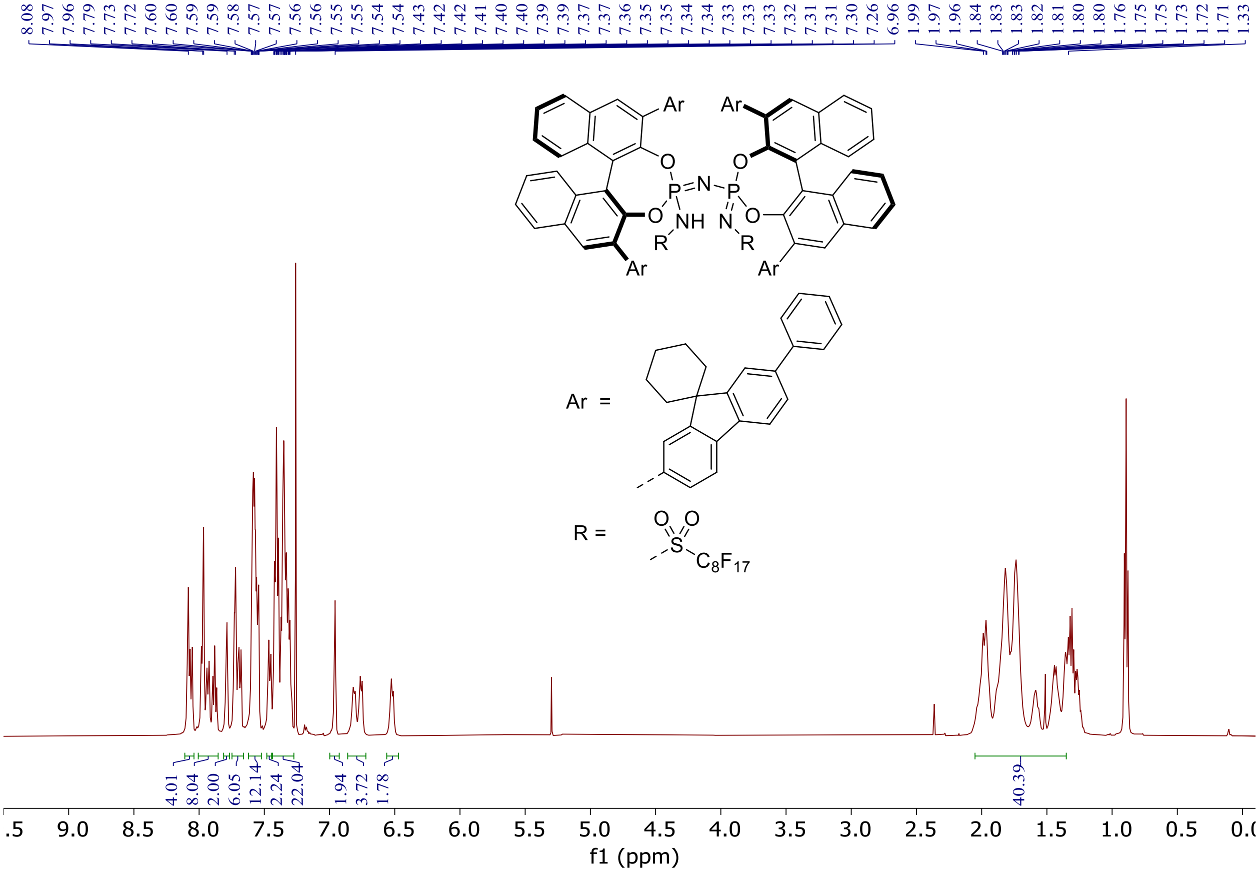
8.08 7.97 7.96 7.79 7.73 7.72 7.60 7.60 7.59 7.59 7.58 7.57 7.57 7.56 7.56 7.55 7.55 7.54 7.54 7.43 7.42 7.42 7.41 7.40 7.40 7.39 7.39 7.37 7.37 7.36 7.35 7.35 7.34 7.34 7.33 7.33 7.33 7.32 7.31 7.31 7.30 7.26 6.96 1.99 1.97 1.96 1.84 1.83 1.83 1.82 1.81 1.80 1.80 1.76 1.75 1.75 1.73 1.72 1.71 1.33
Ar
Ar
O
O
P
N
P
O
O
NH
N
R
R
Ar
Ar
Ar =
R =
O
O
S
C8F17
4.01
8.04
2.00
6.05
12.14
2.24
22.04
1.94
3.72
1.78
40.39
.5 9.0 8.5 8.0 7.5 7.0 6.5 6.0 5.5 5.0 4.5 4.0 3.5 3.0 2.5 2.0 1.5 1.0 0.5 0.(
f1 (ppm)

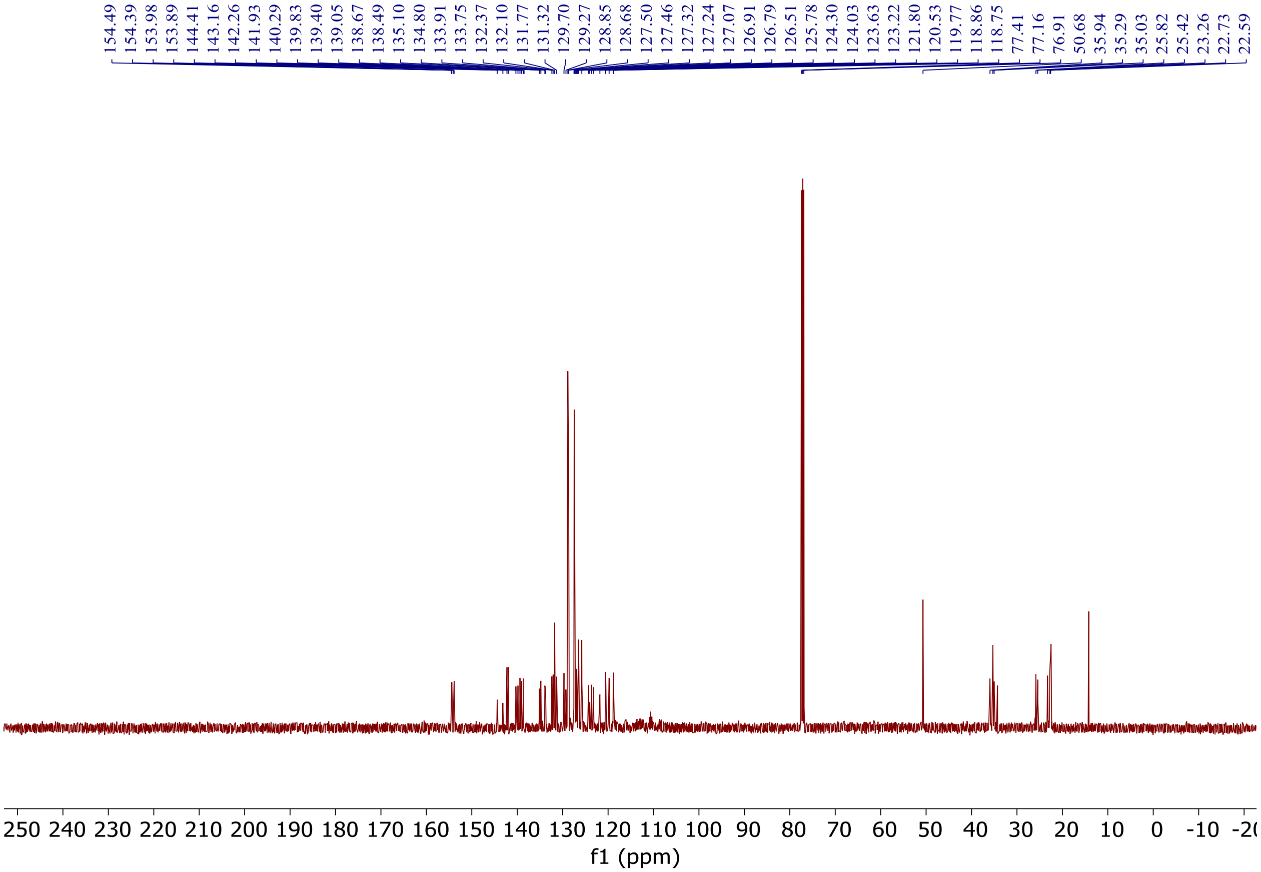
154.49 154.39 153.98 153.89 144.41 143.16 142.26 141.93 140.29 139.83 139.40 139.05 138.67 138.49 135.10 134.80 133.91 133.75 132.37 132.10 131.77 131.32 129.70 129.27 128.85 128.68 127.50 127.46 127.32 127.24 127.07 126.91 126.79 126.51 125.78 124.30 124.03 123.63 123.22 121.80 120.53 119.77 118.86 118.75 77.41 77.16 76.91 50.68 35.94 35.29 35.03 25.82 25.42 23.26 22.73 22.59
250 240 230 220 210 200 190 180 170 160 150 140 130 120 110 100 90 80 70 60 50 40 30 20 10 0 -10 -2(
f1 (ppm)

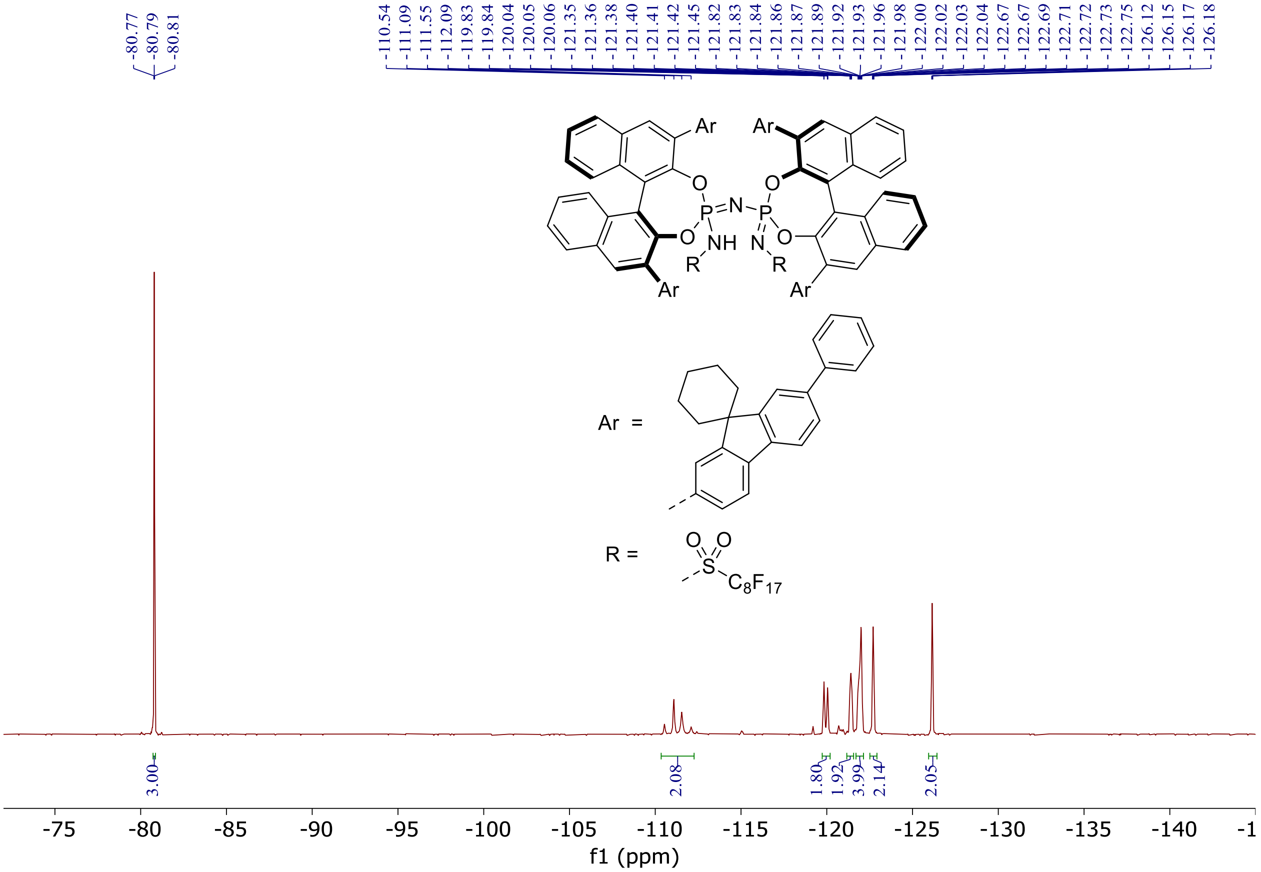
-80.77
-80.79
-80.81
-110.54
-111.09
-111.55
-112.09
-119.83
-119.84
-120.04
-120.05
-120.06
-121.35
-121.36
-121.38
-121.40
-121.41
-121.42
-121.45
-121.82
-121.83
-121.84
-121.86
-121.87
-121.89
-121.92
-121.93
-121.96
-121.98
-122.00
-122.02
-122.03
-122.04
-122.67
-122.69
-122.71
-122.72
-122.73
-122.75
-126.12
-126.15
-126.17
-126.18
Ar
Ar
O
O
P
N
P
O
O
NH
N
R
R
Ar
Ar
Ar =
R =
O
O
S
C_8F_{17}
3.00
2.08
1.80
1.92
3.99
2.14
2.05
-75
-80
-85
-90
-95
-100
-105
-110
-115
-120
-125
-130
-135
-140
-1
f1 (ppm)

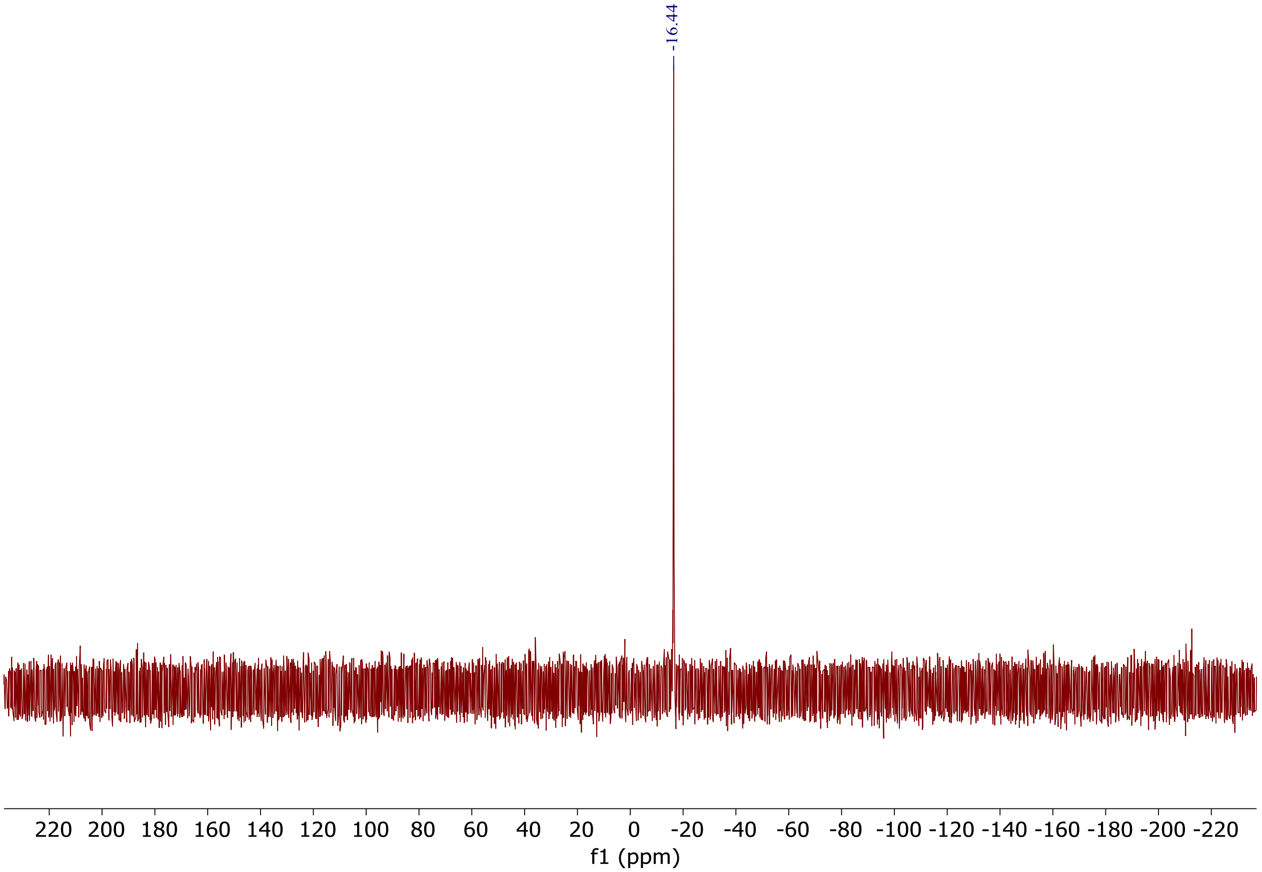
-16.44
220
200
180
160
140
120
100
80
60
40
20
0
-20
-40
-60
-80
-100
-120
-140
-160
-180
-200
-220
f1 (ppm)

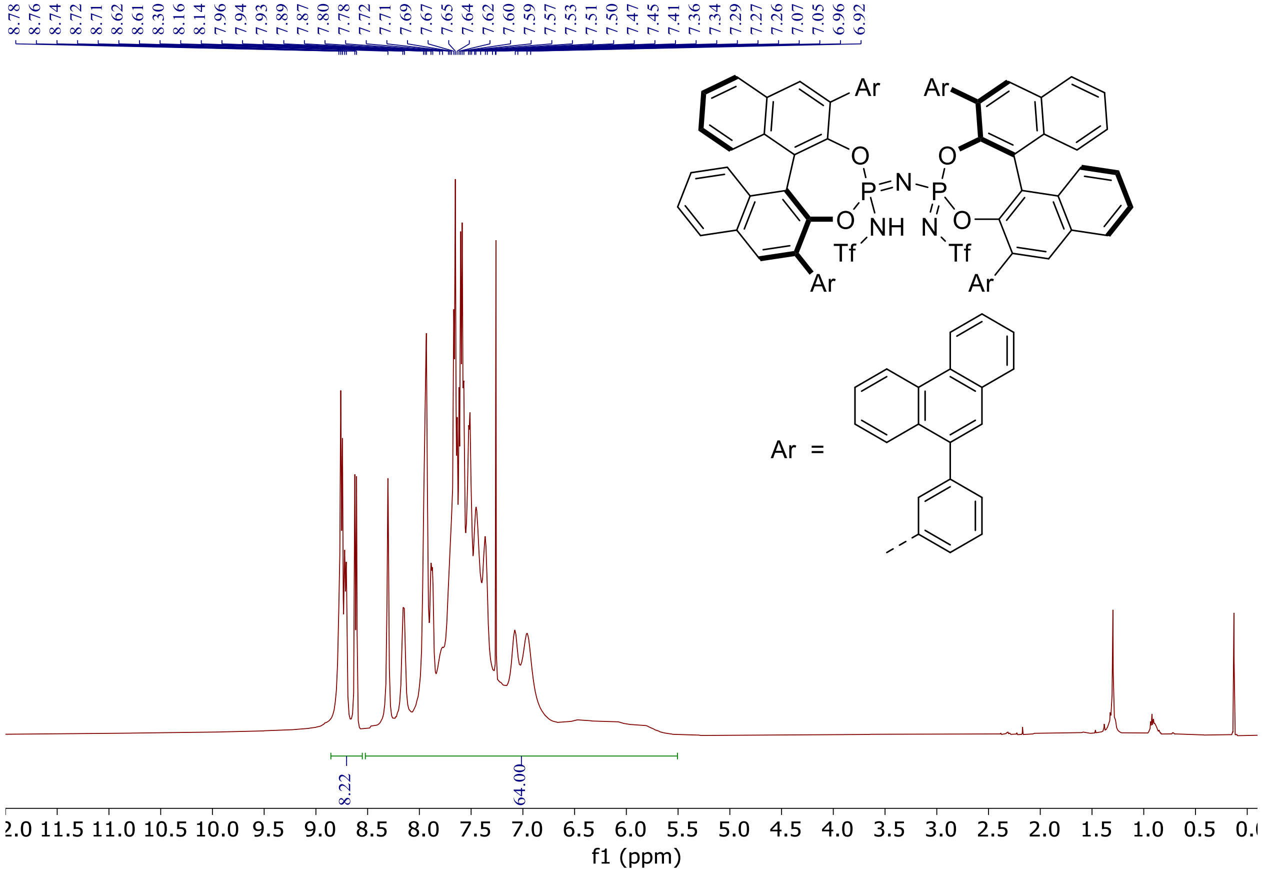
8.78 8.76 8.74 8.72 8.71 8.62 8.61 8.30 8.16 8.14 7.96 7.94 7.93 7.89 7.87 7.80 7.78 7.72 7.71 7.69 7.67 7.65 7.64 7.62 7.60 7.59 7.57 7.53 7.51 7.50 7.47 7.45 7.41 7.36 7.34 7.29 7.27 7.26 7.07 7.05 6.96 6.92
Ar
Ar
O
O
P
N
P
O
O
NH
N
Tf
Tf
Ar
Ar
Ar =
8.22
64.00
2.0 11.5 11.0 10.5 10.0 9.5 9.0 8.5 8.0 7.5 7.0 6.5 6.0 5.5 5.0 4.5 4.0 3.5 3.0 2.5 2.0 1.5 1.0 0.5 0.
f1 (ppm)

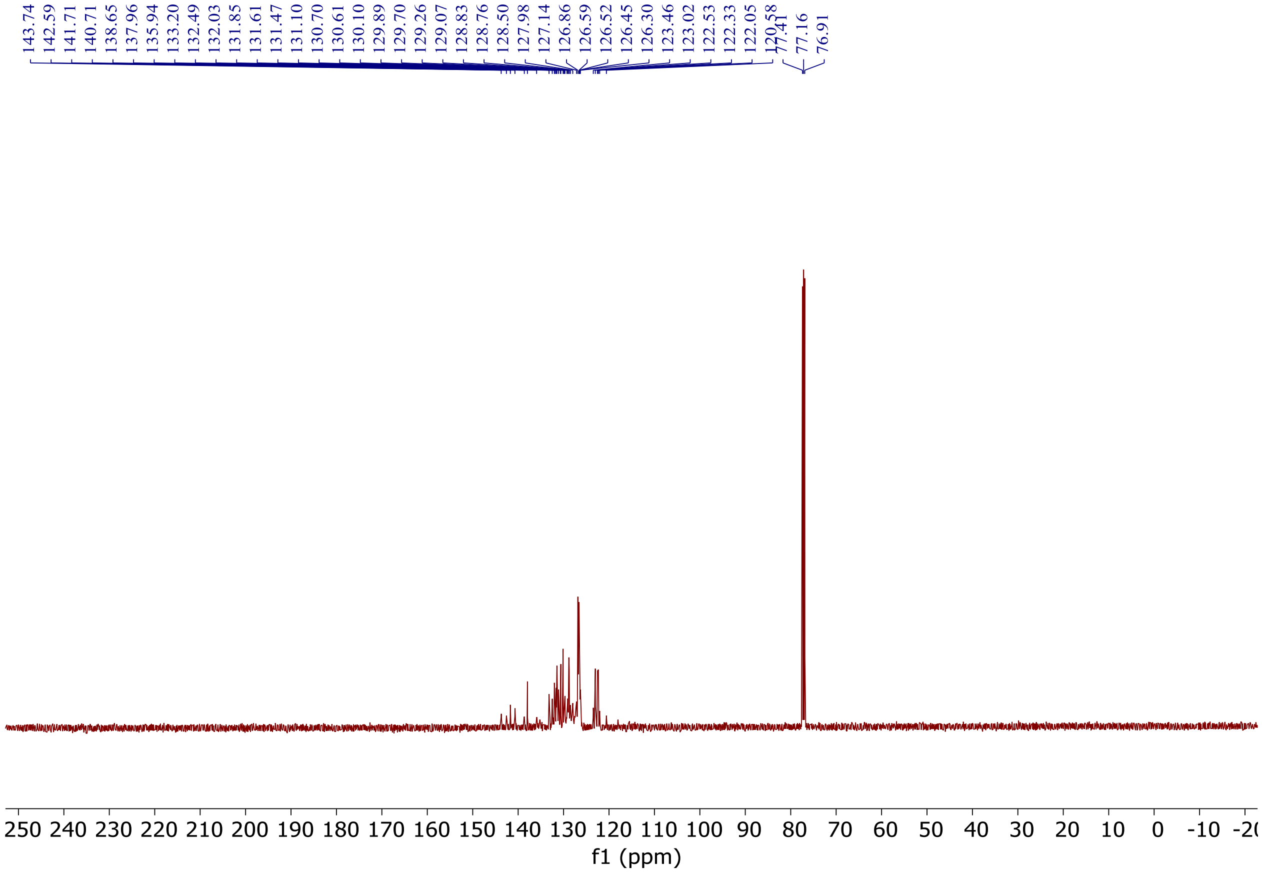
143.74 142.59 141.71 140.71 138.65 137.96 135.94 133.20 132.49 132.03 131.85 131.61 131.47 131.10 130.70 130.61 130.10 129.89 129.70 129.26 129.07 128.83 128.76 128.50 127.98 127.14 126.86 126.59 126.52 126.45 126.30 123.46 123.02 122.53 122.33 122.05 120.58 77.41 77.16 76.91
250 240 230 220 210 200 190 180 170 160 150 140 130 120 110 100 90 80 70 60 50 40 30 20 10 0 -10 -2
f1 (ppm)

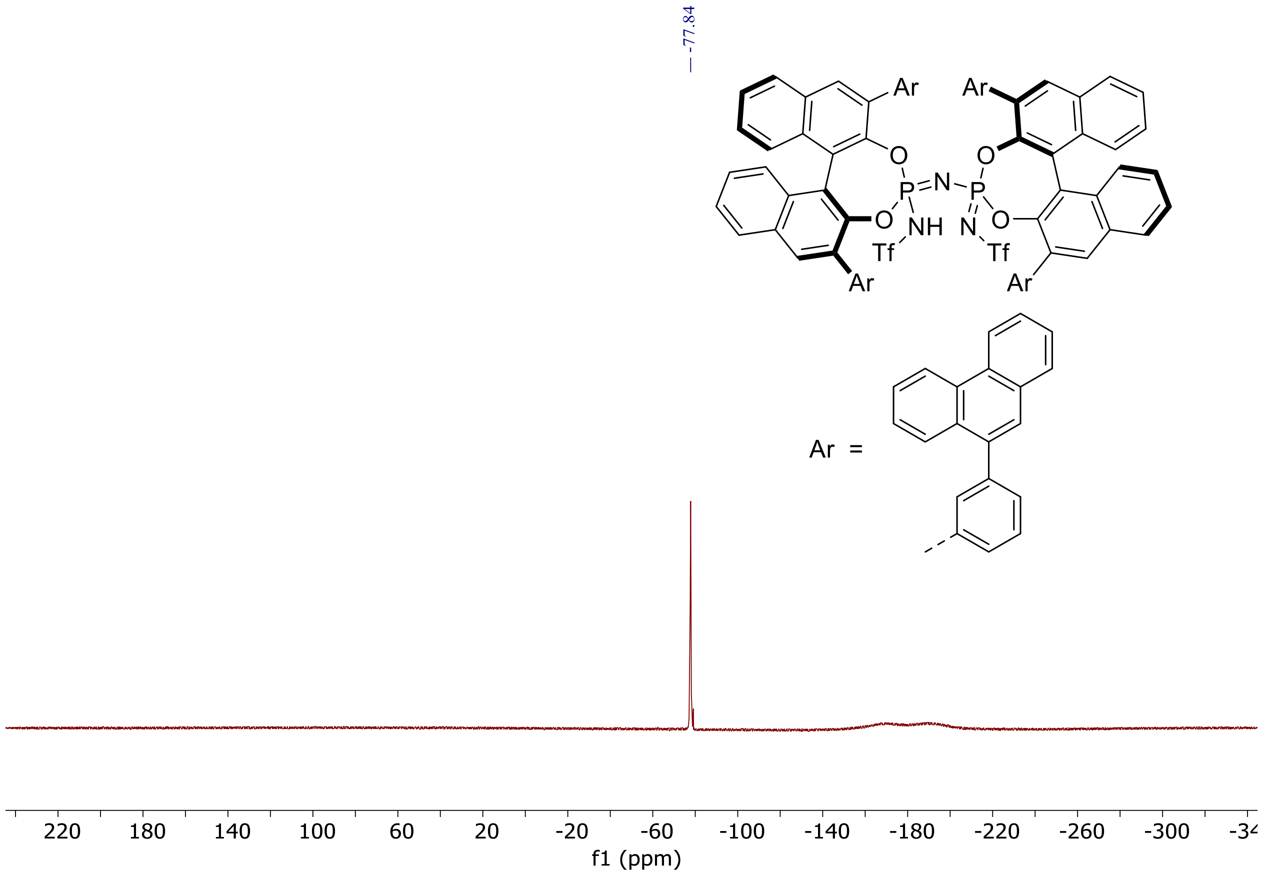
-77.84
Ar
Ar
O
O
P=N-P
O
NH
N
O
Tf
Tf
Ar
Ar
Ar =
220
180
140
100
60
20
-20
-60
-100
-140
-180
-220
-260
-300
-34
f1 (ppm)

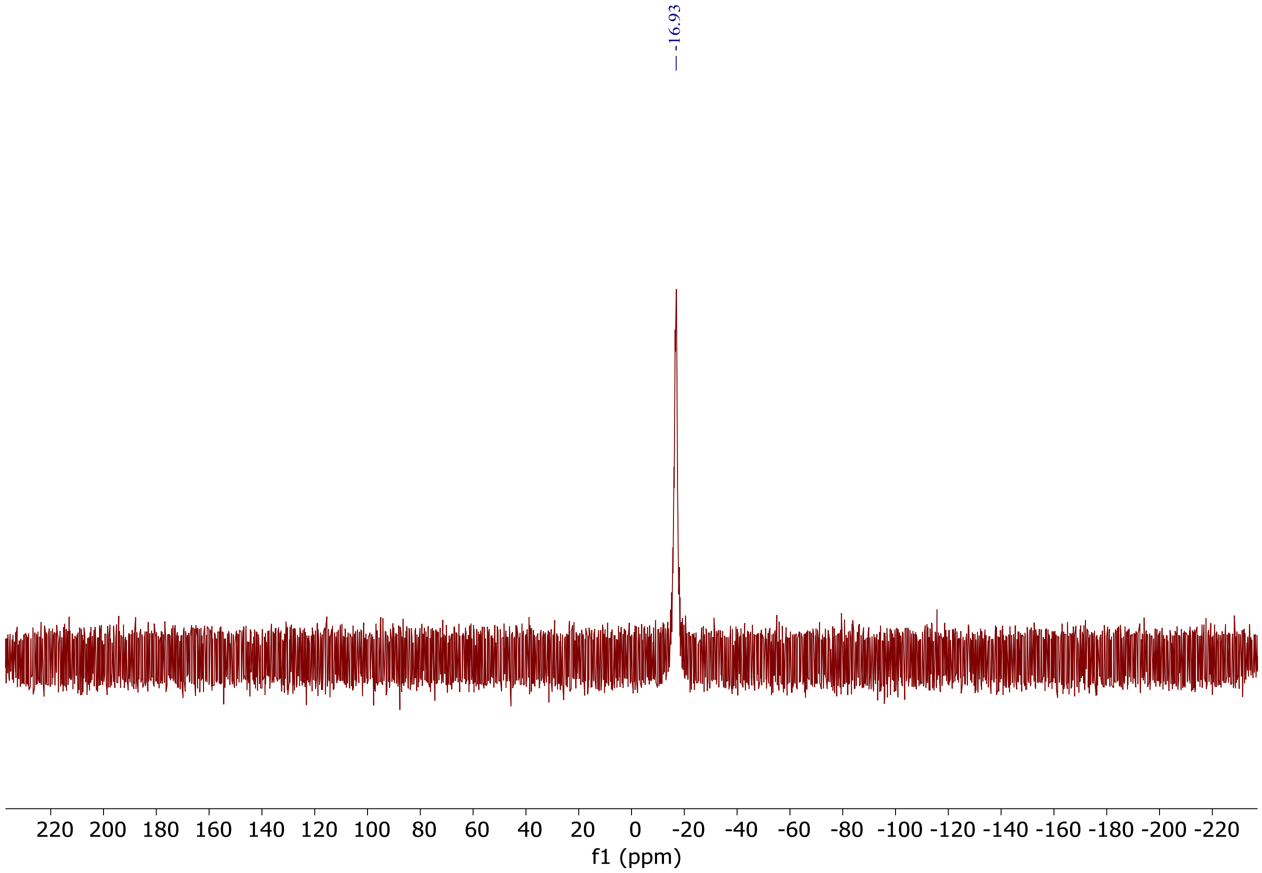
-16.93
220
200
180
160
140
120
100
80
60
40
20
0
-20
-40
-60
-80
-100
-120
-140
-160
-180
-200
-220
f1 (ppm)

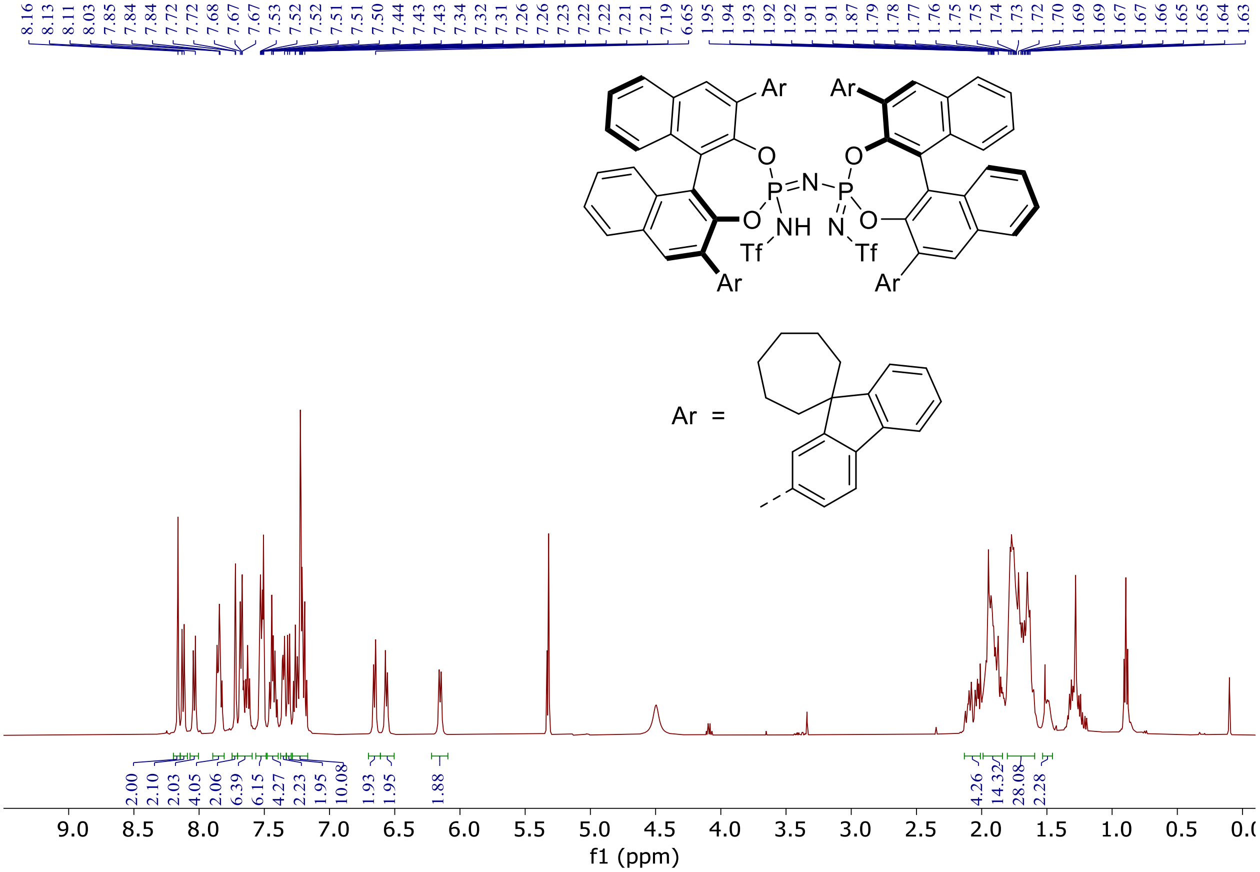
8.16
8.13
8.11
8.03
7.85
7.84
7.84
7.72
7.72
7.68
7.67
7.67
7.53
7.52
7.52
7.51
7.51
7.50
7.44
7.43
7.43
7.34
7.32
7.31
7.26
7.26
7.23
7.22
7.22
7.21
7.21
7.19
6.65
1.95
1.94
1.93
1.92
1.92
1.91
1.91
1.87
1.79
1.78
1.77
1.76
1.75
1.75
1.74
1.73
1.72
1.70
1.69
1.67
1.67
1.66
1.65
1.65
1.64
1.63
Ar
Ar
O
O
P
N
P
O
O
NH
N
Tf
Tf
Ar
Ar
Ar =
2.00
2.10
2.03
4.05
2.06
6.39
6.15
4.27
2.23
1.95
10.08
1.93
1.95
1.88
4.26
14.32
28.08
2.28
9.0
8.5
8.0
7.5
7.0
6.5
6.0
5.5
5.0
4.5
4.0
3.5
3.0
2.5
2.0
1.5
1.0
0.5
0.
f1 (ppm)

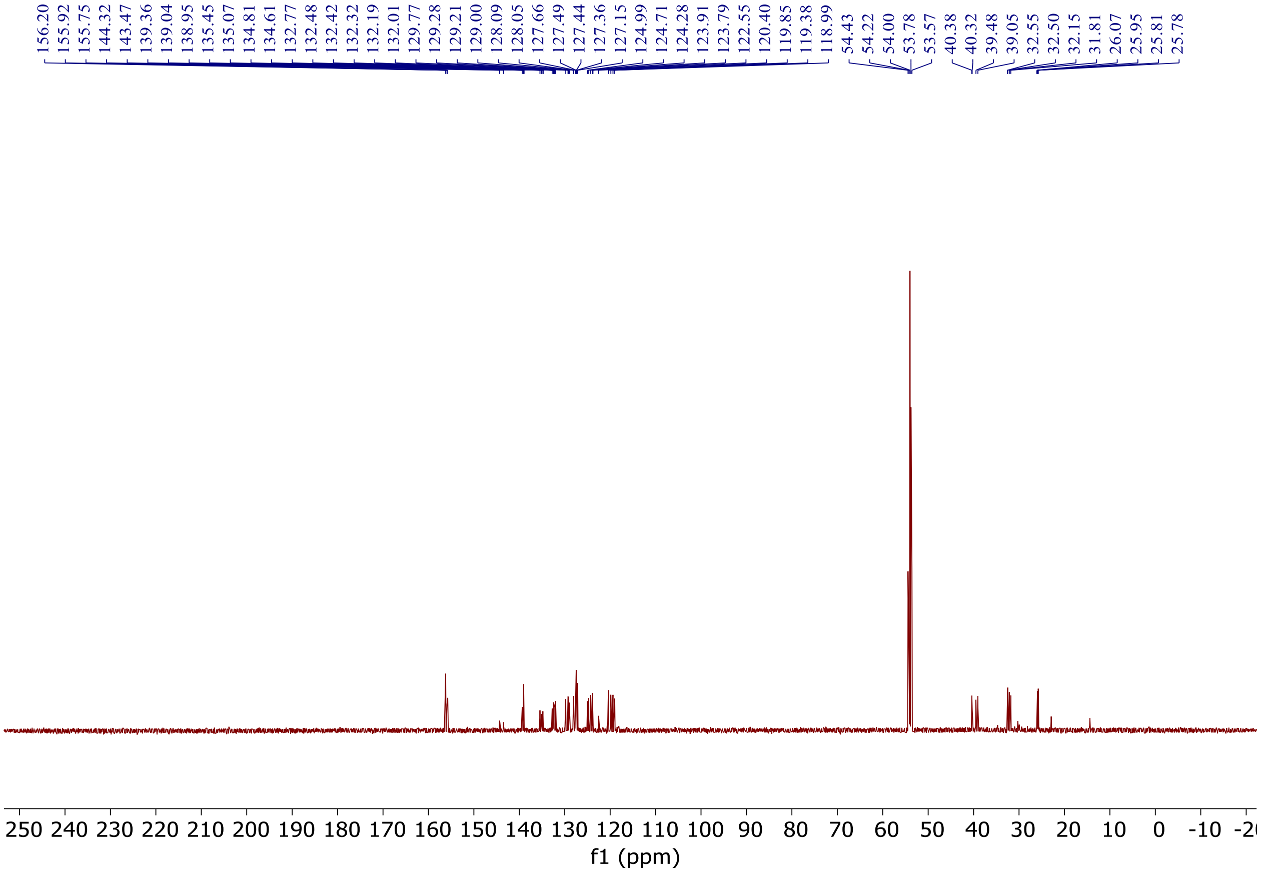
156.20
155.92
155.75
144.32
143.47
139.36
139.04
138.95
135.45
135.07
134.81
134.61
132.77
132.48
132.42
132.32
132.19
132.01
129.77
129.28
129.21
129.00
128.09
128.05
127.66
127.49
127.44
127.36
127.15
124.99
124.71
124.28
123.91
123.79
122.55
120.40
119.85
119.38
118.99
54.43
54.22
54.00
53.78
53.57
40.38
40.32
39.48
39.05
32.55
32.50
32.15
31.81
26.07
25.95
25.81
25.78
250
240
230
220
210
200
190
180
170
160
150
140
130
120
110
100
90
80
70
60
50
40
30
20
10
0
-10
-2
f1 (ppm)

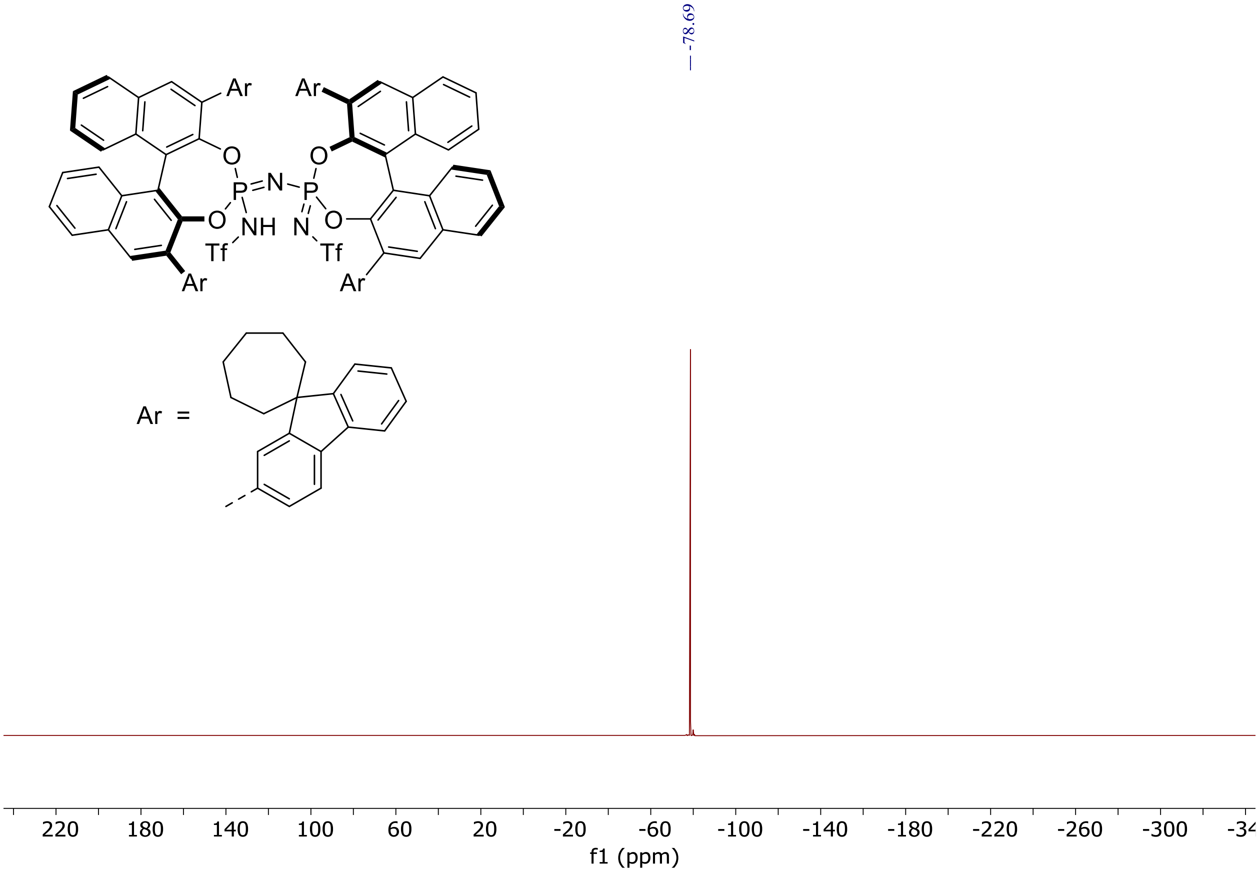
-78.69
Ar
O
P
N
NH
Tf
Ar =
220
180
140
100
60
20
-20
-60
-100
-140
-180
-220
-260
-300
-34
f1 (ppm)

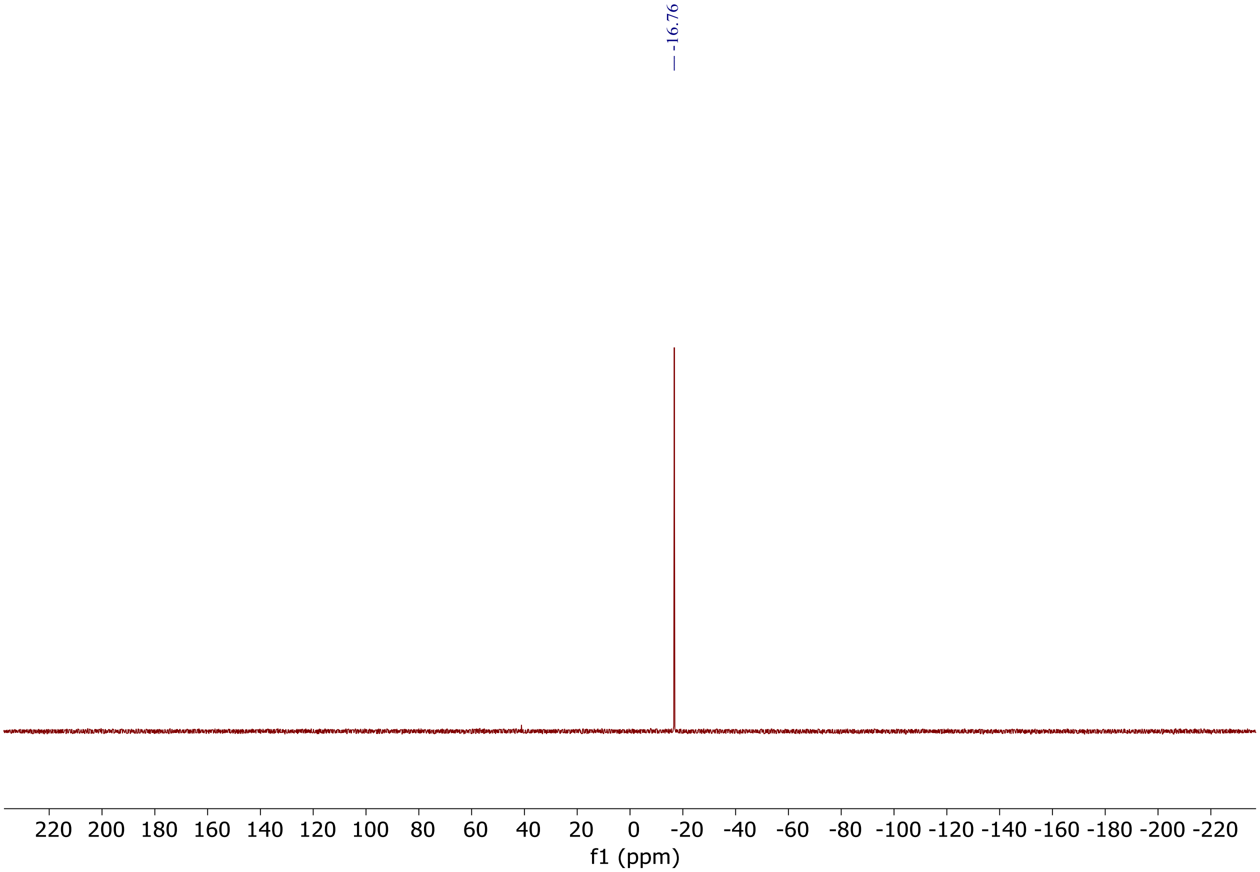
-16.76
220
200
180
160
140
120
100
80
60
40
20
0
-20
-40
-60
-80
-100
-120
-140
-160
-180
-200
-220
f1 (ppm)

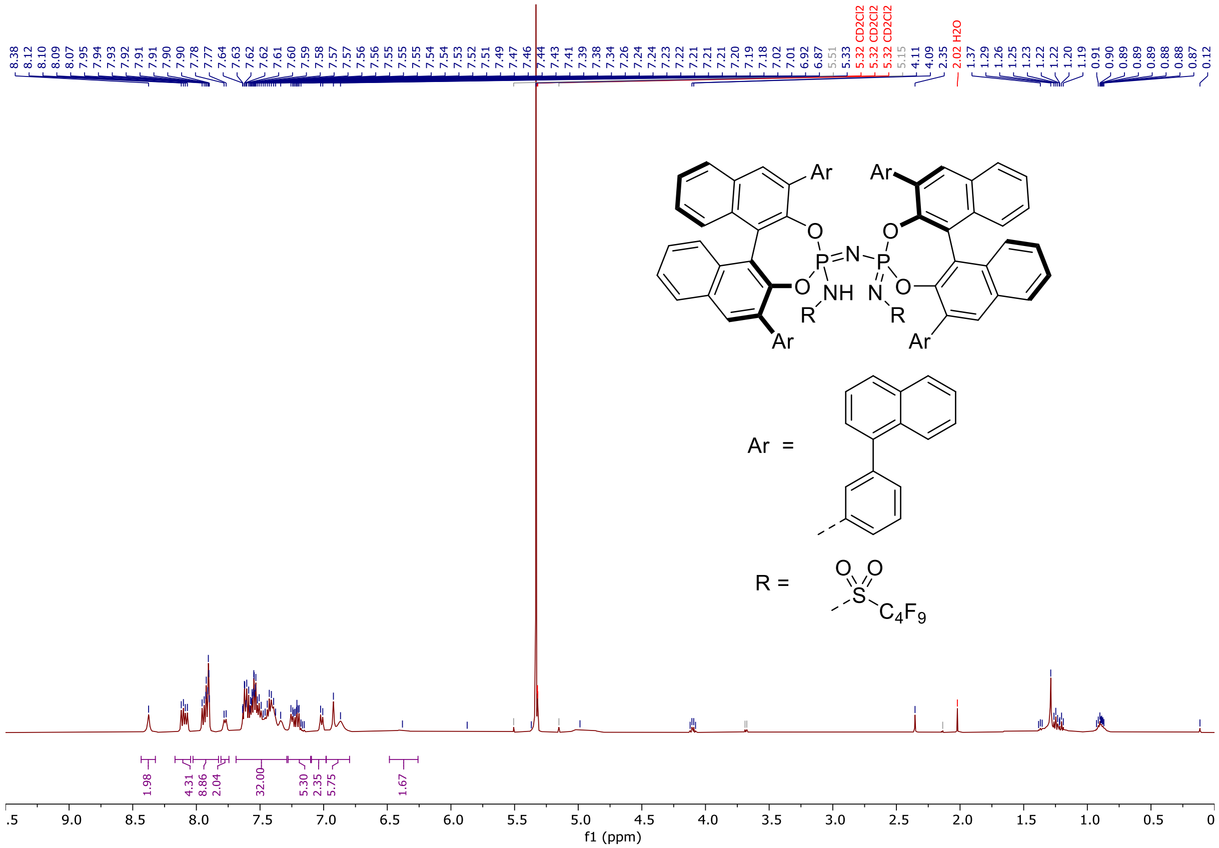
8.38 8.12 8.10 8.09 8.07 7.95 7.94 7.93 7.92 7.91 7.91 7.90 7.78 7.77 7.64 7.63 7.62 7.62 7.61 7.60 7.59 7.58 7.57 7.57 7.56 7.56 7.55 7.55 7.54 7.54 7.53 7.52 7.51 7.49 7.47 7.46 7.44 7.43 7.41 7.39 7.38 7.34 7.26 7.24 7.24 7.23 7.22 7.21 7.21 7.20 7.19 7.18 7.02 7.01 6.92 6.87 5.51 5.33
5.32 CD2Cl2
5.32 CD2Cl2
5.32 CD2Cl2
5.15 4.11 4.09 2.35
2.02 H2O
1.37 1.29 1.26 1.25 1.23 1.22 1.22 1.20 1.19 0.91 0.90 0.89 0.89 0.89 0.88 0.87 0.12
Ar
O
P
N
NH
R
Ar =
R =
O O
S
C4F9
1.98 4.31 8.86 2.04 32.00 5.30 2.35 5.75 1.67
.5 9.0 8.5 8.0 7.5 7.0 6.5 6.0 5.5 5.0 4.5 4.0 3.5 3.0 2.5 2.0 1.5 1.0 0.5 0
f1 (ppm)

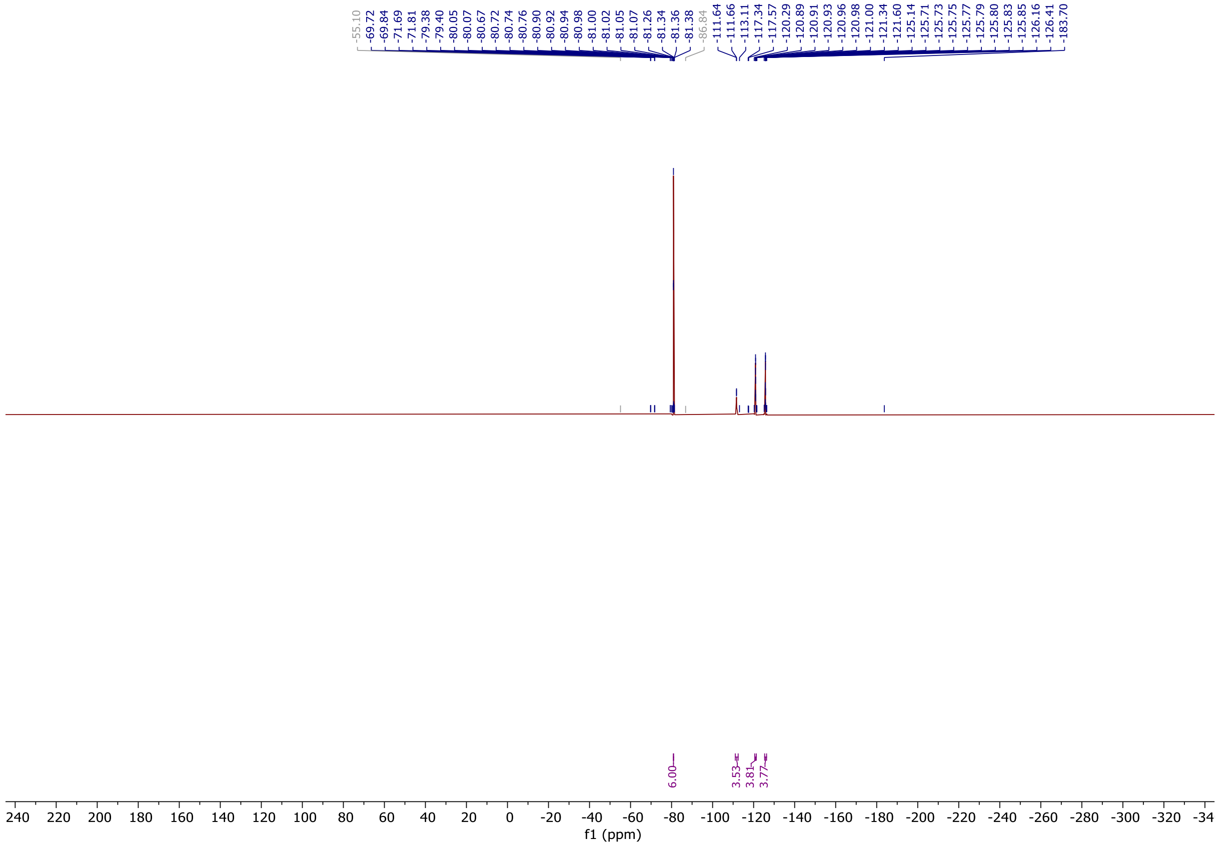
-55.10 -69.72 -69.84 -71.69 -71.81 -79.38 -79.40 -80.05 -80.07 -80.67 -80.72 -80.74 -80.76 -80.90 -80.92 -80.94 -80.98 -81.00 -81.02 -81.05 -81.07 -81.26 -81.34 -81.36 -81.38 -86.84 -111.64 -111.66 -113.11 -117.34 -117.57 -120.29 -120.89 -120.91 -120.93 -120.96 -120.98 -121.00 -121.34 -121.60 -125.14 -125.71 -125.73 -125.75 -125.77 -125.79 -125.80 -125.83 -125.85 -126.16 -126.41 -183.70
6.00 3.53 3.81 3.77
240 220 200 180 160 140 120 100 80 60 40 20 0 -20 -40 -60 -80 -100 -120 -140 -160 -180 -200 -220 -240 -260 -280 -300 -320 -34
f1 (ppm)

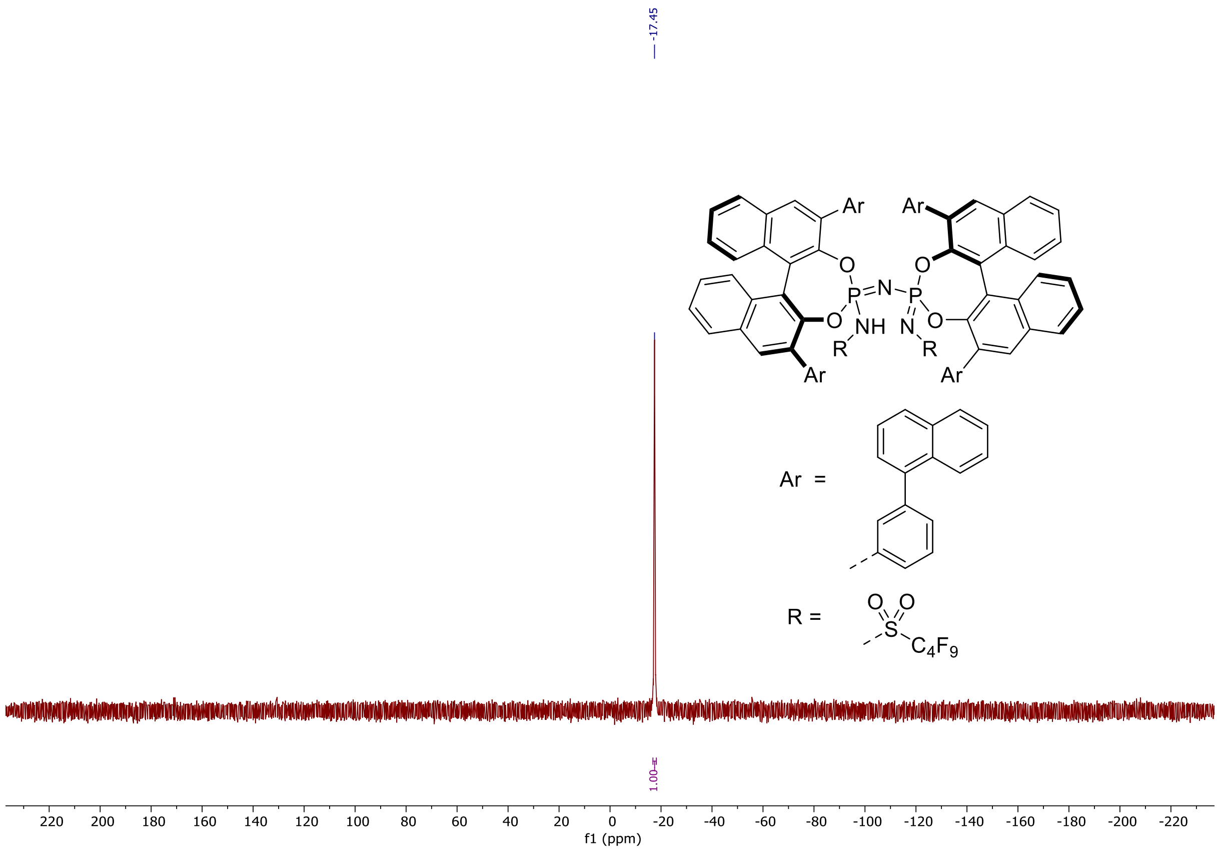
-17.45
Ar
Ar
O
O
P
N
P
O
NH
N
O
R
R
Ar
Ar
Ar =
R =
O O
S
C4F9
1.00
220 200 180 160 140 120 100 80 60 40 20 0 -20 -40 -60 -80 -100 -120 -140 -160 -180 -200 -220
f1 (ppm)

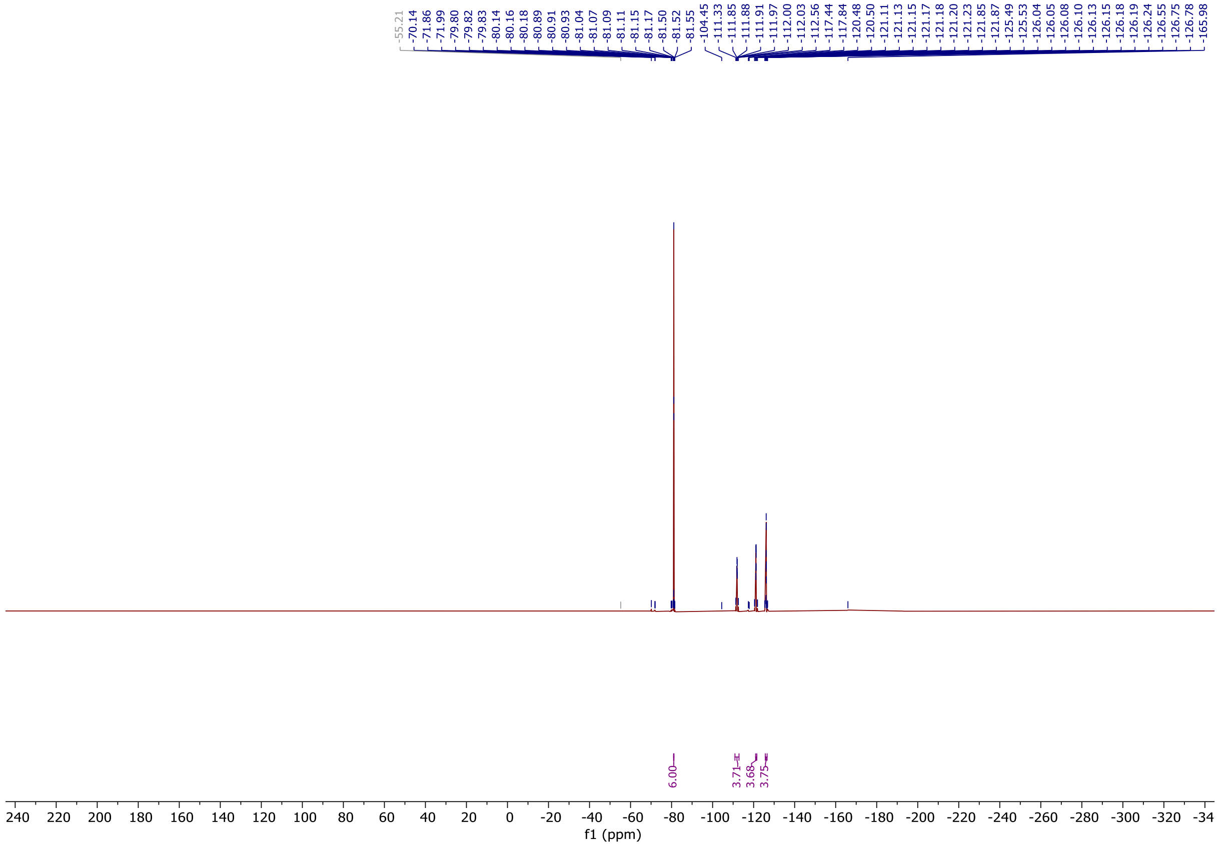
-55.21
-70.14
-71.86
-71.99
-79.80
-79.82
-79.83
-80.14
-80.16
-80.18
-80.89
-80.91
-80.93
-81.04
-81.07
-81.09
-81.11
-81.15
-81.17
-81.50
-81.52
-81.55
-104.45
-111.33
-111.85
-111.88
-111.91
-111.97
-112.00
-112.03
-112.56
-117.44
-117.84
-120.48
-120.50
-121.11
-121.13
-121.15
-121.17
-121.18
-121.20
-121.23
-121.85
-121.87
-125.49
-125.53
-126.04
-126.05
-126.08
-126.10
-126.13
-126.15
-126.18
-126.19
-126.24
-126.55
-126.75
-126.78
-165.98
6.00
3.71
3.68
3.75
240 220 200 180 160 140 120 100 80 60 40 20 0 -20 -40 -60 -80 -100 -120 -140 -160 -180 -200 -220 -240 -260 -280 -300 -320 -34
f1 (ppm)

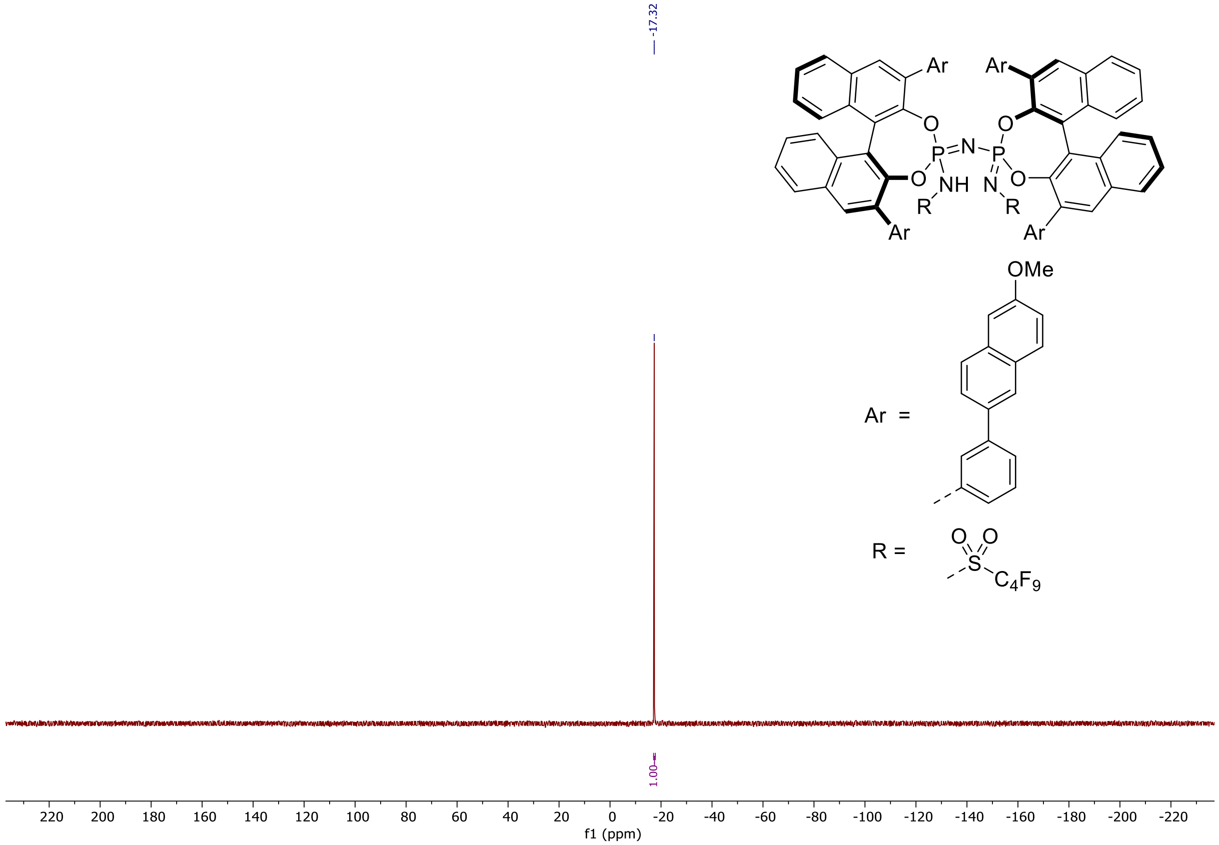
-17.32
Ar
Ar
O
P
N
P
O
O
NH
N
O
R
R
Ar
Ar
OMe
Ar =
R =
O O
S
C_4F_9
1.00
220 200 180 160 140 120 100 80 60 40 20 0 -20 -40 -60 -80 -100 -120 -140 -160 -180 -200 -220
f1 (ppm)

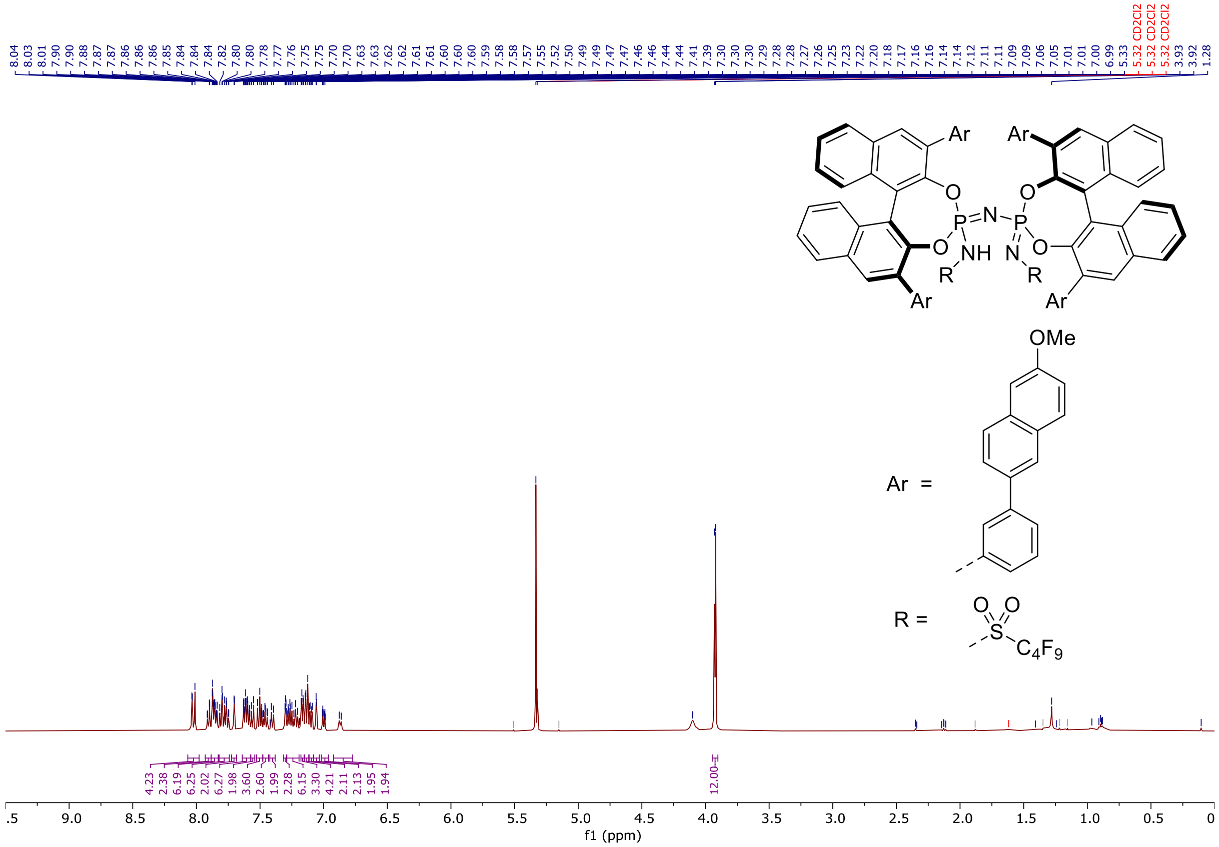
8.04 8.03 8.01 7.90 7.88 7.87 7.86 7.86 7.85 7.84 7.84 7.82 7.80 7.78 7.77 7.76 7.75 7.75 7.70 7.63 7.62 7.61 7.60 7.60 7.59 7.58 7.57 7.55 7.52 7.50 7.49 7.49 7.47 7.46 7.44 7.41 7.39 7.30 7.30 7.29 7.28 7.28 7.27 7.26 7.25 7.23 7.22 7.20 7.18 7.17 7.16 7.16 7.14 7.14 7.12 7.11 7.11 7.09 7.06 7.05 7.01 7.01 7.00 6.99 5.33
5.32 CD2Cl2 5.32 CD2Cl2 5.32 CD2Cl2
3.93 3.92 1.28
Ar
Ar
O
P
N
P
O
O
NH
N
O
R
R
Ar
Ar
OMe
Ar =
R =
O O
S
C_4F_9
4.23 2.38 6.19 6.25 2.02 6.27 1.98 3.60 2.60 1.99 2.28 6.15 3.30 4.21 2.11 2.13 1.95 1.94
12.00
.5 9.0 8.5 8.0 7.5 7.0 6.5 6.0 5.5 5.0 4.5 4.0 3.5 3.0 2.5 2.0 1.5 1.0 0.5 0
f1 (ppm)

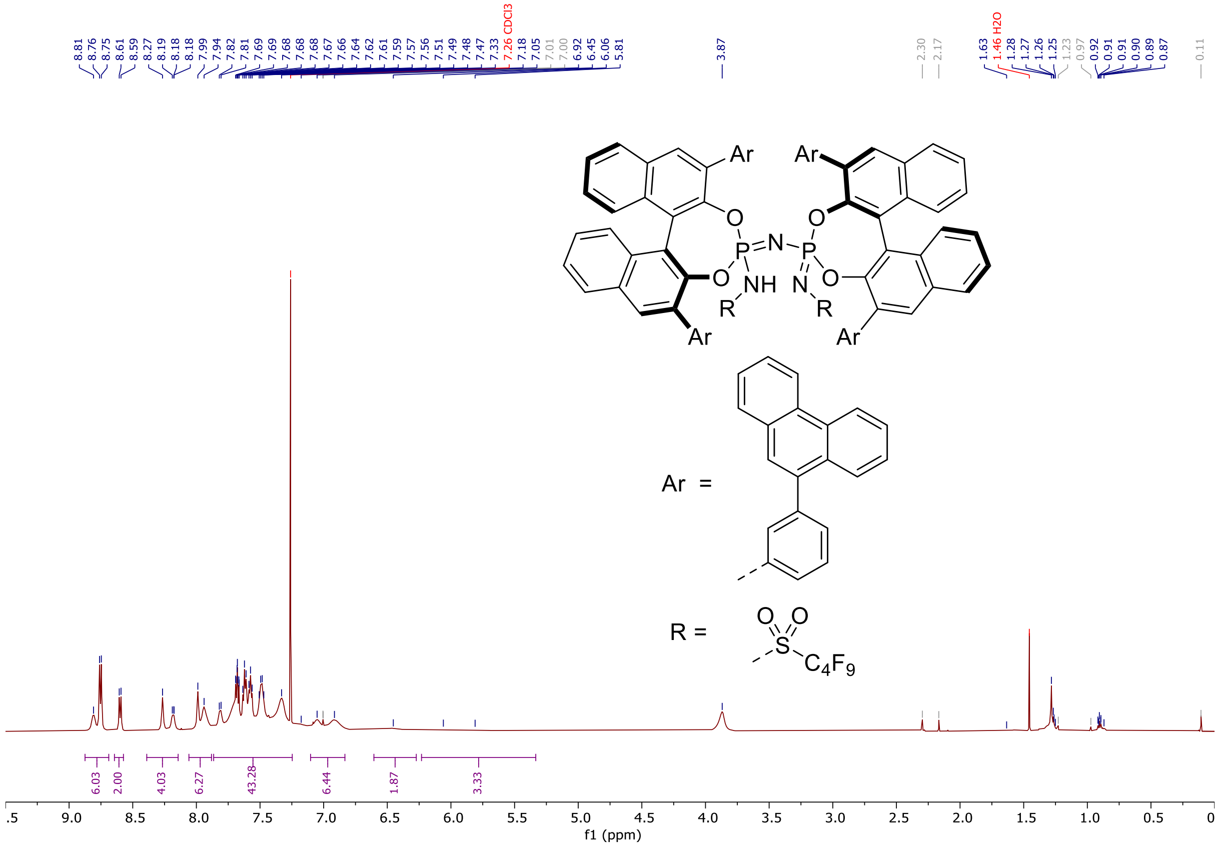
8.81
8.76
8.75
8.61
8.59
8.27
8.19
8.18
8.18
7.99
7.94
7.82
7.81
7.69
7.69
7.68
7.68
7.68
7.67
7.66
7.64
7.62
7.61
7.59
7.57
7.56
7.51
7.49
7.48
7.47
7.33
7.26 CDCl3
7.18
7.05
7.01
7.00
6.92
6.45
6.06
5.81
3.87
2.30
2.17
1.63
1.46 H2O
1.28
1.27
1.26
1.25
1.23
0.97
0.92
0.91
0.91
0.90
0.89
0.87
0.11
Ar
Ar
O
O
P
N
P
O
NH
N
O
R
R
Ar
Ar
Ar =
R =
O
O
S
C4F9
6.03
2.00
4.03
6.27
43.28
6.44
1.87
3.33
.5
9.0
8.5
8.0
7.5
7.0
6.5
6.0
5.5
5.0
4.5
4.0
3.5
3.0
2.5
2.0
1.5
1.0
0.5
0
f1 (ppm)

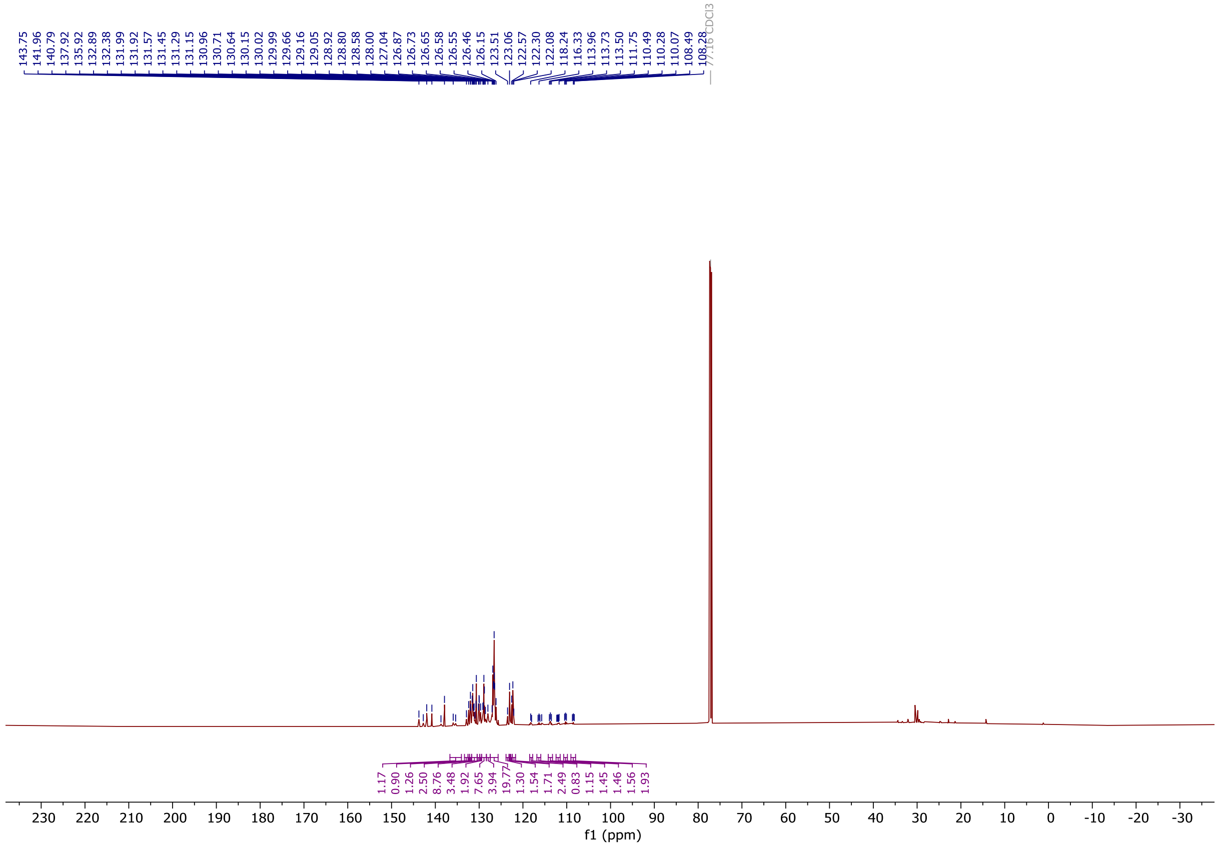
143.75
141.96
140.79
137.92
135.92
132.89
132.38
131.99
131.92
131.57
131.45
131.29
131.15
130.96
130.71
130.64
130.15
130.02
129.99
129.66
129.16
129.05
128.92
128.80
128.58
128.00
127.04
126.87
126.73
126.65
126.58
126.55
126.46
126.15
123.51
123.06
122.57
122.30
122.08
118.24
116.33
113.96
113.73
113.50
111.75
110.49
110.28
110.07
108.49
108.28
77.16 CDCl3
1.17
0.90
1.26
2.50
8.76
3.48
1.92
7.65
3.94
19.77
1.30
1.54
1.71
2.49
0.83
1.15
1.45
1.46
1.56
1.93
230
220
210
200
190
180
170
160
150
140
130
120
110
100
90
80
70
60
50
40
30
20
10
0
-10
-20
-30
f1 (ppm)

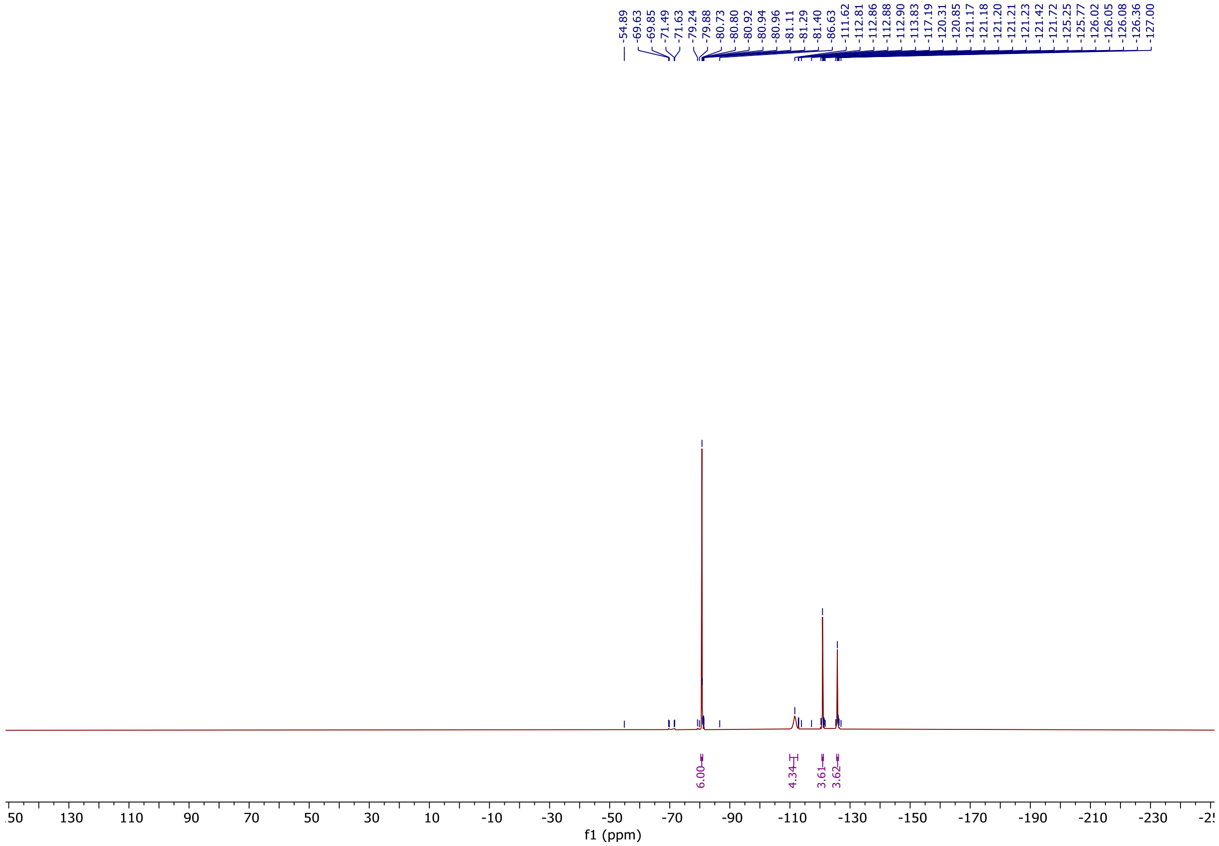
-54.89
-69.63
-69.85
-71.49
-71.63
-79.24
-79.88
-80.73
-80.80
-80.92
-80.94
-80.96
-81.11
-81.29
-81.40
-86.63
-111.62
-112.81
-112.86
-112.88
-112.90
-113.83
-117.19
-120.31
-120.85
-121.17
-121.18
-121.20
-121.21
-121.23
-121.42
-121.72
-125.25
-125.77
-126.02
-126.05
-126.08
-126.36
-127.00
6.00
4.34
3.61
3.62
50
130
110
90
70
50
30
10
-10
-30
-50
-70
-90
-110
-130
-150
-170
-190
-210
-230
-2
f1 (ppm)

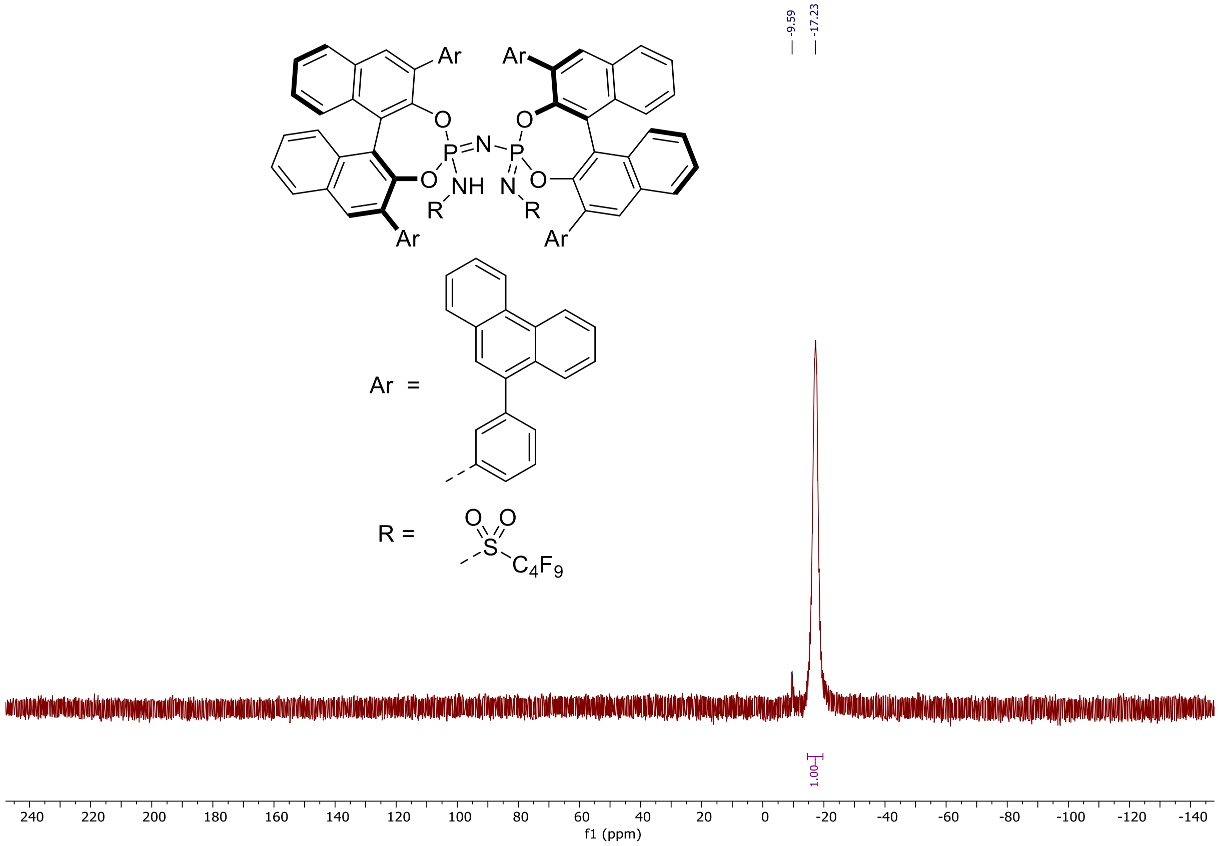
-9.59
-17.23
Ar
Ar
O
O
P
N
P
O
NH
N
O
R
R
Ar
Ar
Ar =
R =
O
O
S
C4F9
1.00
240
220
200
180
160
140
120
100
80
60
40
20
0
-20
-40
-60
-80
-100
-120
-140
f1 (ppm)

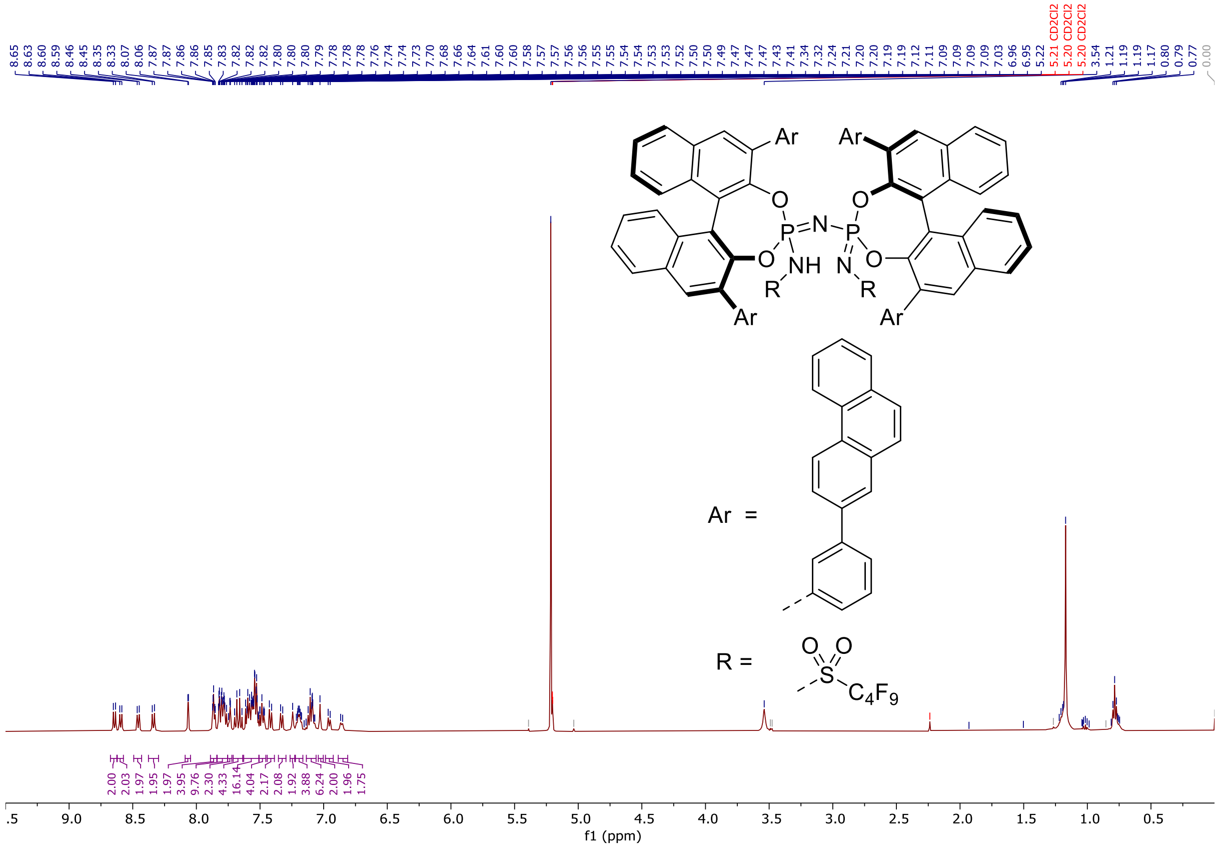
8.65 8.63 8.60 8.59 8.46 8.45 8.35 8.33 8.07 8.06 7.87 7.86 7.86 7.85 7.83 7.82 7.82 7.82 7.80 7.80 7.80 7.79 7.78 7.78 7.78 7.76 7.74 7.74 7.73 7.70 7.68 7.66 7.64 7.61 7.60 7.58 7.57 7.57 7.56 7.55 7.55 7.54 7.54 7.53 7.53 7.52 7.50 7.50 7.49 7.47 7.47 7.43 7.41 7.34 7.32 7.24 7.21 7.20 7.20 7.19 7.19 7.12 7.11 7.09 7.09 7.09 7.03 6.96 6.95 5.22
5.21 CD2Cl2
5.20 CD2Cl2
5.20 CD2Cl2
3.54 1.21 1.19 1.19 1.17 0.80 0.79 0.77 0.00
Ar
O
P
N
NH
R
Ar =
R =
O
S
C4F9
2.00 2.03 1.97 1.95 1.97 3.95 9.76 2.30 4.33 16.14 4.04 2.17 2.08 1.92 3.88 6.24 2.00 1.96 1.75
.5 9.0 8.5 8.0 7.5 7.0 6.5 6.0 5.5 5.0 4.5 4.0 3.5 3.0 2.5 2.0 1.5 1.0 0.5
f1 (ppm)

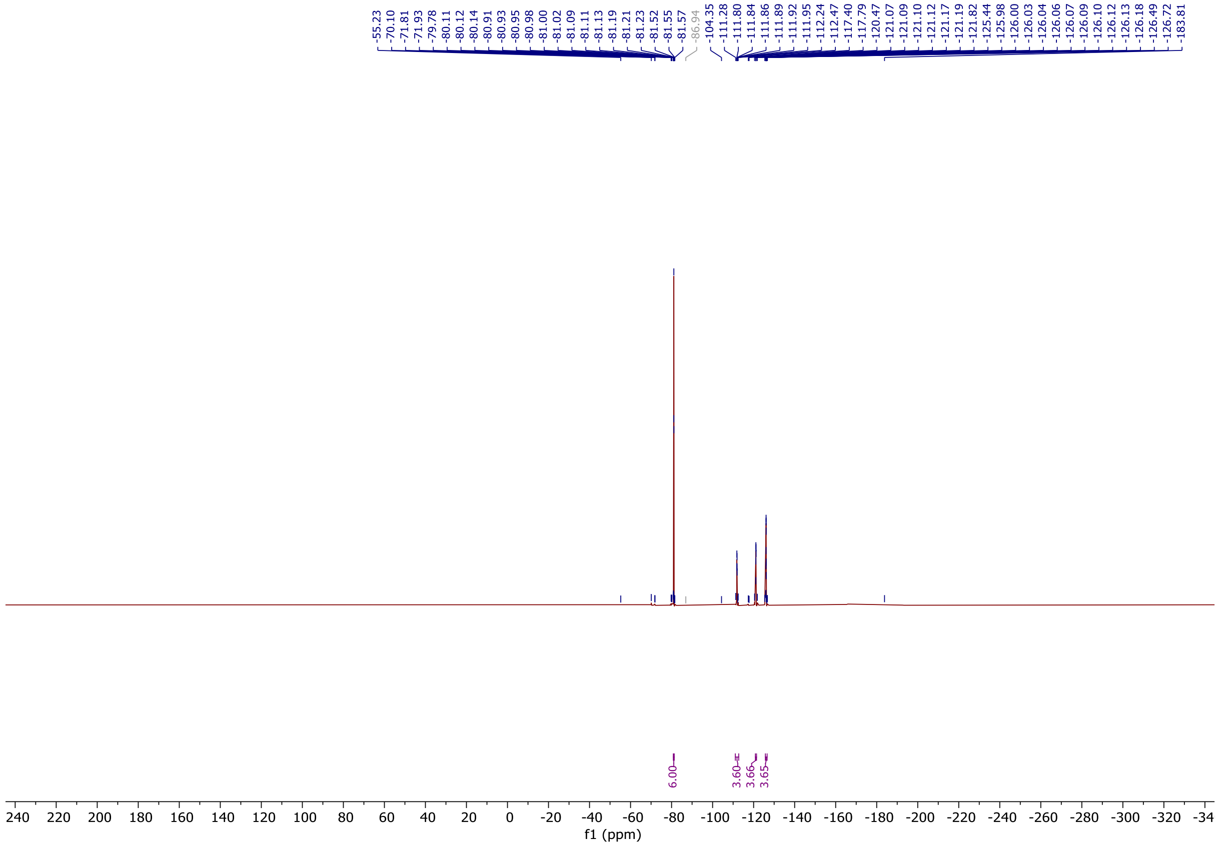
-55.23 -70.10 -71.81 -71.93 -79.78 -80.11 -80.12 -80.14 -80.91 -80.93 -80.95 -80.98 -81.00 -81.02 -81.09 -81.11 -81.13 -81.19 -81.21 -81.23 -81.52 -81.55 -81.57 -86.94 -104.35 -111.28 -111.80 -111.84 -111.86 -111.89 -111.92 -111.95 -112.24 -112.47 -117.40 -117.79 -120.47 -121.07 -121.09 -121.10 -121.12 -121.17 -121.19 -121.82 -125.44 -125.98 -126.00 -126.03 -126.04 -126.06 -126.07 -126.09 -126.10 -126.12 -126.13 -126.18 -126.49 -126.72 -183.81
6.00 3.60 3.66 3.65
240 220 200 180 160 140 120 100 80 60 40 20 0 -20 -40 -60 -80 -100 -120 -140 -160 -180 -200 -220 -240 -260 -280 -300 -320 -34
f1 (ppm)

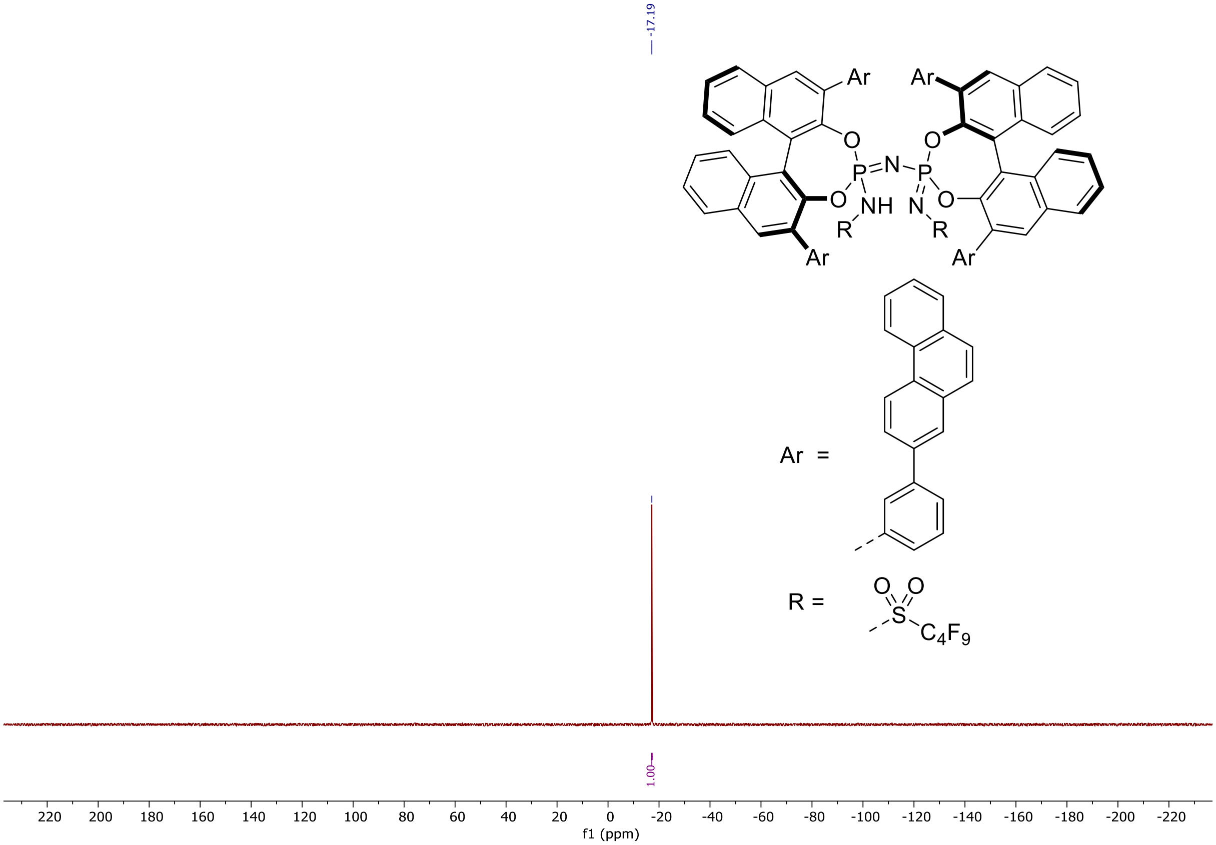
-17.19
1.00
Ar
Ar
Ar
Ar
O
O
O
O
P=N-P
NH
N
R
R
Ar =
R =
O O
S
C4F9
220 200 180 160 140 120 100 80 60 40 20 0 -20 -40 -60 -80 -100 -120 -140 -160 -180 -200 -220
f1 (ppm)

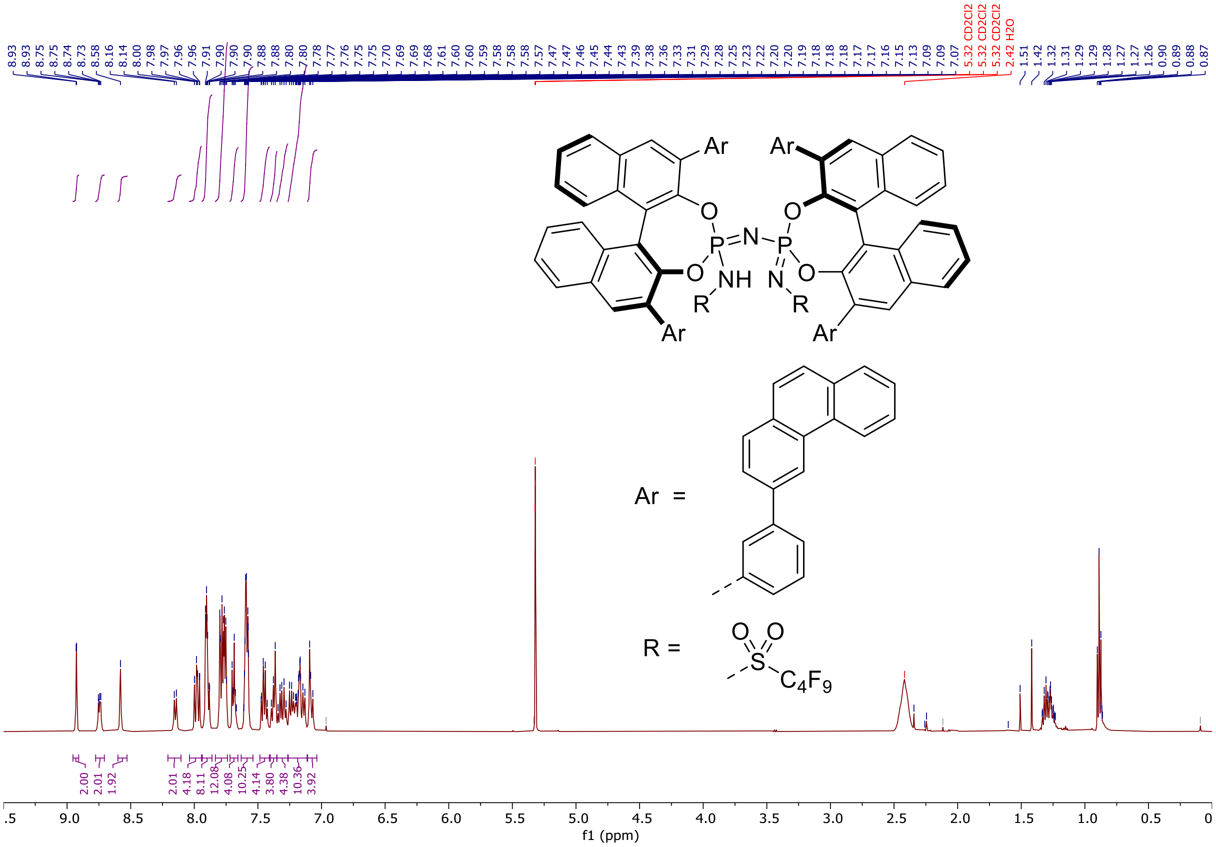
8.93 8.93 8.75 8.75 8.74 8.73 8.58 8.16 8.14 8.00 7.98 7.97 7.96 7.96 7.91 7.90 7.90 7.90 7.88 7.88 7.80 7.78 7.77 7.76 7.75 7.75 7.70 7.69 7.69 7.68 7.61 7.60 7.60 7.59 7.58 7.58 7.58 7.57 7.47 7.47 7.46 7.45 7.44 7.43 7.39 7.38 7.36 7.33 7.31 7.29 7.28 7.25 7.23 7.22 7.20 7.20 7.19 7.18 7.18 7.18 7.17 7.16 7.15 7.13 7.09 7.09 7.07
5.32 CD2Cl2
5.32 CD2Cl2
5.32 CD2Cl2
2.42 H2O
1.51 1.42 1.32 1.31 1.29 1.29 1.28 1.27 1.27 1.26 0.90 0.89 0.88 0.87
2.00 2.01 1.92 2.01 4.18 8.11 12.08 4.08 10.25 4.14 3.80 4.38 10.36 3.92
Ar
Ar
Ar
Ar
O
O
O
O
P=N-P
NH
N
R
R
Ar =
R =
O O
S
C4F9
.5 9.0 8.5 8.0 7.5 7.0 6.5 6.0 5.5 5.0 4.5 4.0 3.5 3.0 2.5 2.0 1.5 1.0 0.5 0
f1 (ppm)

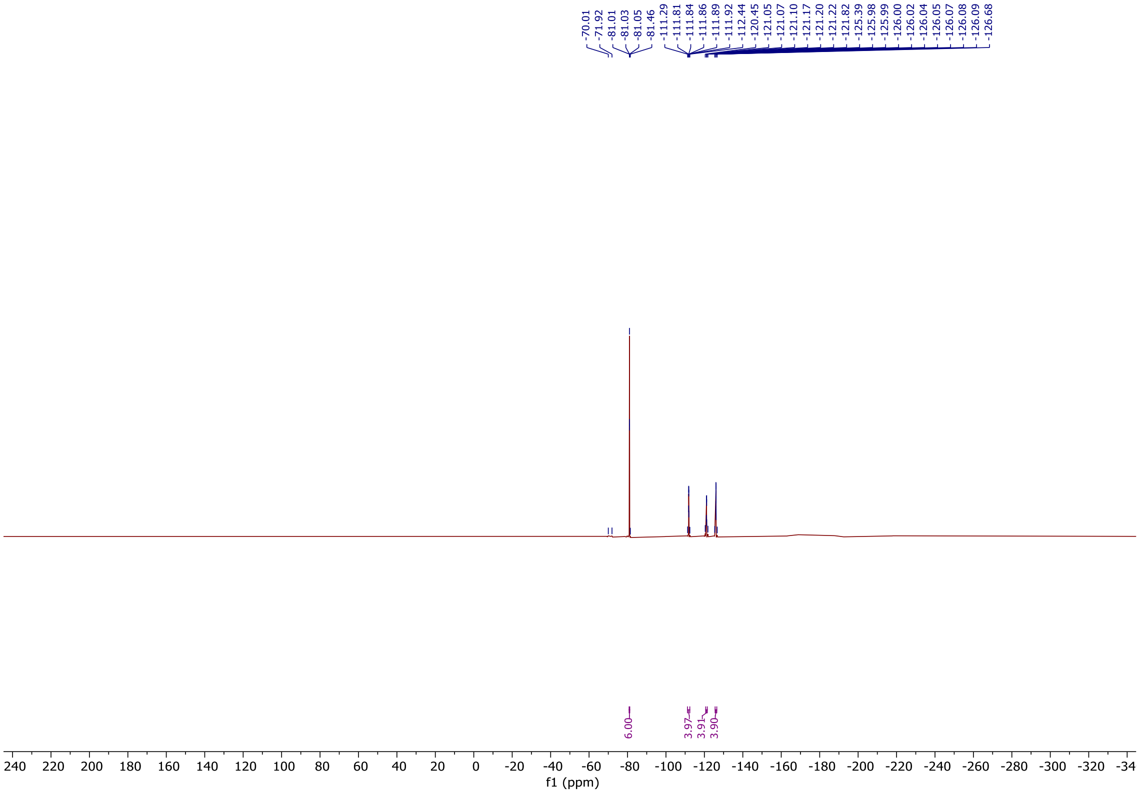
-70.01
-71.92
-81.01
-81.03
-81.05
-81.46
-111.29
-111.81
-111.84
-111.86
-111.89
-111.92
-112.44
-120.45
-121.05
-121.07
-121.10
-121.17
-121.20
-121.22
-121.82
-125.39
-125.98
-125.99
-126.00
-126.02
-126.04
-126.05
-126.07
-126.08
-126.09
-126.68
6.00
3.97
3.91
3.90
240 220 200 180 160 140 120 100 80 60 40 20 0 -20 -40 -60 -80 -100 -120 -140 -160 -180 -200 -220 -240 -260 -280 -300 -320 -34
f1 (ppm)

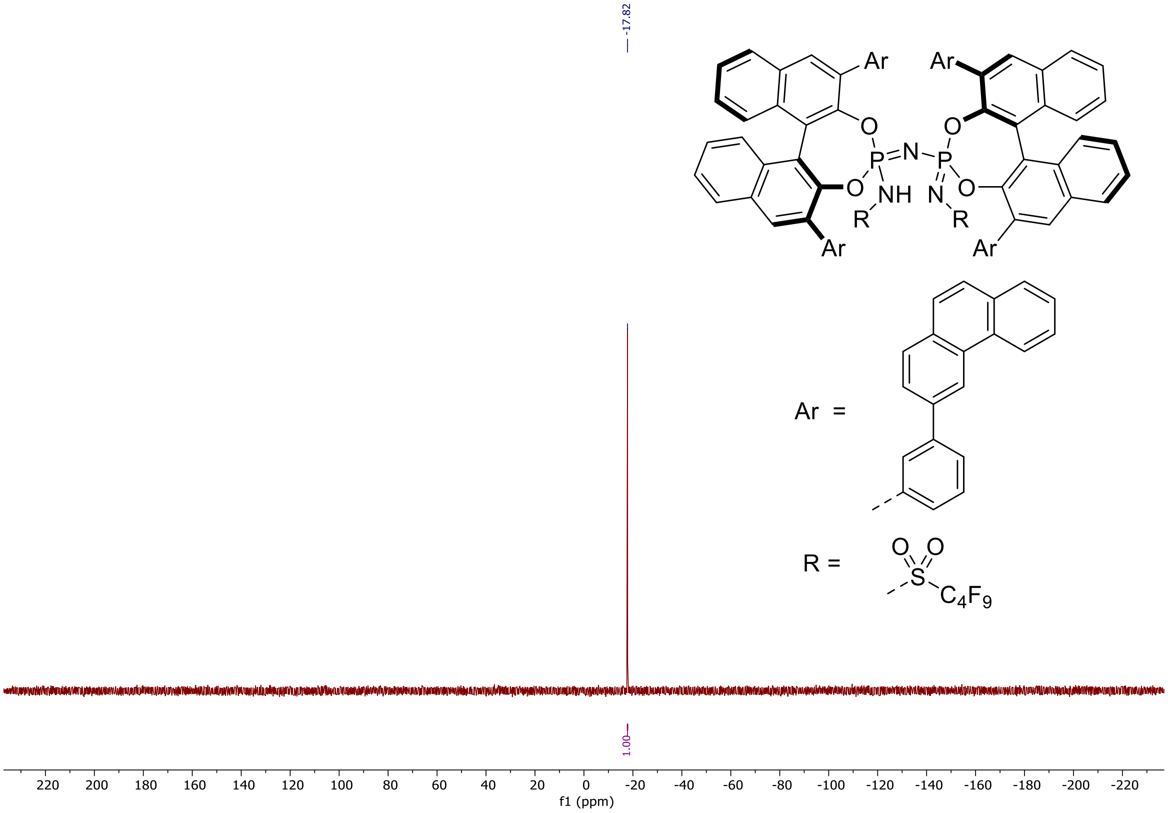
-17.82
Ar
Ar
O
O
P
N
P
O
O
NH
N
R
R
Ar
Ar
Ar =
R =
O
O
S
C_4F_9
1.00
220 200 180 160 140 120 100 80 60 40 20 0 -20 -40 -60 -80 -100 -120 -140 -160 -180 -200 -220
f1 (ppm)

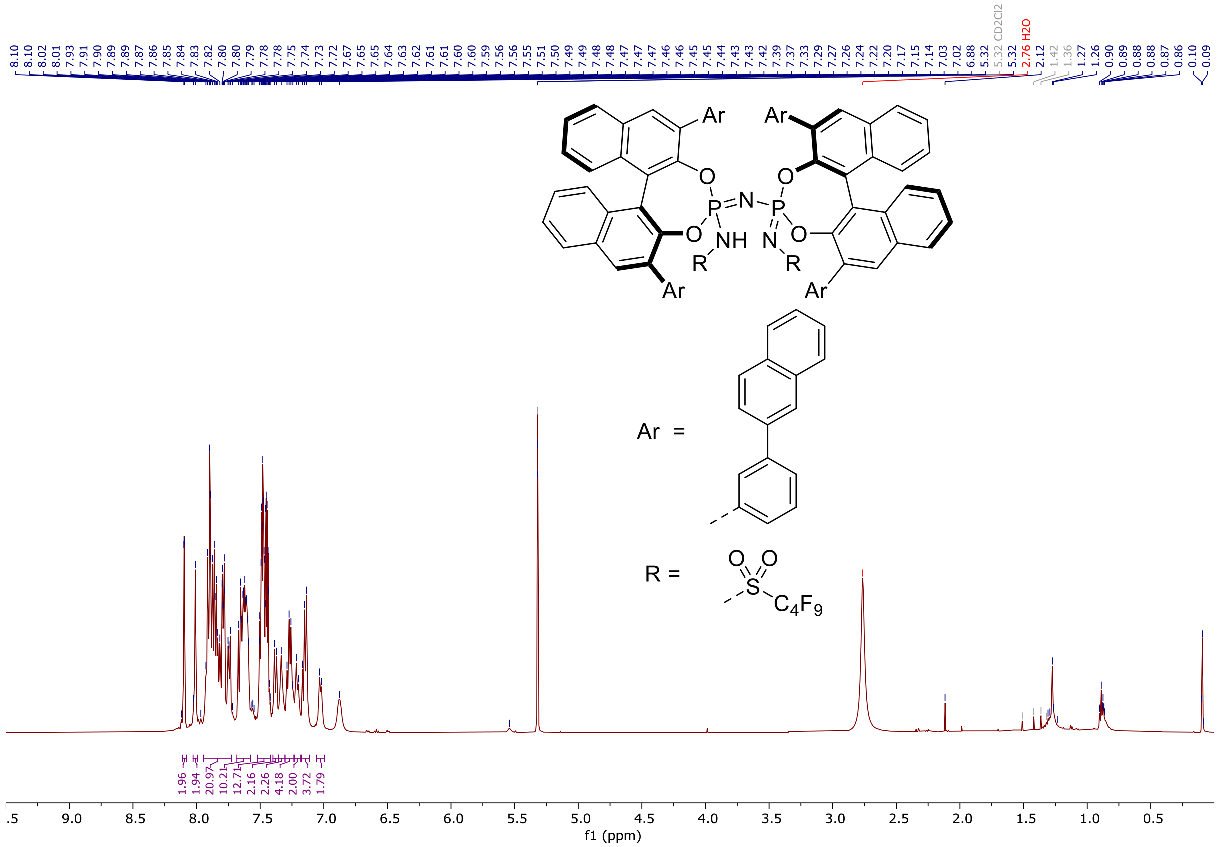
8.10
8.10
8.02
8.01
7.93
7.91
7.90
7.89
7.89
7.87
7.86
7.85
7.84
7.83
7.82
7.80
7.80
7.79
7.78
7.78
7.75
7.74
7.73
7.72
7.67
7.65
7.65
7.64
7.63
7.62
7.61
7.61
7.60
7.59
7.56
7.56
7.55
7.51
7.50
7.49
7.49
7.48
7.47
7.47
7.46
7.45
7.45
7.44
7.43
7.43
7.42
7.39
7.37
7.33
7.29
7.27
7.26
7.24
7.22
7.20
7.17
7.15
7.14
7.03
7.02
6.88
5.32
5.32 CD2Cl2
5.32
2.76 H2O
2.12
1.42
1.36
1.27
1.26
0.90
0.89
0.88
0.88
0.87
0.86
0.10
0.09
Ar
Ar
O
O
P
N
P
O
O
NH
N
R
R
Ar
Ar
Ar =
R =
O O
S
C4F9
1.96
1.94
20.97
10.21
12.71
2.16
2.26
4.18
2.00
3.72
1.79
.5
9.0
8.5
8.0
7.5
7.0
6.5
6.0
5.5
5.0
4.5
4.0
3.5
3.0
2.5
2.0
1.5
1.0
0.5
f1 (ppm)

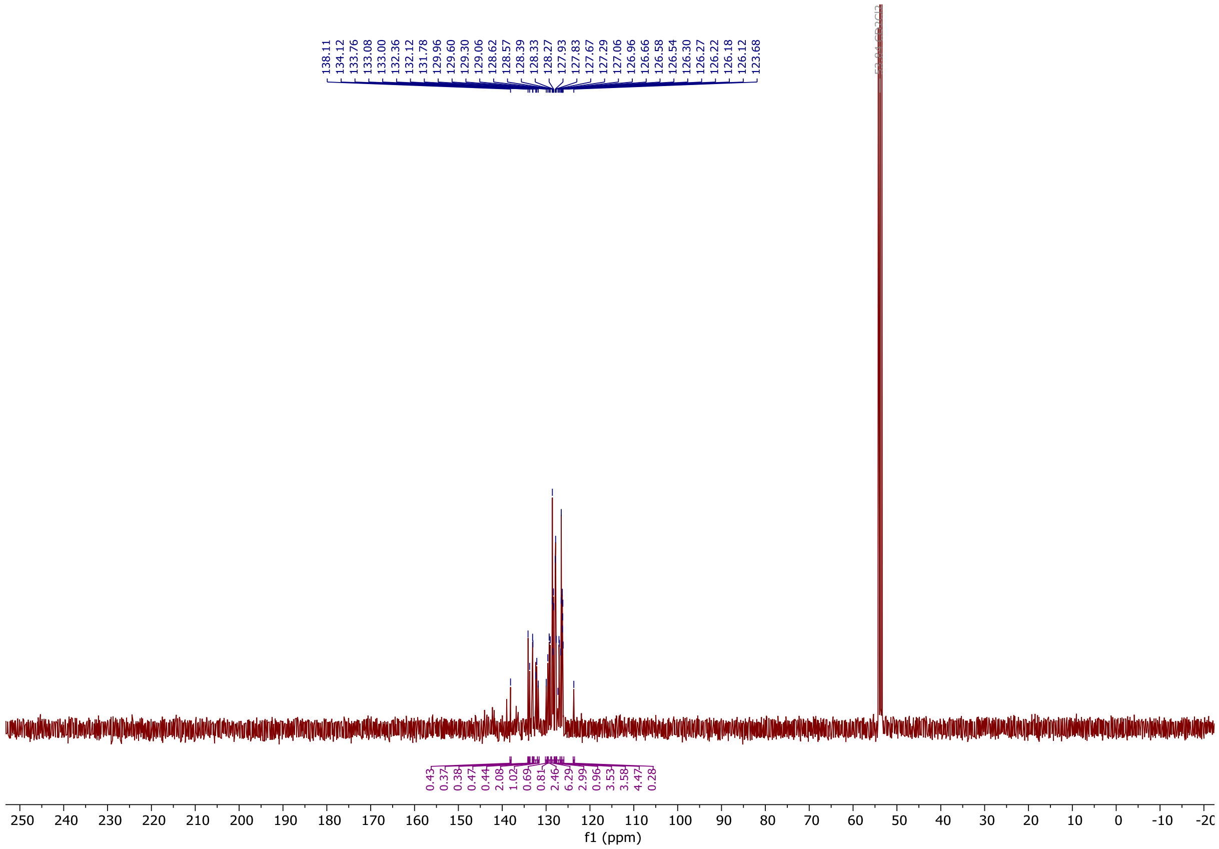
138.11
134.12
133.76
133.08
133.00
132.36
132.12
131.78
129.96
129.60
129.30
129.06
128.62
128.57
128.39
128.33
128.27
127.93
127.83
127.67
127.29
127.06
126.96
126.66
126.58
126.54
126.30
126.27
126.22
126.18
126.12
123.68
0.43
0.37
0.38
0.47
0.44
2.08
1.02
0.69
0.81
2.46
6.29
2.99
0.96
3.53
3.58
4.47
0.28
250
240
230
220
210
200
190
180
170
160
150
140
130
120
110
100
90
80
70
60
50
40
30
20
10
0
-10
-20
f1 (ppm)

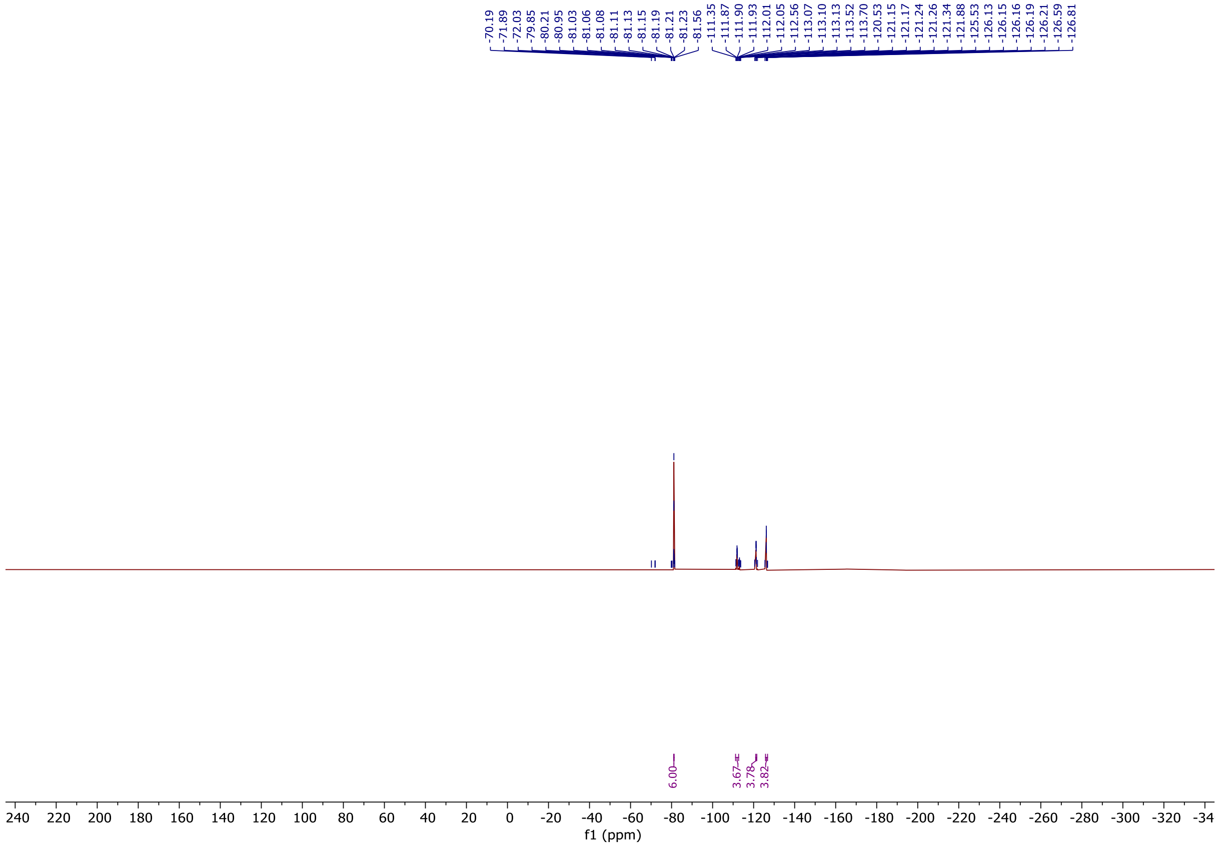
-70.19
-71.89
-72.03
-79.85
-80.21
-80.95
-81.03
-81.06
-81.08
-81.11
-81.13
-81.15
-81.19
-81.21
-81.23
-81.56
-111.35
-111.87
-111.90
-111.93
-112.01
-112.05
-112.56
-113.07
-113.10
-113.13
-113.52
-113.70
-120.53
-121.15
-121.17
-121.24
-121.26
-121.34
-121.88
-125.53
-126.13
-126.15
-126.16
-126.19
-126.21
-126.59
-126.81
6.00
3.67
3.78
3.82
240
220
200
180
160
140
120
100
80
60
40
20
0
-20
-40
-60
-80
-100
-120
-140
-160
-180
-200
-220
-240
-260
-280
-300
-320
-34
f1 (ppm)

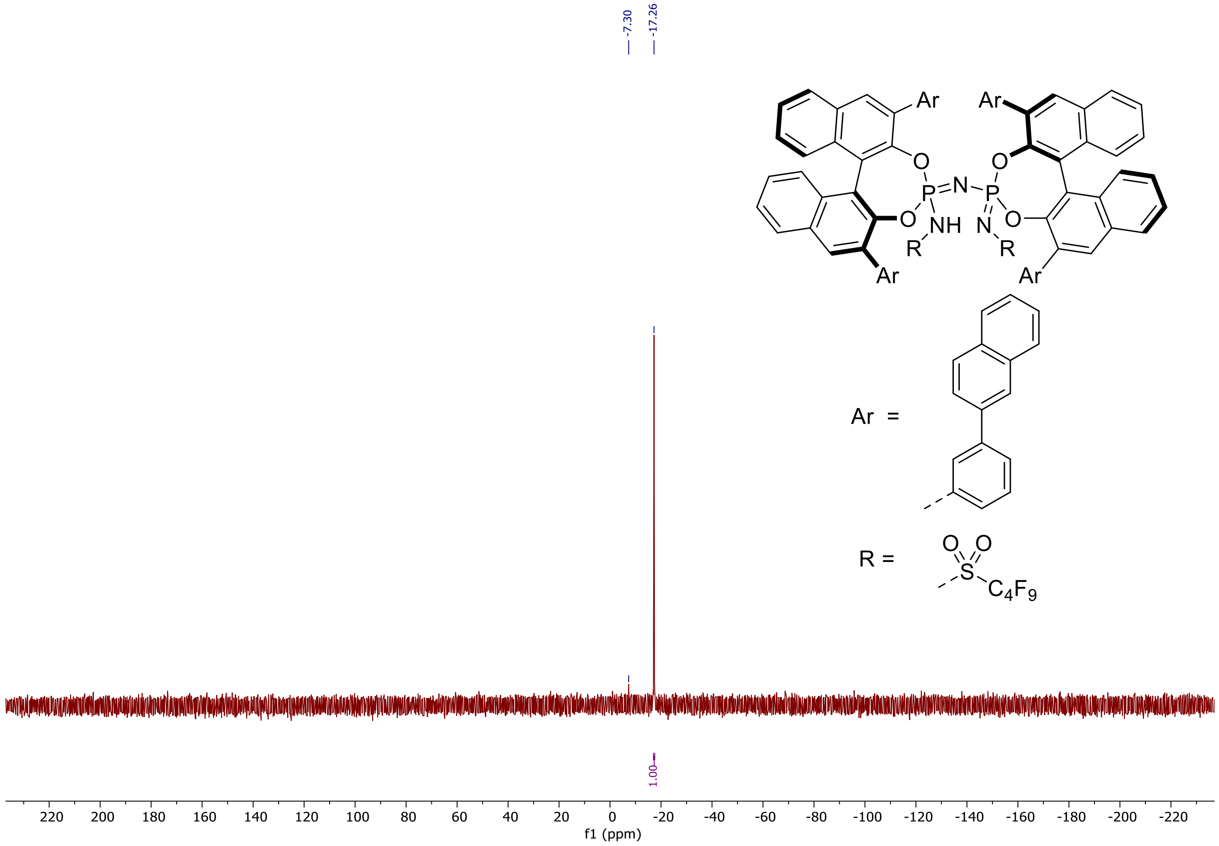
-7.30
-17.26
Ar
Ar
O
P
N
P
O
O
NH
N
O
R
R
Ar
Ar
Ar =
R =
O
O
S
C4F9
1.00
220
200
180
160
140
120
100
80
60
40
20
0
-20
-40
-60
-80
-100
-120
-140
-160
-180
-200
-220
f1 (ppm)

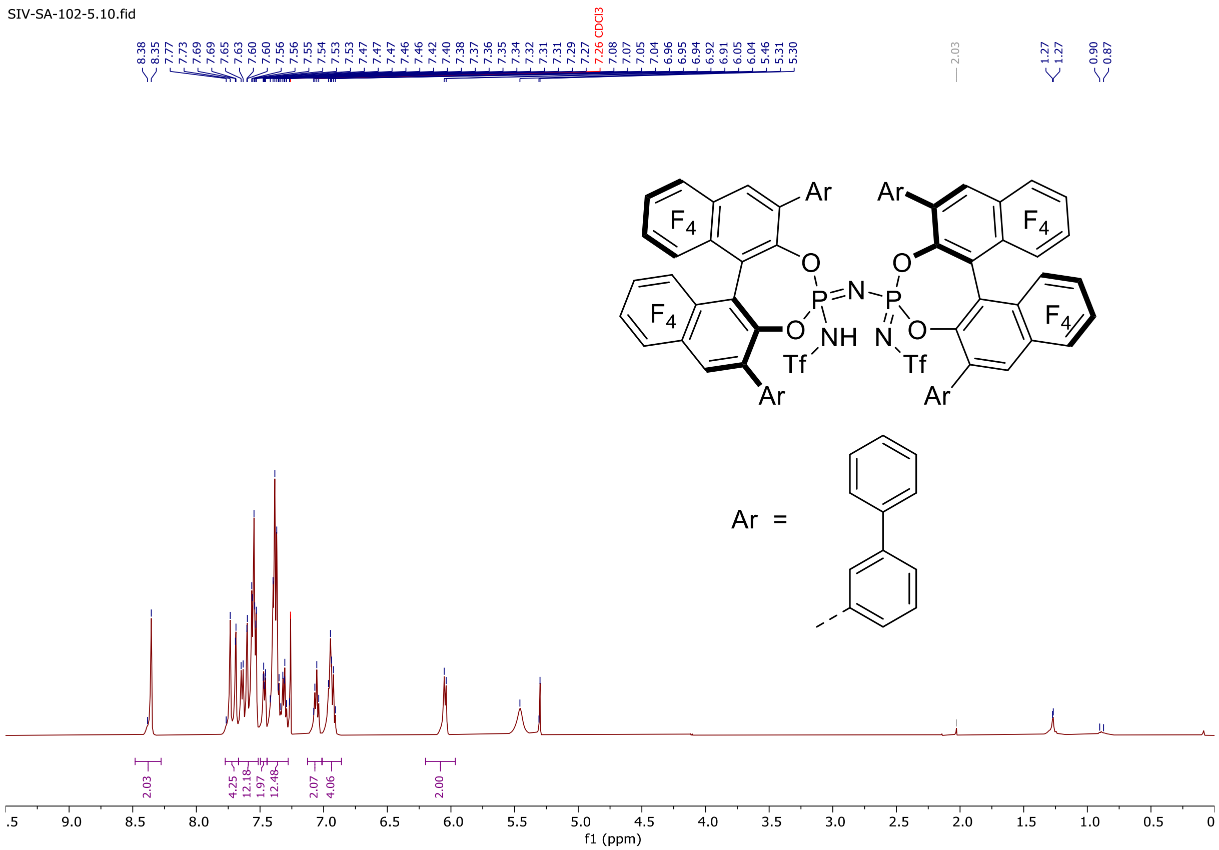
SIV-SA-102-5.10.fid
8.38
8.35
7.77
7.73
7.69
7.69
7.65
7.63
7.60
7.60
7.56
7.56
7.55
7.54
7.53
7.53
7.47
7.47
7.46
7.46
7.42
7.40
7.38
7.37
7.36
7.35
7.34
7.32
7.31
7.31
7.29
7.27
7.26 CDCl3
7.08
7.07
7.05
7.04
6.96
6.95
6.94
6.92
6.91
6.05
6.04
5.46
5.31
5.30
2.03
1.27
1.27
0.90
0.87
Ar
Ar
F4
F4
O
O
P
N
P
O
O
NH
N
Tf
Tf
Ar
Ar
Ar =
2.03
4.25
12.18
1.97
12.48
2.07
4.06
2.00
.5
9.0
8.5
8.0
7.5
7.0
6.5
6.0
5.5
5.0
4.5
4.0
3.5
3.0
2.5
2.0
1.5
1.0
0.5
0
f1 (ppm)

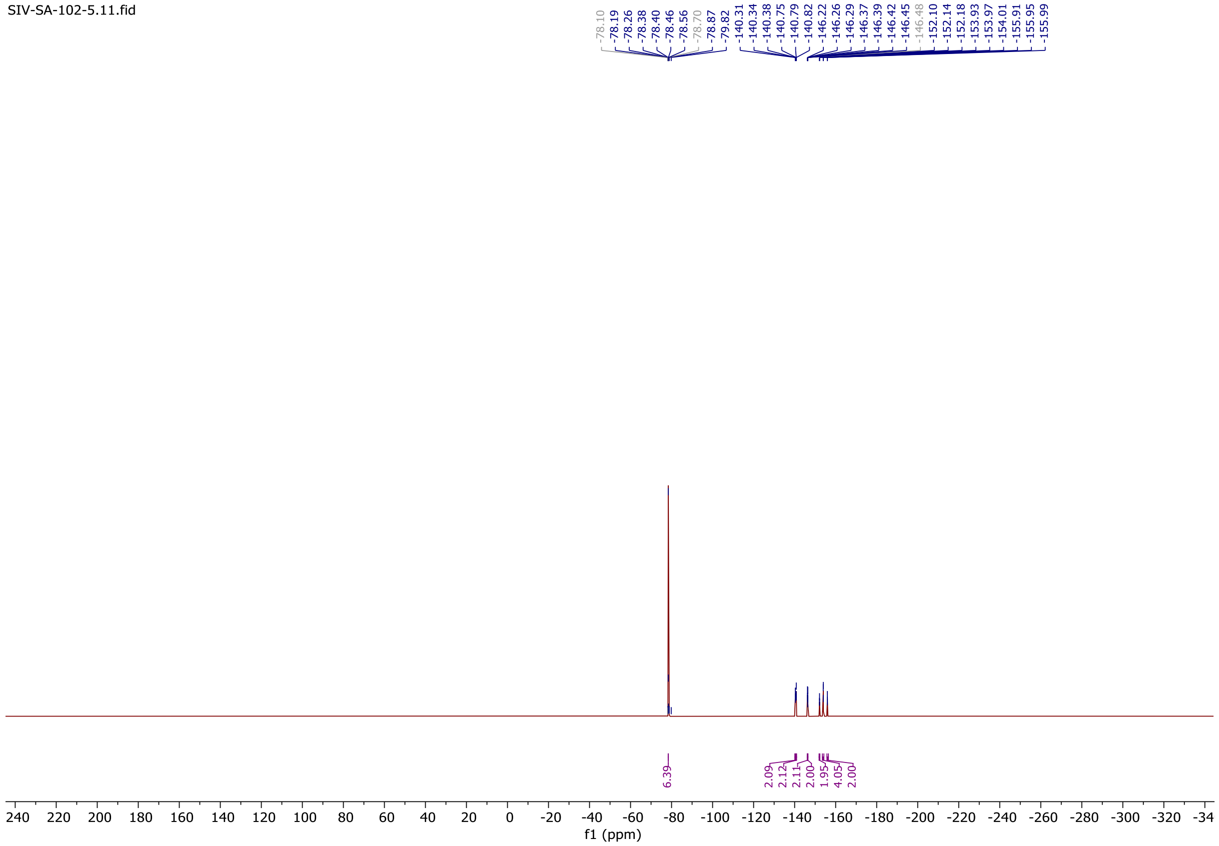
SIV-SA-102-5.11.fid
-78.10
-78.19
-78.26
-78.38
-78.40
-78.46
-78.56
-78.70
-78.87
-79.82
-140.31
-140.34
-140.38
-140.75
-140.79
-140.82
-146.22
-146.26
-146.29
-146.37
-146.39
-146.42
-146.45
-146.48
-152.10
-152.14
-152.18
-153.93
-153.97
-154.01
-155.91
-155.95
-155.99
6.39
2.09
2.12
2.11
2.00
1.95
4.05
2.00
240
220
200
180
160
140
120
100
80
60
40
20
0
-20
-40
-60
-80
-100
-120
-140
-160
-180
-200
-220
-240
-260
-280
-300
-320
-34
f1 (ppm)

SIV-SA-102-5.12.fid

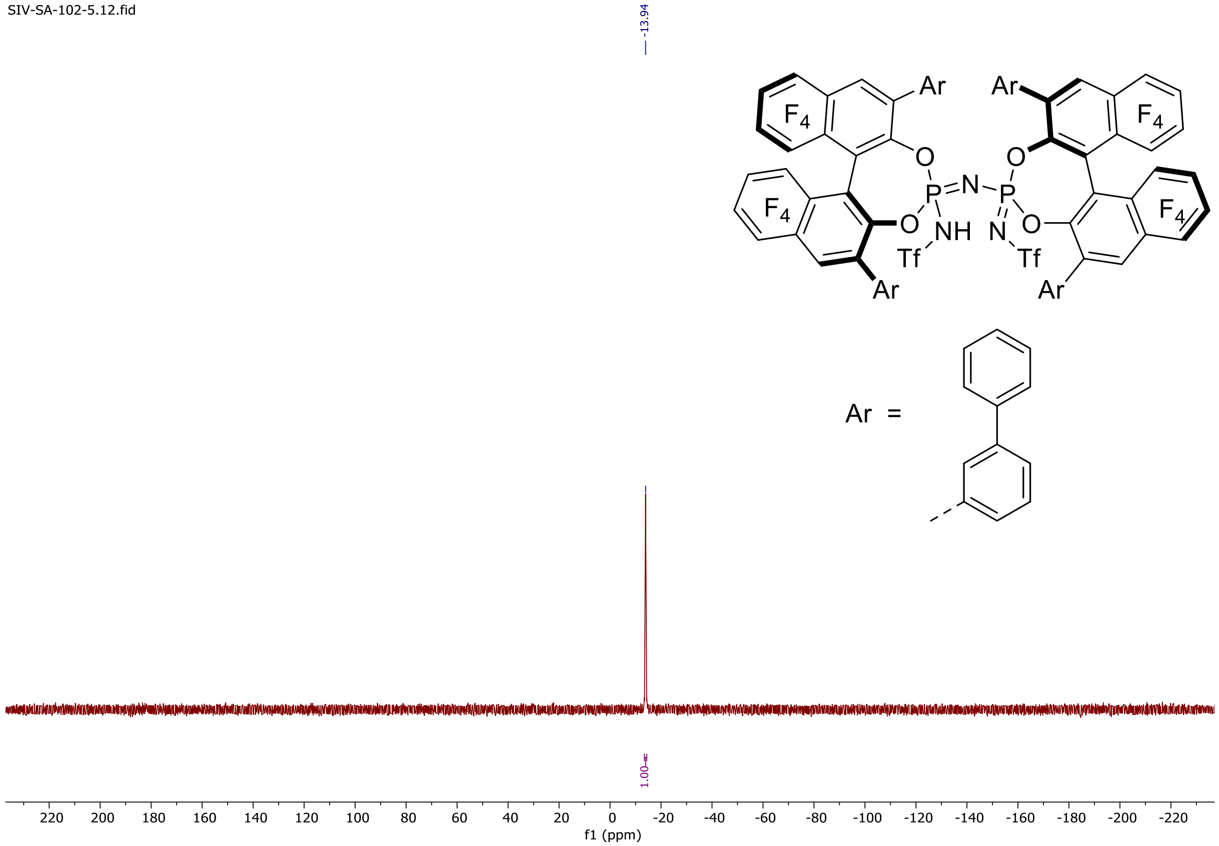

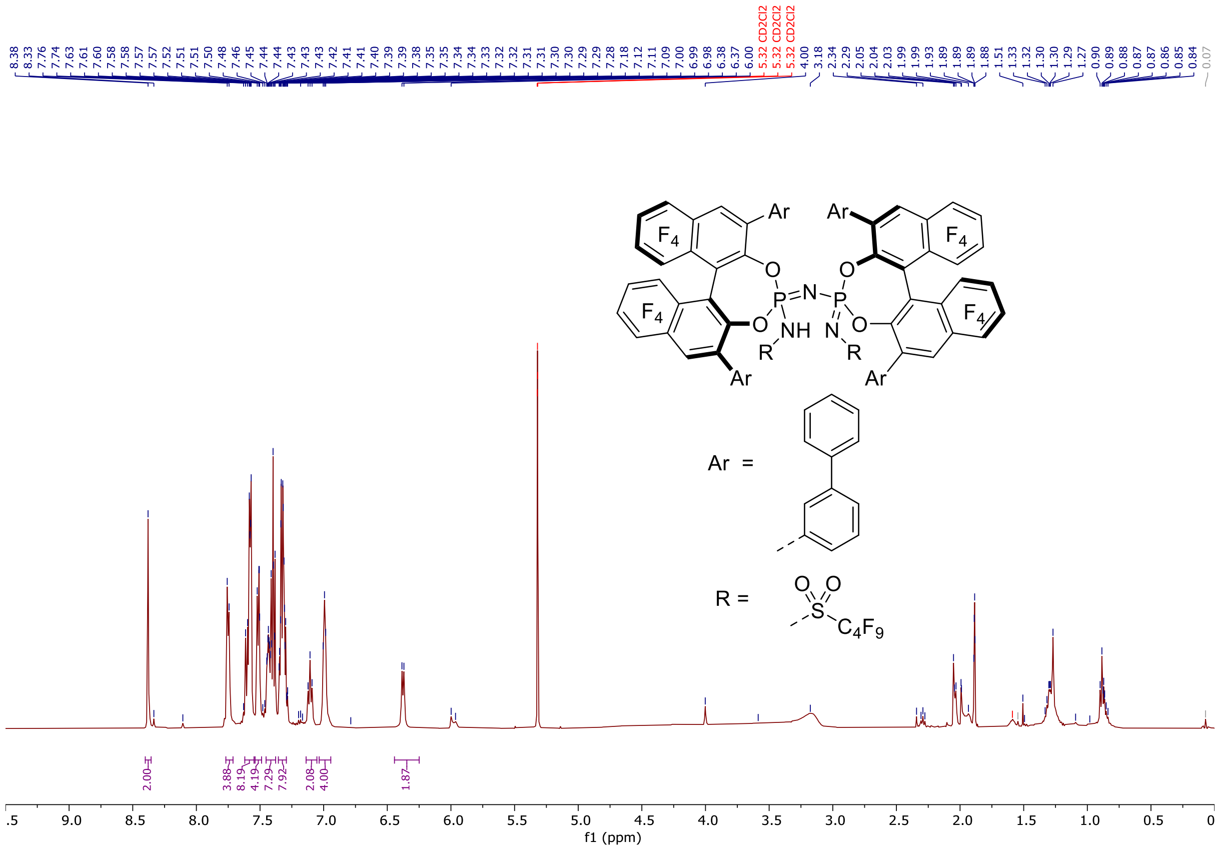

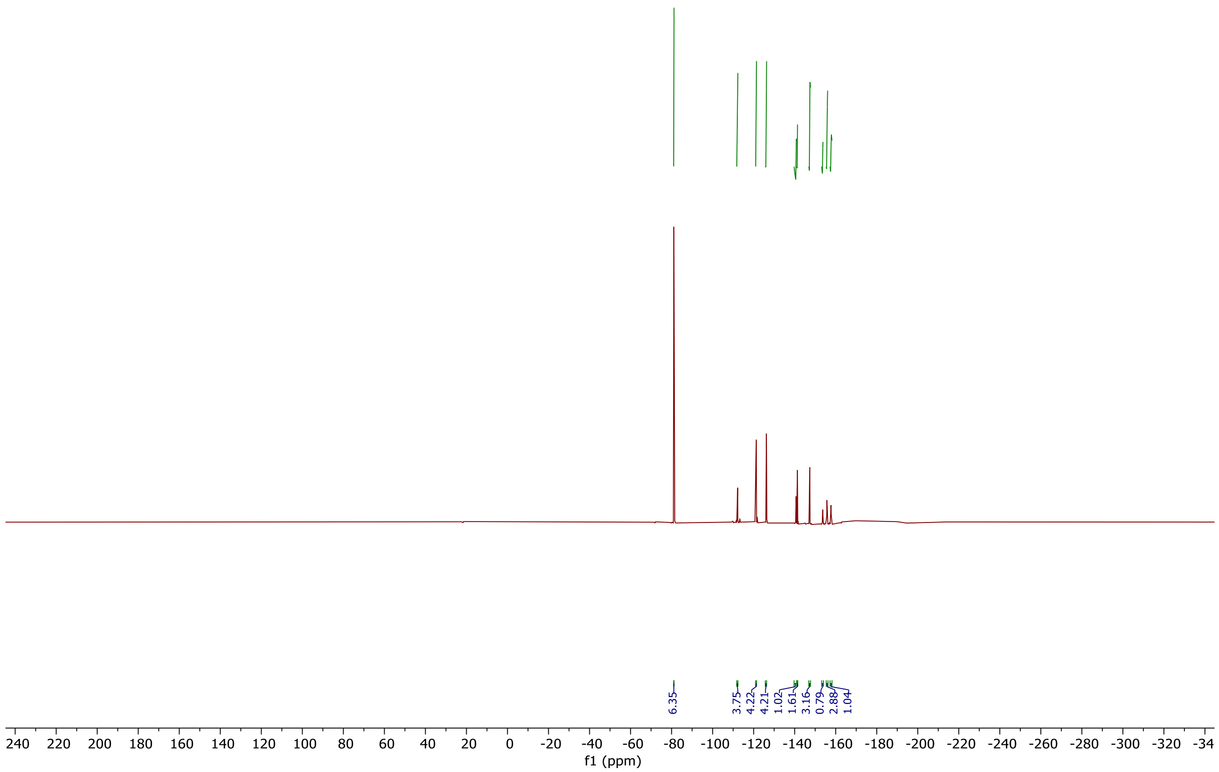
6.35
3.75
4.22
4.21
1.02
1.61
3.16
0.79
2.88
1.04
240 220 200 180 160 140 120 100 80 60 40 20 0 -20 -40 -60 -80 -100 -120 -140 -160 -180 -200 -220 -240 -260 -280 -300 -320 -34
f1 (ppm)

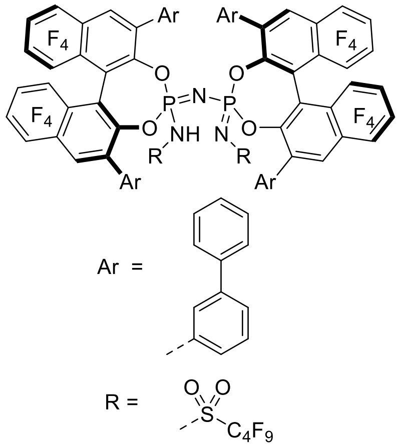
Ar
Ar
F4
F4
F4
F4
O
O
O
O
P
P
N
NH
N
R
R
Ar
Ar
Ar =
R =
O
O
S
C4F9

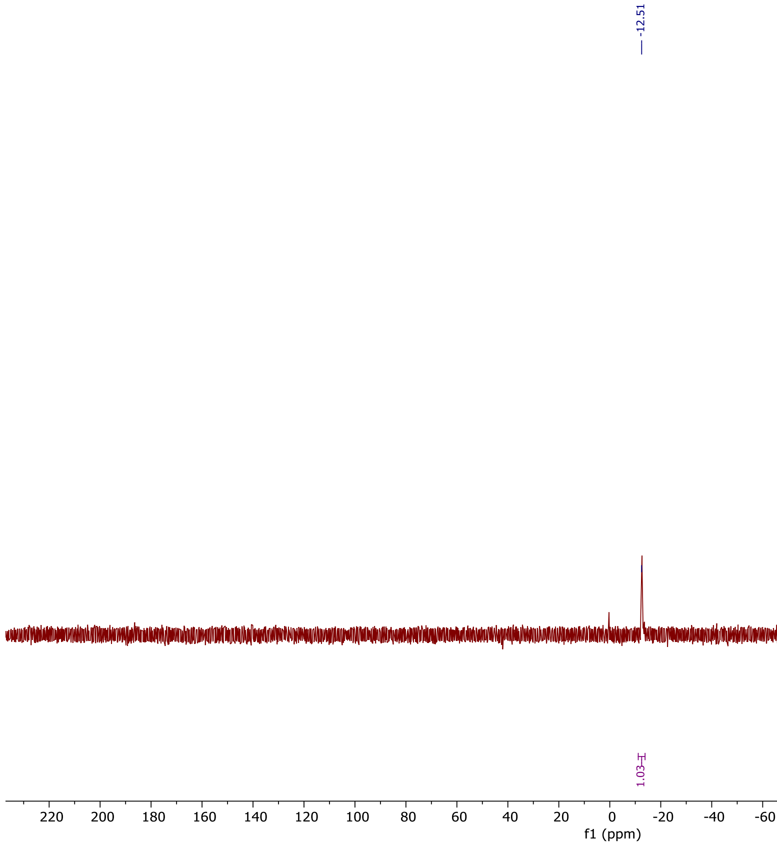
-12.51
1.03
220 200 180 160 140 120 100 80 60 40 20 0 -20 -40 -60 -80 -100 -120 -140 -160 -180 -200 -220
f1 (ppm)

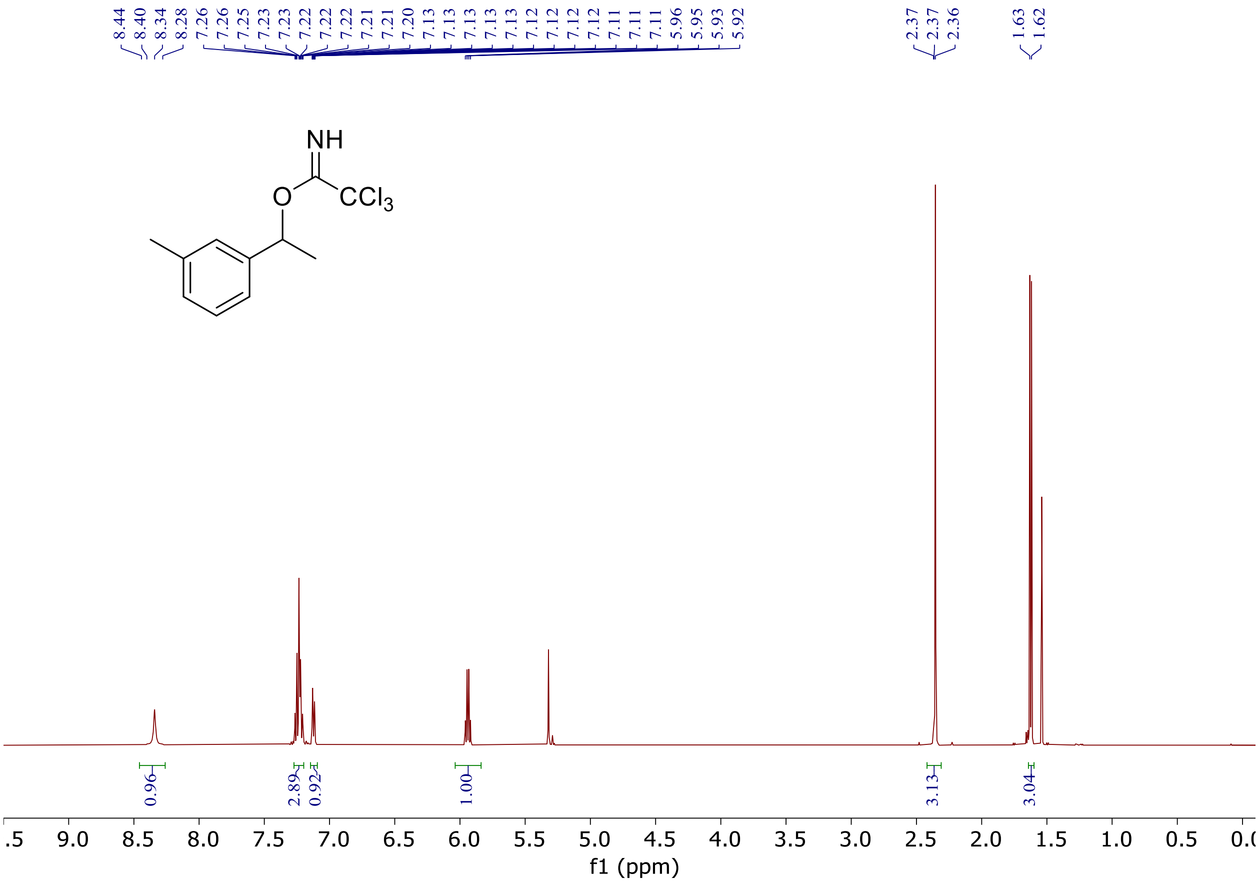
8.44
8.40
8.34
8.28
7.26
7.26
7.25
7.23
7.23
7.22
7.22
7.22
7.21
7.21
7.20
7.13
7.13
7.13
7.13
7.12
7.12
7.12
7.12
7.11
7.11
7.11
5.96
5.95
5.93
5.92
2.37
2.37
2.36
1.63
1.62
NH
O
CCl3
0.96
2.89
0.92
1.00
3.13
3.04
.5 9.0 8.5 8.0 7.5 7.0 6.5 6.0 5.5 5.0 4.5 4.0 3.5 3.0 2.5 2.0 1.5 1.0 0.5 0.
f1 (ppm)

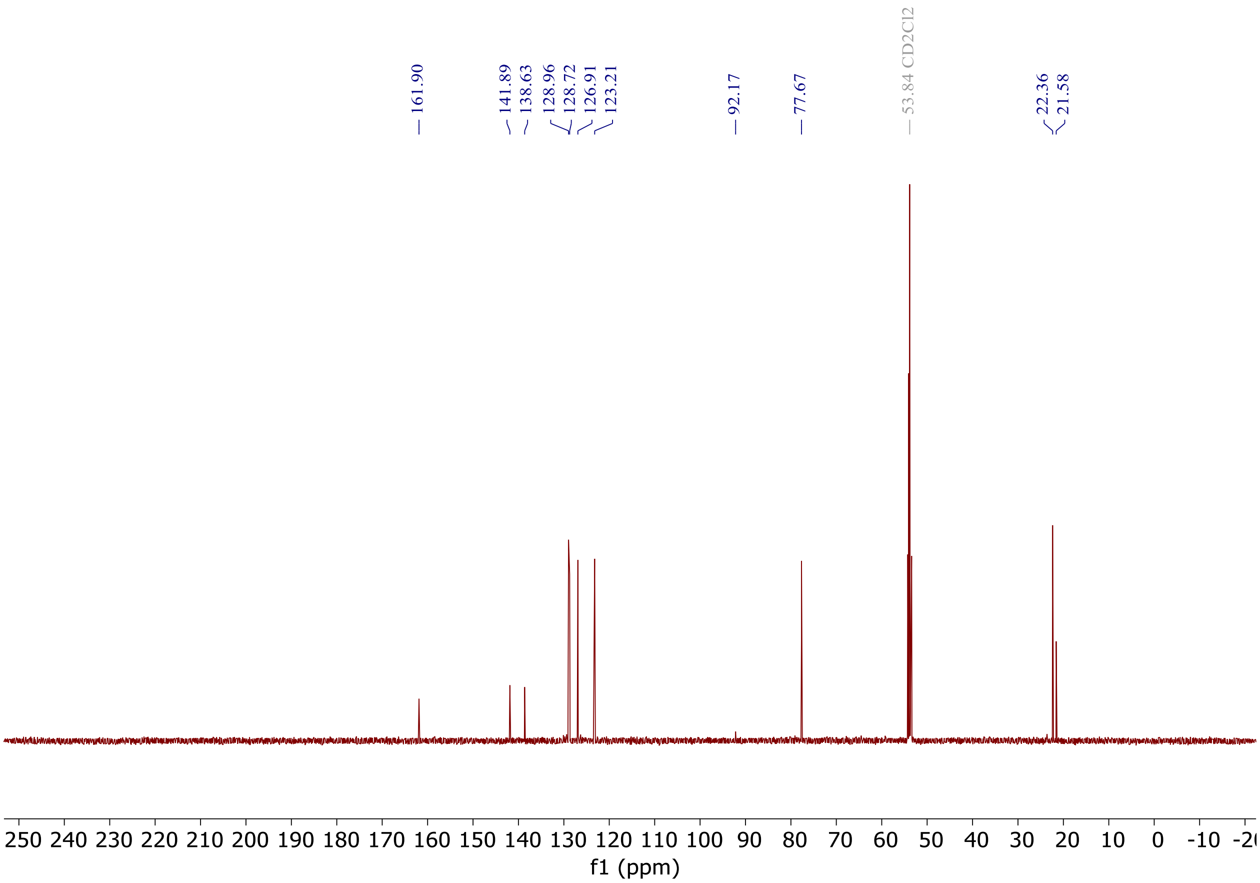
161.90
141.89
138.63
128.96
128.72
126.91
123.21
92.17
77.67
53.84 CD2Cl2
22.36
21.58
250 240 230 220 210 200 190 180 170 160 150 140 130 120 110 100 90 80 70 60 50 40 30 20 10 0 -10 -2
f1 (ppm)

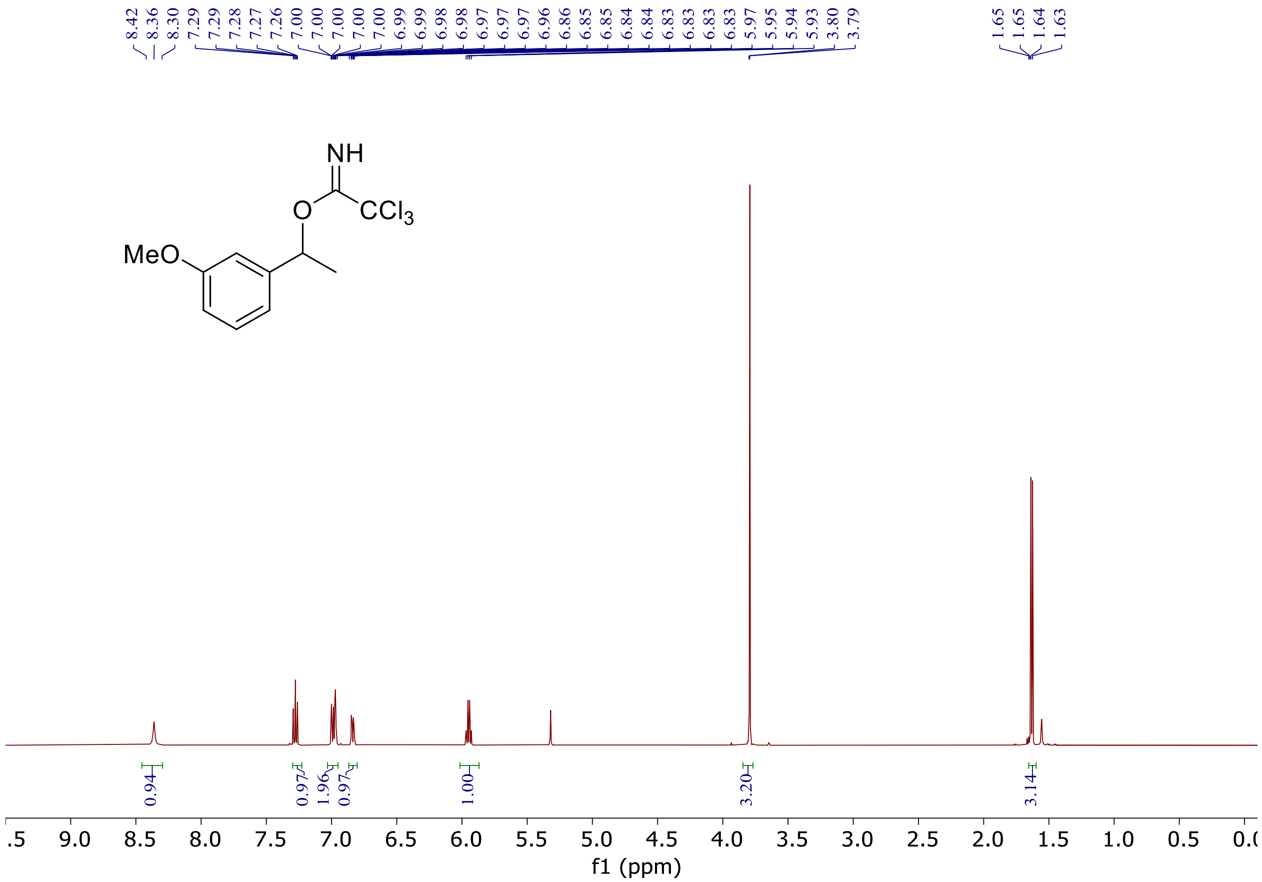
8.42
8.36
8.30
7.29
7.29
7.28
7.27
7.26
7.00
7.00
7.00
7.00
7.00
6.99
6.99
6.98
6.98
6.97
6.97
6.97
6.96
6.86
6.85
6.85
6.84
6.84
6.83
6.83
6.83
6.83
5.97
5.95
5.94
5.93
3.80
3.79
1.65
1.65
1.64
1.63
NH
O
CCl3
MeO
0.94
0.97
1.96
0.97
1.00
3.20
3.14
.5
9.0
8.5
8.0
7.5
7.0
6.5
6.0
5.5
5.0
4.5
4.0
3.5
3.0
2.5
2.0
1.5
1.0
0.5
0.0
f1 (ppm)

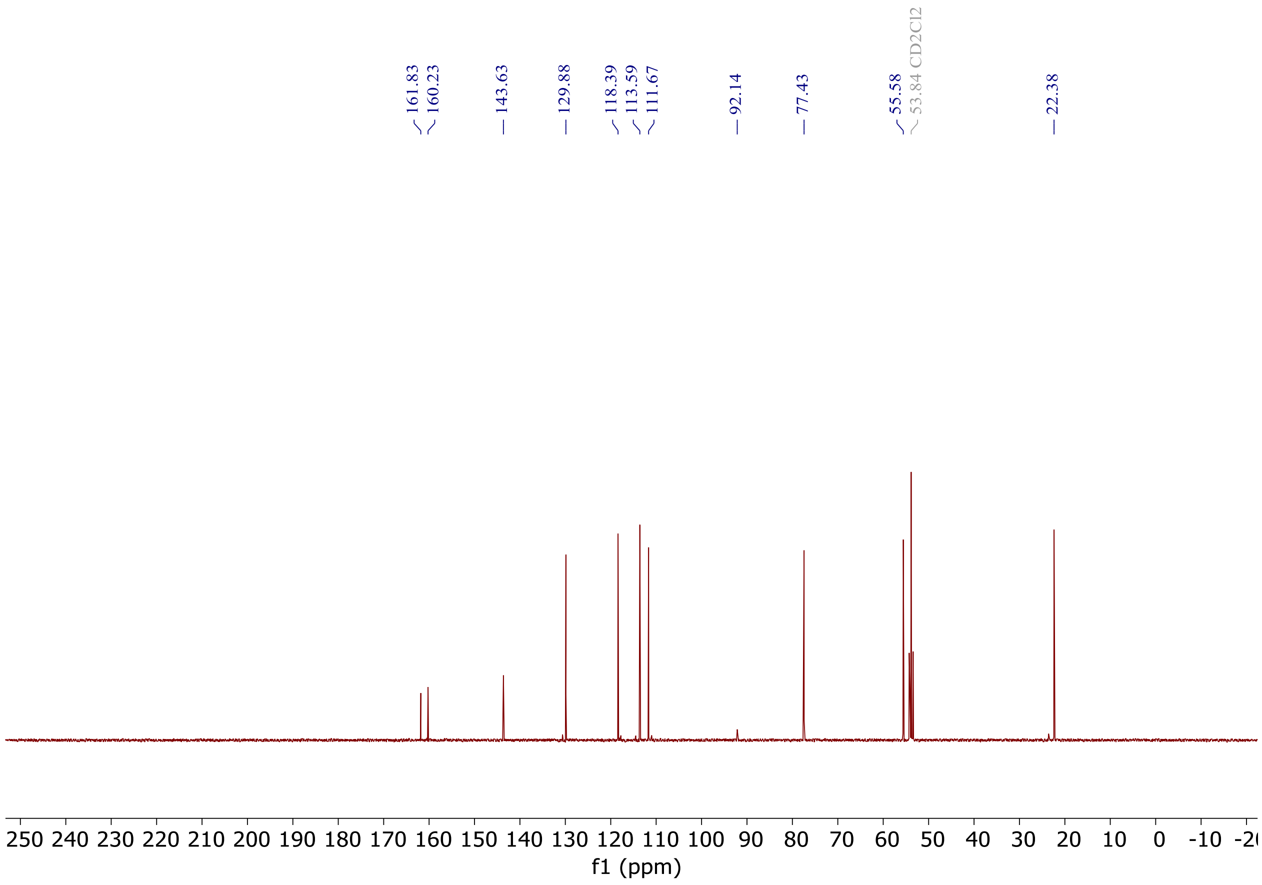
161.83
160.23
143.63
129.88
118.39
113.59
111.67
92.14
77.43
55.58
53.84 CD2Cl2
22.38
250
240
230
220
210
200
190
180
170
160
150
140
130
120
110
100
90
80
70
60
50
40
30
20
10
0
-10
-20
f1 (ppm)

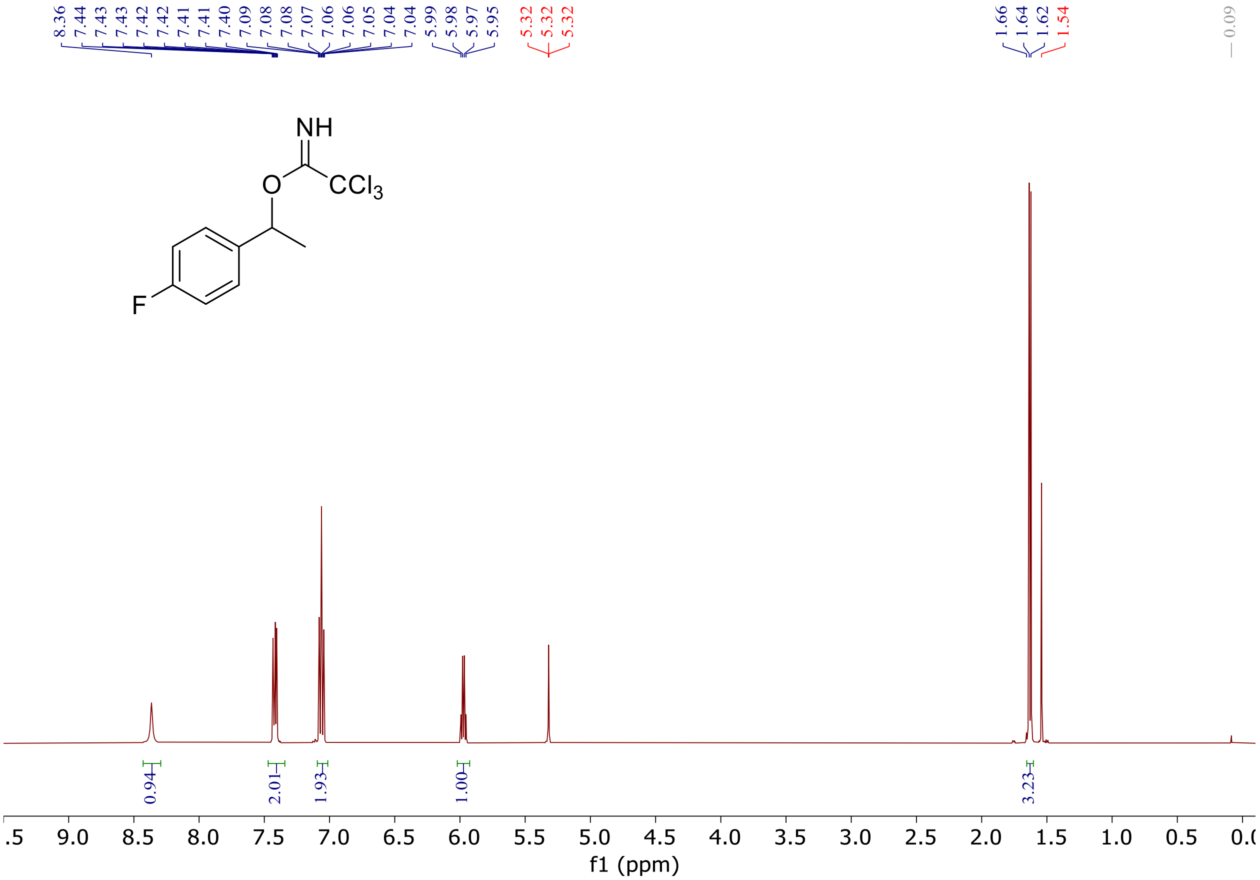
8.36
7.44
7.43
7.43
7.42
7.42
7.41
7.41
7.40
7.09
7.08
7.08
7.07
7.06
7.06
7.05
7.04
7.04
5.99
5.98
5.97
5.95
5.32
5.32
5.32
1.66
1.64
1.62
1.54
0.09
NH
O
CCl3
F
0.94
2.01
1.93
1.00
3.23
.5
9.0
8.5
8.0
7.5
7.0
6.5
6.0
5.5
5.0
4.5
4.0
3.5
3.0
2.5
2.0
1.5
1.0
0.5
0.(
f1 (ppm)

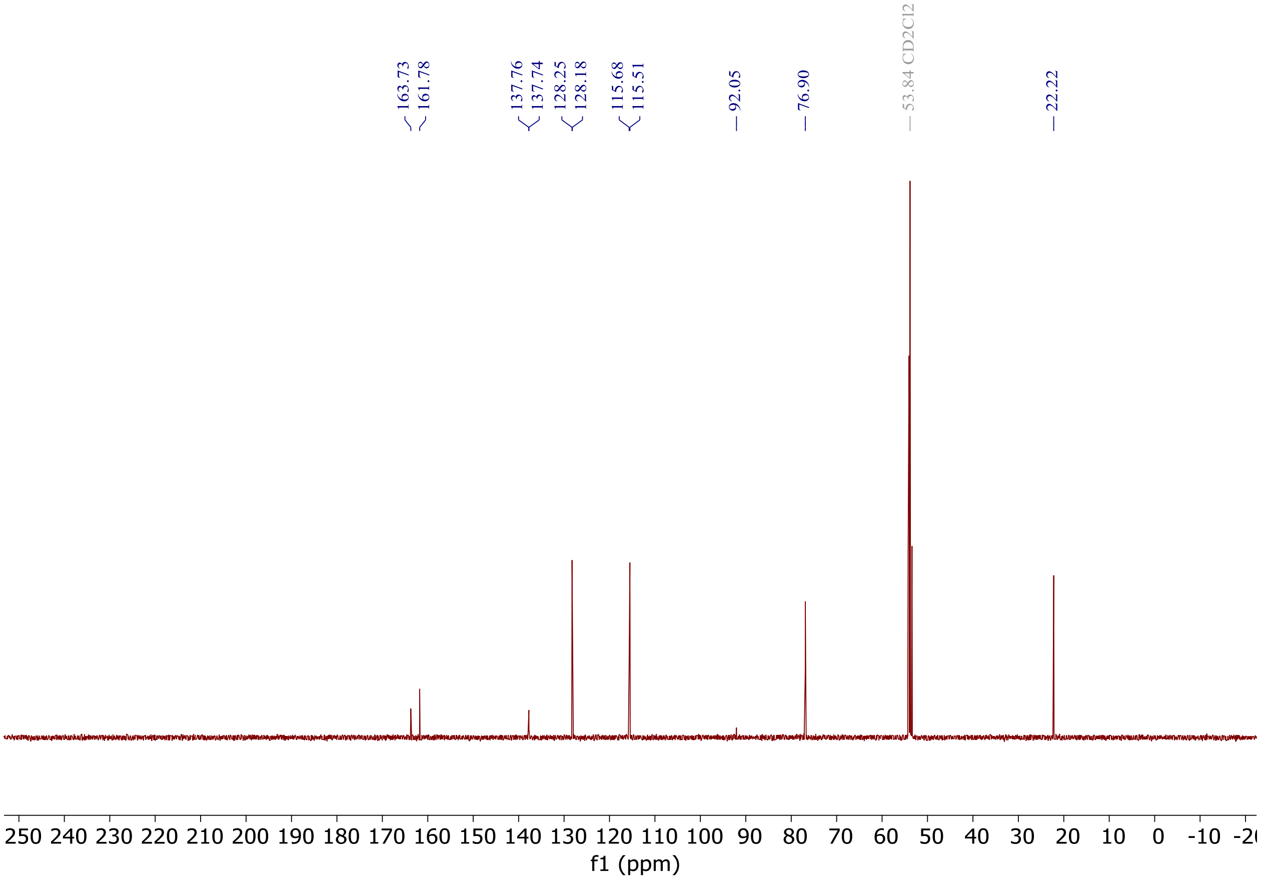
163.73
161.78
137.76
137.74
128.25
128.18
115.68
115.51
92.05
76.90
53.84 CD2Cl2
22.22
250
240
230
220
210
200
190
180
170
160
150
140
130
120
110
100
90
80
70
60
50
40
30
20
10
0
-10
-2(
f1 (ppm)

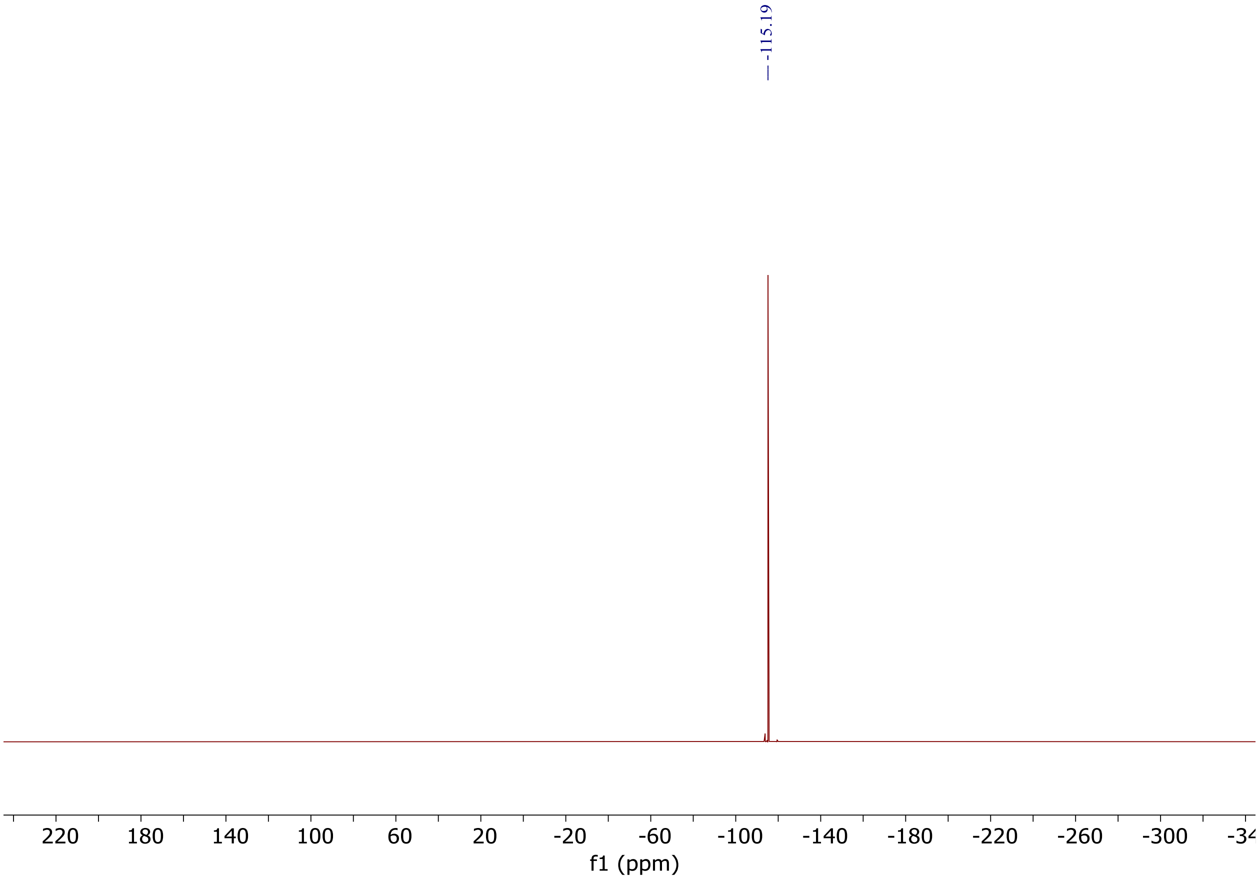
-115.19
220
180
140
100
60
20
-20
-60
-100
-140
-180
-220
-260
-300
f1 (ppm)

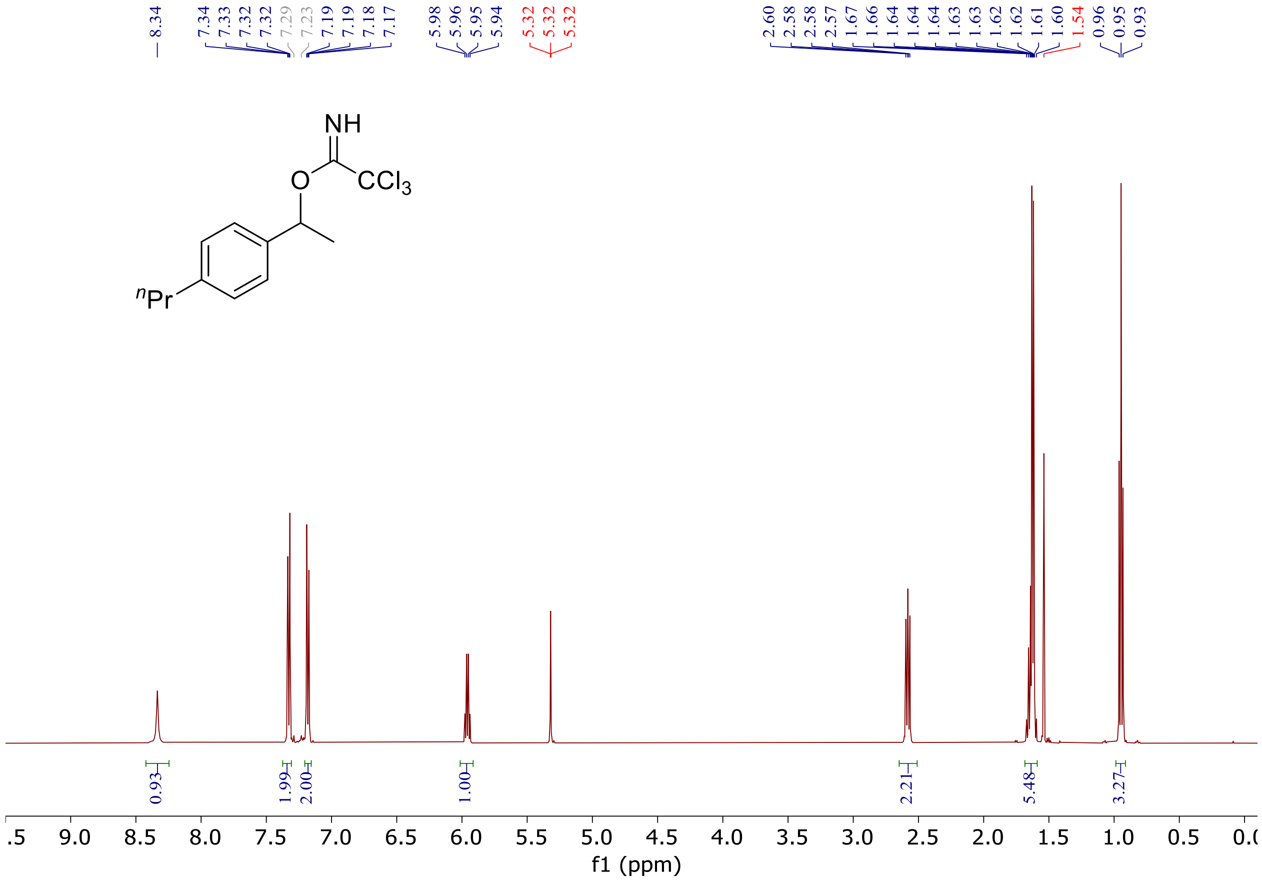
8.34
7.34
7.33
7.32
7.32
7.29
7.23
7.19
7.19
7.18
7.17
5.98
5.96
5.95
5.94
5.32
5.32
5.32
2.60
2.58
2.58
2.57
1.67
1.66
1.64
1.64
1.64
1.63
1.63
1.62
1.62
1.61
1.60
1.54
0.96
0.95
0.93
NH
O
CCl_3
^{n}Pr
0.93
1.99
2.00
1.00
2.21
5.48
3.27
.5
9.0
8.5
8.0
7.5
7.0
6.5
6.0
5.5
5.0
4.5
4.0
3.5
3.0
2.5
2.0
1.5
1.0
0.5
0.(
f1 (ppm)

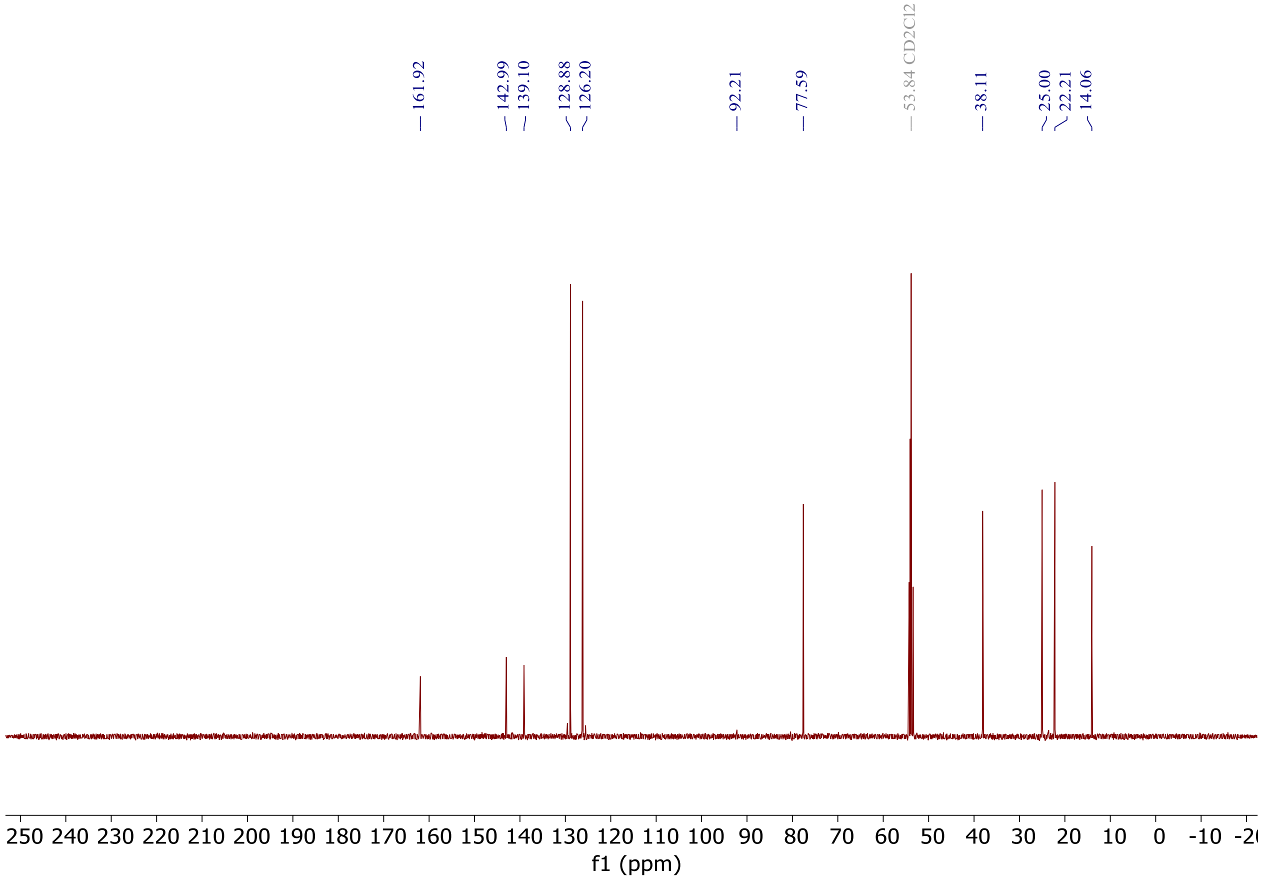
161.92
142.99
139.10
128.88
126.20
92.21
77.59
53.84 CD2Cl2
38.11
25.00
22.21
14.06
250
240
230
220
210
200
190
180
170
160
150
140
130
120
110
100
90
80
70
60
50
40
30
20
10
0
-10
-2(
f1 (ppm)

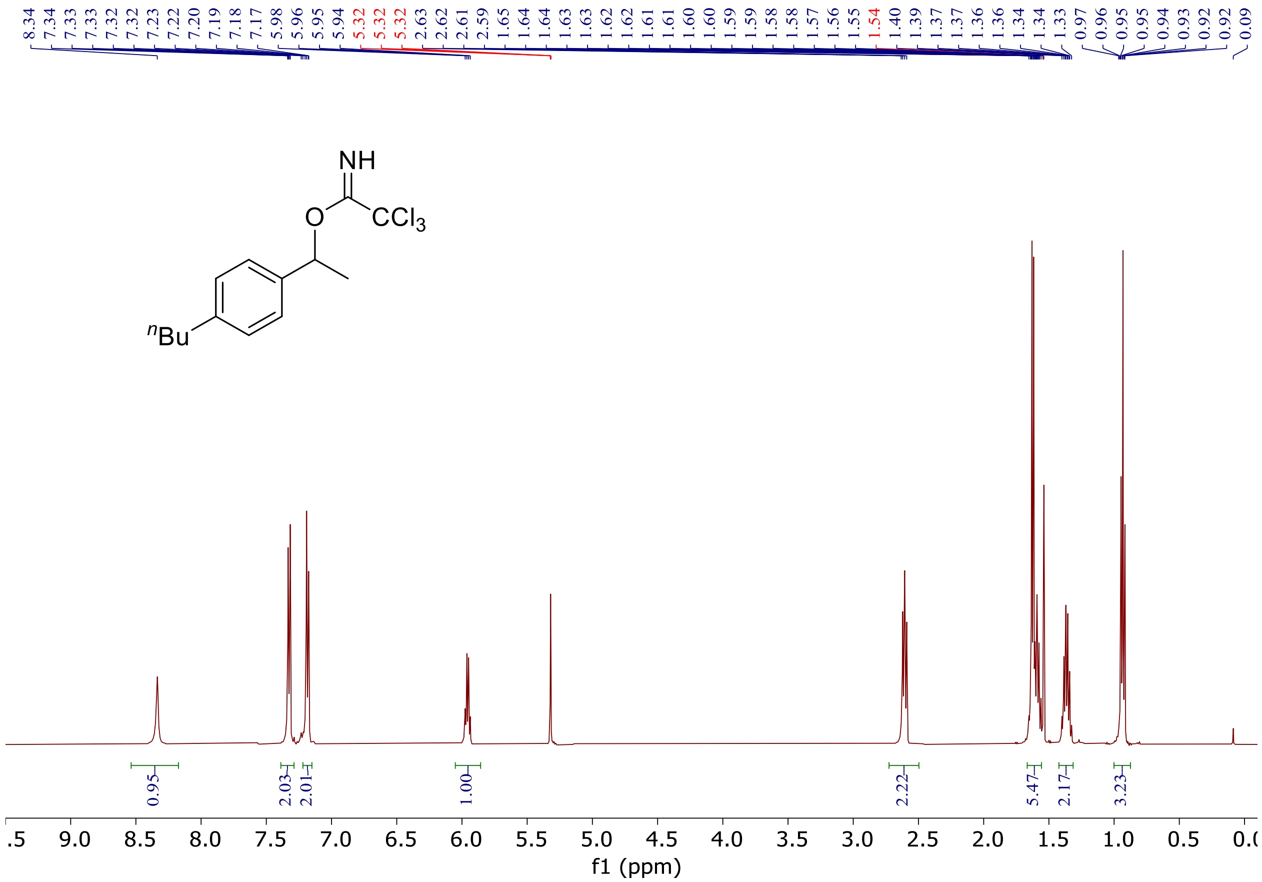
8.34 7.34 7.33 7.33 7.32 7.32 7.23 7.22 7.20 7.19 7.18 7.17 5.98 5.96 5.95 5.94 5.32 5.32 5.32 2.63 2.62 2.61 2.59 1.65 1.64 1.64 1.63 1.63 1.62 1.62 1.61 1.61 1.60 1.60 1.59 1.59 1.58 1.58 1.57 1.56 1.55 1.54 1.40 1.39 1.37 1.37 1.36 1.36 1.34 1.34 1.33 0.97 0.96 0.95 0.95 0.94 0.93 0.92 0.92 0.09
NH
O
CCl3
nBu
0.95
2.03
2.01
1.00
2.22
5.47
2.17
3.23
.5 9.0 8.5 8.0 7.5 7.0 6.5 6.0 5.5 5.0 4.5 4.0 3.5 3.0 2.5 2.0 1.5 1.0 0.5 0.0
f1 (ppm)

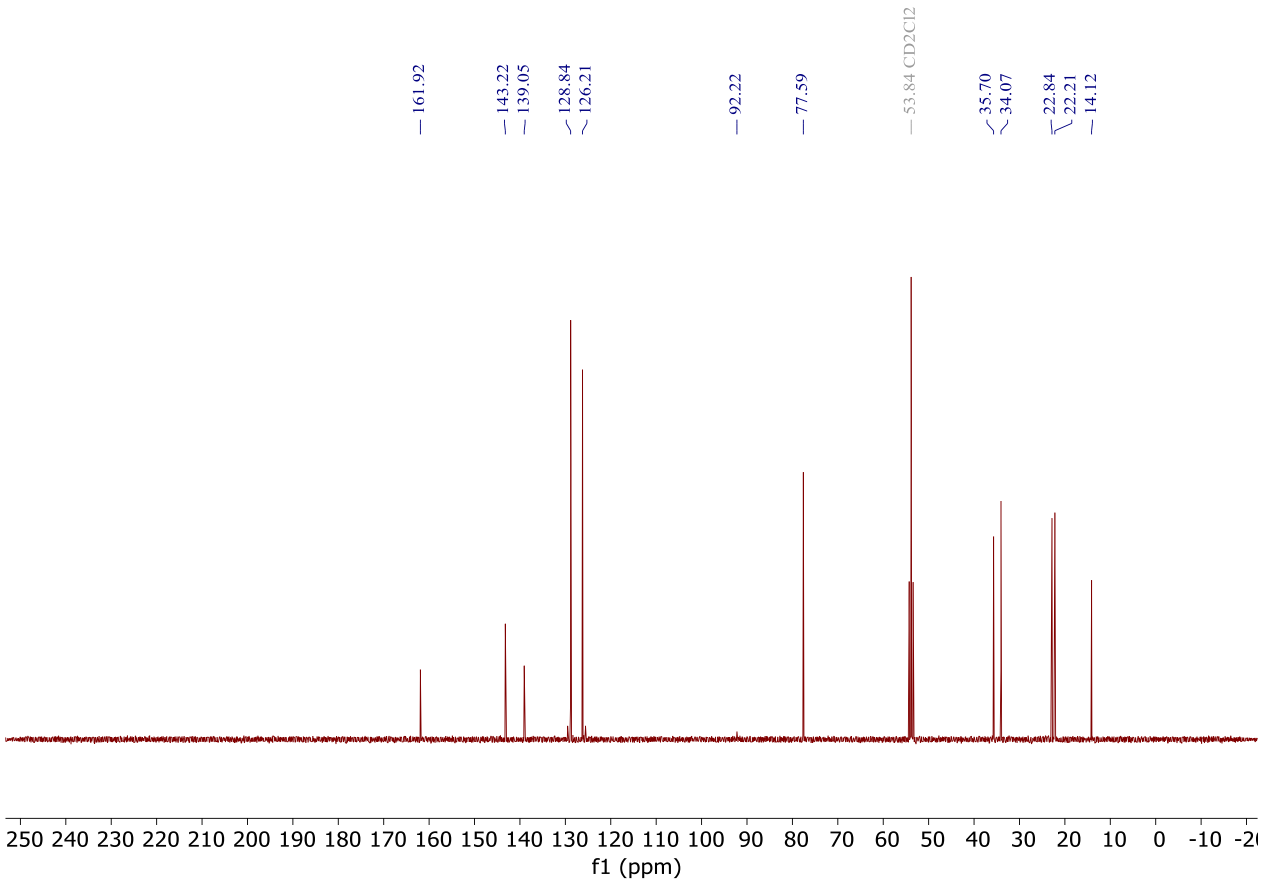
161.92
143.22
139.05
128.84
126.21
92.22
77.59
53.84 CD2Cl2
35.70
34.07
22.84
22.21
14.12
250 240 230 220 210 200 190 180 170 160 150 140 130 120 110 100 90 80 70 60 50 40 30 20 10 0 -10 -20
f1 (ppm)

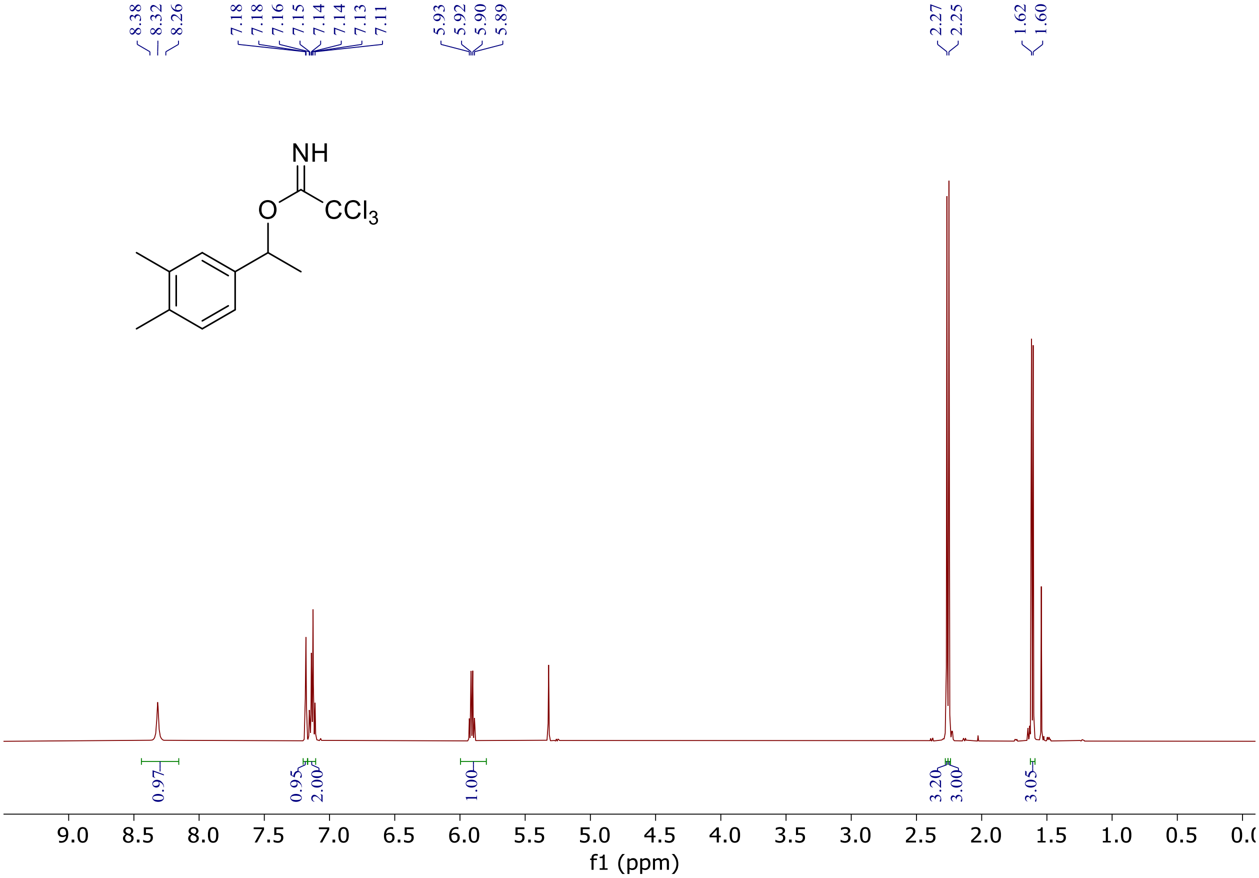
8.38
8.32
8.26
7.18
7.18
7.16
7.15
7.14
7.14
7.13
7.11
5.93
5.92
5.90
5.89
2.27
2.25
1.62
1.60
NH
O
CCl3
0.97
0.95
2.00
1.00
3.20
3.00
3.05
9.0
8.5
8.0
7.5
7.0
6.5
6.0
5.5
5.0
4.5
4.0
3.5
3.0
2.5
2.0
1.5
1.0
0.5
f1 (ppm)

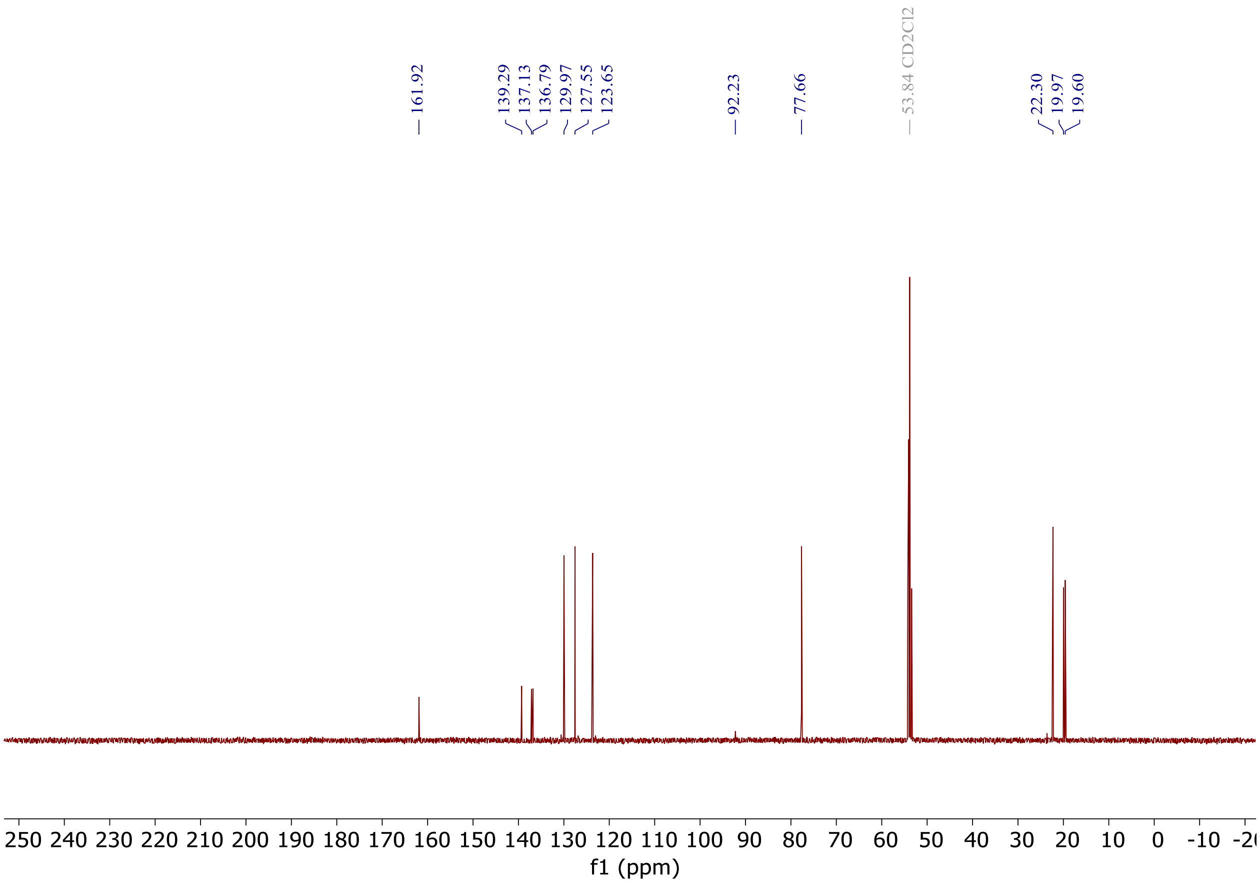
161.92
139.29
137.13
136.79
129.97
127.55
123.65
92.23
77.66
53.84 CD2Cl2
22.30
19.97
19.60
250
240
230
220
210
200
190
180
170
160
150
140
130
120
110
100
90
80
70
60
50
40
30
20
10
0
-10
f1 (ppm)

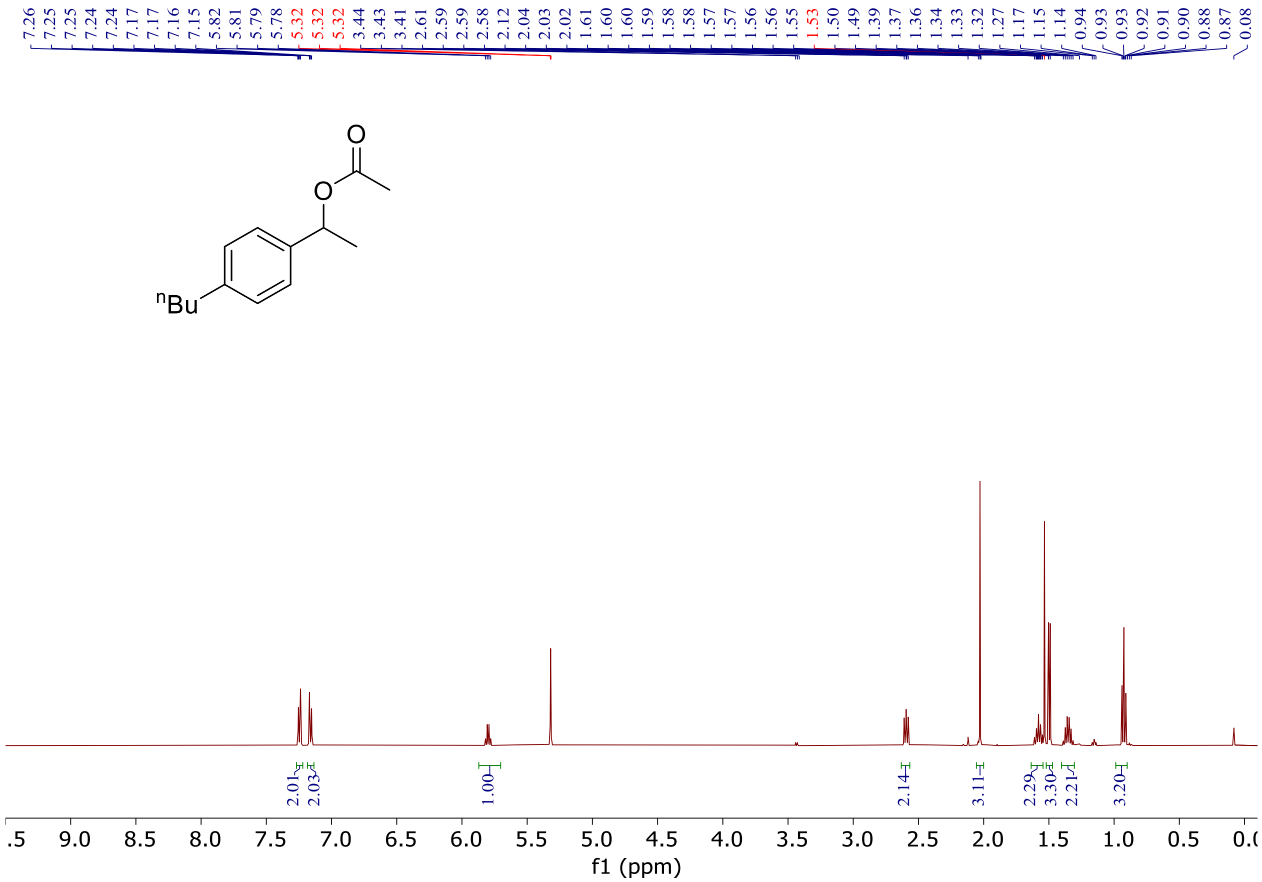
7.26 7.25 7.25 7.24 7.24 7.17 7.17 7.16 7.15 5.82 5.81 5.79 5.78 5.32 5.32 5.32 3.44 3.43 3.41 2.61 2.59 2.59 2.58 2.12 2.04 2.03 2.02 1.61 1.60 1.60 1.59 1.58 1.58 1.57 1.57 1.56 1.56 1.55 1.53 1.50 1.49 1.39 1.37 1.36 1.34 1.33 1.32 1.27 1.17 1.15 1.14 0.94 0.93 0.93 0.92 0.91 0.90 0.88 0.87 0.08
O
O
^{n}Bu
2.01
2.03
1.00
2.14
3.11
2.29
3.30
2.21
3.20
.5 9.0 8.5 8.0 7.5 7.0 6.5 6.0 5.5 5.0 4.5 4.0 3.5 3.0 2.5 2.0 1.5 1.0 0.5 0.(
f1 (ppm)

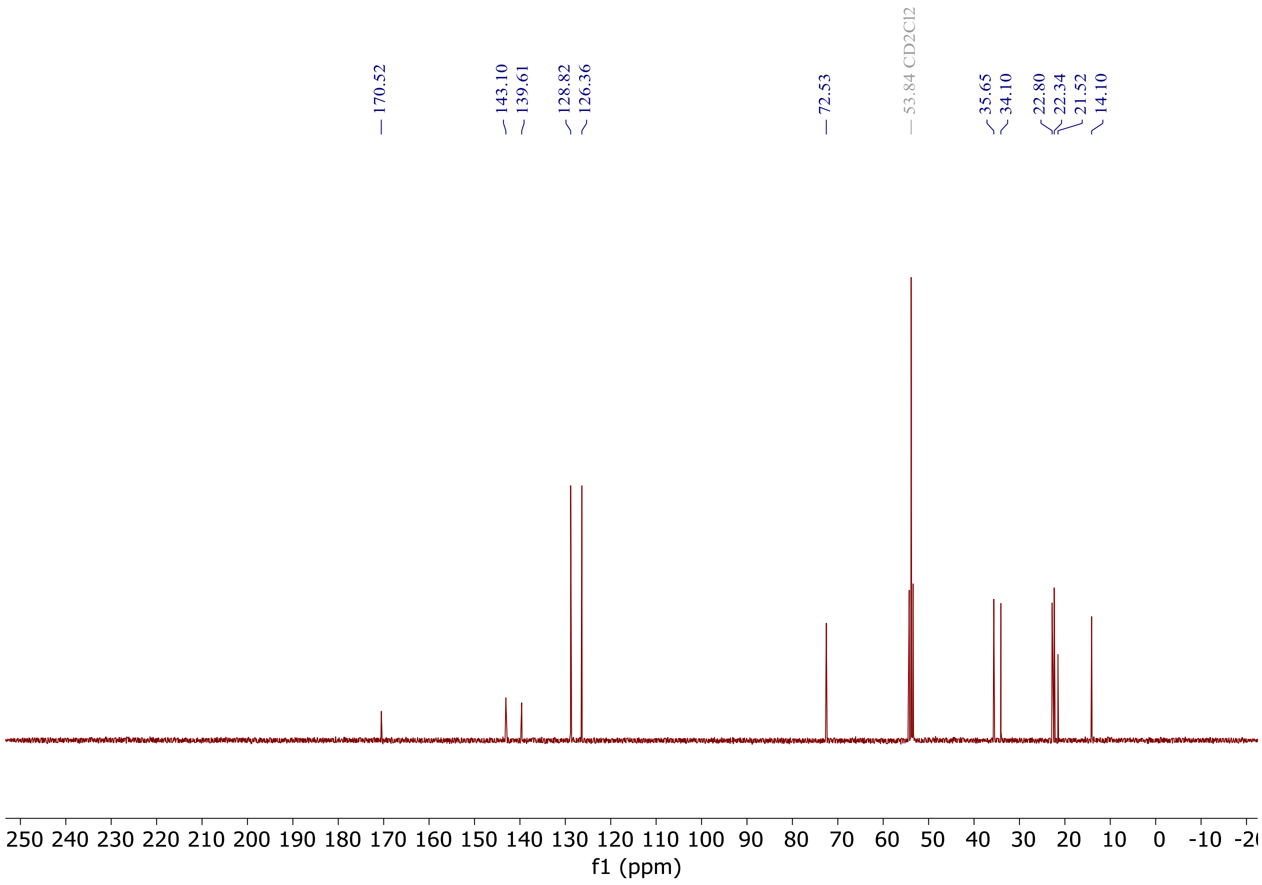
170.52
143.10
139.61
128.82
126.36
72.53
53.84 CD2Cl2
35.65
34.10
22.80
22.34
21.52
14.10
250 240 230 220 210 200 190 180 170 160 150 140 130 120 110 100 90 80 70 60 50 40 30 20 10 0 -10 -2(
f1 (ppm)

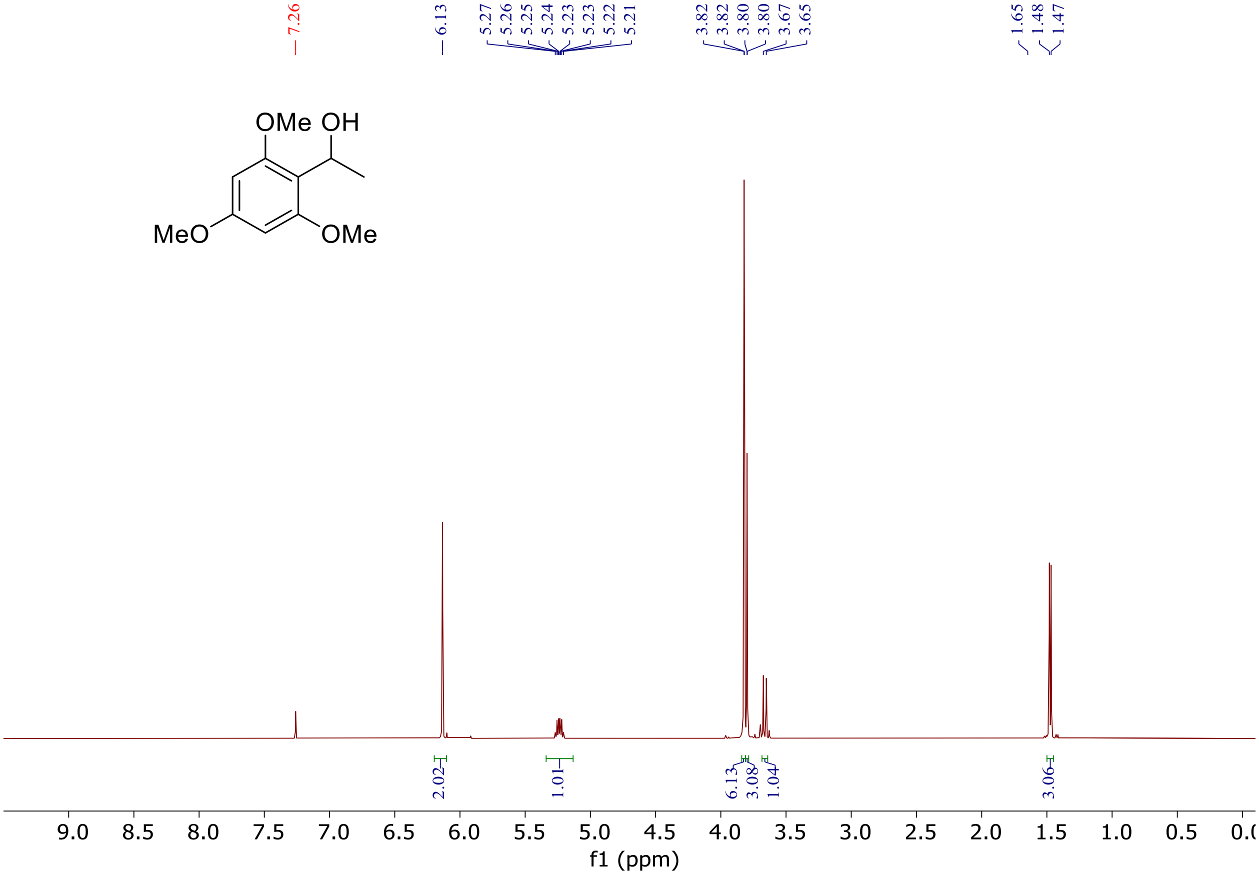
7.26
6.13
5.27
5.26
5.25
5.24
5.23
5.23
5.22
5.21
3.82
3.82
3.80
3.80
3.67
3.65
1.65
1.48
1.47
OMe OH
MeO
OMe
2.02
1.01
6.13
3.08
1.04
3.06
9.0
8.5
8.0
7.5
7.0
6.5
6.0
5.5
5.0
4.5
4.0
3.5
3.0
2.5
2.0
1.5
1.0
0.5
f1 (ppm)

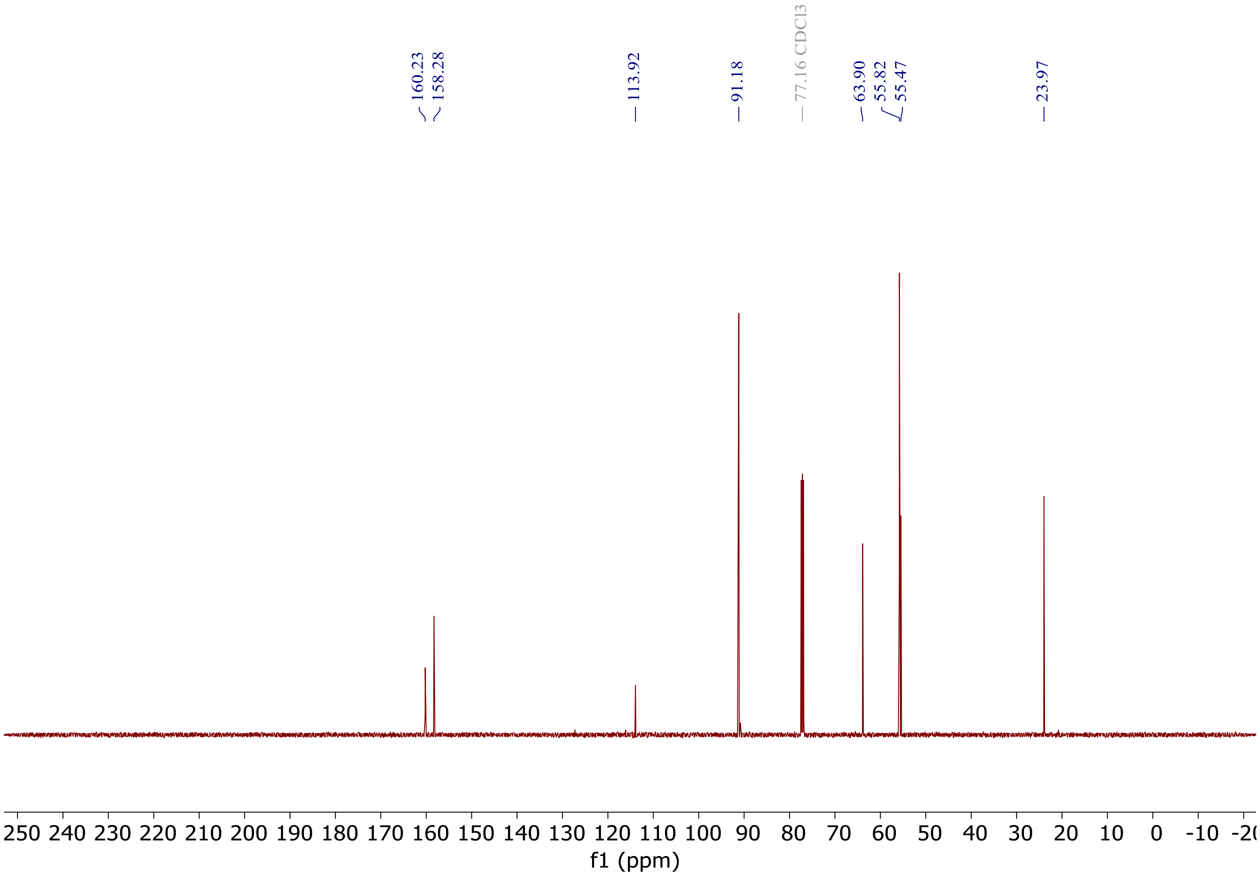
160.23
158.28
113.92
91.18
77.16 CDCl3
63.90
55.82
55.47
23.97
250 240 230 220 210 200 190 180 170 160 150 140 130 120 110 100 90 80 70 60 50 40 30 20 10 0 -10
f1 (ppm)

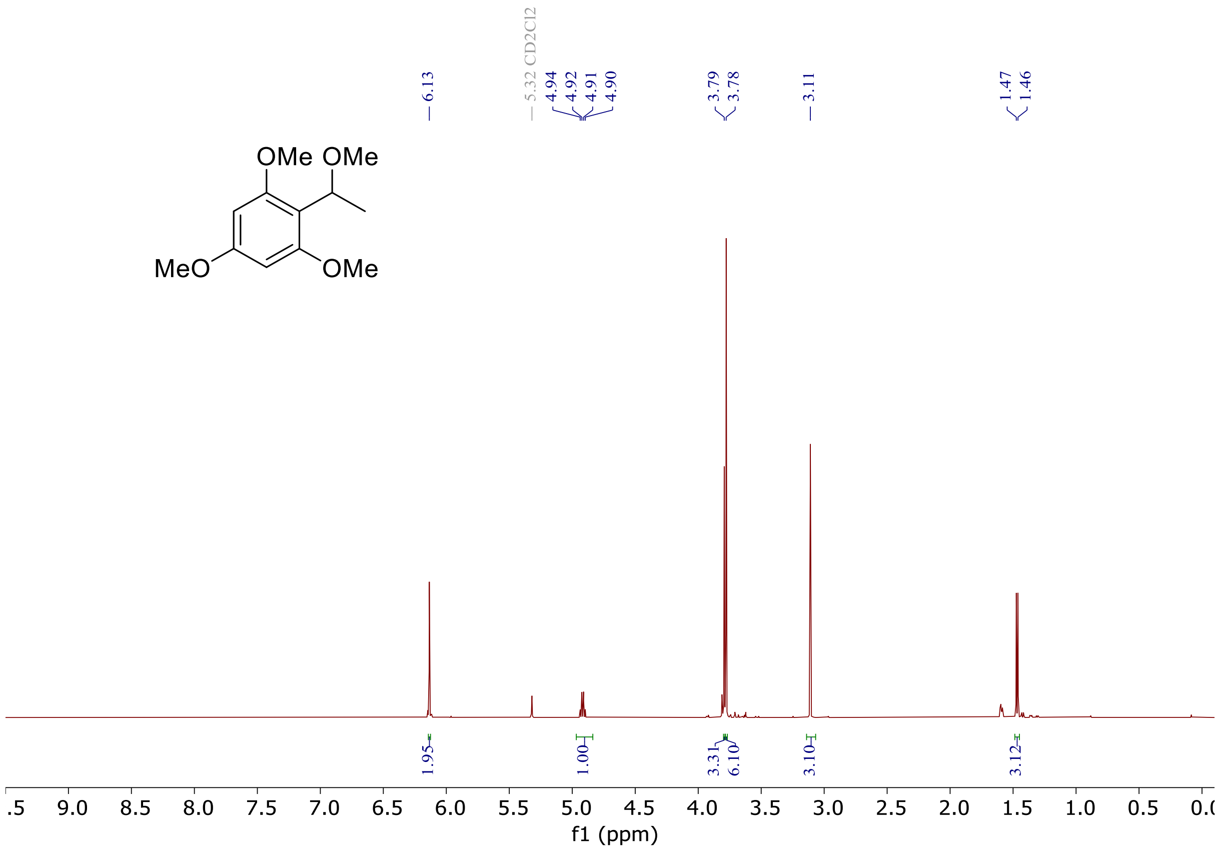
OMe
OMe
MeO
OMe
6.13
5.32 CD2Cl2
4.94
4.92
4.91
4.90
3.79
3.78
3.11
1.47
1.46
1.95
1.00
3.31
6.10
3.10
3.12
.5 9.0 8.5 8.0 7.5 7.0 6.5 6.0 5.5 5.0 4.5 4.0 3.5 3.0 2.5 2.0 1.5 1.0 0.5 0.(
f1 (ppm)

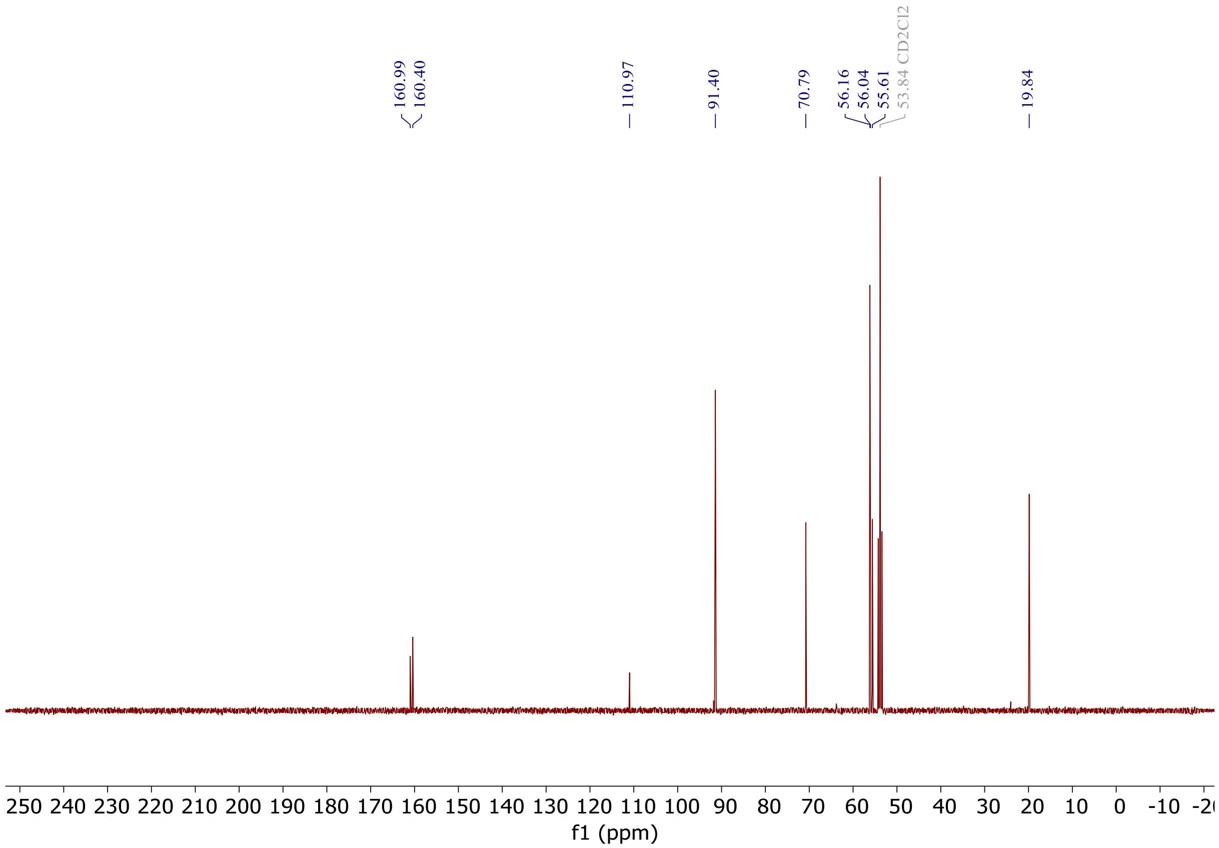
160.99
160.40
110.97
91.40
70.79
56.16
56.04
55.61
53.84 CD2Cl2
19.84
250 240 230 220 210 200 190 180 170 160 150 140 130 120 110 100 90 80 70 60 50 40 30 20 10 0 -10 -2(
f1 (ppm)

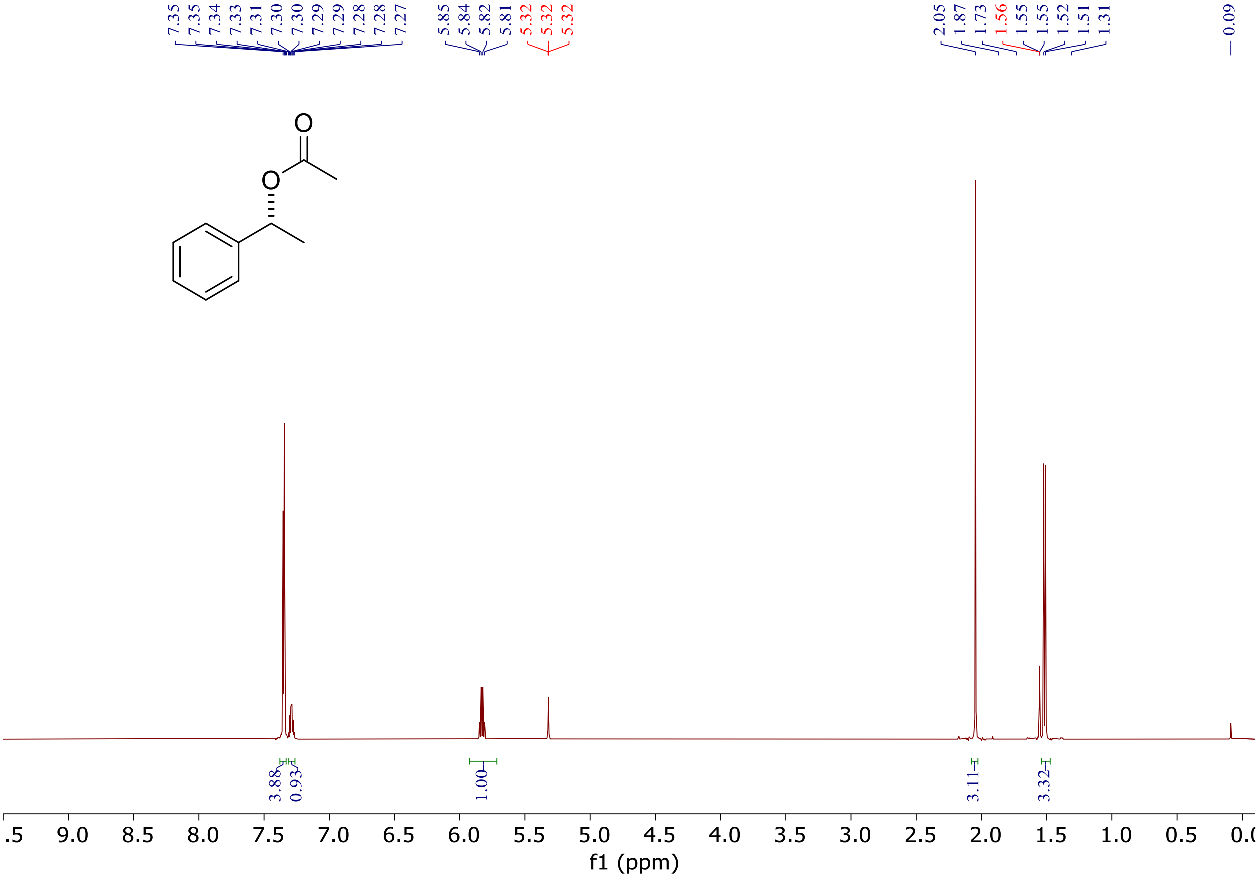
7.35
7.35
7.34
7.33
7.31
7.30
7.30
7.29
7.29
7.28
7.28
7.27
5.85
5.84
5.82
5.81
5.32
5.32
5.32
2.05
1.87
1.73
1.56
1.55
1.55
1.52
1.51
1.31
0.09
O
O
3.88
0.93
1.00
3.11
3.32
.5
9.0
8.5
8.0
7.5
7.0
6.5
6.0
5.5
5.0
4.5
4.0
3.5
3.0
2.5
2.0
1.5
1.0
0.5
0.
f1 (ppm)

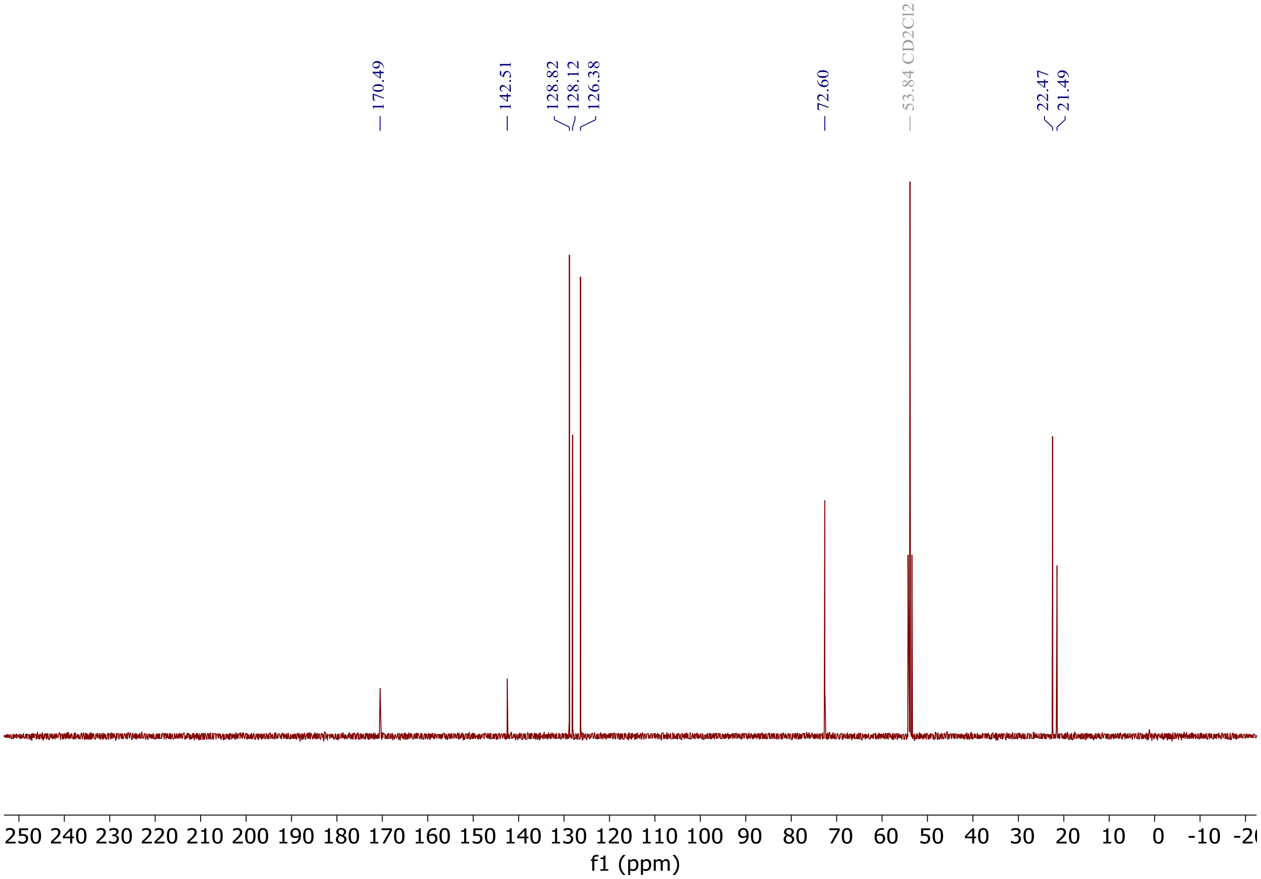
170.49
142.51
128.82
128.12
126.38
72.60
53.84 CD2Cl2
22.47
21.49
250
240
230
220
210
200
190
180
170
160
150
140
130
120
110
100
90
80
70
60
50
40
30
20
10
0
-10
-2
f1 (ppm)

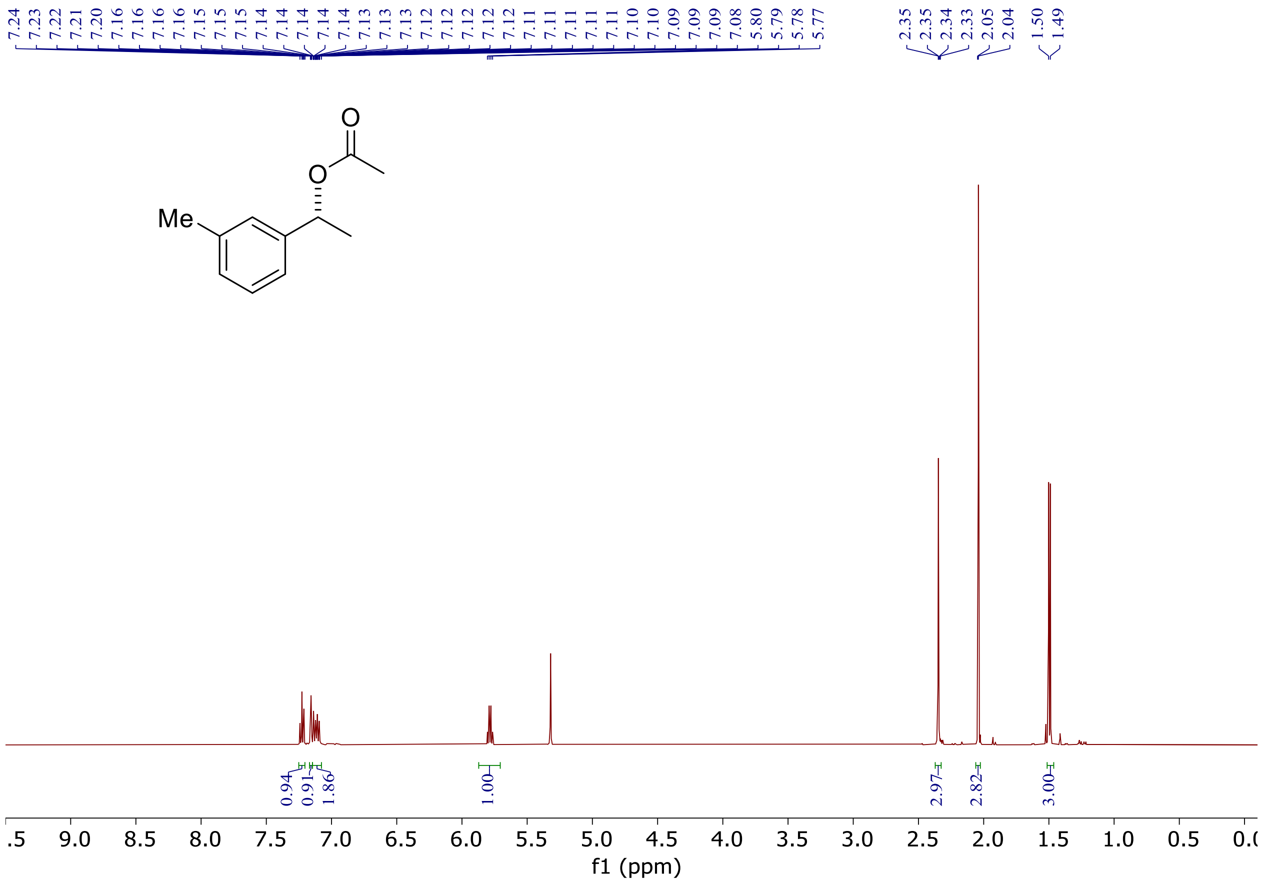
7.24
7.23
7.22
7.21
7.20
7.16
7.16
7.16
7.15
7.15
7.14
7.14
7.14
7.14
7.13
7.13
7.12
7.12
7.12
7.12
7.11
7.11
7.11
7.11
7.11
7.10
7.10
7.09
7.09
7.09
7.08
5.80
5.79
5.78
5.77
2.35
2.35
2.34
2.33
2.05
2.04
1.50
1.49
O
O
Me
0.94
0.91
1.86
1.00
2.97
2.82
3.00
.5
9.0
8.5
8.0
7.5
7.0
6.5
6.0
5.5
5.0
4.5
4.0
3.5
3.0
2.5
2.0
1.5
1.0
0.5
0.0
f1 (ppm)

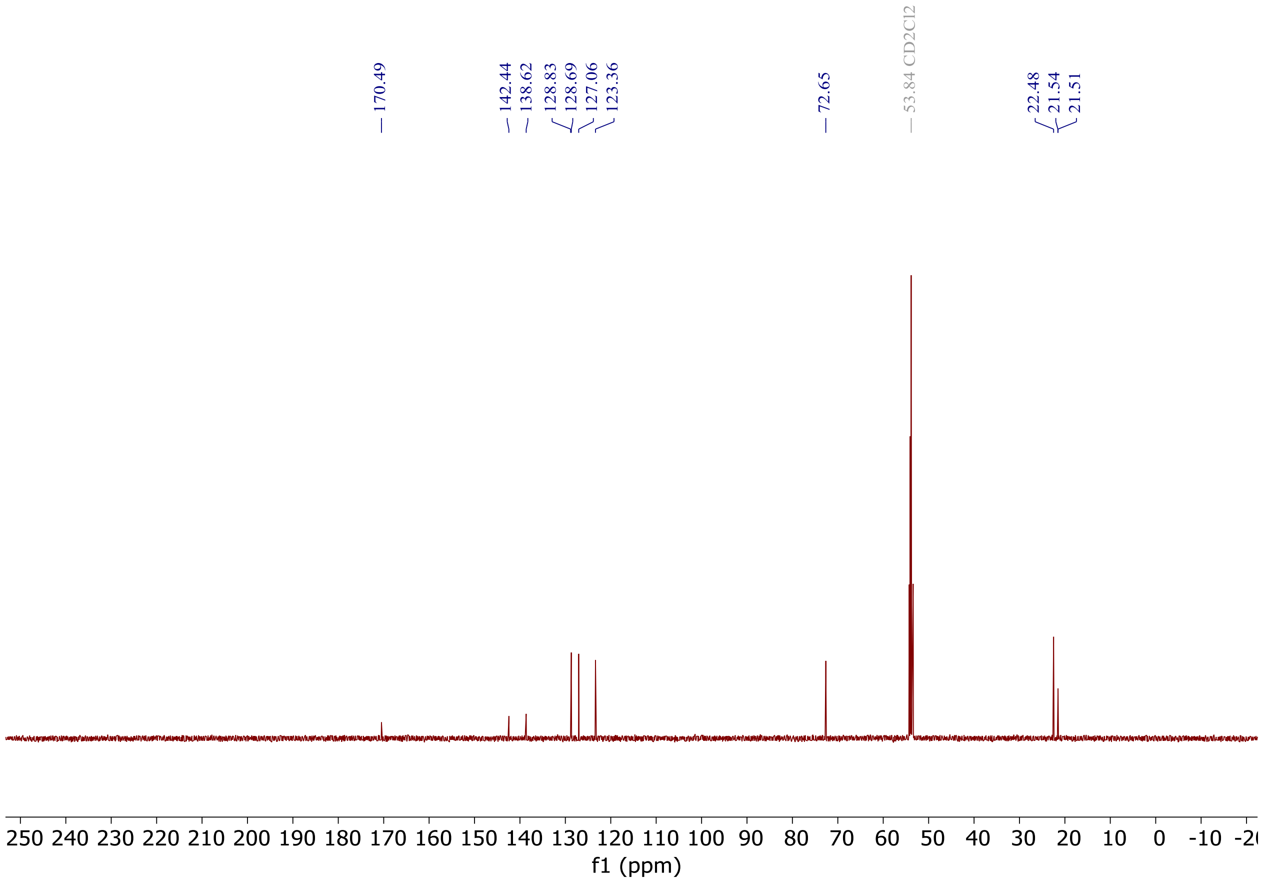
170.49
142.44
138.62
128.83
128.69
127.06
123.36
72.65
53.84 CD2Cl2
22.48
21.54
21.51
250
240
230
220
210
200
190
180
170
160
150
140
130
120
110
100
90
80
70
60
50
40
30
20
10
0
-10
-20
f1 (ppm)

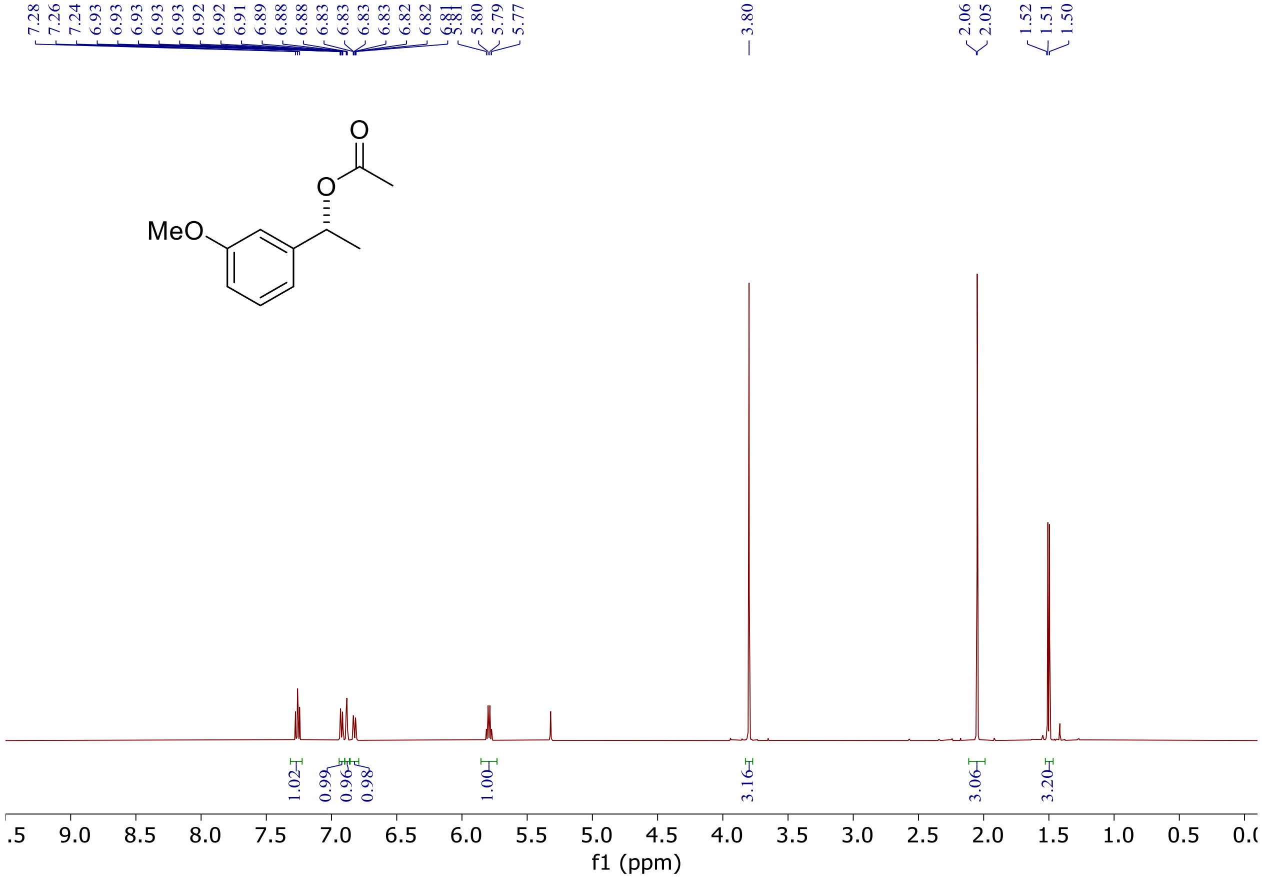
7.28
7.26
7.24
6.93
6.93
6.93
6.93
6.93
6.92
6.92
6.91
6.89
6.88
6.88
6.83
6.83
6.83
6.83
6.82
6.82
6.81
5.81
5.80
5.79
5.77
3.80
2.06
2.05
1.52
1.51
1.50
O
O
MeO
1.02
0.99
0.96
0.98
1.00
3.16
3.06
3.20
.5
9.0
8.5
8.0
7.5
7.0
6.5
6.0
5.5
5.0
4.5
4.0
3.5
3.0
2.5
2.0
1.5
1.0
0.5
0.0
f1 (ppm)

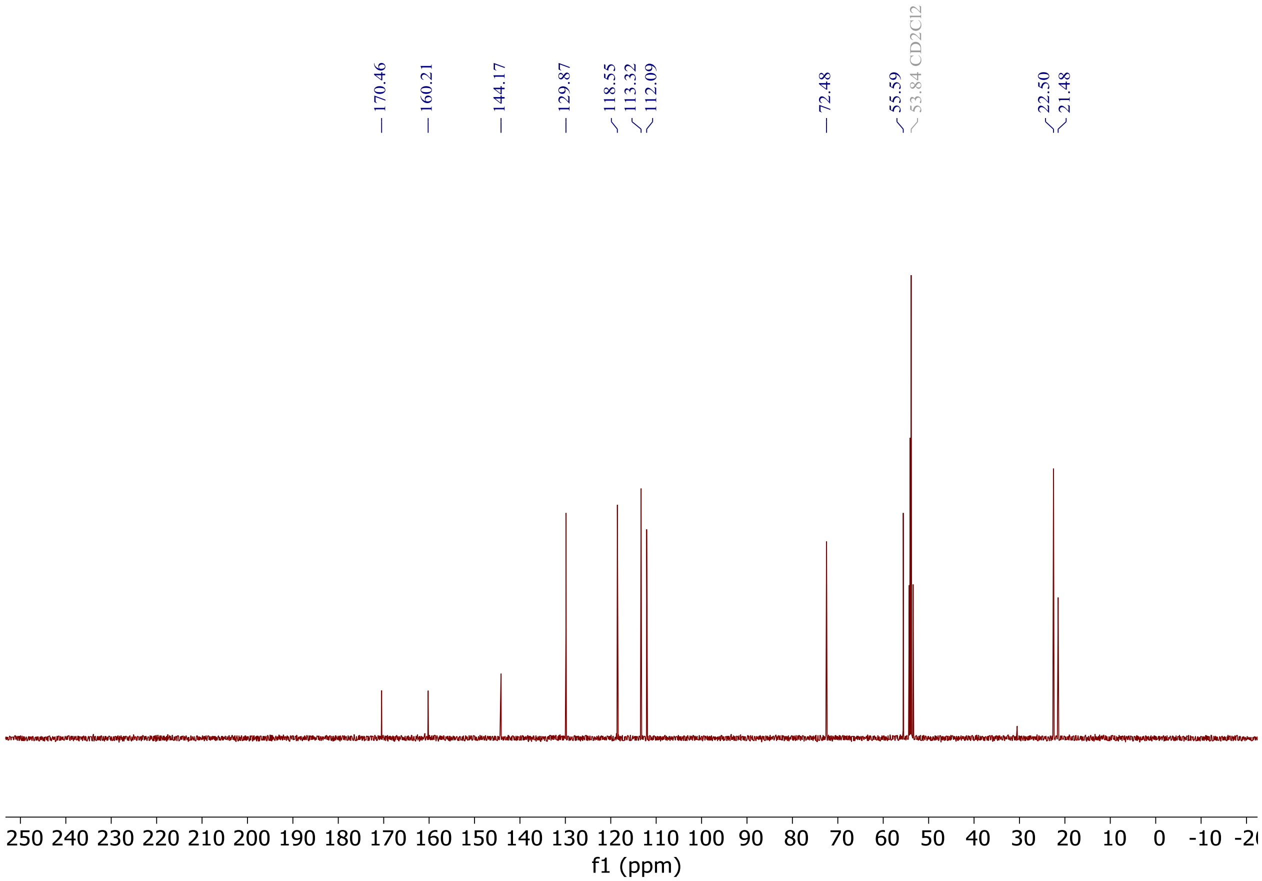
170.46
160.21
144.17
129.87
118.55
113.32
112.09
72.48
55.59
53.84 CD2Cl2
22.50
21.48
250
240
230
220
210
200
190
180
170
160
150
140
130
120
110
100
90
80
70
60
50
40
30
20
10
0
-10
-20
f1 (ppm)

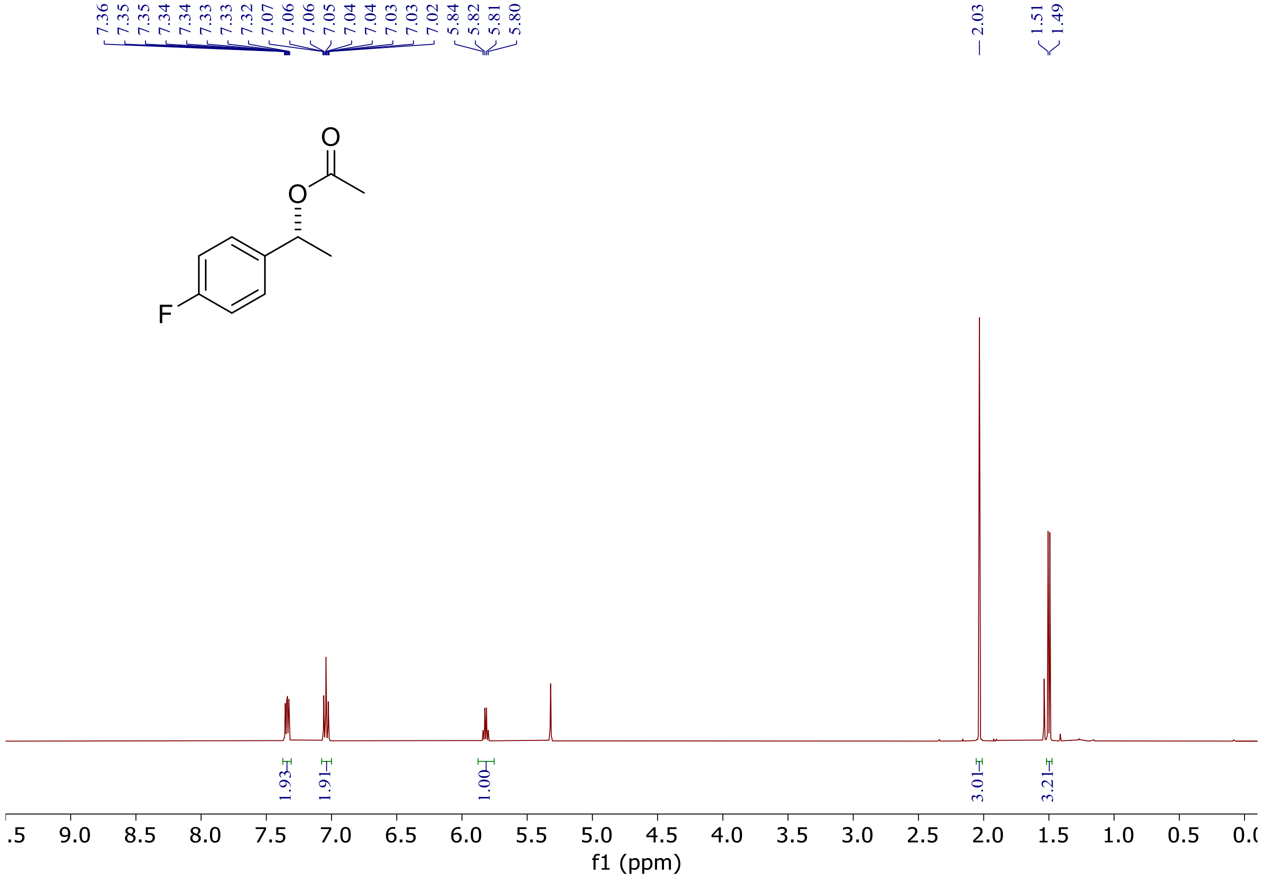
7.36
7.35
7.35
7.34
7.34
7.33
7.33
7.32
7.07
7.06
7.06
7.05
7.04
7.04
7.03
7.03
7.02
5.84
5.82
5.81
5.80
2.03
1.51
1.49
O
O
F
1.93
1.91
1.00
3.01
3.21
.5 9.0 8.5 8.0 7.5 7.0 6.5 6.0 5.5 5.0 4.5 4.0 3.5 3.0 2.5 2.0 1.5 1.0 0.5 0.
f1 (ppm)

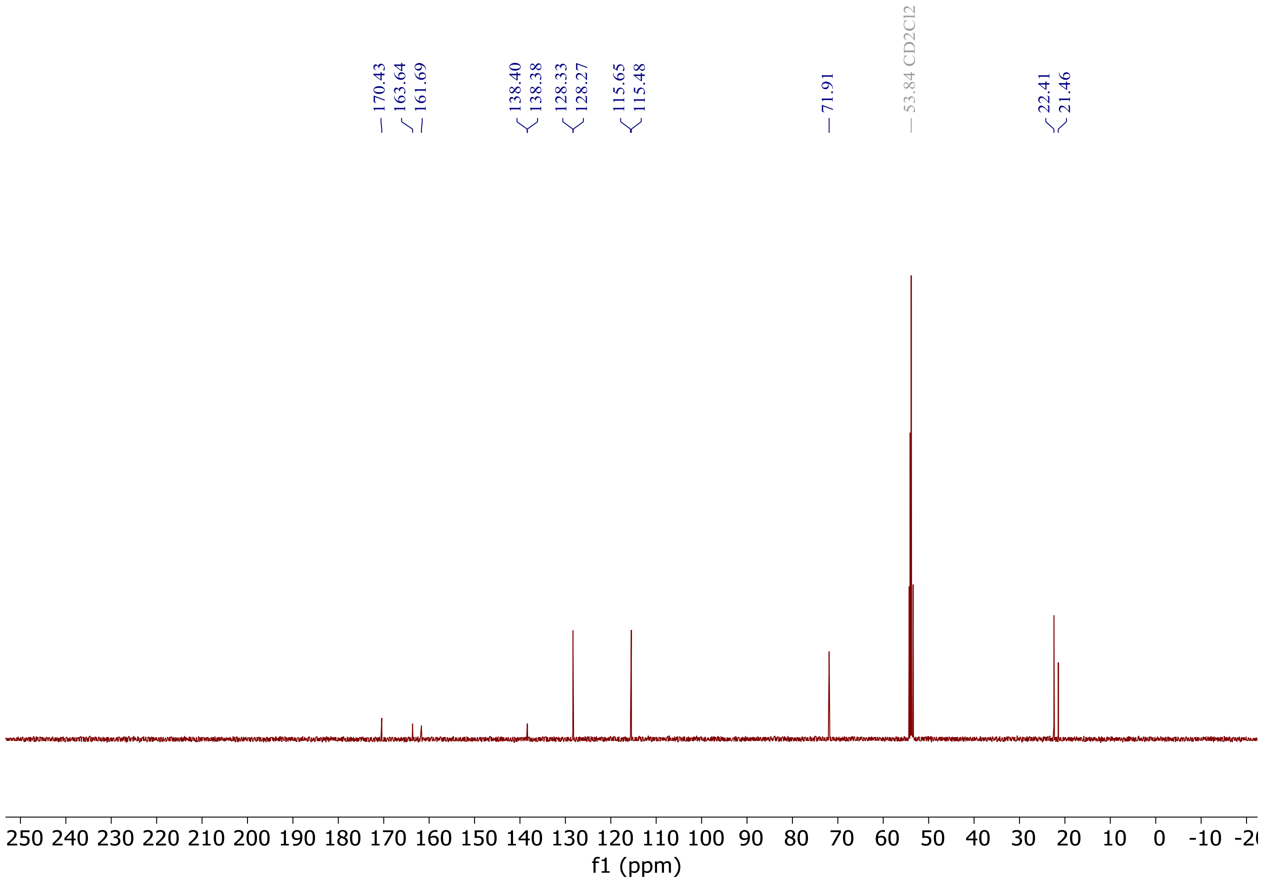
170.43
163.64
161.69
138.40
138.38
128.33
128.27
115.65
115.48
71.91
53.84 CD2Cl2
22.41
21.46
250 240 230 220 210 200 190 180 170 160 150 140 130 120 110 100 90 80 70 60 50 40 30 20 10 0 -10 -2
f1 (ppm)

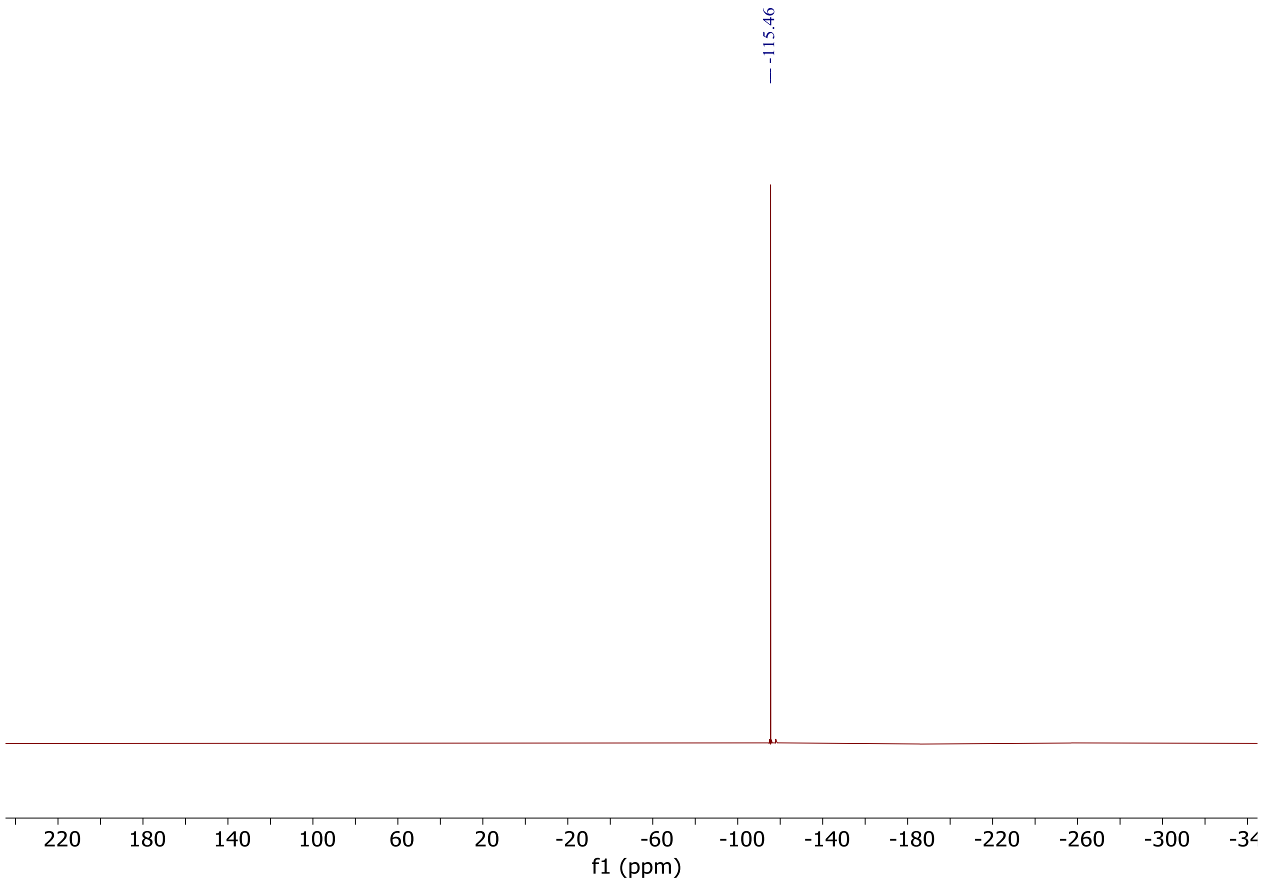
-115.46
220
180
140
100
60
20
-20
-60
-100
-140
-180
-220
-260
-300
f1 (ppm)

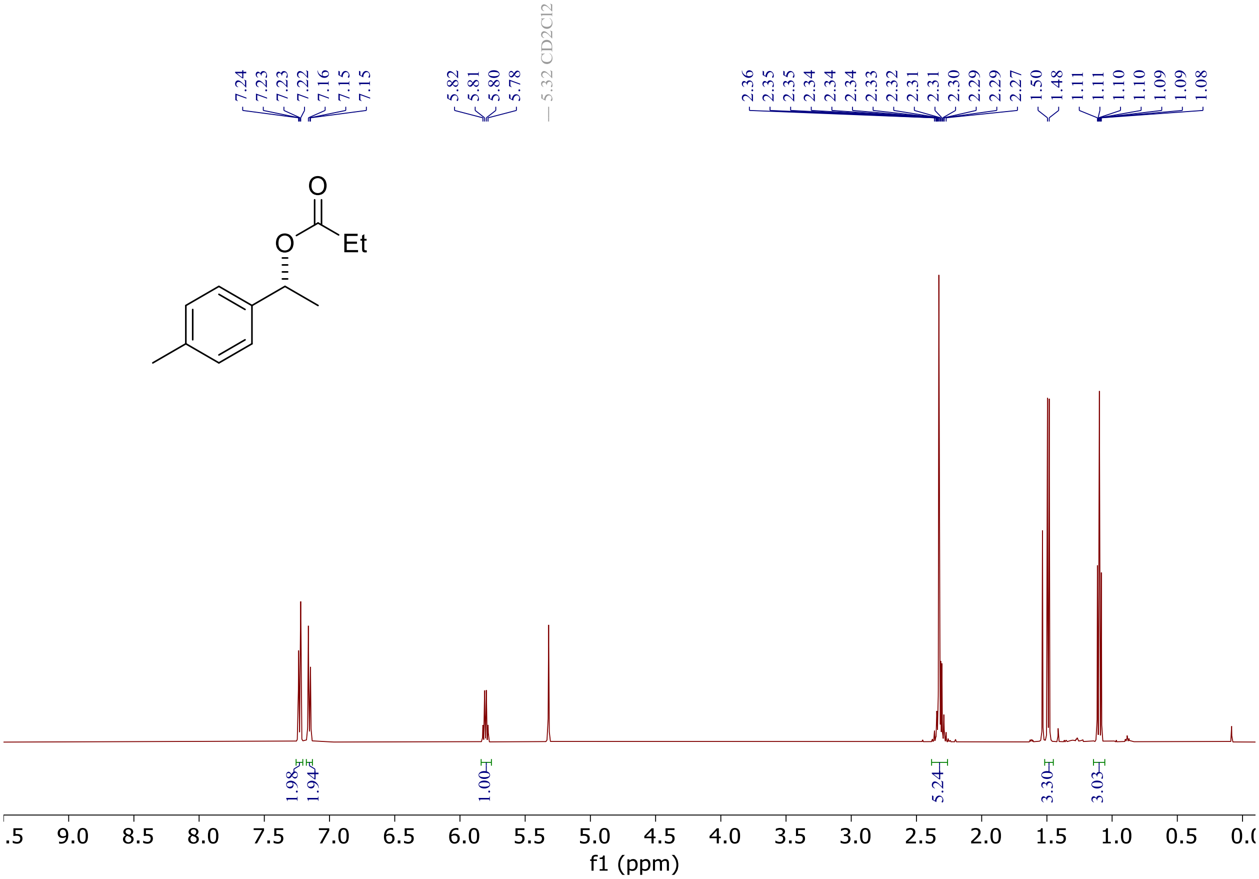
7.24
7.23
7.23
7.22
7.16
7.15
7.15
5.82
5.81
5.80
5.78
5.32 CD2Cl2
2.36
2.35
2.35
2.34
2.34
2.34
2.33
2.32
2.31
2.31
2.30
2.29
2.29
2.27
1.50
1.48
1.11
1.11
1.10
1.10
1.09
1.09
1.08
O
O
Et
1.98
1.94
1.00
5.24
3.30
3.03
.5
9.0
8.5
8.0
7.5
7.0
6.5
6.0
5.5
5.0
4.5
4.0
3.5
3.0
2.5
2.0
1.5
1.0
0.5
0.(
f1 (ppm)

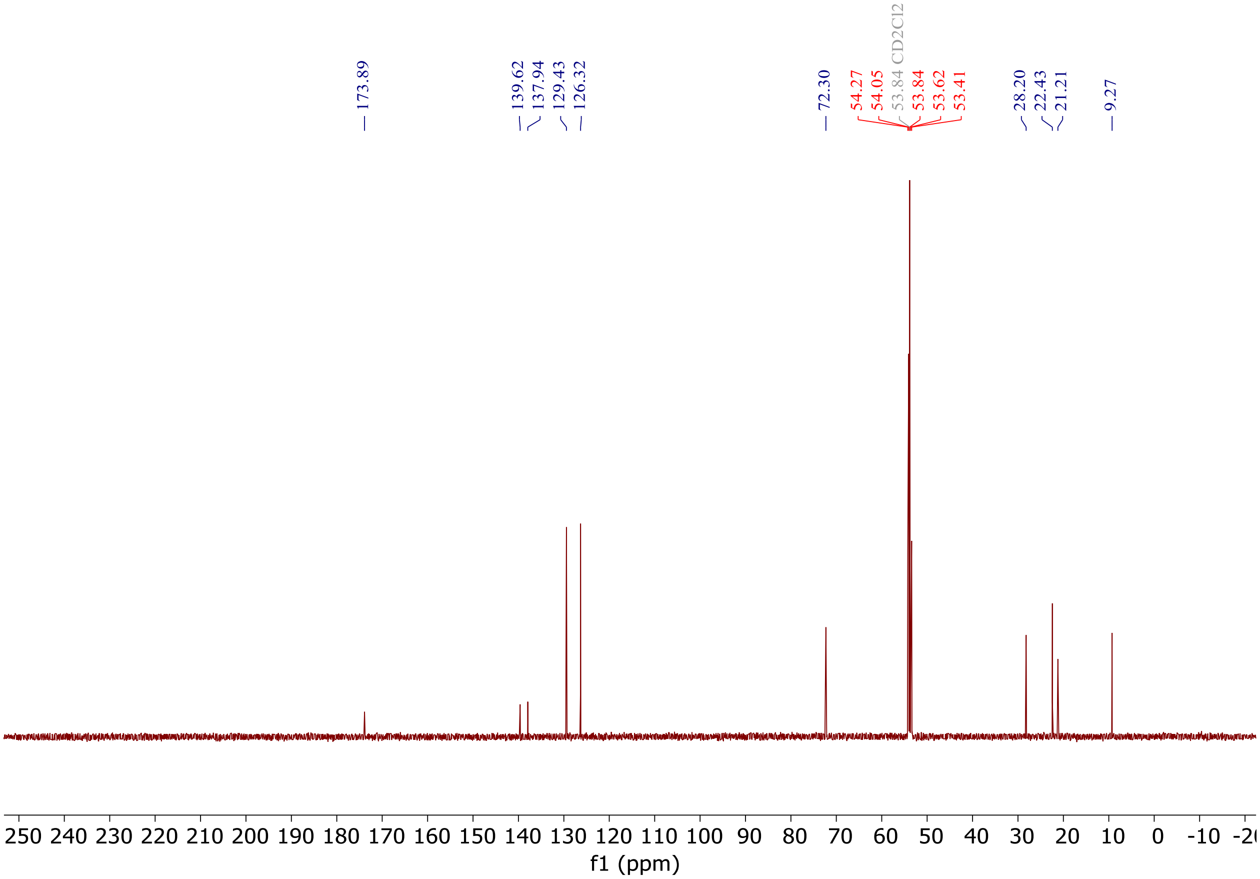
173.89
139.62
137.94
129.43
126.32
72.30
54.27
54.05
53.84 CD2Cl2
53.84
53.62
53.41
28.20
22.43
21.21
9.27
250
240
230
220
210
200
190
180
170
160
150
140
130
120
110
100
90
80
70
60
50
40
30
20
10
0
-10
-2(
f1 (ppm)

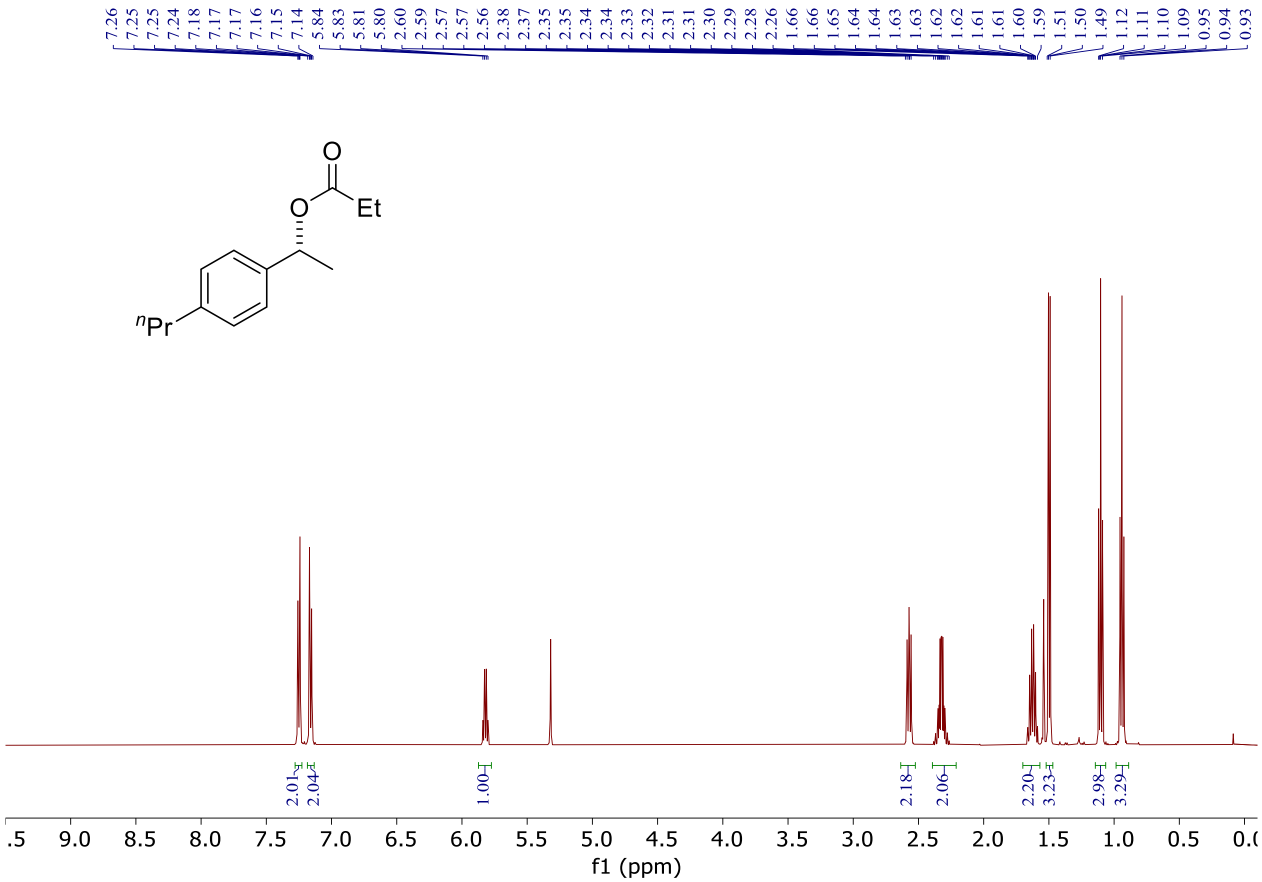
7.26
7.25
7.25
7.24
7.18
7.17
7.17
7.16
7.15
7.14
5.84
5.83
5.81
5.80
2.60
2.59
2.57
2.57
2.56
2.38
2.37
2.35
2.35
2.34
2.34
2.33
2.32
2.31
2.31
2.30
2.29
2.28
2.26
1.66
1.66
1.65
1.64
1.64
1.63
1.63
1.62
1.62
1.61
1.61
1.60
1.59
1.51
1.50
1.49
1.12
1.11
1.10
1.09
0.95
0.94
0.93
O
O
Et
^{n}Pr
2.01
2.04
1.00
2.18
2.06
2.20
3.23
2.98
3.29
.5
9.0
8.5
8.0
7.5
7.0
6.5
6.0
5.5
5.0
4.5
4.0
3.5
3.0
2.5
2.0
1.5
1.0
0.5
0.
f1 (ppm)

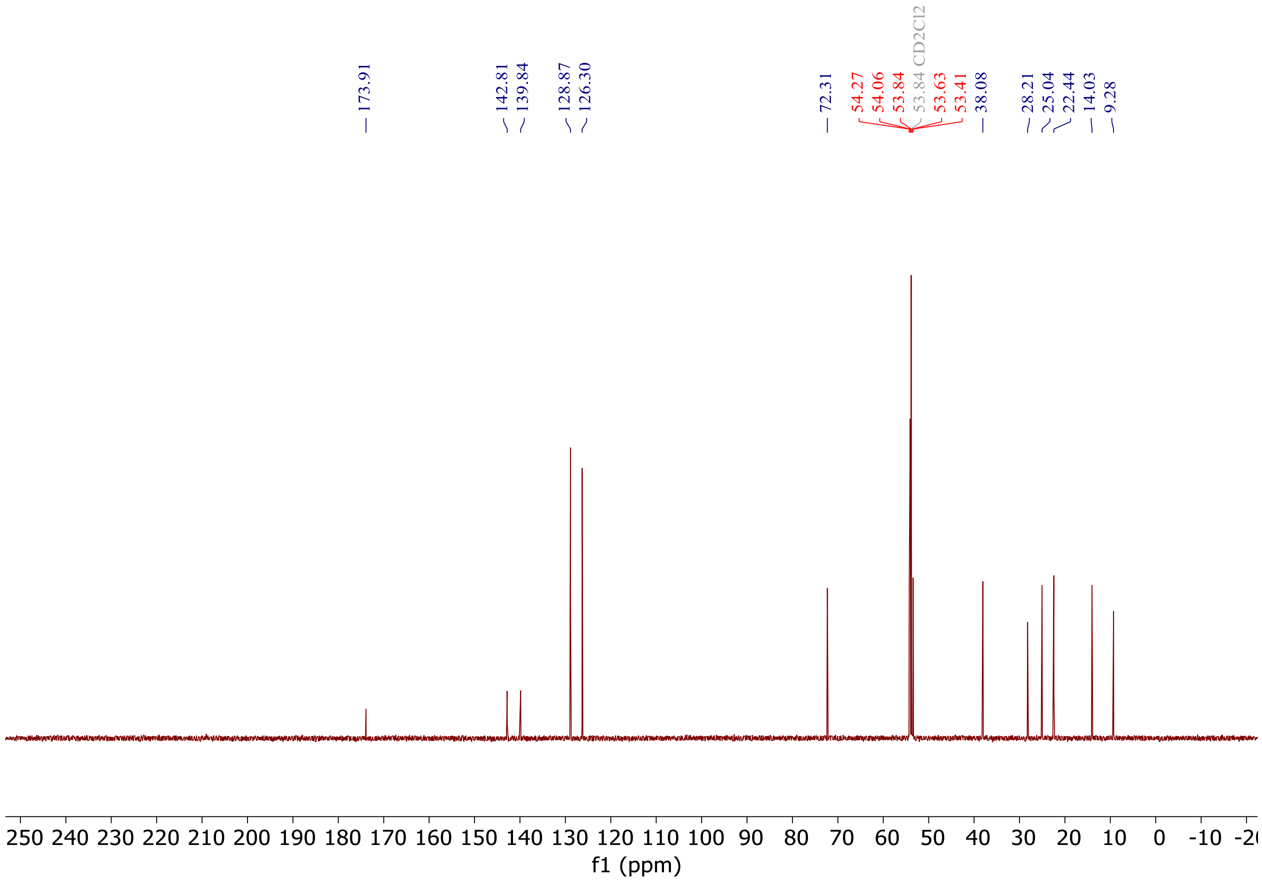
173.91
142.81
139.84
128.87
126.30
72.31
54.27
54.06
53.84
53.84 CD2Cl2
53.63
53.41
38.08
28.21
25.04
22.44
14.03
9.28
250
240
230
220
210
200
190
180
170
160
150
140
130
120
110
100
90
80
70
60
50
40
30
20
10
0
-10
-2
f1 (ppm)

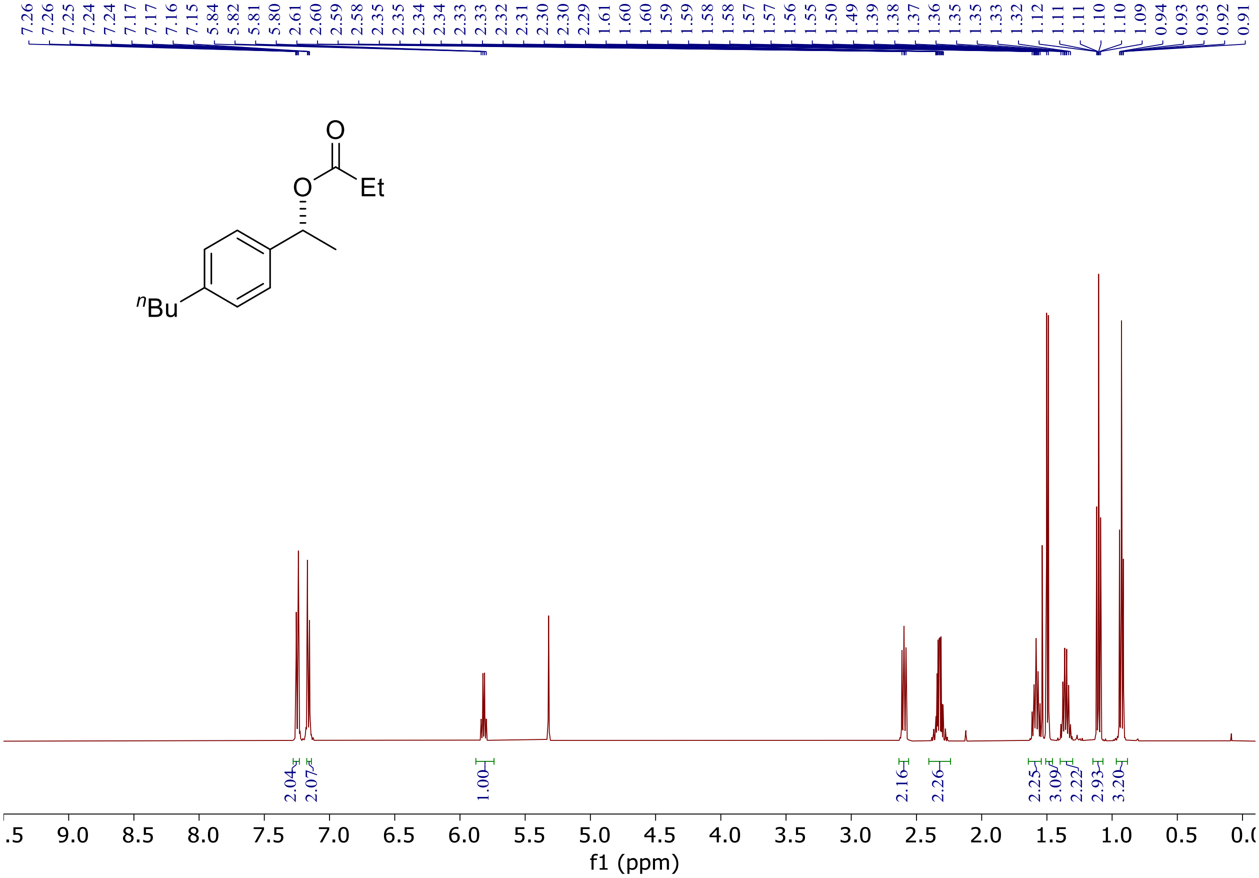
7.26
7.26
7.25
7.24
7.24
7.17
7.17
7.16
7.15
5.84
5.82
5.81
5.80
2.61
2.60
2.59
2.58
2.35
2.35
2.34
2.34
2.33
2.33
2.32
2.31
2.30
2.30
2.29
1.61
1.60
1.60
1.59
1.59
1.58
1.58
1.57
1.57
1.56
1.55
1.50
1.49
1.39
1.38
1.37
1.36
1.35
1.35
1.33
1.32
1.12
1.11
1.11
1.10
1.10
1.09
0.94
0.93
0.93
0.92
0.91
O
O
Et
nBu
2.04
2.07
1.00
2.16
2.26
2.25
3.09
2.22
2.93
3.20
.5 9.0 8.5 8.0 7.5 7.0 6.5 6.0 5.5 5.0 4.5 4.0 3.5 3.0 2.5 2.0 1.5 1.0 0.5 0.(
f1 (ppm)

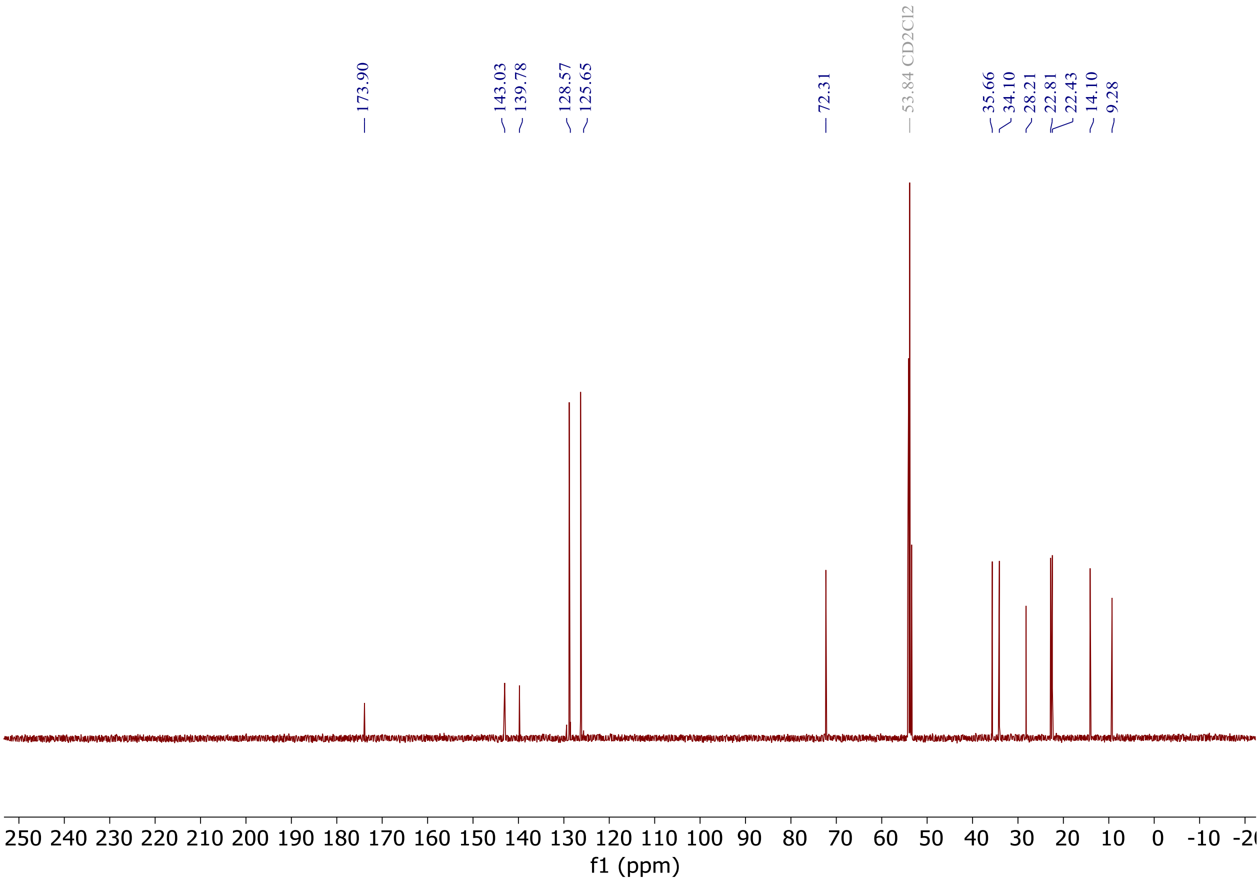
173.90
143.03
139.78
128.57
125.65
72.31
53.84 CD2Cl2
35.66
34.10
28.21
22.81
22.43
14.10
9.28
250 240 230 220 210 200 190 180 170 160 150 140 130 120 110 100 90 80 70 60 50 40 30 20 10 0 -10 -2(
f1 (ppm)

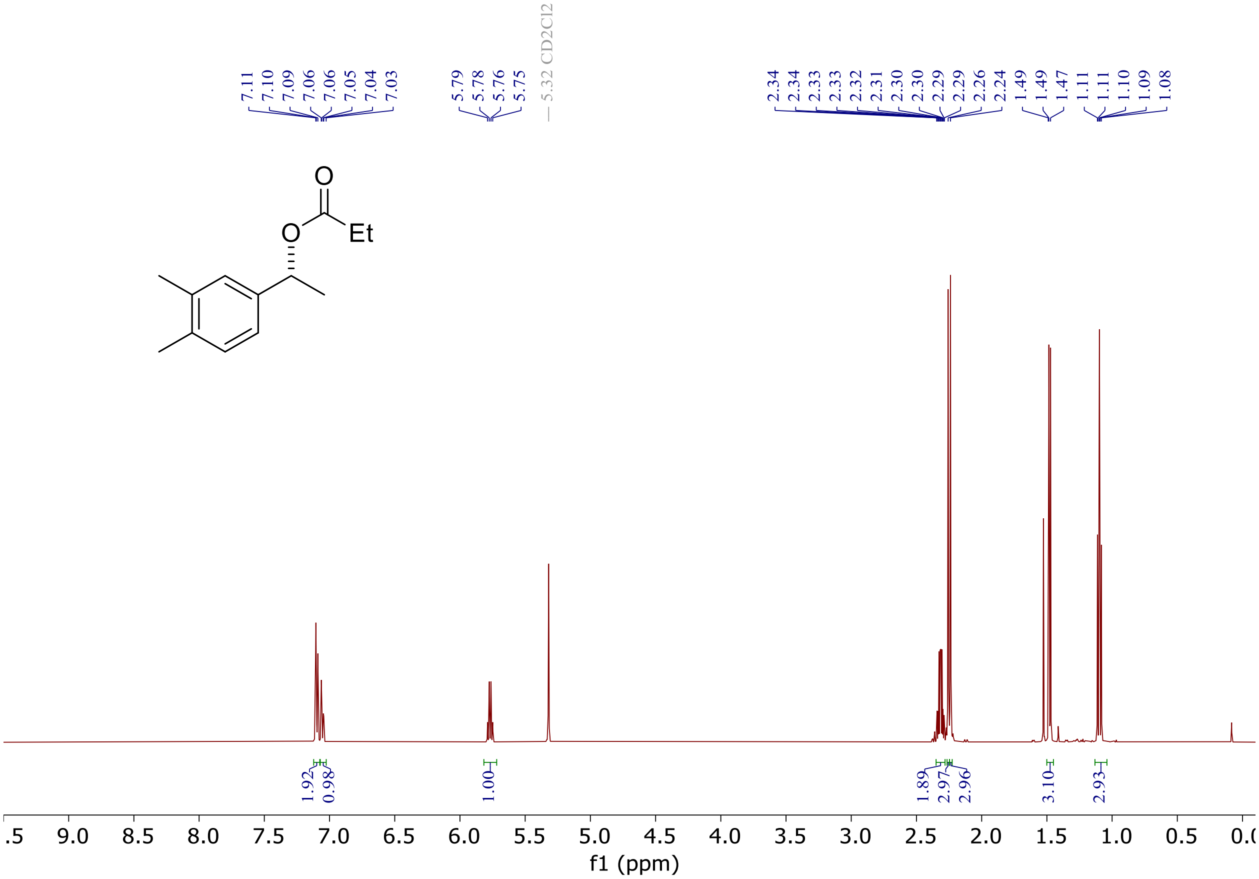
7.11
7.10
7.09
7.06
7.06
7.05
7.04
7.03
5.79
5.78
5.76
5.75
5.32 CD2Cl2
2.34
2.34
2.33
2.33
2.32
2.31
2.30
2.30
2.29
2.29
2.26
2.24
1.49
1.49
1.47
1.11
1.11
1.10
1.09
1.08
O
O
Et
1.92
0.98
1.00
1.89
2.97
2.96
3.10
2.93
.5
9.0
8.5
8.0
7.5
7.0
6.5
6.0
5.5
5.0
4.5
4.0
3.5
3.0
2.5
2.0
1.5
1.0
0.5
0.(
f1 (ppm)

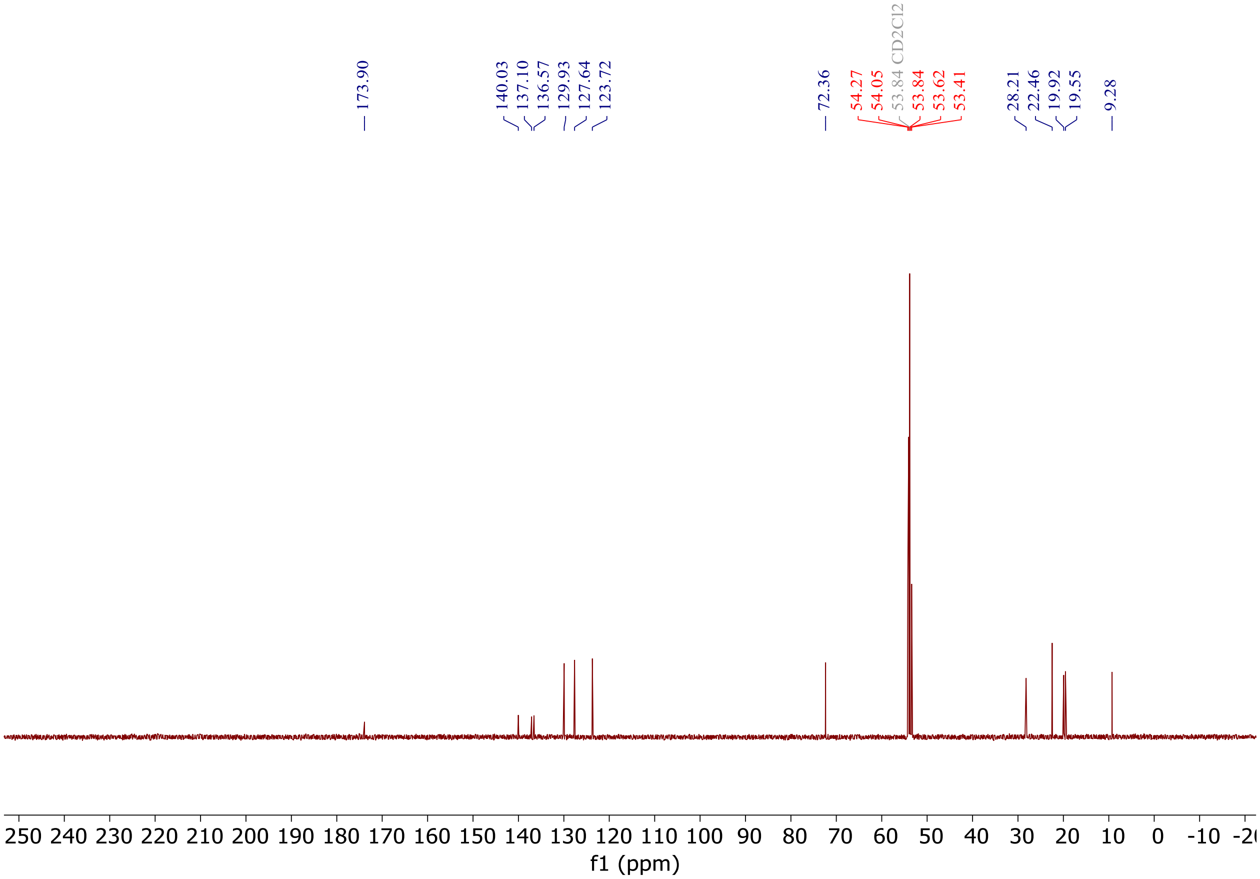
173.90
140.03
137.10
136.57
129.93
127.64
123.72
72.36
54.27
54.05
53.84 CD2Cl2
53.84
53.62
53.41
28.21
22.46
19.92
19.55
9.28
250
240
230
220
210
200
190
180
170
160
150
140
130
120
110
100
90
80
70
60
50
40
30
20
10
0
-10
-2(
f1 (ppm)

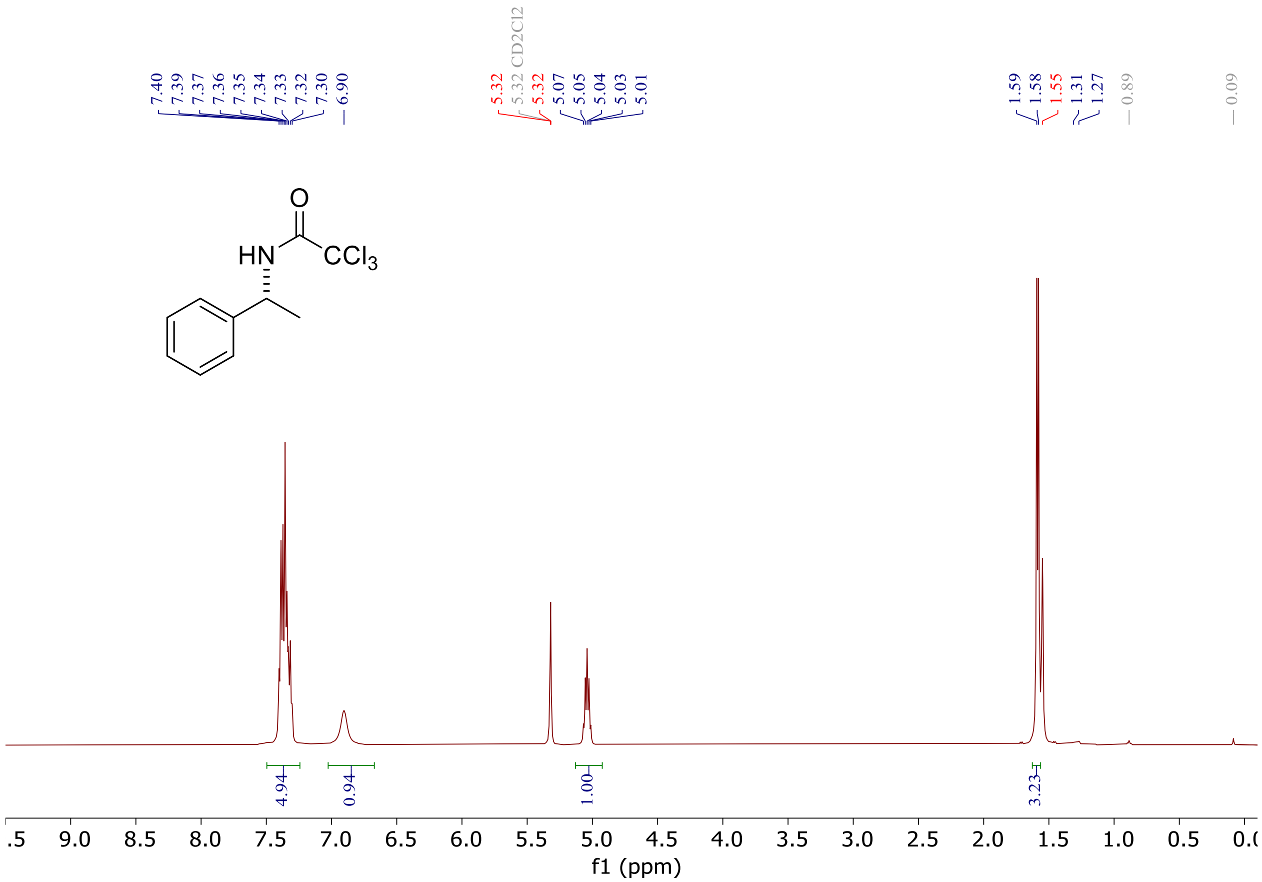
7.40
7.39
7.37
7.36
7.35
7.34
7.33
7.32
7.30
6.90
5.32
5.32 CD2Cl2
5.32
5.07
5.05
5.04
5.03
5.01
1.59
1.58
1.55
1.31
1.27
0.89
0.09
O
HN
CCl3
4.94
0.94
1.00
3.23
.5
9.0
8.5
8.0
7.5
7.0
6.5
6.0
5.5
5.0
4.5
4.0
3.5
3.0
2.5
2.0
1.5
1.0
0.5
0.0
f1 (ppm)

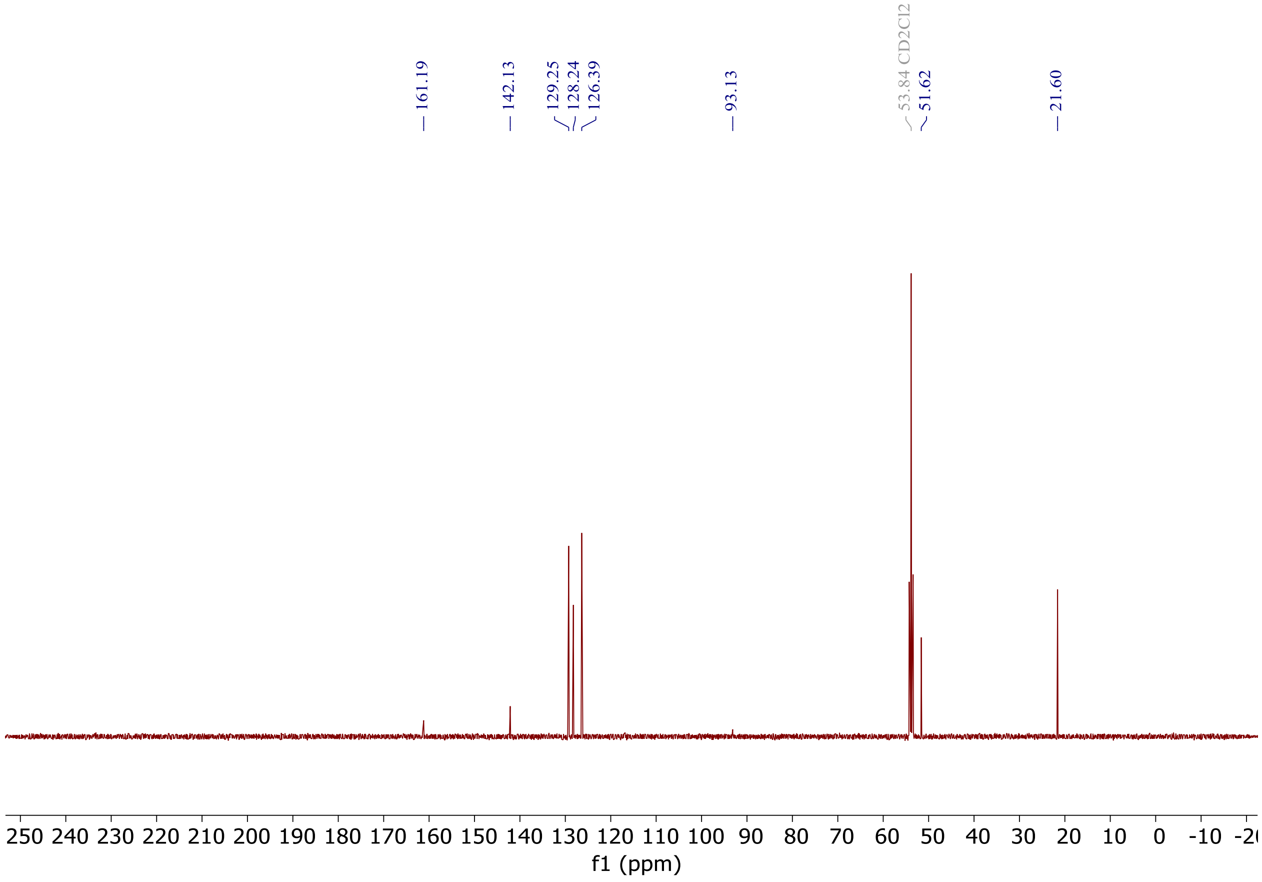
161.19
142.13
129.25
128.24
126.39
93.13
53.84 CD2Cl2
51.62
21.60
250
240
230
220
210
200
190
180
170
160
150
140
130
120
110
100
90
80
70
60
50
40
30
20
10
0
-10
-20
f1 (ppm)

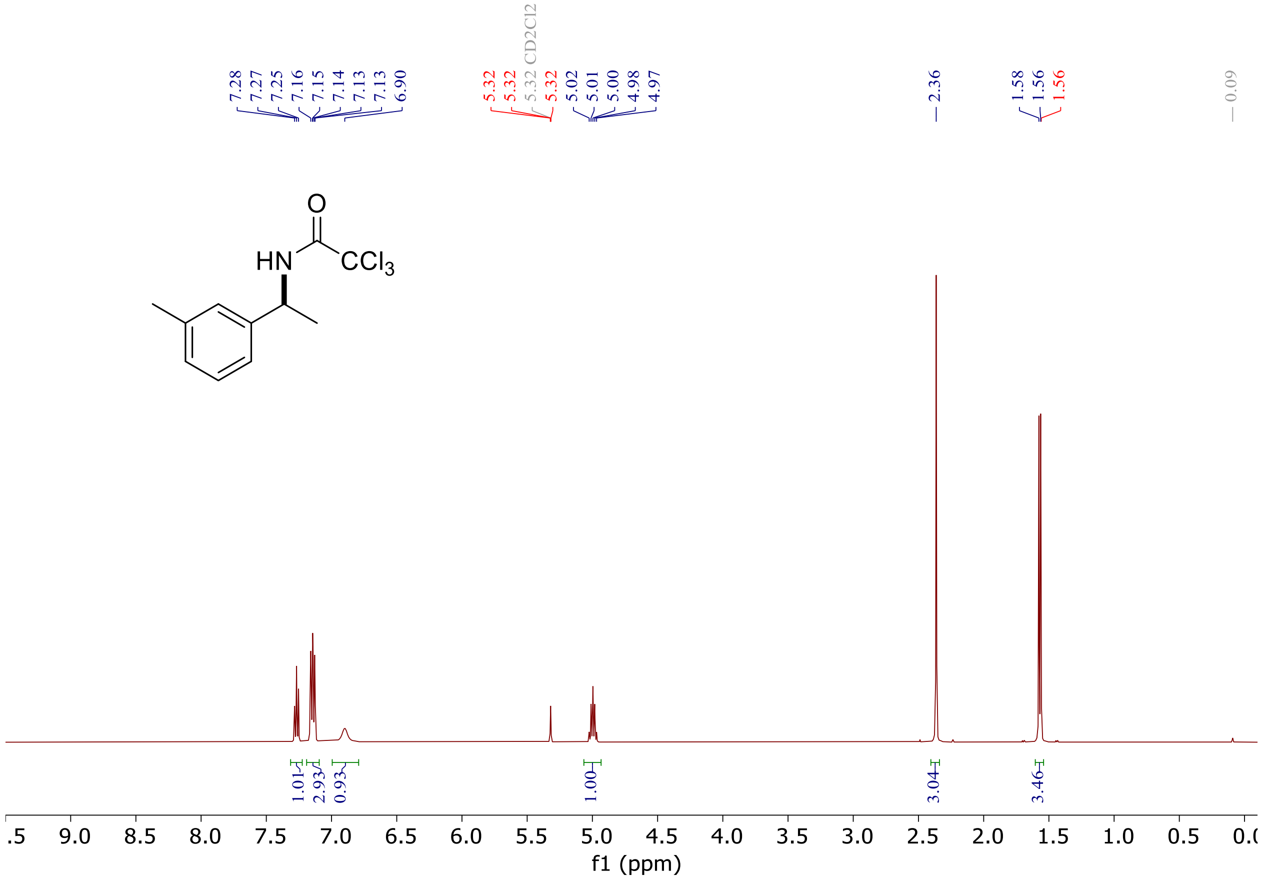
7.28
7.27
7.25
7.16
7.15
7.14
7.13
7.13
6.90
5.32
5.32
5.32 CD2Cl2
5.32
5.02
5.01
5.00
4.98
4.97
2.36
1.58
1.56
1.56
0.09
O
HN
CCl3
1.01
2.93
0.93
1.00
3.04
3.46
.5
9.0
8.5
8.0
7.5
7.0
6.5
6.0
5.5
5.0
4.5
4.0
3.5
3.0
2.5
2.0
1.5
1.0
0.5
0.
f1 (ppm)

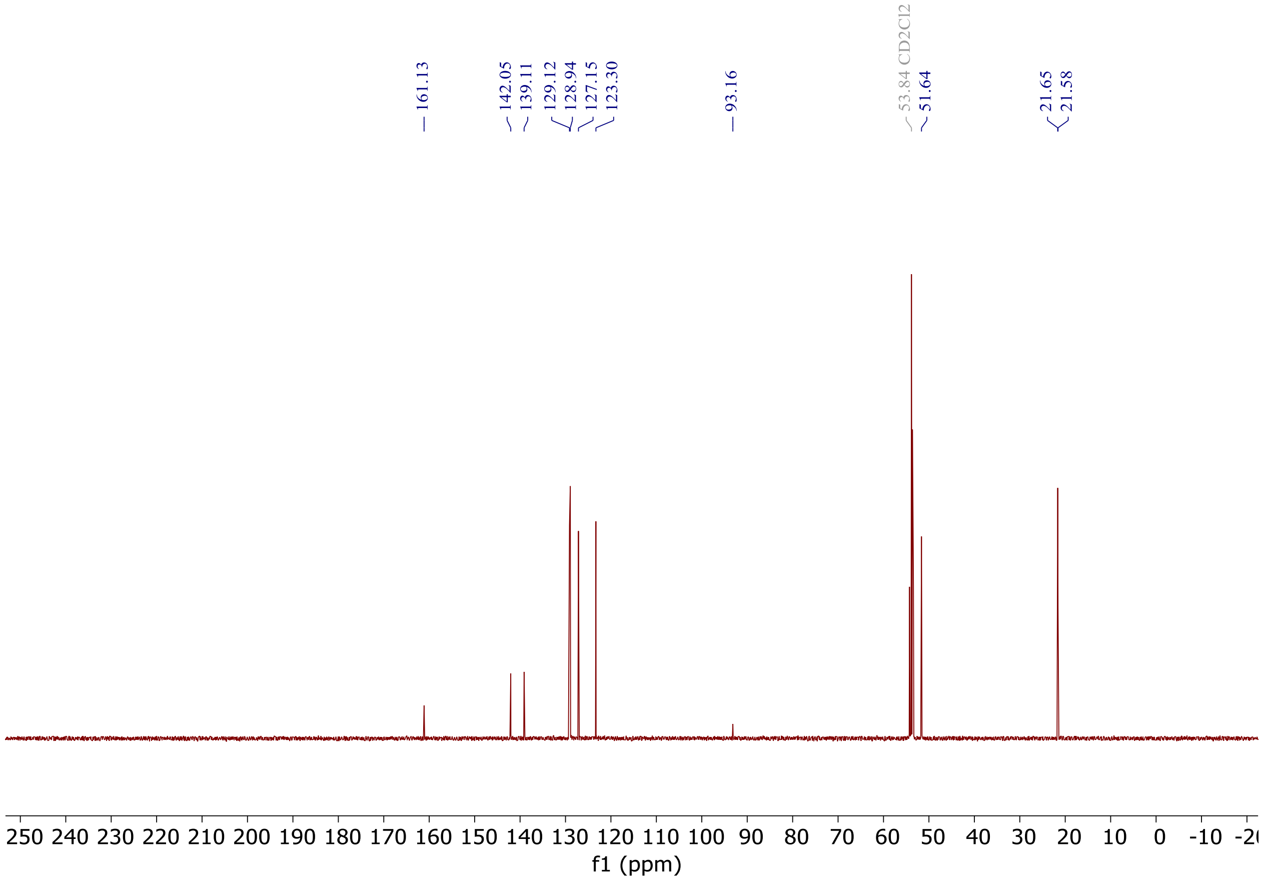
161.13
142.05
139.11
129.12
128.94
127.15
123.30
93.16
53.84 CD2Cl2
51.64
21.65
21.58
250
240
230
220
210
200
190
180
170
160
150
140
130
120
110
100
90
80
70
60
50
40
30
20
10
0
-10
-2
f1 (ppm)

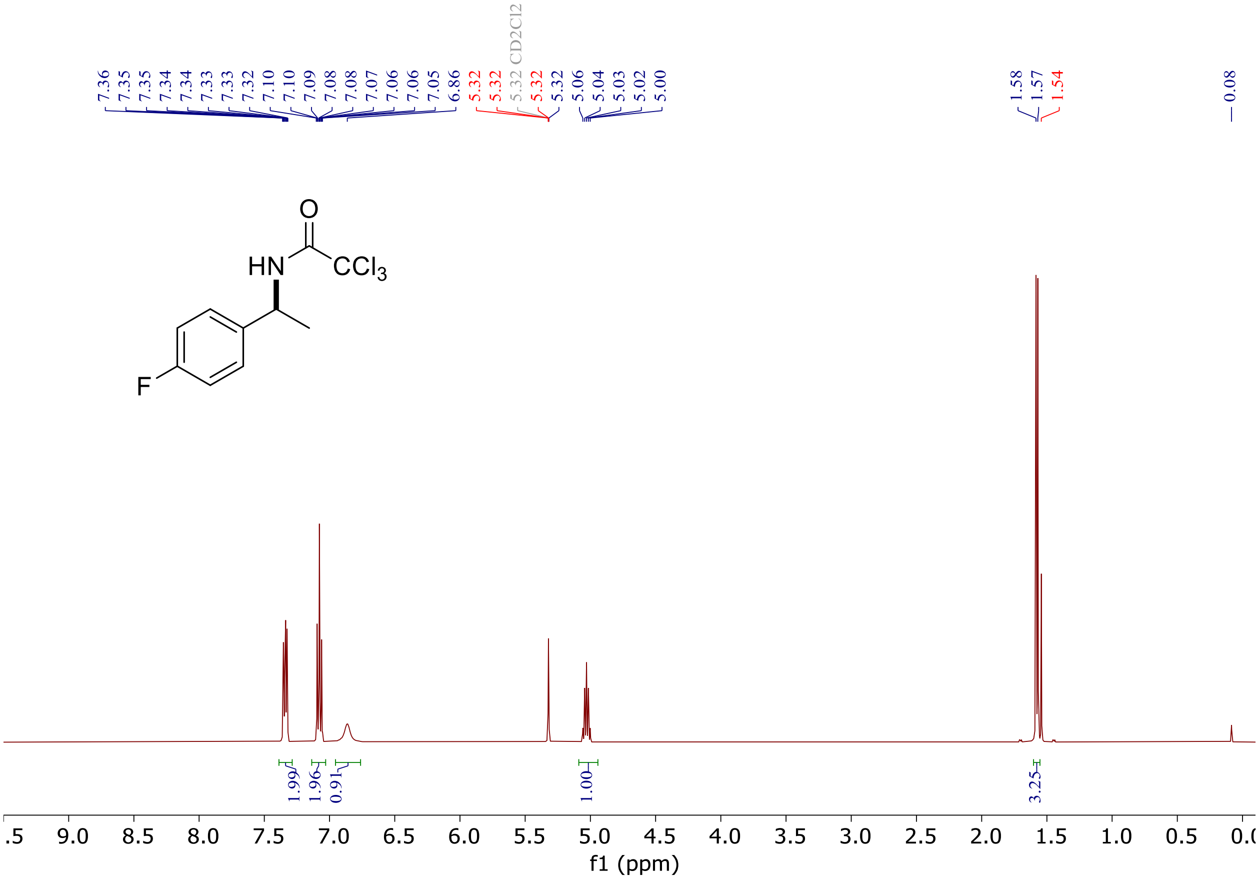
7.36
7.35
7.35
7.34
7.34
7.33
7.33
7.32
7.10
7.10
7.09
7.08
7.08
7.07
7.06
7.06
7.05
6.86
5.32
5.32
5.32 CD2Cl2
5.32
5.32
5.06
5.04
5.03
5.02
5.00
1.58
1.57
1.54
0.08
O
HN
CCl3
F
1.99
1.96
0.91
1.00
3.25
.5
9.0
8.5
8.0
7.5
7.0
6.5
6.0
5.5
5.0
4.5
4.0
3.5
3.0
2.5
2.0
1.5
1.0
0.5
0.
f1 (ppm)

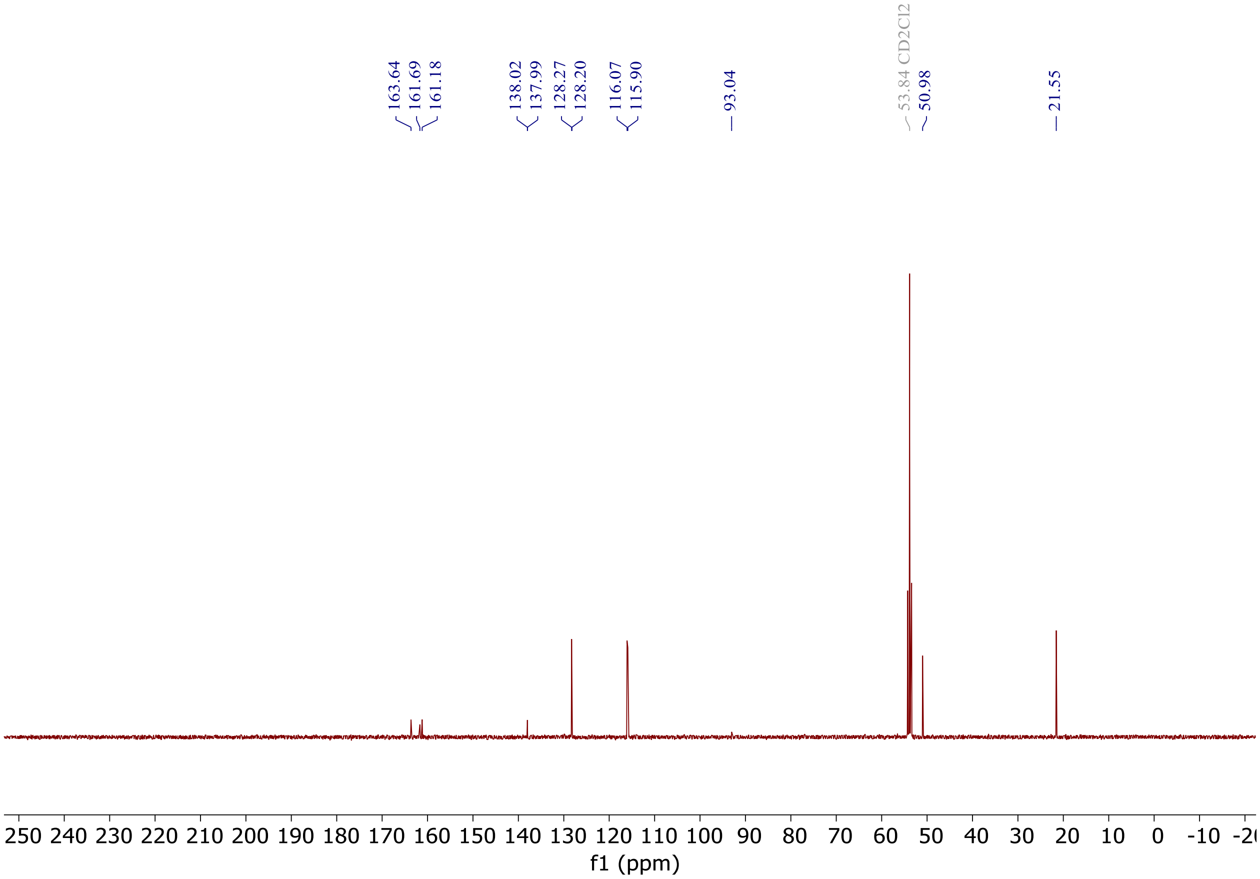
163.64
161.69
161.18
138.02
137.99
128.27
128.20
116.07
115.90
93.04
53.84 CD2Cl2
50.98
21.55
250
240
230
220
210
200
190
180
170
160
150
140
130
120
110
100
90
80
70
60
50
40
30
20
10
0
-10
-2
f1 (ppm)

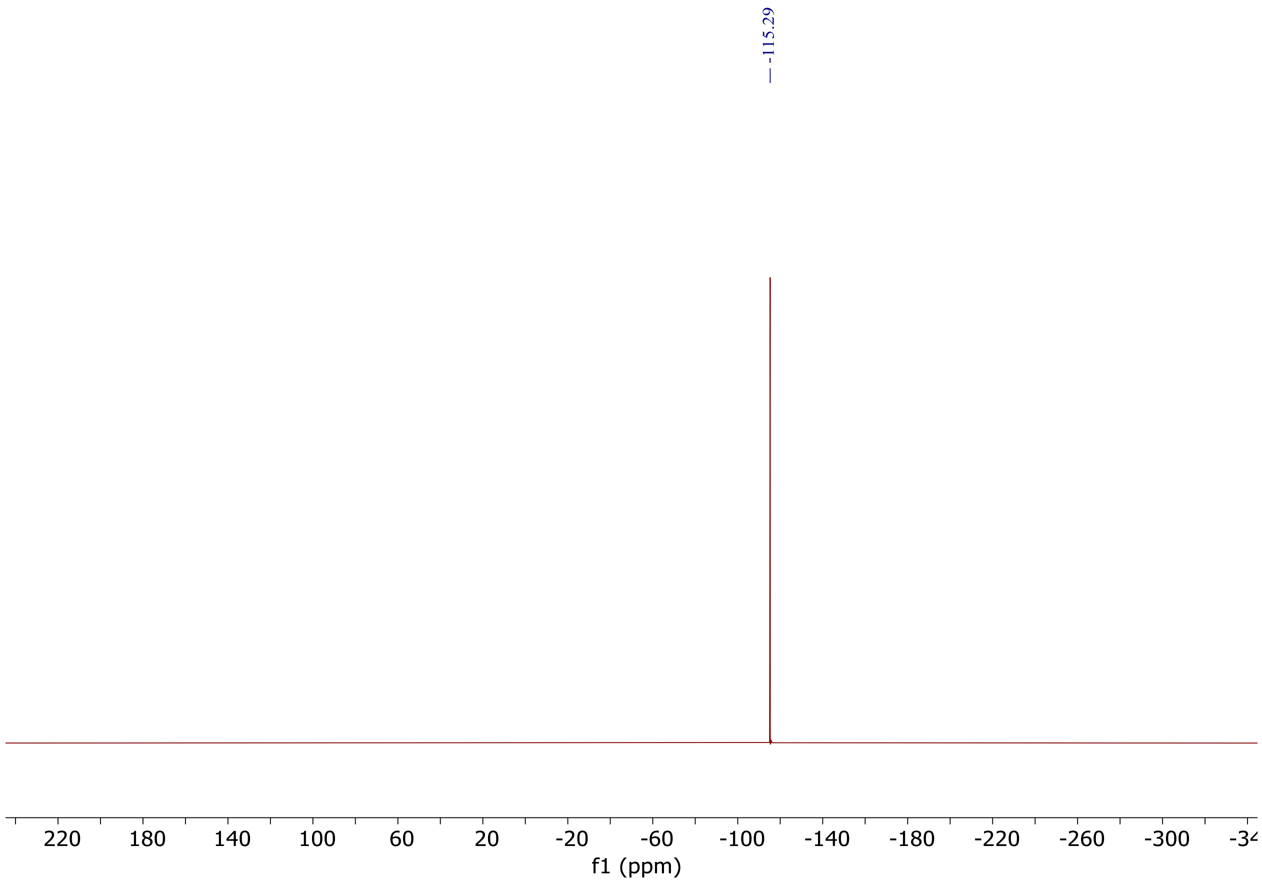
-115.29
220
180
140
100
60
20
-20
-60
-100
-140
-180
-220
-260
-300
-34
f1 (ppm)

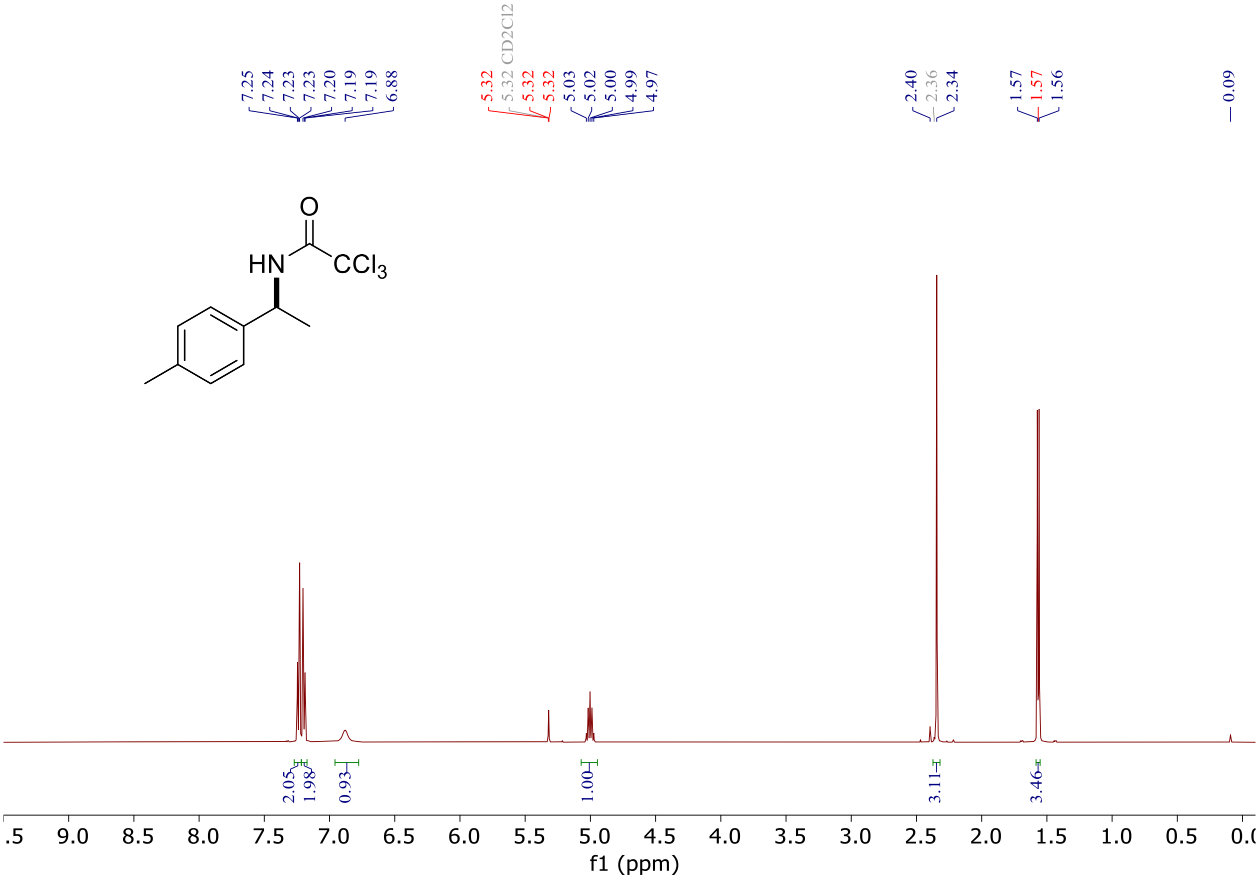
7.25
7.24
7.23
7.23
7.20
7.19
7.19
6.88
5.32
5.32 CD2Cl2
5.32
5.32
5.03
5.02
5.00
4.99
4.97
2.40
2.36
2.34
1.57
1.57
1.56
0.09
O
HN
CCl3
2.05
1.98
0.93
1.00
3.11
3.46
.5
9.0
8.5
8.0
7.5
7.0
6.5
6.0
5.5
5.0
4.5
4.0
3.5
3.0
2.5
2.0
1.5
1.0
0.5
0.(
f1 (ppm)

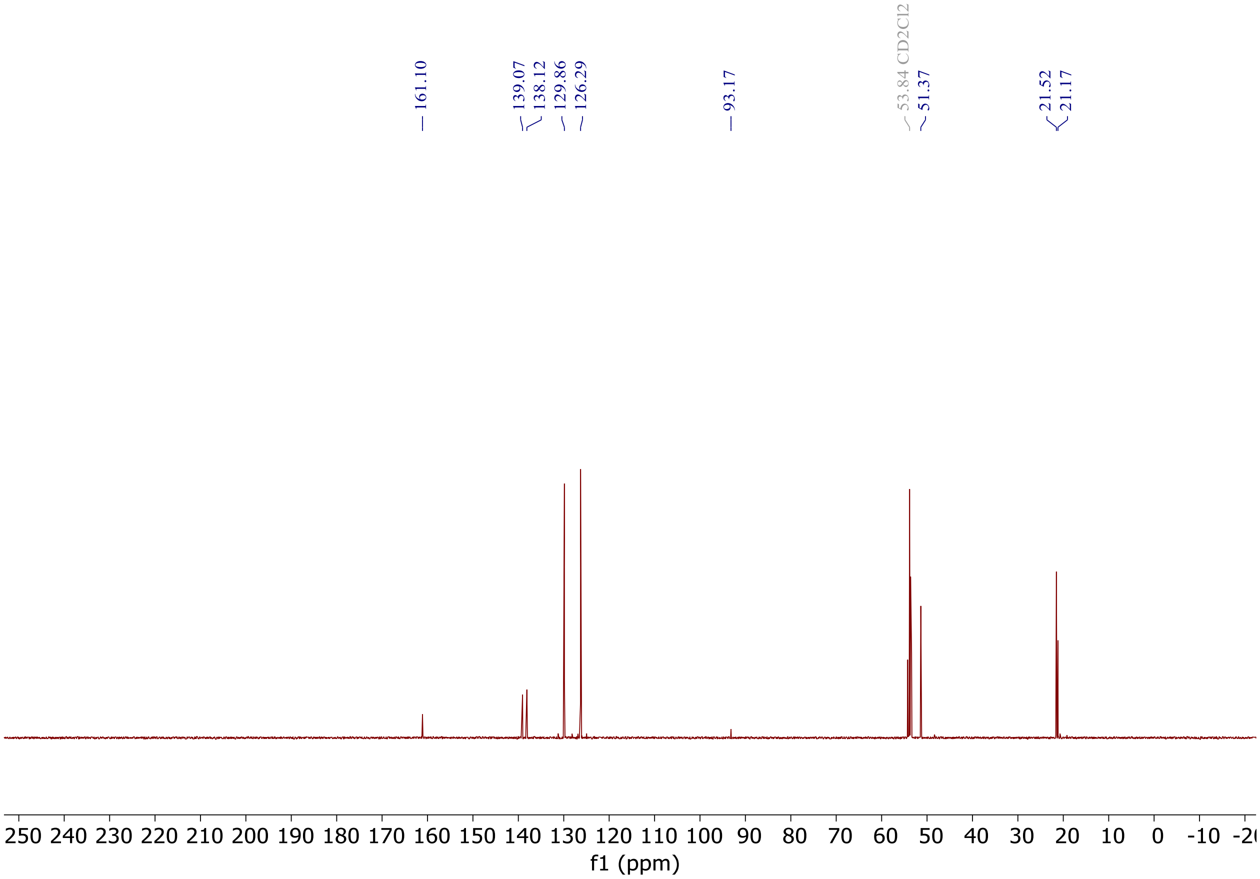
161.10
139.07
138.12
129.86
126.29
93.17
53.84 CD2Cl2
51.37
21.52
21.17
250
240
230
220
210
200
190
180
170
160
150
140
130
120
110
100
90
80
70
60
50
40
30
20
10
0
-10
-2(
f1 (ppm)

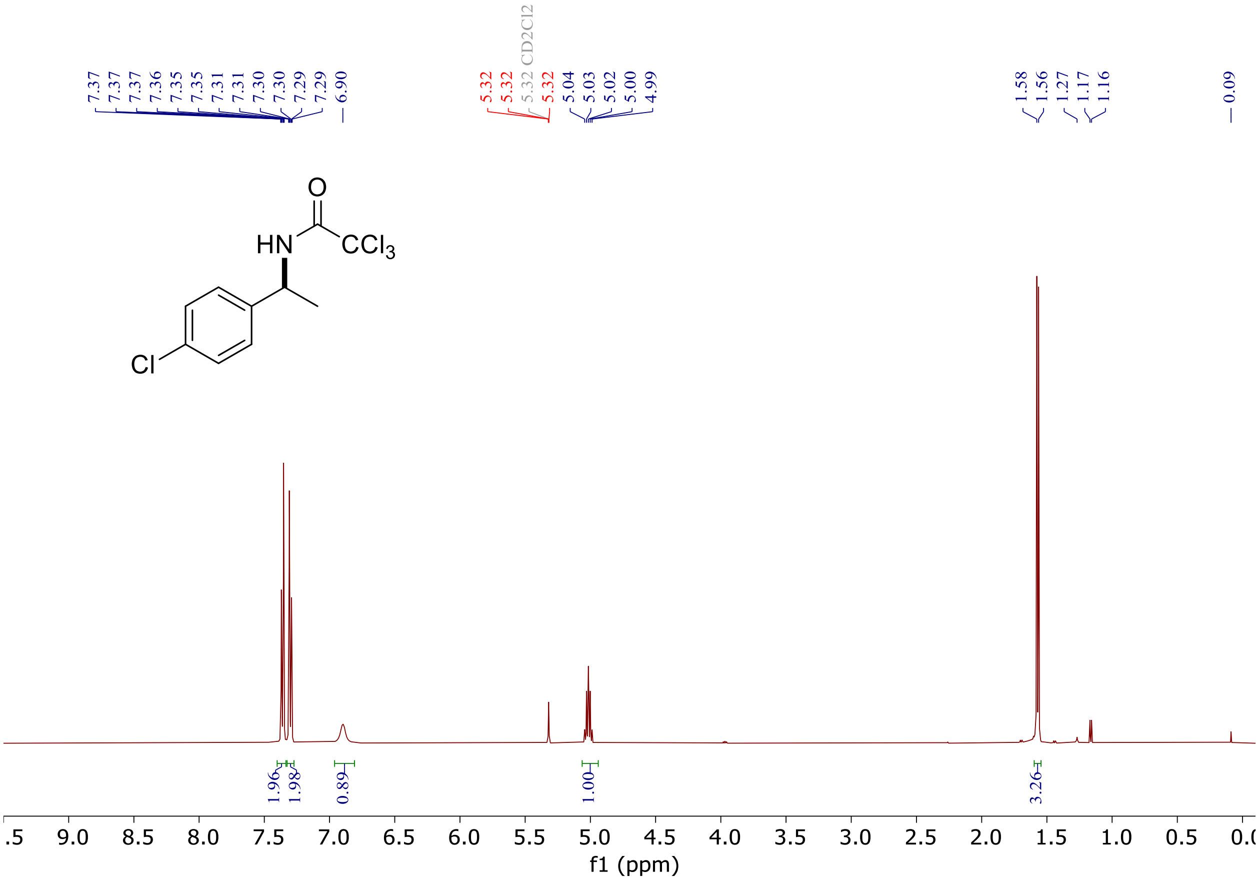
7.37
7.37
7.37
7.36
7.35
7.35
7.31
7.31
7.30
7.30
7.29
7.29
6.90
5.32
5.32
5.32 CD2Cl2
5.32
5.04
5.03
5.02
5.00
4.99
1.58
1.56
1.27
1.17
1.16
0.09
O
HN
CCl3
Cl
1.96
1.98
0.89
1.00
3.26
.5
9.0
8.5
8.0
7.5
7.0
6.5
6.0
5.5
5.0
4.5
4.0
3.5
3.0
2.5
2.0
1.5
1.0
0.5
0.
f1 (ppm)

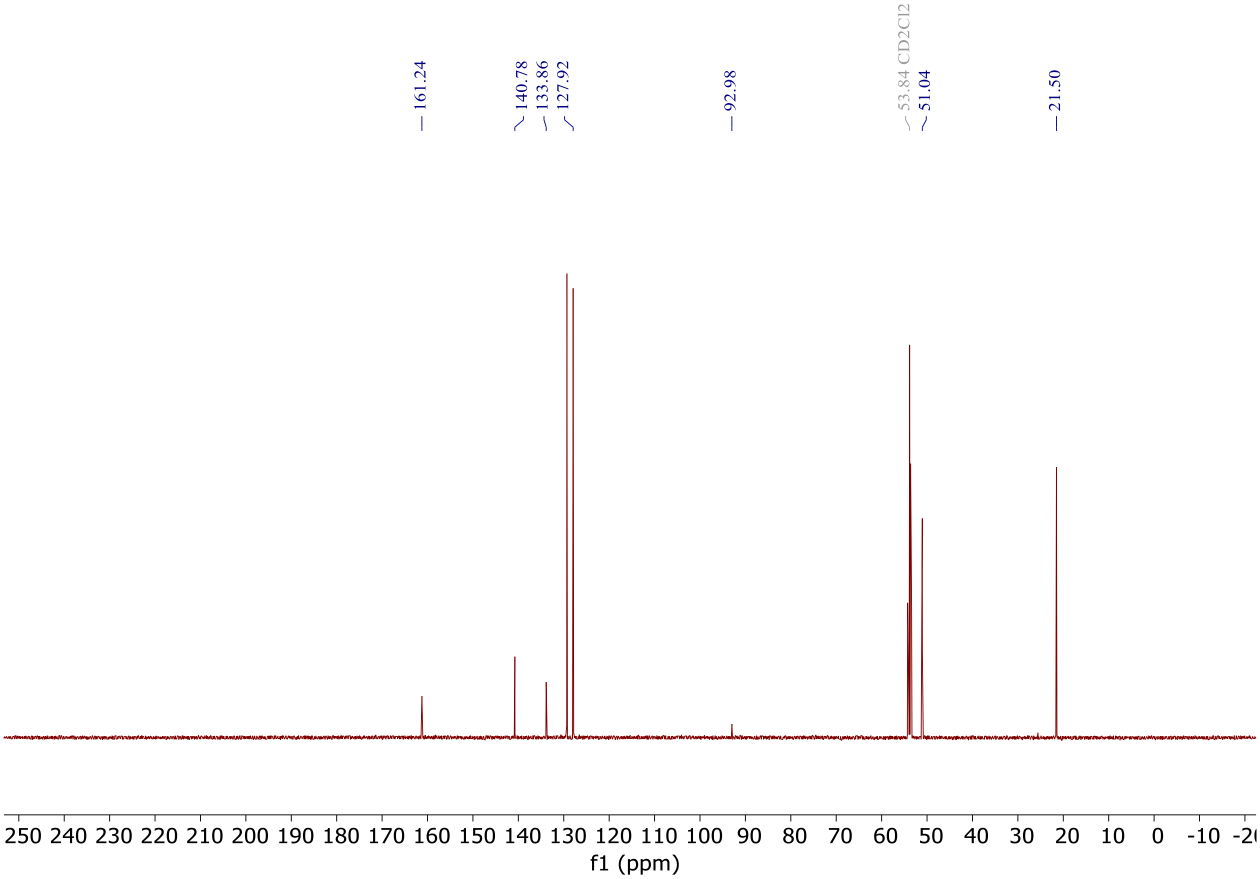
161.24
140.78
133.86
127.92
92.98
53.84 CD2Cl2
51.04
21.50
250
240
230
220
210
200
190
180
170
160
150
140
130
120
110
100
90
80
70
60
50
40
30
20
10
0
-10
-2
f1 (ppm)

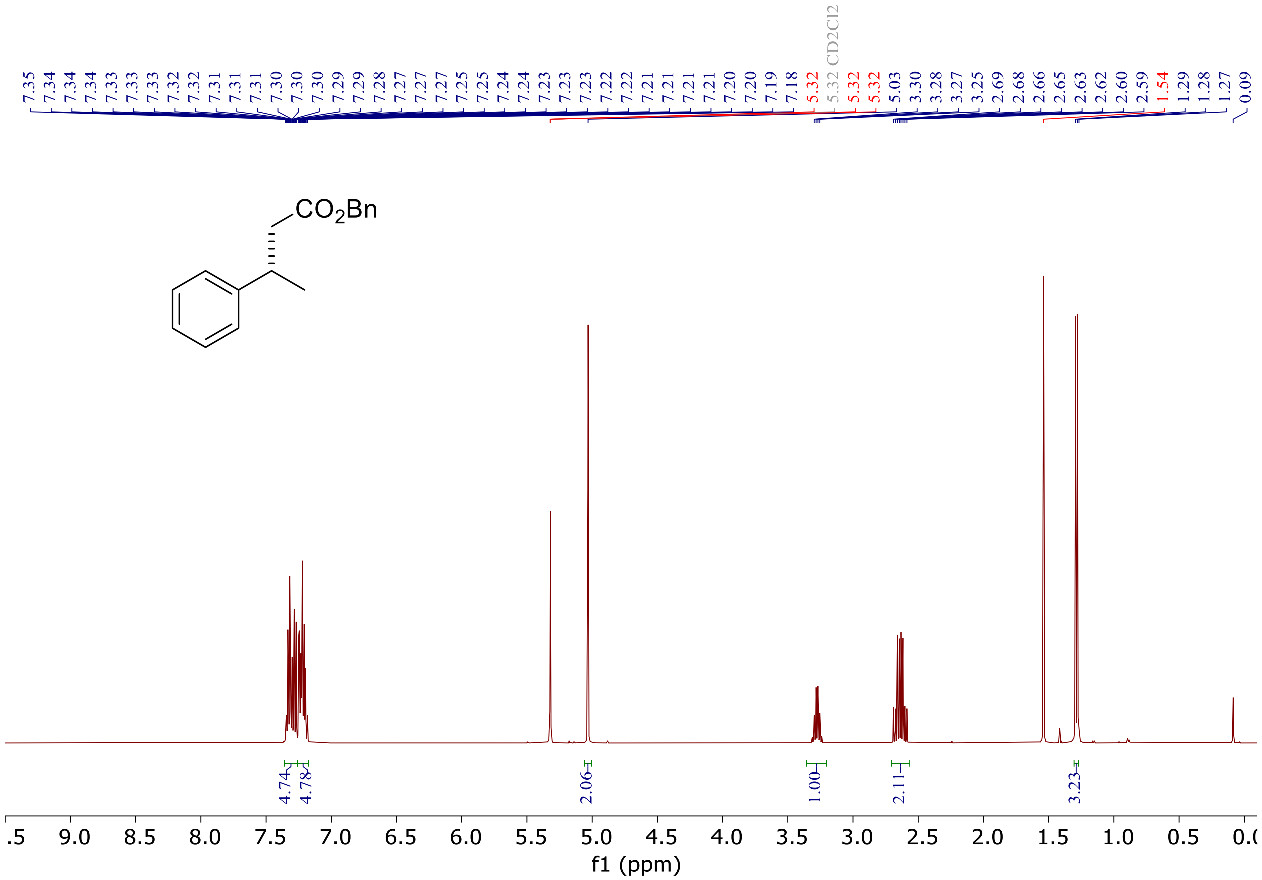
7.35 7.34 7.34 7.34 7.33 7.33 7.33 7.32 7.32 7.31 7.31 7.31 7.30 7.30 7.30 7.29 7.29 7.28 7.27 7.27 7.27 7.25 7.25 7.24 7.24 7.23 7.23 7.23 7.22 7.22 7.21 7.21 7.21 7.21 7.20 7.20 7.19 7.18 5.32
5.32 CD2Cl2
5.32 5.32 5.03 3.30 3.28 3.27 3.25 2.69 2.68 2.66 2.65 2.63 2.62 2.60 2.59 1.54 1.29 1.28 1.27 0.09
CO2Bn
4.74
4.78
2.06
1.00
2.11
3.23
.5 9.0 8.5 8.0 7.5 7.0 6.5 6.0 5.5 5.0 4.5 4.0 3.5 3.0 2.5 2.0 1.5 1.0 0.5 0.
f1 (ppm)

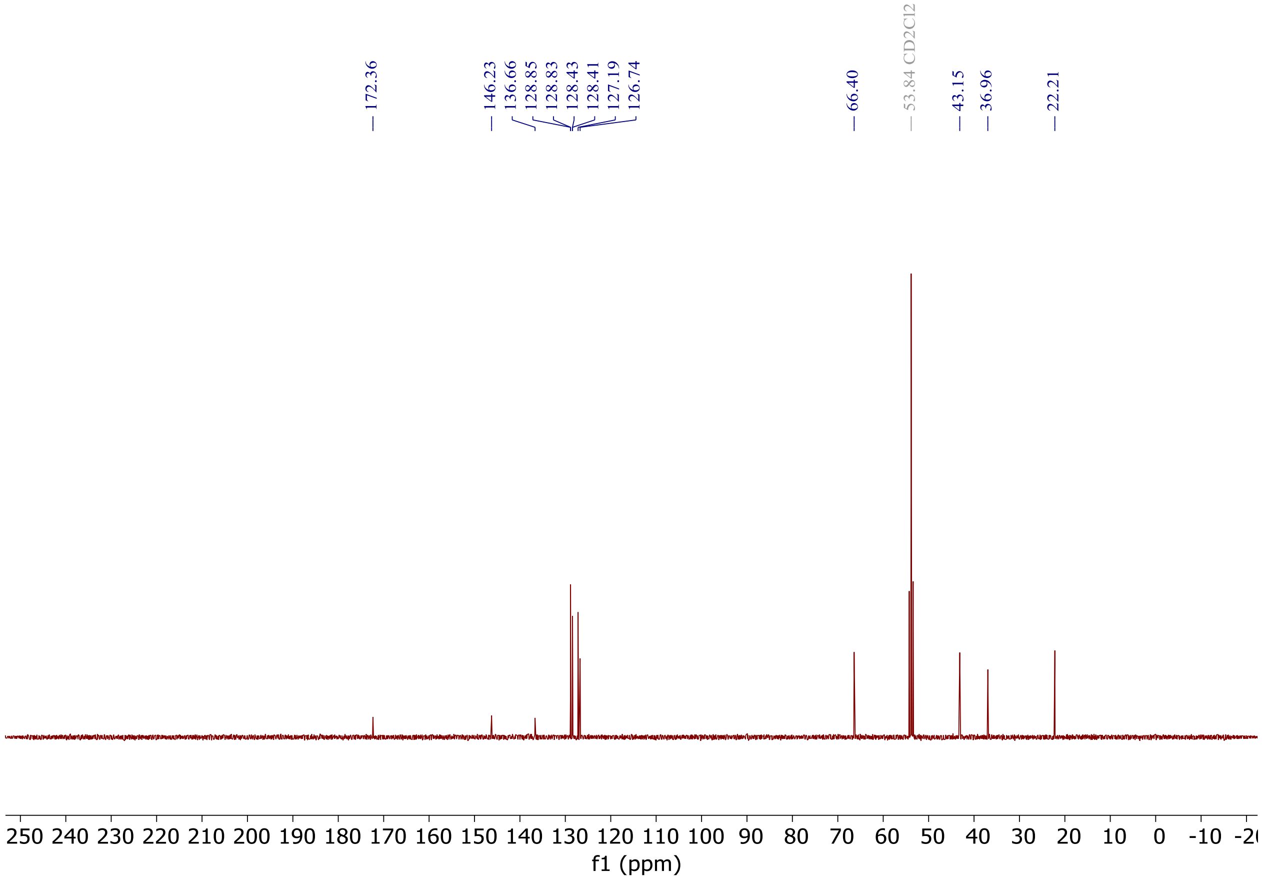
172.36
146.23 136.66 128.85 128.83 128.43 128.41 127.19 126.74
66.40
53.84 CD2Cl2
43.15
36.96
22.21
250 240 230 220 210 200 190 180 170 160 150 140 130 120 110 100 90 80 70 60 50 40 30 20 10 0 -10 -2
f1 (ppm)

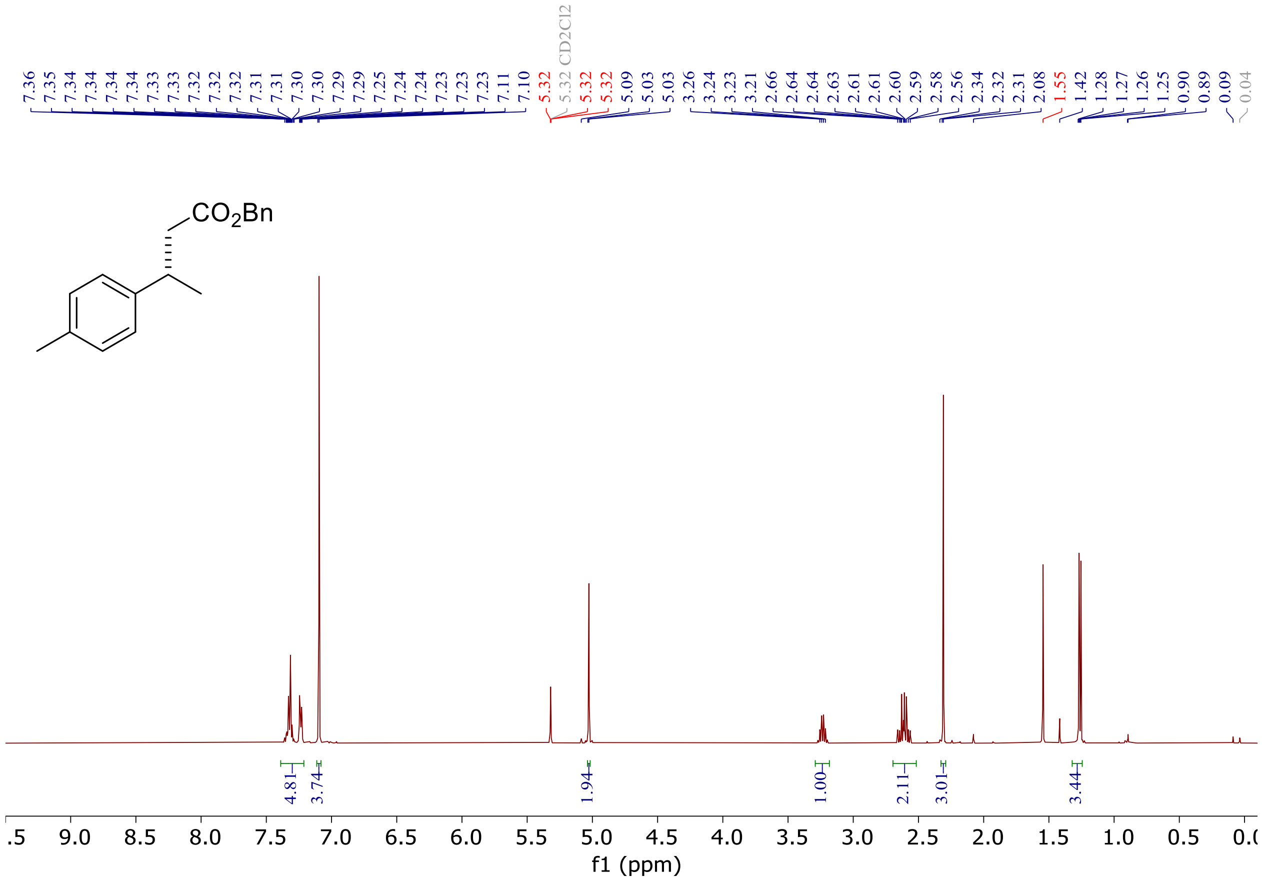
7.36 7.35 7.34 7.34 7.34 7.34 7.33 7.33 7.32 7.32 7.32 7.31 7.31 7.30 7.30 7.29 7.29 7.25 7.24 7.24 7.23 7.23 7.23 7.11 7.10
5.32 5.32 CD2Cl2 5.32 5.32 5.09 5.03 5.03
3.26 3.24 3.23 3.21 2.66 2.64 2.63 2.61 2.61 2.60 2.59 2.58 2.56 2.34 2.32 2.31 2.08
1.55 1.42 1.28 1.27 1.26 1.25 0.90 0.89 0.09 0.04
CO2Bn
4.81
3.74
1.94
1.00
2.11
3.01
3.44
.5 9.0 8.5 8.0 7.5 7.0 6.5 6.0 5.5 5.0 4.5 4.0 3.5 3.0 2.5 2.0 1.5 1.0 0.5 0.
f1 (ppm)

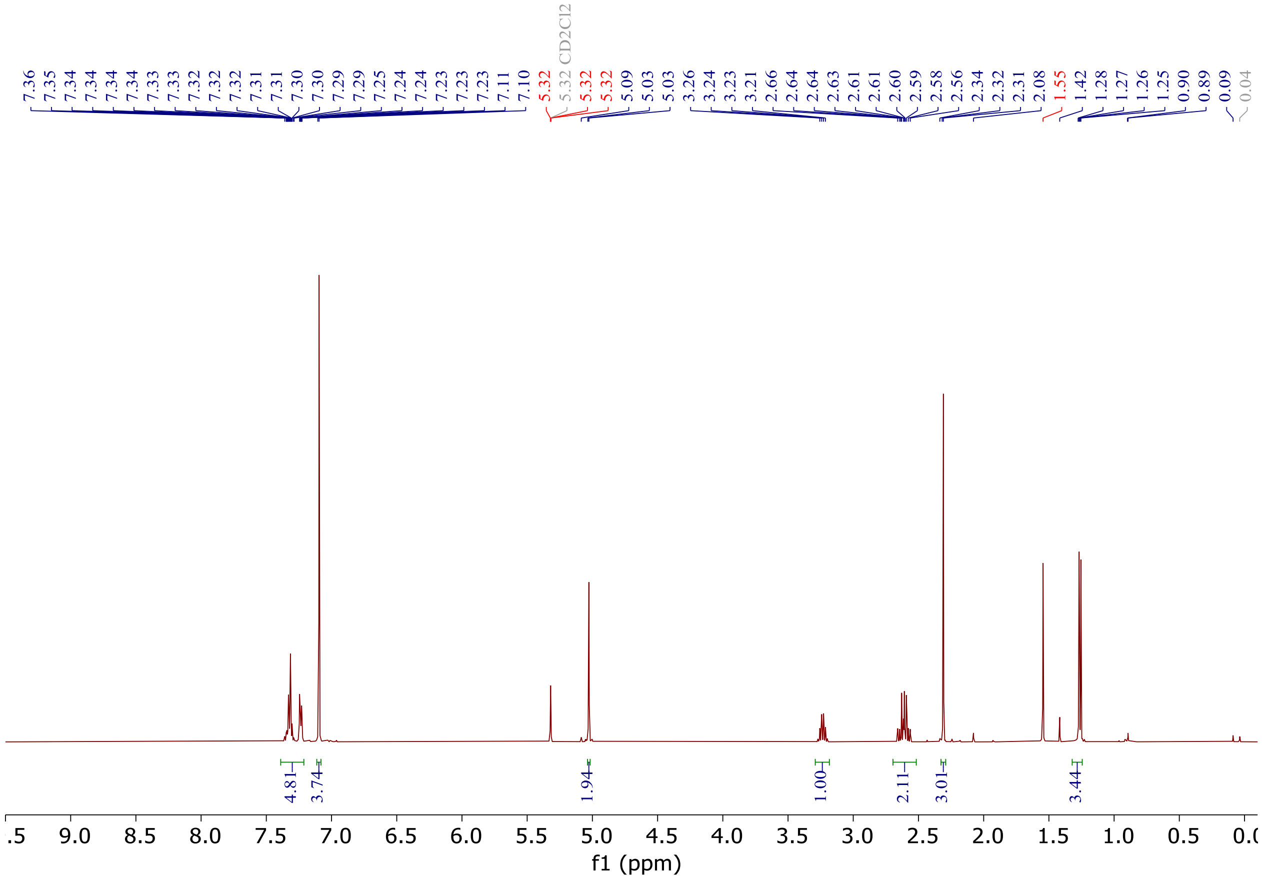
7.36 7.35 7.34 7.34 7.34 7.34 7.33 7.33 7.32 7.32 7.32 7.31 7.31 7.30 7.30 7.29 7.29 7.25 7.24 7.24 7.23 7.23 7.23 7.11 7.10
5.32 5.32 CD2Cl2 5.32 5.32 5.09 5.03 5.03
3.26 3.24 3.23 3.21 2.66 2.64 2.63 2.61 2.61 2.60 2.59 2.58 2.56 2.34 2.32 2.31 2.08
1.55 1.42 1.28 1.27 1.26 1.25 0.90 0.89 0.09 0.04
4.81
3.74
1.94
1.00
2.11
3.01
3.44
.5 9.0 8.5 8.0 7.5 7.0 6.5 6.0 5.5 5.0 4.5 4.0 3.5 3.0 2.5 2.0 1.5 1.0 0.5 0.
f1 (ppm)

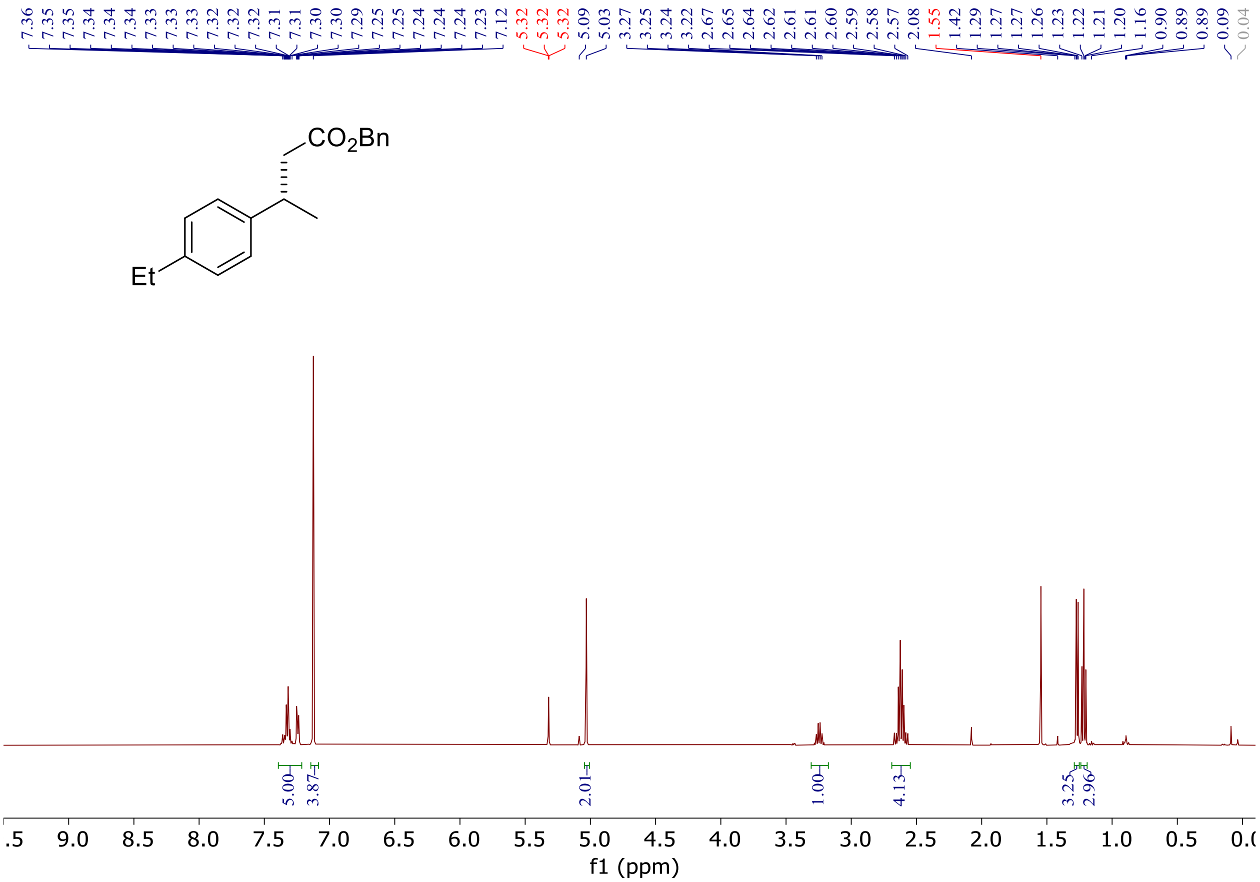
7.36
7.35
7.35
7.34
7.34
7.34
7.33
7.33
7.32
7.32
7.32
7.31
7.30
7.30
7.29
7.25
7.25
7.24
7.24
7.24
7.23
7.12
5.32
5.32
5.32
5.09
5.03
3.27
3.25
3.24
3.22
2.67
2.65
2.64
2.62
2.61
2.61
2.60
2.59
2.58
2.57
2.08
1.55
1.42
1.29
1.27
1.27
1.26
1.23
1.22
1.21
1.20
1.16
0.90
0.89
0.89
0.09
0.04
CO2Bn
Et
5.00
3.87
2.01
1.00
4.13
3.25
2.96
.5 9.0 8.5 8.0 7.5 7.0 6.5 6.0 5.5 5.0 4.5 4.0 3.5 3.0 2.5 2.0 1.5 1.0 0.5 0.
f1 (ppm)

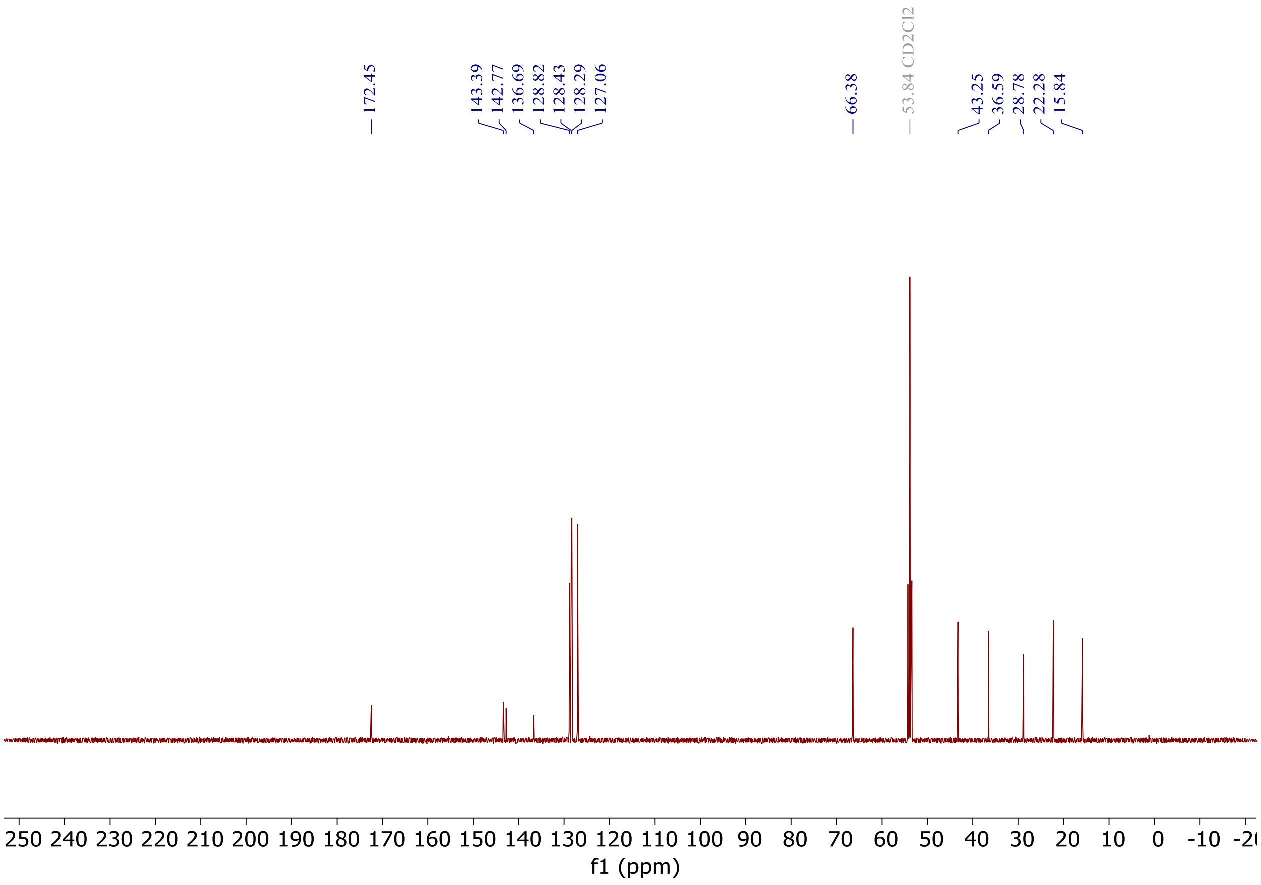
172.45
143.39
142.77
136.69
128.82
128.43
128.29
127.06
66.38
53.84 CD2Cl2
43.25
36.59
28.78
22.28
15.84
250 240 230 220 210 200 190 180 170 160 150 140 130 120 110 100 90 80 70 60 50 40 30 20 10 0 -10 -2
f1 (ppm)

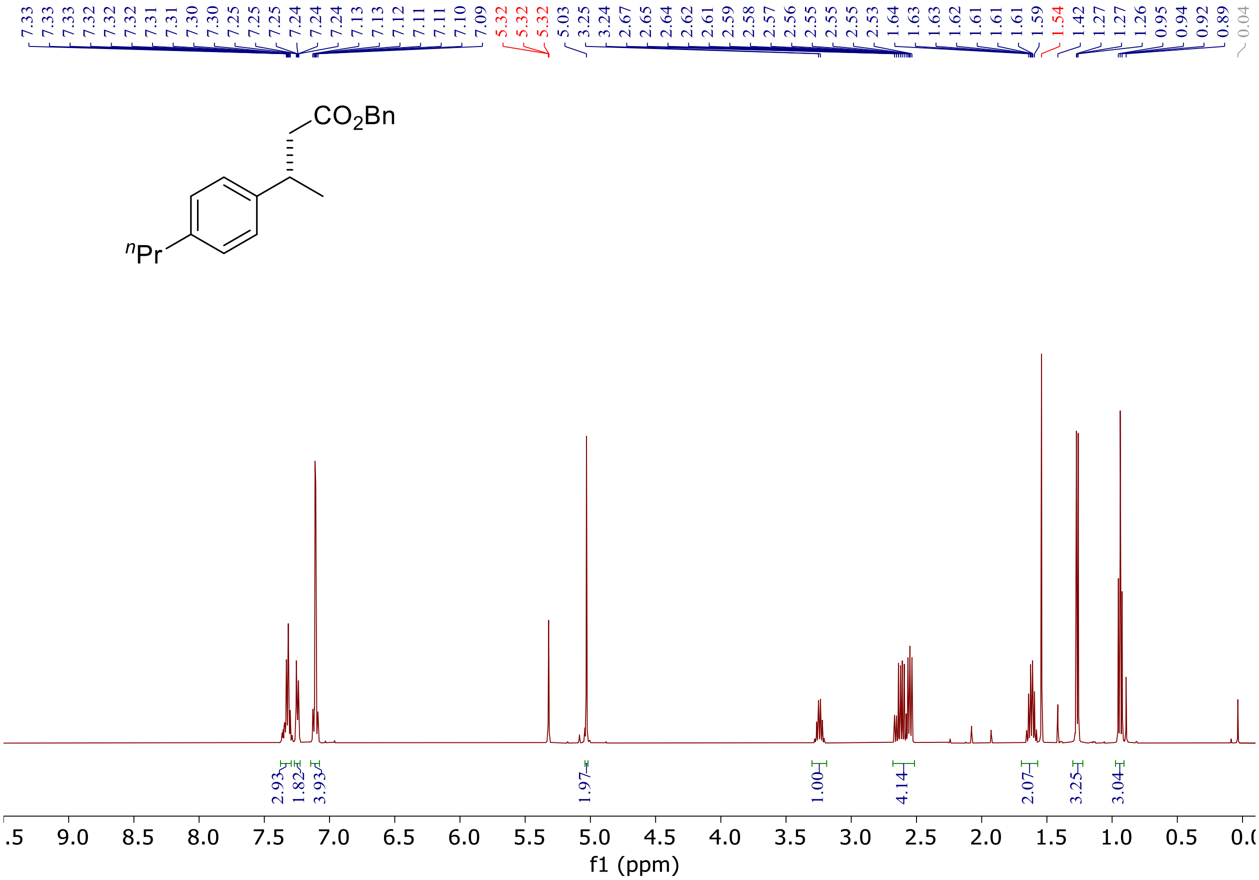
7.33
7.33
7.33
7.32
7.32
7.32
7.31
7.31
7.30
7.30
7.25
7.25
7.25
7.24
7.24
7.24
7.13
7.13
7.12
7.11
7.11
7.10
7.09
5.32
5.32
5.32
5.03
3.25
3.24
2.67
2.65
2.64
2.62
2.61
2.59
2.58
2.57
2.56
2.55
2.55
2.55
2.53
1.64
1.63
1.63
1.62
1.61
1.61
1.61
1.59
1.54
1.42
1.27
1.27
1.26
0.95
0.94
0.92
0.89
0.04
CO2Bn
nPr
2.93
1.82
3.93
1.97
1.00
4.14
2.07
3.25
3.04
.5
9.0
8.5
8.0
7.5
7.0
6.5
6.0
5.5
5.0
4.5
4.0
3.5
3.0
2.5
2.0
1.5
1.0
0.5
0.0
f1 (ppm)

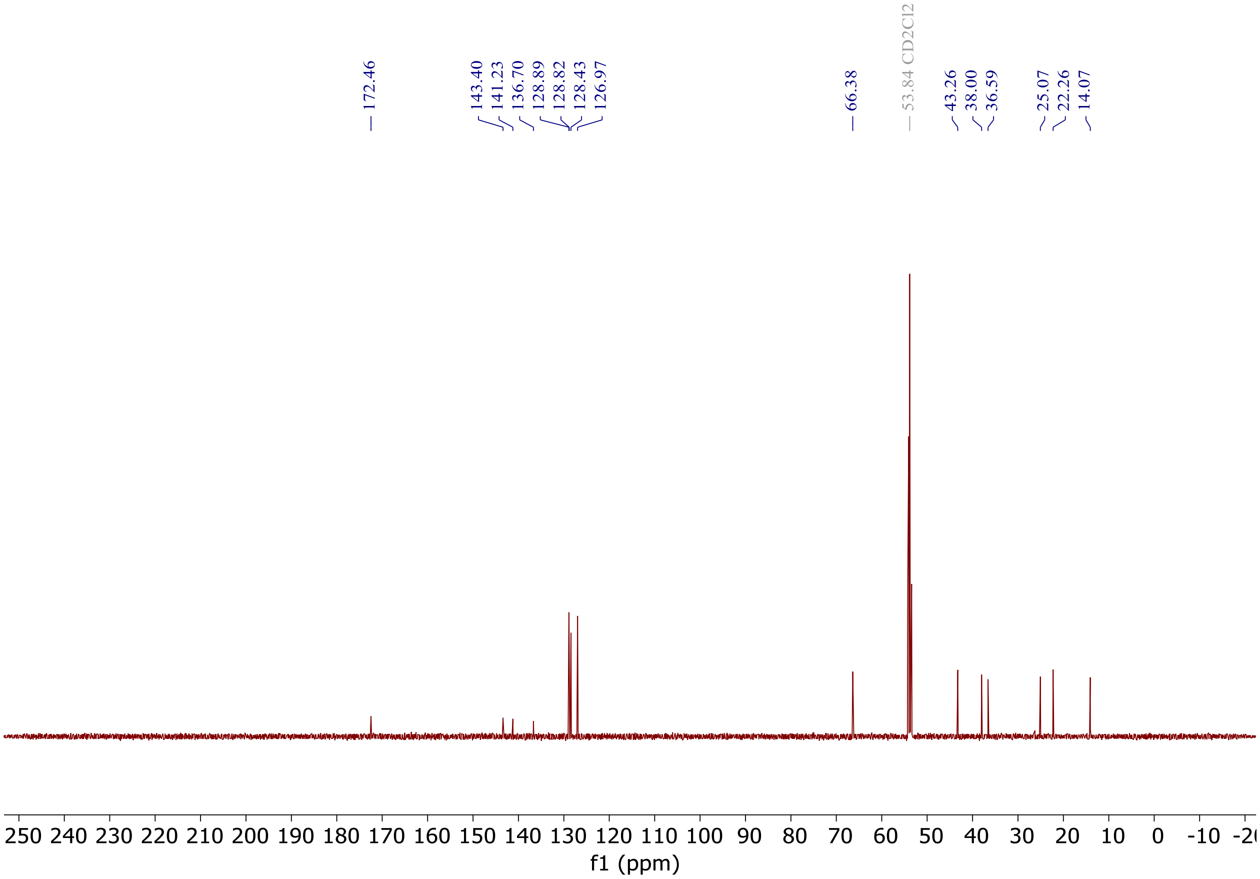
172.46
143.40
141.23
136.70
128.89
128.82
128.43
126.97
66.38
53.84 CD2Cl2
43.26
38.00
36.59
25.07
22.26
14.07
250
240
230
220
210
200
190
180
170
160
150
140
130
120
110
100
90
80
70
60
50
40
30
20
10
0
-10
-20
f1 (ppm)

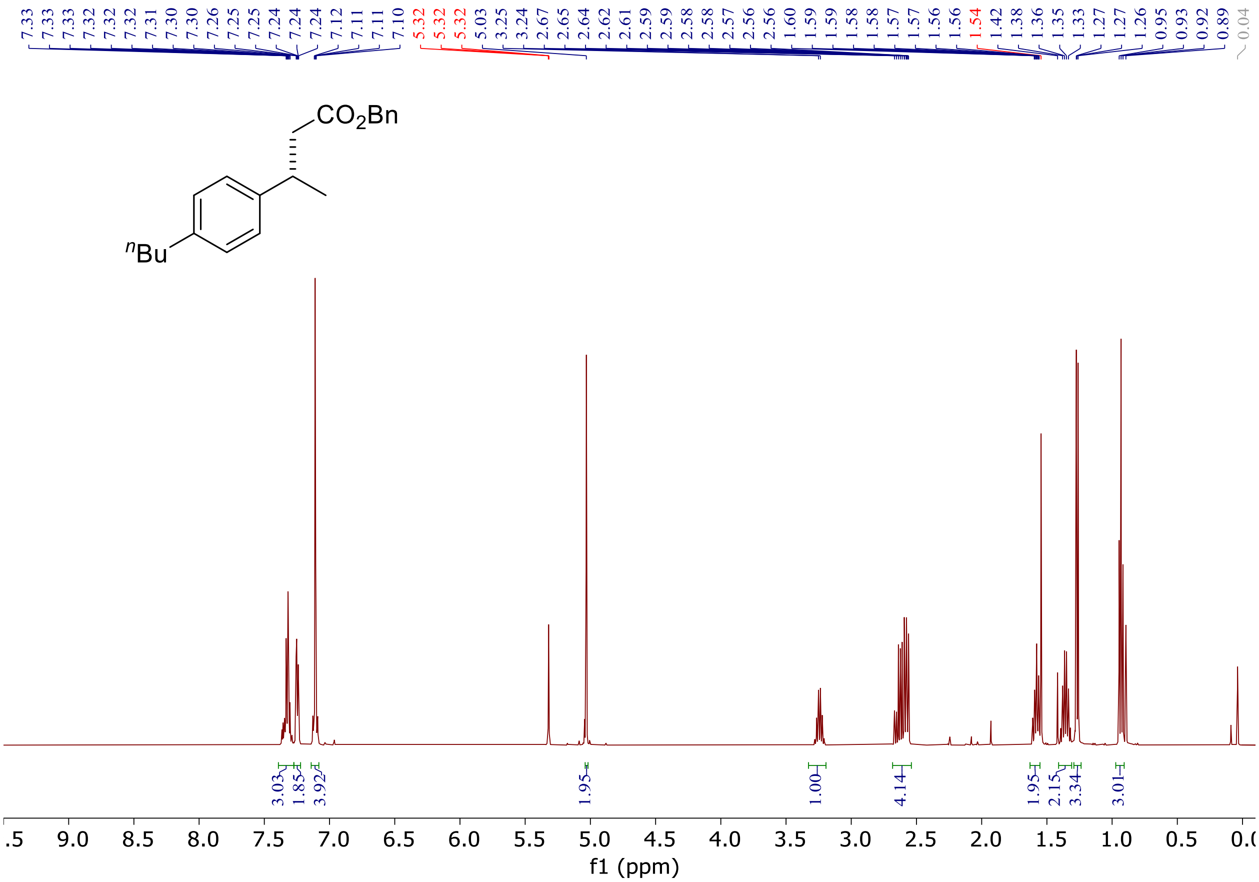
7.33
7.33
7.33
7.32
7.32
7.32
7.31
7.30
7.30
7.26
7.25
7.25
7.24
7.24
7.24
7.12
7.11
7.11
7.10
5.32
5.32
5.32
5.03
3.25
3.24
2.67
2.65
2.64
2.62
2.61
2.59
2.59
2.58
2.58
2.57
2.56
2.56
1.60
1.59
1.59
1.58
1.58
1.57
1.57
1.56
1.56
1.54
1.42
1.38
1.36
1.35
1.33
1.27
1.27
1.26
0.95
0.93
0.92
0.89
0.04
CO2Bn
nBu
3.03
1.85
3.92
1.95
1.00
4.14
1.95
2.15
3.34
3.01
.5
9.0
8.5
8.0
7.5
7.0
6.5
6.0
5.5
5.0
4.5
4.0
3.5
3.0
2.5
2.0
1.5
1.0
0.5
0.0
f1 (ppm)

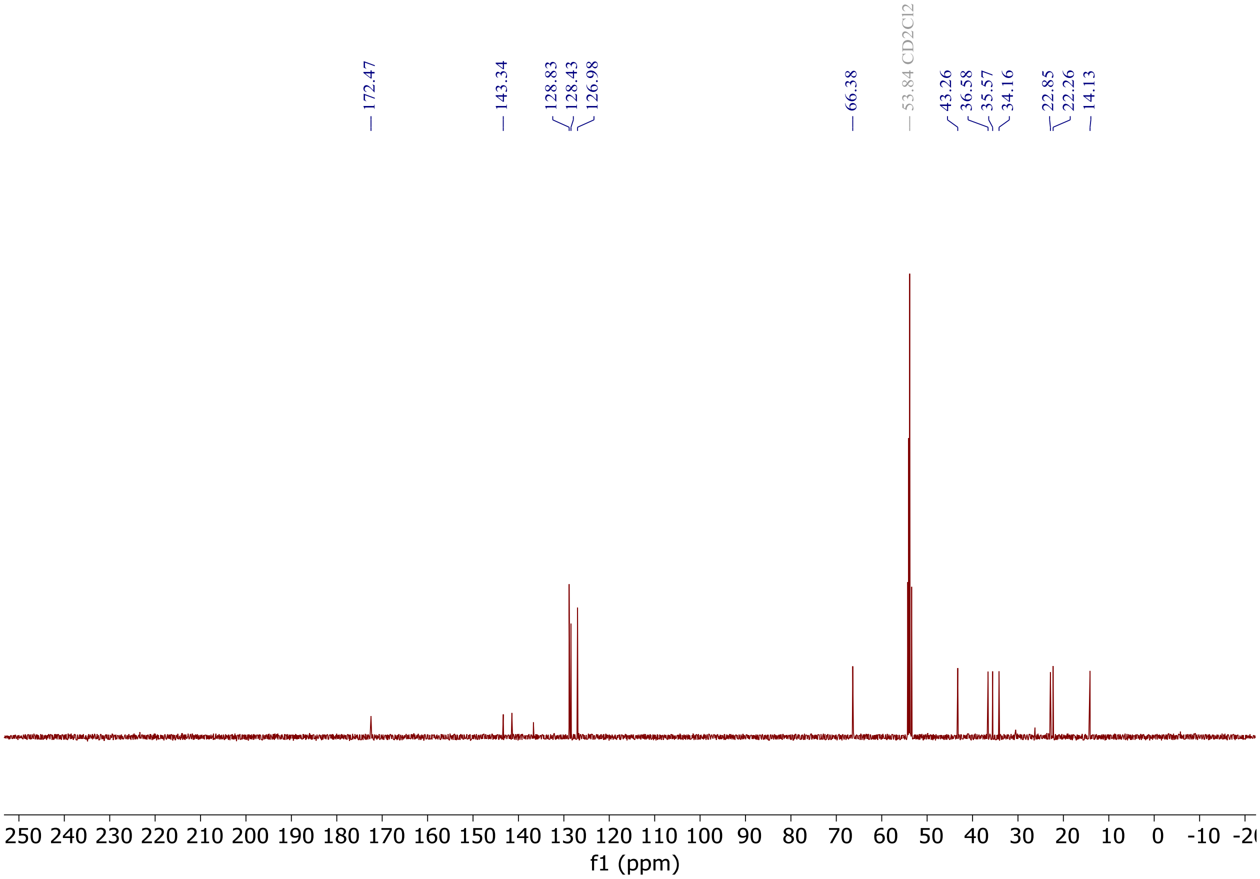
172.47
143.34
128.83
128.43
126.98
66.38
53.84 CD2Cl2
43.26
36.58
35.57
34.16
22.85
22.26
14.13
250
240
230
220
210
200
190
180
170
160
150
140
130
120
110
100
90
80
70
60
50
40
30
20
10
0
-10
-20
f1 (ppm)

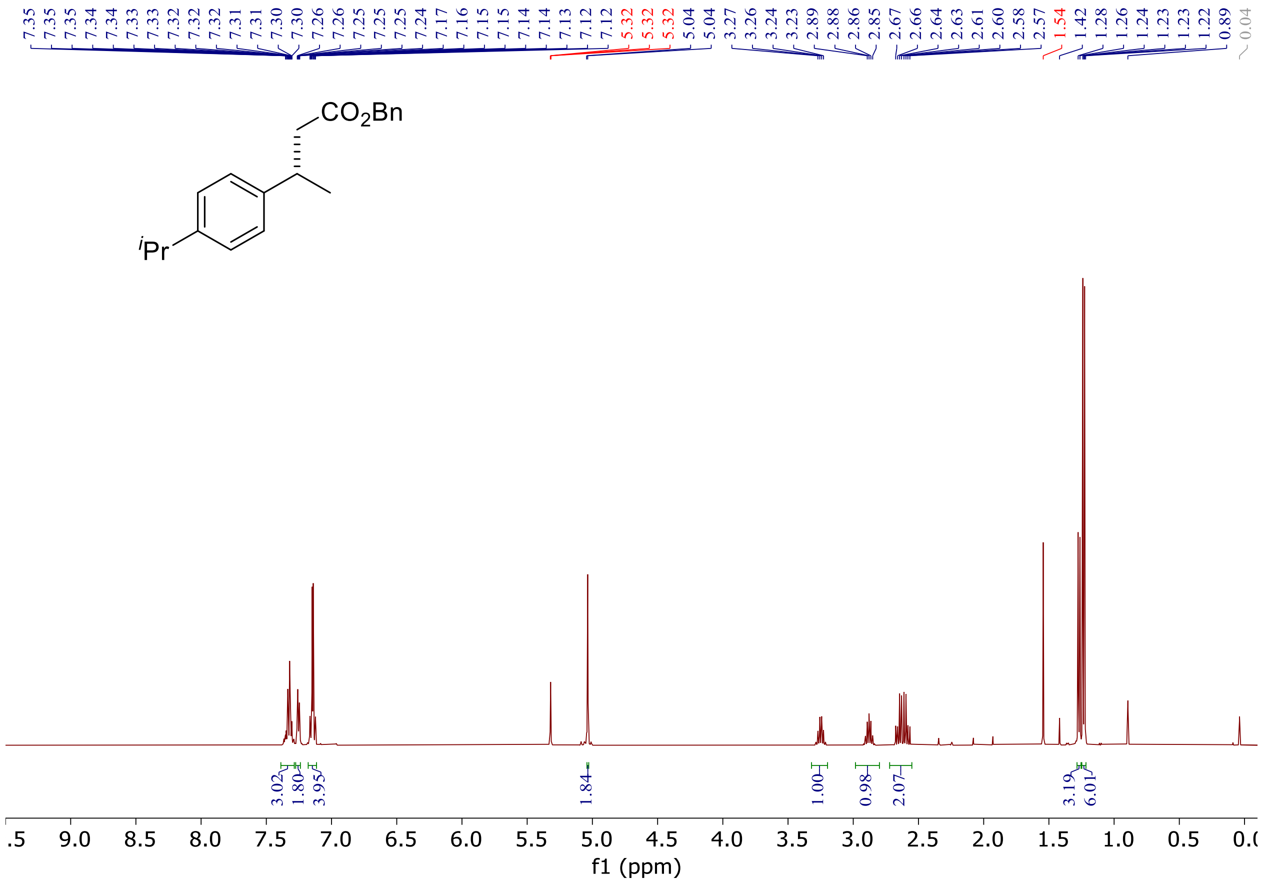
7.35
7.35
7.35
7.34
7.34
7.33
7.33
7.32
7.32
7.32
7.31
7.31
7.30
7.30
7.26
7.26
7.25
7.25
7.25
7.24
7.17
7.16
7.15
7.15
7.14
7.14
7.13
7.12
7.12
5.32
5.32
5.32
5.04
5.04
3.27
3.26
3.24
3.23
2.89
2.88
2.86
2.85
2.67
2.66
2.64
2.63
2.61
2.60
2.58
2.57
1.54
1.42
1.28
1.26
1.24
1.23
1.23
1.22
0.89
0.04
CO2Bn
iPr
3.02
1.80
3.95
1.84
1.00
0.98
2.07
3.19
6.01
.5
9.0
8.5
8.0
7.5
7.0
6.5
6.0
5.5
5.0
4.5
4.0
3.5
3.0
2.5
2.0
1.5
1.0
0.5
0.(
f1 (ppm)

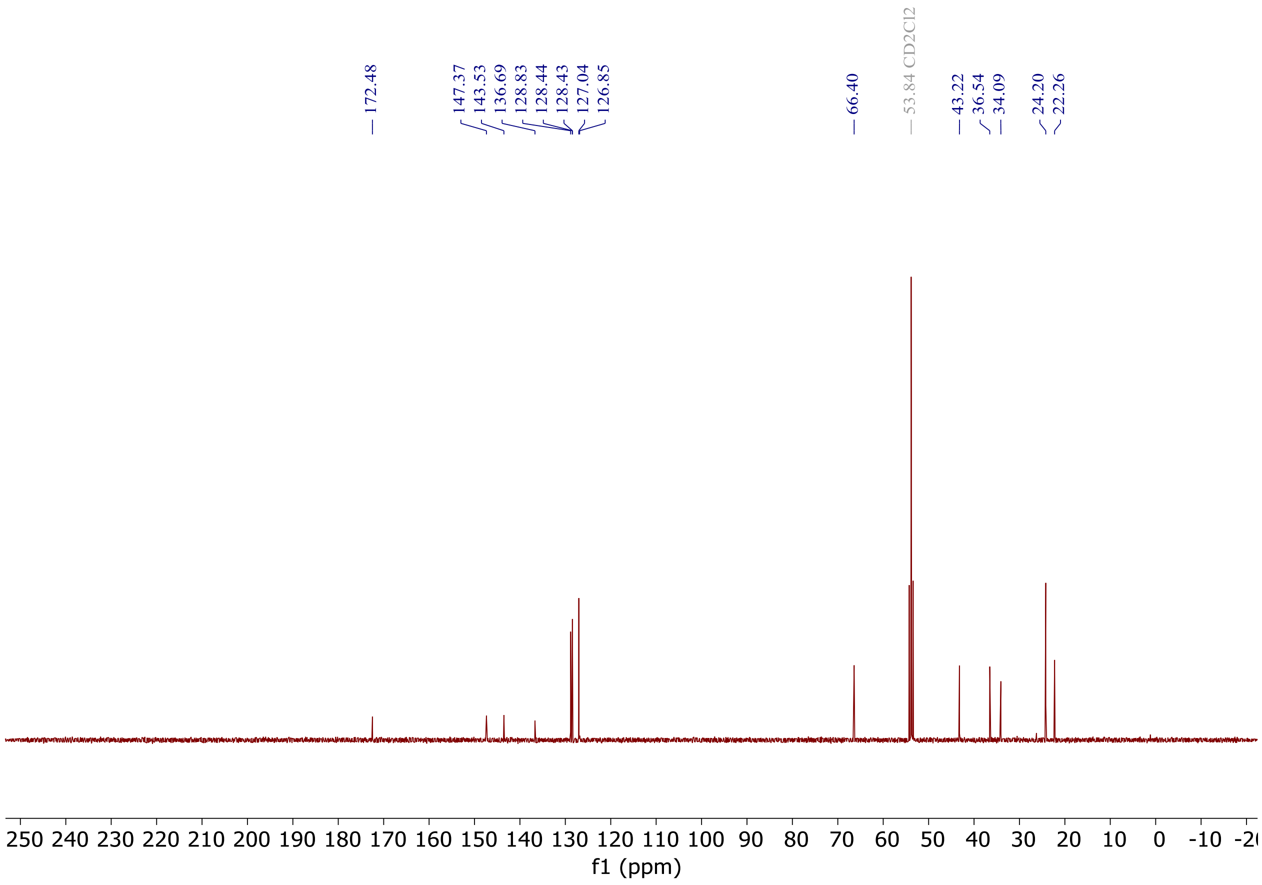
172.48
147.37
143.53
136.69
128.83
128.44
128.43
127.04
126.85
66.40
53.84 CD2Cl2
43.22
36.54
34.09
24.20
22.26
250
240
230
220
210
200
190
180
170
160
150
140
130
120
110
100
90
80
70
60
50
40
30
20
10
0
-10
-2(
f1 (ppm)

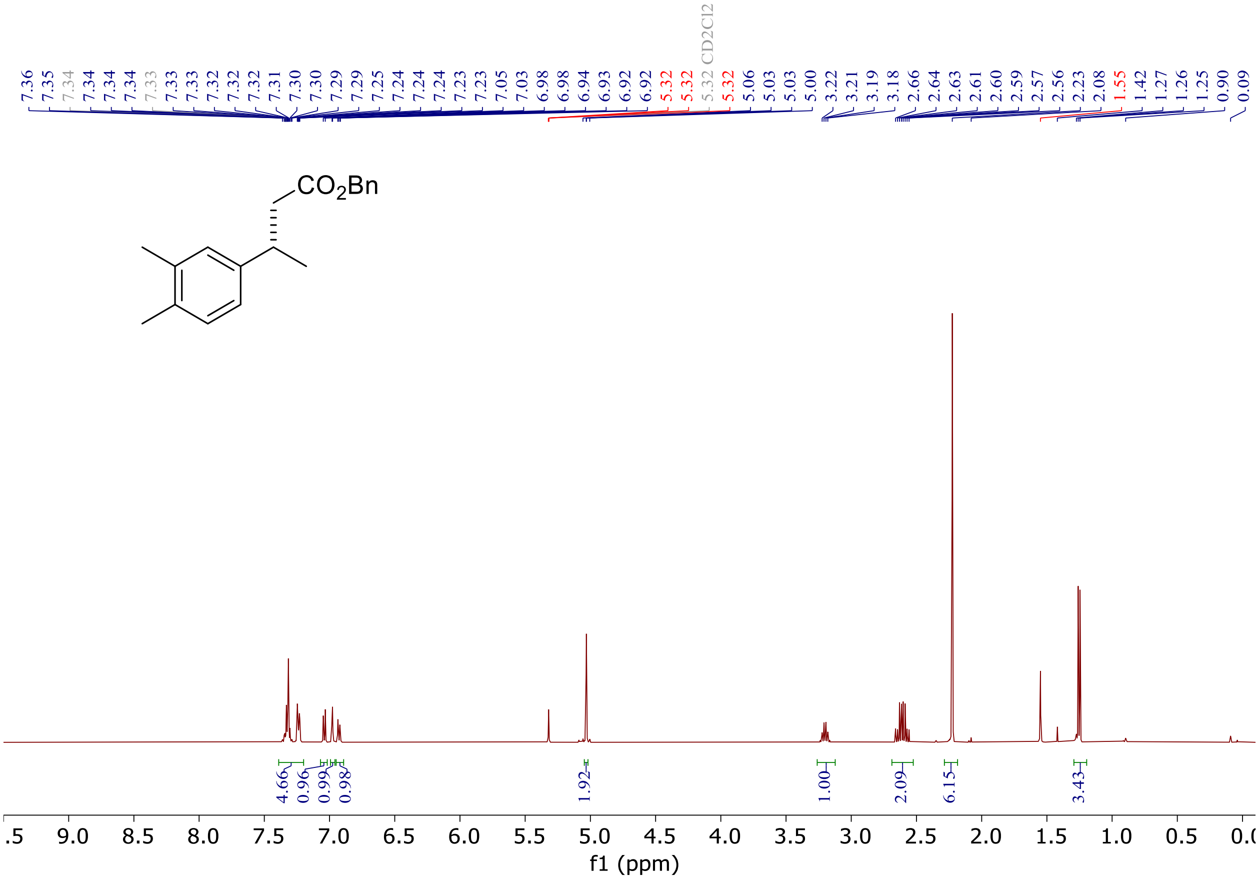
7.36 7.35 7.34 7.34 7.34 7.34 7.33 7.33 7.33 7.32 7.32 7.32 7.31 7.30 7.30 7.29 7.29 7.25 7.24 7.24 7.24 7.23 7.23 7.05 7.03 6.98 6.98 6.94 6.93 6.92 6.92 5.32 5.32 5.32 CD2Cl2 5.32 5.06 5.03 5.03 5.00 3.22 3.21 3.19 3.18 2.66 2.64 2.63 2.61 2.60 2.59 2.57 2.56 2.23 2.08 1.55 1.42 1.27 1.26 1.25 0.90 0.09
CO_2Bn
4.66
0.96
0.99
0.98
1.92
1.00
2.09
6.15
3.43
.5 9.0 8.5 8.0 7.5 7.0 6.5 6.0 5.5 5.0 4.5 4.0 3.5 3.0 2.5 2.0 1.5 1.0 0.5 0.0
f1 (ppm)

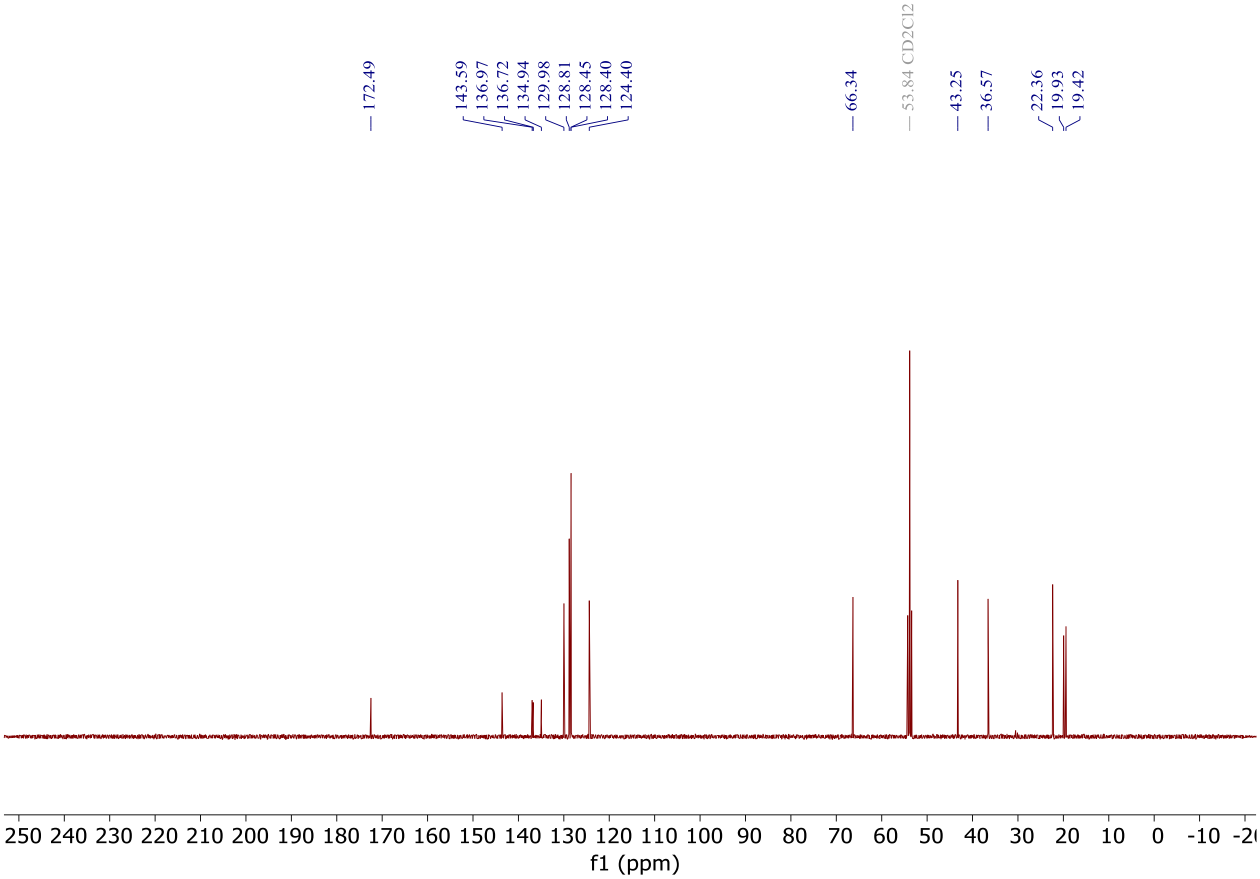
172.49
143.59 136.97 136.72 134.94 129.98 128.81 128.45 128.40 124.40
66.34
53.84 CD2Cl2
43.25
36.57
22.36 19.93 19.42
250 240 230 220 210 200 190 180 170 160 150 140 130 120 110 100 90 80 70 60 50 40 30 20 10 0 -10 -20
f1 (ppm)

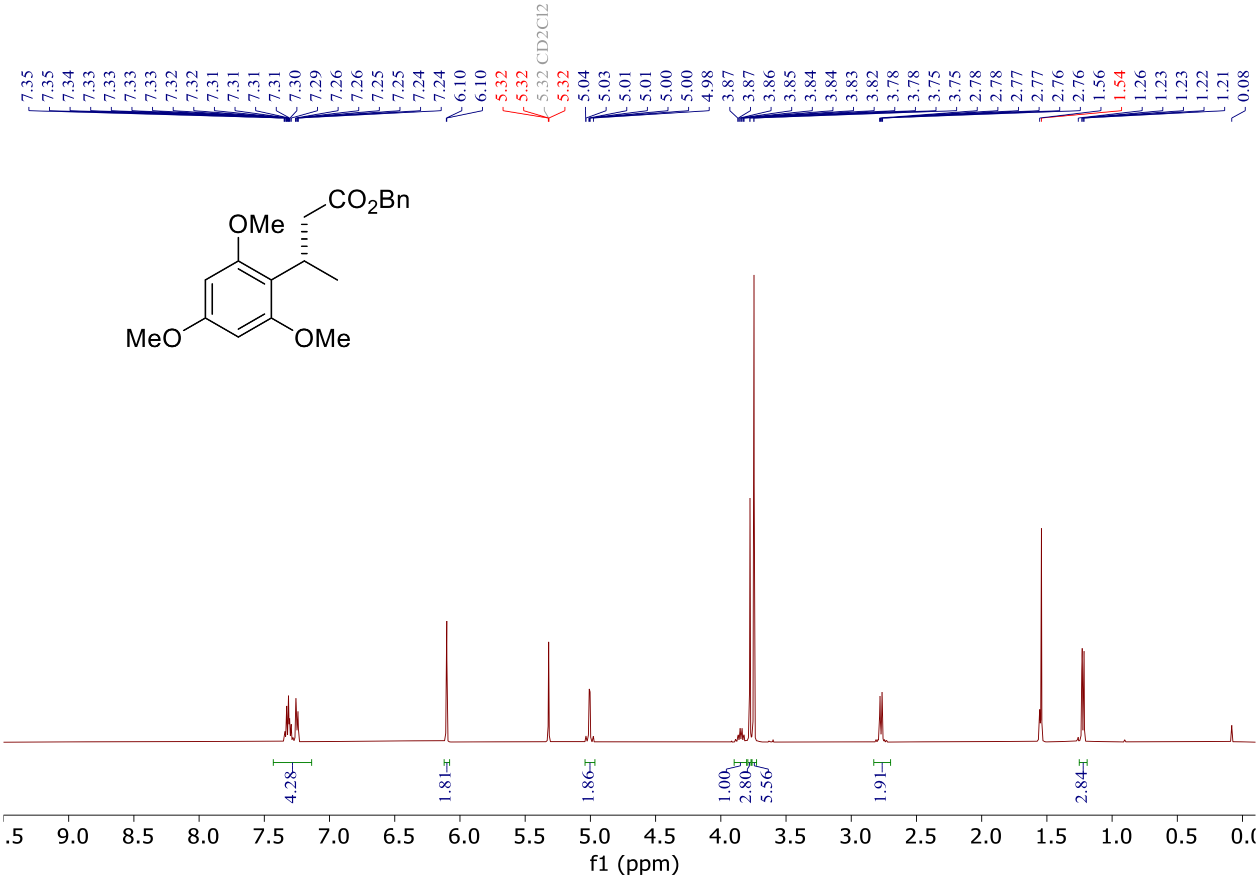
7.35
7.35
7.34
7.33
7.33
7.33
7.33
7.32
7.32
7.31
7.31
7.31
7.31
7.30
7.29
7.26
7.26
7.25
7.25
7.24
7.24
6.10
6.10
5.32
5.32
5.32 CD2Cl2
5.32
5.04
5.03
5.01
5.01
5.00
5.00
4.98
3.87
3.87
3.86
3.85
3.84
3.84
3.83
3.82
3.78
3.78
3.75
3.75
2.78
2.78
2.77
2.77
2.76
2.76
1.56
1.54
1.26
1.23
1.23
1.22
1.21
0.08
CO2Bn
OMe
MeO
OMe
4.28
1.81
1.86
1.00
2.80
5.56
1.91
2.84
.5
9.0
8.5
8.0
7.5
7.0
6.5
6.0
5.5
5.0
4.5
4.0
3.5
3.0
2.5
2.0
1.5
1.0
0.5
0.(
f1 (ppm)

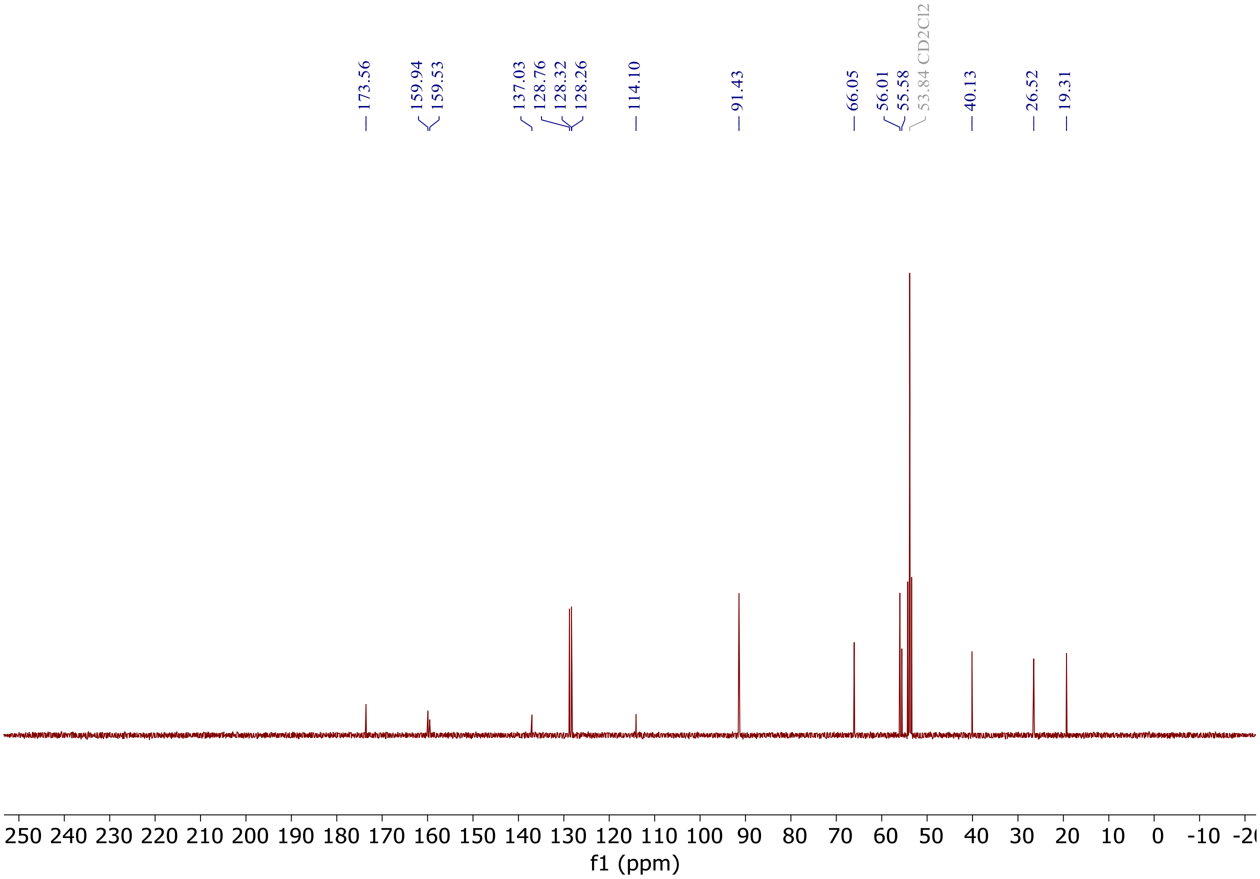
173.56
159.94
159.53
137.03
128.76
128.32
128.26
114.10
91.43
66.05
56.01
55.58
53.84 CD2Cl2
40.13
26.52
19.31
250
240
230
220
210
200
190
180
170
160
150
140
130
120
110
100
90
80
70
60
50
40
30
20
10
0
-10
-2(
f1 (ppm)

7.6. HPLC/GC Chromatograms:

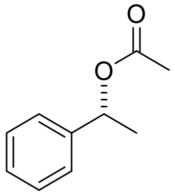

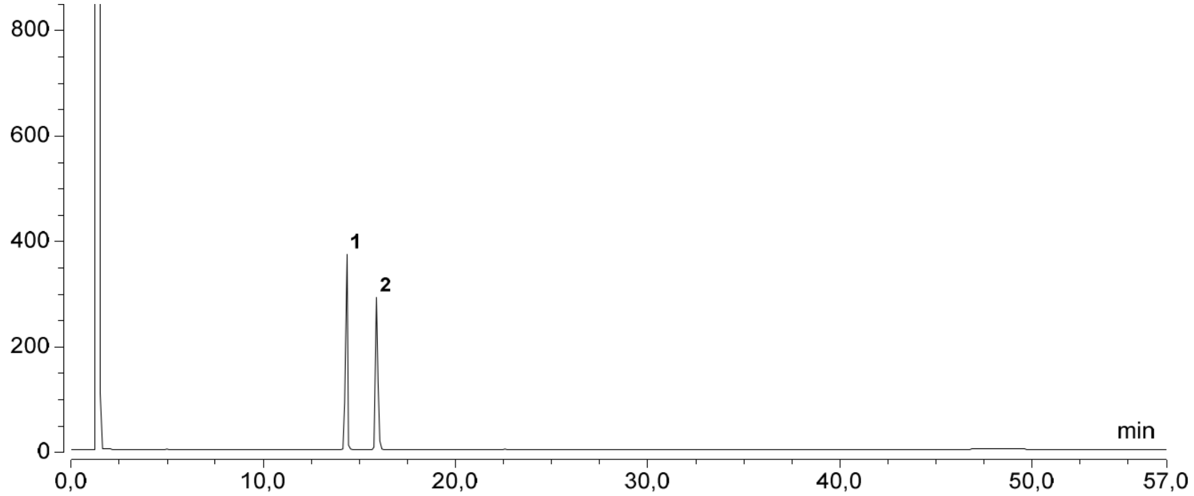

Peak	Time (Min.)	Area %
1	14.34	50.000
2	15.87	50.000
Total		100

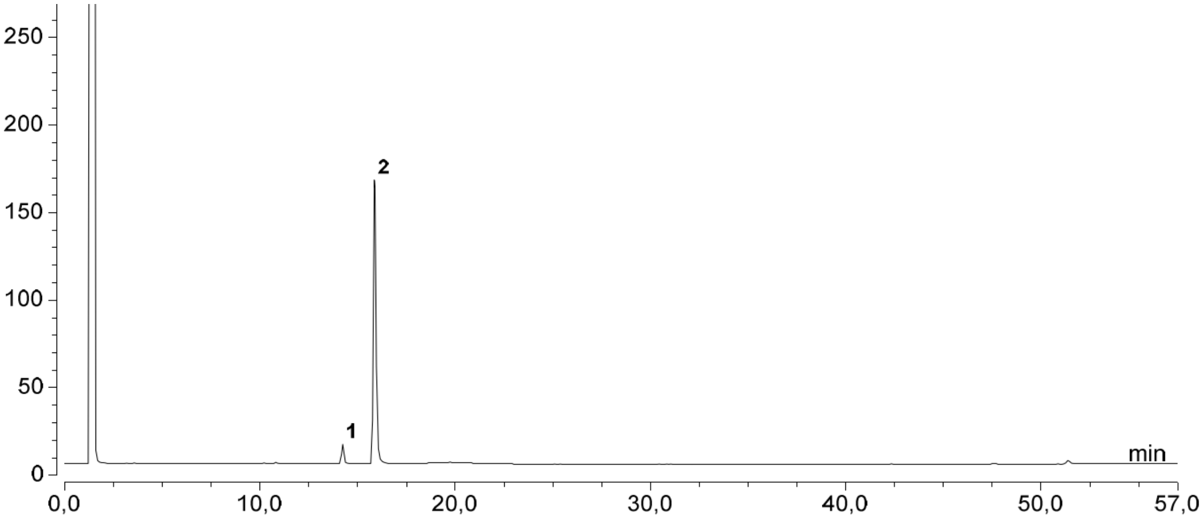

Peak	Time (Min.)	Area %
1	14.24	5.140
2	15.85	94.860
Total		100

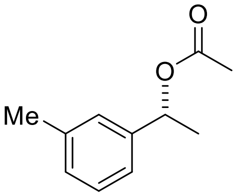

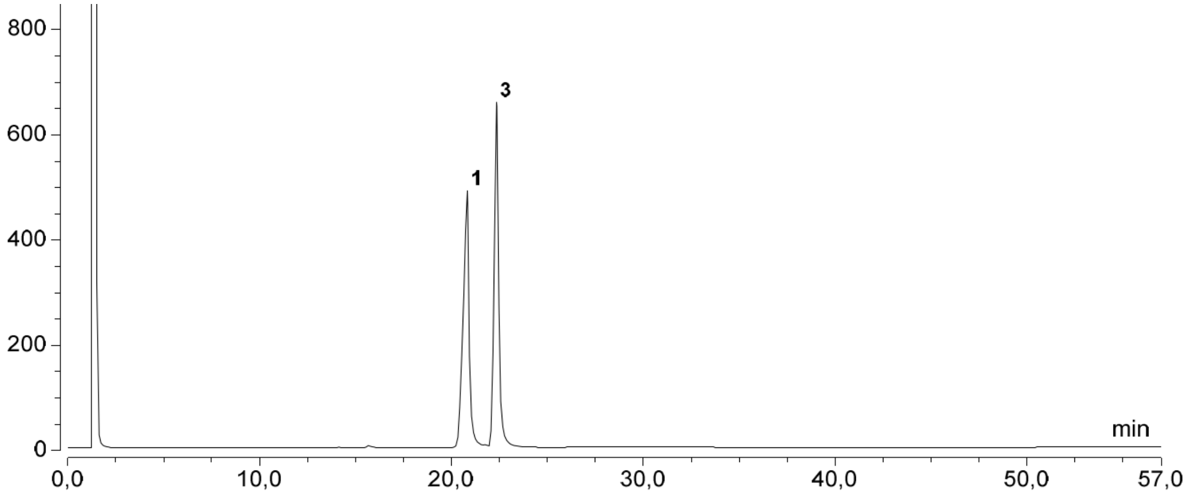

Peak	Time (Min.)	Area %
1	20.83	49.740
2	22.35	50.260
Total		100

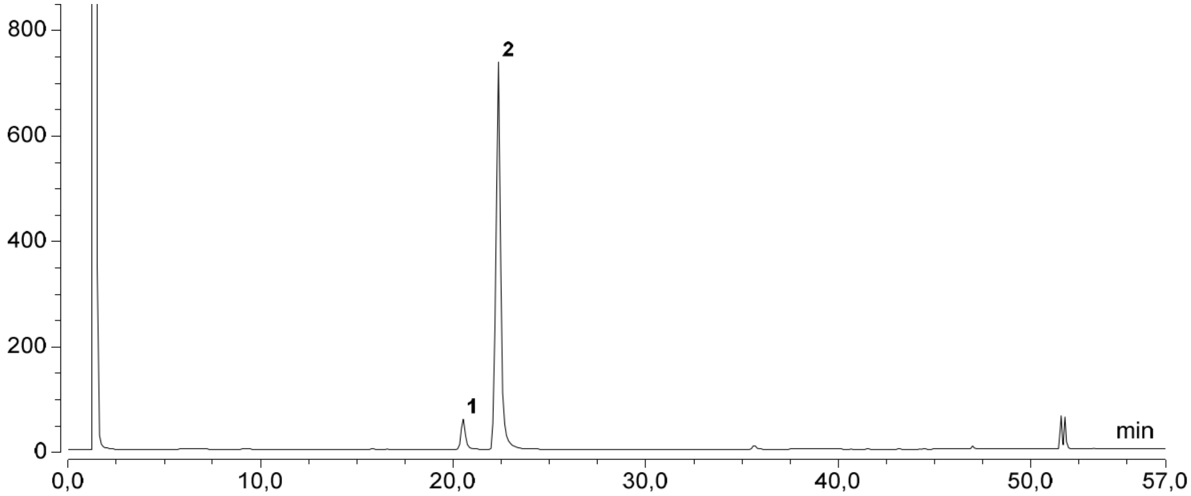

Peak	Time (Min.)	Area %
1	20.52	6.420
2	22.37	93.580
Total		100

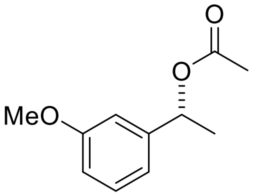

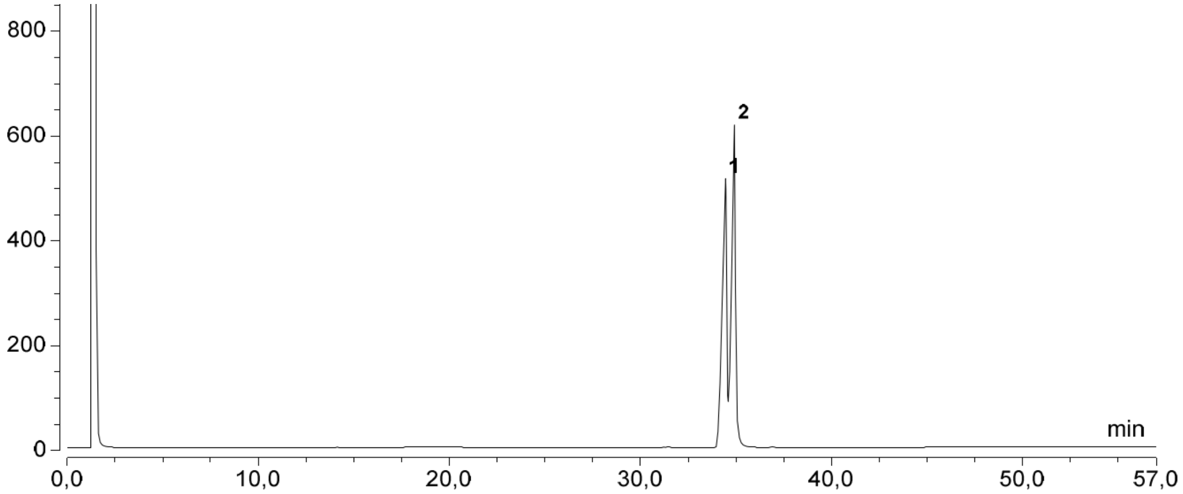

Peak	Time (Min.)	Area %
1	34.45	48.010
2	34.92	51.990
Total		100

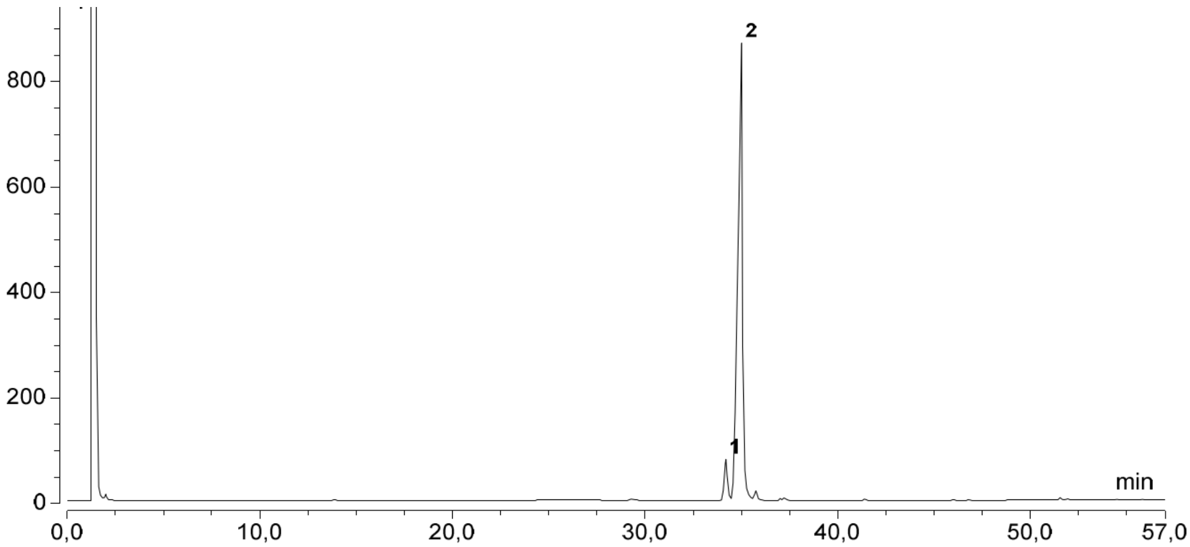

Peak	Time (Min.)	Area %
1	34.20	5.680
2	35.01	94.320
Total		100

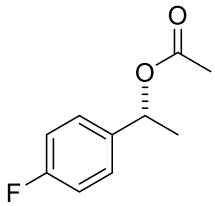

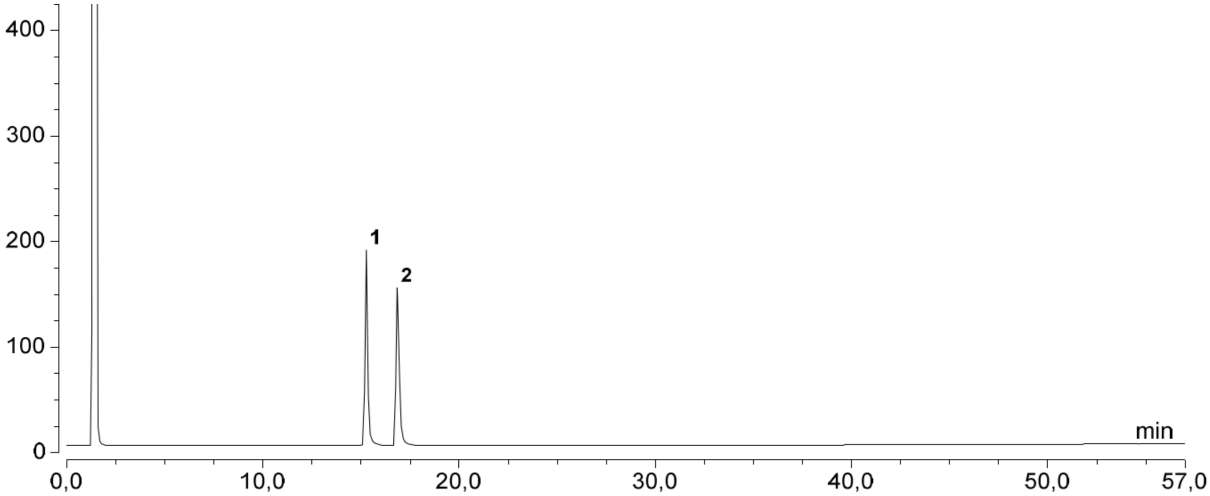

Peak	Time (Min.)	Area %
1	15.27	50.010
2	16.84	49.990
Total		100

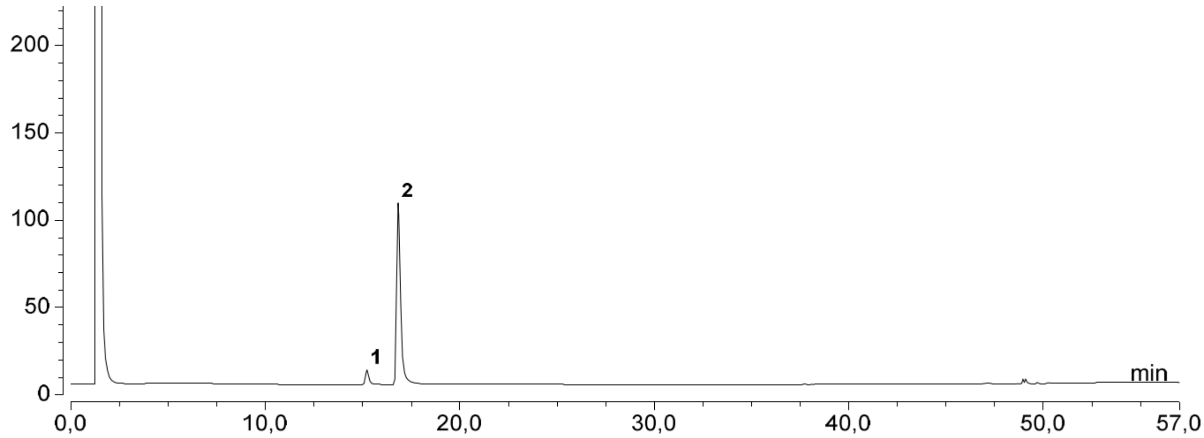

Peak	Time (Min.)	Area %
1	15.23	6.420
2	16.83	93.580
Total		100

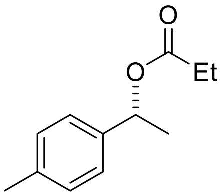

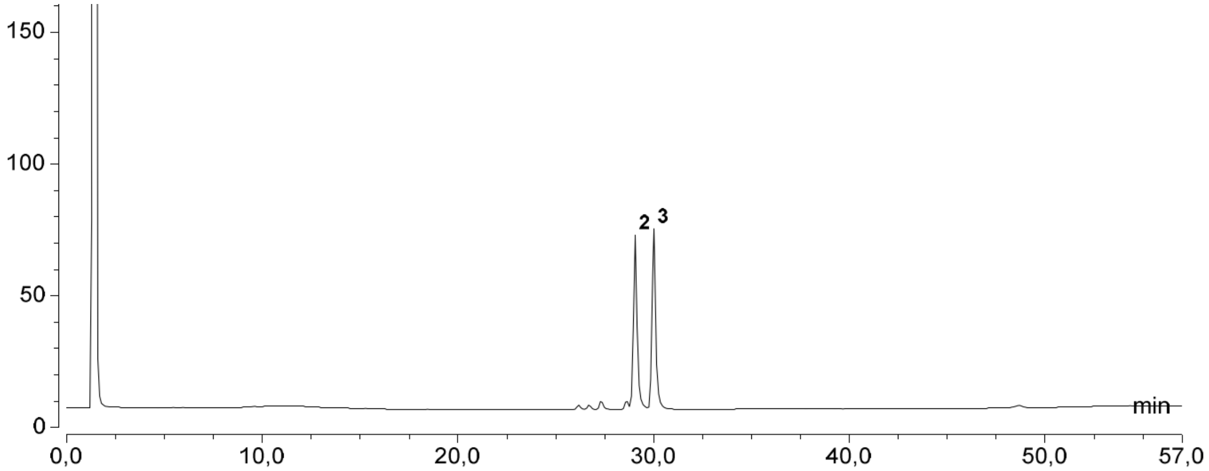

Peak	Time (Min.)	Area %
1	29.06	49.780
2	30.00	50.220
Total		100

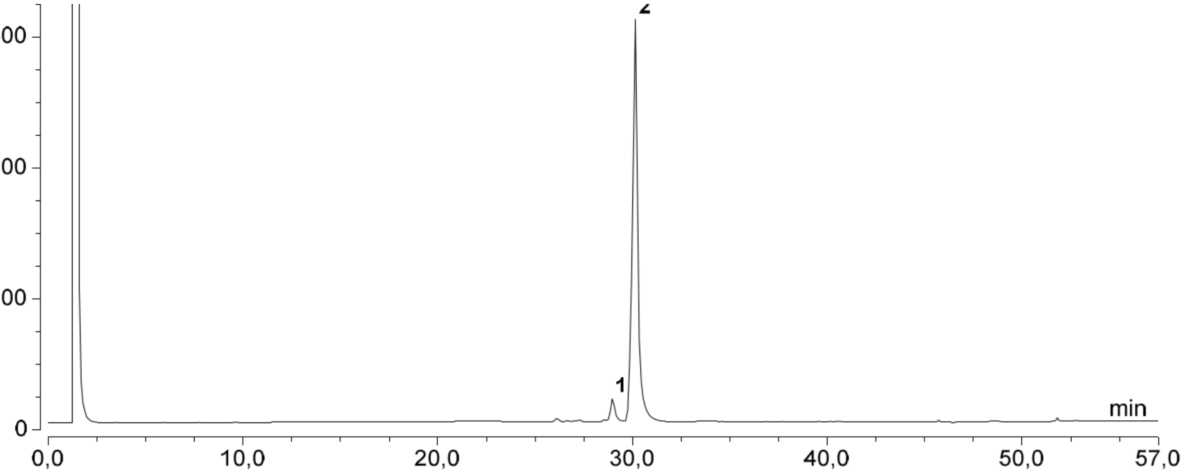

Peak	Time (Min.)	Area %
1	28.96	4.170
2	30.15	95.830
Total		100

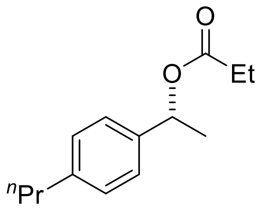

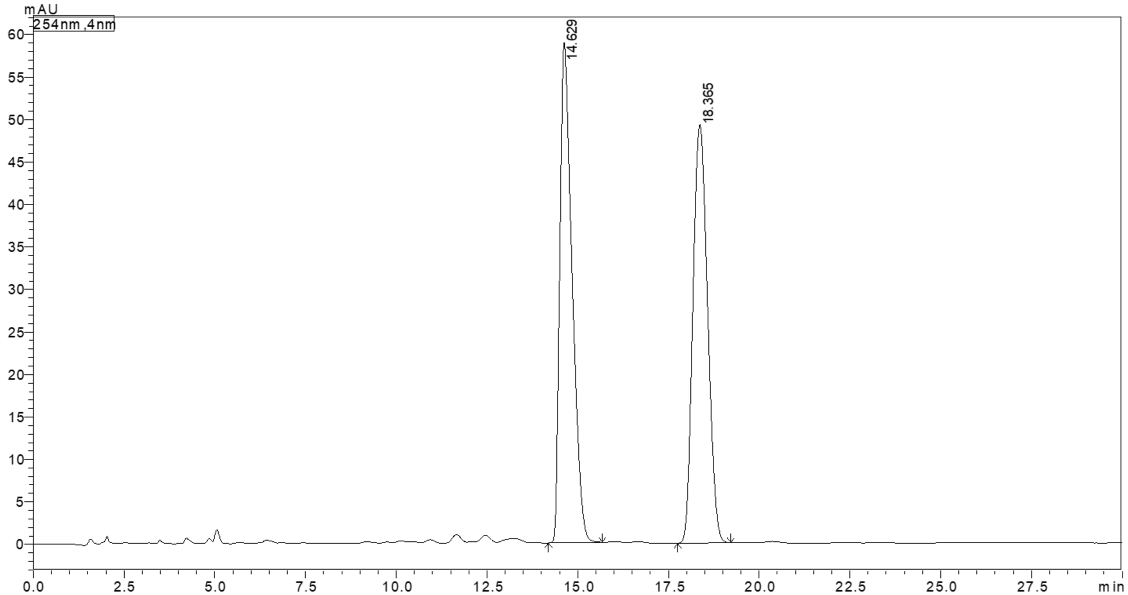

Peak	Time (Min.)	Area %
1	14.63	49.985
2	18.37	50.015
Total		100

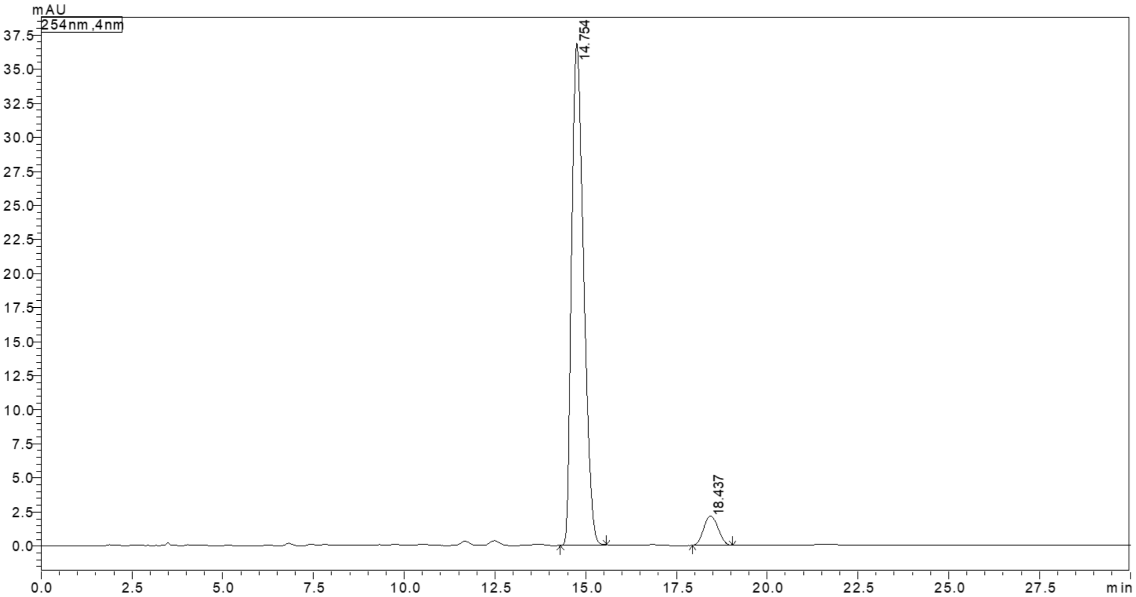

Peak	Time (Min.)	Area %
1	14.75	93.463
2	18.44	6.537
Total		100

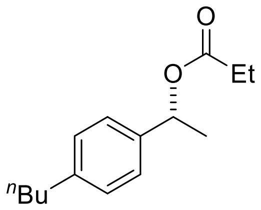

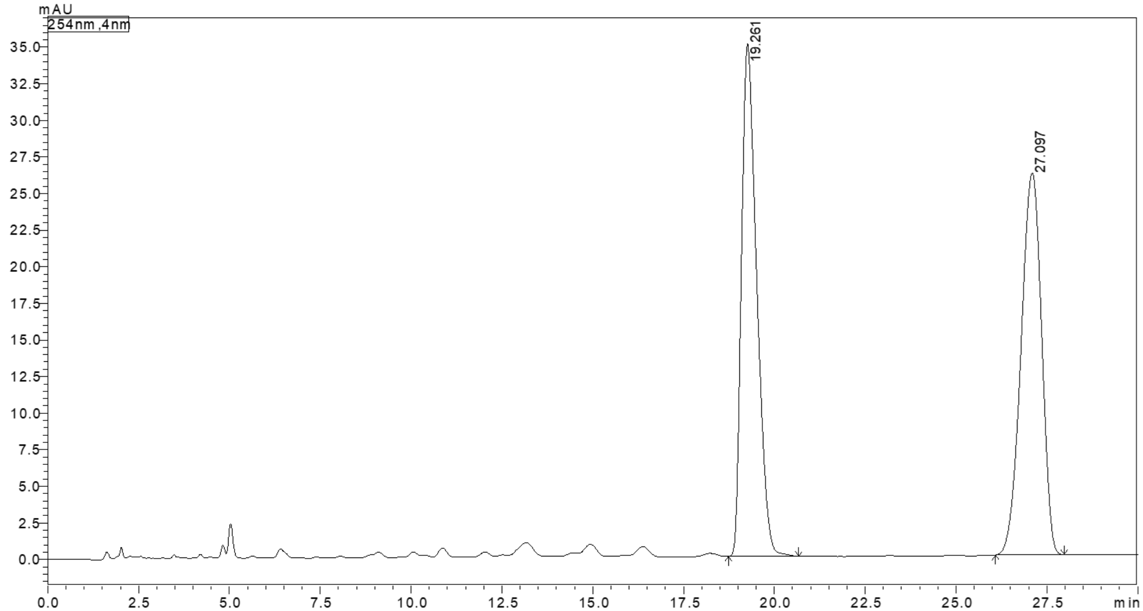

Peak	Time (Min.)	Area %
1	19.26	49.931
2	27.10	50.069
Total		100

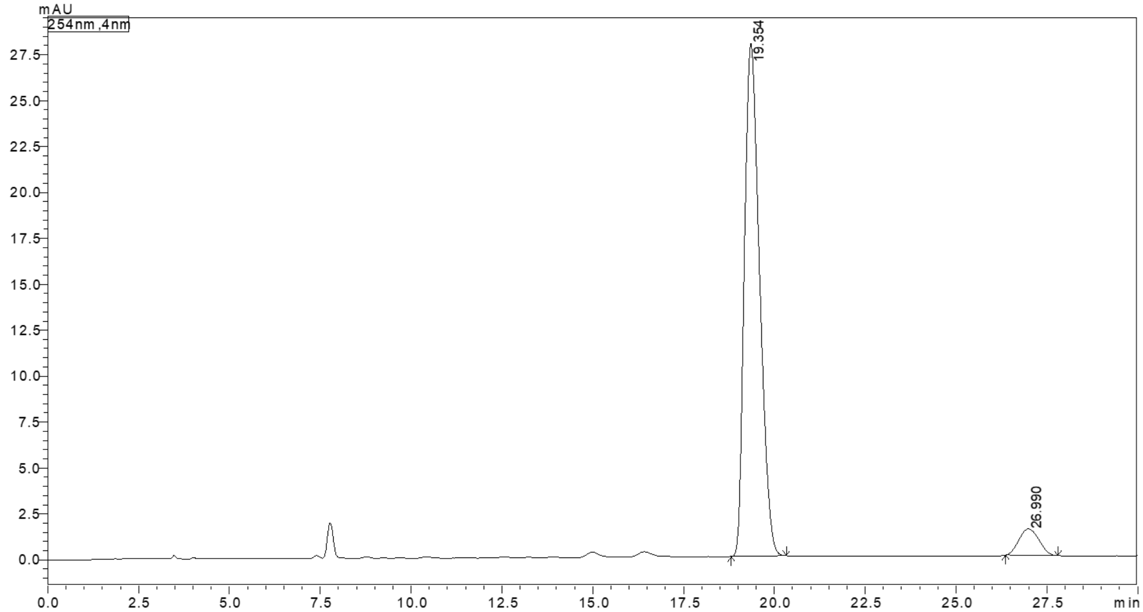

Peak	Time (Min.)	Area %
1	19.35	93.654
2	26.99	6.346
Total		100

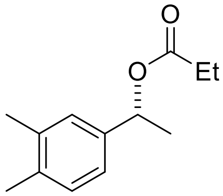

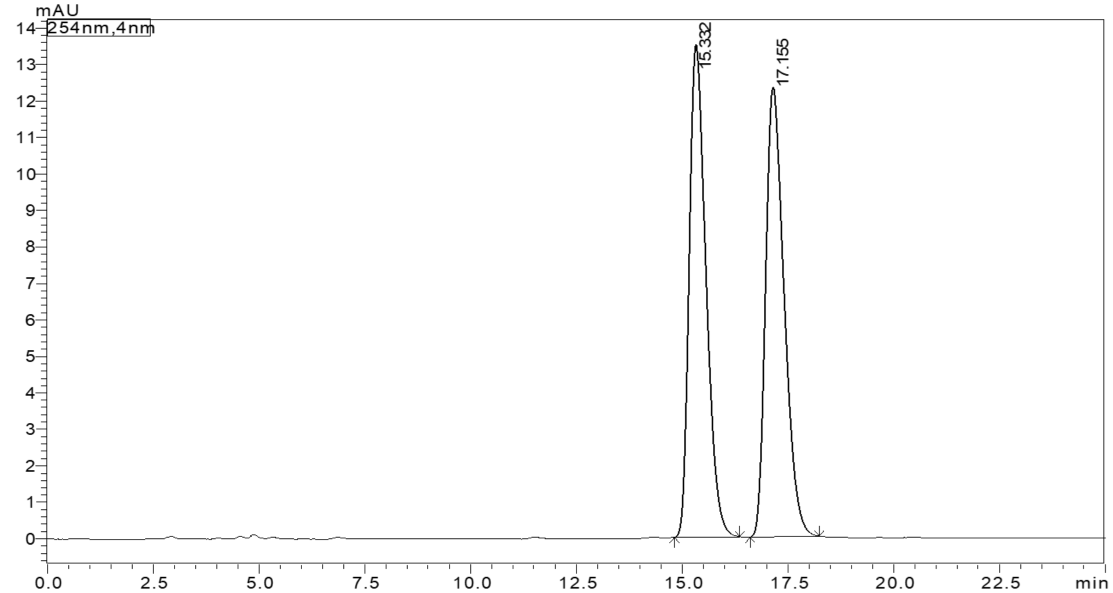

Peak	Time (Min.)	Area %
1	15.33	49.766
2	17.16	50.234
Total		100

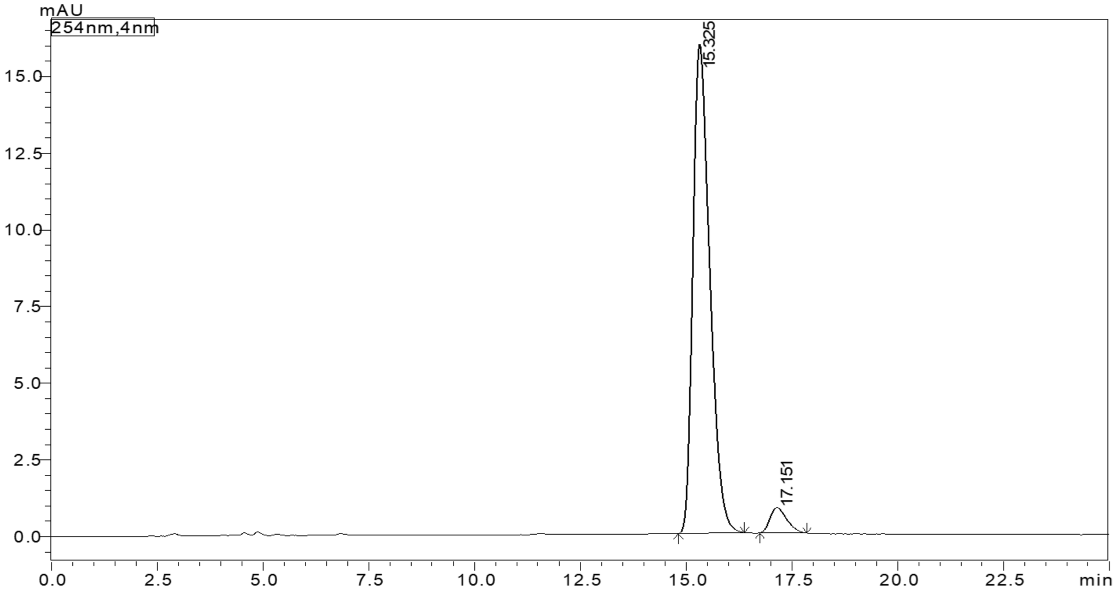

Peak	Time (Min.)	Area %
1	15.32	95.075
2	17.15	4.925
Total		100

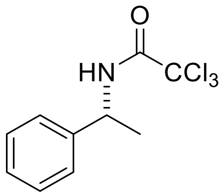

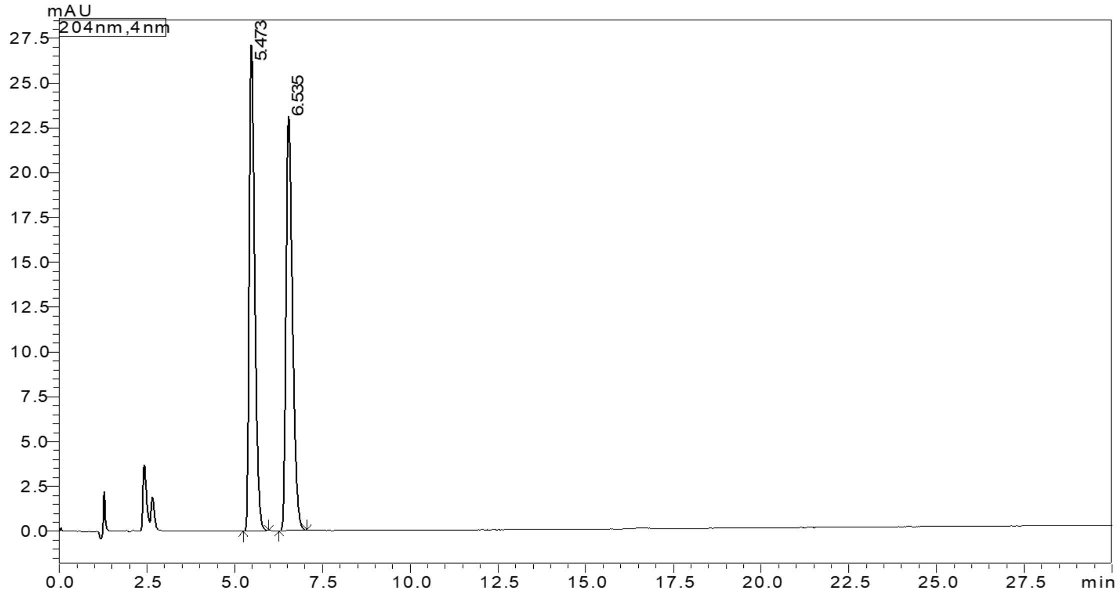

Peak	Time (Min.)	Area %
1	5.47	49.948
2	6.56	50.052
Total		100

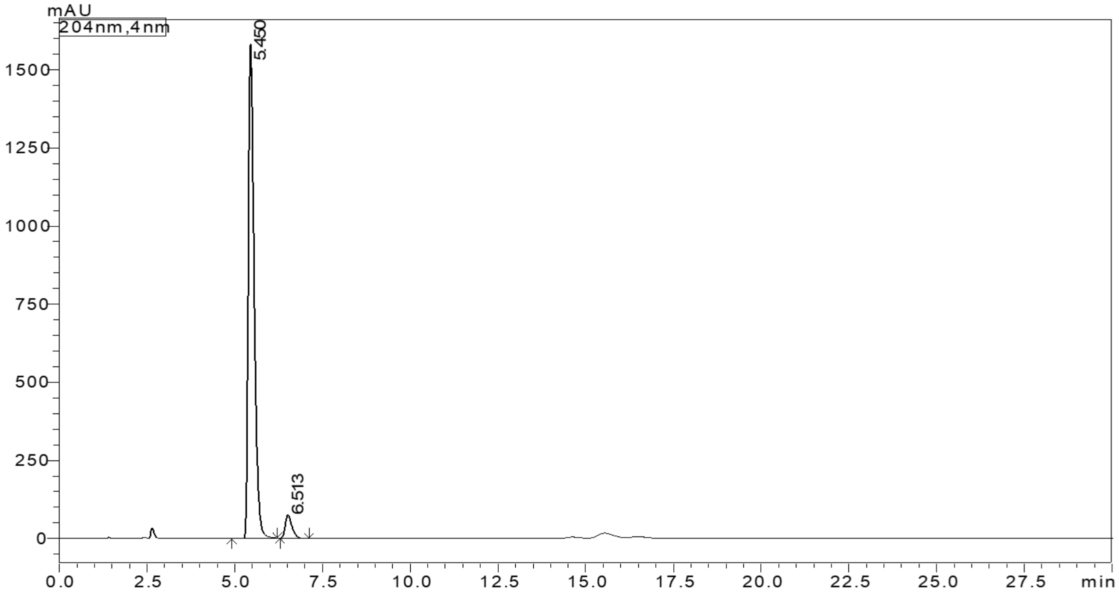

Peak	Time (Min.)	Area %
1	5.45	94.918
2	6.51	5.082
Total		100

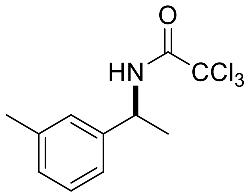

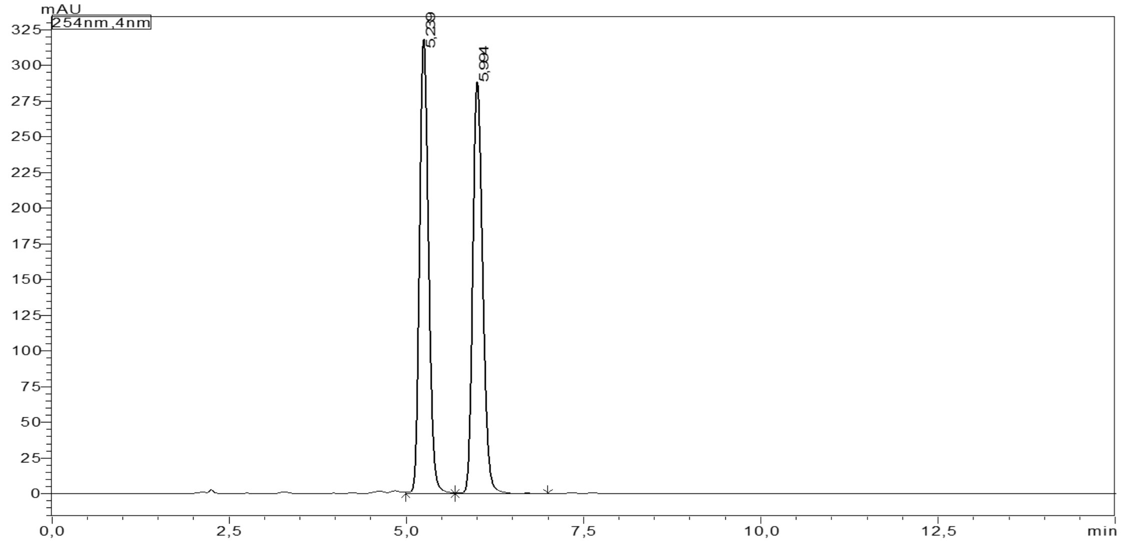

Peak	Time (Min.)	Area %
1	5.24	49.946
2	5.99	50.054
Total		100

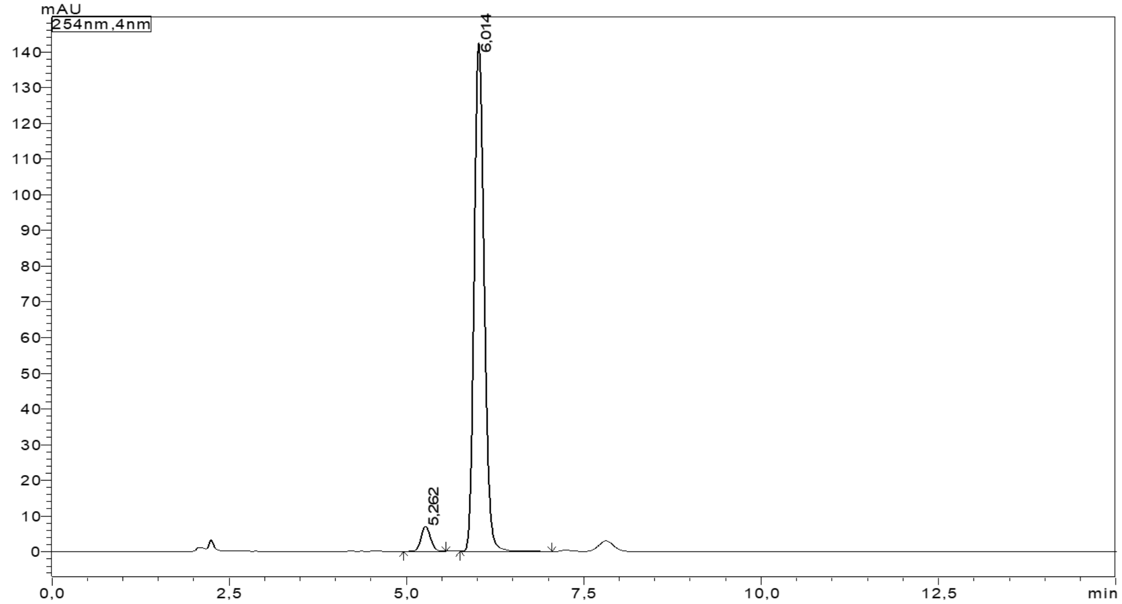

Peak	Time (Min.)	Area %
1	5.26	4.433
2	6.01	95.567
Total		100

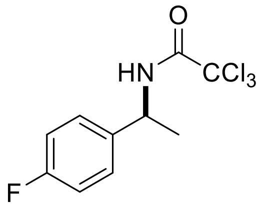

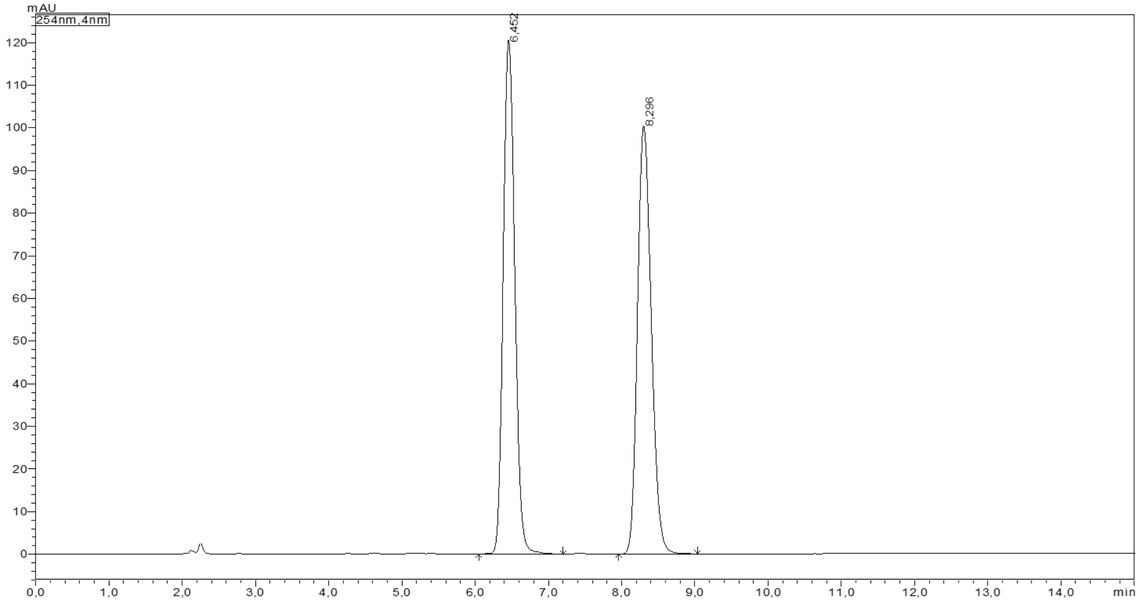

Peak	Time (Min.)	Area %
1	6.45	50.134
2	8.30	49.866
Total		100

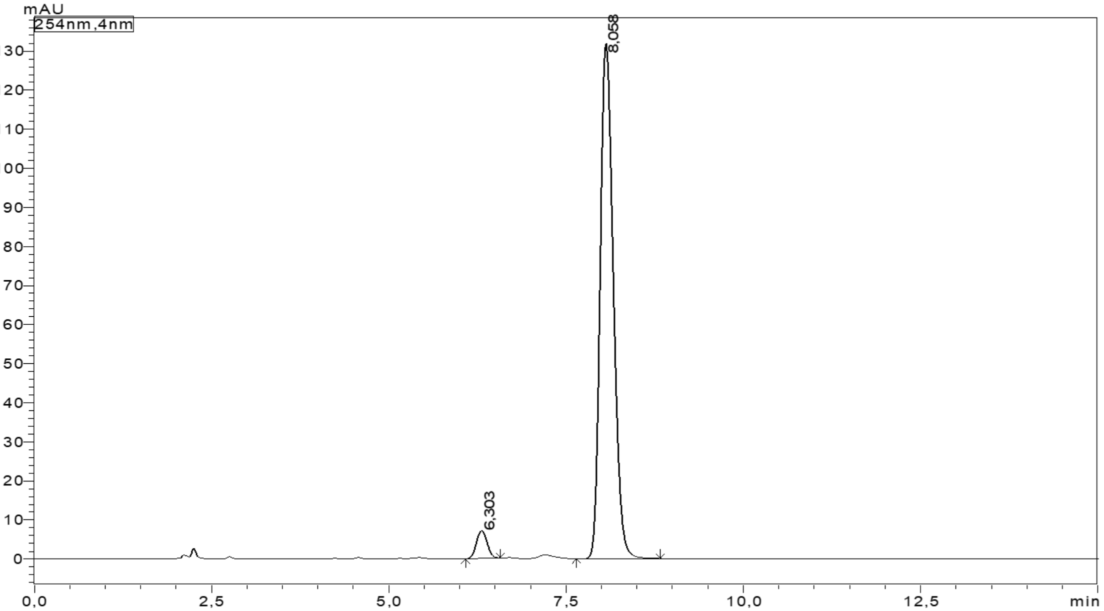

Peak	Time (Min.)	Area %
1	6.30	4.149
2	8.06	95.851
Total		100

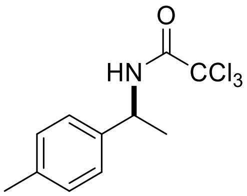

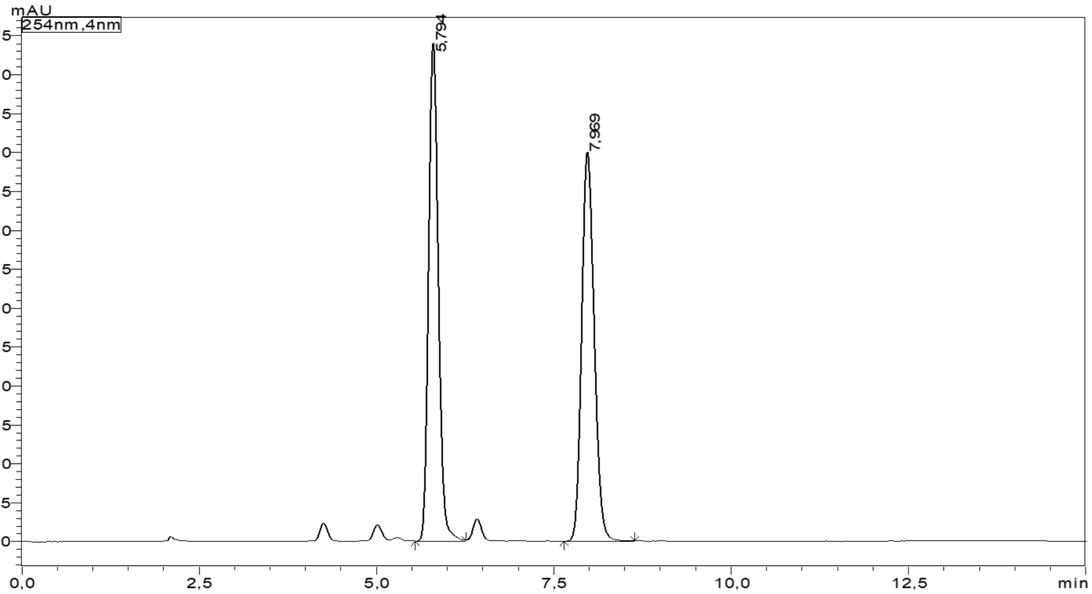

Peak	Time (Min.)	Area %
1	5.79	50.092
2	7.97	49.908
Total		100

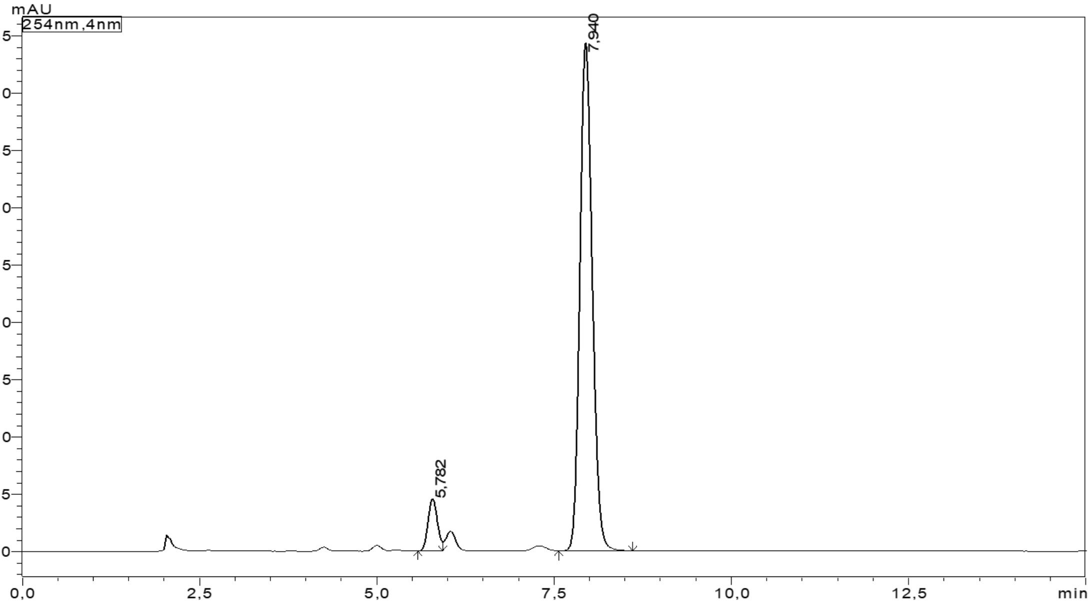

Peak	Time (Min.)	Area %
1	5.78	7.286
2	7.94	92.714
Total		100

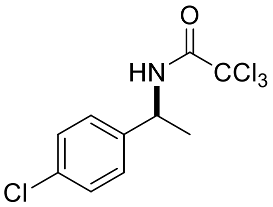

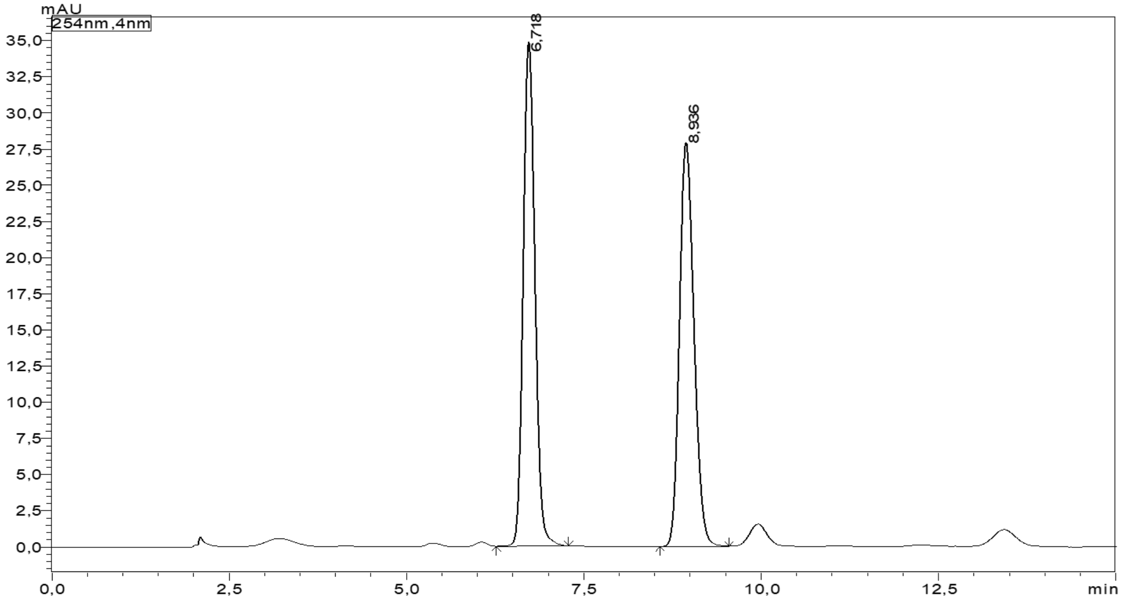

Peak	Time (Min.)	Area %
1	6.72	50.305
2	8.94	49.695
Total		100

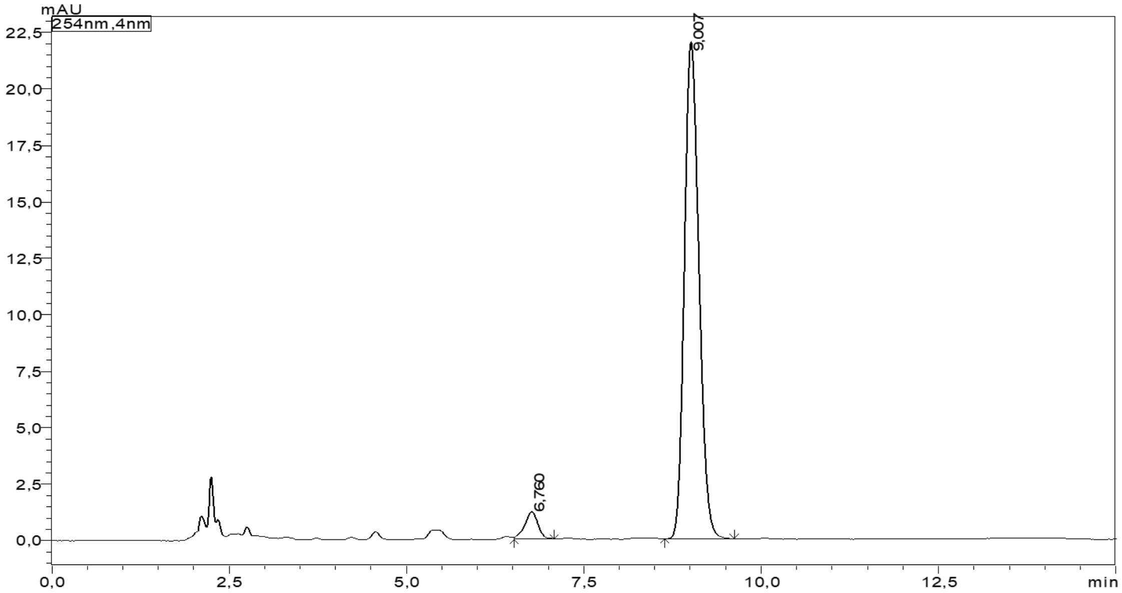

Peak	Time (Min.)	Area %
1	6.76	4.734
2	9.01	95.266
Total		100

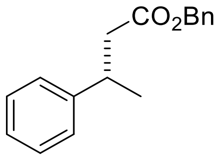

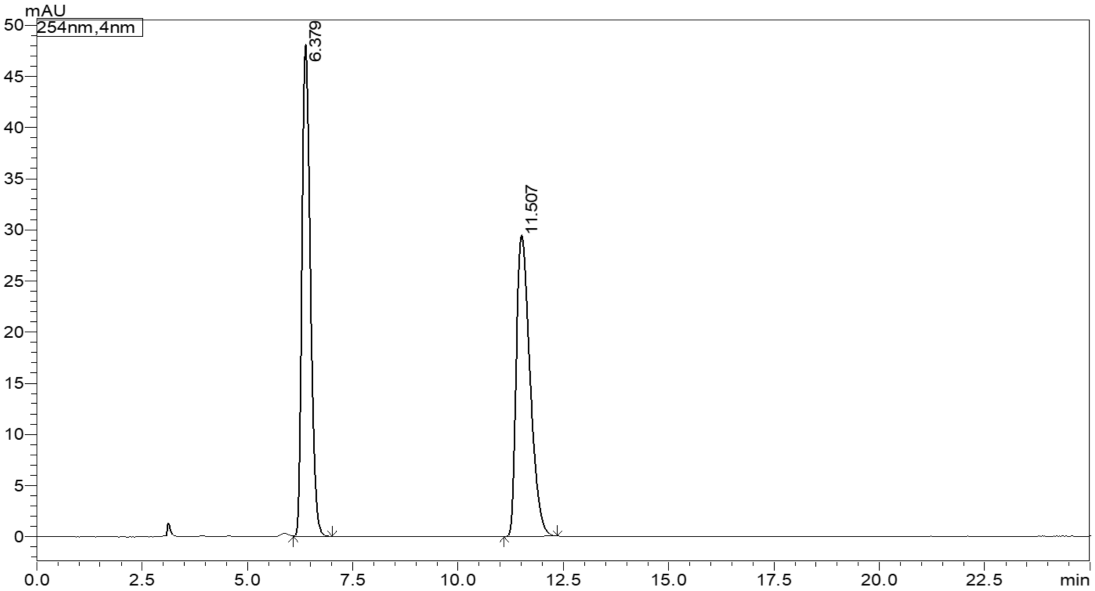

Peak	Time (Min.)	Area %
1	6.38	50.029
2	11.51	49.971
Total		100

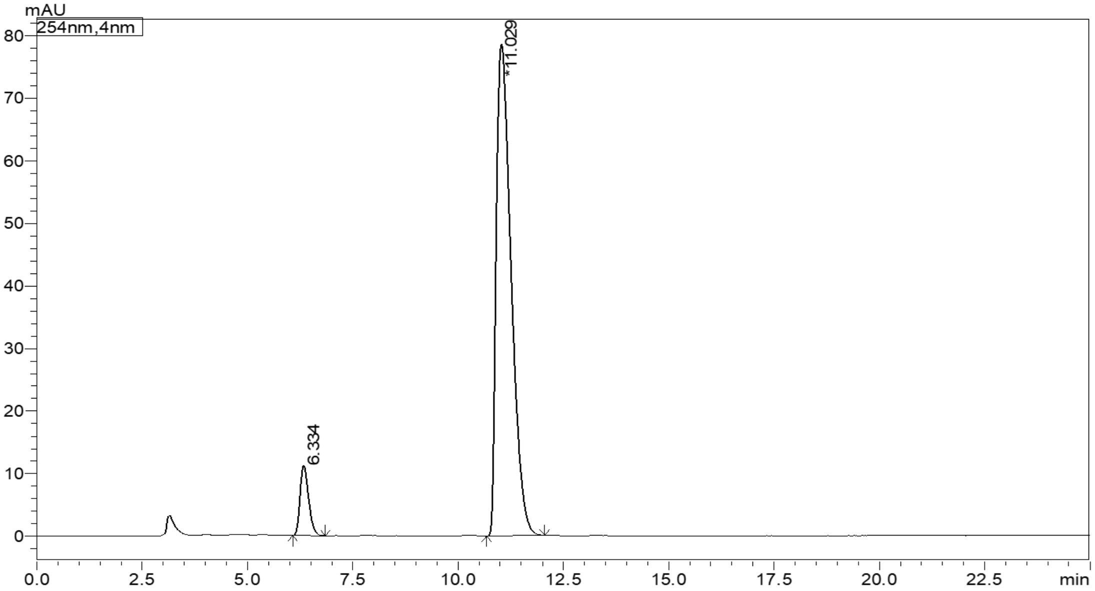

Peak	Time (Min.)	Area %
1	6.33	7.577
2	11.03	92.423
Total		100

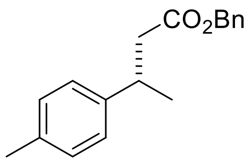

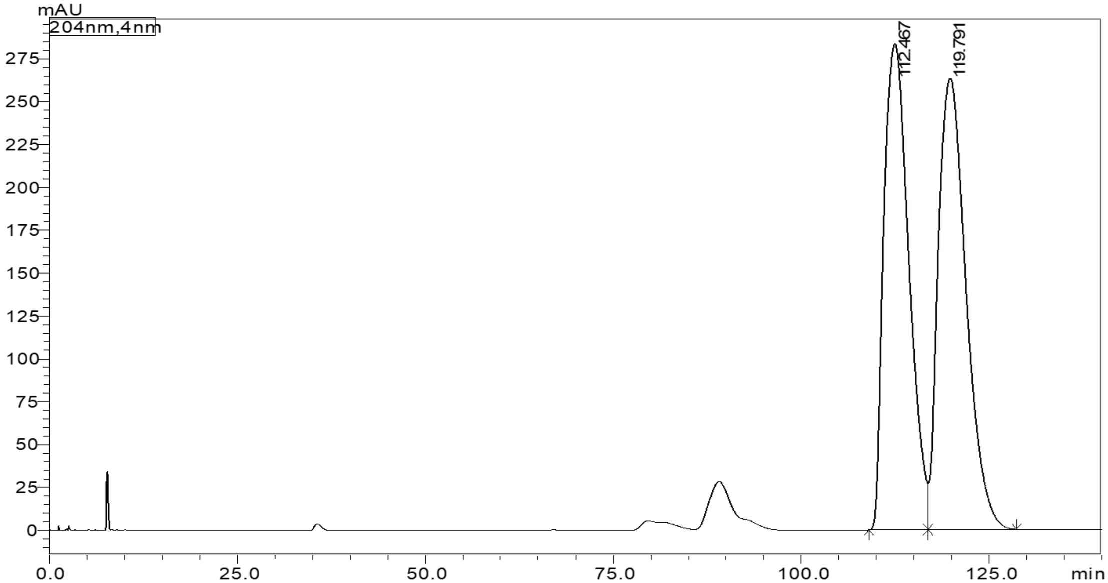

Peak	Time (Min.)	Area %
1	112.47	49.167
2	119.79	50.833
Total		100

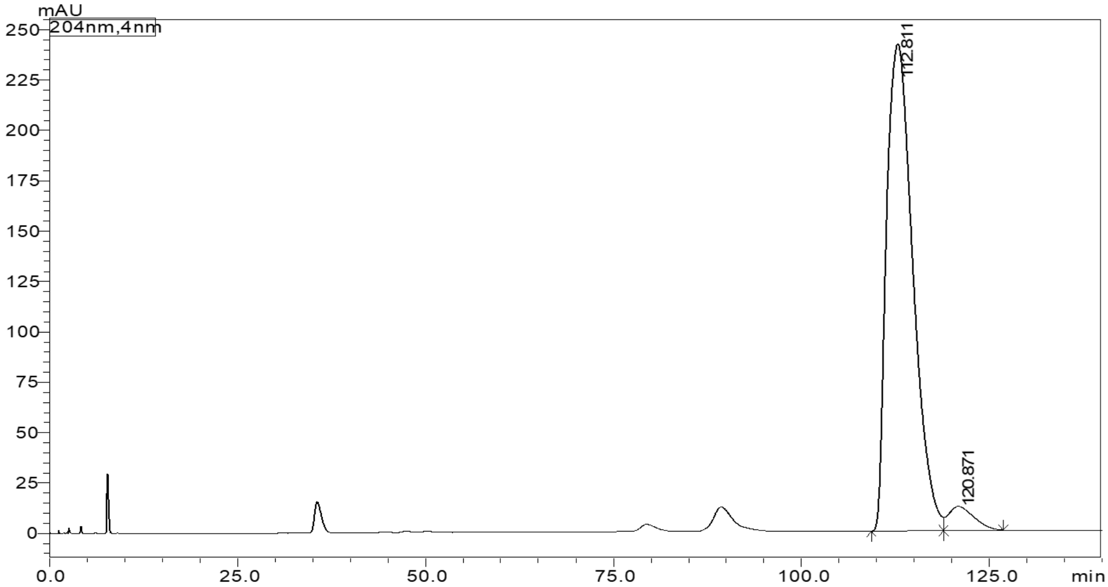

Peak	Time (Min.)	Area %
1	112.81	95.401
2	120.87	4.599
Total		100

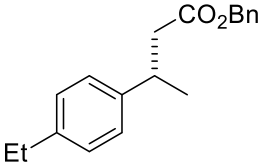

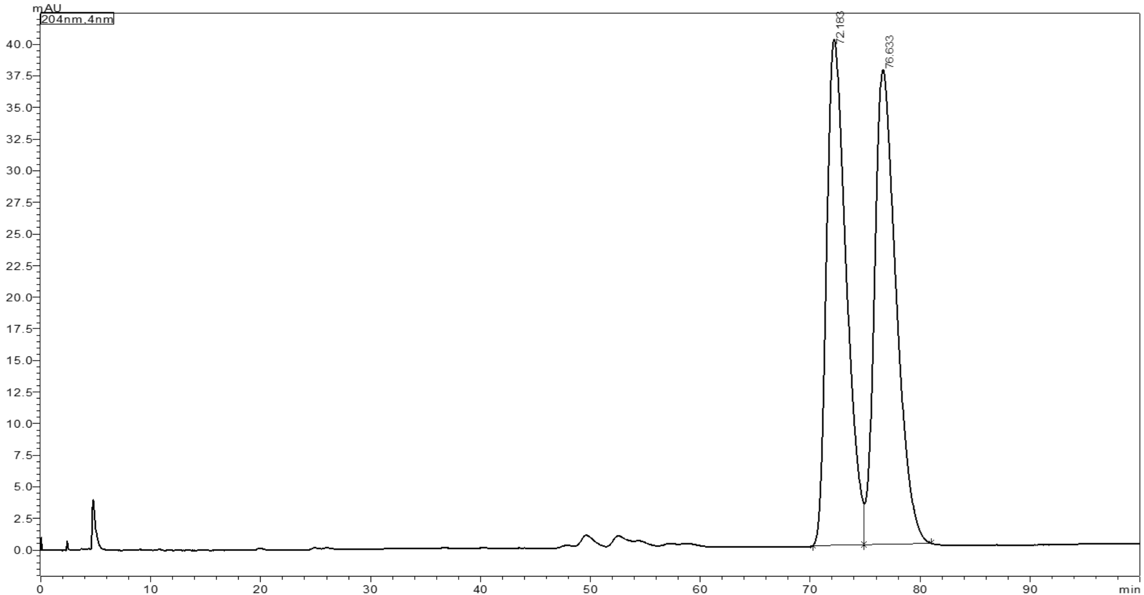

Peak	Time (Min.)	Area %
1	72.18	49.406
2	76.63	50.594
Total		100

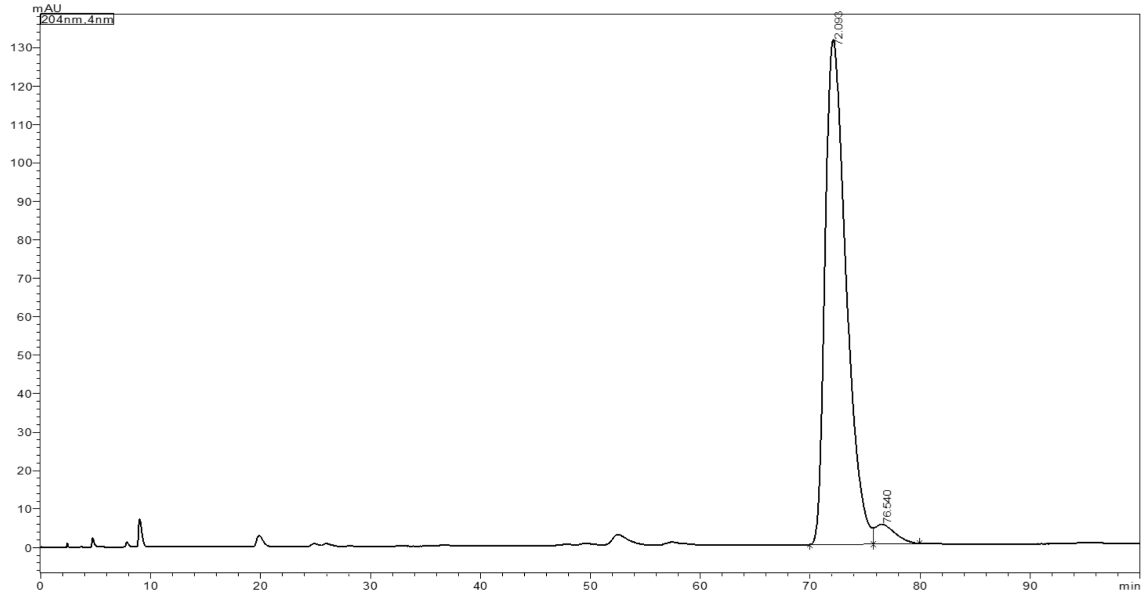

Peak	Time (Min.)	Area %
1	72.10	96.426
2	76.54	3.574
Total		100

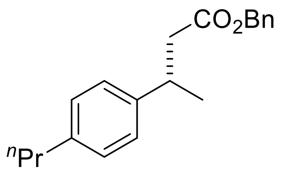

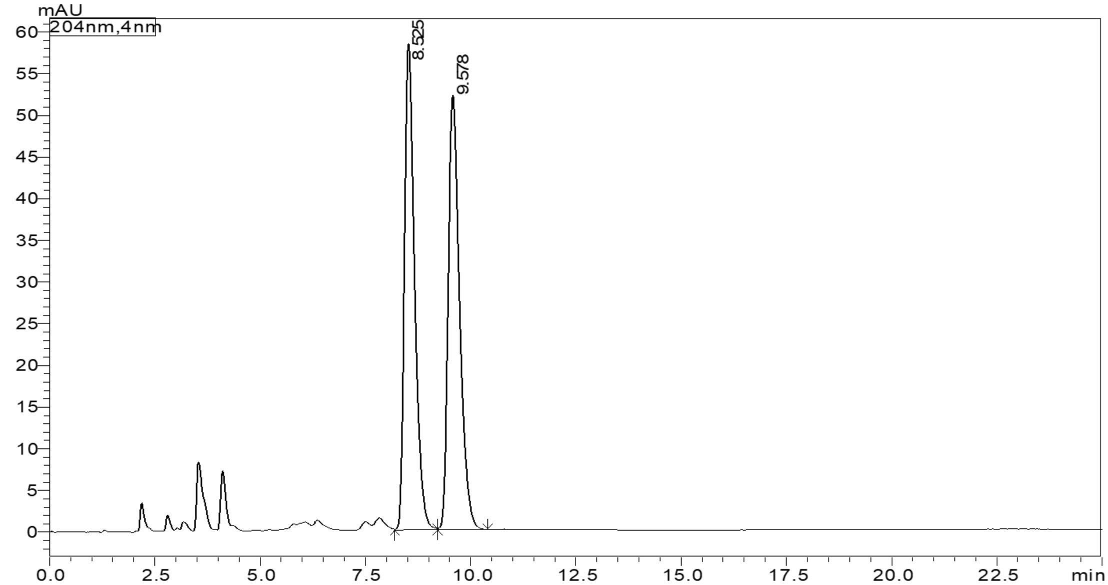

Peak	Time (Min.)	Area %
1	8.53	49.996
2	9.58	50.004
Total		100

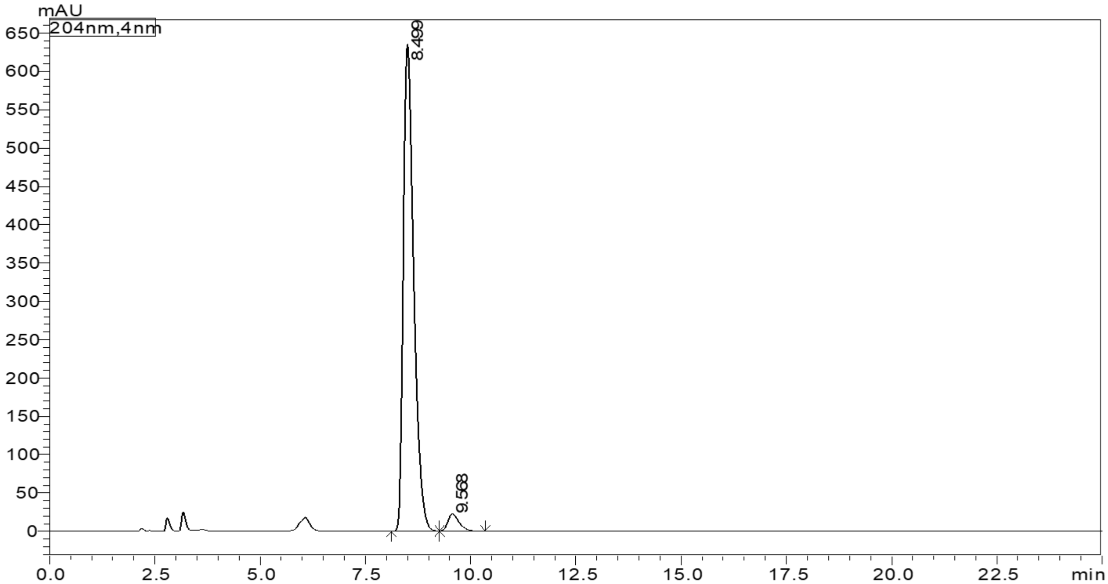

Peak	Time (Min.)	Area %
1	8.50	96.325
2	9.57	3.675
Total		100

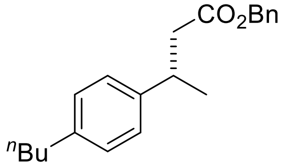

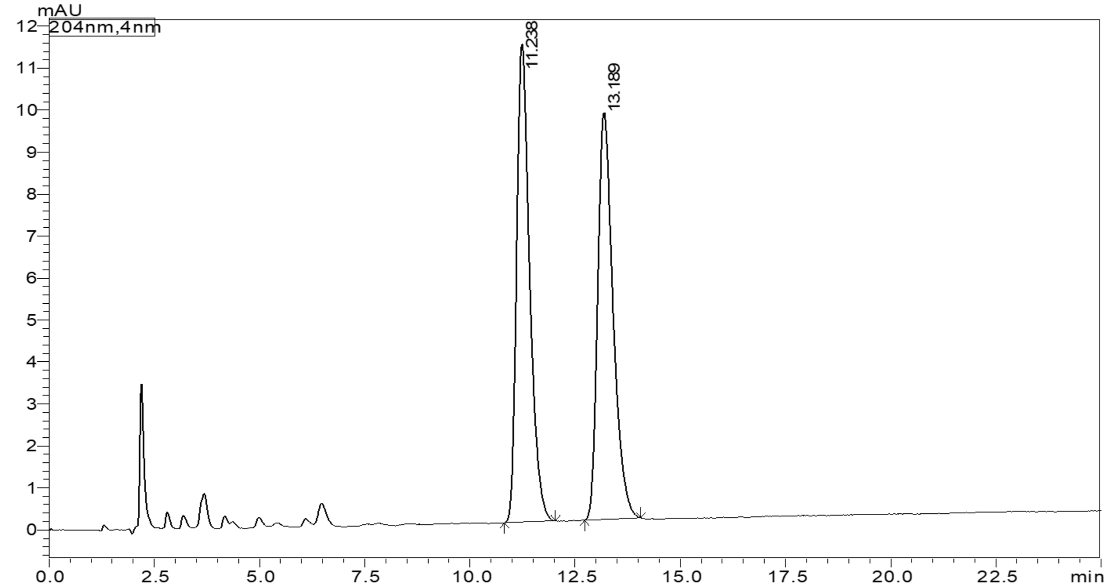

Peak	Time (Min.)	Area %
1	11.24	50.077
2	13.19	49.923
Total		100

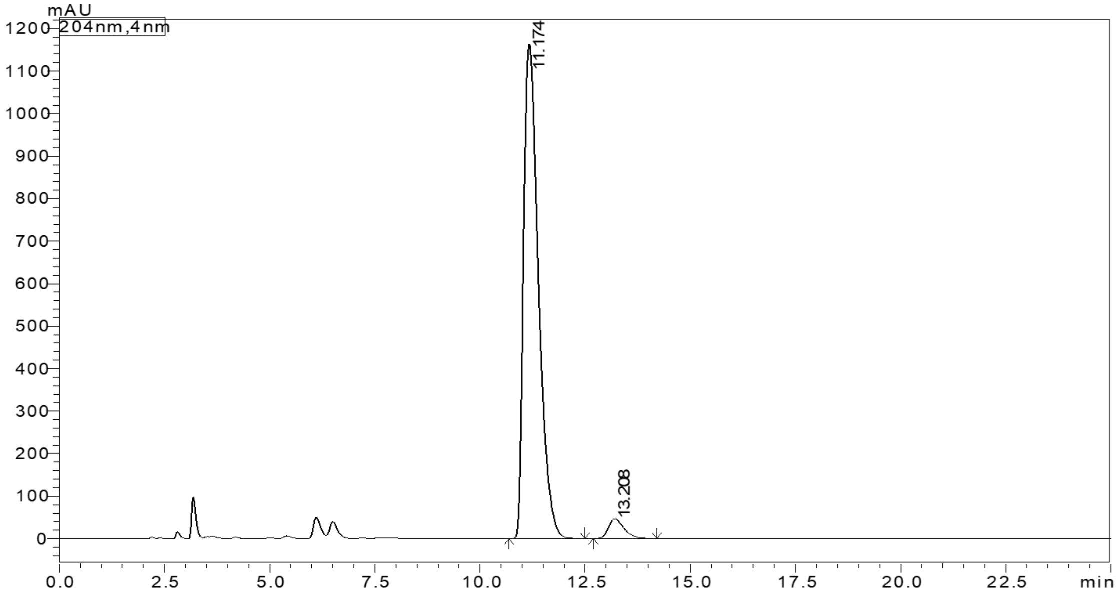

Peak	Time (Min.)	Area %
1	11.17	96.005
2	13.21	3.995
Total		100

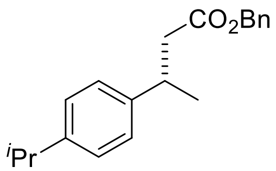

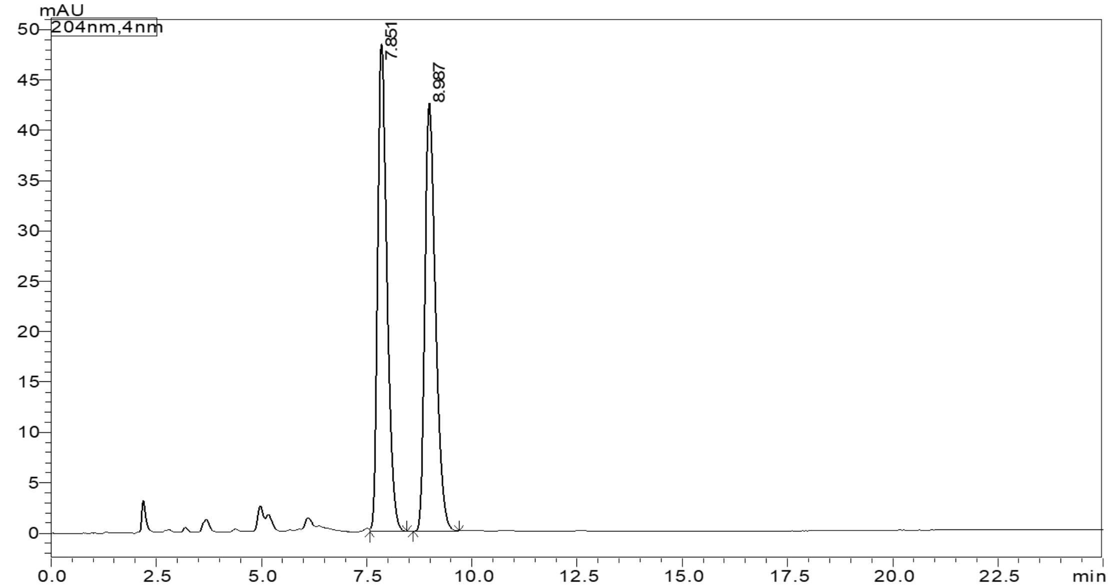

Peak	Time (Min.)	Area %
1	7.85	50.006
2	8.99	49.994
Total		100

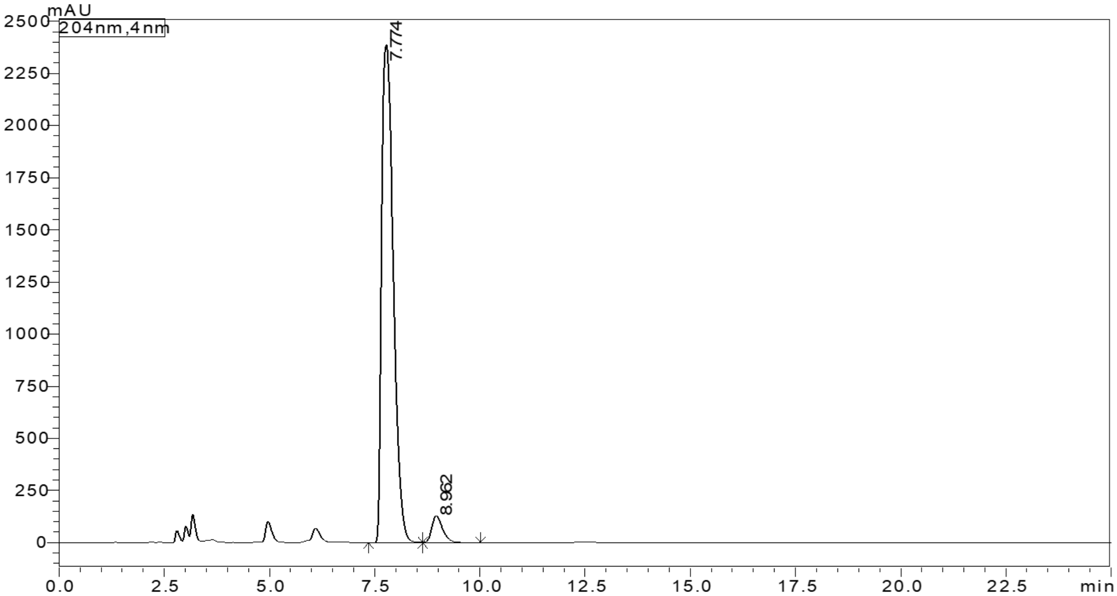

Peak	Time (Min.)	Area %
1	7.77	95.217
2	8.96	4.783
Total		100

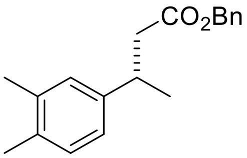

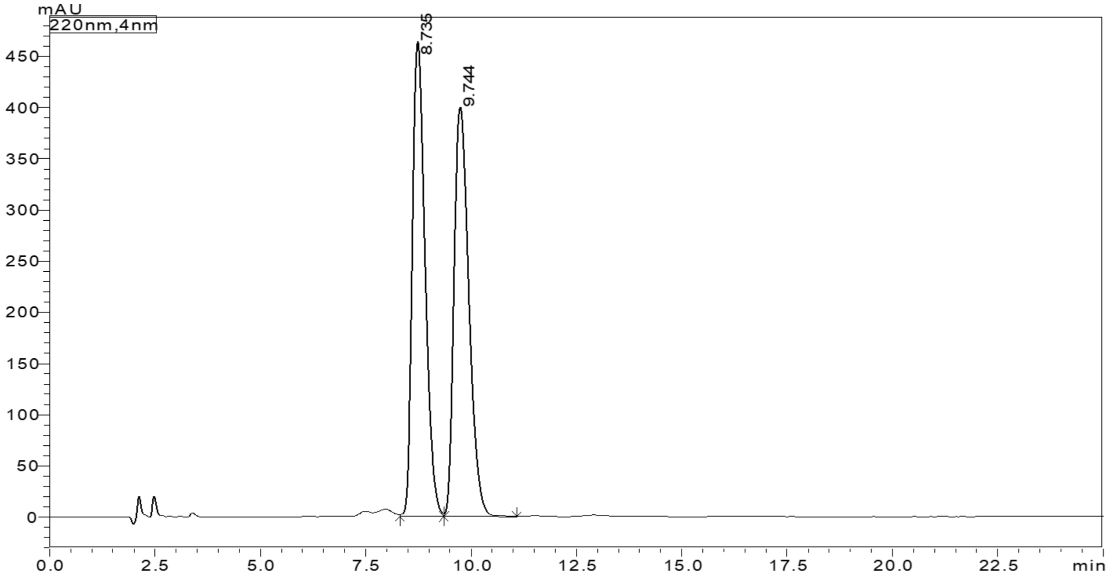

Peak	Time (Min.)	Area %
1	8.74	49.927
2	9.74	50.073
Total		100

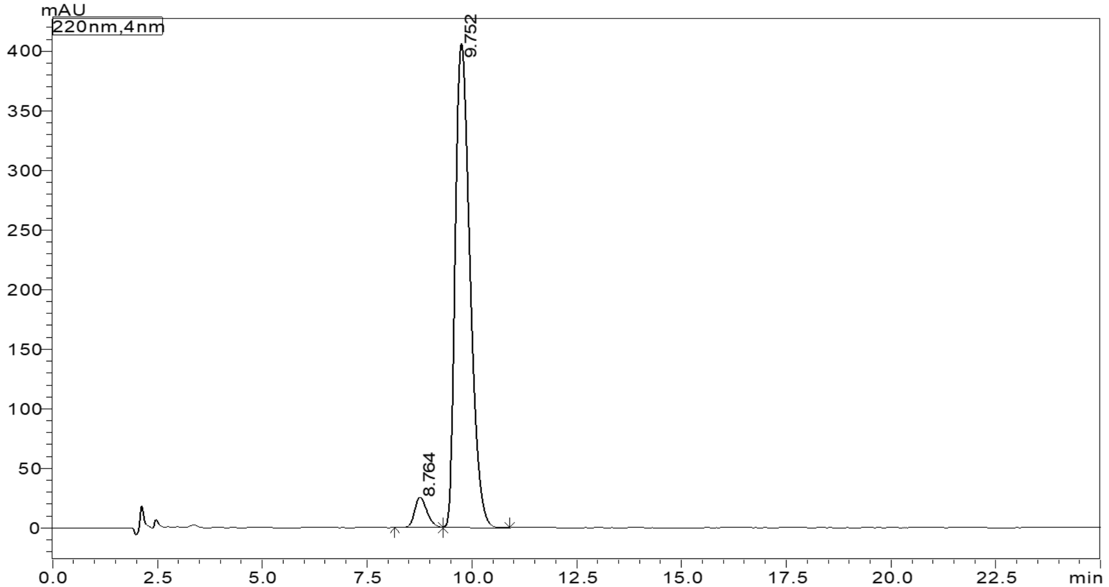

Peak	Time (Min.)	Area %
1	8.76	5.052
2	9.75	94.948
Total		100

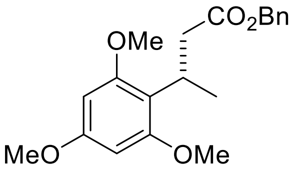
CO$_2$Bn
OMe
MeO
OMe

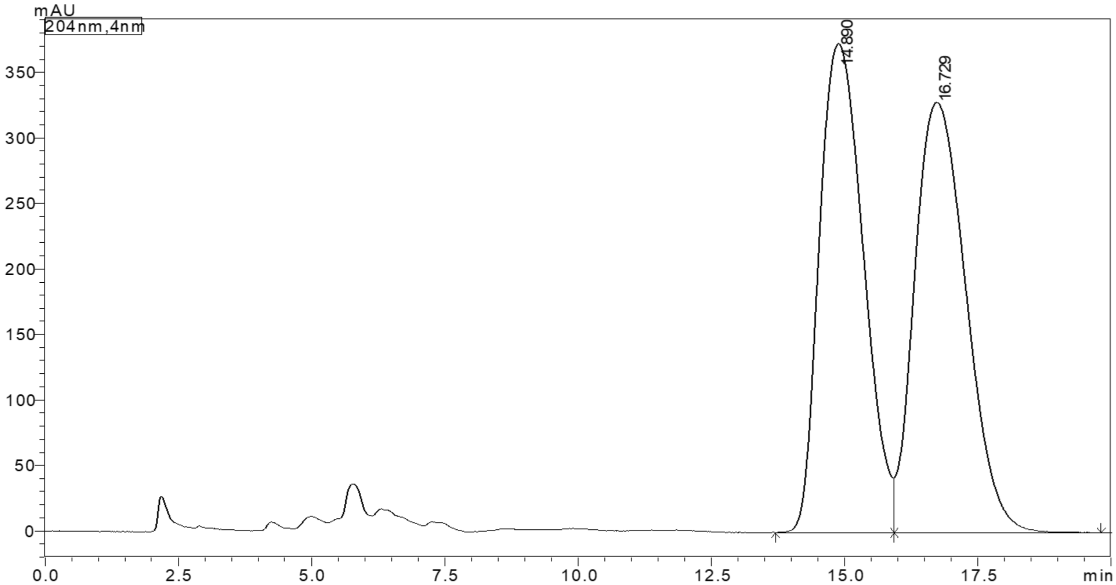

Peak	Time (Min.)	Area %
1	14.89	49.335
2	16.73	50.665
Total		100

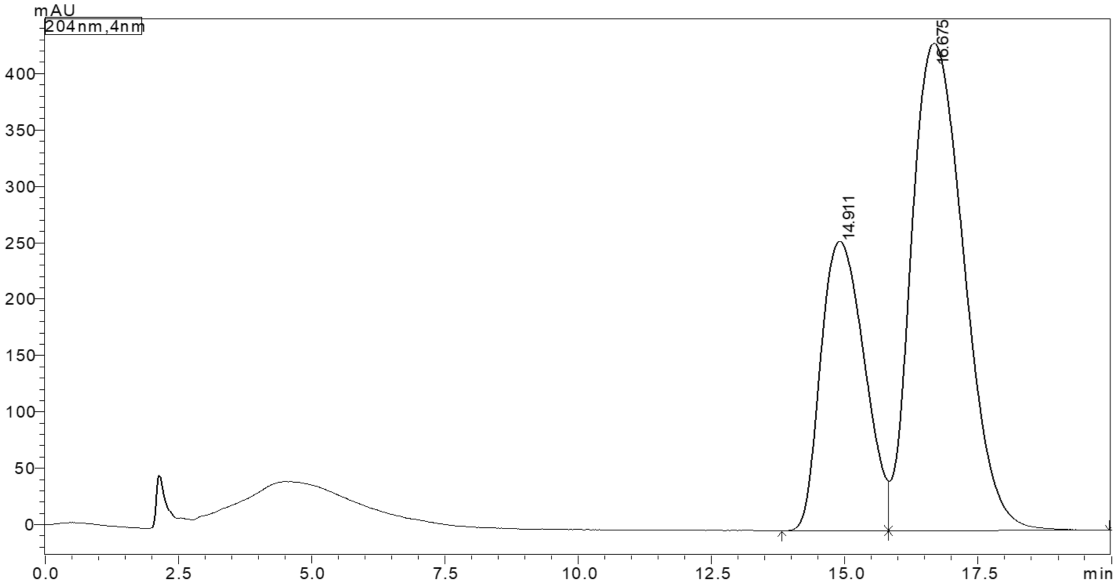

Peak	Time (Min.)	Area %
1	14.91	33.079
2	16.68	66.921
Total		100

7.7. Computational Study Data:

The computed ion pair structure was below.

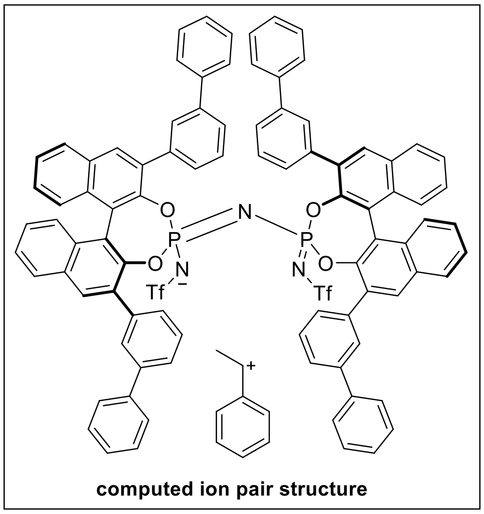
O
P
N
O
N
Tf
−
O
P
N
O
Tf
+

computed ion pair structure

The experimental enantioselectivities and absolute configuration of the corresponding products via this computed ion pair are shown below.

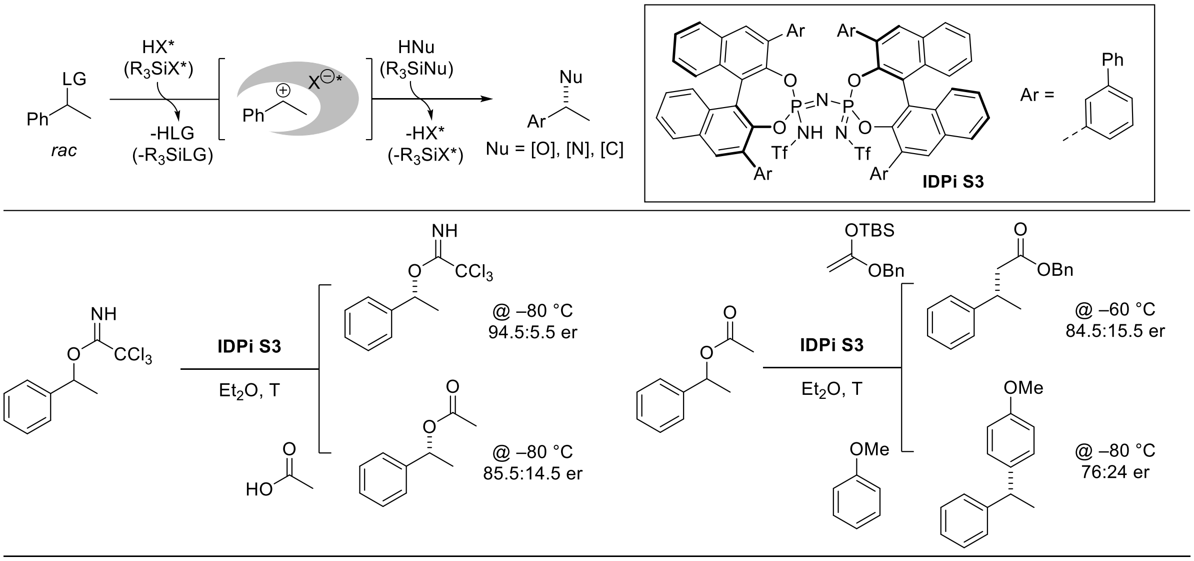
LG
Ph
rac
HX*
(R3SiX*)
-HLG
(-R3SiLG)
Ph
X⊖*
HNu
(R3SiNu)
-HX*
(-R3SiX*)
Nu
Ar
Nu = [O], [N], [C]
Ar
Ar
O
P=N
P
O
O
NH
N
O
Tf
Tf
Ar
Ar
IDPi S3
Ar =
Ph
NH
O
CCl3
IDPi S3
Et2O, T
HO
O
NH
O
CCl3
@ −80 °C
94.5:5.5 er
O
O
@ −80 °C
85.5:14.5 er
O
O
IDPi S3
Et2O, T
OTBS
OBn
OMe
O
OBn
@ −60 °C
84.5:15.5 er
OMe
@ −80 °C
76:24 er

7.7.1 Computational Details

A development version of the ORCA quantum package based on v. 5.0.3 (https://doi.org/10.1002/wcms.1606) was used for all calculations.

The computational protocol used to explore the chemical space for the chiral ion pair is illustrated in Figure 7.2.

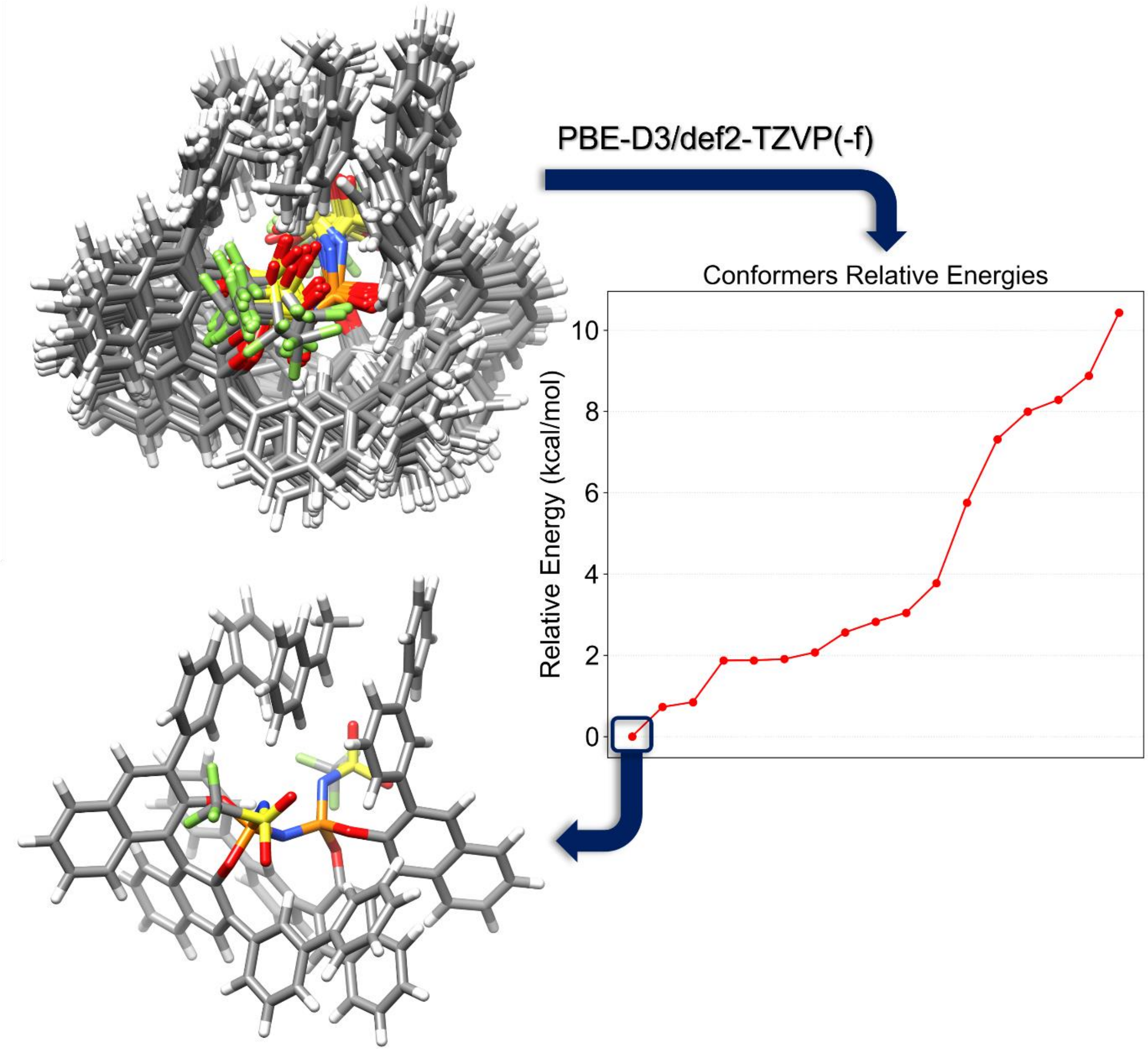

Figure 7.2. Graphical representation of the computational protocol used to determine most stable structures for the chiral ion pair under the experimental conditions.

An initial structural ensemble containing a large number of possible conformations for the chiral ion pair was generated using the CREST algorithm (https://doi.org/10.1039/C9CP06869D). Several CREST runs were carried out using different initial structures and levels of theory.

Specifically, multiple arrangements of the ion pair were modeled manually and used as starting points for the metadynamics simulation. Two different levels of theory were employed, *i.e.*, GFNFF and GFN2-XTB (https://doi.org/10.1002/anie.202004239, https://doi.org/10.1021/acs.jctc.8b01176). For the latter, solvation effects were included with the analytical linearized Poisson-Boltzmann (ALPB) solvation model.

The resulting conformers with unique structural features were refined through geometry optimizations at the DFT level using PBE-D3(BJ) exchange-correlation functional and Ahlrichs def2-TZVP(-f) basis set (https://doi.org/10.1103/PhysRevLett.77.3865, https://doi.org/10.1063/1.3382344, https://doi.org/10.1002/jcc.21759, https://doi.org/10.1016/0009-2614(95)00621-A). These settings have already proven to be reliable in dealing with systems such as the one under study (https://doi.org/10.1021/jacs.9b13725, https://doi.org/10.1021/jacs.8b07092, https://doi.org/10.1002/anie.202000307). For the chiral ion pair interaction analysis, single-point calculations on the previously optimized structures were carried out at B3LYP-D3/def2-QZVP level. Solvation effects in diethyl ether were included using the implicit solvation model CPCM (https://doi.org/10.1021/jp9716997).

NMR single-point calculations were carried out using the B3LYP functional together with the def2-TZVPP basis set on structures previously optimized at PBE-D3(BJ)/ def2-TZVP(-f) level.

Molecular electrostatic potential (MEP) maps were plotted onto electron density isosurfaces (isovalue: 0.002 e Bohr^{-3}). In all cases, the color range for the electrostatic potential is between -0.15 (colored in red) and + 0.15 (colored in blue).

Very tight SCF convergence criteria were used in all calculations. Vibrational frequencies were computed to ensure that all the refined structures were true minima. The resolution of identity (RI) approximation was used for the Coulomb integrals together with the corresponding auxiliary basis set (https://doi.org/10.1016/0009-2614(95)00621-A, https://doi.org/10.1002/jcc.10318, https://doi.org/10.1039/B515623H).

7.7.2 Chiral Ion Pair Interaction Analysis

The computed association free energy between the IDPi anion and benzylic carbocation (ΔG) is slightly negative under the experimental conditions and amounts to -22.08 kcal/mol. In table 7.1, this figure is decomposed into three terms according to the following equation:

$$\Delta G = \Delta E_{int} + \Delta E_{geom} + \Delta G_{therm}$$

In which ΔE_{int} is a stabilizing contribution representing the electronic interaction between the anion and the cation in the ion pair; ΔE_{geom} is the energy penalty required to distort the catalyst and the benzylic carbocation from their ground state structure to the one that is optimal for the interaction with the cation; ΔG_{therm} is the contribution from the thermostatistical corrections and accounts for temperature and entropy effects.

	B3LYP-D3/def2-QZVP (kcal/mol)
ΔG	-22.08
ΔE_{int}	-43.21
ΔE_{geom}	6.46
ΔG_{therm}	14.67

Table 7.1. An energy decomposition analysis of the interaction between the IDPi anion and benzylic carbocation (ΔG). See text for details.

ΔE_{int} is large and negative, demonstrating that the system is held together by strong and attractive noncovalent interactions. While the interaction between the anion and the cation is clearly electrostatically dominated (Figure 7.3), the decomposition of ΔE_{int} into dispersive (ΔE_{disp}) and steric/electrostatic components ($\Delta E_{ster/elec}$) shows that dispersion alone plays a crucial role in favoring the formation of the chiral ion pair, contributing with -27.33 kcal/mol to the overall interaction energy.

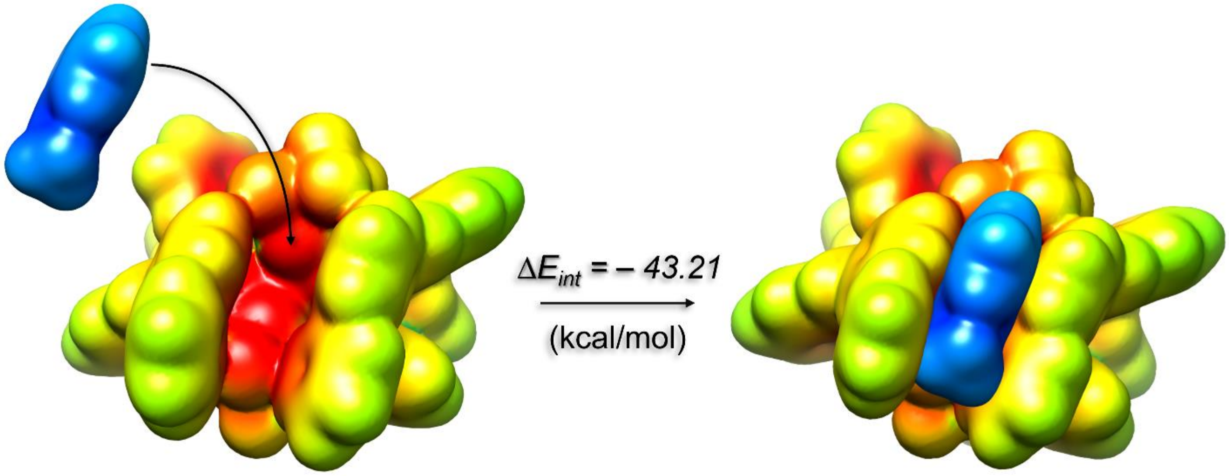

Figure 7.3. Interaction between the IDPi anion and the benzylic carbocation in the chiral ion pair. The molecular electrostatic potential map shows that the region with negative potential is localized in the active site of the IDPi anion.

The negative interaction is at least partially counterbalanced by: (i) the energy penalty required to distort the catalyst to maximize the electrostatic interaction with the cation (Figure 7.4.), (ii) entropy and temperature effects.

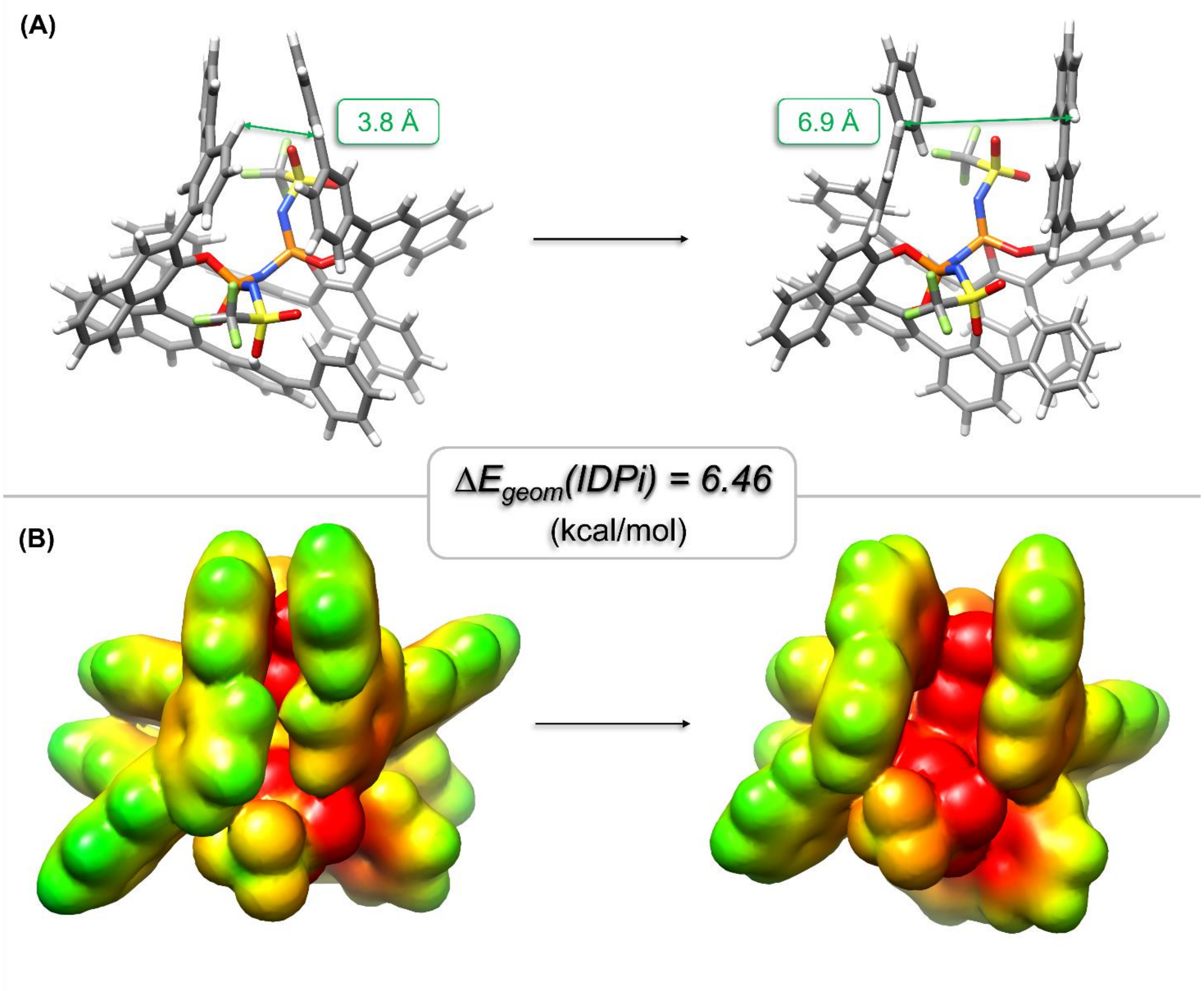
(A)
3.8 Å
6.9 Å
$\Delta E_{geom}(IDPi) = 6.46$
(kcal/mol)
(B)

Figure 7.4. Geometric distortion energy for the IDPi ($\Delta \boldsymbol{E_{geom}(IDPi)}$). **(A)** IDPi in its equilibrium structure (left) and in the chiral ion pair (right). **(B)** Molecular electrostatic potential of the IDPi in both geometries.

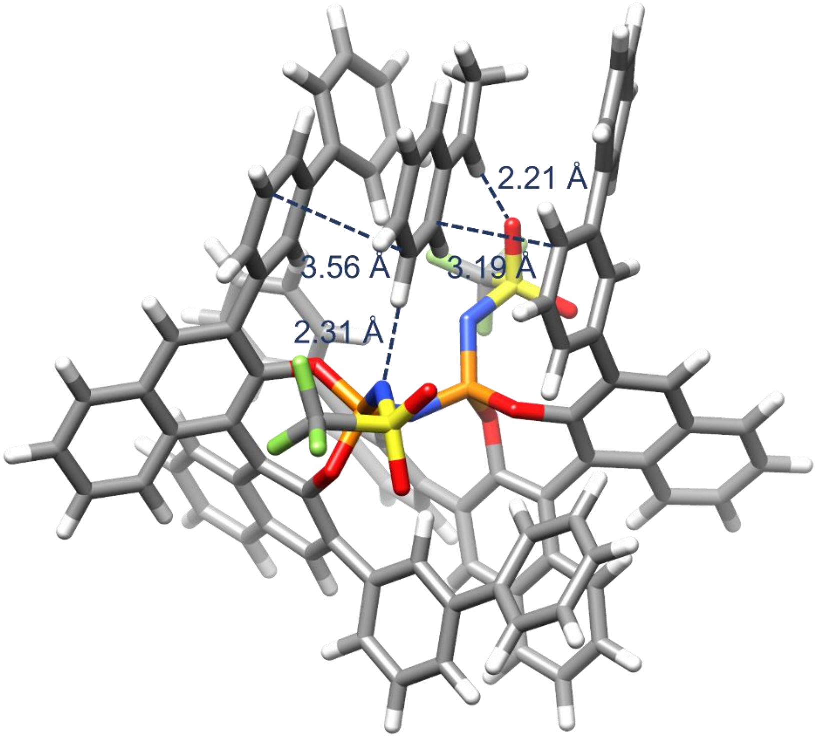

Figure 7.5. Graphic of the ion pair showing crucial interactions between the benzylic cation and the IDPi anion. The distances for the cation–p interaction were chosen so that the atoms of substrate and catalyst are in a as parallel as possible arrangement.

Most notably, the substrate resides between the 3-biphenyl substituents of the BINOL backbone (3.6 Å and 3.2 Å, respectively) that aid in stabilizing the reactive intermediate by virtue of cation–p interactions. Additionally, the benzylic CH group clearly interacts with a sulfonyl oxygen atom (2.2 Å), as well as the phenyl 3-CH with an inner core nitrogen atom (2.3 Å). It is plausible to assume that all of these interactions can be expected to play a vital role in the stabilization of the respective transition states leading to the major enantiomer.

7.7.3 Steric Interactions Analysis and Enantiofacial Discrimination

The topographic steric map (Figure 7.6) of the ion pair reveals that the *re* face of the benzylic is more accessible to the nucleophile for steric reasons. See Figure 7.7 for an illustrative scheme of the nucleophilic attack step.

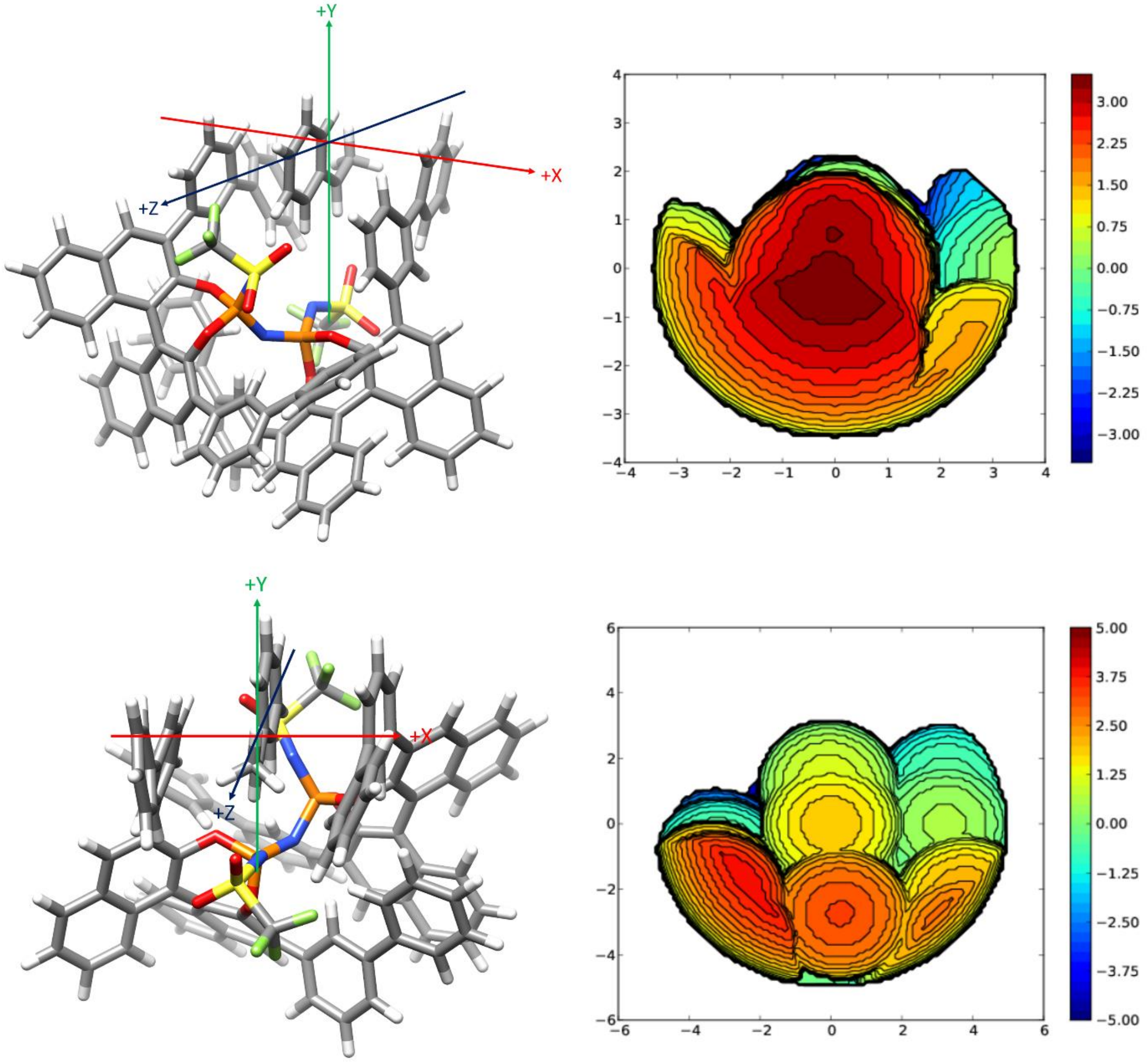

Figure 7.6. Axes orientations in the topographic steric maps highlighting the topology of the region surrounding the nucleophilic attack. The online tool Sambvca 2.1 was used (https://www.nature.com/articles/s41557-019-0319-5). In each steric map, the origin of the axes is close to the stereogenic carbon center, and the xy-plane is perpendicular to the plane where the benzylic cation lies.

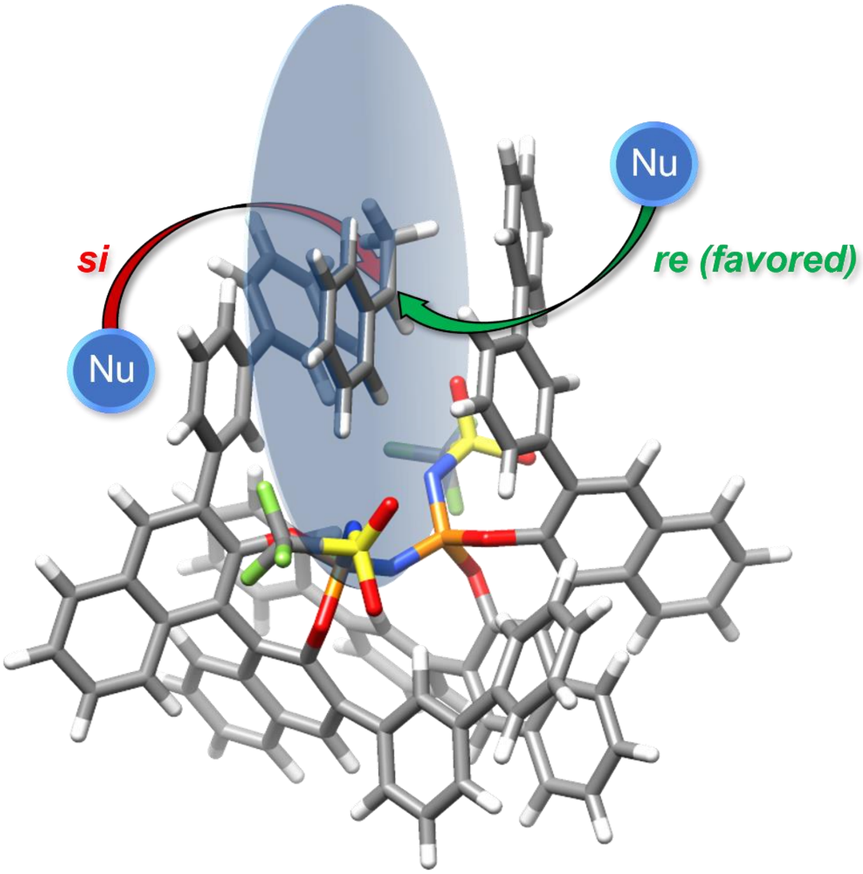

Figure 7.7. Schematic representation of the nucleophilic attack on the *re* face.

Our findings indicate that, in the most stable chiral ion pair structure, the re face of the benzylic carbocation is more accessible to the nucleophile. From this observation, we can reasonably speculate that steric, i.e., 'confinement', is indeed responsible for the observed selectivity. Of course, other effects can play a role here, and a long and detailed analysis of the chemical space for the transition states for multiple nucleophiles would be needed to clearly establish the origin of the selectivity.

We believe the unstable ion pair intermediate should have nearly the same energy content with the consecutive transition state since the products are much more stable, so the transition state should be ion pair like. And according to the Hammond postulate, the structure of the ion pair could make reasonable sense in explaining the enantioselectivities. Indeed, DFT optimized ion pair structure reveals an exposed *re* face of the benzylic cation, and we do observe all our reactions feature the same enantiofacial selectivities attacking from *re* face.

7.7.4 NMR Analysis for Ion Pair 4.4.3e

NMR calculations were carried out for the ion pair consisting of the 1-(2,4,6 trimethoxyphenyl)ethan-1-ylium cation and bistriflimide anion for which the ^{1}H NMR and ^{13}C NMR experimental results are reported in Figure 4.4.2. Table 7.2 shows the computed chemical shifts for the benzylic carbon and the benzylic proton:

Ion pair (4.4.3e)	***Theory***	***Experiment***
$C_{benzylic}$	191.0	173.8
$H_{benzylic}$	9.3	8.7

Table 7.2. Computed and experimental chemical shifts (ppm) for the benzylic carbon and proton of the 1-(2,4,6 trimethoxyphenyl)ethan-1-ylium in ion pair **4.4.3e**

The good agreement between the computed and experimental NMR shifts provides further evidence for the accuracy of our computational protocol. In addition, it serves as a further confirmation that the highly reactive ion pair **4.4.3e** was characterized spectroscopically.

XYZ coordinates

most stable chiral ion pair

184

C	2.23353142336598	-6.51889426953919	-0.46144673103073
C	1.35778569036778	-6.46065621401090	-1.52743958261721
C	0.60892858866529	-5.27131245030345	-1.76981682735137
C	0.79256913168707	-4.15209354968079	-0.90695585177189
C	1.70600681956835	-4.20931377751629	0.13191825619518
C	2.41929687426782	-5.38894772777424	0.35809659764694
C	-0.30564350204760	-5.14706511549848	-2.82603271451808
C	-0.53347178080756	-6.09305212903850	-3.90806461900936
N	1.71176929214933	-1.13974395707741	1.44842728100120
S	2.04402160230071	-1.46682323341374	2.95987168100306
O	1.66138295540666	-2.84685203159850	3.24476859203012
P	1.48352047488582	0.26573336528494	0.72474009913681
N	0.03129275193657	0.72198901027850	0.32708057752772
P	-1.38573199089600	0.13293733940277	-0.00114262020723
N	-1.40602373114017	-0.83781421632764	-1.28153644128837
S	-2.68754427574001	-1.32867044648995	-2.07521656916755
C	-2.81472340169823	-0.13126038992317	-3.52654959623886
F	-3.08421671221755	1.12202226321219	-3.12038389973150
O	2.17720450725879	1.43287234739240	1.61352855468142
C	2.18151497916598	2.70773550035276	1.02394542042696
C	3.04513421654339	2.89998355996428	-0.04361074422975
C	2.98655987373503	4.13562665955213	-0.76310415601995
C	2.08115808324817	5.14751338795344	-0.30272074764060
C	1.33007014713058	4.92866864508826	0.87391318548218
C	1.37498849165755	3.73829973691204	1.58735373904494
C	3.75842421046472	4.39050106349926	-1.92505355930611
C	3.65662233070736	5.59631546338916	-2.58793811564617
C	2.76774059991471	6.59767610213847	-2.13184551068414
C	1.98880541965256	6.37129136419399	-1.01706708704940
C	4.05198920142366	1.85249144587433	-0.36344617673088
C	3.66520742830974	0.56019929458067	-0.69243620885547
C	4.58577239388317	-0.46054212472008	-1.06292378377984
C	5.93402471160856	-0.13963421195491	-1.01808195055126
C	6.39906466194930	1.12846524612448	-0.60300939796761
C	5.45143802307027	2.14819510392386	-0.26140197872753
C	7.78932486076660	1.40803660125051	-0.51347319197915
C	8.23475277056247	2.63567801865215	-0.07276675215367
C	7.30100791070984	3.62948322249607	0.30434877666724
C	5.94426142793946	3.39368565931036	0.21137706270896
C	4.19673944944225	-1.80661848634468	-1.55179542325164
C	3.20682526815783	-1.97953272796207	-2.52908324417663
C	3.01374053751615	-3.21969865523620	-3.16576119301226

C	3.80140004713126	-4.31341588728944	-2.76606147160635
C	4.73648236442179	-4.17088306730265	-1.74499666522349
C	4.94145922413897	-2.92859447492329	-1.14558306731746
O	2.29853912943185	0.25838247757011	-0.68409485333760
C	0.74836224512902	3.66535091145819	2.93365223622404
C	0.15696633594685	2.51876154036098	3.48748824019524
C	-0.34672806067067	2.51261990304864	4.80056427990259
C	-0.28976634862567	3.69816561365089	5.55149307719405
C	0.28164156038424	4.84788529093554	5.01345888015967
C	0.80917502110856	4.83052719905738	3.72584612280238
O	-2.43111379798627	1.33805221106092	-0.28232664088116
C	-2.66961236611532	2.25839542232033	0.75117610581562
C	-2.25004382263375	3.60519704312151	0.55473752108725
C	-2.46951534008168	4.48499051998662	1.60249732746335
C	-3.07998213825585	4.08574418763512	2.81308903870030
C	-3.56397598437431	2.74368166161802	2.95142302120479
C	-3.39811682191395	1.83295882854292	1.85393257345959
C	-4.15507621677480	2.36357109596069	4.18381976526144
C	-4.28900990889151	3.27119891065672	5.21479067174422
C	-3.84122440633770	4.60425859342966	5.06488752841356
C	-3.24203221675125	4.99891551598390	3.88844029165355
C	-1.75511034487980	4.11771227950647	-0.74830828240138
C	-2.31893925800640	5.31272876358172	-1.23304509895834
C	-1.92040320204293	5.83554989374853	-2.46209944600423
C	-0.96874483725782	5.17121091042898	-3.23206380101823
C	-0.38002736067694	3.98115436500453	-2.76970833719190
C	-0.77647962383125	3.47639450026777	-1.52023885191882
C	-4.02938282590701	0.48632113482068	1.86241624156680
C	-3.28260607572267	-0.66192020673523	1.64443321181299
C	-3.81394639369732	-1.97646828531114	1.70667525538576
C	-5.16557451760901	-2.10800635554913	1.96098776286360
C	-6.00755415218865	-0.98005395365679	2.11193902569122
C	-5.44767125903043	0.33946062711140	2.04008260405537
C	-6.33461867034317	1.44748388045561	2.09441836959663
C	-7.69257301910712	1.26414741693631	2.26117591893800
C	-8.23531931919311	-0.03582242008499	2.38520117868911
C	-7.40646151584507	-1.13433940620064	2.30482101508666
O	-1.91380680370391	-0.54131408358428	1.37750367628682
C	-2.96266047506977	-3.16582037325866	1.46139063157076
C	-1.81077664081612	-3.42492949545922	2.22244009302458
C	-1.06868012677468	-4.57896784247330	1.98469313233618
C	-1.43369124349020	-5.46056062830319	0.96711091088745
C	-2.56080443406028	-5.20514365159016	0.16639139845798
C	-3.32580330109779	-4.06078732665637	0.44956542887081
O	-3.97151994289261	-1.18674655397776	-1.39416581313236
O	-2.39133804428409	-2.59873908336541	-2.73721979114052
O	1.71361398689663	-0.43376365739551	3.93206850422025
C	3.92581883292934	-1.53692553572242	2.97491958717181

F	4.46649879712151	-0.34355325263934	2.65458208193192
F	4.35362895160876	-1.88288870701449	4.20832848694480
F	4.38091588986113	-2.45894155974311	2.09485578015830
F	-3.81552921375718	-0.54304424886933	-4.33821298388819
F	-1.67022912529620	-0.11242059104491	-4.24366137035386
C	-0.92927588630701	1.28842496673566	5.39841857317630
H	0.09851719110272	1.60512839768084	2.90439496965090
H	0.32689949635942	5.76355652643890	5.60570949380142
H	1.30371589931098	5.72034226919865	3.33530869112816
H	5.68809125650225	-2.82034613797418	-0.35801396125909
C	2.04763272264224	-3.36259699598991	-4.27476507560274
H	2.63035821832744	-1.11537133580867	-2.85500422133503
H	-0.69897699986238	5.56546198219737	-4.21248689437977
H	-3.09735564829105	5.81220810330798	-0.65433765873934
H	-0.28392099787033	2.58976272573300	-1.12585916590968
C	0.61873770309244	3.26734130935287	-3.59878523719332
H	-1.49859860030328	-2.72908686232437	3.00120533983930
H	-0.17373072774430	-4.76870280136135	2.57768448549427
H	-4.21580681237636	-3.83997262558265	-0.13952417102958
H	4.42343138293468	3.61414071270016	-2.30288746661899
H	4.25182632894361	5.77023162498728	-3.48572261478620
H	2.69182446478500	7.54272643232730	-2.67205905287779
H	1.28783633578682	7.12987506586974	-0.66232980613466
H	0.68919517678126	5.73623676775518	1.23103924253722
H	5.23808190502491	4.16576689409339	0.51357269035231
H	8.49682556352658	0.62319187737434	-0.78950629253309
H	6.66772933520676	-0.88750193562993	-1.32477844860715
H	-4.48720281676410	1.33564824238300	4.32041837480828
H	-4.73612085134648	2.95340268951487	6.15813894118679
H	-3.95424229947151	5.31114473921472	5.88840150413440
H	-2.86774416631392	6.01730820966814	3.76611496437507
H	-2.14742899534360	5.52294110349293	1.49947393911160
H	-5.93512980637175	2.45517296082187	1.99018405609602
H	-8.35411675530428	2.13151227720216	2.29109015838028
H	-9.30944826374604	-0.16606904069860	2.52599893338784
H	-7.81274237385806	-2.14589211537963	2.37190186785019
H	-5.60376063916033	-3.10616540873972	2.02579807074946
H	9.30420415688801	2.83950746294776	-0.00073054349611
H	7.65681712302226	4.59082804518774	0.67853431102158
C	-2.91568827067269	-6.08676074132811	-0.96800505973865
H	5.31607576517213	-5.03371778875808	-1.41313565107720
H	-2.37898080186785	6.75311532400387	-2.83493834313484
H	-0.71333171646748	3.72304107956055	6.55587556676533
H	3.12565883154659	-5.43608292626547	1.18888734860160
H	2.79293071683613	-7.43317285253346	-0.26062602338243
H	1.21809667062378	-7.33014561921167	-2.16922224242701
H	0.20874775773018	-3.24639968440387	-1.08423123762466
H	1.84585776917261	-3.34341071012908	0.77431059927877

H	3.65311055874387	-5.28691273722973	-3.23397563968844
H	-0.80750505512096	-6.33088793175650	0.76736718250902
C	1.42596951722928	3.96129391513812	-4.51850102647512
C	2.34294639133734	3.28856617436303	-5.32434983318309
C	2.46944618924200	1.89973452230565	-5.23703171323337
C	1.67215276592822	1.19744907298863	-4.33002892467230
C	0.76525600237094	1.87168220810089	-3.51347144700778
H	1.35776828200572	5.04759273697674	-4.58103451441992
H	2.96692034547506	3.85303708553303	-6.01985685475578
H	3.17960768455603	1.36832758623439	-5.87292564160167
H	1.73829533503034	0.11039150957073	-4.27736166708700
H	0.14398274625978	1.30197962094246	-2.82247353425103
C	0.83322286178653	-2.64639539168592	-4.29262897080130
C	-0.05554273781671	-2.77174191574912	-5.36221777111646
C	0.24262143401520	-3.62118559957965	-6.42887402920310
C	1.44113889112861	-4.34682467961339	-6.42054817826192
C	2.33061699333861	-4.21902281946298	-5.35638750753845
H	0.57420550896547	-1.99797536332774	-3.45355236097564
H	-0.99374427056104	-2.21867848079485	-5.34718394044507
H	-0.45256835509246	-3.71912059656195	-7.26408167070683
H	1.68639983283030	-5.00736861950641	-7.25395923857011
H	3.27449220693893	-4.76572548136415	-5.37475354556228
C	-2.51197881284321	-7.43725948069034	-0.99916389445271
C	-2.85282126926207	-8.26618787997631	-2.06568009286259
C	-3.61303585955060	-7.76948379651179	-3.13081012330740
C	-4.02033528009755	-6.43122126343326	-3.11672879148402
C	-3.66987043066663	-5.59922934851323	-2.05473885592216
H	-1.94259595886711	-7.84966297823673	-0.16515270420529
H	-2.53307498562553	-9.30968821268072	-2.06228499344967
H	-3.88385243993059	-8.41969949786392	-3.96415325754133
H	-4.60168346539031	-6.02770389089080	-3.94763656911735
H	-3.95432145321522	-4.54810781038495	-2.08575460638418
C	-1.58687828427661	0.33193963048555	4.60953167493733
C	-2.17472973153808	-0.79305616359190	5.18485030836291
C	-2.10080215897440	-1.00139574302022	6.56466808234906
C	-1.42669296985100	-0.07204568466904	7.36124609078548
C	-0.85041995655339	1.06010007882225	6.78425902673662
H	-1.65796277689214	0.48673870528382	3.53502979647736
H	-2.71010362063225	-1.50566162920256	4.55542262167915
H	-2.56059885401849	-1.88315657030384	7.01414634915782
H	-1.34429745652006	-0.23038422034833	8.43817070364621
H	-0.31252853011456	1.76696790507131	7.41800535758793
H	-0.39801301018805	-5.55286224554636	-4.86695582407348
H	-1.60252468236762	-6.38234570530157	-3.91819977833833
H	-0.91580266955134	-4.23752249680360	-2.82986548563991
H	0.09969324147177	-6.98477146137242	-3.89020981304762

ion pair 4.4.3e

44

C	-2.42617397417866	-1.62420007601475	-0.21465969492059
S	-0.57284995189236	-1.86641357164386	0.02924733491158
F	-2.70423233879703	-0.36977295247520	-0.61853862211999
F	-3.09943447778760	-1.86436714770722	0.93081724871725
F	-2.86588913454224	-2.48733256686230	-1.15602581443085
C	2.13478023433872	0.52082597877040	0.94158376247503
F	2.58630185091679	0.00505059965474	2.10455632576565
F	2.67929113776849	1.74608923857199	0.77877013084749
S	0.25712785567809	0.67635513761224	0.95993079662250
F	2.54871644155882	-0.27055963127171	-0.06682123457707
O	-0.07052184765659	1.27498311456363	-0.32804714778265
O	-0.01067286999226	1.43477081085444	2.17737604233966
O	-0.47221090331510	-3.21562359943685	0.57566384185229
O	0.00375033674770	-1.59549554553860	-1.28188318353246
N	-0.22729622075897	-0.83555264763450	1.21373873872358
C	-1.91361884616805	-1.38789639556363	4.44046371221811
C	-2.23334570314122	-2.64706566485582	3.98758658034969
C	-1.19940719439353	-3.56877248764798	3.71082300336830
C	0.16063427526074	-3.26174586752414	3.91366813201763
C	0.49631127976128	-2.00590008576666	4.37668488657559
C	-0.52431355892982	-0.99222576696461	4.66002123776203
O	1.75411939084112	-1.61475984875275	4.59630919638515
O	-2.81876820570894	-0.43639214173637	4.69784643039632
O	-1.62010135042363	-4.74665129655137	3.25020887236111
C	-0.12334086502655	0.25504085282970	5.05880180852814
H	-1.65940079593485	1.22070054922706	6.19365682082988
H	-0.30413297241054	2.28291312770431	5.68491897475683
H	-1.55462429440919	1.73829708274537	4.52318706540194
H	0.95820608995723	0.38317768906013	5.13606241594940
C	-0.94119111345970	1.44287471482163	5.38903632665365
H	-3.25837158546953	-2.95574669065221	3.79934098050242
H	0.92743105739265	-3.99436860411857	3.68508857554274
C	-4.21168109045383	-0.74117334175818	4.46851972664747
H	-4.75142553638771	0.17291460503071	4.73222763027381
H	-4.37758660971671	-0.99094748597898	3.41137352213601
H	-4.53227996899844	-1.57220518213914	5.11243465457698
C	2.82618664510000	-2.52392782113556	4.26739862259040
H	3.74489871861516	-1.97611656457094	4.49545585923537
H	2.76139944225353	-3.43164223240636	4.88377423515786
H	2.79141488619220	-2.78089641707770	3.19966249278916
C	-0.64072648722444	-5.74395038360156	2.87136704009371
H	-1.22743851359818	-6.59148291345395	2.50587508402479
H	0.00231404110149	-5.35228131333492	2.07270172110328
H	-0.04474567290829	-6.04462789796907	3.74367493177960

8 References:

1) N. A. McGrath, M. Brichacek, J. T. Njardarson, *J. Chem. Educ.* **2010**, *87*, 1348–1349.
2) G. C. Fu, *ACS Cent. Sci.* **2017**, *3*, 692–700.
3) D. T. Ziegler, G. C. Fu, *J. Am. Chem. Soc.* **2016**, *138*, 12069–12072.
4) S. Athavale, K. Chen, F. H. Arnold, in Transition Metal–Catalyzed Carbene Transformations, J. Wang, C.-M. Che, M. P. Doyle, Eds. (Wiley, **2022**), chap. 4.
5) D. A. Evans, D. Ennis, D. J. Mathre, *J. Am. Chem. Soc.* **1982**, *104*, 1737–1739.
6) J. N. Brønsted, Recl, *Trav. Chim. Pays-Bas.* **1923**, *42*, 718–728.
7) T. M. Lowry, *Journal of the Society of Chemical Industry* **1923**, *42*, 43–47.
8) M. S. Sigman, E. N. Jacobsen, *J. Am. Chem. Soc.* **1998**, *120*, 4901–4902.
9) A. G. Doyle, E. N. Jacobsen, *Chem. Rev.* **2007**, *107*, 5713–5743.
10) T. J. Auvil, A. G. Schafer, A. E. Mattson, *Eur. J. Org. Chem.* **2014**, *2014*, 2633–2646.
11) Y. Huang, A. K. Unni, A. N. Thadani, V. H. Rawal, *Nature* **2003**, *424*, 146.
12) (a) T. Akiyama, J. Itoh, K. Yokota, K. Fuchibe, *Angew. Chem. Int. Ed.* **2004**, *43*, 1566–1568; (b) D. Uraguchi, M. Terada, *J. Am. Chem. Soc.* **2004**, *126*, 5356–5357.
13) S. Hoffmann, A. M. Seayad, B. List, *Angew. Chem. Int. Ed.* **2005**, *44*, 7424–7427.
14) L. M. Yagupolskii, V. N. Petrik, N. V. Kondratenko, L. Sooväli, I. Kaljurand, I. Leito, I. A. Koppel, *J. Chem. Soc. Perkin Trans.* **2002**, *2*, 1950–1955.
15) D. Nakashima, H. Yamamoto, *J. Am. Chem. Soc.* **2006**, *128*, 9626–9627.
16) S. Vellalath, I. Čorić, B. List, *Angew. Chem. Int. Ed.* **2010**, *49*, 9749–9752.
17) N. Momiyama, H. Okamoto, J. Kikuchi, T. Korenaga, M. Terada, *ACS Catal.* **2016**, *6*, 1198–1204.
18) (a) G. Pousse, A. Devineau, V. Dalla, L. Humphreys, M.-C. Lasne, J. Rouden, J. Blanchet, *Tetrahedron* **2009**, *65*, 10617–10622; (b) N. D. Shapiro, V. Rauniyar, G. L. Hamilton, J. Wu, F. D. Toste, *Nature* **2011**, *470*, 245–249.
19) C. H. Cheon, H. Yamamoto, *J. Am. Chem. Soc.* **2008**, *130*, 9246–9247.
20) P. Kaib, B. List, *Synlett* **2015**, *27*, 156–158.
21) P. García-García, F. Lay, P. García-García, C. Rabalakos, B. List, *Angew. Chem. Int. Ed.* **2009**, *48*, 4363–4366.
22) M. Treskow, J. Neudörfl, R. Giernoth, *Eur. J. Org. Chem.* **2009**, *2009*, 3693–3697.
23) M. van Gemmeren, F. Lay, B. List, *Aldrichimica Acta*. **2014**, *47*, 4–15.

24) T. James, M. van Gemmeren, B. List, *Chem. Rev.* **2015**, *115*, 9388–9409.

25) P. Christ, N. Leconte, J.-M. Neudörfl, M. Schäfer, A. Berkessel, *Eur. J. Org. Chem.* **2010**, *2010*, 5165−5170.

26) D. Kampen, A. Ladépêche, G. Claßen, B. List, *Adv. Synth. Catal.* **2008**, *350*, 962−966.

27) S. C. Pan, B. List, *Chem. Asian J.* **2008**, *3*, 430−437.

28) M. Hatano, T. Maki, K. Moriyama, M. Arinobe, K. Ishihara, *J. Am. Chem. Soc.* **2008**, *130*, 16858−16860.

29) M. Hatano, K. Ishihara, Asian *J. Org. Chem.* **2014**, *3*, 352−365.

30) I. Čorić, B. List, *Nature* **2012**, *483*, 315–319.

31) S. Liao, I. Čorić, Q. Wang, B. List, *J. Am. Chem. Soc.* **2012**, *134*, 10765–10768.

32) J. H. Kim, I. Čorić, S. Vellalath, B. List, *Angew. Chem. Int. Ed.* **2013**, *125*, 4570−4573.

33) J. H. Kim, I. Čorić, C. Palumbo, B. List, *J. Am. Chem. Soc.* **2015**, *137*, 1778−1781.

34) G. C. Tsui, L. Liu, B. List, *Angew. Chem. Int. Ed.* **2015**, *54*, 7703−7706.

35) Z. Sun, G. A. Winschel, A. Borovika, P. Nagorny, *J. Am. Chem. Soc.* **2012**, *134*, 8074−8077.

36) M. H. Aukland, B. List, *Pure and Applied Chemistry* **2021**, *93*, 1371−1381.

37) S. Das, L. Liu, Y. Zheng, M. W. Alachraf, W. Thiel, C. K. De, B. List, *J. Am. Chem. Soc.* **2016**, *138*, 9429−9432

38) L. Liu, P. S. J. Kaib, A. Tap, B. List, *J. Am. Chem. Soc.* **2016**, *138*, 10822−10825.

39) L. Schreyer, R. Properzi, B. *List, Angew. Chem. Int. Ed.* **2019**, *58*, 12761−12777.

40) P. S. J. Kaib, L. Schreyer, S. Lee, R. Properzi, B. List, *Angew. Chem. Int. Ed.* **2016**, *55*, 13200−13203.

41) a) S. Ghosh, S. Das, C. K. De, D. Yepes, F. Neese, G. Bistoni, M. Leutzsch, B. List, *Angew. Chem. Int. Ed.* **2020**, *59*, 12347−12351. b) H. Zhou, H. Y. Bae, M. Leutzsch, J. L. Kennemur, D. Bécart, B. List, *J. Am. Chem. Soc.* **2020**, *142*, 13695−13700. c) R. Properzi, P. S. J. Kaib, M. Leutzsch, G. Pupo, R. Mitra, C. K. De, L. Song, P. R. Schreiner, B. List, *Nat. Chem.* **2020**, *12*, 1174−1179. d) P. Zhang, N. Tsuji, J. Ouyang, B. List, *J. Am. Chem. Soc.* **2021**, *143*, 675−680. e) C. Zhu, F. Mandrelli, H. Zhou, R. Maji, B. List, *J. Am. Chem. Soc.* **2021**, *143*, 3312−3317. f) T. Amatov, N. Tsuji, R. Maji, L. Schreyer, H. Zhou, M. Leutzsch, B. List, *J. Am. Chem. Soc.* **2021**, *143*, 14475−14481. g) S. Das, B. Mitschke, C. K. De, I. Harden, G. Bistoni, B. List, *Nat. Catal.* **2021**, *4*, 1043−1049. h) O. Grossmann, R.

Maji, M. H. Aukland, S. Lee, B. List, *Angew. Chem. Int. Ed.* **2021**, *61*, e20211506. i) S. Ghosh, J. E. Erchinger, R. Maji, B. List, *J. Am. Chem. Soc.* **2022**, *144*, 6703–6708. j) H. Zhou, Y. Zhou, H. Y. Bae, M. Leutzsch, Y. Li, C. K. De, G.-J. Cheng, B. List, *Nature*, **2022**, *605*, 84–89. k) J. Ouyang, R. Maji, M. Leutzsch, B. Mitschke, B. List, *J. Am. Chem. Soc.* **2022**, *144*, 8460–8466. l) H. Zhou, J. T. Han, N. Nöthling, M. M. Lindner, J. Jenniches, C. Kühn, N. Tsuji, L. Zhang, B. List, *J. Am. Chem. Soc.* **2022**, *144*, 10156–10161. m) M. Scharf, B. List, *J. Am. Chem. Soc.* **2022**, *144*, 15451–154456. n) S. K. Nistanaki, C. G. Williams, B. Wigman, J. J. Wong, B. C. Haas, S. Popov, J. Werth, M. S. Sigman, K. N. Houk, H. M. Nelson, carbocations. *Science* **2022**, *378,* 1085–1091. o) H. Zhou, R. Properzi, M. Leutzsch, P. Belanzoni, G. Bistoni, N. Tsuji, J. T. Han, C. Zhu, B. List, *J. Am. Chem. Soc.* **2023**, *145,* 4994–5000. p) R. Maji, S. Ghosh, O. Grossmann, P. Zhang, M. Leutzsch, N. Tsuji, B. List, *J. Am. Chem. Soc.* **2023**, *145*, 8788–8793. q) J. T. Han, H. Zhou, B. List, *Synlett*, **2023**, *34*, 10.1055/a-2100-1575. r) S. Brunen, B. Mitschke, M. Leutzsch, B. List, *J. Am. Chem. Soc.* **2023**, *145*, 15708–15713.

42) L.-Y. Chen, H. He, W.-H. Chan, A. W. M. Lee, *J. Org. Chem.* **2011**, *76*, 7141–7147.

43) S. Prévost, N. Dupré, M. Leutzsch, Q. Wang, V. Wakchaure, B. List, *Angew. Chem. Int. Ed.* **2014**, *53*, 8770–8773.

44) Y. Xie, G.-J. Cheng, S. Lee, P. S. J. Kaib, W. Thiel, B. List, *J. Am. Chem. Soc.* **2016**, *138*, 14538–14541.

45) L. Liu, H. Kim, Y. Xie, C. Farès, P. S. J. Kaib, R. Goddard, B. List, *J. Am. Chem. Soc.* **2017**, *139*, 13656–13659.

46) J. Ouyang, J. L. Kennemur, C. K. De, C. Farès, B. List, *J. Am. Chem. Soc.* **2019**, *141*, 3414–3418.

47) N. Tsuji, J. L. Kennemur, T. Buyck, S. Lee, S. Prévost, P. S. J. Kaib, D. Bykov, C. Farès, B. List, *Science* **2018**, *359*, 1501–1505.

48) L. Ratjen, P. García-García, F. Lay, M. E. Beck, B. List, *Angew. Chem. Int. Ed.* **2011***, 50*, 754–758.

49) A. Tap, A. Blond, V. N. Wakchaure, B. List, *Angew. Chem. Int. Ed.* **2016**, *55*, 8962–8965.

50) J. Guin, C. Rabalakos, B. List, *Angew. Chem. Int. Ed.* **2012**, *51*, 8859–8863.

51) Z. Zhang, H. Y. Bae, J. Guin, C. Rabalakos, M. Van Gemmeren, M. Leutzsch, M. Klussmann, B. List, *Nat. Commun.* **2016**, *7,* 12478.

52) M. Mahlau, P. García-García, B. List, *Chem. Eur. J.* **2012**, *18*, 16283–16287.

53) J. Guin, Q. Wang, M. Van Gemmeren, B. List, *Angew. Chem. Int. Ed.* **2015**, *54*, 355–358.

54) Q. Wang, M. Leutzsch, M. van Gemmeren, B. List, *J. Am. Chem. Soc.* **2013**, *135*, 15334–15337.

55) Q. Wang, M. Van Gemmeren, B. List, *Angew. Chem. Int. Ed.* **2014**, *53*, 13592–13595.

56) S. Gandhi, B. List, *Angew. Chem. Int. Ed.* **2013**, *52*, 2573–2576.

57) S. Lee, P. S. J. Kaib, B. List, *J. Am. Chem. Soc.* **2017**, *139*, 2156–2159.

58) D. S. Allgäuer, H. Jangra, H. Asahara, Z. Li, Q. Chen, H. Zipse, A. R. Ofial, H. Mayr, *J. Am. Chem. Soc.* **2017**, *139*, 13318–13329.

59) T. Gatzenmeier, P. S. J. Kaib, J. B. Lingnau, R. Goddard, B. List, *Angew. Chem. Int. Ed.* **2018**, *57*, 2464–2468.

60) T. Gatzenmeier, M. Turberg, D. Yepes, Y. Xie, F. Neese, G. Bistoni, B. List, *J. Am. Chem. Soc.* **2018**, *140*, 12671–12676.

61) H. Y. Bae, D. Höfler, P. S. J. Kaib, P. Kasaplar, C. K. De, A. Dçhring, S. Lee, K. Kaupmees, I. Leito, B. List, *Nat. Chem.* **2018**, *10*, 888–894.

62) L. Schreyer, P. S. J. Kaib, V. N. Wakchaure, C. Obradors, R. Properzi, S. Lee, B. List, *Science* **2018**, *362*, 216–219.

63) S. A. Schwengers, C. K. De, O. Grossmann, J. A. A. Grimm, N. R. Sadlowski, G. G. Gerosa, B. List, *J. Am. Chem. Soc.* **2021**, *143*, 14835–14844.

64) J. A. A. Grimm, H. Zhou, R. Properzi, M. Leutzsch, G. Bistoni, J. Nienhaus, B. List, *Nature* **2023**, *615*, 634–639.

65) M. Mahlau, B. List, *Angew. Chem. Int. Ed.* **2013**, *52*, 518–533.

66) E. V. Anslyn, D. A. Dougherty, Modern Physical Organic Chemistry, University Science Books, **2005**, pp. 164–180.

67) S. Mayer, B. List, *Angew. Chem. Int. Ed.* **2006**, *45*, 4193–4195.

68) G. L. Hamilton, E. J. Kang, M. Mba, F. D. Toste, *Science* **2007**, *317*, 496–499.

69) S. Mukherjee, B. List, *J. Am. Chem. Soc.* **2007**, *129*, 11336–11337.

70) M. S. Taylor, E. N. Jacobsen, *J. Am. Chem. Soc.* **2004**, *126*, 10558–10559.

71) Z. Wang, J. Sun, *Synthesis* **2015**, *47*, 3629–3644.

72) A. A. Jaworski, K. A. Scheidt, *J. Org. Chem.* **2016**, *81*, 10145–10153.

73) W. Li, X. Xu, P. Zhang, P. Li, *Chem. Asian. J.* **2018**, *13*, 2350–2359.

74) J. Kikuchi, M. Terada, *Chem. Eur. J.* **2021**, *27*, 10215–10225.

75) C. Dorsch, C. Schneider, *Synthesis* **2022**, *54*, 3125−3141.

76) X. Li, Z. Li, J. Sun, *Nat. Synth.* **2022**, *1*, 426–438.

77) J. Ouyang, R. Maji, M. Leutzsch, B. Mitschke, B. List, *J. Am. Chem. Soc.* **2022**, *144*, 8460−8466.

78) M. Braun, W. Kotter, *Angew. Chem. Int. Ed.* **2004**, *43*, 514–517.

79) C. Zhao, F. D. Toste, K. N. Raymond, R. G. Bergman, *J. Am. Chem. Soc.* **2014**, *136*, 14409–14412.

80) A. E. Wendlandt, P. Vangal, E. N. Jacobsen, *Nature* **2018**, *556*, 447–451.

81) X. Tan, Z. Deng, Q. Wang, S. Chen, G. Zhu, J. Sun, *Nat. Synth.* **2023**, *2*, 275–285.

82) S. D. Walker, C. J. Borths, E. DiVirgilio, L. Huang, P. Liu, H. Morrison, K. Sugi, M. Tanaka, J. C. S. Woo, M. M. Faul, *Org. Process Res. Dev.* **2011**, *15*, 570−580.

83) a) W. Oppolzer, H. J. Löher, *Helv. Chim. Acta.* **1981**, *64*, 2808–2811. b) W. Oppolzer, T. Stevenson, *Tetrahedron Lett.* **1986**, *27*, 1139–1140. c) C. Fang, T. Ogawa, H. Suemune, K. Sakai, *Tetrahedron: Asymmetry* **1991**, *2*, 389–398. d) A. Alexakis, R. Sedrani, P. Mangeney, J. F. Normant, *Tetrahedron Lett.* **1988**, *29*, 4411–4414. e) F. Xu, R. D. Tillyer, D. M. Tschaen, E. J. J. Grabowski, P. J. Reider, *Tetrahedron: Asymmetry* **1998**, *9*, 1651−1655. f) K. Tanaka, M. Nuruzzaman, M. Yoshida, N. Asakawa, X.-S. Yang, K. Tsubaki, K. Fuji, *Chem. Pharm. Bull.* **1999**, *47*, 1053−1055.

84) G., Lonardi, R. Parolin, G. Licini, M. Orlandi *Angew. Chem. Int. Ed.* **2023**, *62*, e202216649.

85) J. D. White, Q. Xu, C. S. Lee, F. A. Valeriote, *Org. Biomol. Chem.* **2004**, *2*, 2092–2102.

86) B. López-Pérez, M. A. Maestro, A. Mouriño, *Chem. Commun.* **2017**, *53*, 8144–8147.

87) U. Leutenegger, A. Madin, A. Pfaltz, *Angew. Chem. Int. Ed.* **1989**, *28*, 60−61.

88) D. H. Appella, Y. Moritani, R. Shintani, E. M. Ferreira, S. L. Buchwald, *J. Am. Chem. Soc.* **1999**, *121*, 9473–9474.

89) B. H. Lipshutz, J. M. Servesko, B. R. Taft, *J. Am. Chem. Soc.* **2004**, *126*, 8352−8353.

90) a) Y. Tsuchiya, Y. Kanazawa, T. Shiomi, K. Kobayashi, H. Nishiyama, *Synlett* **2004**, *14*, 2493–2496. b) Y. Kanazawa, Y. Tsuchiya, K. Kobayashi, T. Shiomi, J.-i. Itoh, M. Kikuchi, Y. Yamamoto, H. Nishiyama, *Chem. Eur. J.* **2006**, *12*, 63–71.

91) C.-J. Hou, W.-L. Guo, X.-P. Hu, J. Deng, Z. Zheng, *Tetrahedron: Asymmetry* **2011**, *22*, 195–199.

92) S. Guo, J. (Steve) Zhou, *Org. Lett.* **2016**, *18*, 5344−5347.

93) R. Itooka, Y. Iguchi, N. Miyaura, *J. Org. Chem.* **2003**, *68*, 6000–6004.

94) a) Y. Takaya, T. Senda, H. Kurushima, M. Ogasawara, T. Hayashi, *Tetrahedron: Asymmetry* **1999**, *10*, 4047–4056. B) R. K. Rit, H. Li, S. P. Argent, K. M. Wheelhouse, S. Woodward, H. W. Lam, *Adv. Synth. Catal.* **2023**, *365*, 1629–1639.

95) a) S. Sakuma, M. Sakai, R. Itooka, N. Miyaura, *J. Org. Chem.* **2000**, *65*, 5951–5955. b) R. Itooka, Y. Iguchi, N. Miyaura, *J. Org. Chem.* **2003**, *68*, 6000–6004.

96) F. López, S. R. Harutyunyan, A. Meetsma, A. J. Minnaard, B. L. Feringa, *Angew. Chem. Int. Ed.* **2005**, *44*, 2752–2756.

97) J.-F. Paquin, C. R. J. Stephenson, C. Defieber, E. M. Carreira, *Org. Lett.* **2005**, *7*, 3821–3824.

98) S.-Y. Wang, S.-J. Ji, T.-P. Loh, *J. Am. Chem. Soc.* **2007**, *129*, 276–277.

99) a) A. Lightfoot, P. Schnider, A. Pfaltz, *Angew. Chem. Int. Ed.* **1998**, *37*, 2897–2899. b) D. Liu,W. Tang, X. Zhang, *Org. Lett.* **2004**, *6*, 513–516. c) J. Zhao, K. Burgess, *J. Am. Chem. Soc.* **2009**, *131*, 13236–13237. d) X. Cui, K. Burgess, *Chem. Rev.* **2005**, *105*, 3272–3296. e) T. L. Church, P. G. Andersson, Coord. *Chem. Rev.* **2008**, *252*, 513–531. f) D. H. Woodmansee,A. Pfaltz, Iridium Catalyzed Asymmetric Hydrogenation of Olefins with Chiral N,P and C,N Ligands, Springer, Berlin Heidelberg, **2010**. g) S. J. Roseblade, A. Pfaltz, *Acc. Chem. Res.* **2007**, *40*, 1402–1411. h) D. H. Woodmansee, A. Pfaltz, *Chem. Commun.* **2011**, *47*, 7912–7916. i) D. Rageot, D. H. Woodmansee, B. Pugin, A. Pfaltz, *Angew. Chem. Int. Ed.* **2011**, *50*, 9598–9601. j) S.-M. Lu, C. Bolm, *Angew. Chem. Int. Ed.* **2008**, *47*, 8920–8923. k) J. Mazuela, O. Pàmies, M. Diéguez, *ChemCatChem* **2013**, *5*, 2410–2417.

100) D. H. Woodmansee, M.-A. Müller, L. Tröndlin, E. Hörmann, A. Pfaltz, *Chem. Eur. J.* **2012**, *18*, 13780–13786.

101) M. Shevlin, M. R. Friedfeld, H. Sheng, N. A. Pierson, J. M. Hoyt, L.-C. Campeau, P. J. Chirik, *J. Am. Chem. Soc.* **2016**, *138*, 3562−3569.

102) R. K. Zhang, K. Chen, X. Huang, L. Wohlschlager, H. Renata, F. H. Arnold, *Nature* **2019**, *565*, 67–72.

103) S. D. Laffoon, Z. Wu, K. L. Hull, *Chem. Commun.* **2018**, *54*, 7814–7817.

104) D. H. Aue, Dicoordinated carbocations; Rappoport, Z., Stang, P. J., Eds.; John Wiley and Sons: Chichester, 1997, pp 105–156.

105) E. V. Anslyn, D. A. Dougherty, Modern physical organic chemistry, page 88, (2006) ISBN: 978-1-891389-31-3.

106) Z. Li, Z. Zhou, L. Wang, Q. Zhou, C. Tang, *Tetrahedron: Asymmetry* **2002**, *13*, 145–148.

107) K. Tauber, M. Fuchs, J. H. Sattler, J. Pitzer, D. Pressnitz, D. Koszelewski, K. Faber, J. Pfeffer, T. Haas, W. Kroutil, *Chem. Eur. J.* **2013**, *19*, 4030–4035.

108) F. G. Mutti, T. Knaus, N. S. Scrutton, M. Breuer, N. J. Turner, *Science* **2015**, *349*, 1525–1529.

109) F.-F. Chen, Y.-Y. Liu, G.-W. Zheng, J.-H. Xu, *ChemCatChem* **2015**, *7*, 3838–3841.

110) E. Liardo, N. R.-Lombardía, F. Morís, F. Rebolledo, J. G.-Sabín, *ACS Catal.* **2017**, *7*, 4768−4774.

111) L. J. P. Martyn, S. Pandiaraju, J. Zheng, A. Lough, A. K. Yudin *Org. Lett.* **2000**, *2*, 1, 41–44.

112) R. J. Detz, Z. Abiri, R. le Grile. H. Hiemstra, J. H. van Maarseveen, *Chem. Eur. J.* **2011**, *17*, 5921–5930.

113) a) E. J. Corey, D. H. Lee, *J. Am. Chem. Soc.* **1991**, *113*, 4026–4028 b) E. J. Corey, S. S. Kim, *J. Am. Chem. Soc.* **1990**, *112*, 4976–4977.

114) a) M. Roeder, O. Spiegelstein, V. Schurig, M. Bialer, B. Yagen, *Tetrahedron: Asymmetry* **1999**, *10*, 841–853. b) B.-F. Li, R. M. Hughes, J. Le, K. McGee, D. J. Gallagher, R. S. Gross, D. Provencal, J. P. Reddy, P. Wang, L. Zegelman, Y. Zhao, S. E. Zook, *Org. Process Res. Dev.* **2009**, *13*, 463–467.

115) M. P. Sibi, J. Chen, *J. Am. Chem. Soc.* **2001**, *123*, 9472–9473. b) H.-C. Guo, J.-A. Ma, *Angew. Chem. Int. Ed.* **2006**, *45*, 354–366. c) P. Tian, H.-Q. Dong, G.-Q. Lin, *ACS Catal.* **2012**, *2*, 95–119. d) T. Jia, P. Cao, J. Liao, *Chem. Sci.* **2018**, *9*, 546–559.

116) S. P. Miller, J. P. Morken, *Org. Lett.* **2002**, *4*, 2743–2745. b) K. C. Wong, E. Ng, W.-T. Wong, P. Chiu, *Chem. Eur. J.* **2016**, *22*, 3709–3712.

117) Y.-Q. Han, X. Yang, K.-X. Kong, Y.-T. Deng, L.-S. Wu, Y. Ding, B.-F. Shi, *Angew. Chem. Int. Ed.* **2020**, *59*, 20455–20458.

118) E. J. Corey, A. Guzman-Perez, *Angew. Chem., Int. Ed.* **1998**, *37*, 388–401. (b) C. J. Douglas, L. E. Overman, *Proc. Natl. Acad. Sci. U. S. A.* **2004**, *101*, 5363–5367. (c) K. W. Quasdorf, L. E. Overman, *Nature* **2014**, *516*, 181–191. (d) Y. Liu, S.-J. Han, W.-B. Liu, B. M. Stoltz, *Acc. Chem. Res.* **2015**, *48*, 740–751. (e) X.-P. Zeng, Z.-Y. Cao, Y.-H. Wang, F. Zhou, J. Zhou, Chem. Rev. **2016**, *116*, 7330–7396. (f) C. G. Newton, S.-G. Wang, C. C. Oliveira, N. Cramer, *Chem. Rev.* **2017**, *117*, 8908–8976. (g) Z. Dong, Z. Ren, S. J. Thompson, Y. Xu, G. Dong, *Chem. Rev.* **2017**, *117*, 9333–9403. (h) J. Feng, M. Holmes, M. J. Krische, *Chem. Rev.* **2017**, *117*, 12564–12580. (i) Y. Li, S. Xu, *Chem. Eur. J.* **2018**, *24*, 16218–16245. (j) Y. Ping, Y. Li, J. Zhu, W. Kong, *Angew. Chem. Int. Ed.* **2019**, *58*, 1562–1573. (k) Q. Li, Z.-X. Yu, *Angew. Chem., Int. Ed.* **2011**, *50*, 2144–2147. (l) B. Ye, P. A. Donets, N. Cramer, *Angew. Chem., Int. Ed.* **2014**, *53*, 507–511. (m) C. Zhang, C. B. Santiago, J. M. Crawford, M. S. Sigman, *J. Am. Chem. Soc.* **2015**, *137*, 15668–15671.

119) R. M. Wilson, W. S. Jen, D. W. C. MacMillan, *J. Am. Chem. Soc.* **2005**, *127*, 11616–11617.

120) a) S. Krautwald, D. Sarlah, M. A. Schafroth, E. M. Carreira, *Science* **2013**, *340*, 1065–1068. b) C. D. Behenna, B. M. Stoltz, *J. Am. Chem. Soc.* **2004**, *126*, 15044–15045. c) J. J. Murphy, D. Bastida, S. Paria, M. Fagnoni, P. Melchiorre, *Nature* **2016**, *532*, 218–222.

121) P. Zhang, H. Le, R. E. Kyne, J. P. Morken, *J. Am. Chem. Soc.* **2011**, *133*, 9716–9719.

122) B. Jung, A. H. Hoveyda, *J. Am. Chem. Soc.* **2012**, *134*, 1490–1493.

123) T.-S. Mei, H. H. Patel, M. S. Sigman, *Nature* **2014**, *508*, 340–344.

124) D. R. Wallach, J. D. Chisholm, *J. Org. Chem.* **2016**, *81*, 8035–8042.

125) A. A. Adhikari, T. Suzuki, R. T. Gilbert, M. R. Linaburg, J. D. Chisholm, *J. Org. Chem.* **2017**, *82*, 3982–3989.

126) K. Ikeuchi, K. Murasawaa, H. Yamada, *Synlett* **2019**, *30*, 1308–1312.

127) C. Zhang, G. Zhang, S. Luo, C. Wang, H. Li, *Org. Biomol. Chem.* **2018**, *16*, 8467–8471.

128) K. Nguyen, V. Nguyen, H. Trau, P. Pham, *RSC Adv.* **2023**, *13*, 7168–7178.

129) B. M.-Matute, M. Edin, K. Bogár, F. B. Kaynak, J.-E. Bäckvall, *J. Am. Chem. Soc.* **2005**, *127*, 8817–8825.

130) G. A. B. Vieira, T. L. G. Lemos, M. C. de Mattos, M. da. C. F. de Oliveira, V. M. M. Melo, G. de Gonzalo, V. G.-Fernández, V. Gotor, *Tetrahedron:Asymmetry* **2009**, *20*, 214–219.

131) B. Wang, X. Tang, J. Liu, H. Yu, *Tetrahedron Lett.* **2010**, *51*, 6360–6364.

132) A. Vandenberghe, I. E. Markó, F. Lucaccioni, S. Lutts, *Industrial Crops and Products* **2013**, *42*, 380–385.

133) A. Kinens, S. Balkaitis, O. K. Ahmad, D. W. Piotrowski, E. Suna, *J. Org. Chem.* **2021**, *86*, 7189−7202.

134) M.-J. Kim, H. M. Kim, D. Kim, Y. Ahn., *J. Park, Green Chem.* **2004**, *6*, 471–474.

135) P. Yuan, J. Chen, J. Zhao, Y. Huang, *Angew. Chem. Int. Ed.* **2018**, *57*, 8503–8507.

136) S. Pal, A. Khatua, M. K. Das, V. Bisai, *Tetrahedron Lett.* **2021**, *65*, 152790.

Appendix:

ERKLÄRUNG ZUR DISSERTATION

Hiermit versichere ich an Eides statt, dass ich die vorliegende Dissertation selbstständig und ohne die Benutzung anderer als der angegebenen Hilfsmittel und Literatur angefertigt habe. Alle Stellen, die wörtlich oder sinngemäß aus veröffentlichten und nicht veröffentlichten Werken dem Wortlaut oder dem Sinn nach entnommen wurden, sind als solche kenntlich gemacht. Ich versichere an Eides statt, dass diese Dissertation noch keiner anderen Fakultät oder Universität zur Prüfung vorgelegen hat; dass sie – abgesehen von unten angegebenen Teilpublikationen und eingebundenen Artikeln und Manuskripten- noch nicht veröffentlicht worden ist sowie, dass ich eine Veröffentlichung der Dissertation vor Abschluss der Promotion nicht ohne Genehmigung des Promotionsausschusses vornehmen werde. Die Bestimmungen dieser Ordnung sind mir bekannt. Darüber hinaus erkläre ich hiermit, dass ich die Ordnung zur Sicherung guter wissenschaftlicher Praxis und zum Umgang mit wissenschaftlichem Fehlverhalten der Universität zu Köln gelesen und sie bei der Durchführung der Dissertation zugrundeliegenden Arbeiten und der schriftlich verfassten Dissertation beachtet habe und verpflichte mich hiermit, die dort genannten Vorgaben bei allen wissenschaftlichen Tätigkeiten zu beachten und umzusetzen. Ich versichere, dass die eingereichte elektronische Fassung der eingereichten Druckfassung vollständig entspricht.

Vikas Kumar Singh

Mülheim an der Ruhr, 13.12.2023

Unterschrift

Vikas Kumar Singh

Homogenous Catalysis (Organic Chemistry)
Ph.D. student

Max-Planck-Institut für Kohlenforschung

Male **DOB: 05/07/1996**

Academic Summary

Examination	University	Institute	Year	CPI / %
Integrated M.Sc.	IIT Bombay	IIT Bombay	2018	7.52
Higher Secondary	UP Board	S.P.I. College	2012	74
Secondary	UP Board	S.P.I. College	2010	69

Research Publications

Taming Secondary Benzylic Cations in Catalytic Asymmetric S_N1 Reactions.

V. K. Singh, C. Zhu, C. K. De, M. Leutzsch, L. Baldinelli, R. Mitra, G. Bistoni, B. List, *Science* **2023**, *382*, 325–329.

Alkyne Linchpin Strategy for Drug:Pharmacophore Conjugation: Experimental and Computational Realization of a *meta*-Selective Inverse Sonogashira Coupling.

S. Porey, X. Zhang, S. Bhowmick, **V. K. Singh**, S. Guin, R. S. Paton, D. Maiti, *J. Am. Chem. Soc.*, **2020**, *142*, 3762–3774.

Iterative Arylation of Amino Acids and Aliphatic Amines *via* δ-C(sp^3)−H Activation: Experimental and Computational Exploration.

S. Guin, P. Dolui, X. Zhang, S. Paul, **V. K. Singh**, S. Pradhan, H. B. Chandrashekar, S. S. Anjana, R. S. Paton, D. Maiti, *Angew. Chem. Int. Ed.*, **2019**, *58*, 5633–5638.

Promoting Highly Diastereoselective *γ*-C−H Chalcogenation of *α*-Amino Acids and Aliphatic Carboxylic Acids.

S. Guin, A. Deb, P. Dolui, S. Chakraborty, **V. K. Singh**, D. Maiti, *ACS Catal.*, **2018**, *8*, 2664–2669.

Experimental and Computational Exploration of *para*-Selective Silylation Involving H-Bonded Template.

A. Maji, S. Guin, S. Feng, A. Dahiya, **V. K. Singh**, P. Liu, D. Maiti, *Angew. Chem. Int. Ed.*, **2017**, *56*, 14903–14907.